

1994

| Paper No | Paper Title | Author Details | Company | Page |
|----------|--|---|--|------|
| | Keynote Address: Hydrocarbon Mixture Equations of State and Their Impact on Gas Flow Measurement | Kenneth Starling | Univ of Oklahoma | 4 |
| 1.1 | The Use of Calculated Density on an Offshore High Pressure Wet Gas Metering System | M Emms | British Gas | 13 |
| 1.2 | Wet Gas Flow Measurement by Means of a Venturi Meter and a Tracer Technique | H de Leeuw | Shell Research | 46 |
| 1.3 | Do We Need to Use Gas Density Meters in North Sea Metering Stations | Dr P L Wilcox | SGS | 59 |
| 1.4 | Agip – Trecate Multiphase Test Loop Facility Description and Specification | A Mazzoni M Bonuccelli | Agip C.P.R.-TEA | 69 |
| 2.1 | Shortening Installation Lengths Using a Low Loss Vaned Flow Conditioner | E M Laws and A K Ouazzane A Erdal | University of Salford K-Lab | 85 |
| 2.2 | Development of a Flow Conditioner | A Erdal D Lindholm and D Thomassen | K-Lab IFE | 96 |
| 2.3 | Design of a Tube Bundle Conditioner from Aerodynamic Concepts | P Gajan and A Strzelecki M Bosch D Donat | ONERA/CERT/DERMES Gaz de Sud Ouest Gaz de France | 108 |
| 2.4 | The Gallagher Flow Conditioner | James Gallagher Paul J LaNasa Ronald E Beaty | Shell USA CPL Aramco Production | 119 |
| 3.1 | North Sea Field Test of a Multiphase Flowmeter | Andreas Hatlo Sven Sørensen | Kongsberg Maersk Oil & Gas | 138 |
| 3.2 | Using the MFI Multiphase Meter for Well Testing at Gullfaks B | Ole Økland and Hans Berentsen | Statoil | 148 |
| 3.3 | BP Multiphase Meter Test Experience | W J Priddy | BP Exploration | 159 |
| 3.4 | An Evaluation of Some Static Mixers in Multiphase Flow | Sigmund Hjermann and Eivind Dykesteen | CMR | 172 |
| 3.5 | Development and Trial of Multiphase Flow Meters for Oil, Water and Gas in Pipelines | S L Ashton, N G Cutmore, G J Roach, J S Watt and H W Zastawny | CSIRO | 189 |

1994

| Paper No | Paper Title | Author Details | Company | Page |
|-----------------|--|---------------------------------------|--|-------------|
| 4.1 | V-Cone Meter: Gas Measurement for the Real World | Maron Dahlstrom | Phillips AS | 217 |
| 4.2 | Installation Effects on Multi-Path Ultrasonic Flow Meters: The "ULTRAFLOW" Project | K van Bloemendaal and P M van der Kam | Gasunie | 233 |
| 4.3 | Developments of Multipath Transit Time Ultrasonic Gas Flow Meters | K J Zanker W R Freund Jr | Daniel Industries UK Daniel Electronics USA | 243 |
| 4.4 | The Effect of Different Path Configurations on Ultrasonic Flow Measurement | T Cousins | Stork Flow Measurement | 255 |
| 5.1 | Water-in-Oil: On-Line Measurement. The MFI Water Cut Meter in Offshore Applications | R Purvey | BP Research | 275 |
| 5.2 | Field Testing of the Fluenta WIOM 300 – Water-in-Oil | L Farestvedt | Fluenta | 291 |
| 5.3 | Framo Multiphase Flow Meter – Field Testing Experience from Statoil Gullfaks A and B Platforms and Texaco Humble Test Facilities | A B Olsen and Birger V Hanssen | Framo Engineering AS | 301 |
| 5.4 | A Cooperative Approach to New Product Development | W Letton | Daniel Electronics | 311 |

SESSION 1

QUALITY GAS MEASUREMENT

Chairman - G J Stobie, Phillips UK

HYDROCARBON MIXTURE EQUATIONS OF STATE AND THEIR IMPACT ON GAS FLOW MEASUREMENT

Kenneth E. Starling

School of Chemical Engineering and Materials Science, University of Oklahoma, Norman, Oklahoma, USA

SUMMARY

Discussion is presented summarizing recently developed equations of state for hydrocarbon mixtures for use in high accuracy gas flow measurements. The accuracies of these equations of state and the ranges of their application are summarized. The impact of these equations of state on gas flow measurement also is discussed. Special attention is given to the impact of the accuracy of calculated gas densities using these equations of state on flow measurement accuracy. Another topic discussed is the impact of these equations of state on electronic flow measurement, including the computation time and resultant impact on gas volume calculation frequency. Also, the calculation of sonic velocity for use with sonic provers and meters which require sonic velocity is discussed.

1 INTRODUCTION

1.1 Background

Cooperative worldwide research has been performed in recent years to improve the accuracy of flow measurement. This research has led to numerous developments, including more accurate hydrocarbon gas mixture equations of state. Two high accuracy equations of state, the SGERG-88 equation and the AGA8-92DC equation, have been selected for implementation as standards in gas flow measurement^(1,2). The AGA8-92DC equation of state uses the molar composition for characterization of a gas mixture. The SGERG-88 equation of state uses for the characterization of a gas mixture a simplified analysis comprising superior calorific value (volumetric basis), relative density, carbon dioxide content and (if non-zero) hydrogen content. It is anticipated that ISO 12213 will utilize both of these equations of state with these two specific characterization methods⁽²⁾. A.G.A. Report No. 8 utilizes these two equations of state with these two characterization methods and also utilizes the SGERG-88 equation with natural gas characterization comprising relative density, nitrogen content and carbon dioxide content⁽¹⁾.

1.2 Previous Methods

Since 1962, when A.G.A. Report NX-19 was published,⁽³⁾ the NX-19 method and variations of this method have been used extensively for natural gas compressibility in flow measurement. The 1985 A.G.A. Report No. 8 provided much greater accuracy than the NX-19 method.⁽⁴⁾ However, the 1985 API Manual of Petroleum Measurement Standards⁽⁵⁾ did not require the use of the 1985 A.G.A. Report No. 8 and so the NX-19 method has remained in extensive use. The 1992 API Manual of Petroleum Measurement Standards⁽⁶⁾ specifies the use of the 1992 A.G.A. Report No. 8 methods. In fact, Section 2 of Chapter 14 of API MPMS⁽⁷⁾ is equivalent to the 1992 A.G.A. Report No. 8. It should also be noted that Section 3 of Chapter 14 of the API MPMS⁽⁶⁾ and A.G.A. Report No. 3 are equivalent.

1.3 Equations of State

The equations of state in the 1992 A.G.A. Report No. 8 and anticipated in ISO 12213 can be represented in the form of Equation (1).

$$Z = 1 + Bd + Cd^2 + \text{higher order terms in } d$$

(1)

In Equation (1), Z is the compressibility factor, d is the molar density (moles per unit volume) and B and C are coefficients which are functions of absolute temperature and gas characteristics. The coefficients B and C commonly are referred to as the second and third virial coefficients, respectively. The SGERG-88 equation does not have terms of higher order than d^2 , while the AGA8-92DC equation has numerous higher order terms. In the AGA8-92DC equation, the coefficients B and C and all coefficients in the higher order terms are calculated from the gas composition and absolute temperature. In the SGERG-88 equation, the coefficients B and C are calculated from absolute temperature and the gas characterization information utilized, for example, superior calorific value, relative density, carbon dioxide content and (if non-zero) hydrogen content). Both the SGERG-88 equation and the AGA8-92DC equation represent experimental natural gas density data very accurately in the range of temperatures from 263K to 338K at pressures up to 12 MPa. The AGA8-92DC equation has a more complex form to allow its use at conditions beyond the above range, usually for purposes other than flow measurement.

2 IMPACTS ON FLOW MEASUREMENT

The implementation of ISO 12213 and A.G.A. Report No. 8 will have numerous technical and economic impacts on gas flow measurement. The improved accuracy of these new methods over the A.G.A. Report NX-19 method and other methods in current use justifies the cost of implementation. A number of specific technical impacts are discussed below.

2.1 Types of Gases

The SGERG-88 and AGA8-92DC equations of state used in the new standards can be utilized for flow measurement of pipeline quality natural gases in the range from 263K to 338K at pressures up to 12 MPa with essentially equivalent absolute uncertainties which average less than 0.1%. The average absolute uncertainty for pipeline quality natural gases increases outside of this range of conditions. Although not specifically intended for manufactured (synthetic) gases, the SGERG-88 and AGA8-92DC equations can both be used (with increased uncertainties) for these gases and admixtures of these gases with natural gases. The AGA8-92DC equation can be used for wet and/or sour gases and an extension of the AGA8-92DC equation can be used for extremely rich gases.

It is anticipated that ISO 12213 will specify the allowable limits on mole fractions of components given in Table 1 for the purposes of the ISO 12213 standard. For ISO 12213 calculations using the SGERG-88 method, the anticipated ranges are 30 to 45 MJ/m³ for superior calorific value and 0.55 to 0.80 for relative density. The 1992 A.G.A. Report No. 8 defines two ranges of gas composition, the "normal" range and the "expanded" range, both of which are shown in Table 2. Although the composition limits in Table 1 and in the "normal" range in Table 2 differ, both of these ranges encompass the range of natural gas composition commonly referred to as pipeline quality gas and both ranges have an average absolute uncertainty which is less than 0.1% for 263K to 338K up to 12 MPa. In A.G.A. Report No. 8, it is recommended that calculations in the "expanded" range be performed using the AGA8-92DC equation. It should be noted that although A.G.A. Report No. 8 does not present text information regarding the use of the SGERG-88 method for gases containing hydrogen and carbon monoxide, the computer program listing does allow this computation. Calculation uncertainties using the AGA8-92DC method in the expanded range are largest for natural gases containing high concentrations of hydrocarbons heavier than pentanes (hexanes plus). An extension of the AGA8-92DC method⁽¹⁰⁾ which is not part of A.G.A. Report No. 8 has been developed for calculations when the hexanes plus content exceeds 0.2 mole percent.

Table 1

Allowable Limits on Mole Fractions of Components Consistent with ISO 12213

| Component | Mole Fraction |
|----------------------------------|---------------|
| Main Components | |
| Methane | ≥ 0.70 |
| Nitrogen | ≤ 0.20 |
| Carbon Dioxide | ≤ 0.20 |
| Ethane | ≤ 0.10 |
| Propane | ≤ 0.035 |
| Butanes | ≤ 0.015 |
| Pentanes | ≤ 0.005 |
| Hexanes | ≤ 0.001 |
| Heptanes | ≤ 0.0005 |
| Octanes and above | ≤ 0.0005 |
| Hydrogen | ≤ 0.10 |
| Carbon Monoxide | ≤ 0.03 |
| Helium | ≤ 0.005 |
| Minor and Trace Component | |
| Ethylene | ≤ 0.001 |
| Benzene | ≤ 0.0005 |
| Toluene | ≤ 0.0002 |
| Water Vapor | ≤ 0.0002 |
| Hydrogen Sulfide | ≤ 0.0002 |
| Oxygen | ≤ 0.0002 |
| Total Unspecified Components | ≤ 0.0001 |

Table 2

Ranges of Gas Mixture Characteristics
Consistent with A.G.A. Report No. 8

| Quantity | Normal Range | Expanded Range |
|-------------------------------|--------------------------------|---------------------------|
| Relative Density | .56 to .87 | 0.07 to 1.52 |
| Gross Heating Value* | 477 to 1150 Btu/scf | 0 to 1800 Btu/scf |
| Gross Heating Value** | 18.7 to 45.1 MJ/m ³ | 0 to 66 MJ/m ³ |
| Mole Percent Methane | 45.0 to 100.0 | 0 to 100.0 |
| Mole Percent Nitrogen | 0 to 50.0 | 0 to 100.0 |
| Mole Percent Carbon Dioxide | 0 to 30.0 | 0 to 100.0 |
| Mole Percent Ethane | 0 to 10.0 | 0 to 100.0 |
| Mole Percent Propane | 0 to 4.0 | 0 to 10.0 |
| Mole Percent Butanes | 0 to 1.0 | 0 to 6.0 |
| Mole Percent Pentanes | 0 to 0.3 | 0 to 4.0 |
| Mole Percent Hexanes Plus | 0 to 0.2 | 0 to Dew Point |
| Mole Percent Helium | 0 to 0.2 | 0 to 3.0 |
| Mole Percent Hydrogen | # | 0 to 100.0 |
| Mole Percent Carbon Monoxide | # | 0 to 3.0 |
| Mole Percent Argon | # | 0 to 1.0 |
| Mole Percent Oxygen | # | 0 to 21.0 |
| Mole Percent Water | 0 to 0.05 | 0 to Dew Point |
| Mole Percent Hydrogen Sulfide | 0 to 0.02 | 0 to 100.0 |

* Reference conditions: Combustion at 60°F, 14.73 psia; density at 60°F, 14.73 psia.

** Reference conditions: Combustion at 25°C, 0.101325 MPa; density at 0°C, 0.101325 MPa.

The normal range is considered to be zero for these compounds.

It is obvious that the differences in the SGERG-88 method and the AGA8-92DC method create important impacts on gas flow measurement decisions because of the need for selecting the appropriate computation method based on gas mixture composition and operating conditions.

2.2 Accuracy

There is ample documentation on the impact on gas flow measurement accuracy due to improved gas compressibility accuracy. ISO 12213 and A.G.A. Report No. 8 both provide summaries of expected compressibility factor uncertainties and references for detailed evaluations^(1,2). Table 3 shows comparisons of deviations of calculated compressibility factors from experimental values for the NX-19 method, the SGERG-88 method and the AGA8-92DC method. The comparisons in Table 3 are from Gas Institute Report No. GRI-91/0184 by Starling, et al.⁽⁸⁾. The experimental data are from GERG Technical Monograph 4 by Jaeschke and Humphreys⁽⁹⁾. The gas groupings in Table 3 are designated as Lean Gases (methane content greater than 94 mole percent), Rich Gases (ethane content greater than 8 mole percent), High Nitrogen Gases (nitrogen content greater than 9.5 mole percent) and High Carbon Dioxide Gases (carbon dioxide content greater than 4 mole percent).

The relative deviation of the calculated compressibility factor at the i th data point, $Z_{i \text{ calc}}$ from the experimental value $Z_{i \text{ exp}}$ is $RDEV_i$

$$RDEV_i = \frac{(Z_{i \text{ calc}} - Z_{i \text{ exp}}) \times 100\%}{Z_{i \text{ exp}}} \quad (2)$$

The maximum value of $RDEV_i$ is the MaxDev and the average absolute deviation, AAD, for N data points is

$$AAD = \frac{1}{N} \sum_{i=1}^N [(RDEV_i)^2]^{1/2} \quad (3)$$

The range of conditions for the data in Table 3 is 263 to 338K at pressures up to 12 MPa. The NX-19 method has an AAD of 0.095% for lean gases and 0.130% for high nitrogen gases and thus is reasonably accurate for these gases. For high carbon dioxide gases, the NX-19 method AAD is 0.283% and the maximum deviation is -1.043%. For high ethane content rich natural gases, the NX-19 deviations are even larger, with an AAD of 0.585% and a maximum deviation of -2.057%. Thus, the NX-19 method is badly in error for high ethane rich natural gases and has fairly large errors for high carbon dioxide natural gases. On the other hand, for the conditions of Table 3, both the SGERG-88 method and the AGA8-92DC method have average absolute deviations which are less than 0.1% and maximum deviations which are less than $\pm 0.32\%$. Thus, for the ranges of gases and conditions in Table 3, the impact of the equation of state on flow measurement uncertainty should not exceed $\pm 0.32\%$ and for orifice meters should not exceed $\pm 0.16\%$.

2.3 Computation Complexity

The complexity of calculations using either ISO 12213 or A.G.A. Report No. 8 is much greater than the computation complexity of A.G.A. Report NX-19. The accuracy improvement of the new methods over the accuracy of A.G.A. Report NX-19 justifies this increased computational overhead, but requires use of a computer, while A.G.A. Report NX-19 calculations can be performed with hand-held calculators. The fact that the new calculation methods must be programmed is having a noticeable impact on the speed of implementation of A.G.A. Report No. 8 by the U.S. gas industry. Although efficient FORTRAN language algorithms are presented in A.G.A. Report No. 8, implementation has been relatively slow.

Table 3

Summary of Deviations of Calculated Natural Gas Compressibility Factors
from Experimental Data

| Gas Group | No. of Natural Gases | No. of Points | Method | AAD% | MaxDev% |
|---------------------------|----------------------|---------------|-----------|-------|---------|
| Lean Gases | 8 | 448 | NX-19 | 0.095 | -0.615 |
| | | | SGERG-88 | 0.022 | -0.137 |
| | | | AGA8-92DC | 0.020 | -0.136 |
| Rich Gases | 23 | 1278 | NX-19 | 0.585 | -2.057 |
| | | | SGERG-88 | 0.037 | -0.319 |
| | | | AGA8-92DC | 0.031 | 0.253 |
| High Nitrogen Gases | 13 | 625 | NX-19 | 0.130 | -0.452 |
| | | | SGERG-88 | 0.039 | -0.154 |
| | | | AGA8-92DC | 0.059 | -0.198 |
| High Carbon Dioxide Gases | 8 | 477 | NX-19 | 0.283 | -1.043 |
| | | | SGERG-88 | 0.035 | 0.148 |
| | | | AGA8-92DC | 0.033 | 0.163 |

Reasons for slow implementation are numerous. One reason is the fact that source code algorithms have not been published for the orifice discharge coefficient calculations required for implementation of the 1992 API MPMS, Chapter 14, Section 3 methods. Most U.S. companies have implemented A.G.A. Report No. 8 only as a part of the implementation of new orifice meter standards. Because the new calculation methods are much more complex than earlier standards, the effort and monetary costs involved have delayed implementations in some U.S. companies.

2.4 Accounting Systems

Regardless of the source of the basic flowrate data, i.e., chart data or electronic flow meter data, the capability for calculations and/or recalculations must be incorporated in the accounting system used. Software implementing the 1992 A.G.A. Report No. 8 calculations has been installed in numerous U.S. accounting systems, including mainframe, minicomputer and PC based systems. Few quantitative problems are encountered when care is taken to properly pass the data and calculation results across computation modules, whether the modules are subroutines, libraries of subroutines or dynamic link libraries (DLLs). Checks, of course, are needed for proper variable ranges and unreasonable variable values such as negative absolute pressure.

2.5 Electronic Flow Measurement

Electronic flow measurement (EFM) software must be efficient to allow for frequent flow calculations. The algorithms in the 1992 A.G.A. Report No. 8 were designed to minimize redundant calculations with the anticipation of EFM applications. The natural gas properties depend on three quantities, (1) gas composition, (2) temperature and (3) pressure. Quantities which depend on composition but not on temperature or pressure are calculated in one computation block (a group of subroutines). Quantities which depend on temperature but not pressure are calculated in a second computation block.

Quantities which depend on pressure are calculated in a third computation block. If between two successive EFM calculations the flowing pressure changes but the temperature and composition remain unchanged, then computations of composition dependent and temperature dependent quantities are not performed as these calculations would be redundant. Most EFM applications have utilized C-language for the source code algorithms; the FORTRAN language algorithms in A.G.A. Report No. 8 can of course be used for checking the C-language algorithms.

2.6 EFM Editing

The editing of flow measurement data, especially for final accounting and monthly billings, is a necessary activity regardless of whether the flow data is from charts or electronic flow meters. However, because of the large quantity of data entries associated with EFM data, it is not feasible to edit each individual entry from a computer keyboard. It is more efficient to upload the EFM data to a computer with resident EFM editing software, enter the edit information (e.g., change of orifice diameter from first to second part of month) and allow the many recalculations of flow for the edited period. This edit can be performed while retaining the original data for archival purposes and updating the event log for the meter, so that a complete audit trail is maintained. EFM editing software using dynamic link libraries (DLLs) for the new orifice discharge coefficient and gas density calculations have been developed for PC applications, making it feasible for EFM editing as part of field or office operations. Installations also have been implemented to send the EFM data from the meter to the EFM editing in a real-time mode using dynamic data exchange (DDE).

2.7 Applications Outside Pipeline Quality Range

Both the SGERG-88 method and the AGA8-92DC method can be used outside the pipeline quality range. For many applications there is a paucity of accurate experimental gas density data for determining the uncertainties of predicted densities. Nevertheless, for many applications, the AGA8-92DC method probably is as accurate as other available methods. An exception is rich natural gases with hexanes plus content greater than 0.2 mole percent. However, an extension of the AGA8-92DC method allows calculations up to the dew point concentration for rich gases⁽¹⁰⁾. The maximum hexanes plus concentration of the data utilized in developing the extension of AGA8-92DC is 9.8 mole percent.

2.7.1 Synthetic Gases

Both the SGERG-88 method and the AGA8-92DC method have been evaluated using experimental data⁽⁹⁾ for gas mixtures containing as much as 35 mole percent hydrogen. For thirteen natural gases with more than 2 mole percent hydrogen, the average absolute deviations are 0.021% for the SGERG-88 method and 0.027% for the AGA8-92DC method⁽⁸⁾. It is clear that these equations can be used for admixtures of natural gas and manufactured gas up to at least 10 mole percent hydrogen with high accuracy and beyond 10 mole percent hydrogen at reduced accuracy.

2.7.2 Wet Gases

The AGA8-92DC method has been evaluated using natural gas compressibility factor data⁽¹¹⁾ with a maximum water content of 10 mole percent. These data cover the range 348K to 483K for pressures up to 16 MPa. Compressibility factors calculated using the AGA8-92DC method have an average absolute deviation of less than 0.1% from the experimental values. Because of this excellent agreement and the fact that the experimental data range to such high water mole fractions, it is probable that the AGA8-92DC method remains accurate for water concentrations as high as the water dew point.

2.7.3 Sour Gases

Two data sources were utilized to evaluate the AGA8-92DC method for compressibility factors of natural gas containing hydrogen sulfide. For the compressibility factor data reported by Scheloske⁽¹¹⁾,

with up to 3.0 mole percent hydrogen sulfide, the average absolute deviation is less than 0.1%. For proprietary data for a sour natural gas with 26.4 mole percent hydrogen sulfide, the average absolute deviation is 0.6%, which is probably close to the uncertainty of the experimental data. Although these deviations are much larger than for pipeline quality natural gas, it is probable that the AGA8-92DC method yields the lowest uncertainties of available correlations for high hydrogen sulfide natural gas compressibility factors at the present time.

3 EXTENSION OF AGA8-92DC FOR RICH GASES

The maximum concentration of hexanes plus for the "normal" range in Table 2 is 0.2 mole percent. An extension of the AGA8-92DC method has been developed for hexanes plus concentrations as high as the hydrocarbon dew point⁽¹⁰⁾. This extension is not a part of A.G.A. Report No. 8 but can be used conveniently as an extension of the AGA8-92DC method for rich gases. The compressibility factor data used in developing this extension to the AGA8-92DC method includes data for mixtures containing as much as 9 mole percent hexanes plus⁽¹⁰⁾. Portions of the data are for gas condensate fluids at pressures above the upper dew point. The range of conditions for the data is 273K to 409K for pressures up to 94 MPa. The average absolute deviation of calculated compressibility factors from the experimental values is 1.15%. The experimental compressibility factors probably have uncertainties near $\pm 1\%$. Therefore, this extension of the AGA8-92DC method probably is about as accurate a correlation as is possible at present for gases with more than 0.2 mole percent hexanes plus.

4 SONIC VELOCITY

Sonic velocity calculations for use with sonic nozzle provers and flow meters which require the sonic velocity can be performed using the AGA8-92DC equation of state. Although experimental sonic velocity data were used in the development of the AGA8-92DC equation, calculated sonic velocities have greater uncertainties than calculated compressibility factors, especially near dew point conditions. This fact has an impact on the choice of operating conditions for sonic provers. For conditions well away from dew points, pipeline quality natural gas sonic velocities calculated using the AGA8-92DC method generally will have uncertainties of less than $\pm 0.2\%$ in the range 250K to 350K at pressures up to 7 MPa.

5 CONCLUSIONS

It is clear that implementations of ISO 12213 and A.G.A. Report No. 8 will have decided impacts on gas flow measurements. The fact that the SGERG-88 method and the AGA8-92DC method are significantly more accurate than the A.G.A. Report NX-19 method, especially for rich gases and high carbon dioxide gases, justifies the costs of implementing ISO 12213 and A.G.A. Report No. 8. The timing for this implementation is appropriate because of coincidence with major revisions in orifice discharge coefficient equations. The fact that computer computations are required for both orifice discharge coefficients and gas densities is no longer a deterrent to implementation in light of increased usage of computers in flow measurement.

REFERENCES

- 1 STARLING, K.E. and SAVIDGE, J.L., Compressibility factors of natural gas and other related hydrocarbon gases, A.G.A. Transmission Measurement Committee Report No. 8, American Gas Association, 1992.
- 2 ISO 12213 Natural gas - calculation of compression factor, ISO/TCH3/SG1/WG7 draft of 93-11-01, International Standards Organization, 1993.
- 3 ZIMMERMAN, R.H., Manual for determination of supercompressibility factors for natural gas, A.G.A. Report NX-19, American Gas Association, 1962.

- 4 STARLING, K.E., Compressibility and supercompressibility for natural gas and other hydrocarbon gases, A.G.A. Transmission Committee Report No. 8, American Gas Association, 1985.
- 5 Natural gas fluids measurement, Manual of Petroleum Measurement Standards, Chapter 14, Section 3, American Petroleum Institute, 1985.
- 6 Natural gas fluids measurement, Manual of Petroleum Measurement Standards, Chapter 14, Section 3, American Petroleum Institute, 1992.
- 7 STARLING, K.E. and SAVIDGE, J.L., Compressibility factors of natural gas and other related hydrocarbons, Manual of Petroleum Measurement Standards, Chapter 14, Section 2, American Petroleum Institute, 1992.
- 8 STARLING, K.E., R.T. JACOBSEN, S.W. BEYERLEIN, C.W. FITZ, W.P. CLARKE, E. LEMMON, Y.C. CHEN and E. RONDON, GRI high accuracy natural gas equation of state for gas measurement applications - 1991 revision of A.G.A. No. 8 equation, technical reference document, Annual Report to Gas Research Institute Report No. GRI-91/0184, June 1991.
- 9 JAESCHKE, M. and A.E. HUMPHREYS, GERG databank of high accuracy compressibility factor measurements, GERG Technical Monograph 4, Fortschritt-Berichte VDI Reihe 6, No. 251, 1990.
- 10 STARLING, K.E., MARTIN, J.W., SAVIDGE, J.L., BEYERLEIN, S.W. and LEMMON, E., Application of A.G.A. Report No. 8 equation of state to rich natural gas mixtures and retrograde condensates, Proceedings of the Seventy Second Annual Gas Processors Association Convention, 1993.
- 11 SCHELOSKE, J.J., HALL, K.R. EUBANK, P.T. and HOLSTE, J.C., Experimental densities and enthalpies for water-natural gas systems, Research Report RR-53, Gas Processors Association, 1981.

THE USE OF CALCULATED DENSITY ON AN OFFSHORE HIGH PRESSURE WET GAS METERING SYSTEM

M. A Emms

British Gas plc

SUMMARY

The paper details an investigation into the use of calculated density on an offshore high pressure wet gas metering system. The condition of the gas at the metering system, including the presence of water and methanol, is considered for a typical wellstream and minimum process system. Likely changes in gas composition are calculated and the methods currently used for obtaining gas composition are reviewed. Data from offshore chromatographs is used to estimate the uncertainty in gas composition. The methods available for the calculation of density are reviewed, with consideration given to the inclusion of water and methanol and the high operating pressure. The uncertainty of calculated density is estimated using the uncertainty of the gas composition and methods available to calculate compressibility.

NOTATION

- ρ_1 = Calculated upstream density (kg/m³)
 Z_1 = Compressibility at line conditions
 Z_b = Compressibility at base conditions (P_b & T_b)
 P_1 = Upstream measured pressure (barA)
 P_b = Pressure at base conditions (1.01325 barA)
 T_1 = Upstream temperature (°K)
 T_b = Temperature at base conditions (288.15 °K)
 M_w = Molecular weight of the gas (kg/kmol)
 R = Universal gas constant (bar m³ kmol K)

1 INTRODUCTION

In the Southern Basin of the North Sea calculated density is used on offshore 'wet gas' metering systems because live measurement, using conventional vibrating element densitometers, has proved to be unsuccessful due to liquid contamination.

On earlier metering systems density was often calculated from the live measurement of Real Relative Density (RD), Pressure and Temperature with Compressibility (Z) and Base Compressibility (Z_b) obtained from sampling.

$$\rho_1 = \text{Real RD} * \text{Density of air} * \frac{P_1 * T_b * Z_b}{P_b * T_1 * Z_1}$$

The density of air is also at the same base conditions as P_b , T_b and Z_b .

In essence the Molecular Weight (MW) is measured by the live measurement of RD with Z and Z_b calculated from a fixed composition that is manually entered into the flowcomputer system. The accuracy of this method is dependent on the change in gas composition and the frequency of sampling.

With the introduction of gas chromatography on offshore metering systems density is now calculated from live measurement of pressure and temperature with the MW and Z calculated from the most recent chromatograph analysis.

$$\rho_1 = \frac{P_1 * \text{Mw}}{R * T_1 * Z_1}$$

2 THE WELLSTREAM

In order to establish the condition of the metered gas stream, and any possible variations in the gas composition, a typical gas reservoir wellstream and process facility was considered. The reservoir contains gas, liquid hydrocarbons (condensate) and water. The produced wellstream, although mainly gaseous, is at its hydrocarbon and water dewpoints and is likely to contain some free water. The composition of the wellstream depends on the equilibrium conditions in the reservoir and hence pressure and temperature. Due to the drop in pressure and temperature at the wellhead condensate will be formed in the wellstream. This is best illustrated by the phase envelope, which for the typical wellstream is detailed on Figure 1.

The bubble point and dewpoint lines are calculated from the wellstream composition. The shape and location of the phase envelope changes with composition but not pressure, temperature or flow. The C7+ components have a significant effect on the dewpoint curve of the phase envelope. CO₂ and H₂S lower the cricondenbar. N₂ raises the cricondenbar whilst H₂O does not have much effect except at high pressure and temperature.

3 THE PROCESS SYSTEM

In most gas/condensate reservoirs the wellhead condition is within the two phase region as shown on Figure 1. It is therefore necessary to separate the gas and condensate to allow the gas and condensate to be individually metered and the flow from the reservoir controlled. A typical process system is detailed on Figure 2.

The wellstream from individual wells is controlled by a choke valve before entering the production manifold. Methanol is often injected into each wellstream to prevent the formation of hydrates.

The wellstream leaving the production manifold enters a separator, often three phase, where gas, condensate and water are separated. The gas and condensate streams are metered before being commingled, sometimes with the water, for transportation to shore. The separator is often operated over a range of pressures depending on the pipeline operating pressure. The pressure drop across the choke valves will result in a drop in gas temperature. Due to the process of separation the gas leaving the separator is at its dew point and the condensate at its bubble point.

The ratio of gas to condensate varies with different separator operating pressures and temperatures and is indicated by the position in respect to the quality lines, as detailed on Figure 3. For the typical wellstream the normal wellhead conditions was between 98% and 99.8% vapour. As the ratio of gas to condensate varies the gas and condensate compositions will also vary. The quantity and composition of both gas and condensate streams were obtained from 'flash calculations' at the separator operating pressure and temperature.

4 VARIATIONS IN GAS COMPOSITION

From the typical wellstream composition and separator operating conditions a series of flash calculations were performed, using the 'Hysim' process simulator, with the Soave, Redlich, Kwong equation of state. The short term changes in gas composition and possible errors in density are detailed on Figure 4. The resulting gas composition at the typical operating pressure and temperature of 130 Bar, 30 °C respectively was used as the base case. Further flash calculations were performed at 10 Bar intervals, with the corresponding drop in temperature. In each case the true density was calculated from the resulting gas composition at the pressure and temperature. The possible error in density was then calculated by comparing the true density with the density calculated from the base composition at the operating pressure and temperature. As shown the gas composition did change with separator operating conditions, particularly the C5+ components. For a change of 10 Bar the error in calculated density was 1.2 % if the composition is not changed in the calculations.

The typical wellstream used has a Condensate to Gas Ratio (CGR) of 1.92 Barrels/MMSCF. CGR's for other gas/condensate fields vary between 1 to 6 Barrels/MMSCF. The variation in gas composition due to changes in separator operating conditions did not appear to be directly related to the CGR.

It can therefore be concluded that for a 'single reservoir' there are two causes for changes in gas composition :-

a) The longer term change as the reservoir depletes and the pressure drops. The change in equilibrium between the gas and condensate in the reservoir will result in a change in wellstream composition. This change is, however, relatively small and slow.

b) The short term change due to different separator operating conditions, which in this case did cause a change in gas composition significant enough to introduce an error in calculated density.

There are also fields that consist of a number of small individual reservoirs where individual wells produce wellstreams of different compositions. For both single or multiple reservoir fields changes in gas composition can occur in the short term.

5 CONDITION OF THE GAS STREAM

Although the gas stream leaving the separator is at its hydrocarbon and water dewpoints it is the condition as it passes through the orifice plate that is of interest. Therefore the pressure drop along the pipework between the separator and the orifice plate was considered, at worst case with a flow conditioner installed in the upstream pipework.

An upstream pipe configuration of 20 metres of 12" pipe and 4 bends was used to calculate the pressure drop between the separator and the flow conditioner. The larger 12" pipe was used to minimise the pressure drop. The pressure drop across the flow conditioner was calculated using a pressure loss coefficient of 2.2. The resulting temperature drop was calculated assuming an Isenthalpic expansion. The pressure and temperature drop between the separator and the meter was calculated to be 0.153 Bar and 0.04 °C respectively.

Again flash calculations were performed using the 'Hysim' process simulator. The results detailed on Figure 5 show that although a relatively small amount of condensate was produced (0.0306 m³/hr, which is 0.0026% of the total flow) the calculated gas composition did not appreciably change. It is, however, not clear whether the condensate passes through the orifice in the form of a mist, droplets or as a liquid flowing along the bottom of the pipe, and therefore its affect on density.

The formation of condensate could be reduced by minimising the pressure drop by installing fewer bends and larger diameter pipe and installing lagging to prevent further heat loss by radiation. It could also be prevented by heating the gas which would result in additional plant and cost.

The amount of water produced was calculated and found to be insignificant.

As methanol is injected into the wellstream upstream of the separator to prevent hydrate formation the gas stream will contain water and methanol in the gaseous state.

5.1 WATER CONTENT

It is very likely that water will be present in the reservoir and therefore the wellstream. Any 'free water' will be removed in the separator. The amount of water vapour present in the gas from the separator will be dependent on the pressure, temperature and composition of the gas. As there is free water in the wellstream it was assumed that the gas is saturated with

water vapour at the operating pressure and temperature and is therefore always at its water dewpoint. As detailed on Figure 6 at the typical operating conditions the water content of the gas was calculated to be 0.056 mol%. The error on calculated density when water is not included was calculated to be -0.1 % of reading.

Water content can be derived from sampling, on-line measurement or calculation/empirical methods.

Sampling

A gas sample would be analysed for dewpoint/water content at an onshore laboratory using a direct method, probably the Karl Fischer or Dewscope (Chilled Mirror) method. A direct method has a direct relationship between the measured quantity and the water vapour content. The Karl Fischer method uses the titration of absorbed water vapour with iodine and measures directly the water content per unit volume of gas. In the Dewscope the chilled mirror is used to measure the temperature at which water condenses on its surface, as it is gradually cooled, and hence the water dewpoint of the gas.

The major problem with sampling is the precautions necessary to ensure that the gas sample is at the sampling pressure and temperature and therefore representative. The sample should not be contaminated with moisture from the atmosphere or any residual moisture present in the sample container before the sample is taken.

On-Line Measurement

Most on-line water content measuring instruments use hygroscopic sensors that respond to the water vapour in the gas stream. Measurement is based on either Electrolytic, Capacitance, Mass Change (quartz crystal) or Conductivity principles. As the measurements are indirect, i.e. do not have a direct relationship with water content, calibration of the sensor is necessary. Calibrations are performed by either replacing the sensor with a pre-calibrated sensor or by calibration with a dry inert purge gas. The measurement accuracy can be affected by contamination of the sensors by CO₂, H₂S and methanol present in the gas stream. It has suggested [1] that variations in gas composition can produce dewpoint measurement errors of between 2°C to 3°C with hygroscopic instruments.

Some on-line direct measuring instruments are available using the chilled mirror or automatic high pressure Karl Fischer methods. The chilled mirror instruments often have operational problems due to the contamination of the mirror by heavy hydrocarbons and other components present in the gas. The Karl Fischer instrument although automated, requires the reagents used to be constantly checked.

When measuring the water dewpoint it is necessary to perform further calculations to obtain the water content.

Calculated Methods

The water content of the gas can be calculated from the gas composition using an equation of state. This is, however, a reasonably complex calculation that requires specialist software, which although available for off-line calculations is not available in flowcomputers for on-line

calculations of water content. It is also questionable whether the amount, or effect of water content, would justify the cost of incorporating this type of software in a flowcomputer.

An empirical method for obtaining the water content of lean sweet natural gas is detailed in Gas Conditioning and Processing Volume 1 by John M Campbell [2]. It consists of a graph of water content versus water dewpoint for different pressures.

The water content in kg/10⁶ std m³ (100 kPa and 15°C) is converted to mol fraction of water yw using :-

$$yw = \frac{\text{water content kg/10}^6 \text{ std m}^3}{\text{MW water} * \text{kmol gas / 10}^6 \text{ std m}^3}$$

$$yw = \frac{\text{water content kg/10}^6 \text{ std m}^3}{18 * 41740}$$

The likely error associated with this method is quoted as 3 to 5 %. There are further corrections to apply if there is CO₂ and H₂S present in the gas.

An alternative method is that detailed in the paper Equilibrium Moisture Content of Natural Gases by R.F Bukacek ref [3]. The method uses the equation :-

$$W = A/P + B$$

where

W = the water content in pounds per MMCF (14.7 psia 60°F)

P = the pressure in psia

A = a constant proportional to the vapour pressure of water.

B = a constant depending on temperature and composition.

Values for A and B are given in tables for varying temperature. The equation is based on tests carried out on a series of binary mixtures and natural gases in the pressure range 69 to 680 Bar and at a temperature of 220°F. This temperature was chosen to ensure that the heavier hydrocarbons were kept in the vapour phase. However, the constants are stated for a temperature range of -40°F to 460°F although there is an element of doubt as to the validity of this correlation at temperatures below the critical temperature.

The results, obtained for typical operating conditions, from the Campbell and Bukacek methods are detailed below. As shown there is very little difference between the methods.

| Pressure | Temperature | Campbell | Bukacek |
|----------|-------------|----------|---------|
| BarsA | °C | mol % | mol % |
| 130 | 30 | 0.059 | 0.056 |
| 120 | 25 | 0.044 | 0.045 |
| 110 | 20 | 0.037 | 0.036 |
| 100 | 15 | 0.028 | 0.029 |

5.2 METHANOL CONTENT

In the absence of offshore dehydration it is necessary to inhibit the formation of hydrates. Hydrates are formed by the combination of free water and hydrocarbon molecules into an ice like solid. The temperature at which hydrates form is dependent on pressure and gas composition. The higher the pressure the higher the temperature at which hydrates form. To suppress the hydrate formation temperature below the operating temperature either glycol or methanol is injected into the wellbore, or the wellstream upstream of the separator.

Methanol is most commonly used due to its suitability at low temperatures and its corrosion inhibiting properties but has one disadvantage in that it is volatile and is therefore distributed between the water, condensate and gas phases. The quantity of methanol injected has to be sufficient to compensate for this whilst maintaining the water/methanol concentration to ensure adequate hydrate suppression in any part of the system. This includes the wellbore, wellhead, separator, pipeline and reception facilities. It is often necessary to inject up to 3 times that required in the water phase to maintain the required methanol/water concentration. The amount of methanol in the gas stream is dependent on the pressure, temperature and methanol/water concentration and can be calculated, using methods such as that detailed in the GPSA Engineering Data Book [4] or be determined from sample analysis using chromatography [5].

On some wet gas systems a minimum of 25 weight % of methanol in the free water is used which equates to 0.4 mol% of methanol being present in the gas stream leaving the separator.

In the early years when the wellhead pressure is high hydrates could form in the wellbore or wellhead. It is, however, the conditions at the reception facilities that usually dictates the methanol injection rate during the rest of the field life. This is primarily due to the drop in temperature along the pipeline to shore. It was therefore assumed that the methanol content of the metered gas stream will be in the order of 0.2 to 0.6 mol% over the life of the field.

Although the methanol content is relatively small it is thought that methanol is detected by some gas chromatographs and is included in the C₆₊ peak. It was calculated that not including 0.6% mol% methanol in the gas composition used to calculate density would introduce a density error of +0.32% of reading.

6 METHODS TO OBTAIN GAS COMPOSITION

Currently there are 3 methods used to obtain the gas composition; spot sampling, automatic sampling and on-line gas chromatography.

6.1 SPOT SAMPLING

Spot samples are taken manually from a sample point located at a position that gives a representative homogeneously mixed sample. Samples are collected in stainless steel cylinders that have been thoroughly purged with line gas. The sample cylinder is then shipped onshore, usually to a recognised laboratory, for analysis. On receipt at the laboratory the cylinder is checked for leaks and placed in an oven, usually to soak for at least 24 hours at 20°C above the sampling temperature. A sample is then analysed in a laboratory chromatograph to provide an analysis to C₁₀. Samples can also be analysed to determine the water and methanol content.

6.2 AUTOMATIC SAMPLING

An Automatic Sampler collects a sample from the gas stream and passes it to a sample cylinder on a time or flow proportional basis. The sample is either 'grabbed' from the flowing stream, or collected from a sidestream, by a solenoid initiated sample valve. When full, or after a set time period, the sample cylinder is removed and transported to shore for analysis at an approved laboratory. Although the gas composition represents the average over the sample period it typically takes one month to collect the sample and one month to obtain the sample analysis. This delay is undesirable when using the gas composition to calculate physical properties. When sampling is used density is often calculated from the measured RD with Z and Z_b calculated from the last gas composition. Although this does reduce the dependence on gas composition significant errors can still exist on calculated density.

6.3 GAS CHROMATOGRAPHY

A continuous gas sample is taken from the gas stream by a sample probe and conditioned before entering the gas chromatograph. The gas chromatograph consists of a sample injection system, a chromatographic column and detector as shown on Figure 7.

A precise volume of sample gas is injected into the column. The column contains a stationary phase, either an active solid (gas solid chromatography) or an inert solid coated with a liquid phase (gas liquid chromatography). The gas sample is transported through the column by a carrier gas. As the gas sample passes through the column the stationary phase retards the components of the sample. Therefore each component moves through and elutes from the column at different times. The separated components are measured by a detector that produces an electrical output proportional to the concentration of the component which is shown, as detailed on Figure 8, as a series of peaks on a chromatogram. The area under each component peak is proportional to the total mass of that component. Therefore the weight percent compositions are calculated from the area ratios on the chromatogram, or from the peak height.

The sample valve, column and detector are housed in a temperature controlled oven. To separate all of the components in a typical natural gas, and provide a fast response, multiple columns are often used. An analysis time of 7 to 8 minutes is typical for an on-line gas chromatograph. The analysis would include C_1 to C_6+ , N_2 and CO_2 .

The chromatograph is calibrated by routine analysis of a calibration gas of known composition. The calibration gas would be representative of the gas stream and be either gravimetrically prepared or sales quality line gas analysed at an approved laboratory. From the analysis of the calibration gas response factors, based on either peak area or height, are calculated for each component. The response factors are then averaged, depending on the number of calibration runs, and stored in the chromatograph. The component concentrations in each subsequent analysis is calculated from the response factor and the measured component area or peak height.

The use of gas chromatographs on offshore platforms has increased in recent years. However the major problem in using on-line gas chromatography on a wet gas metering system is the design and efficiency of the sampling and pressure reduction system.

It is necessary to reduce the sample from line pressure to between 1.0 to 2.0 Bar before introduction to the analyser. This large reduction in pressure is a potential problem as the drop in pressure and hence temperature would certainly result in the formation of condensate and water. This would result in a change in gas composition and hence physical properties and more importantly could contaminate the chromatograph columns causing failure and the need for lengthy maintenance.

To overcome the problem the pressure is usually dropped in multiple stages, introducing heat at each stage to keep the sample above the hydrocarbon dewpoint and the initial sample temperature, to avoid condensate and water drop out. The setting of the pressure regulators and the amount of heat introduced would be calculated to ensure that the sample temperature is always above the dewpoint line on the phase envelope as shown on Figure 9.

7 COMPARISON OF METHODS

7.1 ACCURACY

The accuracy of each method was investigated and the results shown on Figure 10. A statistical analysis of the gas compositions obtained by gas chromatography, spot and time proportional automatic sampling, on an onshore terminal and a number of offshore platforms was carried out. The standard deviation gives an indication of the degree to which individual component concentration vary from the mean. As shown the standard deviations are generally one order greater for sampling than gas chromatography. This indicates that the gas composition obtained from sampling varied more than that obtained from on-line chromatography.

Due to the long time period over which the samples were taken it is not clear whether the variance is due to the method or genuine changes in gas composition. Unfortunately it was not possible to compare data from all methods, for the same field, over the same time period.

It was assumed that for Field A the variance in composition was a result of the method as the field has very consistent physical properties.

The data from time proportional sampling and on-line gas chromatography was compared for Field B, which has a relatively constant composition. However data was not obtained over the same length of time. In order to establish a reference the gas chromatograph calibration data was used. The chromatograph performs daily three consecutive calibration runs. The first run is ignored and the mean of the second and third runs are used to update the response factors and hence calibrate the chromatograph. The mean of the second and third calibration runs, using the previous days response factors, are reported by the chromatograph. This is therefore an analysis of a sample of constant composition and over a period of time is a good measure of the long term stability of the chromatograph. As shown over a period of 4 months, the component standard deviations for calibration gas are small. The hourly averages over a day also gave comparable component standard deviations and it is assumed that separator operating conditions and hence gas composition did not change significantly during the day. The component standard deviations of daily averages from the chromatograph over a period of 4 months and the monthly automatic samples are significantly higher. The results therefore confirm that the gas composition did change with time. It also gave an indication of the

stability of the gas chromatograph operating in an offshore environment which was confirmed by the data obtained from Fields E and F .

7.2 RELIABILITY

It is difficult to quantify and therefore compare the reliability between methods. It is fair to say that the reliability of a gas chromatograph or an RD analyser is primarily dependent on the design and operation of the sample system. The contamination of either device by condensate carried over from the separator, which does happen, is a potential problem which must be taken into consideration during the design of the sample system.

7.3 COST AND MAINTENANCE

Although spot sampling is the most cost effective and maintenance free solution it is unlikely that all parties would agree to this method being adopted. At the time of contract negotiation there is often only very preliminary well test data available to determine any likely variations in gas composition. It can be argued that even if the gas composition was constant, to verify it would require a high frequency of spot sampling. The method is not suitable if there are short term change in gas composition .

Automatic sampling has the disadvantage of high capital cost, the maintenance necessary to achieve the required reliability and the time taken to collect, transport and analyse the sample. This delay is undesirable, particularly when the gas composition is used in the calculation of physical properties.

The gas chromatograph has the advantage that an analysis is provided every 7 to 8 minutes and can be automatically transferred to the flowcomputer system for the calculation of physical properties and the daily composition for allocation. There is, however, a need for routine spot samples to be taken to define the split of the C₆+ component. Spot samples are typically taken every 3 months for this purpose.

The use of manual samples for obtaining water content is not really practicable due to the complex procedure and precautions necessary to obtain a representative sample. The cost of an on-line instrument, maintenance and calibration is difficult to justify. The use of calculated water content is normally adequate for most applications.

If present in sufficient quantities it was considered necessary to include methanol in the gas composition when calculating density. The amount of methanol injected into the wellstream is often measured for control purposes. The methanol content in the gas stream can be calculated for the likely flowrates, pressures and temperatures. The calculated data can be verified by the analysis of the spot samples taken to define the C₆+ component.

8 THE FULL GAS COMPOSITION

A typical on-line gas chromatograph has the capability to calculate RD, CV, ρ_b and Z_b from the sample analysis. It does however have limitations primarily the breakdown of the C₆+ components and addition of components not in the chromatograph analysis. The components not present in the sample analysis, in this case water and methanol, cannot be included. These

limitations, although not likely to introduce large errors, combined with the need to calculate line density in each meter run often necessitates the transfer of data and further calculations not available in the chromatograph.

Modern chromatographs have the capability to communicate with host computers through a serial link. It is therefore possible to transfer both the normalised or un-normalised composition and alarms to the flowcomputer system. The favoured method is to transfer the un-normalised composition.

The un-normalised composition is then normalised to 100 - the sum of additional components not in the chromatograph analysis. This would include H₂O, CO, H₂, H₂S and He.

The C₆+ component is then split into the ratios of C₆, C₇, C₈, C₉, C₁₀ & C₁₁ and where applicable methanol. The amounts and hence % split would be determined from occasional spot samples and along with water and methanol entered into the computer system as fixed values.

As each analysis is transferred from the chromatograph the full gas normalised gas composition is calculated and used in the computer system to calculate density.

9 UNCERTAINTY OF GAS COMPOSITION USING CHROMATOGRAPHY

As the gas chromatograph is in essence a 'comparator', comparing sample gas with calibration gas it was assumed that the uncertainty in gas composition obtained from a gas chromatograph consists of a systematic uncertainty due to the accuracy of the calibration gas and a random uncertainty due to the repeatability of the chromatograph.

Calibration gas can either be gravimetrically prepared or sales quality line gas or a prepared sample analysed at an approved laboratory. In this instance the calculations are based on the use of a gravimetrically prepared calibration gas with manufacturers stated component accuracies. Ideally the calibration gas should contain the components present in the chromatograph analysis at the same levels as the sample gas.

To estimate the repeatability of a gas chromatograph in an offshore environment the data from a number of existing installations detailed previously was used as shown on Figure 11. It is assumed that the repeatability is the random uncertainty, both expressed at a 95% confidence level. The repeatability of each component was calculated using :-

$$\text{Repeatability} = \text{Students } t * \text{Estimated Standard Deviation}$$

where :-

Repeatability is in +/- mol%

Students t is at a confidence level of 95% and takes into account the number of measurements 'n'.

The Estimated Standard Deviation is calculated in accordance with ISO 5168 [6] 3.2.1.1.

The component repeatability from each of the offshore chromatographs were added in quadrature to give an overall estimated component repeatability. Individual results were ignored if the ratio of the lowest to highest value was greater than 2.0. The Field B Daily

Averages were also not used as the repeatability over that time period could not be solely attributed to the chromatograph.

The repeatability and systematic uncertainties were combined quadratically to give an overall chromatograph uncertainty for each component. The results are detailed on Figure 12.

10 CALCULATED DENSITY

When calculating line density it is necessary to calculate the compressibility factor Z at line pressure and temperature. Most of the methods available use an equation of state, with combination rules, to calculate Z and density. In some cases the full gas composition is used whilst other methods use a measured physical property, usually CV or RD, to characterise the hydrocarbon content of the mixture. The equation of state then uses the 'characterised' hydrocarbon content with the nitrogen and/or carbon dioxide content to calculate Z and density. In all cases the methods are derived from actual measurements of Z for given gas compositions within a pressure and temperature range. The extent and accuracy of the database on which the methods are based have a significant impact on the suitability and the accuracy of the method and have to be taken into consideration. For this application consideration was given to use at high pressures and the inclusion of methanol and water.

10.1 GENERALISED EQUATIONS OF STATE

A number of P-V-T equations of state have been developed that correlate to specific test data using empirical constants. Examples are Van der Waals, Benedict-Webb-Rubin (BWR), Redlich-Kwong (R-K) and the Peng- Robinson equations of state.

There are however limitations on the ability of each of the methods to calculate accurately Z and density over a wide range of gas compositions, pressures and temperatures.

10.2 SPECIFIC EQUATIONS

The specific equations are based on accurate data which by regression methods is used to determine virial coefficient constants for use in Virial Equations. Virial equations are derived using statistical mechanics and consideration of intermolecular forces between gas molecules.

10.2.1 AGA NX 19

In 1962 the American Gas Association (AGA) published the NX-19 Report [7] which calculates the supercompressibility factor F_{pv} from a combination of specific gravity or calorific value and the carbon dioxide and nitrogen content of the gas. The compressibility factor Z is then calculated using :-

$$Z = 1/F_{pv}^2$$

The NX-19 calculation has been modified a number of times by users to suit specific gas compositions and is still in use. It is, however, generally limited to a pressure range of 0 to 80 Bar and a temperature range of 0 to 40°C. Examples are AGA NX-19-mod technique[8] for lean natural gases and AGA NX-19-mod/3H [9] for rich natural gases. Test results published

in Gerg TM5 [10] show that the difference between the calculated Z and measured Z using the above methods for lean and rich natural gases can be as much as 0.8 and 1.0 % respectively at a pressure of 120 Bar.

In the 1980's it was recognised that a method was required to calculate compressibility over a wider range of pressures, temperatures and gas compositions. Projects were started in America by the Gas Research Institute (GRI) and in Europe by the Group Européen de Recherches Gazieres (GERG) using a common database. The Americans headed by Professor Starling of the University of Oklahoma published two reports (GRI Interim and GRI Final) before final publication of the method in American Gas Association (AGA) Report No 8 1985 [11]. Although both GRI Interim and Final methods are available they have been superseded by AGA 8 1985 , which has become an industry standard. AGA 8, however, has recently been revised and AGA 8 Second Edition, November 1992 [12] published.

10.2.2 AGA 8 1985

The AGA 8 1985 report details the calculation of compressibility and supercompressibility factors for natural and other hydrocarbon gases over a range of gas compositions. Other components including water are mentioned and can be included without additional uncertainty provided they do not sum to more than 1 mol%. The characterisation parameters (energy, size and orientation) for the other components are included in the report. Although methanol is not mentioned it can be included with the binary interaction parameters U, V and W taken to be 1.0 . The size, energy and orientation parameters for methanol can be calculated using the methods detailed in the report and data readily available from other sources.

A primary method using the full gas composition is recommended for optimum accuracy. Live measurements of pressure, temperature and the full gas composition are therefore required.

AGA 8 1985 also includes five alternative methods that estimate the methane and other hydrocarbon components in the gas. The five methods use combinations of CV, RD, and mol fractions of carbon dioxide, nitrogen and methane. Method 1 requiring inputs of RD, carbon dioxide and nitrogen content appears to be the most practical option but has the disadvantage that there is additional uncertainty, which is not stated in the report. Water and methanol content are not included which also increases the uncertainty.

The uncertainty limits for the computation of supercompressibility against pressure and temperature are detailed for gas compositions within the stated range. For high pressure applications (130 Bar) the uncertainty in supercompressibility is +/-0.3%.

The uncertainty in computed compressibility factor is detailed in AGA 8 Section 8.3 on the basis of comparisons between computed and experimental compressibility for a number of natural gases. It states that as a general guideline the uncertainties in computed compressibility factors for most natural gases at typical pipeline conditions are expected to be less than +/-0.1%, provided the composition of the natural gas is known accurately. Uncertainties in computed compressibility factors are expected to exceed +/-0.1% in some instances (at pressures above 35 Bar) when the gas composition is not accurately known or when the alternative methods for characterisation are used. The relationship between compressibility and supercompressibility uncertainties is detailed in AGA 8 Sections 8.1 and 8.4 where it

states that the relative uncertainty in the supercompressibility factor is one half the relative uncertainty in the compressibility. It is therefore assumed that the uncertainty in compressibility factor Z , for a pressure of 130 barA using the primary method is

$$= 2 * 0.3 = +/-0.6 \% \text{ of reading.}$$

10.2.3 GERG TM2

The GERG TM2 [13] report was published in 1988 following collaboration between the GERG members, who provided the data set, and Van der Waals Laboratory University of Amsterdam who carried out the correlation. The data set contained over 13,000 high accuracy compressibility measurements from pure, binary, ternary and natural gas mixtures. The resulting Master GERG-88 Virial Equation calculates the compressibility Z with an uncertainty of +/-0.1% over a pressure range of 0 to 120 Bar, a temperature range of -8 to 62°C and a 13 component gas composition .

Minor components, (typically less than 0.1 mol%) not detailed above, can be included by adding them to the major components above that have the most similar PVT behaviour. The groupings are detailed in the report Table 6.1 and include water with carbon dioxide but do not include methanol.

The report does state that the +/- 0.1% uncertainty is applicable to gas phase mixtures and is not applicable to natural gas near a phase separation surface particularly in the vicinity of the critical point.

Use of the GERG equation at pressures and temperatures outside of those stated introduces errors. For the pressure range 120 to 150 BarA the error on Z is predicted to be less than 0.5%. It is therefore assumed that the overall uncertainty in Z due to the high pressure, being outside some of the component ranges, not including water and methanol and the gas being at its hydrocarbon dewpoint, is going to be in excess of +/- 0.5%.

10.2.4 GERG TM5

GERG have also published report TM5 which calculates the compressibility factor Z from a restricted set of input variables and not the full gas composition. The Standard (or Simplified) GERG-88 Virial Equation was developed from the Master GERG-88 Virial Equation detailed in TM2 . The input variables are any three from the following : CV, RD, carbon dioxide and nitrogen content with pressure and temperature. The compressibility factor Z is calculated over the same pressure and temperature ranges and with the same uncertainty as the Master GERG Virial Equation in TM2. The same limitations apply with the exception of the uncertainty at pressures above 120 BarA. From tests on five natural gases at higher pressures it states that the uncertainty at a pressure of 130 BarA would be between +/-0.1 and 0.2%. There is, however, the uncertainty in the measurement of CV, RD, CO₂ and N₂ content, and not including methanol and water. It is also not clear what additional uncertainty should be included due to the gas being at its hydrocarbon dewpoint.

10.2.5 AGA 8 SECOND EDITION NOVEMBER 1992

AGA 8 1992 details two methods to calculate Z and density, the Detail Characterisation Method that uses the gas composition and the Gross Characterisation Method that uses CV or RD, N₂ and CO₂ content. Both methods have utilised the GERG database and are significantly different from those detailed in AGA 8 1985. Both methods are applicable for a range of gas compositions but are only suitable for the gas phase and should not be used if the gas is within 5 °C and 2 Bar of the Critical Point.

The Detailed Characterisation Method can also be used outside of this range of gas compositions as it includes correlation specifically for gases from hydrocarbon separators containing heavy hydrocarbons (C₆+ hydrocarbon dewpoint up to 10 mol%) and water (water dewpoint up to 10 mol%). Methanol is not included as a component nor is any provision made for the inclusion of additional components other than H₂S. The method is applicable for the gas phase for temperatures between -130 to 400 °C and pressures up to 2800 Bar, although the uncertainty does increase at high pressures and extreme temperatures.

The uncertainty in computed Z at an operating pressure of 130 BarA and a temperature of 30 °C is stated to be +/- 0.3%.

The Gross Characterisation Method is based on the method used in GERG TM2 and is only suitable for gases within the specified composition, pressure and temperature range (< 120 BarA & 82°C). Within these limits the accuracy of the method is the same as the Detailed Characterisation Method and is estimated to be less than +/- 0.1%. It is stated that outside of these limits the Detail Characterisation Method is more accurate and should be used.

10.3 SELECTION OF METHOD

It is evident that to achieve optimum accuracy, particularly when operating at higher pressures, a full gas compositional method should be used. This excludes both AGA NX -19 and GERG TM-5.

A comparison of the remaining compositional methods is detailed on Figure 13. It could be argued that the later methods AGA 8 1992 and GERG TM 2 will be more accurate as they are derived from and tested against a larger database and hence wider range of gas compositions, pressure and temperatures. There is also the inclusion of other components, in this case water and methanol, to consider.

As shown AGA 8 1985 covers the full gas composition and has the provision to include both water and methanol. Although when including methanol the binary interaction parameters are taken to be 1.0 the size, energy and orientation parameters for methanol are calculated. With the exception of binary temperature interaction parameter the parameters used in the second virial coefficient, which contributes 90% of the final compressibility value, are therefore calculated and included which does give a degree of confidence. However the disadvantage of this method for pressures above 103 Bar is the targeted uncertainty in compressibility of +/- 0.6%.

GERG TM 2 covers the full gas composition with the exception of pentane and additional components. Water can be included by adding it to CO₂. The uncertainty in Z increases above 120 Bar to +/- 0.5 % due to the truncation of the virial equation after the third term.

AGA 8 1992 covers the full gas composition with the exception of pentanes and methanol and specifically mentions the inclusion of water and higher concentrations of C6+ components. The uncertainty in Z increases above 120 Bar to +/- 0.3% which is less than the other methods.

To include methanol in both GERG TM 2 and AGA 8 1992 it has to be added to an existing component. As the effect of methanol on Z is due to the mass and the interaction potential there are options :-

- 1) Add methanol to hexane as they have similar 2nd Virrial Coefficients.
- 2) Add methanol to Ethane as they have similar molecular weights.
- 3) Add methanol to water as both are associating compounds which interact with other components.

The differences between Z calculated by GERG TM 2 and AGA 8 1992 are compared on Figure 14 for a composition without methanol or water and each of the above options for including methanol, over the operating pressure range. As shown there is a larger than expected % difference between the methods even for the composition without water and methanol. The % differences due to the method of including water and methanol were much smaller. It was therefore concluded that the major difference was due to the high operating pressure. This was confirmed on Figure 15 which details the % difference for the composition without water and methanol at a lower operating pressure.

For all cases when compared with AGA 8 1985 GERG TM2 gave a lower value and AGA 8 1992 a higher value of Z.

10.4 UNCERTAINTIES

AGA 8 1992 AND GERG TM2 FULL COMPOSITION METHODS

$$\text{where } \rho = \frac{P_1 Mw}{RTZ}$$

Having reviewed the uncertainty associated with the calculation of Z the uncertainty of calculated density is the combination of the uncertainties for each of the terms in the above equation.

Compressibility Z - The uncertainty in Z is due to the method of calculation and the uncertainty of the gas composition.

Molecular Weight MW - The uncertainty in MW is due to the method of calculation and the uncertainty of the gas composition. The former is assumed to be negligible and was ignored.

The uncertainties in Z and MW, due to the gas composition, were estimated by varying each component in the typical composition by the chromatograph uncertainty and then normalising the composition. The compressibility and molecular weight were then calculated from each normalised composition. The largest deviations in compressibility and molecular weight were then used as the uncertainty due to the uncertainty of the gas composition.

Uncertainty in Universal Gas Constant R - The uncertainty in R was assumed to be negligible and was ignored.

Uncertainty in Pressure Measurement

The uncertainty of pressure measurement Ep is a combination of the transmitter accuracy, ambient temperature effect and the flowcomputer ADC accuracy

$$E_p = [(E_t * P_{fs}/P_m)^2 + (E_{te} * \text{mod } t/28)^2 + (E_{adc} * P_{fs}/P_m)^2]^{0.5} \text{ \% of reading}$$

where :-

Et = the manufacturer's stated accuracy in % of span or URV

Pfs = the calibrated span or URV in barA

Pm = the measured pressure barsA

Ete = the manufacturer's stated temperature effect in % of span or URV per 28°C

mod t = the change in ambient temperature from that during calibration °C

Eadc = the flowcomputer adc accuracy in % of span or URV

For a typical pressure transmitter operating in analogue mode :-

Et = +/- 0.15 % of span

Pfs = 150 BarA

Pm = 130 BarA

Ete = +/- 0.175% of span per 28°C

mod t = 5°C

Eadc = 0.1% full scale

$$E_p = +/- [(0.15 * 150/130)^2 + (0.175 * 5/28)^2 + (0.1 * 150/130)^2]^{0.5}$$

$$= +/- 0.21 \text{ \% of reading (at 130 BarA)}$$

Uncertainty in Temperature Measurement.

The uncertainty of temperature measurement ET when using a Class A platinum resistance thermometer in accordance with BS 1904 as a direct input into the flowcomputer is :-

$$ET = +/- [(0.15 + (0.35 - 0.15) * \text{mod } T)^2 + (E_{adc})^2]^{0.5} \text{ °C}$$

where :-

mod T = the measured temperature
= 30°C

Eadc = the flowcomputer temperature adc
= +/-0.1°C

$$\begin{aligned} ET &= \pm \left[\frac{(0.15 + (0.35-0.15) * 30)^2}{100} + (0.1)^2 \right]^{0.5} \text{°C} \\ &= \pm 0.23 \text{°C} \\ &= \pm 0.23 \text{K} \end{aligned}$$

$$ET = \pm 0.076 \% \text{ of reading. (at 303.15 K)}$$

There is an interdependence of terms due to pressure and temperature affecting both the compressibility and the density. To overcome this sensitivity coefficients were calculated for each of the variables. The sensitivity coefficient θ_j is the percentage change in ρ as a result of a 1% change in variable Y_j . This was achieved by varying each variable by 1% and calculating the resulting percentage change in density.

The uncertainties were then combined using :-

$$E_\rho^2 = \sum_i^k (\theta_j * e_j)^2$$

where :-

θ_j = the dimensionless sensitivity coefficient of variable Y_j
 e_j = the uncertainty of each variable
 E_ρ = the % uncertainty in density

At 130 BarA the uncertainty using the GERG TM2 Method was estimated to be +/- 0.55 % of reading.

At 130 BarA the uncertainty using the AGA 8 1992 Detail Characterisation Method was estimated to be +/- 0.38 % of reading.

The calculations are detailed on Figure 16 but do not include an additional uncertainty on Z due to the method used to include methanol.

11 CONCLUSIONS

The gas composition does vary with separator operating conditions. It is therefore desirable to measure the gas composition with an on-line gas chromatograph.

The gas at the metering system will be at its hydrocarbon dewpoint and depending on the presence of free water, be at its water dewpoint. The use of sampling or live measurement of water content on an offshore platform does present problems. Assuming the gas is at its water dewpoint the water content can be calculated using a method such as Campbell or Bukacek. On wet gas systems it is likely that methanol will be injected to inhibit the formation of hydrates and corrosion and will therefore be present in the gas stream. Although the effect of water and methanol on density counteract each other ignoring them, in the calculated concentrations, would result in a systematic bias of +0.22% of reading. It is therefore concluded that to achieve optimum accuracy, if present in sufficient quantities, water and methanol should be included in the gas composition used to calculate density.

The methanol content could be calculated or determined from sample analysis using chromatography. There is conflicting opinion on the effect of water and methanol on the C6+ peak of some gas chromatographs. Tests are required to establish the effect relative to concentration.

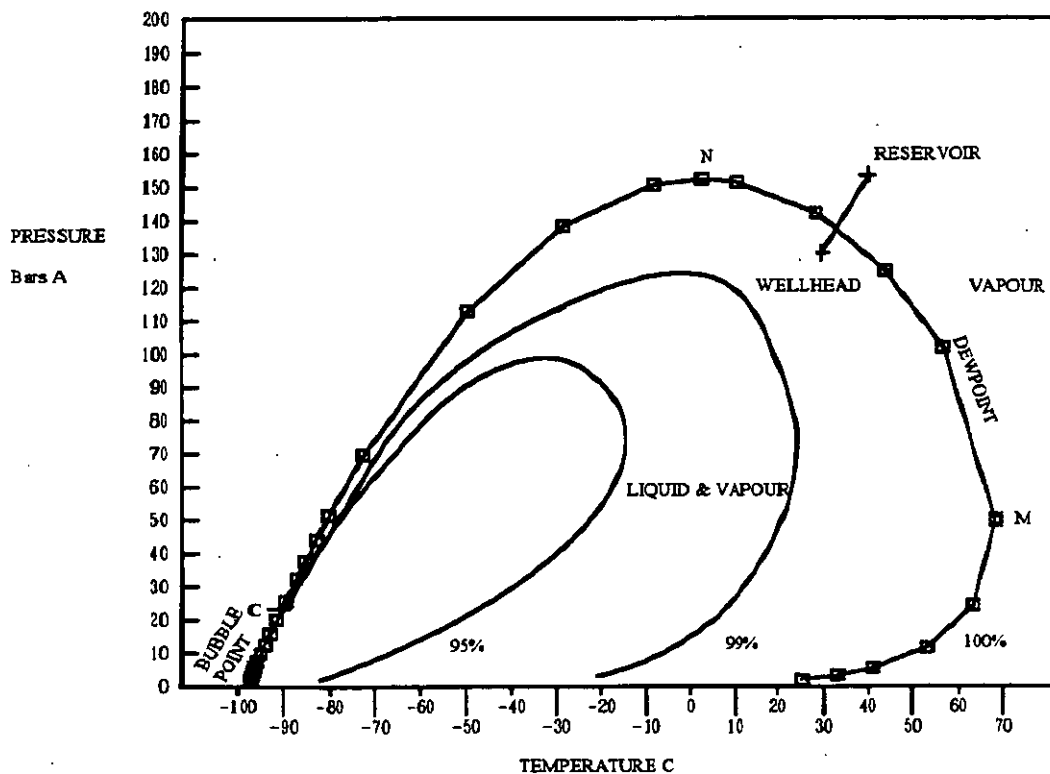
A full compositional method should be used to calculate Z with due regard given to the range of components, and the operating pressure and temperature. Generally the more recent methods should be more accurate as they are derived and tested against a larger database and hence wider range of gas compositions, pressures and temperatures. For the typical composition used there were differences between the Z calculated by the more recent methods, GERG TM2 and AGA8 1992, particularly at high operating pressures. Ideally the method chosen should be tested against measurements of Z over the full gas composition and operating range of pressures and temperatures. The inclusion of additional components, in this case methanol is often not detailed. The method chosen to include methanol did have an effect on the calculated Z and density. It is not clear to the user which method is correct.

The effects on the calculation of Z and density of the condensate present at the orifice, or the use of an equation of state near a phase boundary, are not clear. Although the sampled gas is in this condition, the gas entering the chromatograph will have been conditioned in the pressure reduction system. The condensate will have been removed either by a coalescer or by heating. The condition of the gas entering the chromatograph with respect to the dewpoint line will depend on the amount of heat introduced as shown on Figure 9. The use of either GERG TM2 or AGA 8 1992 equations of state near a phase boundary is discouraged, although it is not clear whether this is due to the lack of test data or the unpredictability of the gas in this condition. If the gas sample is heated so that it is not near the dewpoint line is the gas composition obtained from the chromatograph representative of the metered stream? Clearly there is a need to investigate the behaviour of gas in this condition and the suitability of calculated density.

12 REFERENCES

- [1] A.W. JAMIESON and H.J. SIKKENGA On-line Water Dewpoint Measurement in Natural Gas.
Gas Quality Elsevier Science Publishers B.V Amsterdam 1986.
- [2] Gas Conditioning and Processing - Volume 1 1984
The Basic Principles by John M Campbell
- [3] R.F. BUKACEK Equilibrium Moisture Content of Natural Gases - Pipeline Research Committee of the American Gas Association 1955
- [4] Engineering Data Book - Volume 1 - Tenth Edition 1987
Gas Processors Suppliers Association (GPSA)
- [5] British Gas Analytical Method (BGAM) 9.2.5 Methanol in Gas.
- [6] ISO 5168-1978(E) Measurement of Fluid Flow - Estimation of Uncertainty of a Flow-rate Measurement.
- [7] Manual for the Determination of Supercompressibility Factors for Natural Gas.
American Gas Association (1963).
- [8] F. Herning and E. Wolowski
Kompressibilitatzahlen und Realgasfaktoren von Erdgasen nach neuen amerikanischen Berechnungsmethoden
Ges. Ber Ruhrgas no 15 7-14 (1966).
- [9] M. Jaeschke and B Harbrink
gwf-gas/erdgas 123 (1) 20-27 (1982).
- [10] GERG TMS 1991 Standard GERG Virial Equation for Field Use.

- [11] K.E. STARLING Compressibility and Supercompressibility for Natural Gas and Other Hydrocarbon Gases.
A.G.A. Transmission Measurement Committee report No. 8 (Dec 1985).
- [12] Compressibility Factors of Natural Gas and Other Related Hydrocarbon Gases.
A.G.A. Transmission Measurement Committee report No. 8 Second Edition
November 1992.
- [13] GERG TM2 1988 High Accuracy Compressibility Factor
Calculation for Natural Gases and Similar Mixtures by use of a Truncated Virial
Equation.



N = Cricondensar - the maximum pressure at which liquid and vapour may exist
M = Cricondentherm - the maximum temperature at which liquid and vapour may coexist in equilibrium
C = Critical Point - Critical Pressure and Critical Temperature

**FIGURE 1 - WELLSTREAM PHASE ENVELOPE
RESERVOIR & WELLHEAD CONDITIONS**

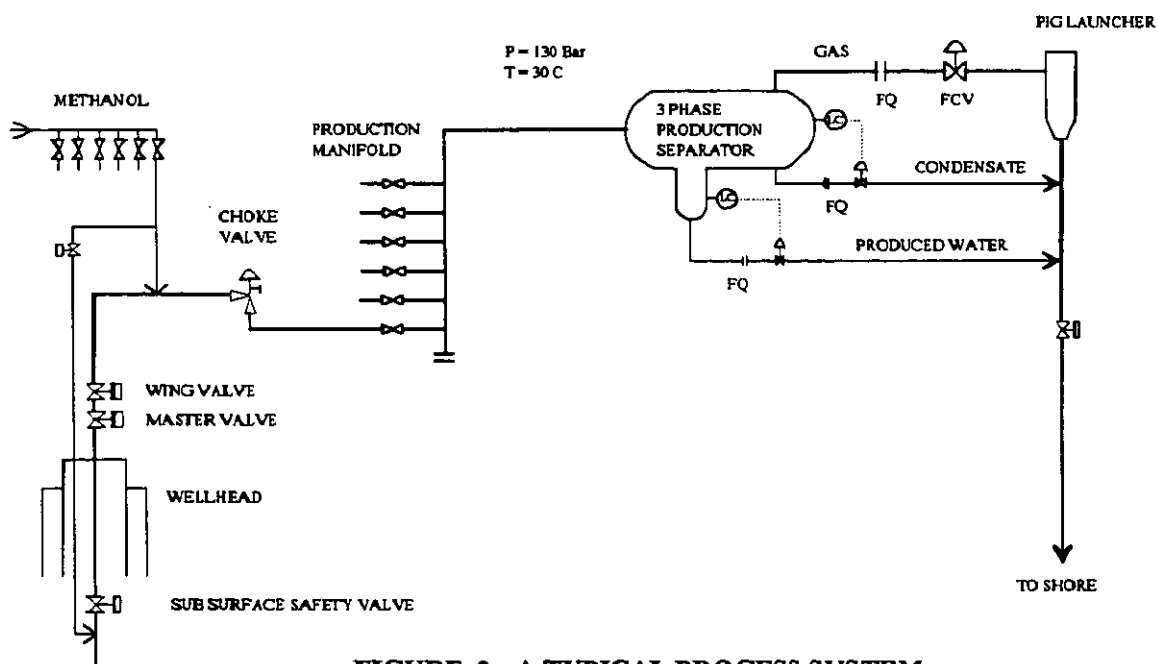


FIGURE 2 - A TYPICAL PROCESS SYSTEM

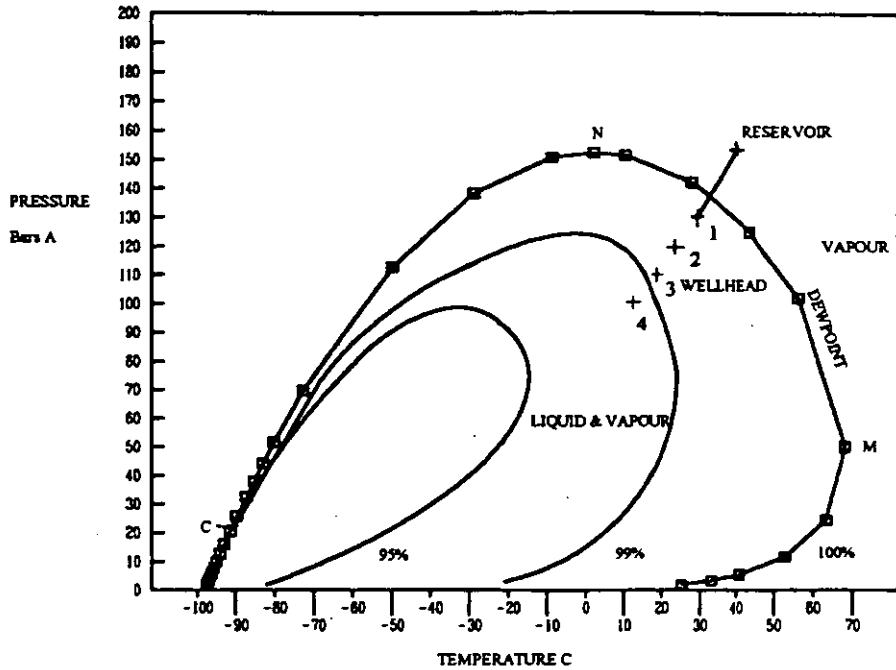


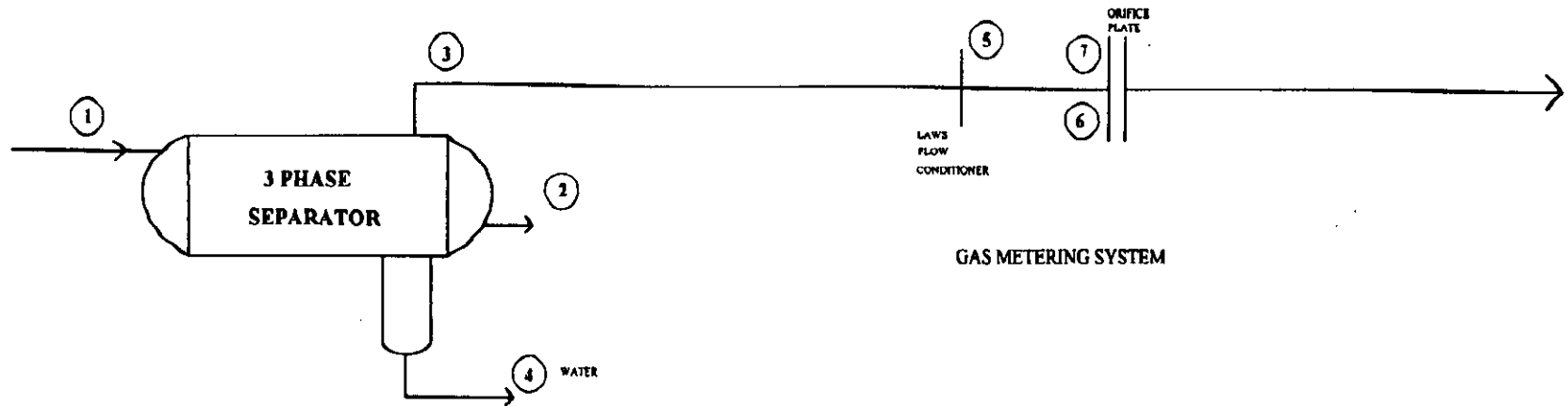
FIGURE 3 - WELLSTREAM PHASE ENVELOPE
CONDENSATE TO GAS RATIO (CGR)

| COMPONENT | YEAR 1 | | | |
|-----------------|------------------------------|------------------------------|------------------------------|------------------------------|
| | 1 P = 130 Bar T = 30 C | 2 P = 120 Bar T = 25 C | 3 P = 110 Bar T = 20 C | 4 P = 100 Bar T = 15 C |
| Nitrogen | 2.02 | 2.02 | 2.03 | 2.03 |
| Carbon Dioxide | 0.65 | 0.65 | 0.65 | 0.65 |
| Water | 0.06 | 0.06 | 0.06 | 0.05 |
| Methane | 91.21 | 91.38 | 91.56 | 91.76 |
| Ethane | 3.03 | 3.02 | 3.02 | 3.01 |
| Propane | 0.69 | 0.68 | 0.68 | 0.67 |
| I-Butane | 0.14 | 0.13 | 0.13 | 0.13 |
| N-Butane | 0.2 | 0.2 | 0.2 | 0.19 |
| I-Pentane | 0.77 | 0.75 | 0.71 | 0.66 |
| N-Pentane | 0.77 | 0.74 | 0.7 | 0.64 |
| Hexane | 0.1 | 0.09 | 0.08 | 0.07 |
| Heptane | 0.15 | 0.13 | 0.1 | 0.08 |
| Octane | 0.1 | 0.08 | 0.05 | 0.03 |
| Nonane | 0.05 | 0.03 | 0.02 | 0.01 |
| Decane | 0.04 | 0.02 | 0.01 | 0.01 |
| Undecane | 0.01 | 0.01 | 0 | 0 |
| True Density | 121.53854 | 113.79646 | 105.44496 | 98.65294 |
| Comp. 1 Density | 121.53854 | 115.15993 | 108.08732 | 100.27758 |
| % Difference | 0.00 | 1.20 | 2.51 | 3.75 |

Notes

1) Condensate to Gas Ratio = 1.92 Barrels per MMSCF

FIGURE 4 - CHANGES IN GAS COMPOSITION WITH CHANGING
SEPARATOR OPERATING CONDITIONS



| STREAM | 1 | 2 | 3 | 5 | 6 | 7 |
|--------------------------------|-----------|---------------------------|--------------------|-------------------|------------------------|-----------------|
| WELLSTREAM | 130.00 | CONDENSATE FROM SEPARATOR | GAS FROM SEPARATOR | INPUT TO METERING | CONDENSATE TO METERING | GAS TO METERING |
| PRESSURE Bar A | 130.00 | 130.00 | 130.00 | 129.847 | 129.847 | 129.847 |
| TEMPERATURE C | 30.0 | 30.0 | 30.0 | 29.96 | 29.96 | 29.96 |
| MASS FLOW kg/h | 137445.00 | 11099348 | 136335.08 | 136335.08 | 17.6345 | 136317.44 |
| GAS DENSITY kg/m ³ | | | 122.263 | | | 122.138 |
| STD VOL FLOW m ³ /h | | | 173141.5 | | | 173119.1 |
| LIQ DENSITY kg/m ³ | | 554.91 | | | 554.98 | |
| LIQ VOL FLOW m ³ /h | | 1.9276 | | | 0.0306 | |
| NITROGEN | 2.00 | 0.53 | 2.01 | 2.01 | 0.53 | 2.01 |
| CARBON DIOXIDE | 0.65 | 0.58 | 0.65 | 0.65 | 0.58 | 0.65 |
| WATER | 0.06 | 0.06 | 0.06 | 0.06 | 0.06 | 0.06 |
| METHANE | 90.84 | 46.62 | 90.96 | 90.96 | 46.59 | 90.96 |
| ETHANE | 3.29 | 4.42 | 3.29 | 3.29 | 4.42 | 3.29 |
| PROPANE | 0.69 | 1.85 | 0.69 | 0.69 | 1.85 | 0.69 |
| I-BUTANE | 0.14 | 0.61 | 0.14 | 0.14 | 0.61 | 0.14 |
| N-BUTANE | 0.21 | 1.12 | 0.21 | 0.21 | 1.13 | 0.21 |
| I-PENTANE | 0.79 | 7.03 | 0.77 | 0.77 | 7.06 | 0.77 |
| N-PENTANE | 0.79 | 8.07 | 0.77 | 0.77 | 8.09 | 0.77 |
| HEXANE | 0.11 | 2.08 | 0.10 | 0.10 | 2.09 | 0.10 |
| HEPTANE | 0.17 | 5.70 | 0.15 | 0.15 | 5.71 | 0.15 |
| OCTANE | 0.12 | 6.84 | 0.10 | 0.10 | 6.85 | 0.10 |
| NONANE | 0.07 | 6.48 | 0.05 | 0.05 | 6.47 | 0.05 |
| DECANE | 0.05 | 5.08 | 0.04 | 0.04 | 5.07 | 0.04 |
| UNDECANE | 0.02 | 2.90 | 0.01 | 0.01 | 2.89 | 0.01 |

NOTES

- 1) PRESSURE DROP BETWEEN SEPARATOR AND ORIFICE CALCULATED TO BE 0.153 BAR.
- 2) PIPE BETWEEN SEPARATOR AND FLOW CONDITIONER 20 METRES, WITH 4 BENDS AND SIZED AT 12 INCH DIAMETER. PRESSURE DROP 0.075 BAR
- 3) PRESSURE DROP ACROSS LAWS CONDITIONER 0.078 BAR
- 4) PRESSURE DROP ACROSS ORIFICE 0.550 BAR
- 5) PRESSURE LOSS ACROSS ORIFICE 0.342 BAR
- 6) TEMPERATURE DROPS CALCULATED USING ISENTHALPIC CONSTANT OF 0.298 K/BAR

FIGURE 5 - THE CONDITION OF GAS STREAM AT THE ORIFICE

24

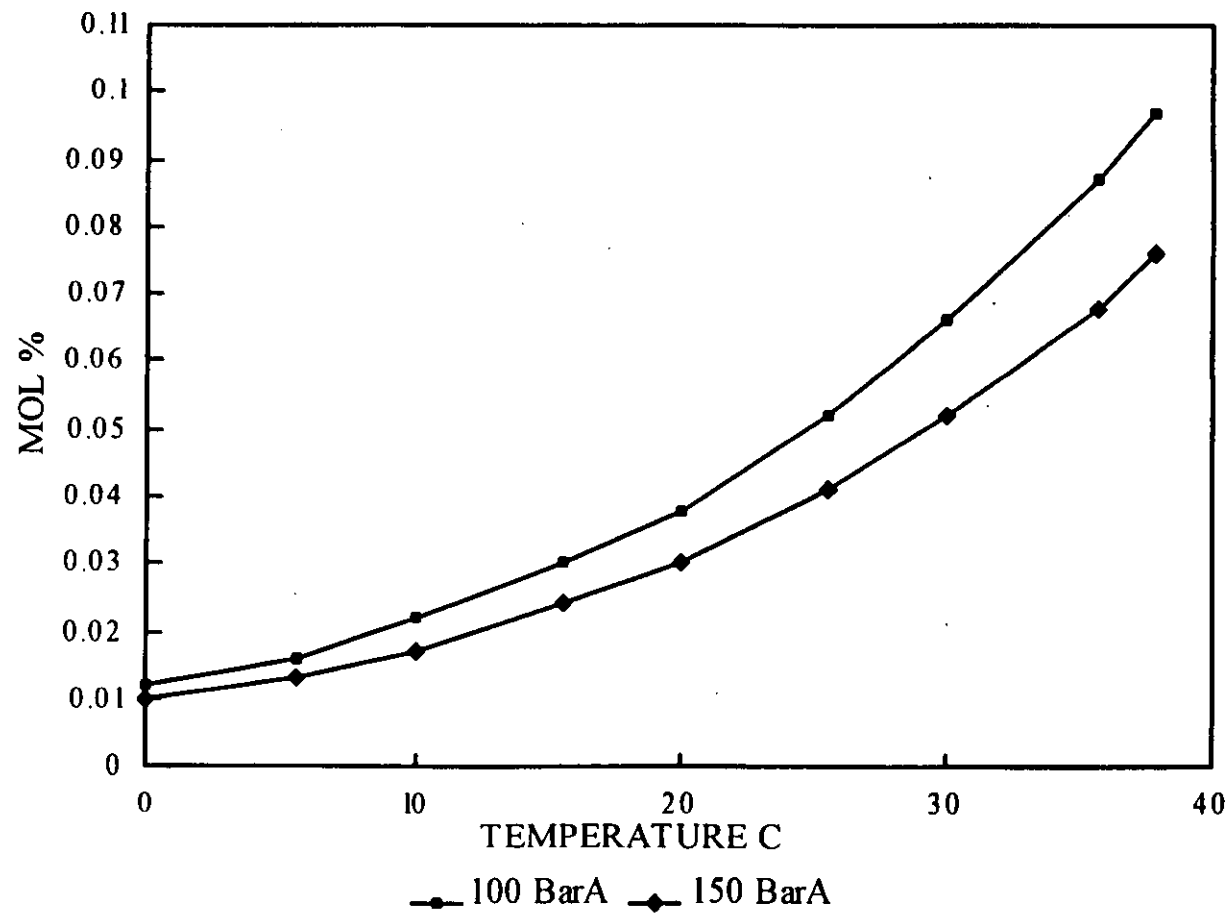


FIGURE 6 - WATER CONTENT OF NATURAL GAS

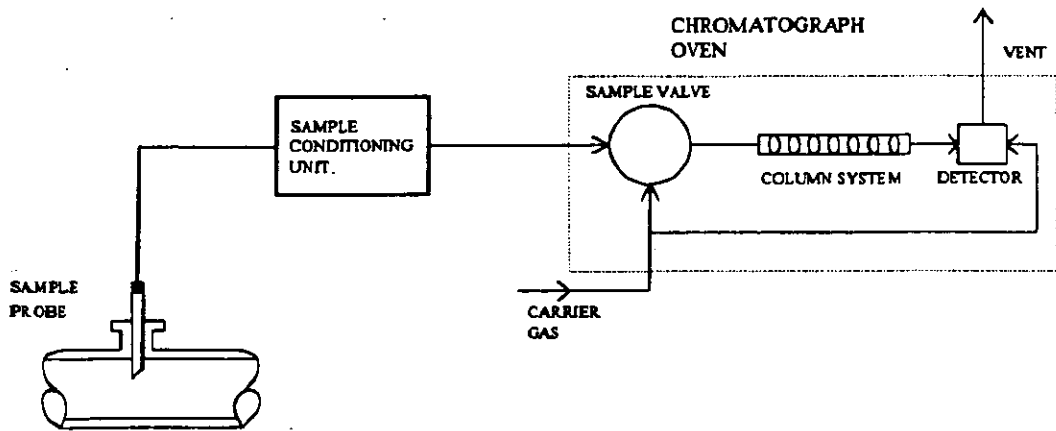


FIGURE 7 - A GAS CHROMATOGRAPH

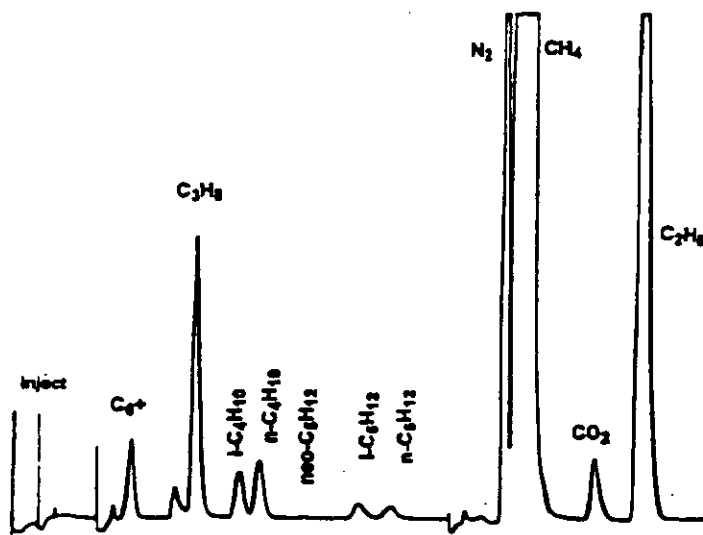
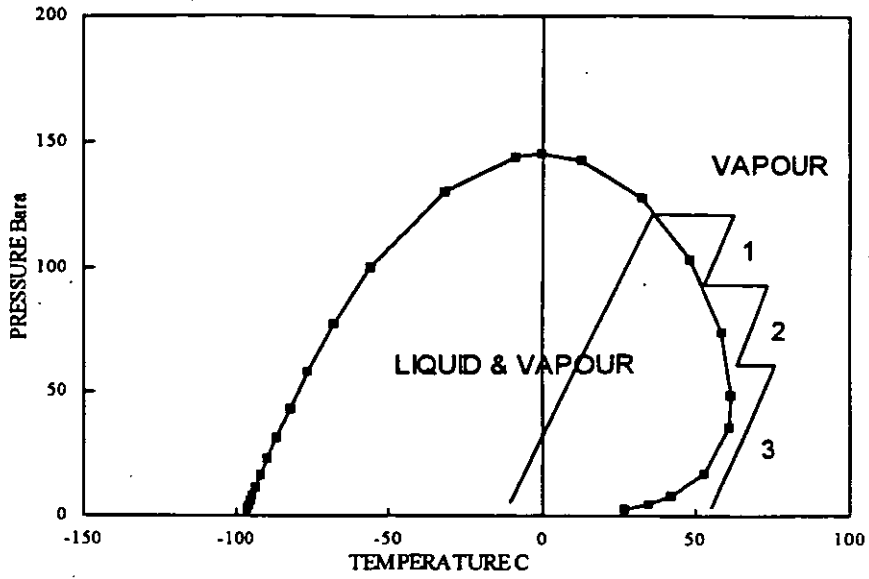


FIGURE 8 - A CHROMATOGRAM



**FIGURE 9 - GAS STREAM PHASE ENVELOPE
PRESSURE REDUCTION STAGES**

| COMPONENT | SPOT SAMPLING | | AUTO SAMPLING | | | |
|----------------|----------------------------|---------------------------------|---------------------------------|---------------------------------|--|--|
| | FIELD A | FIELD B | FIELD C | FIELD D | | |
| | BI-MONTHLY OVER 6 YEARS | TIME WEIGHTED OVER 15 MONTHS | TIME WEIGHTED OVER 15 MONTHS | FLOW WEIGHTED OVER 21 MONTHS | | |
| Nitrogen | 0.02 | 0.0739 | 0.0252 | 0.255 | | |
| Carbon Dioxide | 0.08 | 0.018 | 0.0225 | 0.031 | | |
| Methane | 0.059 | 0.0673 | 0.094 | 0.4755 | | |
| Ethane | 0.04 | 0.0623 | 0.0434 | 0.1954 | | |
| Propane | 0.04 | 0.0191 | 0.0213 | 0.0375 | | |
| N-Butane | 0.01 | 0.0041 | 0.0034 | 0.0161 | | |
| I-Butane | 0.01 | 0.0123 | 0.0046 | - | | |
| N-Pentane | 0.028 | 0.0021 | 0.0014 | 0.0114 | | |
| I-Pentane | 0.008 | 0.0016 | 0.0019 | - | | |
| Hexane + | 0.042 | 0.0318 | 0.0501 | 0.041 | | |

NOTE - Field A samples were taken at the onshore terminal.
All other samples were taken offshore.

SPOT AND AUTO SAMPLING COMPONENT STANDARD DEVIATIONS

| COMPONENT | CHROMATOGRAPH | | | | |
|----------------|----------------------------------|------------------------------|---------------------------------|-------------------------------|----------------------------|
| | FIELD B | FIELD B | FIELD B | FIELD E | FIELD F |
| | CALIBRATION GAS OVER 4 MONTHS | HOURLY AVERAGE OVER 1 DAY | DAILY AVERAGES OVER 4 MONTHS | HOURLY AVERAGE OVER 4 DAYS | ALL ANALYSIS OVER 1 DAY |
| Nitrogen | 0.0014 | 0.0016 | 0.0189 | 0.0104 | 0.0027 |
| Carbon Dioxide | 0.0017 | 0.0058 | 0.0167 | 0.0015 | 0.0006 |
| Methane | 0.0062 | 0.0097 | 0.0685 | 0.011 | 0.0105 |
| Ethane | 0.0029 | 0.0015 | 0.0299 | 0.005 | 0.0028 |
| Propane | 0.0014 | 0.0008 | 0.0144 | 0.001 | 0.0012 |
| N-Butane | 0.0003 | 0.0003 | 0.0039 | 0.0006 | 0.0005 |
| I-Butane | 0.0002 | 0.0002 | 0.0024 | 0.0005 | 0.0003 |
| N-Pentane | 0.0004 | 0.0004 | 0.0014 | 0.0004 | 0.0002 |
| I-Pentane | 0.0003 | 0.0003 | 0.0014 | 0.0001 | 0.0002 |
| Hexane + | 0.0029 | 0.0037 | 0.015 | 0.0037 | 0.0058 |

ON-LINE GAS CHROMATOGRAPHY COMPONENT STANDARD DEVIATIONS

FIGURE 10

| CHROMATOGRAPH | | | | | | CALCULATED CHROMATOGRAPH REPEATABILITY +/- mol% |
|---|---|--|--|---------------------------------------|-------------|--|
| FIELD B CALIBRATION GAS OVER 4 MONTHS | FIELD B HOURLY AVERAGE OVER 1 DAY | FIELD B DAILY AVERAGES OVER 4 MONTHS | FIELD E HOURLY AVERAGE OVER 4 DAYS | FIELD F ALL ANALYSIS OVER 1 DAY | | |
| n = t = | 98 1.96 | 21 2.086 | 53 2.011 | 70 1.96 | 183 1.96 | |
| COMPONENT | | | | | | |
| Nitrogen | 0.0027 | 0.0033 | 0.0380 | 0.0204 | 0.0053 | 0.0068 |
| Carbon Dioxide | 0.0033 | 0.0121 | 0.0336 | 0.0029 | 0.0012 | 0.0044 |
| Methane | 0.0122 | 0.0202 | 0.1378 | 0.0218 | 0.0208 | 0.0380 |
| Ethane | 0.0057 | 0.0031 | 0.0601 | 0.0098 | 0.0056 | 0.0126 |
| Propane | 0.0027 | 0.0017 | 0.0290 | 0.0020 | 0.0024 | 0.0044 |
| N-Butane | 0.0008 | 0.0008 | 0.0078 | 0.0012 | 0.0010 | 0.0018 |
| I-Butane | 0.0004 | 0.0004 | 0.0048 | 0.0010 | 0.0008 | 0.0008 |
| N-Pentane | 0.0008 | 0.0008 | 0.0028 | 0.0008 | 0.0004 | 0.0014 |
| I-Pentane | 0.0008 | 0.0008 | 0.0028 | 0.0002 | 0.0004 | 0.0008 |
| Hexane + | 0.0057 | 0.0077 | 0.0302 | 0.0073 | 0.0114 | 0.0120 |

NOTE SHADED RESULTS NOT INCLUDED

**FIGURE 11 - CHROMATOGRAPH REPEATABILITY +/- MOL%
CALCULATED AT 95% CONFIDENCE LEVEL**

| COMPONENT | mol % | CHROMATOGRAPH REPEATABILITY +/- mol % | CALIBRATION GAS UNCERTAINTY +/- mol % | CHROMATOGRAPH UNCERTAINTY +/- mol % |
|----------------|-------|---|---|---|
| Nitrogen | 2.02 | 0.0068 | 0.0101 | 0.0122 |
| Carbon Dioxide | 0.85 | 0.0044 | 0.0065 | 0.0078 |
| Methane | 91.21 | 0.0380 | 0.0621 | 0.0728 |
| Ethane | 3.03 | 0.0126 | 0.0152 | 0.0197 |
| Propane | 0.69 | 0.0044 | 0.0069 | 0.0082 |
| N-Butane | 0.20 | 0.0018 | 0.0020 | 0.0027 |
| I-Butane | 0.14 | 0.0008 | 0.0014 | 0.0016 |
| N-Pentane | 0.77 | 0.0014 | 0.0077 | 0.0078 |
| I-Pentane | 0.77 | 0.0009 | 0.0077 | 0.0078 |
| Hexane + | 0.46 | 0.0120 | 0.0046 | 0.0129 |
| | 99.94 | | | |

FIGURE 12 - UNCERTAINTY IN GAS COMPOSITION MEASURED BY A GC

| COMPONENT | mol % | AGA8 1985 | GERG TM2 | AGA8 1992 |
|----------------|-----------|--|--|--|
| Nitrogen | 2.020 | 0 - 50 | 0 - 50 | 0.3 - 53.6 |
| Carbon Dioxide | 0.650 | 0 - 50 | 0 - 30 | 0.04 - 28.94 |
| Water | 0.060 | *1) | *2) | *4) |
| Methane | 91.210 | 50 - 100 | 50 - 100 | 45.2 - 98.3 |
| Ethane | 3.030 | 0 - 20 | 0 - 20 | 0.24 - 9.53 |
| Propane | 0.690 | 0 - 5 | 0 - 5 | 0.02 - 3.57 |
| N-Butane | 0.200 | } 0 - 3 | } 0 - 1.5 | } 0.01 - 1.08 |
| I-Butane | 0.140 | | | |
| N-Pentane | 0.770 | } 0 - 2 | } 0 - 0.5 | } 0.002 - 0.279 |
| I-Pentane | 0.770 | | | |
| Hexane | 0.090 | } 0 - 1 | 0 - 0.1 | } *5) |
| Heptane | 0.130 | | 0 - 0.1 | |
| Octane | 0.090 | | 0 - 0.1 | |
| Nonane | 0.040 | | | |
| Decane | 0.040 | | *3) | |
| Undecane | 0.010 | | | |
| Methanol | 0.060 | *1) | *2) | not included |
| PRESSURE BarA | 100 - 150 | | | |
| TEMPERATURE C | 15 - 30 | | | |
| UNCERTAINTY Z | | +/- 0.2 % 0 - 130 Bar +/- 0.6 % 103 - 172 Bar | +/- 0.1 % 0 - 120 Bar +/- 0.5 % 120 - 150 Bar | +/- 0.1 0 - 120 Bar +/- 0.3 % 120 - 170 Bar |

NOTES

- 1) Additional components can be included provided they do not sum to more than 1 mol %
- 2) Additional components (typically less than 0.1 mol %) are added to major components with similar PVT behaviour i.e. those with similar second virial coefficients.
- 3) All hydrocarbons higher than C8 are added to C8.
- 4) Water Dewpoint up to 10 mol %
- 5) Hydrocarbon Dewpoint up to 10 mol %.

FIGURE - 13 A COMPARISON OF METHODS FOR THE CALCULATION OF Z FROM FULL GAS COMPOSITION

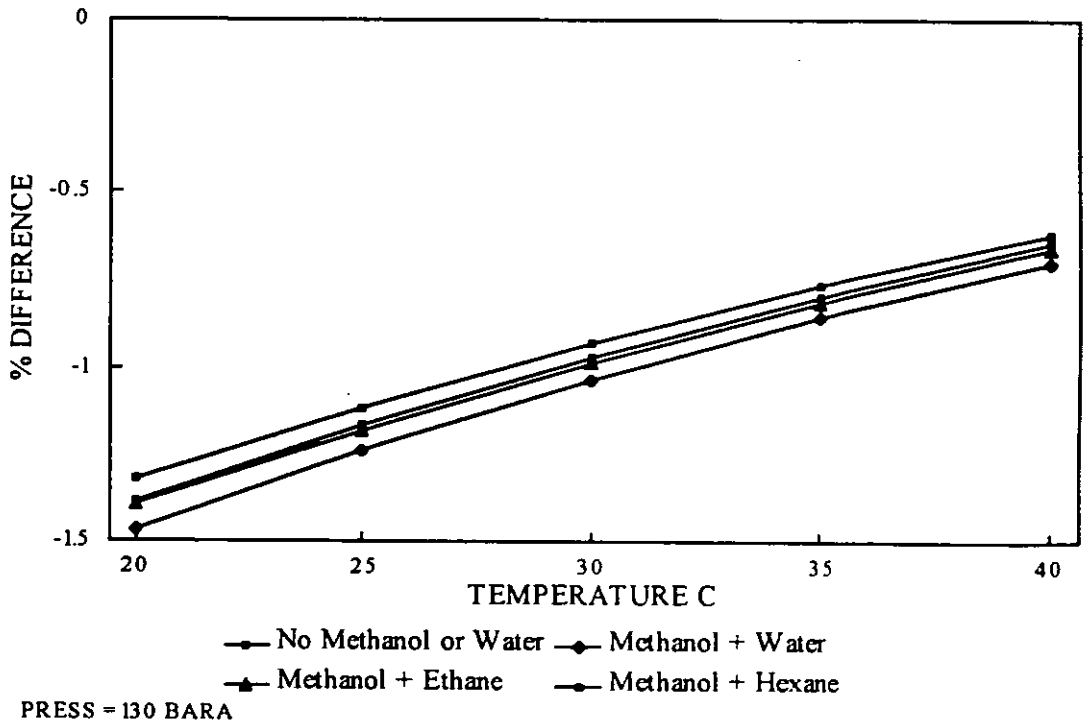
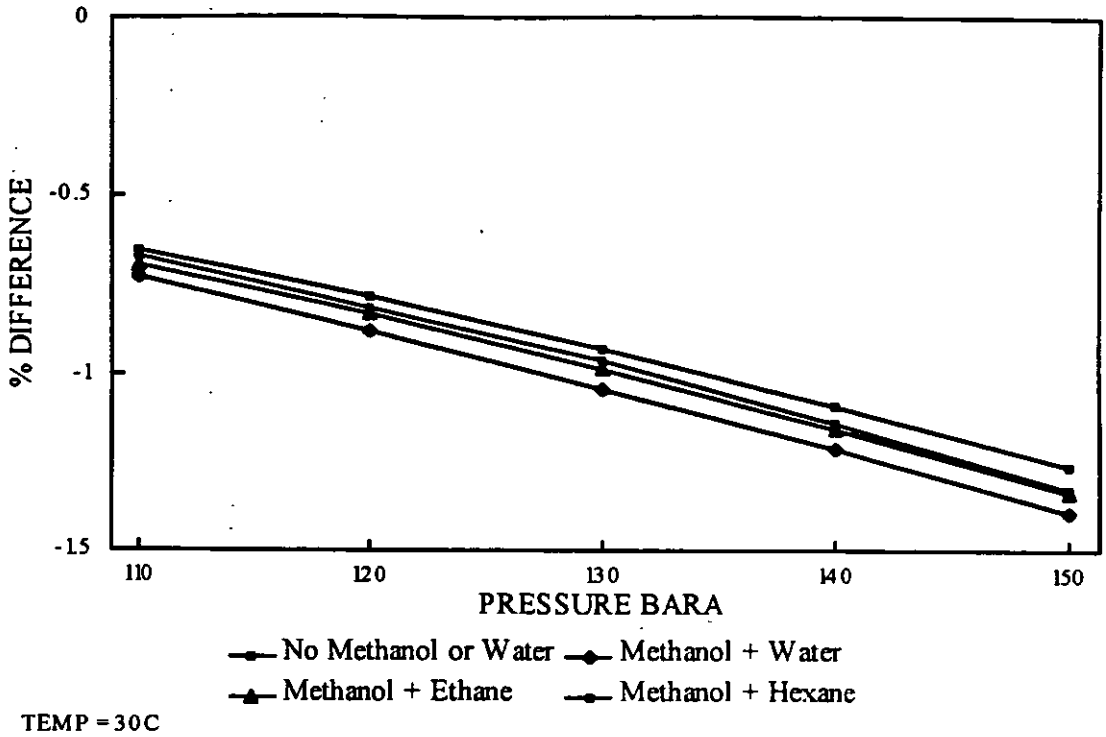
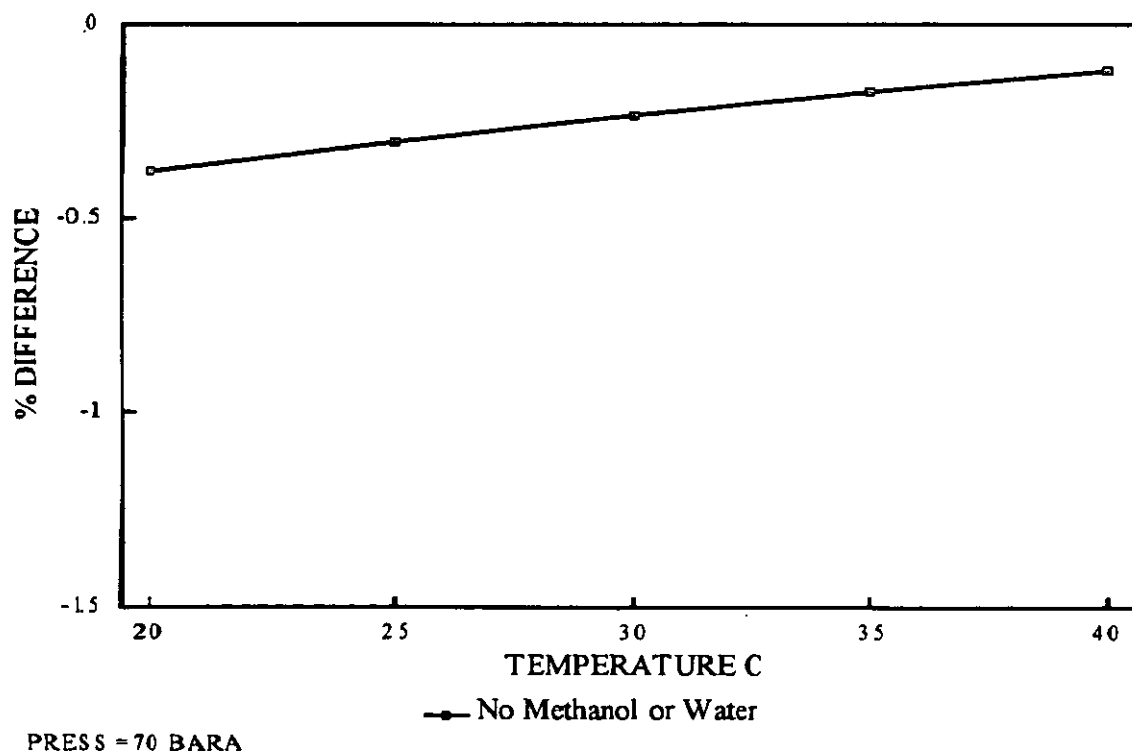
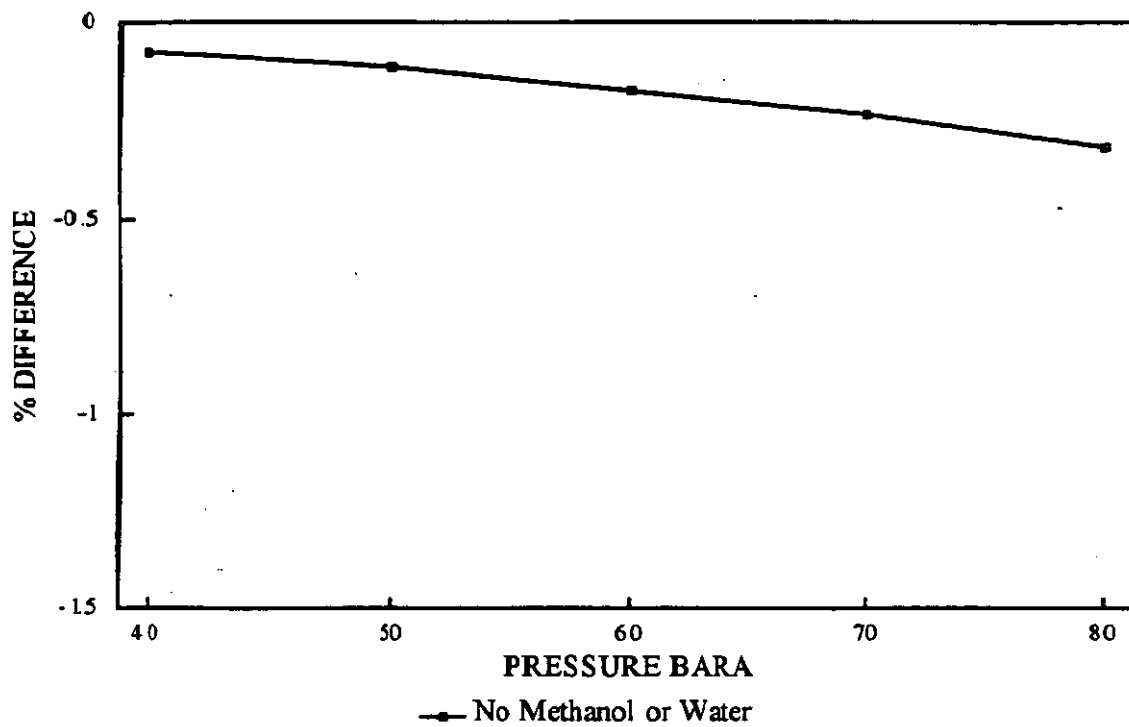


FIGURE - 14 % DIFFERENCE IN Z BETWEEN AGA 8 1992 & GERG TM 2
HIGH OPERATING PRESSURE



**FIGURE - 15 % DIFFERENCE IN Z BETWEEN AGA 8 1992 & GERG TM 2
LOW OPERATING PRESSURE**

GERG TM 2

| PARAMETER | VALUE | 1% CHANGE | DENSITY kg/m3 | SENS. sj % | UNCERT. ej % | VARIANCE (sj ej) ^ 2 |
|-------------|---------|--------------|------------------|---------------|-----------------|-------------------------|
| Base Case | - | - | 121.6862 | - | | |
| Pressure | 130 | 131.3 | 122.9031 | 1.00 | 0.21 | 0.044102 |
| Temperature | 303.15 | 306.1815 | 120.4814 | -0.99 | 0.076 | 0.005662 |
| Zcomp | 0.78297 | 0.7907997 | 120.4814 | -0.99 | 0.039 | 0.001491 |
| Zcalc | 0.78297 | 0.7907997 | 120.4814 | -0.99 | 0.5 | 0.245064 |
| MW comp | 18.473 | 18.65773 | 122.9031 | 1.00 | 0.065 | 0.004225 |

Total Uncertainty = +/- 0.300544) ^0.5 %
= +/- 0.55 %

AGA 8 1992

| PARAMETER | VALUE | 1% CHANGE | DENSITY kg/m3 | SENS. sj % | UNCERT. ej % | VARIANCE (sj ej) ^ 2 |
|-------------|----------|--------------|------------------|---------------|-----------------|-------------------------|
| Base Case | - | - | 120.5010 | - | | |
| Pressure | 130 | 131.3 | 121.7060 | 1.00 | 0.21 | 0.044101 |
| Temperature | 303.15 | 306.1815 | 119.3080 | -0.99 | 0.076 | 0.005662 |
| Zcomp | 0.790671 | 0.79857771 | 119.3080 | -0.99 | 0.039 | 0.001491 |
| Zcalc | 0.790671 | 0.79857771 | 119.3080 | -0.99 | 0.3 | 0.088222 |
| MW comp | 18.473 | 18.65773 | 121.7060 | 1.00 | 0.065 | 0.004225 |

Total Uncertainty = +/- 0.143702) ^0.5 %
= +/- 0.38 %

FIGURE 16 - UNCERTAINTY IN CALCULATED DENSITY

WET GAS FLOW MEASUREMENT BY MEANS OF A VENTURI METER AND A TRACER TECHNIQUE.

H. de Leeuw

Koninklijke/Shell Exploratie & Productie Laboratorium, Rijswijk, The Netherlands

SUMMARY

Experiments in wet gas flow have demonstrated that venturi flow meter readings can be corrected to give the actual gas rate, provided the entrained liquid flow rate or wetness is known. A technique has been developed to measure the liquid flow rate in a wet gas stream, which is based on the tracer dilution technique using fluorescent dyes. Laboratory experiments and field tests under various operating conditions have demonstrated that the liquid flow rate can be determined within the target accuracy of 10%. Hence the gas flow rate measurement can be corrected to within approximately 2% to 4% accuracy. The new technique makes it possible to develop satellite gas fields without (test-)separators and manifolds, thereby offering substantial capital savings and enhancing the economics of marginal fields.

1 INTRODUCTION

To make the development of small gas fields economically viable, costs have to be reduced significantly. If the flow measurement of the produced gas can be made before, rather than after any entrained liquids have been removed, then satellite field developments could be set up without conventional separation facilities. The production streams from a number of small fields can then be simply commingled prior to transportation and processing by shared facilities. Evidently, the gas flow meters should handle some liquid in the flow. Also, as the gas price and ownership of each field is often different, these meters should have a sufficiently high accuracy to allow commercial custody transfer¹.

Previous tests at a NAM location in the Netherlands demonstrated that both venturi meters and orifice meters can be used to accurately measure the flow of wet gas, provided the liquid fraction is known². The over-reading of those meters, compared to the actual dry gas measurement, at pressures around 90 bar and with liquid fractions up to 4% by volume closely followed the relationships developed by Chisholm³ and Murdock⁴. However, recent venturi meter tests at a Norwegian test site performed at different line pressures and with liquid fractions up to 10% by volume, showed that for other pressures than around 90 bar above relationships do not predict the correct over-reading. The recent experimental data enable a more accurate wet gas correlation to be developed. This is, however, beyond the scope of this paper.

Correction of the venturi meter readings using a wet gas correlation, requires the total liquid fraction of the gas stream to be measured. This measurement needs to be neither very accurate, $\pm 10\%$ will be sufficient, nor continuous as the wetness only gradually changes with time.

A technique has been developed to measure the liquid fraction of a wet gas stream, which is based on the tracer dilution technique. Fluorescent dyes have been identified as suitable tracers. The tracer dilution technique and the fluorescent tracer dyes have been successfully tested at both the laboratory and a NAM field location.

2 VENTURI METER PERFORMANCE IN WET GAS FLOW

Empirical correlations currently in use with venturi meters in wet gas are limited in their experimental range. The well-known relationships published by Murdock and by Chisholm for example have been established in steam/water flow at low to moderate pressures, and formally apply to orifice plates only. Previous experiments at Coevorden², a NAM location in the Netherlands, have shown that the over-reading of venturi and orifice meters measuring natural gas at pressures around 90 bar and with liquid fractions up to 4% by volume closely followed the coinciding predictions by Chisholm and Murdock.

However, extrapolation of the above correlations show that they only coincide for pressures around 90 bar. For all other pressures each correlation gives a different predicted over-reading. This can be explained by the fact that the correlations are based on different physical models. To examine the physics behind the behaviour of a venturi in wet gas flow, flow conditions have to be expressed by their gas and liquid Froude numbers instead of the corresponding gas and liquid velocities. The gas and liquid Froude numbers are given by:

$$Fr_g = \frac{v_{sg}}{\sqrt{gD}} \sqrt{\frac{\rho_g}{(\rho_l - \rho_g)}} \quad (1) \quad Fr_l = \frac{v_{sl}}{\sqrt{gD}} \sqrt{\frac{\rho_l}{(\rho_l - \rho_g)}} \quad (2)$$

According to theory, flow conditions which have identical Froude numbers are located in approximately the same position in the two-phase flow map. The liquid to gas ratio expressed in Froude numbers is the Lockhart-Martinelli parameter (X):

$$X = \frac{Q_l}{Q_g} \sqrt{\frac{\rho_l}{\rho_g}} \quad \left(= \frac{Fr_l}{Fr_g} \right) \quad (3)$$

With the equations of Murdock and Chisholm expressed in terms of the Lockhart-Martinelli parameter, it shows that the over-reading predicted by Murdock is independent of the line pressure and flow regime. The over-reading predicted by Chisholm is independent of flow regime, but dependent on the line pressure.

The experiments at Coevorden were conducted within a narrow range of pressure and flow regimes. The line pressure could only be varied slightly. The flow conditions were all located in only a small part of the flow map. Stratified wavy with almost no entrainment.

Therefore, it was recognised that additional experiments, covering different line pressures and flow regimes, were required to address the problem. Recently, such experiments were performed at the SINTEF multiphase flow laboratory, located near Trondheim, Norway. Tests were performed at line pressures of 90, 45, 30 and 15 bar, with liquid fractions up to respectively 10%, 8%, 6% and 4%. In total, about 100 different flow conditions were covered.

To indicate the difference between the experimental range at Trondheim for 90 bar and the experimental range at Coevorden, both ranges are indicated in a two-phase flow map, as shown in figure 1. As can be seen, the tests at Trondheim cover a much larger range than the previous experiments at Coevorden. Flow conditions at Trondheim were both in the stratified and annular dispersed flow regime.

The experimental ranges at Trondheim for the other three pressures (45, 30 and 15 bar) were selected by taking identical gas and liquid Froude numbers as for the 90 bar tests.

Some typical results from the venturi tests at Trondheim are shown in figure 2, in which the results of the Coevorden tests are also shown. The over-reading of the venturi meter is plotted against the Lockhart-Martinelli parameter. As can be seen from the data in figure 2, there is a clear line pressure dependency. From more Trondheim results, which are not presented, it can be seen that there is also a Froude number i.e. flow regime dependency.

It can be concluded from the Trondheim experiments that the correlations of Murdock and Chisholm do not predict the venturi meter over-reading correctly, and that their apparent similarity at approximately 90 bar stratified wavy flow is a coincidence. However, the extensive data set gathered at Trondheim will enable a more accurate correlation to be developed. Which is, however, beyond the scope of this paper.

3 PRINCIPLES OF THE TRACER METHOD

Measuring flow by means of the tracer dilution technique, which is a well-established method in single phase flow applications, is simple. A suitably chosen tracer is injected into a flowing stream at a precisely metered rate. Downstream of the injection point, where the tracer has mixed thoroughly with the fluid, a sample is taken. The sample is analysed to determine the concentration of the tracer, whereupon the flow rate (Q) can be calculated from the following relationship:

$$Q = \frac{(C_0 - C_s)}{(C_s - C_b)} \cdot q \quad (4)$$

in which C_0 is the concentration of tracer in the solution injected into stream Q , C_s the plateau of the concentration-time curve as measured in the downstream sample, C_b the background tracer concentration of the stream, and q the injection flow rate of the tracer solution.

The liquid flow rate to be measured is in practice much larger than the tracer injection flow rate. This means that the initial tracer concentration C_0 is much larger than the sample concentration C_s . If it is further assumed that the background concentration is zero, then the above formula can be reduced to:

$$Q = \frac{C_0}{C_s} \cdot q \quad (5)$$

From this equation it can be seen that no absolute concentration, but in fact a dilution measurement is required, which is much more precise and repeatable. The accuracy of the tracer dilution method is therefore only dependent on the following factors: (a) the accuracy of the injection flow rate; and (b) the accuracy of determining the dilution ratio of injection and sample concentration. With the tracer dilution method neither pressure, nor temperature, nor gas or liquid velocity has any influence on the results.

The tracer dilution technique as described above, has been used to measure the liquid flow rate in a wet gas stream. See the schematic overview in figure 3. As the liquid phase can contain water as well as condensate, two tracers are required. One selective for the water phase and one selective for the condensate phase. Note that the liquid samples taken from the flow line do not have to be representative as the tracers will distribute themselves selectively into the phase of interest. The only requirement is that the samples should contain enough water and condensate for analysis.

Tracer dilution measurements require that the flowing section, between the injection point and the sample point, should be of sufficient length for the tracer to mix fully with the phase of interest. There should not be any inflow or outflow of liquid within the section. The minimum measuring section for single phase flows is listed in ISO 2975/1⁵. To achieve an allowable variation in tracer concentration at the sample point of less than 1%, approximately 150 diameters of straight pipe are required. For multiphase flow, however, no data is available. For wet gas flow, where the liquid is only occupying a small portion of the pipe area, lateral mixing will obviously require less effort. Therefore, by specifying a measurement section that is at least as long as that for single phase flow and includes at least one component that introduces additional mixing like a bend or valve, one will probably be on the safe side.

The liquid samples taken from the flowing stream are flashed to atmospheric conditions before analysis. This means that the tracer method determines the liquid flow rate at ambient conditions. To determine the venturi meter correction factor, however, the liquid flow rate under actual conditions needs to be known. Therefore, the shrinkage factor of both the water and the condensate phase have to be taken into account.

4 FLUORESCENT TRACERS

4.1 Fluorescent dyes

The best tracers are those which mix well with the fluid and which are easily detected at the sample point. Tracer loss in the measurement section, for example due to absorption on the pipe wall or chemical degradation should be minimum. A tracer should preferably be readily available, cheap and safe to use. Due to the presence of two different liquid phases, i.e. water and condensate, suitable tracers should have a

good partitioning between those phases. They should also be non-volatile because of the presence of the gas phase.

Fluorescent dyes were identified as the most suitable tracers for our application. Particularly because of the following advantages:

- the detection limits for fluorescence are extremely low, allowing that only very small quantities of tracer need to be used. This is of particular importance with respect to tracer handling, cost and environmental considerations.
- suitable fluorescent tracers are available for the water and condensate phase. This makes it possible to use a single detection technique for both phases.
- portable fluorometers for field use are available. These instruments are simple to use, not too expensive, and combine the accuracy of a research instrument with rugged simplicity.

Initially, four fluorescent tracer dyes were selected. Two for the water phase and two for the condensate phase. Suitable water tracers were selected from a large set of fluorescent dyes commonly used in hydrology. The suitability of a large number of these dyes was investigated by Smart and Laidlaw⁶ (1977) and Viriot and André⁷ (1989). Suitable condensate tracers were selected from the dye product ranges of various chemical companies. These dyes are sold to colour fuels and greases.

In contrast to above mentioned applications, the amount of tracer that will be required for a flow measurement is very low: typically 0.1 gram of tracer per measurement. These relatively low quantities involved, in combination with their low environmental and health impact make the use of these tracers fully acceptable.

4.2 Concentration measurement

Fluorescence occurs when a dye absorbs light at a certain wavelength range and emits light at a longer range. Fluorescence is measured by means of a fluorometer. A laboratory spectrofluorometer has been used for all measurements up till now, but its cost, complexity and delicacy make it unsuitable for general application in the field. For field measurements a filter fluorometer should be used. This instrument combines the accuracy, sensitivity and stability of a research instrument with rugged simplicity.

The optimum dye concentration in the sample lies in the range of 50 to 500 ppb (parts per billion). The upper value originates from the fact that for larger concentrations the relationship between the measured fluorescence intensity and dye concentration becomes non-linear. Although a concentration of 1ppb can easily be measured, the lower value is arbitrarily set at 50 ppb as very dilute solutions (≤ 1 ppb) are relatively unstable. Also, a somewhat larger concentration makes additional dilution of the samples with a clear liquid possible in case of turbid or opaque solutions.

The reference dilutions, against which the samples are compared, should be prepared using actual produced water and condensate. This will eliminate systematic errors, made in both the sample and reference measurements, as the calculation of the liquid flow rate is essentially determined from a dilution ratio. For all four tracers, a plot of fluorescence intensity against reference dilution ratio is shown in figure 4.

5 TRACER EXPERIMENTS

The tracer dilution method and the selected dyes have been tested at the laboratory and at a NAM field location. Both experiments have shown that the tracer technique is capable of determining liquid flow rates in a wet gas stream. The results of the laboratory tests showed that an accuracy of about $\pm 2\%$ is achievable. The results of the field test showed an accuracy of $\pm 8\%$. The difference between these results is mainly due to the fact that the reference measurements in the field had larger uncertainties than those at the laboratory.

5.1 Laboratory experiments

5.1.1 Test set up

Laboratory tests in a 3" line were performed with water as the liquid phase. Experiments with condensate were not possible since recirculation of the condensate would lead to its gradual pollution with tracer.

Tracer solutions were injected by means of a calibrated metering pump. The injection rates were varied between 1 ml/min and 5 ml/min, with an uncertainty of approximately 0.3%. The initial concentrations were around 1500 ppm for tracer W1 and 1000 ppm for tracer W2.

The air flow rates ranged from 4800 m³/d to 17000 m³/d, equivalent to superficial gas velocities of respectively 9 m/s and 40 m/s in the 3" line. The water flow rates were in the range of 12 m³/d to 24 m³/d. The flow regimes were observed to be stratified wavy for all conditions tested. At the larger air flow rates some wall wetting was observed. The experiments were conducted at atmospheric pressure.

5.1.2 Discussion of the results

The results for tracer W1 are shown in figure 5. The error in the calculated water flow rate is plotted against the air flow rate. It can be seen that the errors are within $\pm 2\%$ for all conditions tested. The measuring section in this case consisted of 250 pipe diameters including three bends.

The results for tracer W2 are shown in figure 6. The mixing distance for these tests consisted of 150 pipe diameters including only a single bend. The errors in the calculated water flow rate are within $\pm 2\%$, which is comparable to the previous results.

It was concluded from the laboratory tests that the tracer method is capable of determining the water flow rate in an air/water stream far better than the required accuracy of $\pm 10\%$. A field test with both the water and condensate tracers was required to demonstrate the method also works under field conditions.

5.2 Field experiments

5.2.1 Test set up

Field tests were carried out in July 1993 at De Wijk 16, a NAM field location in the Netherlands (figure 7).

A movable well test unit was connected to the well to provide the means of setting the gas flow, measure the gas and liquid flow rates, and the flow line in which to install the tracer injection nozzle and the liquid sample nozzle. The distance between the two nozzles was 150 pipe diameters including four bends. This meant that the mixing was expected to be better than in the laboratory tests.

An additional liquid injection nozzle, installed upstream of the tracer injection nozzle, made it possible to adjust the water and condensate fraction of the well stream. Water and/or condensate was injected using two, high pressure, positive displacement pumps. The liquid reference flow rates were determined by measuring the amount of liquid pumped into the flow line. To determine the total flow of liquid in the flow line, the background water and condensate flow rates had to be taken into account. The background water flow was found to be negligible. The background condensate production was approximately 1.5 m³ of condensate per million normal m³ of gas. These background flow rates were determined by using the test separator.

No gas production was lost during the tests. The test facilities were set up in such a way that the gas from the separator was injected back into the regular production system.

The gas flow rate was varied between 120,000 normal m³/d to 240,000 normal m³/d, corresponding to superficial gas velocities in the 3" flow line of 5 m/s and 11 m/s respectively. The pressure at the test section was around 73 bar for all experiments.

The liquid flow rate ranged from approximately 2.4 m³/d to 90 m³/d, which corresponds to liquid to gas ratios between 20 and 420 m³ of liquid per million normal m³ of gas. The availability of two liquid injection pumps made it possible to vary the watercut of the liquid phase. The watercut was arbitrarily varied between 0%, 40% and approximately 99%. A watercut of 100% was not possible as the well was producing some background condensate.

The tracer solutions were injected by means of a high pressure metering pump, connected to the flow line by a high pressure flexible hose, as shown in figure 8. The injection rates lay between 10 ml/min and 12.5 ml/min. The concentration of the dye in the injection solution was around 100 ppm for all four tracers.

5.2.2 Discussion of the results

Samples at the sample point were taken every 5 minutes, after the start of the injection, for a period of 30 minutes. The results for a number of tests are shown in figure 9. It can be seen that a sufficiently stable tracer concentration at the sample point already exists after 5 minutes.

The overall test results are shown in figure 10, in which the deviation between the calculated and injected liquid flow rates is plotted against the liquid to gas ratio. Each

data point is the average of all samples taken at that particular flow condition. It can be seen from this figure that the results for tracer W1 and C1 are within the target accuracy of $\pm 10\%$. The other two tracers, W2 and C2, show disappointing results. The results for tracer C2 are not even on the graph as the deviations involved were too large. The explanation for the poor performance of these tracers has been found to lie in the fact that their fluorescent capability had been degraded by the influence of sun light. The capillary tubing at the suction side of the injection pump was made of transparent plastic, allowing sun light to pass and damage the tracer dyes. Therefore, it is expected that the tracers W2 and C2 can be used successfully as well, provided the injection solution and the samples are not exposed to sun light.

It can also be seen from figure 10 that the liquid flow rates as measured by the test separator are approximately 10% low. Apparently, 10% of the liquid injected disappeared with the gas stream. The separator measurements at the low liquid to gas ratios are considered unreliable as relatively low flow rates were involved.

6 CONCLUSIONS

Laboratory and field trials have demonstrated that the tracer dilution technique is capable of determining the water and condensate flow rates in a wet gas stream within a 10% accuracy. These flow rates are required to correct the venturi meter readings in order to determine the actual gas rate.

Suitable fluorescent tracer dyes for both the water and condensate phase are available, as well as portable fluorometers for field use.

Recent venturi meter experiments have shown that existing wet gas correlations, such as developed by Chisholm and Murdock, do not predict the correct over-reading. Further work is required to develop a more accurate relationship.

7 REFERENCES

- [1] A.W. Jamieson, P.F. Dickinson, High accuracy wet gas metering, North Sea Flow Metering Workshop, Peebles, Oct. 1993.
- [2] G.V. Washington, Measuring the flow of wet gas, North Sea Flow Metering Workshop, Haugesund, Norway, Oct. 1989.
- [3] D. Chisholm, Two phase flow through sharp-edged orifices, Research note, Journal mechanical engineering science, 1977.
- [4] J.W. Murdock, Two phase flow measurements with orifices, Journal of basic engineering, Dec. 1962.
- [5] ISO 2975 Measurement of water flow in closed conduits-Tracer methods.
- [6] P.L. Smart, I.M.S. Laidlaw, An evaluation of some fluorescent dyes for water tracing. Water Resources Research, v. 13, no. 1, Feb. 1977.
- [7] M.L. Viriot, J.C. André, Fluorescent dyes: a search for new tracers for hydrology. Analysis, v.17, no. 3, 1989.

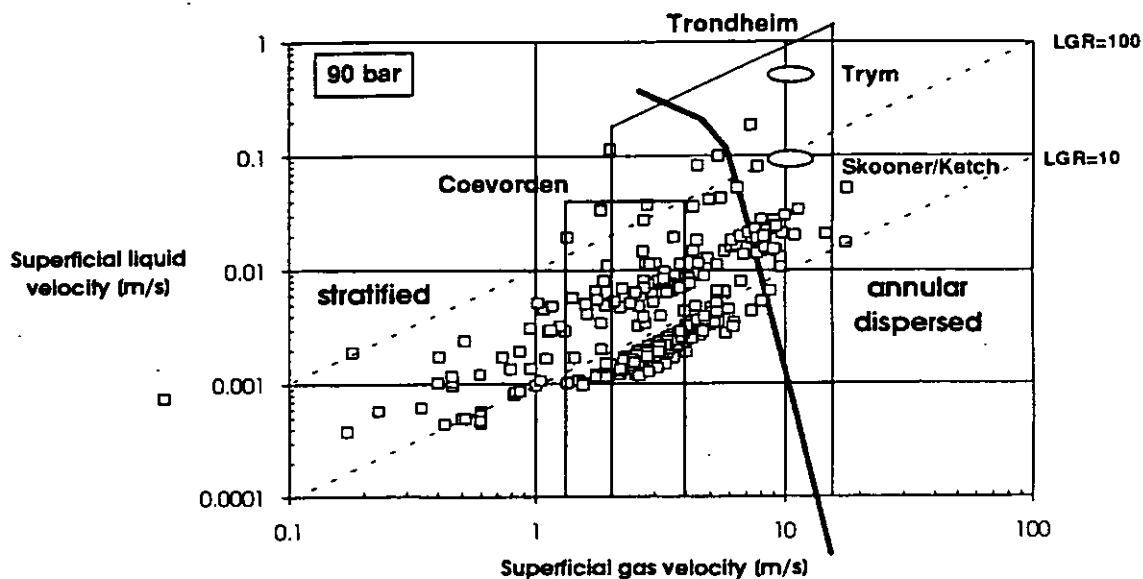


Figure 1. Experimental test range at Trondheim at 90 bar, compared to the Coevorden test range, a distribution of NAM wells and two recent developments of Shell Expro and Norske Shell.

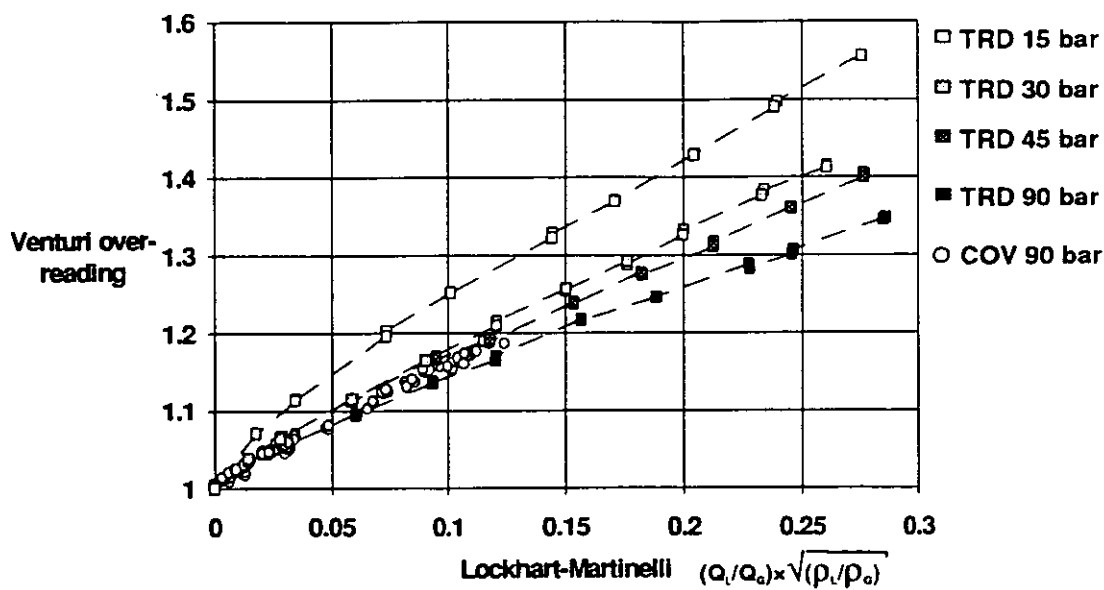


Figure 2. Typical test results from Trondheim and Coevorden indicating a line pressure dependency. The gas Froude number is the same for all data.

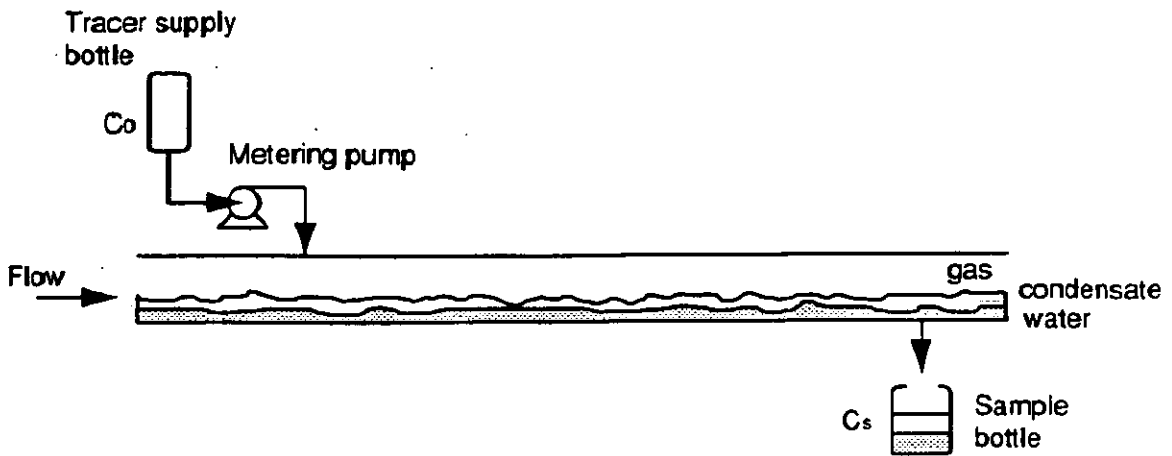


Figure 3. The tracer dilution technique for measuring the water and condensate flow rates in a wet gas stream.

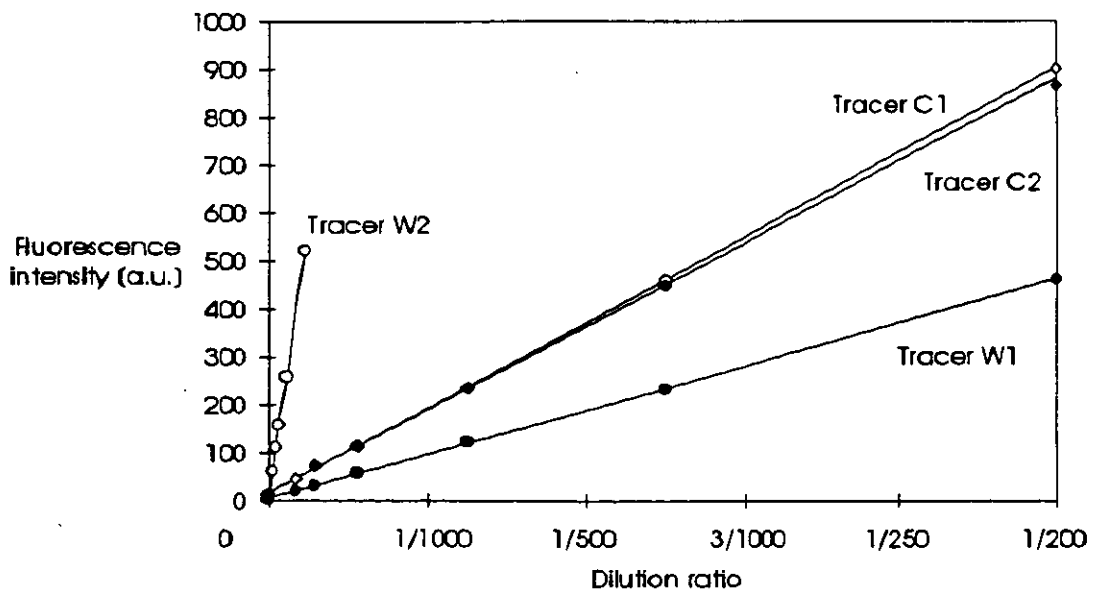


Figure 4. Plots of fluorescence intensity against tracer dilution ratio.

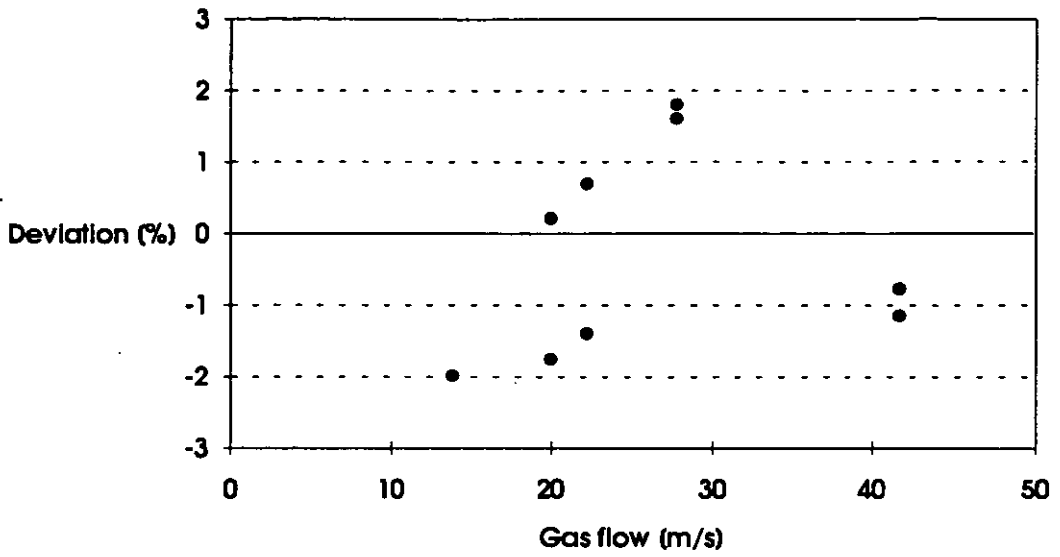


Figure 5. Laboratory test results for water tracer W1. The measuring section consisted of 250 diameters of pipe including three bends.

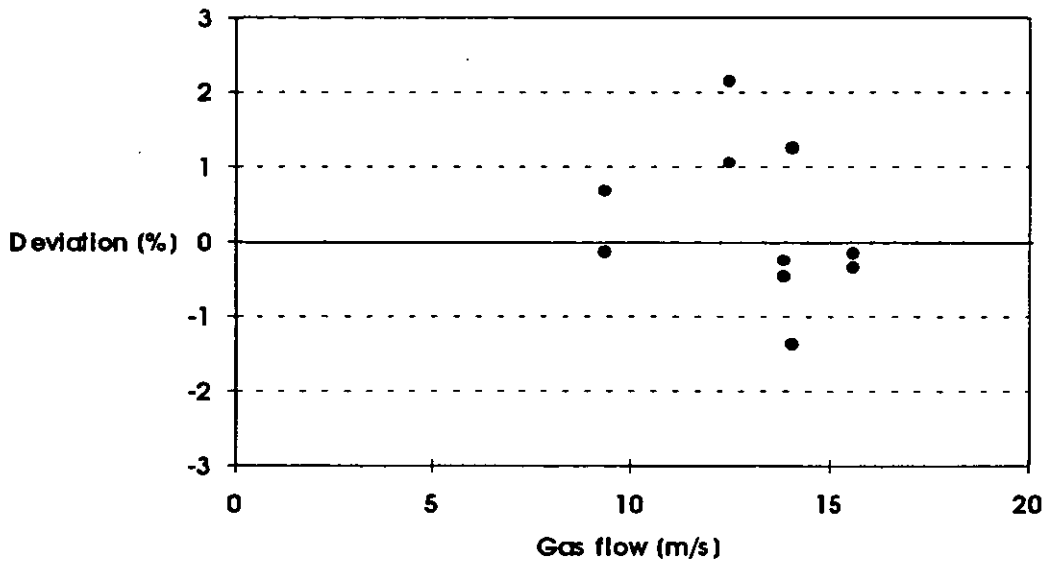


Figure 6. Laboratory test results for water tracer W2. The measuring section consisted of 150 diameters of pipe including a single bend.



Figure 7. Overview of the field test location De Wijk 16, NAM, the Netherlands.

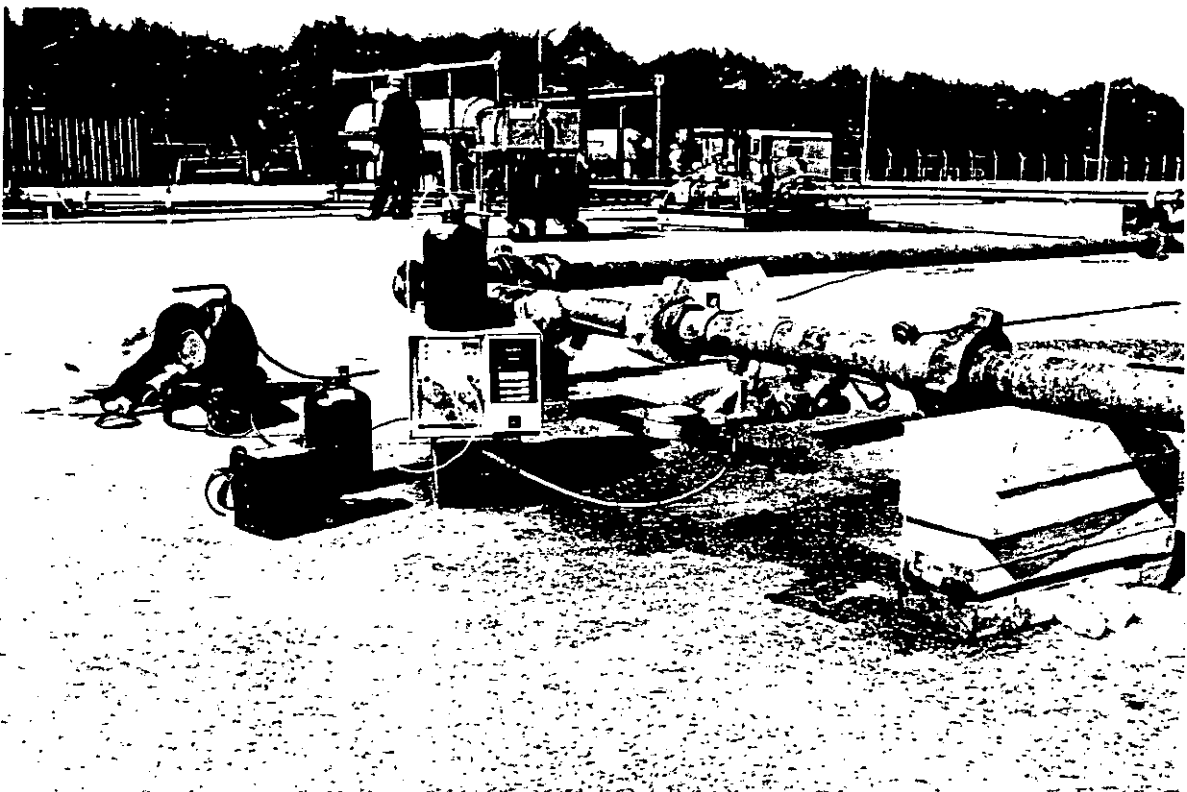


Figure 8. Tracer injection pump connected to the flow line by means of a high pressure flexible hose.

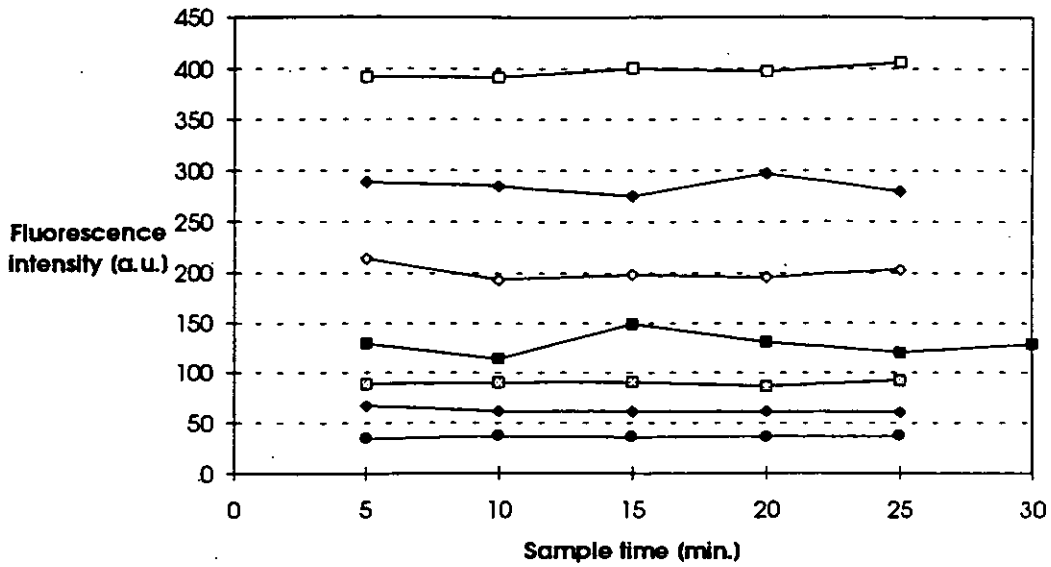


Figure 9. Variation of the tracer concentration at the sample point for a number of tests. Samples were taken at 5 minute intervals after the start of the injection.

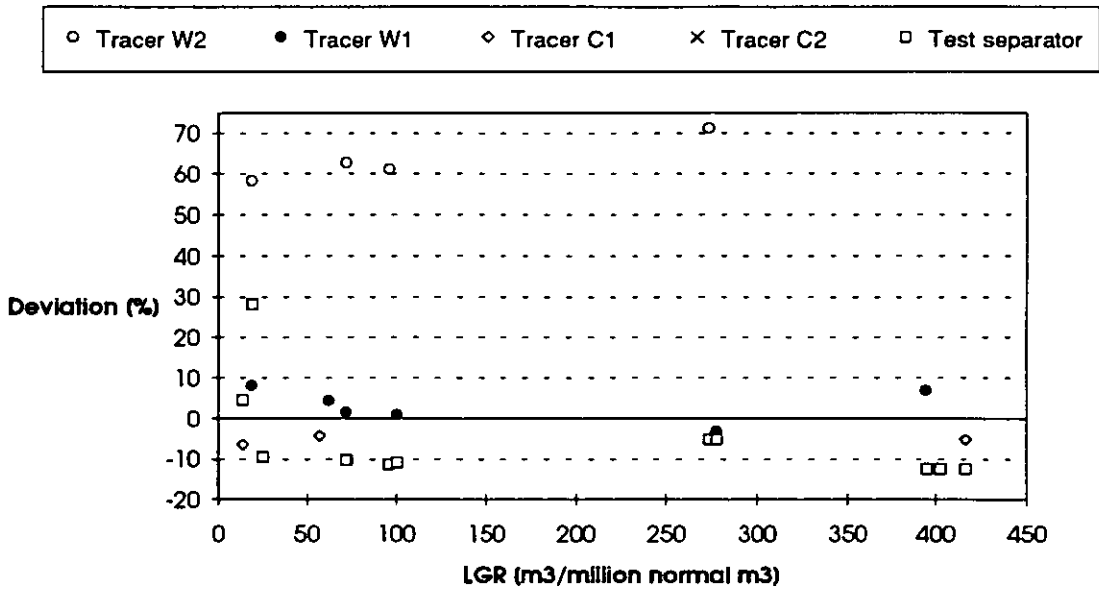


Figure 10. Overview of the field test results. The results for tracer W1 and C1 are within the target accuracy of 10%. Each data point represents the average result of all samples taken at that particular test condition.

DO WE NEED TO USE GAS DENSITY METERS IN NORTH SEA METERING STATIONS?

Dr. P. L. Wilcox - SGS Redwood Limited

SUMMARY

A review is made of the practical problems being experienced when trying to measure gas density accurately. The advantages and disadvantages of using calculated density based on the American Standard AGA 8 for computing compressibility are discussed. A comparison is also made of the reduction in the uncertainty of calculated density to be gained from using improvements in basic metering instrumentation. The conclusion of the paper is that measuring density is probably no longer necessary.

NOTATION

| | | |
|---------------|---|---|
| A | - | Location of inlet of gas sampling system |
| B | - | Location of outlet of gas sampling system |
| p | - | Upstream pressure |
| Δp | - | Differential pressure across the orifice plate |
| ρ | - | Density |
| ρ_{corr} | - | Density at the plane of the upstream pressure tapping on the orifice carrier. |
| ρ_{meas} | - | Density measured by the transducer |
| ρ_{calc} | - | Calculated density using AGA 8 |
| K | - | A contractual number (could be the isentropic exponent) |
| MW | - | Molecular weight of gas |
| Z | - | Compressibility factor |
| T | - | Temperature |
| R | - | Universal gas component |

1 INTRODUCTION

This short paper has been written to promote discussion on the topic of the necessity for gas density measurement. As part of the author's working brief over the past 10 years, numerous audits have been made on orifice plate gas metering systems in the North Sea, and world-wide. A recurring common problem that has been seen on these audits is the problem of obtaining a representative density measurement. Over almost the same 10 year time span the possibility to accurately calculate gas density has arrived with the publication of the American Standard AGA 8 for calculating natural gas compressibility factors. This standard has brought the uncertainty in calculating density to the same order of magnitude as the uncertainty on measuring density over a wide range of operating conditions.

The typical problems at present being experienced when measuring density are reviewed, and then the advantages and disadvantages of calculating density rather than measuring density are discussed. A comparison is also made of the reduction in the uncertainty of calculated density to be gained when better instrumentation is used in place of the normally accepted standard of instrumentation used in the North Sea.

2 DENSITY MEASUREMENT

Figure 1 shows a sketch of a typical layout for performing density measurement in a metering station. The method shown is the downstream recovery method which is used to overcome the upstream straight lengths restriction of the gas metering standard ISO 5167 (reference 3). The measured density from the density transducer is corrected to conditions at the plane of the upstream orifice plate tapping by the equation :-

$$\rho_{corr} = \rho_{meas} * \left(\frac{p}{p - \Delta p} \right)^{1/K} \quad (1)$$

where:-

| | | |
|---------------|---|---|
| ρ_{corr} | = | density at the plane of the upstream orifice plate pressure tapping |
| ρ_{meas} | = | density measured by the transducer |
| p | = | upstream pressure |
| Δp | = | differential pressure measured across the orifice plate |
| K | = | a contractual number (could be the isentropic exponent) |

Referring to the sketch, the obvious possible sources of errors in the measurement of density are :-

1. Temperature difference between the gas sample in the density transducer and stream conditions.
2. Pressure difference between the gas sample in the density transducer and the pressure at location B, the return point for the gas sample in the plane of the downstream orifice plate pressure tapping.
3. The flow rate of the gas sample through the density transducer.
4. The gas sample taken is not a representative sample.
5. Filtration in the gas sample line to keep the density transducer clean.
6. Effects of velocity of sound, ie. calibration.
7. Gas condensation effects.

Each of these problems will now be discussed.

2.1 Temperature Difference

Let us consider a typical offshore gas metering system operating under the following conditions :-

| | |
|---------------------|---------------|
| Stream temperature | 50°C to 60°C |
| Ambient temperature | 10°C (Summer) |
| Stream pressure | 100 bara |

What is found by experience, even with substantial lagging around the pipework, is that, unless steps are taken to remedy the situation, the gas sample in the density transducer is only at a temperature of approximately 20°C due to the combined effects of :

- * the heat sink effect of the density transducer, the pocket, and surrounding pipework.
- * the heat sink effect of the isolation valves.
- * the wind chill factor.

The accepted method of overcoming this temperature difference between the gas sample in the density transducer and the stream condition is to enclose the density transducer in a box and heat the air inside the box to line conditions, with a thermostat set within the box to stream temperature.

An alternative method used to overcome the problem is to measure the temperature of the gas leaving the density transducer, and to heat up the incoming gas sample to the density transducer until the exit gas temperature corresponds to the stream temperature.

However, if the stream temperature is constantly fluctuating, it requires a very sophisticated temperature compensation system to keep up with changes. So sophisticated, I believe no system exists today!

2.2 Pressure Difference

For the system of density measurement to operate correctly, there must be a flow through the transducer from the pipeline offtake at location A in the sketch, to the pipeline return at location B. This changing flow brings to the density transducer information on changes in stream gas composition and stream gas temperature, but it must be recognised that these changes will not be instantaneous. To have a flow through the gas sample line it is obvious that the pressure at location A must be higher than the pressure at location B. In addition, because the density transducer lies in between locations A and B, we must have :-

$$P_A > P_{\text{transducer location}} > P_B \quad (2)$$

What is normally assumed is that the pressure at the transducer location is the same as that at location B, which is at the downstream pressure tapping location of the orifice plate. This of course is not true, and few studies have been made to determine the actual pressure at the density meter location. A quick test is to close off the inlet sample valve whilst leaving the outlet valves open. This will provide information on the effect of the magnitude of the pressure difference between gas transducer and sample outlet on the measured density.

As with the temperature difference effect, the pressure difference effect will tend to give higher density values, and hence over-metering of the flow will occur through the metering station.

2.3 Gas Sample Flow Rate

As stated previously, a flow of sample gas is required through the density transducer to bring information on changes in gas composition and stream temperature to the transducer. If the flow rate is too low, in the absence of any additional external temperature correction, there can be a considerable heat loss from the sample gas. On the other hand, if the flow rate is too high, there can be a considerable pressure loss through the sample line. Again, there appears to be few studies made on what the optimum sample flow rate should be.

2.4 Taking A Relevant Gas Sample

The most commonly used gas sample take off method is simply a wall tapping, unlike the sample probes commonly used in conjunction with liquid density meters which take samples from the middle portion of the main stream flow.

It is debatable whether a wall tapping does take a representative sample of the main stream flow.

2.5 Filtration

Filters in the sample line are necessary to keep dirt or condensate off the sensitive innards of the density transducer. However, filters will cause a pressure drop through the sample line - particularly when they become clogged with debris. This will cause a change in density measurement.

2.6 Velocity of Sound Effects

This is one area in gas density measurement where there has been considerable progress. The problem was originally caused by calibrating transducers on a different gas (Argon or Nitrogen) to that in which it was be going to be used (Natural gas). With calibration services now being able to calibrate at high pressure using Nitrogen and able to provide User Gas Certificates at temperatures close to that at which a density transducer will operate in the field, it is felt that velocity of sound effects are no longer a problem.

2.7 Gas Condensation Effects

Operating conditions sometimes occur where the gas is completely gaseous at the metering system operating conditions, (say at 100 barg and 50°C), but undergoes partial condensation at atmospheric pressure and ambient temperature. Thus it has been known to occur on some metering systems that condensates are deposited within the density transducer every time the metering tube is depressurised, or the density transducer is depressurised, to enable the regular monthly calibration to be performed.

In some instances, the condensates will evaporate when a vacuum is pulled on the transducer. On other metering stations, the vibrating tube within the density transducer has been affected and must be cleaned before again re-calibrating.

3 CALCULATING GAS DENSITY

The upsurge in calculating density occurred with the arrival of the American Standard AGA 8 for calculating compressibility factors of natural gas and other hydrocarbon gas mixtures, reference (1). Prior to the arrival of this standard, gas calculation routines were only used as back-up routines to give a comparison with the measured density.

The second edition of AGA 8 produced in 1992, reference (2), extended the data bank used to compile the first edition of AGA 8. This together with additional velocity of sound data and more GRI and GERG compressibility factor data resulted in two new equations of state. However, it has modified inwards the boundaries for which an uncertainty in calculated compressibility can be expected to be 0.1%.

The required starting point for the AGA 8 calculations is a gas composition, which would normally be obtained from a periodic flow proportioned gas sample analysis if the gas constant is fairly constant with time. Alternatively, the gas composition can

be obtained from an on-line chromatograph analysis. The gas composition, together with AGA 8 and measured values of stream pressure and stream temperature, enables the gas density to be calculated.

4 COMPARING MEASURED AND CALCULATED DENSITY

Figure 2 gives a comparison table of the advantages and disadvantages between measured and calculated density. Although it should be clear from the comparison that calculating density has more advantages than disadvantages compared with measuring density, what the table does not bring out is the simplicity and time and cost saving in calculating density.

5 COMPARISON OF PREDICTED UNCERTAINTIES FOR MEASURED AND CALCULATED DENSITY

5.1 Measured Density

The uncertainty value associated with measuring density of natural gases using vibrating tube transducers is accepted to be : 0.2% of reading.

Many laboratory tests performed in Denmark in the '90's, at the Institute formerly named DANTEST, have confirmed this value of uncertainty. However, it is debatable whether such an uncertainty can be directly attributed to density measured on a metering system in the field.

More realistically, in a gas metering station the uncertainty on the measured density would additionally be affected by temperature and pressure differences between the transducer and the stream as previously discussed. If we assume that the temperature difference and pressure difference is, say, 1°C and 0.1 bar respectively, then the uncertainty on measured density becomes :-

$$\begin{aligned} \text{Unc. } \rho_{\text{meas}} &= \sqrt{(0.2)^2 + \left(\frac{1}{323.15} \times 100\right)^2 + \left(\frac{0.1}{100} \times 100\right)^2} \\ &= \underline{\underline{0.38\%}} \end{aligned} \quad (3)$$

5.2 Calculated Density

In this section, the uncertainty predicted for calculating density will be obtained using two sets of measuring instruments. "Standard" instruments consist of the normally accepted type of instruments used for measuring pressure and temperature, whereas the "upgraded" instruments are slightly more expensive instruments, still off-the-shelf, but which Operators do not usually purchase. The corresponding uncertainties for each package are as follows :-

| PARAMETER | UNCERTAINTY | |
|------------------------|------------------|------------------|
| | NORMAL | UP-GRADED |
| Static Pressure | 0.25% of span | 0.1% of span |
| Temperature | 0.5°C of reading | 0.2°C of reading |
| Molecular Weight | 0.1% of value | 0.1% of value |
| Compressibility Factor | 0.1%* | 0.1%* |

* What is at present unclear to the author and many of his colleagues is : How does the uncertainty associated with the analysis of each gas component using a gas chromatograph relate to the uncertainty of calculating z from AGA 8?

Let us assume the operating conditions are 50°C and 100 bara, with the span for the pressure instruments as 200 bara.

Ignoring the uncertainty involved in computing the formula :

$$\rho = \frac{p}{ZT} \cdot \frac{MW}{R}, \quad (4)$$

where :-

| | | |
|--------|---|------------------------|
| ρ | = | density |
| p | = | pressure |
| MW | = | molecular weight |
| Z | = | compressibility factor |
| T | = | temperature |
| R | = | universal gas constant |

and also the uncertainty involved in the value of the universal gas constant, it is found that the predicted uncertainty for calculated density when using "normal" and when using "up-graded instruments" is :

"Normal Instruments"

$$\begin{aligned} \text{Uncertainty for } \rho_{calc} &= \sqrt{(0.5)^2 + \left(\frac{0.5}{323.15} \times 100\right)^2 + (0.1)^2 + (0.1)^2} \quad (5) \\ &= \underline{0.54\%} \end{aligned}$$

"Up-graded Instruments"

$$\begin{aligned} \text{Uncertainty for } \rho_{calc} &= \sqrt{(0.2)^2 + \left(\frac{0.2 \times 100}{323.15}\right)^2 + (0.1)^2 + (0.1)^2} \quad (6) \\ &= \underline{0.25\%} \end{aligned}$$

Comparing these calculated uncertainty values against the measured density uncertainty values of 0.2% and 0.38% obtained under laboratory conditions and typical metering conditions, it is felt that the calculated values are very close to the measured values of uncertainty. In particular, a metering system using "up-graded" instruments would have an extremely low value of uncertainty for calculated density which approaches that obtained under laboratory conditions for measured density.

6 CONCLUSION

The practical problems arising when attempting to measure gas density accurately in metering systems are significant. The standard AGA 8 enables density to be calculated with a comparable value of uncertainty to that obtained using density transducers, particularly if the more accurate readily available instruments for measuring pressure and temperature are used.

It is concluded that gas density measurement is probably no longer necessary.

REFERENCES

- 1 "Compressibility and super-compressibility for natural gas and other hydrocarbon gases", AGA Transmission Measurement Committee Report No. 8, 1985.
- 2 "Compressibility factors of natural gas and other related hydrocarbon gases", AGA Transmission Measurement Committee Report No. 8, Second Edition, November 1992.
- 3 "Measurement of fluid flow by means of pressure differential devices - Part 1: Orifice plates, nozzles and venturi tubes inserted in circular cross-section conduits running full", ISO 5167-1, First Edition, 15 Dec. 1991.

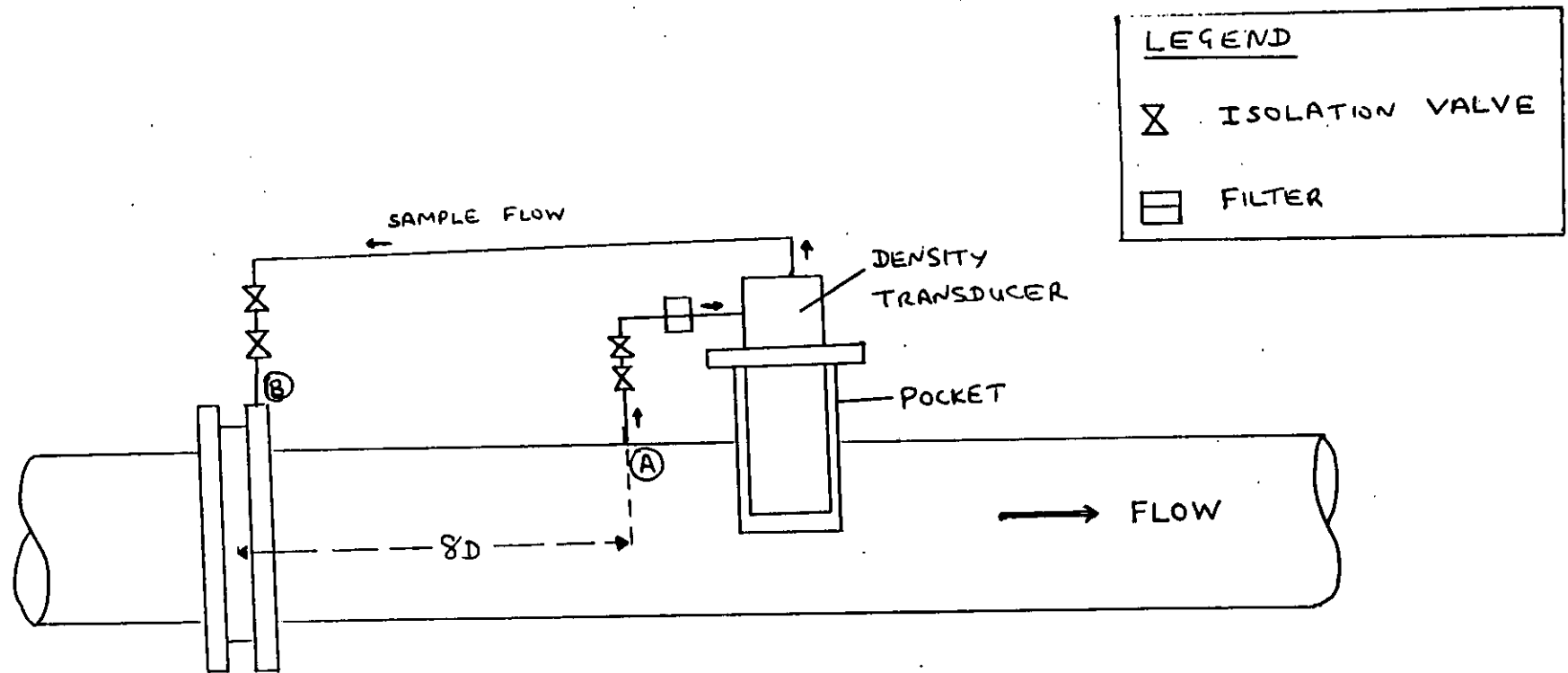


FIGURE 1 - DENSITY MEASUREMENT USING THE DOWNSTREAM RECOVERY METHOD

FIGURE 2 - COMPARISON BETWEEN MEASURED AND CALCULATED DENSITY

| MEASURED DENSITY | |
|--|---|
| ADVANTAGE | DISADVANTAGE |
| On-line Measurement | Prone to temperature, pressure, installation, ambient surroundings effects. |
| Knowledge of gas composition not required. | Density transducer needs periodic re-calibration off-site. |
| | High maintenance and re-calibration costs. |

| CALCULATED DENSITY | |
|--|---|
| ADVANTAGE | DISADVANTAGE |
| Not prone to temperature, pressure, installation, ambient surroundings effects | Need to know gas composition. |
| Minimal maintenance and re-calibration costs. | (However, if using an on-line chromatograph to obtain gas composition, regular in-situ re-calibration is possible). |

AGIP-TRECCATE MULTIPHASE TEST LOOP TEST FACILITY DESCRIPTION AND SPECIFICATION

A Mazzoni, M Villa
AGIP S.p.A. , Milan, Italy

M Bonuccelli
C.P.R.-TEA, Pisa, Italy

SUMMARY

The test loop is located in the Treccate-Villafortuna on shore oil field that is at about 60 Km from Milan and is fed with crud oil coming directly from the wells. This is obtained through two test separators connected respectively to two interface skids, which allow to change and to meter the flow rates of each phase (oil, water, gas), feeding the loop, in the full range (0-100 % of the test separators flows). Two test sections, interconnected mainly by three flow lines ($\Phi=4",6",6"$; $L\cong 450$ m), are available for the tests. These flow lines can be used as single lines, or in parallel and series; in this last case the total length of the flow lines , before the test section, becomes of about 1 Km. This allows to obtain developed flow and all the main flow regimes at the test sections. The loop is working normally at the local pressure of the main transportation line ($\cong 55$ bar) but is possible also to perform tests at different pressures, directly in line or in close loop, using a multiphase pump.

1 INTRODUCTION

The Treccate Multiphase Test Loop (TMTL) has been built by AGIP with the EEC support in order to test in real conditions a multiphase metering developed by ENEA and CPR, which are two Italian Research Institutes involved in the multiphase technology development.

The loop being an upgrading of an existing test facility, built in order to test multiphase pumps, has the capacity to test not only multiphase flow metering but also other multiphase components as pumps, ejectors, valves and separators. Being the loop full integrated with the field flow lines, it also allows to perform specific fluid dynamic tests to qualify the multiphase computer codes. Since the main objective of the loop was to qualify multiphase metering, considerable effort has been put in the selection of the reference single phase flow meters and in the selection of the control and data acquisition system. Two consoles to control independently the overall test loop (only the ON/OFF valves are operated manually) are used. The two consoles also allow the generation on the screenings of the tests configurations and their memorisation. These configurations are then printed and given to the operators to set up the tests. For the long time period a PC-486 to store (for several weeks) the data is used. The control room of the loop is located in a cabin where other two rooms are available to install the computers of the systems to be tested. Instead 4 junction boxes (2 for each test sections), are already installed close to the two test sections, to connect the systems to be tested. Because the complexity of the loop and the strong interface with the production plant a crew of at least four people is need to run the tests. Fig. 12 shows same main components of the test loop.

2 TEST LOOP DESCRIPTION

The test loop (see fig. 5) is located in the TR2, satellite area of the Trecate-Villafortuna field. Fig 1 shows schematically the configuration of the transportation lines and the location of the loop. In fig. 2, 3 and 4 are shown respectively the typical configurations of the well and satellite areas and of the slugcatchers in the oil centre. The field, till under development, is presently producing by 19 wells. At the cluster in the TR2 satellite area, where the loop is connected, there are 9 producing wells. The field is producing from two reservoirs but the characteristics of the oils are very similar. The oil is light with a density of 700-750 Kg/cm and a viscosity ranging between 1 and 3 cp. The GOR is about 70 and the gas oil ratio at the actual conditions (55 bar, 60 °C) is about 0.6. The water cut of the producing wells is normally lower than 3%. The loop is connected through a manifold (SBS) to 4 wells upstream the production manifold (see fig. 5). In order to perform the tests a selected number of these 4 wells are bypassed from the production manifold to the SBS manifold. The flow then is delivered to the test sections(2) through the field test separator or the test loop separator or through both the test separators and the respective interface skids at which the test separators are connected. The maximum measured hydrocarbon flow (about 100 cm/hr of oil; 60 cm/hr of gas) is obtained using both the test separators. The flow limits are connected to the maximum separation capacity of the two equal test separators. If is not required to measure all the test flow in real time, but the well testing data are enough, two additional wells can be deliver to the test loop, bypassing the test separators. In this case it is possible to reach about 150 cm/hr of oil and 90 cm/hr of gas. In the interface skids (MULTIPHASE METERING UNIT; SBS INTERFACE SKID) three control valves are installed (one for each line) to control the single phase flows and single phase flow meters to measure the flow rates. The test flow conditions are obtained fixing the flow rates set points of each phase (oil, gas, water) at the required test values, then the flow controllers act on the control valves in order to meet, with the actual flow rates, the set points values. Since the water flow coming directly from the wells is presently to low for the tests, an outside system is used to inject additional water into the loop. This is obtained by using the reinjection system of the oil centre (see fig. 6). The maximum water flow rate that is possible to obtain with this system is about 50 cm/hr. This limit is connected to the maximum capacity of the reinjection pumps(2) used to boost the water from the storage tank into the reservoir. The well flow ,before to be delivered into the loop and at the oil centre, must be cooled through air coolers. For this, dedicated air coolers which can be used independently by the production are installed in the loop. In addition, the loop is connected to an air cooler bank of the production plant (one air cooler for the test , two for the production). The temperature of the crud at the manifolds is normally about 120 °C and the delivery temperature must be bellow 80 °C. The flow from the SBS manifold is delivered first to the air coolers and then to the test separator(s). If all the flow delivered to the test separator(s) is used for the tests, the single phase flow rates are measured in the test separators and also in the interface skid, otherwise (test flow lower than the test separator flow) the single phase flow rates (oil, water, gas) are measured only in the interface skids. The SBS interface skid was built in the 1987 in order to test only multiphase pumps, instead the new interface skid (MULTIPHASE METERING UNIT), just completed, has been built in order to test mainly multiphase metering. For this reason particular effort has been put to design this last skid, in order to have a stable flow at the test sections and to measure the single flow rates with the best accuracy. In the loop there are two test sections, (shown in fig. 5 with the connections of the METERING UNIT 1 and 2), which allow to test more than one multiphase flow meter in the same time. Having two test sections, interconnected by sufficient long flow lines, is possible to use one of them to meet the test conditions and the second one to test the components. This allows the generation of several flow regimes at the second test section, including the slug flow. The INTERCONNECTING SKID also allows to test multiphase pumps. The connections of the SCREW PUMP UNIT (not in field actually) and of the MEMBRANE PUMP UNIT (see fig. 5)

show the two positions where the pumps can be tested. The two positions are interconnected allowing also to test systems of pumps in series or in parallel. The tests in the loop may be performed mainly with three test loop configurations:

- in line
- in line with multiphase pump
- in close loop with multiphase pump

2.1 Tests in line

These tests are performed at the local main flow lines pressure, which is defined by the pressure set point of the slugcatcher (see fig. 4) and by the pressure drop through the flow line used to perform the tests. The flow at the outlet of the loop may be delivered to the slugcatcher through a 10" or 12" line (see fig 5). The actual set point of the slugcatcher at the oil centre is set at 50 bar and the pressure drop through the 12" flow line is about 5 bar. This brings to have in the loop a pressure of about 55 bar. This pressure may be increased up to about 70 bar increasing the pressure drop through the control valves at the outlet of the loop. This upper limit is due to the blocks, for high pressure, of the wells feeding the test loop. The pressure in the loop may be also decreased down to about 45 bar decreasing the set point pressure of the slugcatcher at 40 bar. This operation can be done only for short time and in agreement with the exercise requirements. A typical configuration of the loop for these tests is shown in fig. 7. Collecting field data through the lines upstream the loop (well heads, manifolds) and downstream (slugcatcher), it is possible also to perform fluid dynamic tests for the multiphase computer codes qualification. In this case all the test loop becomes a test section where it is possible to measure the pressures and temperatures in several points of the loop and to verify, using multiphase metering, the flow regimes in two points (test sections) of the line. Figure 8 shows a very schematic configuration of the transportation system involved in these tests.

2.2 Test in line with multiphase pump

These tests are performed using the diaphragm pump (MEMBRANE PUMP UNIT) that has been already tested and is still installed in the field. A typical configuration for these tests is shown in fig. 9. The pump allows to decrease the loop pressure down to 20 bar, that is the minimum inlet pressure accepted by the pump. The pump then increases again the fluid pressure up to the flow line pressure (55 bar) required to deliver the flow to the oil centre. With this loop configuration it is possible to perform tests in a wide range of pressure (20-70 bar), allowing also to test choke and control valves in critical and sub critical conditions. In this case the maximum test flow rate is about 120 cm³/hr correspondent to the maximum capacity of the pump.

2.3 Tests in close loop with the multiphase pump

These tests are performed in close loop using the test loop separator (see fig. 10) or using the field test separator (see fig. 11). In this case the multiphase pump must supply the differential pressure required for the flow recirculation. The tests can be done in the pressure range of operability of the pump (20-65 bar), with a temperature variable in the range (20-80 °C). With these configurations it is possible also to replace the oil in the separator(s) with more heavy oil and to verify the fluid effects (specially the viscosity) on the multiphase components and on the fluid dynamic of the transport. This can be done replacing, at low pressure, the Trecate oil with stabilised oil and adding then field gas in order to obtain a live oil.

3 TEST LOOP SINGLE PHASE FLOW METERING STATIONS

In the loop there are mainly four single phase flow metering stations:

- test field separator
- test loop separator
- SBS interface skid
- multiphase metering unit

The two test separators have the same capacity and are used as reference stations for the flow measurement when all the test separator flow is delivered to the test section(s). In these conditions they are also used to verify the accuracy of the flow meters in the interface skids, since the test separators flow meters are in series with those in the skids and the same flows are passing through them. The reference flow meters in the test separators are:

- oil flow rate: positive displacement
- gas flow rate: orifices
- water flow rate: positive displacement

The single phase flow meters in the SBS interface skid (orifices) are not used as reference, since their accuracy is presently considered not acceptable to test multiphase flow metering. For this scope, at partial flow (not all the separator flow), only the multiphase metering unit is used as single phase metering station. In order to verify the PVT package (used normally in the multiphase metering to calculate the oil and gas densities versus the measured pressures and temperatures), in this skid the oil and gas densities also are measured. The reference meters are:

- oil flow rate: positive displacements
- gas flow rate: turbines
- water flow rate: magnetic meters
- oil density: resonance densitometer
- gas density: resonance densitometer

The overall accuracy on the single phase flow rates (oil, water and gas) and on the densities is:

- flow rates: $\geq 1\%$
- densities: ± 0.5 kg/cm for oil
 ± 0.04 kg/cm for gas

4 CONCLUSIONS

The Trecate multiphase test loop is now available to test the following multiphase components or multiphase systems:

- flow metering,
- pumps and systems of pumps,
- ejectors,
- choke and control valves,
- novel separators and

-to perform fluid dynamic tests for the multiphase computer codes qualification.

The operating conditions of the loop are:

- pressure: 20-70 bar
- temperature: 40-70 °C
- oil flow rate: 0-150 cm/hr
- gas flow rate: 0-90 cm/hr
- water flow rate: 0-50 cm/hr
- oil viscosity: 1-3 cp (1)
- all flow regimes

Given the wide range of variation of the operative parameters the loop is particularly indicated for the characterisation of the multiphase components especially for the multiphase flow metering.

(1) replacing the Trecate oil is possible to perform tests also at higher viscosity

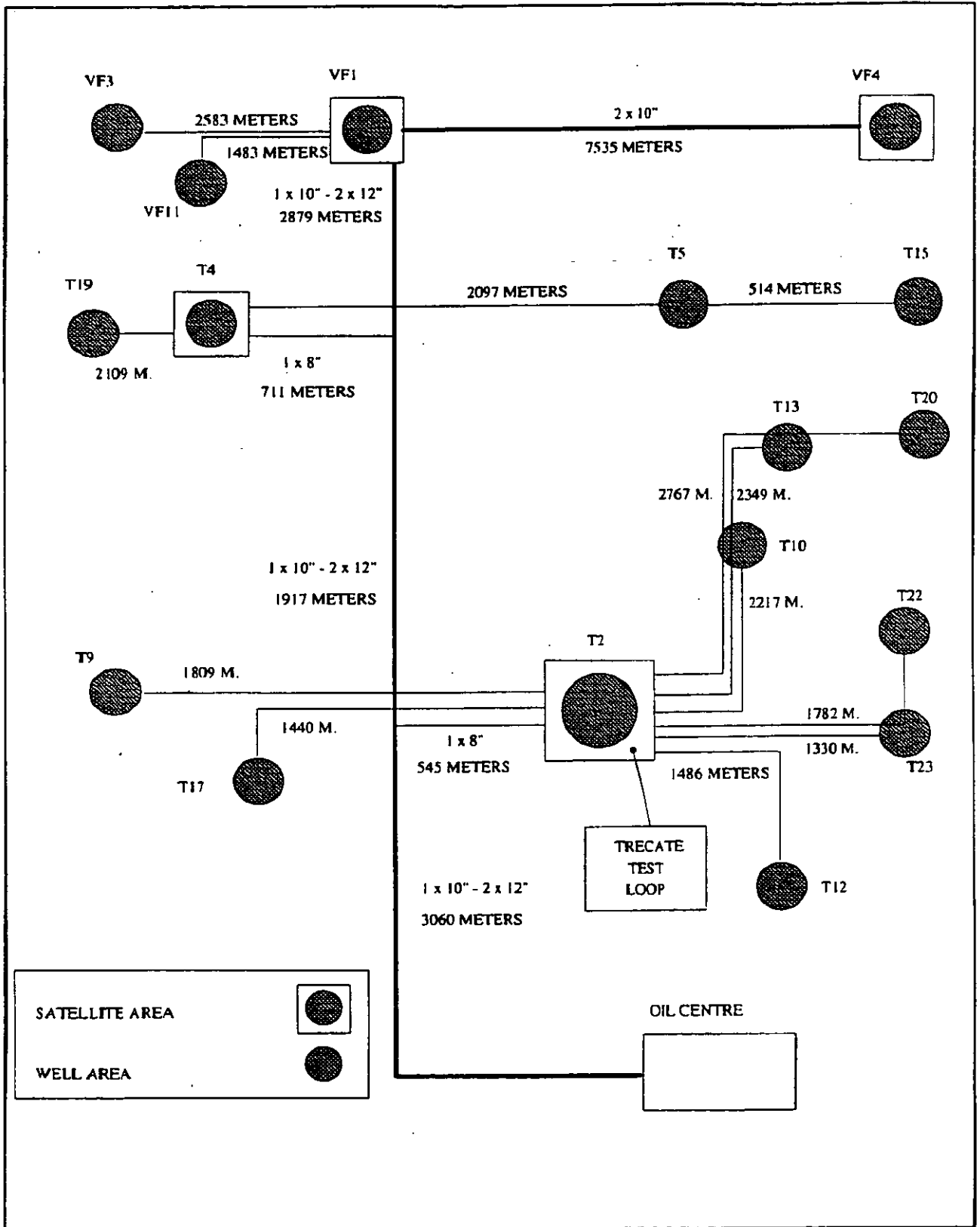


Fig. 1 - Trecate-Villafortuna overall field configuration

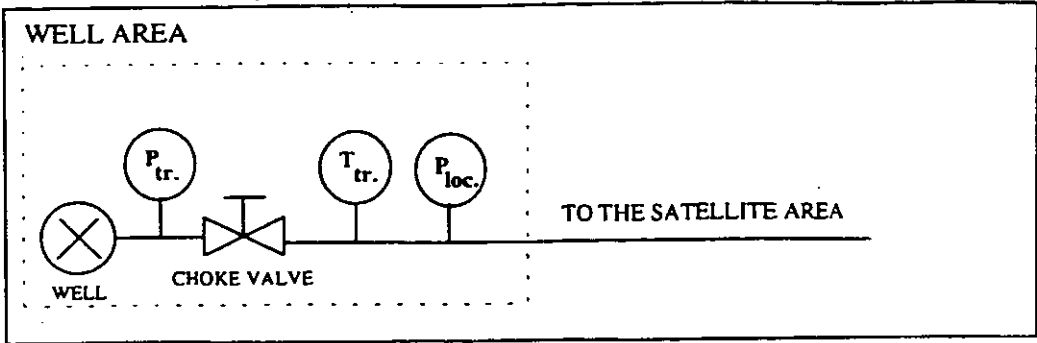


Fig. 2 - Typical configuration of a well area

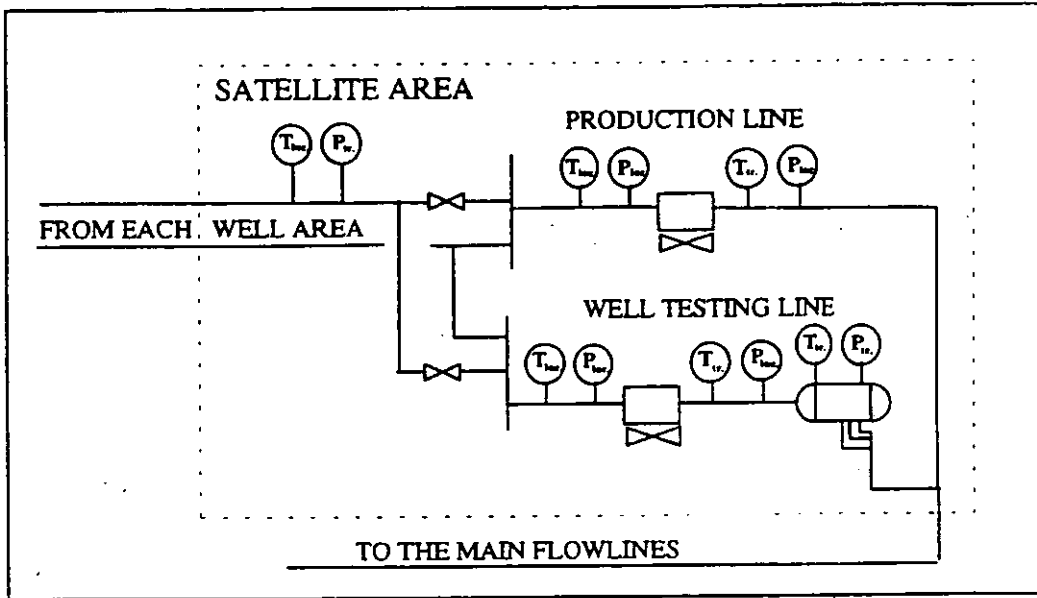


Fig. 3 - Typical configuration of a satellite area

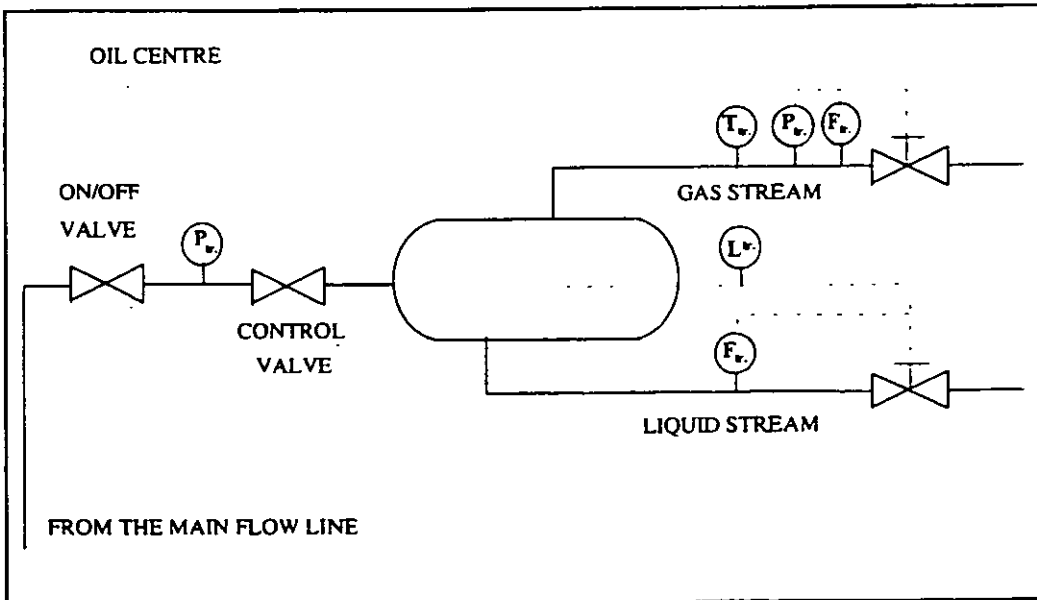


Fig. 4 - Slug catcher configuration

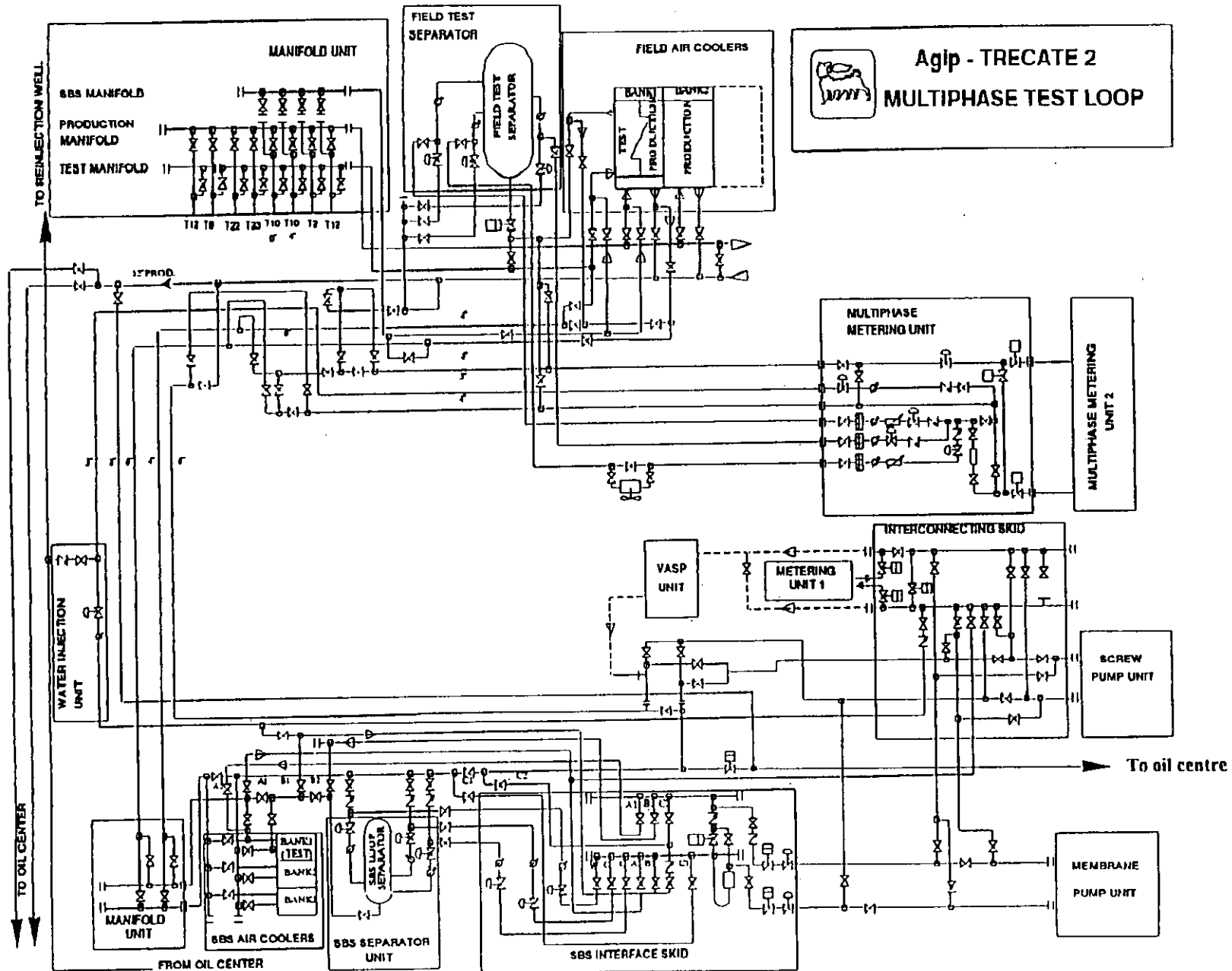


Fig. 5-Trecate multiphase test loop

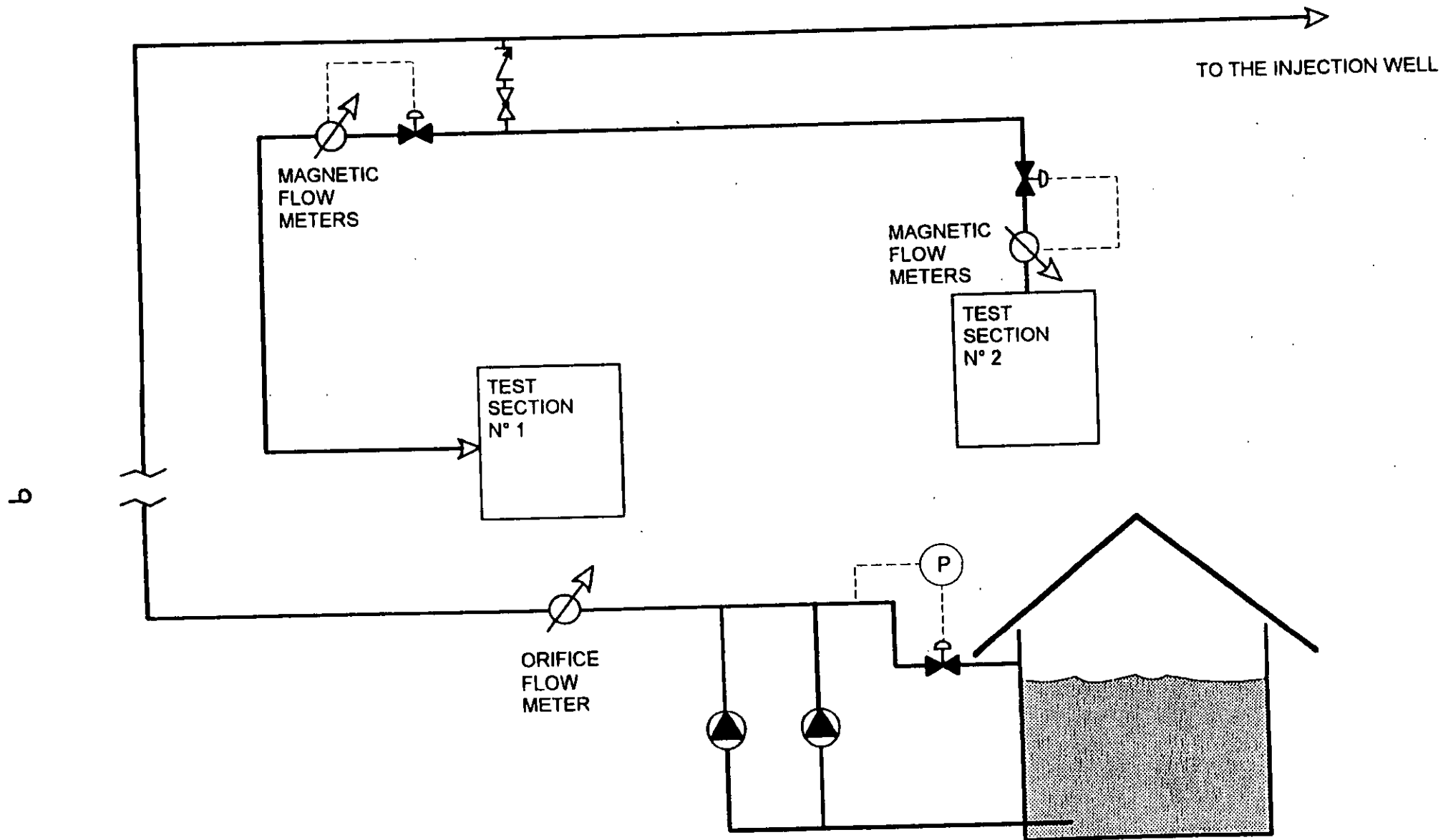


Fig. 6 - Water injection system

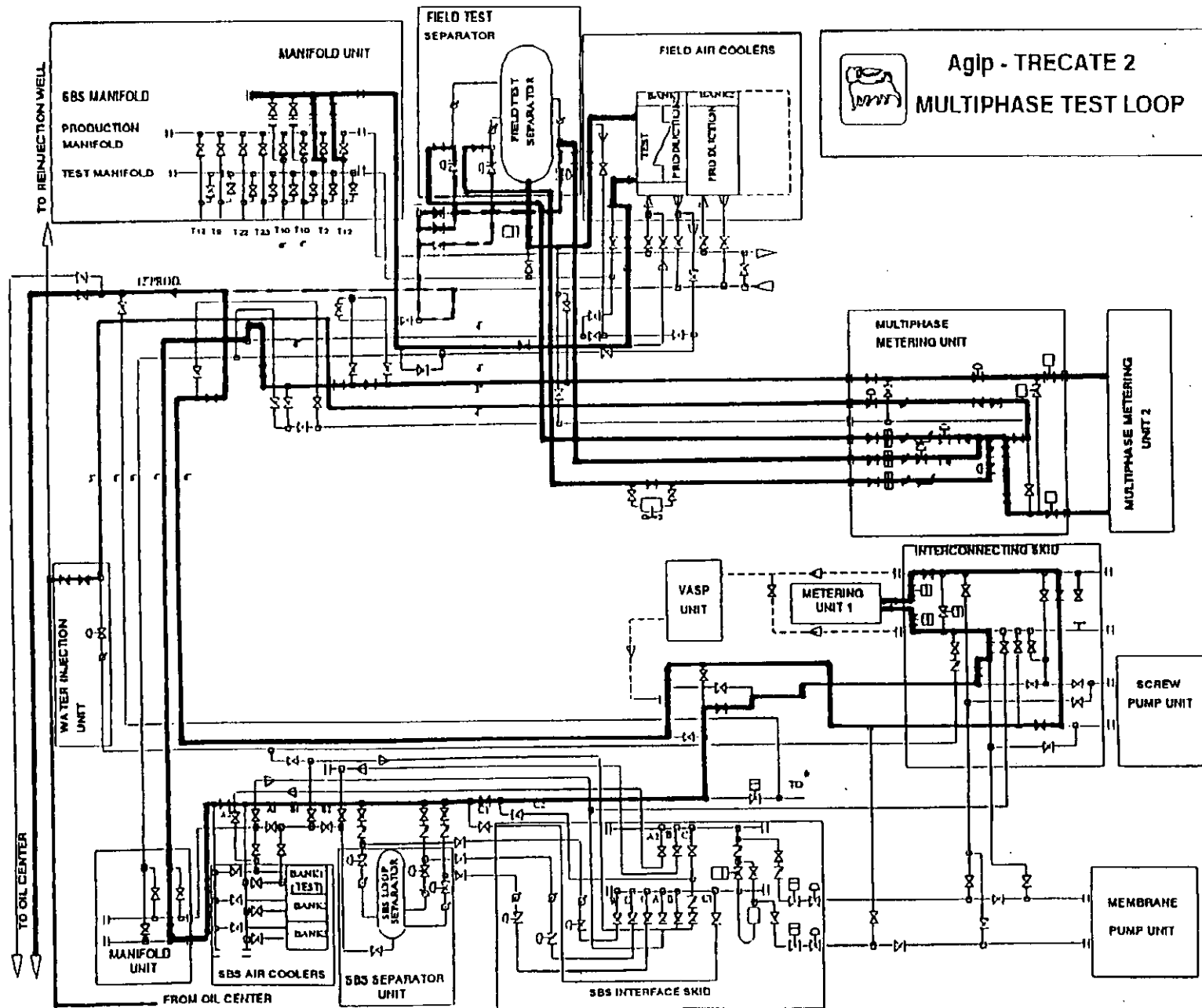


Fig. 7-Test on line

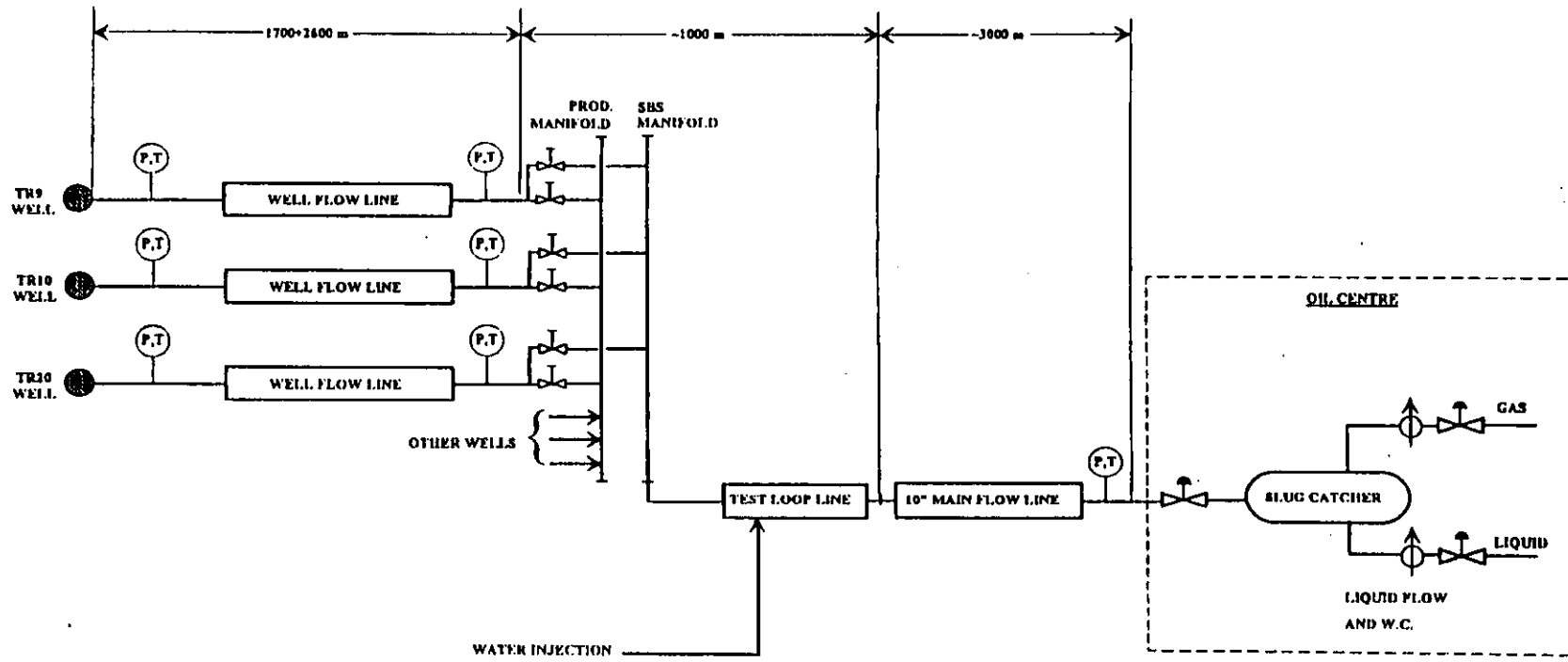


Fig. 8 - Plant configuration for fluid dynamic tests

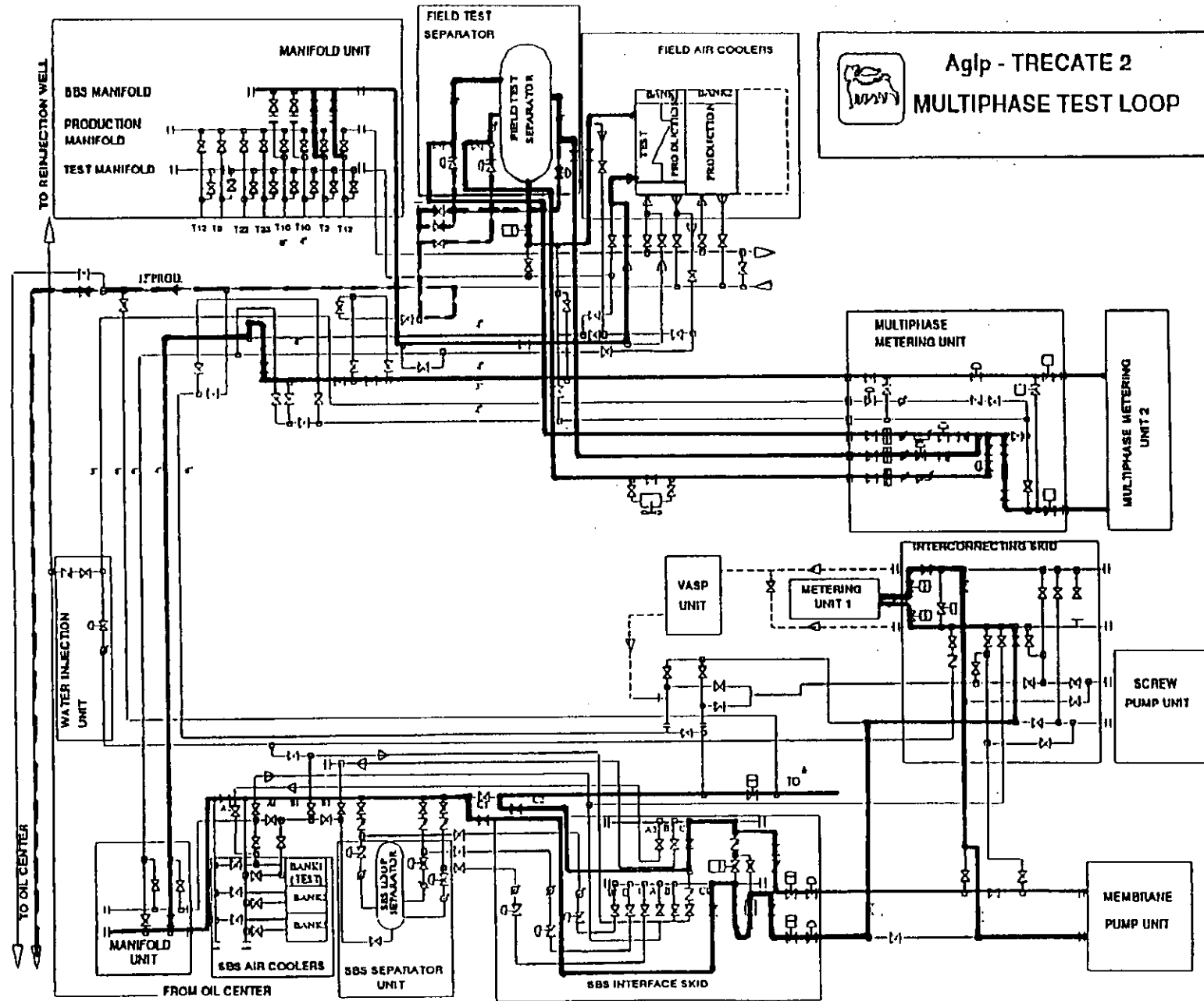


Fig. 9-Test on line with multiphase pump

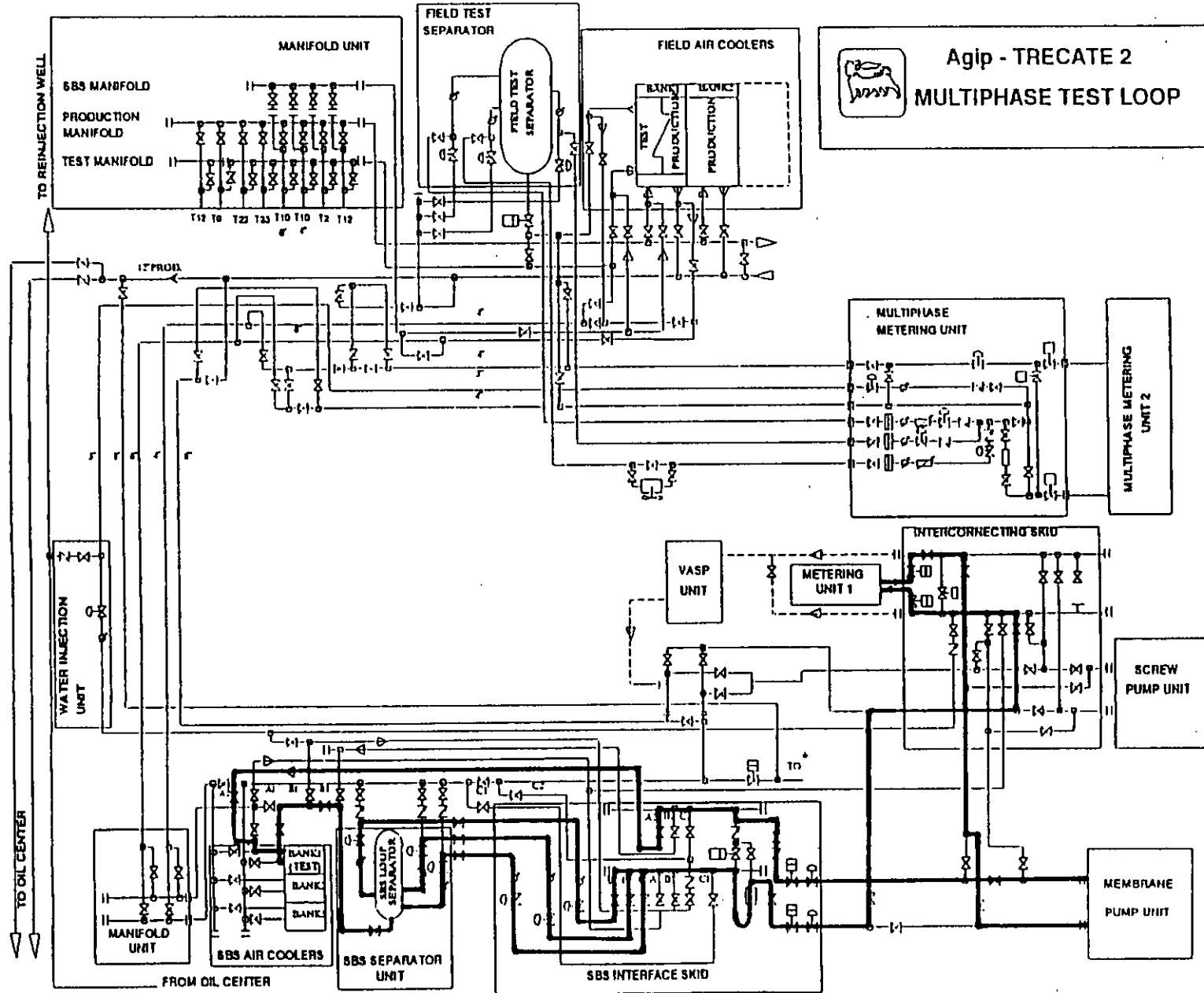


Fig. 10-Test in close loop with multiphase pump, using the test loop separator

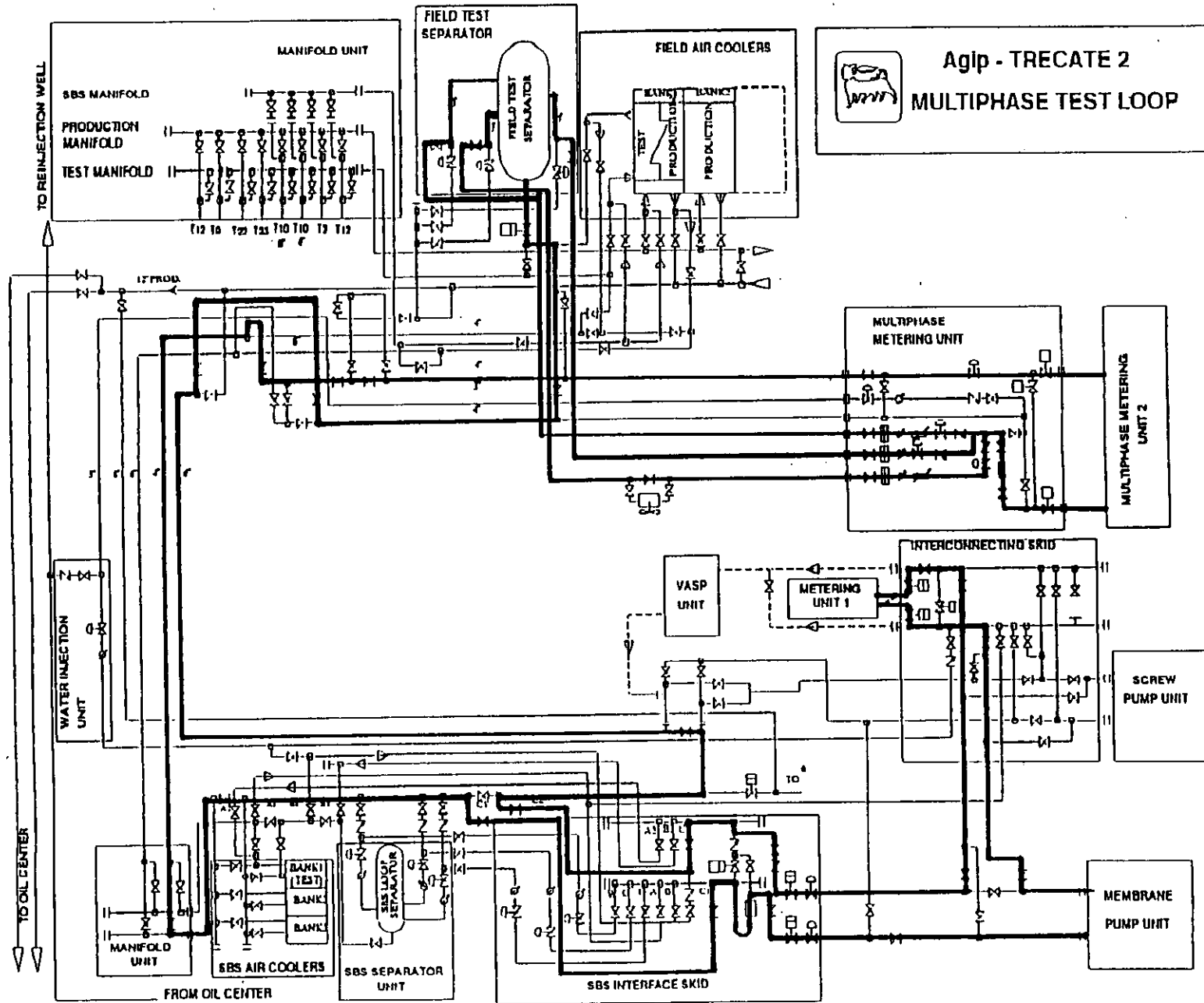
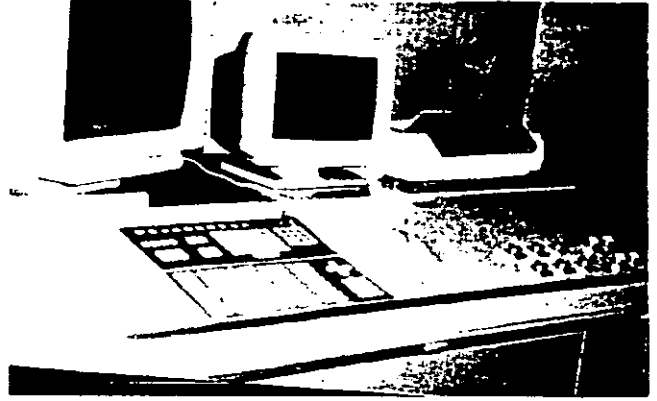
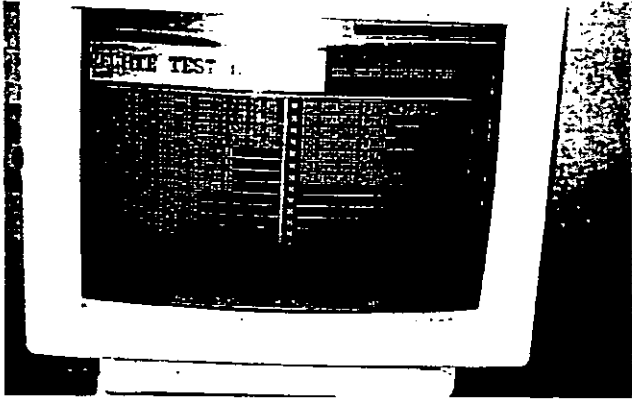
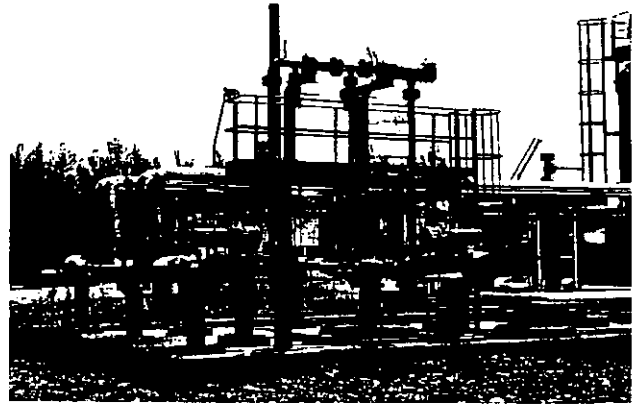


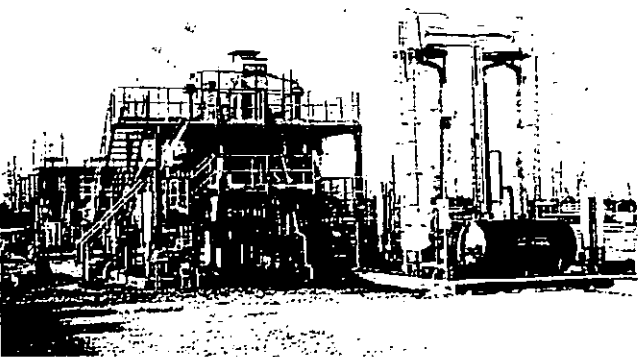
Fig. 11-Test in close loop with multiphase pump, using the field test separator



Operators console



Interface skids (test sections)



Diaphragm multiphase pump



Trecate 2 well (TR2)

Fig 12-Same Trecate test loop main components

SESSION 2

INSTALLATION EFFECTS

Chairman - Dr R J W Peters, Daniel Industries

SHORTENING INSTALLATION LENGTHS USING A LOW LOSS VANED FLOW CONDITIONER

E.M.Laws*, A K Ouazzane* and A Erdal⁺

*Department of Aeronautical, Mechanical and Manufacturing Engineering
University of Salford
Salford M5 4WT, UK.

+ K-Lab, Haugesund Norway

SUMMARY

Recent developments in flow conditioning have shown that pre conditioning a disturbed flow prior to a perforated plate flow conditioner can produce a device capable of producing 'ideal' flow conditions within very short installation lengths. Whilst this approach involves combining two devices and thus complicates the installation the benefits gained in terms of shortened installation lengths and improved downstream flow quality far outweigh this disadvantage. The present paper is concerned with a further investigation into the vaned plate described by Laws & Ouazzane(1) and Laws et al(2) resulting in a low loss integrated design capable of operating within very short installation lengths. The improved performance of orifice plates with β ratios between 0.4 and 0.7 when installed 3 diameters downstream of this conditioner is demonstrated. Preliminary results obtained in natural gas at a pressure of 100 bar for a 60% porosity plate in conjunction with a $\beta = 0.5$ orifice plate confirm the beneficial effects of the vaned plate on orifice plate performance.

Key Words: Flow straightener, flow conditioner, installation errors.

NOTATION

| | |
|-----------|---|
| Cd | Orifice plate discharge coefficient. |
| K | Pressure loss coefficient = $(\frac{\Delta p}{2}) / (0.5 \rho \bar{u})$. |
| D | Pipe diameter. |
| r | Radial distance measured from pipe centre line. |
| R | Pipe radius. |
| Re | Reynolds number |
| u,u' | time mean local, fluctuating velocity. |
| \bar{u} | average time mean velocity. |
| y | Distance measured radially from pipe wall |
| z | axial distance measured from plane of conditioner (- upstream, + downstream). |
| β | Orifice plate diameter ratio. |
| ρ | Density. |

1. INTRODUCTION

The technology of flow conditioning has developed rapidly in recent years. The devices included in the flow standards have now been complemented by a number of short perforated plate devices involving porosity grading capable of producing acceptable time mean flow conditions within an overall installation length of 12-15 pipe diameters.

Such perforated plate devices are usually effective with an upstream settling length of 3-4 pipe diameters and can produce acceptable time mean flow conditions within 8-9 pipe diameters dependant on the nature of the approach flow (the degree of asymmetry, swirl magnitude etc.). Immediately downstream of the plate in the first 2-3 diameters of the development there is a highly turbulent jet

mixing zone in which both the swirl and asymmetry in the upstream flow are destroyed and the flow re-distributed by the porosity grading of the plate. This mixing zone contributes to an increase in the turbulence intensity of the downstream flow. Consequently a longer development length is usually required before an established turbulence structure can be developed.

The Mitsubishi perforated plate described by Akashi et al (3) was the first short, perforated plate to be developed. The plate consists of 35 holes each of diameter, $d = 0.13D$, distributed hexagonally over the plate surface and is of depth, d . This plate has not however been widely used in industry and has been shown by a number of investigators to, in certain cases, both fail to produce acceptable time mean profile quality and to reduce swirl effectively, (see refs 4,5). Nevertheless this plate can be considered as the first stage in the evolution of an efficient, short perforated plate design indicating to the flow measurement community that the recommended lengths of the devices included in the flow standards ISO 5167 and AGA/API 3 (6,7) may be unnecessary.

The Laws plate (see fig 2) described in Laws(8,9) has a central hole and two surrounding rings of holes. The hole sizes in the centre, inner and outer rings and the number of holes in the inner and outer ring are such as to distribute the downstream flow to produce fully developed flow in a relatively short downstream length. Details on the plate geometry are given in Laws(9) and a comparison between the performance of the Mitsubishi and Laws plates is given in Laws (8,9).

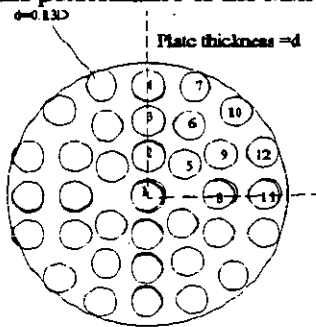


FIG 1. MITSUBISHI PERFORATED PLATE

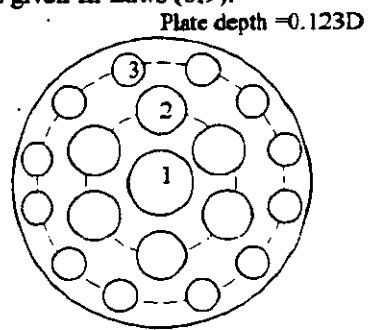


FIG 2 LAWS PERFORATED PLATE

The Zanker flow conditioner included in ISO 5167 (see fig 3) which consists of a thin perforated plate followed by a boxed honeycomb section 1 pipe diameter in length is a hybrid device combining the grading of porosity introduced by the perforated plate with the swirl removing capabilities of a honeycomb section. Though several investigations have concentrated on the effect of the Zanker conditioner on orifice plate discharge coefficient errors few have focused on the flow quality produced by the Zanker conditioner or attempted to distinguish between the contribution due to the plate and that of the honeycomb. Laws and Ouazzane (10) however looked in detail at the effect of the depth of the plate in the Zanker conditioner on the performance of the conditioner and have shown that as the perforated plate is thickened the downstream honeycomb becomes effectively redundant. Thus a Zanker plate of a depth similar to the Laws and Mitsubishi plates appeared to be capable of both removing swirl and improving flow quality.

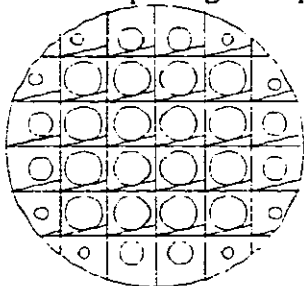


FIG 3. THE ZANKER FLOW CONDITIONER

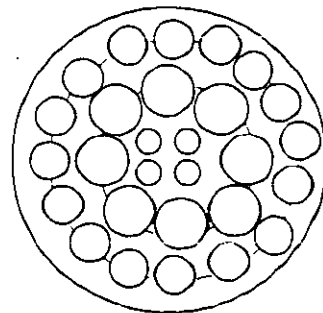


FIG 4. THE NEL PLATE

More recently a perforated plate conditioner has been designed by Spearman et al (11) working at NEL (see fig 4). This plate can be regarded as a combination of the Laws and Zanker plates having the graded porosity and hole sizes equivalent to a graded 1:8:16 Laws plate but replacing the central hole of the Laws design with the square grid hole arrangement of the Zanker design. The selection of the square central geometry limits the usefulness of this design since the need to maintain, for manufacturing purposes, some solid material between the central holes prevents the porosity of this plate being increased significantly above its present value. Thus the pressure loss of this plate is significantly higher than that for the Laws or Mitsubishi design though comparable with that of a thick Zanker design at a value of about 3.5.

The paper presented discusses the performance of the perforated plates currently available in terms of their effectiveness in meeting the ISO 5167 time mean flow criteria. This requires conditions within $\pm 5\%$ of the profile of u/u_{max} profile obtained after a development length of 100 pipe diameters to be attained together with a swirl angle within $\pm 2^\circ$.

Recently Laws & Ouazzane(1), and Laws et al(2) have shown that the addition of vanes upstream of, or actually on the plate itself, produces a significant improvement in the plate capability. The refined device is illustrated in figure 5.

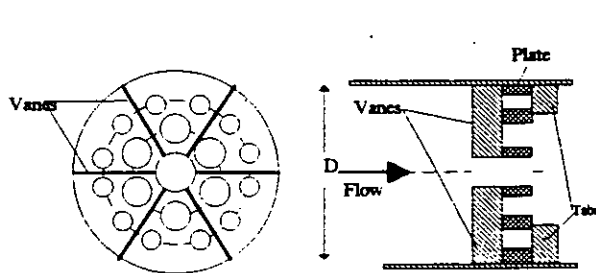


FIG 5 MODIFIED LAWS PLATE WITH VANES AND TABS ON PLATE

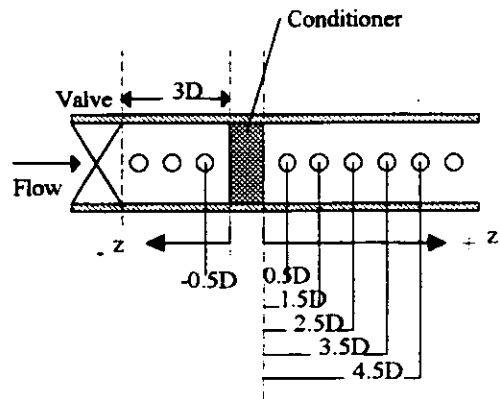


FIGURE 6 TEST ARRANGEMENT USED

They have shown that the vanes reduce significantly the asymmetry in a distorted upstream flow leaving the plate to operate in a less hostile flow environment. The additional feature of vanes on the plate improves the overall component performance significantly giving a device which can produce both acceptable time mean flow and axial turbulence intensity profiles within short upstream and downstream installation lengths with very low overall pressure loss. The flow quality produced by a vaned Laws' plate with a porosity of 70% (having a loss coefficient of approximately 0.7) will be presented and compared with the equivalent results for the perforated plates discussed previously.

2 TEST CONFIGURATION

The open circuit air rig used was of 0.103m diameter. The test section was preceded by a ball valve which was used to generate different upstream flow conditions. Three different valve settings were used, valve open, 50% closed and 70% closed. The conditioner tested was placed 3 pipe diameters downstream of the valve outlet plane. Each test section consisted of pipe sections 3 pipe diameters in length, each pipe section contained 3 instrument ports at a 1 diameter pitch along the axial length. The pipe sections, which were made from cast aluminium were designed with carefully machined flange faces enabling a number of sections to be linked together to give a smooth leak-free assembly of selected length. Measurements of time mean velocity and axial turbulence intensity were made at a number of axial locations downstream of the devices tested over a test length extending to 7.5 diameters downstream of the device. The time mean profiles were obtained using pressure probes and

the turbulence intensity measurements made using a constant temperature hot-wire anemometer using straight single hot-wire sensors. The measurements were made in air at a test Reynolds number based on the pipe diameter of 1.8×10^5 . The experimental data is presented in the form of profiles of non-dimensional velocity u/\bar{u} and also profiles of axial turbulence intensity $\sqrt{u'^2}/u$. On the figures the plane of the conditioner has been taken as $z=0$ with the distance upstream of the conditioner denoted by $z < 0$ and downstream by $z > 0$. (see figure 6). Orifice discharge coefficient errors for a series of orifice plates placed 3 diameters downstream of the vaned 70% porosity Laws plate are presented for tests in atmospheric air. Preliminary results obtained at K-Lab are also presented for tests conducted at a pressure of 100bar in natural gas for a 60% porosity vaned Laws plate in conjunction with a $\beta = 0.5$ orifice plate.

3. EXPERIMENTAL RESULTS FOR PERFORATED PLATES

Space prohibits the inclusion of detailed experimental data for the different plates tested. However for each plate tested the results obtained when the device was placed 3 pipe diameters from the ball valve set either fully open or 50% closed are presented. Figs 7a,b show the results for the Mitsubishi plate which can clearly cope well with the well behaved upstream flow when the valve was set fully open but less well when the upstream flow is distorted as for the case when the valve was set 50% closed. The pressure loss for the Mitsubishi plate is however low at a value of about 1.4 dynamic heads.

The equivalent results for a 60% porosity Laws plate with a pressure loss again of around 1.4 dynamic heads are shown in figs 8a and b. These show that the Laws plate appears capable of coping with both the clean and disturbed approach flow case. Both plates however require the first 2-3 pipe diameters of downstream development length before the turbulent mixing from the individual jets to be completed.

Figs 9a,b show the results for the thick Zanker plate (no honeycomb) which again can cope well with the valve fully open but yielded a slight asymmetry when the valve was set 50% closed. The pressure loss coefficient for this device is also high at around 4.

Figs 10a, b show the corresponding results for the NEL plate which gives rise to a slight central wake associated with the central blocking of the plate which mixes out quickly resulting in a well behaved though slightly overpeaked profile when the valve was set fully open and a similar central wake and slightly underpeaked profile when the valve was set 50% closed. The pressure loss coefficient for this plate is also relatively high at around 3.5.

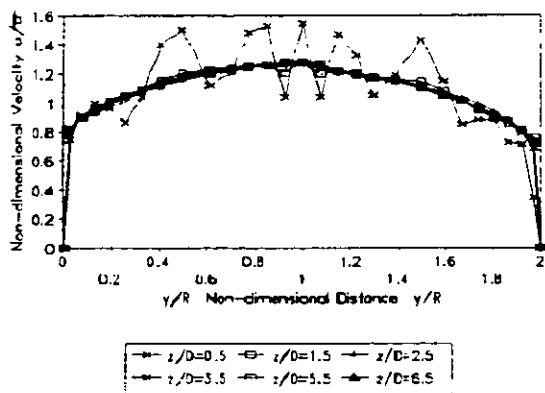


FIG 7a TIME MEAN PROFILES MEASURED DOWNSTREAM OF MITSUBISHI PLATE VALVE OPEN

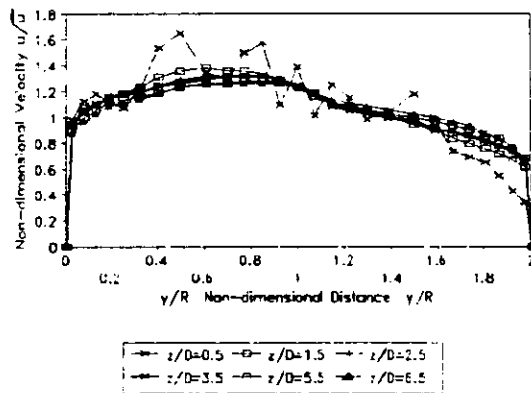


FIG 7b TIME MEAN PROFILES MEASURED DOWNSTREAM OF MITSUBISHI PLATE VALVE 50% CLOSED

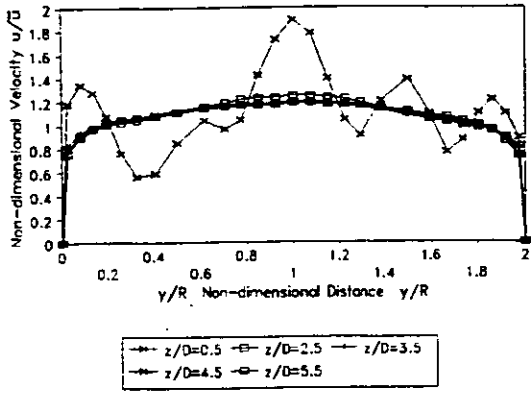


FIG 8a TIME MEAN VELOCITY PROFILES DOWNSTREAM OF 60% LAWS PLATE VALVE FULLY OPEN

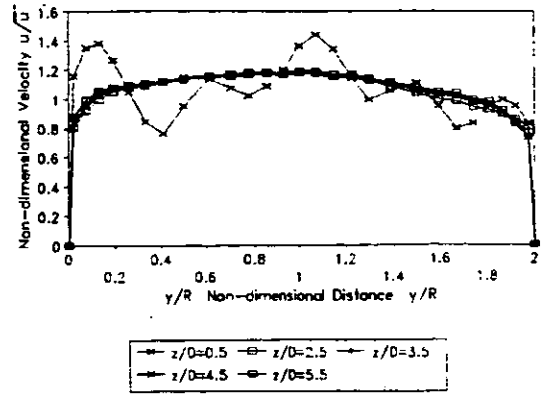


FIG 8b TIME MEAN VELOCITY PROFILE DOWNSTREAM OF 60% LAWS PLATE VALVE 50% CLOSED

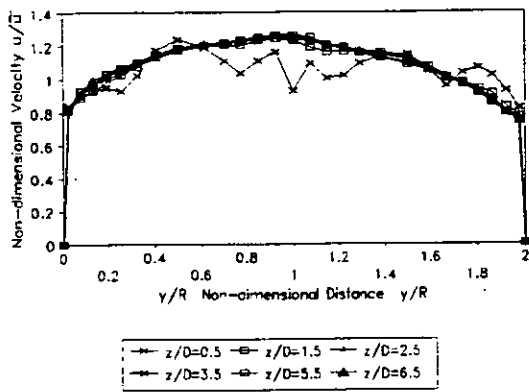


FIG 9a TIME MEAN VELOCITY PROFILES MEASURED DOWNSTREAM OF THICK ZANKER PLATE VALVE FULLY OPEN

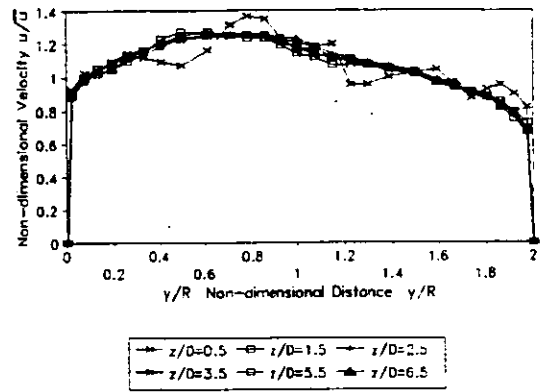


FIG 9b TIME MEAN VELOCITY PROFILES MEASURED DOWNSTREAM OF THICK ZANKER PLATE VALVE 50% CLOSED

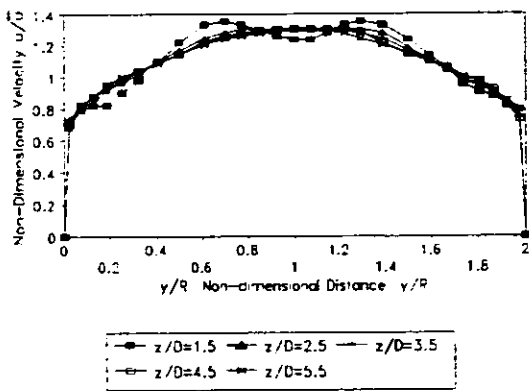


FIG 10a TIME MEAN VELOCITY PROFILES MEASURED DOWNSTREAM OF NEL PLATE VALVE FULLY OPEN

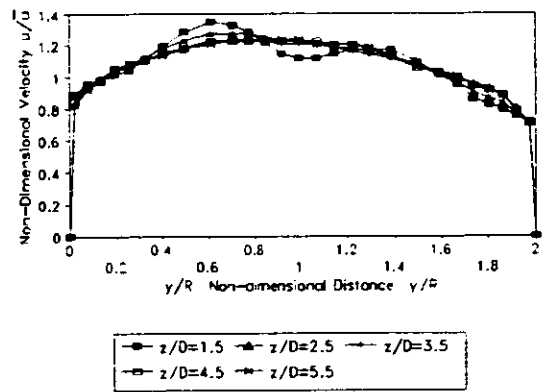


FIG 10b TIME MEAN VELOCITY PROFILES MEASURED DOWNSTREAM OF NEL PLATE VALVE 50% CLOSED

All the plates tested exhibited certain common features related to their method of operation suggesting that no matter how refined the hole design a perforated plate alone would not be capable of satisfying all the desirable features of an ideal flow conditioner. For all the plates a comparative study of the axial turbulence intensity profiles indicated that though a time mean profile meeting the ISO 5167 requirements could be produced within an overall length of some 12-15 diameters a much longer length would be required to develop an associated 'fully developed' turbulence distribution. Similarly none of the plates tested proved capable of operating efficiently when the upstream settling length was significantly reduced below 3 pipe diameters or the severity of the upstream distortion significantly increased. Thus to produce any significant improvement in conditioner performance an alternative to the perforated plate alone is required.

4. EXPERIMENTAL RESULTS FOR THE VANED LAWS' PLATE (70% POROSITY)

Laws and Ouazzane have demonstrated that by combining the graded porosity Laws plate with a series of radial vanes mounted on the surface of the plate, resulting in a device as shown in fig 5, it is possible to produce a flow conditioner which performs significantly better than the perforated plate alone in that a vaned plate appears capable of producing conditions very close in both time mean flow and axial turbulence intensity structure with those associated with fully developed flow. Figs 11a-c show the time mean profiles measured downstream of a 70% porosity vaned Laws' plate for three different upstream distortions. Settings 1, 2 and 3 correspond to the valve set fully open, 50% closed and 70% closed. clearly for all three cases the downstream profiles quickly become well established. The significant effect of the upstream vanes on the initial turbulent jet mixing can be clearly seen by comparing the profiles obtained at $z/D=0.5$ with those already presented in figs 8a,b for the Laws plate alone.

With this 'hybrid' arrangement it is possible to produce conditions within the ISO 5167 limits within a downstream settling length as short as 1.5 diameters as fig 11d illustrated, although better agreement is achieved if the downstream length is increased to 2.5 diameters. Similarly it is possible to shorten the upstream length considerably down to a length of 1 pipe diameter.

The porosity of the plate can be varied (results for 50% and 60% porosity plates have already been presented in Laws & Ouazzane(1,2)) though the 70% porosity plate appeared to be marginally better than the other versions tested.

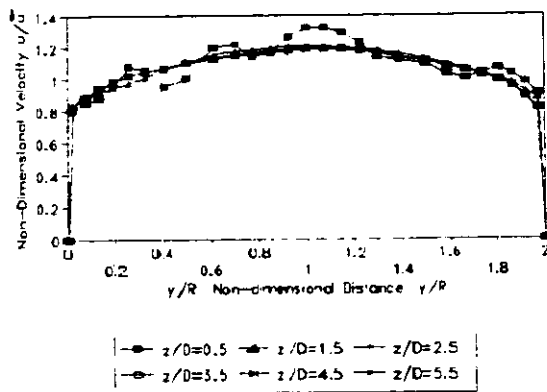


FIG 11A VELOCITY PROFILES
DOWNSTREAM OF 70% LAWS PLATE
WITH VANES AND FINS VALVE OPEN

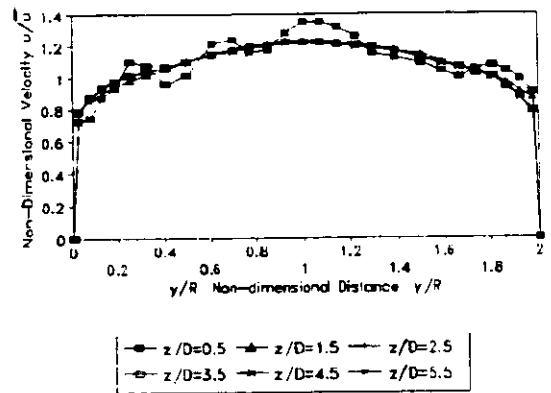


FIG 11B VELOCITY PROFILES
DOWNSTREAM OF 70% LAWS PLATE
WITH VANES AND FINS VALVE 50%
CLOSED

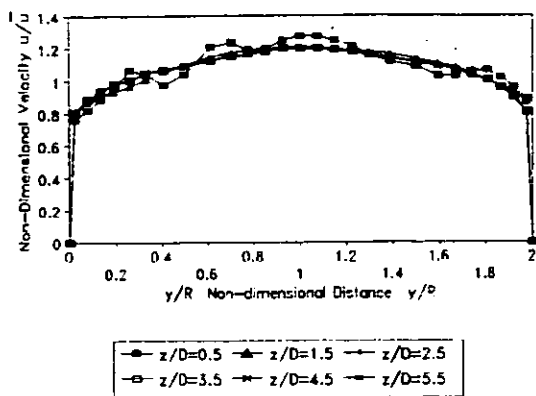


FIG 11C VELOCITY PROFILES
DOWNSTREAM OF 70% LAWS PLATE
WITH VANES AND FINS VALVE 70%
CLOSED

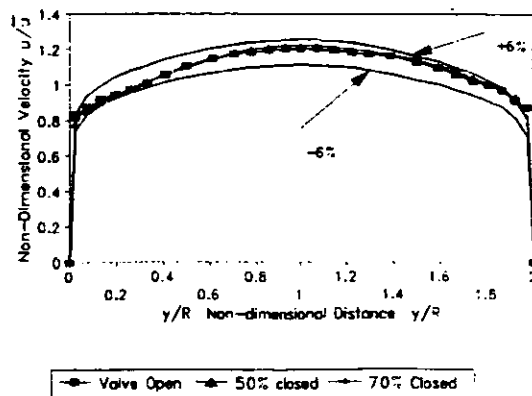


FIG 11D COMPARISON OF TIME MEAN
VELOCITY MEASURED AT $Z/D=1.5$
DOWNSTREAM OF 70% LAWS PLATE
WITH VANES AND FINS

5. EFFECT ON ORIFICE PLATE DISCHARGE COEFFICIENT ERROR

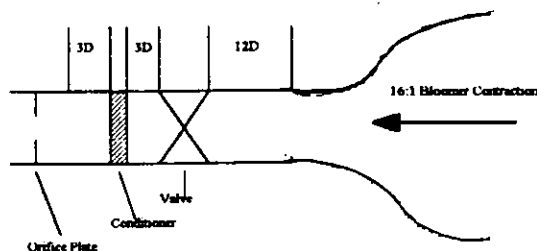


FIG 12 ORIFICE PLATE TEST LAYOUT

The test configuration used is shown in fig 12. The 70% porosity Laws plate with vanes and tabs as described previously was positioned 3 pipe diameters downstream of the exit plane of a sliding vane valve and the orifice plate positioned downstream of the conditioner so that there was 3 pipe diameters between the conditioner and the upstream tapping of the orifice plate. The valve was positioned 12 pipe diameters from the pipe inlet. The pipe inlet was preceded by a well designed 16:1 area ratio Bloomer contraction and the pressure drop across the contraction was used as the primary measuring device. Thus the mean velocity as determined from the pressure drop across the contraction was used to determine the orifice plate discharge coefficient as obtained from the pressure drop across the orifice plate. Recognising that with this measurement technique absolute accuracy could not be achieved it being estimated that the mean velocity could not be determined to within an accuracy of $\pm 0.4\%$ it was considered to be more appropriate to compare the discharge coefficient of the orifice plates as determined in the installation in fig 12 with the equivalent discharge coefficient values when the plate was installed at 100 pipe diameters from the pipe inlet. Thus the discharge coefficient errors referred to subsequently refer to differences between measured values and those determined from a calibration of the orifice plate at $z/D=100$.

The orifice discharge coefficient with and without the flow conditioner installed has been determined for three valve positions. Note that when the flow conditioner was removed the orifice plate was maintained in the same position i.e. then with approximately 6 pipe diameters between the valve exit plane and the upstream tapping of the orifice plate.

For all the orifice plates tested the maximum error in C_d was 0.15% with the conditioner in line compared to values upto 4% without the inclusion of the conditioner.

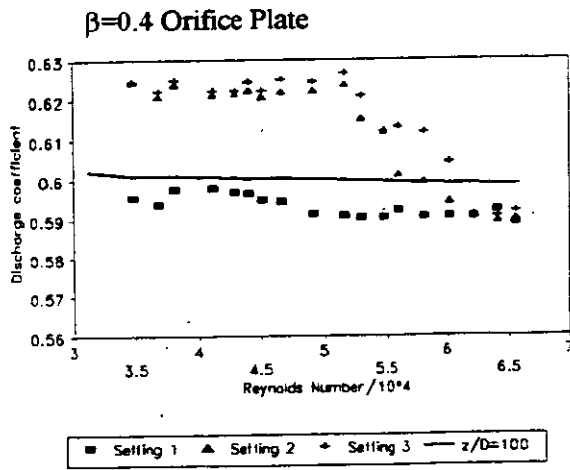


FIG 12A DISCHARGE COEFFICIENT VARIATION DIFFERENT CASES WITHOUT THE CONDITIONER

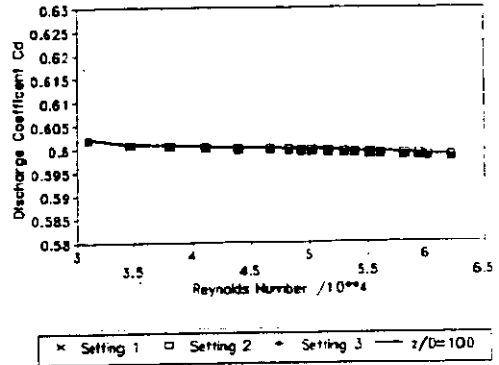


FIG 12B DISCHARGE COEFFICIENT VARIATION DIFFERENT CASES WITH THE CONDITIONER

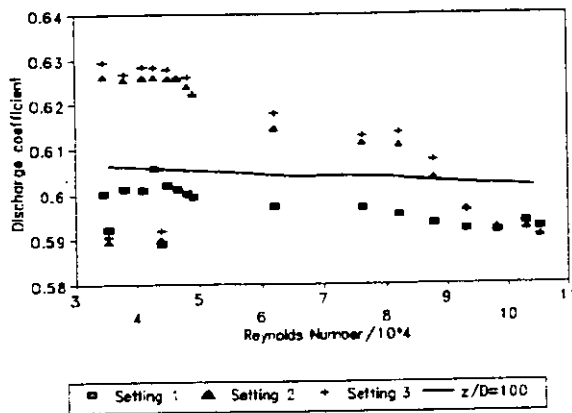


FIG 13A COMPARISON OF DISCHARGE COEFFICIENTS WITHOUT FLOW CONDITIONER

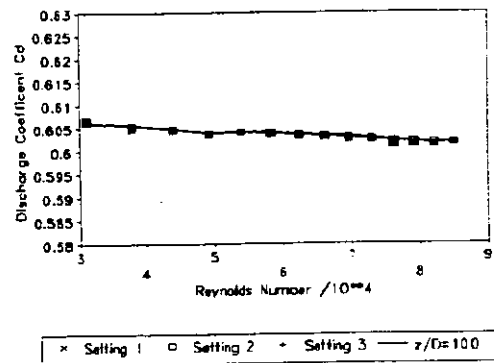


FIG 13B DISCHARGE COEFFICIENT VARIATION FOR THE DIFFERENT CASES WITH THE CONDITIONER

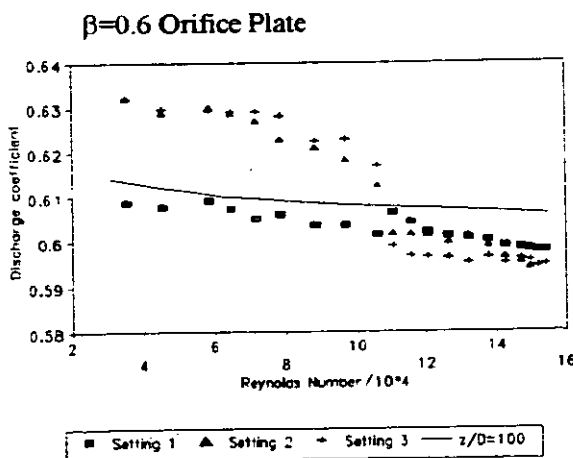


FIG 14A DISCHARGE COEFFICIENT VARIATION DIFFERENT CASES WITHOUT THE CONDITIONER

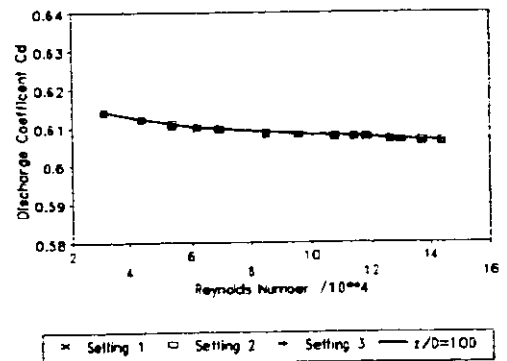


FIG 14B DISCHARGE COEFFICIENT VARIATION DIFFERENT CASES WITH THE CONDITIONER

$\beta=0.7$ Orifice Plate

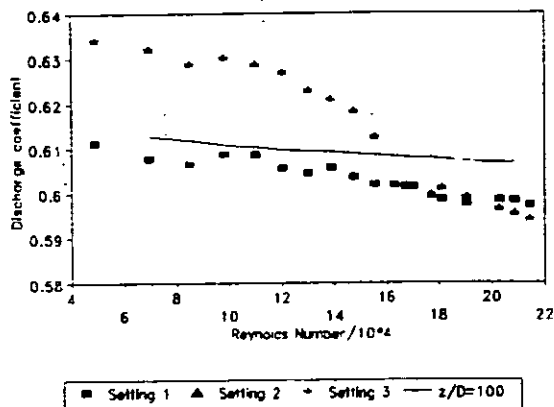


FIG 15A COMPARISON OF DISCHARGE COEFFICIENT FOR DIFFERENT VALVE SETTINGS WITHOUT CONDITIONER

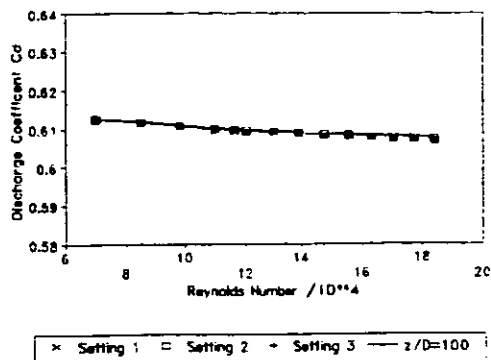


FIG 15B COMPARISON OF DISCHARGE COEFFICIENT FOR DIFFERENT VALVE SETTINGS WITH CONDITIONER

The results for the 70% porosity plate appear marginally better than those for the 60% porosity plate presented in Laws et al(2). In the line size used in the present tests i.e. 0.103m, 70% was the maximum porosity that could be achieved whilst maintaining the structural rigidity of the plate. In larger line sizes a higher plate porosity could be practical and it would be of interest to assess the performance of a higher porosity plate in these circumstances.

Complete confidence in the vaned plate behaviour requires more detailed testing at different pressures, Reynolds numbers and in different line sizes. Preliminary results at high pressure for a $\beta = 0.5$ orifice plate installed downstream of single and double 90° bends are shown in fig 16. These test were carried out at K-Lab in natural gas in a 0.1397m diameter pipe using a 60% porosity vaned plate installed 3.1D downstream of the bend outlet flange with the orifice plate located 5.3D downstream of the conditioner. Repeatability in the measurements is estimated as $\pm 0.5\%$.

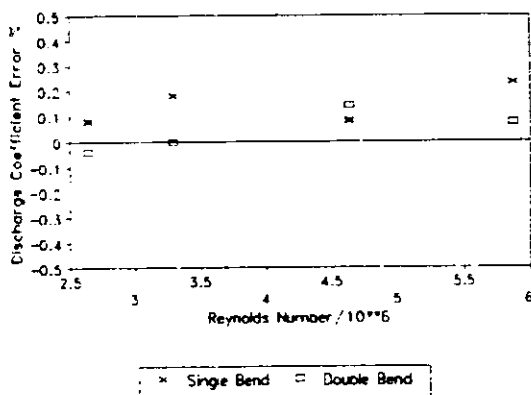


FIG 16 DISCHARGE COEFFICIENT ERROR FOR $\beta = 0.5$ ORIFICE PLATE OBTAINED IN NATURAL GAS AT 100BAR.

6. ENHANCEMENT IN PERFORMANCE OF PERFORATED PLATES

Whilst a more fundamental study into the mechanism by which the vanes and plate interact is required before the behaviour of the vaned plate can be fully understood a careful study of the turbulence intensity measured upstream and downstream of a perforated plate with and without vanes indicates that the vanes have a significant effect on the turbulence structure of the flowfield both

upstream and downstream of the plate. In consequence vanes can be used upstream of other perforated plates to enhance the plate performance. Preliminary results are presented here for the axial turbulence intensity measured downstream of the thick Zanker plate with and without radial vanes installed 1 pipe diameter upstream of the plate for the case when the valve is set 50% closed.

Fig 17a shows the axial turbulence intensity profiles measured at different stations downstream of the thick version of the Zanker plate installed 3 diameters from the outlet plane of the valve. Fig 17b shows the same plate preceded by a set of eight radial vanes of depth $D/8$. The improvement in the form and magnitude of the turbulence profiles is clear. Figs 18a and 18b show the equivalent results when the valve is 70% closed. The improvement in the turbulence profile is again evident.

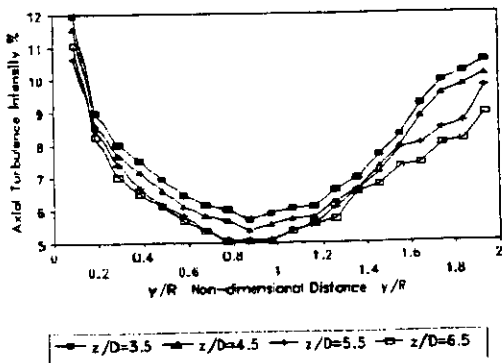


FIG 17A AXIAL TURBULENCE INTENSITY DOWNSTREAM OF THICK ZANKER PLATE VALVE 50% CLOSED

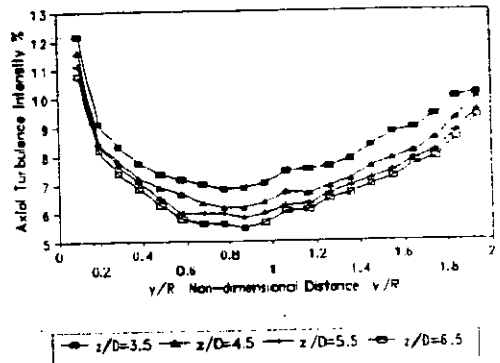


FIG 18A AXIAL TURBULENCE INTENSITY DOWNSTREAM OF THICK ZANKER PLATE VALVE 70% CLOSED

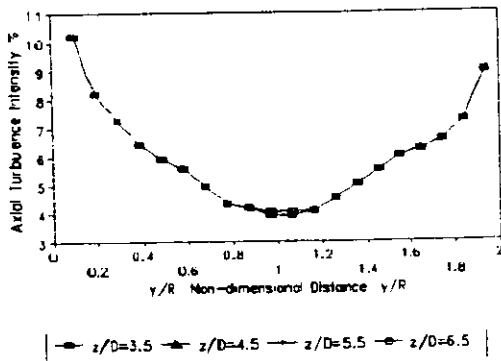


FIG 17B AXIAL TURBULENCE INTENSITY DOWNSTREAM OF THICK ZANKER PLATE PRECEDED BY RADIAL VANES VALVE 50% CLOSED
CONCLUSIONS

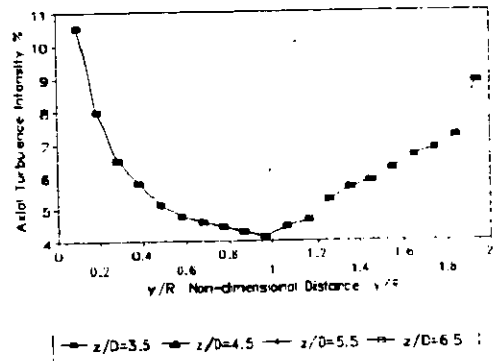


FIG 18B AXIAL TURBULENCE INTENSITY DOWNSTREAM OF THICK ZANKER PLATE PRECEDED BY RADIAL VANES VALVE 70% CLOSED

A modified vaned Laws plate, easy to manufacture and install, has been introduced which has been demonstrated to be capable of delivering flow conditions which meet the ISO 5167 requirements within an overall installation length of some 5-6 pipe diameters incurring a pressure loss of approximately 0.7 dynamic heads. The improvement in the performance of orifice plates of area ratios of 0.4-0.7 installed in close proximity to this vaned perforated plate flow conditioner has been demonstrated in atmospheric air. Preliminary tests conducted at high pressure using a 60% porosity plate with a pressure loss coefficient of approximately 1.4 give confidence in the behaviour of the vaned plate geometry.

The findings reported here are covered by British Patent Application No: 9319025.4.

REFERENCES

- 1 Laws, E M and Ouazzane, A K. Compact Installations for Differential Flowmeters. Flow Measurement for the Utilities, Amsterdam, November 1993. (Published in J Flow Measurement and Instrumentation 1994)
- 2 Laws, E M, Ouazzane, A.K and Erdal A, Compact Installations for Orifice Plate Flowmeters, Flow Measurement in the Mid 90s, Flomeko '94, NEL, Glasgow, 1994
- 3 Akashi, K, Watanabe, H and Koga, K, Development of a New Rectifier for Shortening Upstream Pipe Length of Flowmeter. Proceedings of IMEKO Symposium Flow Measurement and Control in Industry, pp 279-284, 1979.
- 4 Lake, W.T and Reid, J. Optimal Flow Conditioner, Proceedings North Sea Workshop. 1992.
- 5 Laws, E M. Flow Conditioning a New Development. J of Flow Measurement and Instrumentation, Vol 1, 1990, pp 165-170.
- 6 ISO 5167: 1991. Measurement of Fluid Flow by means of Orifice Plates, Nozzles and Venturi Tubes inserted in Circular Cross-section Conduits Running Full
- 7 ASME/ANSI 2530/API 3, 1980. Orifice metering of natural gas and other related hydrocarbon fuels.
- 8 Laws, E.M. Development of a Perforated Plate Flow Conditioner, Presented at IBC. Flow Measurement in Industry and Science, London, 1990.
- 9 Laws, E.M. Flow conditioning a new development, J of Flow Measurement and Instrumentation, Vol 1, 1990, pp 165-170.
- 10 Laws, E. M and Ouazzane, A.K. The Performance of the Zanker Straightener, J of Flow Measurement and Instrumentation, Vol 4, 1992.
- 11 Spearman, E P, Sattary, J.A and Reader-Harris, M J. Comparison of Velocity Profiles Downstream of Perforated Plate Flow Conditioners, Flow Measurement in the Mid-90's, Flomeko '94, NEL Glasgow.

DEVELOPMENT OF A FLOW CONDITIONER

Asbjørn Erdal, Kårstø Metering and Technology Laboratory, K-Lab, Haugesund, Norway
 Dag Lindholm, Institute for Energy Technology, IFE, Kjeller, Norway
 Dag Thomassen, Institute for Energy Technology, IFE, Kjeller, Norway

ABSTRACT

This paper gives a review of the major activities of the systematic process to develop a flow conditioner (FC) which can be used to reduce the required length of an orifice metering station.

A theoretical design procedure for the development of a FC is presented together with the main findings from experiments performed in test rigs using air at atmospheric pressure and natural gas at high pressure. Orifice meter discharge coefficient (Cd) measurements at 100 bar in natural gas show that Short Metering Systems (SMS) of 15D with the Mark 5 FC installed have very good performance.

NOMENCLATURE

| | |
|-----------|---|
| A | : Cross section area [m ²] |
| a | : Hole diameter [mm] |
| Cd | : Discharge coefficient [-] |
| D | : Internal pipe diameter [m] |
| K | : Pressure loss coefficient [] |
| n | : Number of holes [] |
| m | : Number of area rings [] |
| P | : Pressure [Pa] |
| R | : Pipe radius or ring radius [mm] |
| Re | : Reynolds number [-] |
| U | : Axial velocity [m/s] |
| Y | : radial position referred to the wall [m] |
| β | : Diameter ratio of the orifice meter [-] |
| Φ | : Ratio of the flow area in vena contracta to the pipe area [-] |
| λ | : Porosity [-] |
| ρ | : Density [kg/m ³] |

subscripts:

| | |
|----|--------------------|
| i | : Ring number |
| m | : Mean value |
| o | : Stagnation value |
| vc | : Vena contracta |

1. INTRODUCTION

1.1 BACKGROUND

For over sixty years, the concentric orifice meter has remained the predominant meter for natural gas metering applications. Even if more modern flowmeters appear on the market, orifice meters continue to be a preferred choice by many users because of the simple technology, the existence of well-known standards and the long experience with the meters. Unfortunately, the accuracy of an orifice meter is affected by flow perturbances, especially swirl, and even 100D may not be enough to fulfil the ISO-5167 requirement of less than +/- 2° swirl (ref. 1).

Orifice metering stations offshore are very heavy and expensive installations because of the long upstream pipelength that are required in ISO-5167 (ref. 2). Therefore a lot of effort is put into developing FCs that can reduce the upstream length required to eliminate swirl and develop a fully developed velocity profile. A review of the work done so far is presented by Gallagher and Beaty (ref. 3).

K-Lab has since 1987 co-operated with IFE and University of Salford on the development of a series of FCs. This paper deals only with the development of the Mark series of FC and testing at IFE and K-Lab.

The development was inspired by section 7.4 of ISO-5167. This section states that if the flow conditions immediately upstream of the primary device can be demonstrated to sufficiently approach those of a fully developed velocity profile (within $\pm 5\%$) and be free from swirl (within $\pm 2^\circ$), then the uncertainty range claimed by the standard remains applicable. It was decided to attempt to design a new FC to reach this condition within $15D$ downstream of a flow disturbance, independently of the velocity and swirl profiles existing upstream of the FC.

1.2 GOALS FOR THE FC DEVELOPMENT

In the early days of the project, the following goals were listed :

The new FC should :

- Eliminate swirl (within $\pm 2^\circ$).
- Generate a fully developed velocity profile (within $\pm 5\%$) maximum $15D$ downstream of the flow perturbation.
- Give low pressure drop across the FC.
- Be simple and cheap to manufacture.
- Give similar or better measurement accuracy compared to a standard ISO-5167 installation.

1.3 DEVELOPMENT PROGRAM

When the design objectives for the FC development were identified, a research plan with several activities was established. The main ones are listed below :

- Develop a theoretical model for the design of the FCs.
- Manufacture FCs according to the theoretical model.
- Test the FCs in air at atmospheric pressure.
- Develop a tool to measure velocity and swirl (swirl probe) which can be used in natural gas at North Sea conditions (up to 150 bar).
- Test the FC in natural gas at high pressure.
- Acquire orifice meter performance data (C_d) in natural gas at high pressure.
- Make a result database for FCs.
- Obtain general acceptance for the technology.

2. DESIGN OF THE FLOW CONDITIONERS

2.1 A THEORETICAL DESIGN MODEL

Initially a simple theoretical model for the flow through the holes in the FC was established. Based on formulas deducted from his theory and some practical modifications the new FC was designed.

A design procedure for the FCs is presented below. It is based on a simplified theoretical model which calculates the pressure loss through the holes in the FC.

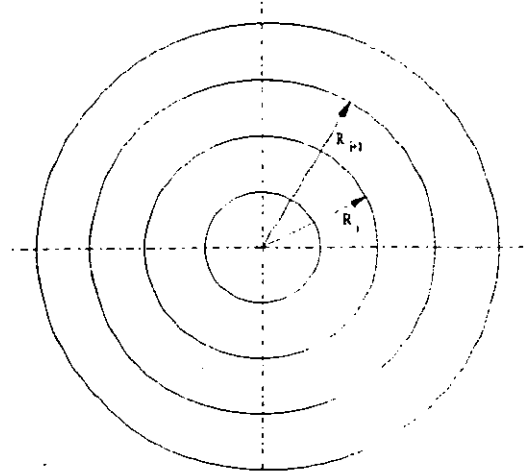


Figure 1.
Discretisation of the flow area

The cross sectional area in the flow conditioner is first discretised into rings as shown in figure 1. Each ring area is then described by an inner and outer radius, and includes one or more holes.

The velocity profile immediately upstream of the flow conditioner is assumed flat, while the velocity profile downstream is assumed fully developed. A "quasi one-dimensional" illustration of the flow profile through the flow conditioner is shown in figure 2.

The area of the flow conditioner is divided into rings, and each ring is regarded as a separate flow channel. The outlet velocity shall correspond to the discrete velocity in the fully developed profile. The flow through each ring is treated separately, and the holes are dimensioned to introduce a sufficient pressure loss to give near fully developed flow downstream. The pressure loss from a distance upstream of the flow conditioner to a distance downstream through all flow channels are equal.

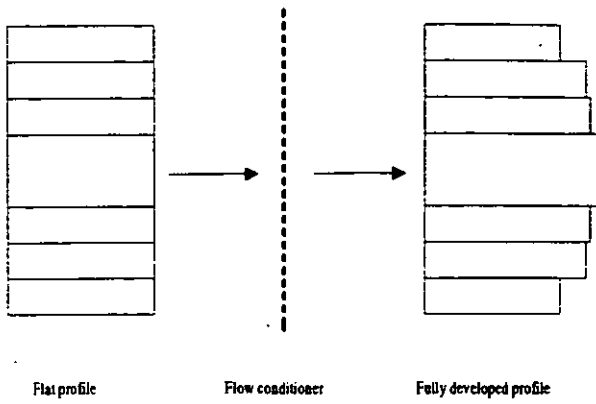


Figure 2.
Discretisation of the velocity profile

Consider the flow through one of these flowchannels. It can be divided into flow through a sudden contraction, figure 3, and flow through a sudden enlargement, figure 4. The two parts are first treated separately and then coupled through the total pressure loss. The flow is considered one-dimensional and incompressible.

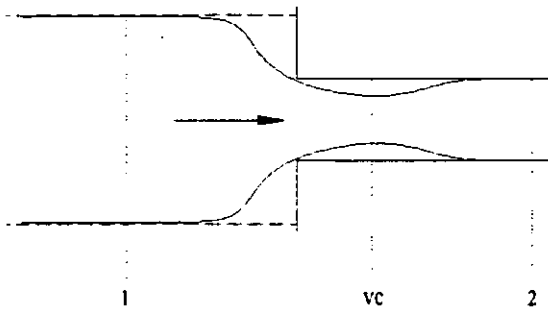


Figure 3.
Turbulent flow through a sudden contraction

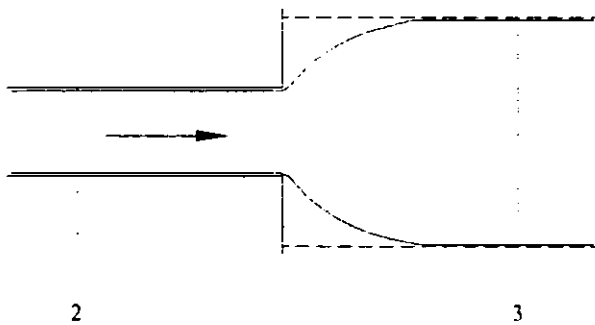


Figure 4.
Turbulent flow through a sudden enlargement

An equation which relates the total pressure coefficient of the flow conditioner, K_0 , to the ring porosity, λ_i , and the ratio between the local velocity in the fully developed profile, U_i , corresponding to the location of

the ring to the mean velocity, U_m , can now be derived. The equation reads

$$K_0 = \frac{0.7(1-\lambda_i)}{\lambda_i^2} + [(1-\lambda_i)/\lambda_i]^2 \cdot (U_i/U_m)^2 \quad (1)$$

The two terms on the right hand side of eq. (1) express the pressure loss due to the sudden area contraction and enlargement caused by the holes in the ring, respectively. The equation does not take into account the friction against the hole walls. For FC plates in which the length of the holes are typically 2-6 times the hole diameter, this is a reasonable simplification.

The total pressure loss coefficient is defined as

$$K_0 \equiv \frac{\Delta P_0}{0.5 \rho U_m^2} \quad (2)$$

where ρ is the fluid density and P_0 the total pressure difference over the FC in terms of the stagnation pressures.

The porosity of a ring flowchannel is defined as the ratio between the area of the holes to the total ring area. Thus, the porosity of ring no. i can be calculated as

$$\lambda_i = \frac{n(\pi/4) \cdot a^2}{\pi(R_{o,i}^2 - R_i^2)} \quad (3)$$

where n is the number of holes in the ring, a is the diameter of each hole, and $R_{o,i}$ and R_i the outer and inner radius of the ring.

Eq. (1) forms the basis of the design procedure. The porosity of each ring will be determined to get a predefined velocity profile and total pressure loss.

The shape of a fully developed velocity profile will change with the Reynolds number up to about $3 \cdot 10^7$ (for smooth pipes to even higher Re-numbers). According to Wilcox et al. (ref. 4) the ratio U/U_m can be represented as a function of the radial distance from the pipe axis by the equation

$$\frac{U}{U_m} = 1.173 \cdot \left(\frac{Y}{R}\right)^{1/9} \quad (4)$$

Here Y is the distance from the pipe wall and R is the internal pipe radius. This formula can be employed for determination of the U_i -values in eq. (1).

The area of each ring is divided into n holes, each with a diameter a . Physical limitations restrict the diameter and the number of holes by the following constraints:

$$R_{i+1} - R_i > a + 2 \tag{5}$$

and

$$n(a + 2) < 2\pi \cdot (R_{i+1} + R_i)/2 \tag{6}$$

where R_i is the inner radius and R_{i+1} the outer radius of ring i . These constraints ensure that the diameter of each hole is smaller than the width of the ring, and that the sum of the hole diameters is less than the circumference of the ring. An additional requirement is of course that the number of holes, n , must be an integer.

For a given porosity there is normally not a unique solution to the above equations. To solve the equations either the size of each hole or the number of holes have to be maximised.

The design of a flow conditioner geometry can then be determined by the following steps:

1. Define the porosity (or pressure loss) for the flow conditioner. Calculate the pressure loss (or porosity) by eq. (1) applied at the radial position where the upstream velocity equals the downstream velocity, i.e. $U/U_m=1.0$.
2. Define the number of rings. Select m axial velocities to represent the fully developed axial velocity profile and determine the radial location of each corresponding ring using eq. (4).
3. Calculate the porosity of each ring using eq. (1).
4. Calculate the area of each hole and the number of holes in each ring by either maximising the hole diameter or the number of holes. For this purpose eq. (3), (5) and (6) are employed.

2.2 THE DIFFERENT MODELS

The results from the examination of the performance of Mark 2 have been presented in ref. 4 and 5. This FC show excellent performance as swirl remover, but was not equally good in straightening out asymmetric velocity profiles. Therefore the design of Mark 2 was gradually improved resulting in the Mark 3, Mark 4, Mark 4 ch (chamfered) and culminating in the Mark 5 FC. At an early stage, the decision was taken to maintain a thickness of 50mm for the FC when it was installed in a test rig having an internal pipe diameter equal to 140mm. This eliminated one of the variables in the problem, leaving only the layout of the holes in the cross-section to be optimised.

The design of the FCs was based on the theory above. For Mark 3 the hole diameters were maximised (point 4 above). Plate thickness, porosity and the number of rings were copied from the Mark 2 conditioner.

Mark 4 was designed to introduce higher pressure loss in order to increase the ability to handle more asymmetric inlet profiles than the previous versions. The porosity was defined to be 0,40 in this model.

Mark 5 was designed from the same concept as Mark 3 and Mark 4, but was given larger porosity in order to reduce the pressure loss coefficient. For Mark 5 the hole diameters were maximised. A pressure loss coefficient equal to 2,0 was specified which yields an overall porosity equal to 0.53.

Some design data are listed in table 1 below :

| FC | Porosity | Pressure loss coefficient |
|------------|----------|---------------------------|
| Mark 2 | 0,51 | 2,38 |
| Mark 3 | 0,51 | 2,57 |
| Mark 4 | 0,40 | 4,65 |
| Mark 4, ch | 0,40 | 3,28 |
| Mark 5 | 0,53 | 2,13 |

Table 1.
The prescribed overall porosity of the FCs and the measured pressure loss coefficients obtained from experiments using air at atmospheric pressure.

All FCs have one centrehole and 4 concentric rings with holes. The thickness is common for all FCs and equal to 0.357D. Figure 5 shows the basic layout.

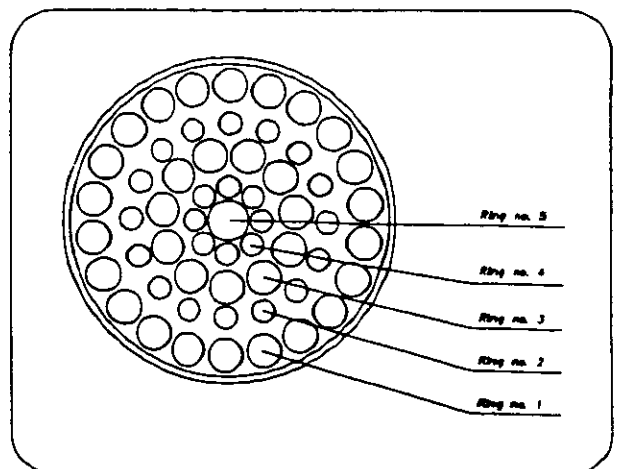


Figure 5.
K-Lab Mark 2 flow conditioner

3. EXPERIMENTAL SET UP FOR THE ATMOSPHERIC TESTS

3.1 THE TEST SECTION

The experiments using air at atmospheric pressure were done in a test rig of plexiglas having an internal pipe diameter equal to 140mm. Air is sucked through the loop by a positive displacement pump yielding constant volumetric flowrate. The pipe Reynolds number in the test section is $2.6 \cdot 10^5$. In this project three different geometrical disturbances at the inlet to the test section have been used.

3.2 THE SINGLE BEND RIG

In the single 90°-bend geometry a 9D straight pipe with a perforated plate at the inlet followed by a 90° bend is connected to the test section. The radius of curvature of the bend is 1.5D. The set up is shown in figure 6. Axial velocity profiles and swirl angle profiles can be measured at 1D, 3D, 5D, 10D and 15D, while the FC can be installed 3D, 4D, 5D, 6D, 7D and 8D downstream of the bend.

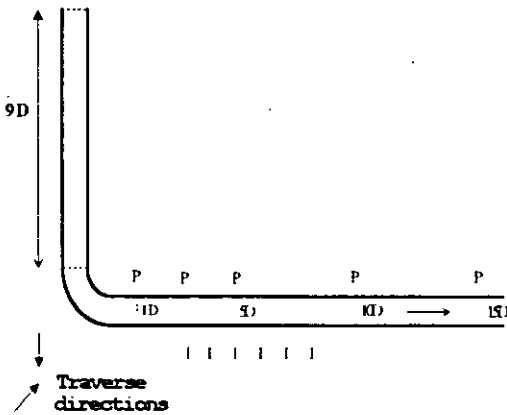


Figure 6.
The single 90° bend geometry. The points P represent the traverse positions, the points I the positions for flow conditioner installation. The curvature of the bend is 1.5D.

3.3 THE TWISTED S-BEND RIG

A twisted S-bend with a perforated plate at the inlet is connected to the test section, and traverses to measure the axial velocity profile and the swirl angles can be done at 1D, 3D, 5D, 10D and 15D downstream from the second bend. The flow conditioner can be positioned at 3D, 4D, 5D, 6D, 7D and 8D, see figure 7. The length of straight pipe between the two bends is 1.25D, and the radius of curvature of the bends is 1.5D.

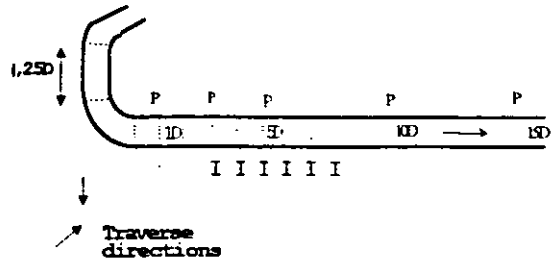


Figure 7.
The twisted S-bend geometry. The points P represent the traverse positions and the points I the positions for flow conditioner location. The curvature r/D of the bends is 1.5D.

3.4 THE FLAT PROFILE TEST RIG

In order to study the flow disturbances caused by the flow conditioner itself, a special set up referred to as the flat profile test rig, was built. The rig consists of a 10D long straight pipe upstream of the flow conditioner with a perforated plate positioned at the pipe inlet. Downstream of the flow conditioner the velocity profiles can be measured at 5D, 6D, 7D, 8D, 9D, 10D and 12D. A drawing of the set up is shown in figure 8.

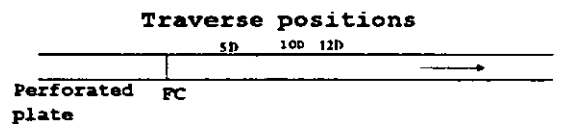


Figure 8.
The flat profile test rig

3.5 PRIMARY MEASUREMENT DEVICES

A pitot static tube was used for the axial velocity profile measurements. The swirl angles were measured by a 10mm thick 2 hole cylinder pitot tube. Both these instruments were connected to a differential pressure manometer type 5 Airflow manufactured by Airflow Development.

4. ATMOSPHERIC TEST RESULTS

4.1 INTRODUCTORY REMARKS

Mark 2, Mark 3, Mark 4 and Mark 5 which all have the same basic layout with one centerhole and 4 concentric rings with holes were tested in the air loop. Only the main conclusions from these experiments will be presented here.

The results obtained with Mark 2 are presented in ref. 4. With Mark 2 the ISO-5167 section 7.4 requirements were fulfilled 15D downstream from the single bend and the twisted S-bend.

Mark 3 gave better results than Mark 2. With Mark 3 the ISO-5167 requirements were fulfilled 12D downstream from the bend. Mark 4 was even better and the required length between the bend and the orifice plate was reduced to 11D.

Mark 5 exhibited the lowest pressure loss coefficient which is considered as a very important property for a FC. If a Short Metering System with Mark 5 fulfils the ISO-5167 requirements at 15D downstream of the tested disturbances and has good orifice meter performance, this FC-model can therefore be considered as an optimum design based upon our requirements mentioned in Section 1.2. In the following attention will only be given to the results obtained using Mark 5.

4.2 REFERENCE VELOCITY PROFILE

The fully developed velocity profile measured downstream from 101D lengths of straight pipe is shown in figure 9. The pipe Reynolds number was $2.6 \cdot 10^5$. The profile will be used as "reference profile" in the subsequent graphs.

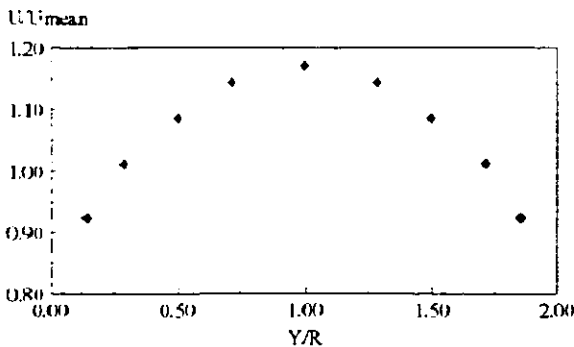


Figure 9.
Fully developed velocity profile measured downstream of 101D straight pipe. $Re = 2.6 \cdot 10^5$.

4.3 TEST OF THE DISTURBANCE INTRODUCED BY THE FLOW CONDITIONER ITSELF

Axial velocity profiles measured downstream of the Mark 5 FC in the Flat Profile Rig are shown in Figure 10. The profile at 5D has almost recovered to fully developed but is still too peaked. At 12D the measured profile is identical to the fully developed velocity profile in Figure 9.

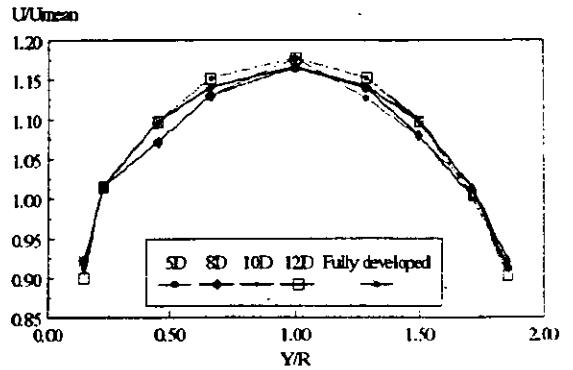


Figure 10.
Axial velocity profiles. Mark 5 positioned downstream of flat velocity profile.

4.4 SINGLE BEND TESTS

Figure 11 and 12 show the velocity profiles in two perpendicular planes when no flow conditioner was installed. The corresponding swirl angles are presented in Figure 13. The traverse directions are defined in Figure 5. In Figure 14 the results obtained with the flow conditioner located at 8D are presented as percentage deviations in U/U_{mean} from the corresponding ratios in the fully developed profile. The dotted lines visualise the ISO-5167 requirement to the deviation of the axial velocity profile from the fully developed profile.

The swirl angles were measured at the same positions as the velocities. Maximum deviation between the swirl angles measured within the same traverse was 0.5 degrees, which is comfortably within the ISO-5167 requirement. However, the relative swirl along each traverse is measured to within ± 0.5 degree uncertainty. Thus, a maximum variation in the swirl angle measurements of 1 degree means that no swirl actually has been detected in the flow.

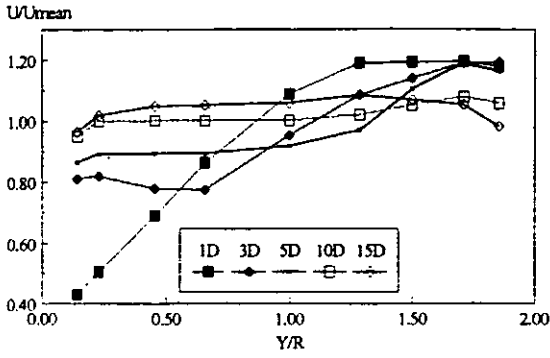


Figure 11.
Measured axial velocity profiles downstream of the single 90° bend. Vertical traverses. No FC was installed downstream of the flow disturbance.

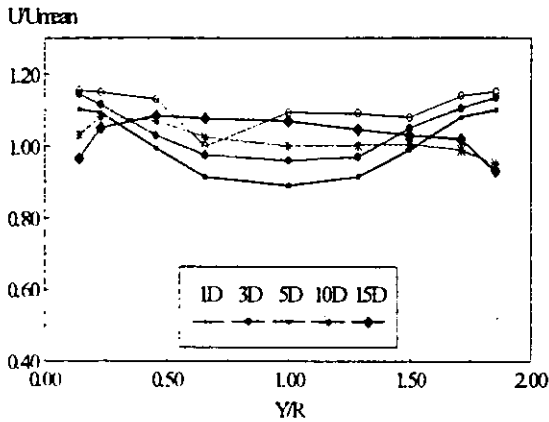


Figure 12.
Measured axial velocity profiles downstream of the single 90° bend. Horizontal traverses. No FC was installed downstream of the flow disturbance.

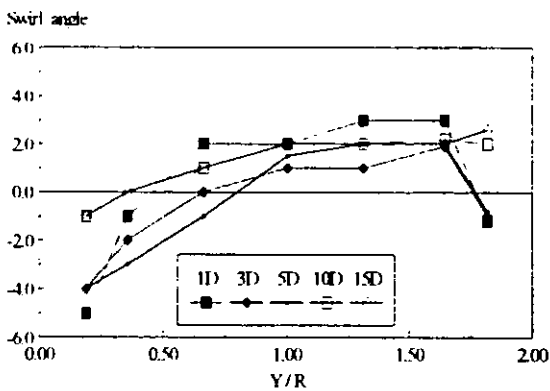


Figure 13.
Measured swirl angle profiles downstream of the single 90° bend. Horizontal traverses. No FC was installed downstream of the flow disturbance.

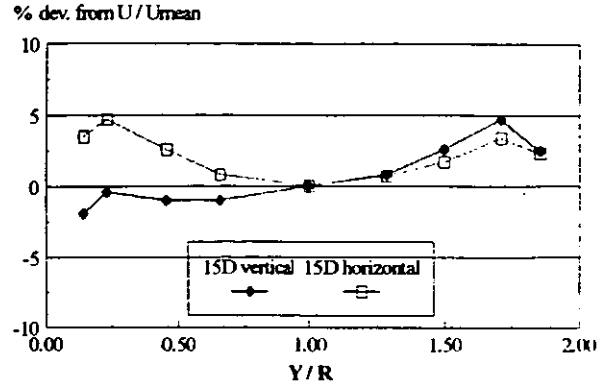


Figure 14.
Deviation of the measured axial velocity profile from the fully developed profile downstream of the 90° bend. Mark 5 was installed 8D downstream of the flow disturbance.

4.5 TWISTED S-BEND

The axial velocity profiles measured downstream of the twisted S-bend with no FC installed in the rig are shown in figure 15 and 16. The corresponding swirl angle profiles are plotted in figure 17. The traverse directions are defined in Figure 7. Figure 18 presents the deviation in U/U_{mean} from the corresponding ratios in the fully developed velocity profiles when the FC was installed 8D downstream from the last bend. The measurements were done at 15D.

Also for this configuration traverses of the swirl angles were measured, and again the maximum swirl angle found was 0.5 degrees, which mean that no swirl has been detected in the flow.

4.6 CONCLUSION OF AIR TESTS

The ISO-5167 requirements are satisfied both with respect to the axial velocity profile and the swirl angles 15D downstream of a single 90° bend and a twisted S-bend when Mark 5 is installed 8D downstream of the flow disturbance. Figure 14 and 18 show that the velocity profile is not completely developed. The aim was however, to satisfy the ISO-requirements, and therefore this performance is acceptable.

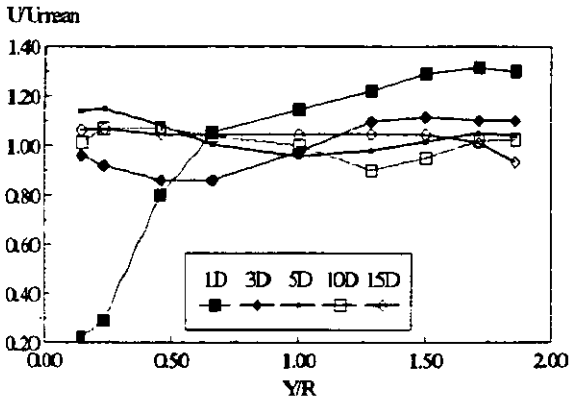


Figure 15.
Measured axial velocity profiles downstream of twisted S-bend. Vertical traverses. No FC was installed downstream of the flow disturbance.

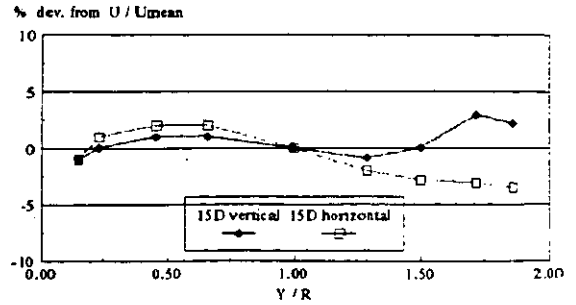


Figure 18.
Deviation of the measured axial velocity profile from the fully developed profile downstream of twisted S-bend. Mark 5 was installed 8 D downstream of the flow disturbance.

5 EXPERIMENTAL SET-UP FOR THE HIGH PRESSURE TESTS

5.1 HIGH PRESSURE TEST LOOP

The high pressure tests were performed at 100 bar and 37°C in dry natural gas (85% methane, 13% ethane and 2% other components).

All the tests were carried out in a 6 inch nominal bore test section with an internal pipe diameter of 140mm. The FCs were tested downstream of a single 90° bend and a twisted S-bend similar to those used in the atmospheric air rig.

The reference flowmeters are a bank of sonic nozzles, built according to ISO-9300, which have been primary calibrated in a gravimetric calibration rig over the range 20 to 100 bar. For the discharge coefficient (C_d) measurements a 6" Daniel Orifice meter (model M7591) was used. All applied instruments had calibration certificates traceable to international standards.

5.2 SWIRL PROBE

A swirl probe was designed and manufactured to measure velocity and swirl in natural gas up to 150 bar in the test-section. Before the final design was made, the performance of 3 cylindrical Pitot probe was investigated.

The following probes were tested :

- 10mm diameter 2-holes probe with 60° between the holes
- 17mm diameter 2-holes probe with 60° between the holes
- 17mm diameter 3-holes probe with 36.2° between the holes

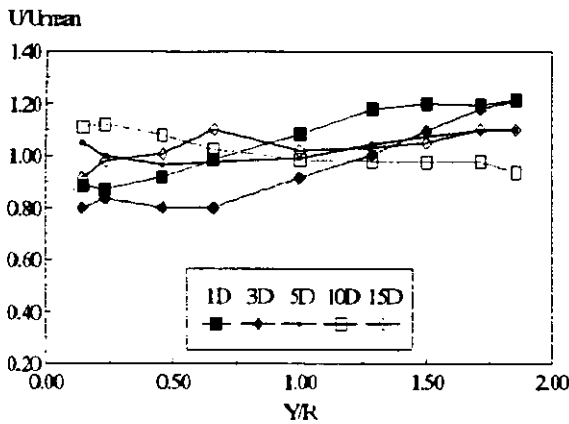


Figure 16.
Measured axial velocity profiles downstream of twisted S-bend. Horizontal traverses. No FC was installed downstream of the flow disturbance.

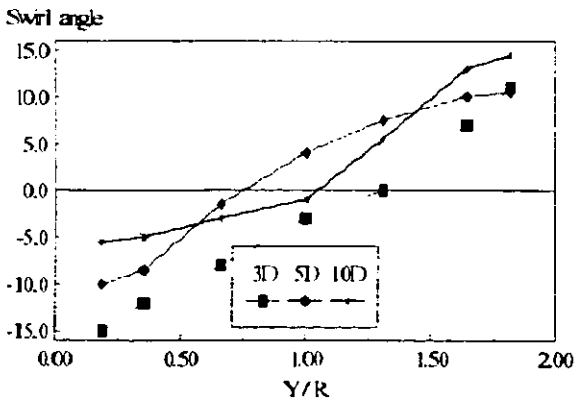


Figure 17.
Measured swirl angle profiles downstream of twisted S-bend. Horizontal traverses. No FC was installed downstream of the flow disturbance.

The results are described and discussed in ref. 6. Based upon this study the swirl probe was designed with a 12mm cylinder and 3 holes with 35.4° between the holes.

6.0 HIGH PRESSURE TEST RESULTS

6.1 REFERENCE VELOCITY PROFILE

As mentioned earlier, the Mark 2 to Mark 5 FCs have been designed to produce a 9th power law velocity profile given by equation (4). From figure 19 it can be seen that the 9th power law velocity profile fits the measured velocity profile 341D downstream of a twisted S-bend at a Reynolds number $1.5 \cdot 10^7$ very well.

Thus the 9th power law profile has been used as reference profile for the high pressure tests.

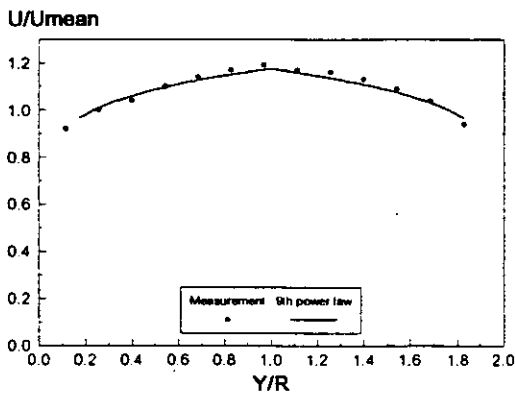


Figure 19.
Fully developed velocity profile. $Re = 1.5 \cdot 10^7$

6.2 SINGLE BEND TESTS

Figure 20 shows the horizontal velocity profile 15D downstream of the single bend at 2 different Reynolds numbers when no FC was installed in the rig. It can be seen that some of the measurements are outside the ISO-5167 recommendation. Figure 21 shows the velocity profile when Mark 5 is used. The results are now within the 5% band of the fully developed velocity profile. Both with and without the FC the swirl measured at this position is well within the ISO-5167 requirements.

6.3 TWISTED S-BEND TESTS

The horizontal velocity profile 15D downstream of the twisted S-bend can be seen in Figure 22. The same profile when Mark 5 is used is shown in Figure 23.

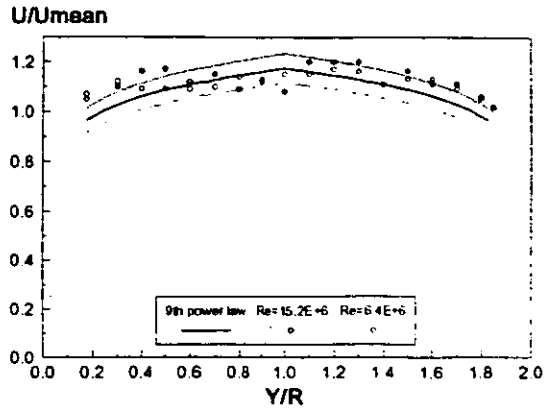


Figure 20.
Horizontal velocity profile 15D downstream of a single 90° bend.

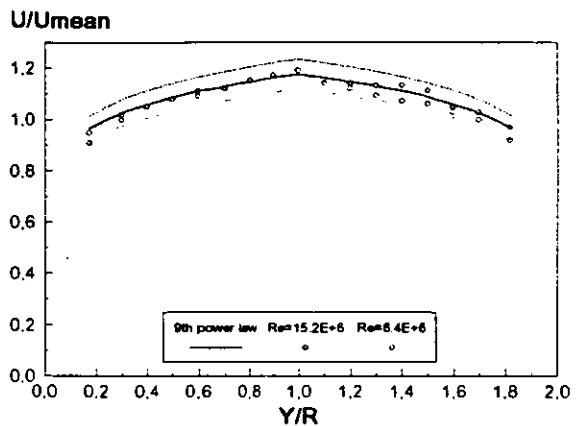


Figure 21.
Horizontal velocity profile 15D downstream of a single 90° bend when Mark 5 is used.

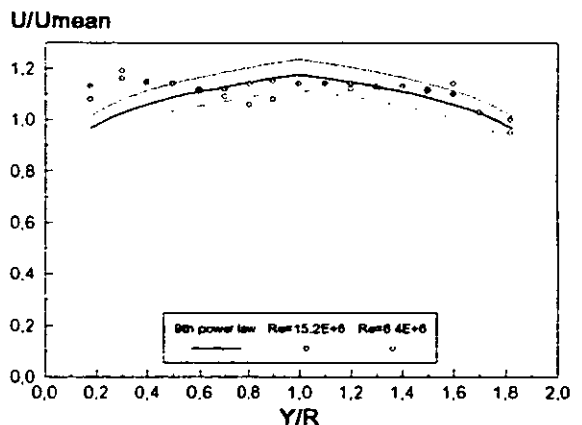


Figure 22.
Horizontal velocity profile 15D downstream of a twisted S-bend.

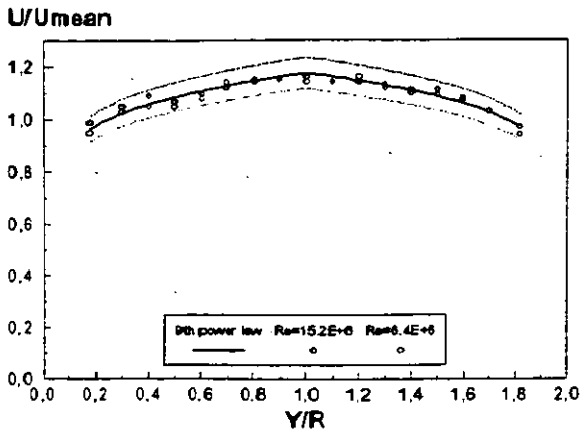


Figure 23.
Horizontal velocity profile 15D downstream of a twisted S-bend when Mark 5 was used.

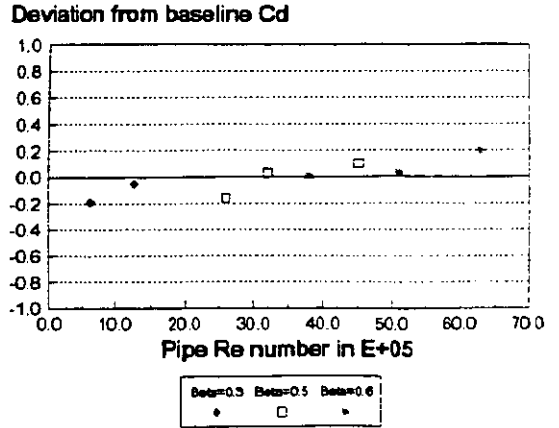


Figure 26.
 ΔC_d for a 15D SMS with Mark 5. Deviation from "baseline" C_d measurements.

The swirl angle for this configuration with and without the FC is shown in Figure 24. From the results presented above it is demonstrated both how Mark 5 transforms the velocity profile from distorted to nearly fully developed and how it removes the swirl.

6.4 MEASUREMENTS OF DISCHARGE COEFFICIENT

The aim of the ISO-5167 recommendation is to describe how to build an orifice gas metering station and obtaining a gas measurement-error within +/- 1.0%.

The ultimate question is then how well a Short Metering System (SMS) with Mark 5 FC and an overall length of 15D behaves when it is calibrated. In figure 25 tests between the flow element and the upstream disturbances are shown for β -ratios equal to 0.2, 0.6 and 0.75. The results show that the C_d deviations from the reference sonic nozzles are within +/- 0.5%. The tests were done at 100 bar with Reynolds number between $5 \cdot 10^4$ and $2 \cdot 10^7$.

Normally the performance of the FCs is compared against some "base-line" C_d calibrations. For some common β -ratios (0.3, 0.5 and 0.6) these calibrations were carried out at 48D lengths of straight pipe with Mark 5 installed at the inlet. Then the results obtained at 15D downstream of a twisted S-bend were checked against these "baseline" data. The results are found in figure 26. It can be seen that all the results are within +/- 0.2%.

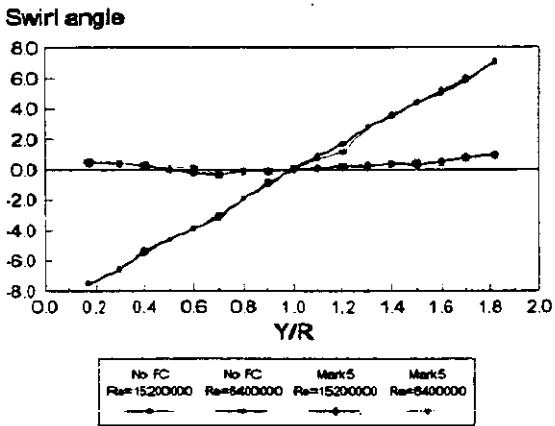


Figure 24.
Horizontal swirl angle profile 15D downstream of a twisted S-bend. Results with and without Mark 5.

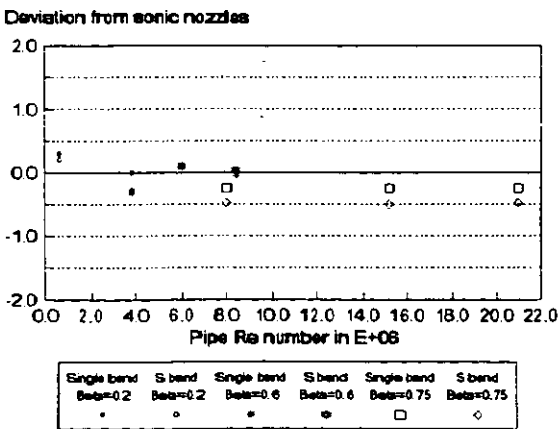


Figure 25.
Calibration of a 15D SMS with Mark 5. Results for different configurations and different beta-ratios.

These "baseline" Cds are also compared against data obtained with the upstream length required by ISO-5167 downstream of a twisted S-bend. The results are shown in figure 27. It can be seen that all these Cds are lower than the "baseline" data, and in the worst case the deviation is nearly 0.5%.

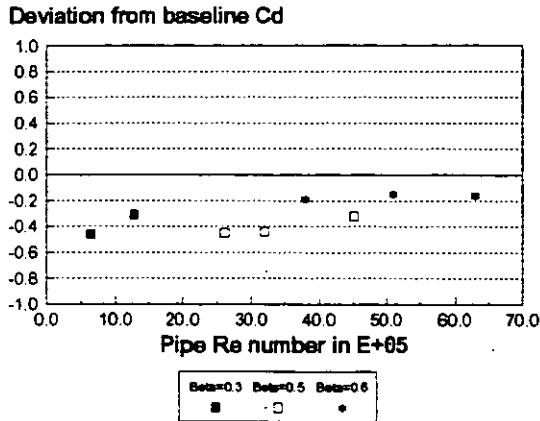


Figure 27.
Cd between normal ISO-5167 installation length downstream from a twisted S-bend and "baseline" Cd measurements.

6.5 DISCUSSION

It has been shown that also at high pressure (100 bar) Mark 5 effectively eliminates the swirl 15D downstream of a single bend and a twisted S-bend. The velocity profile at this position for the 2 configurations examined is not 100% developed but well within the ISO-5167 recommendation which was the objective to reach for the development project.

The measurements of the discharge coefficient show that the performance of a SMS with a total length of 15D compares with the sonic nozzles within +/- 0.5%. This is good results as a normal ISO-installation may have an uncertainty up to 1%.

The Cd-shift between the "base-line" calibration and the SMS-system is within +/- 0.2% at Reynolds number between $6.4 \cdot 10^5$ and $6.3 \cdot 10^6$. Also these results are considered very satisfactory as they have been obtained at high pressure (100 bar). However this Cd-shift is wanted as low as possible, and there is still some room for improvement here (+/- 0.1%).

Another finding during these tests is that today's ISO-5167 recommendation does not require long enough upstream lengths after twisted S-bends for the removal of swirl. It is well known that swirl cause

undermeasuring of the flow (ref. 7) which is also shown in figure 27. These testresults (fig. 24) demonstrate that Mark 5 is an efficient swirl-remover and avoid this undermeasuring.

To summarise, this SMS shows small deviation (within +/- 0.2%) from the "base-line" Cd-data. It also gives better results than a standard ISO-5167 installation downstream of a twisted S-bend, confirming that the SMS-concept with Mark 5 installed fully compares with an ISO-5167 installation as was the project objective.

The interest for FCs in the metering community is increasing continuously because the large demand for cheaper and better metering systems. The challenge now is therefore to further collect performance data for a result-database and work for general acceptance of this technology. All the attention the FCs have received the last couple of years confirms the promising potential of this technology.

The metering technology evolves all the time, and it is still possible to slightly improve the performance of the FCs. The new tabs/vanes FC is an example of an encouraging improvement (ref. 8) where K-Lab and University of Salford co-operate.

7.0 CONCLUSION

In this paper the main research activities in developing a good FC is described. The aim was to build a Short Metering Systems (SMS) of maximum 15D which fulfilled the ISO-5167 requirements.

- First a theoretical design model was developed.
- From that model FCs with different porosity (between 0.4 and 0.51) and pressure loss coefficients (between 2.13 and 4.65) have been designed.
- The different FCs were then tested in air at atmospheric pressure. Mark 5, which has the lowest pressure loss coefficient of 2.1, fulfilled the ISO-5167 requirements 15D downstream of a single 90° bend and a twisted S-bend.
- A cylindrical Pitot probe with 3 holes for measuring velocity and swirl in a 6 inch pipe up to 150 bar was designed and manufactured.
- The performance of the SMS with Mark 5 was tested at 15D at high pressure. The ISO-5167 requirements for fully developed flow were fulfilled.
- The SMS with β -ratios equal to 0.2, 0.6 and 0.75 were tested against sonic nozzles at 100 bar for Reynolds numbers between $5 \cdot 10^4$ and $2 \cdot 10^7$. The results showed a deviation within +/- 0.5%.
- The SMS was also compared against "base-line" Cd data for common β -ratios, (0.3, 0.5 and 0.6). All

the results were within +/- 0.2%.

- The comparison between a 15D SMS with Mark 5 and an ordinary installation with normal ISO requirements for upstream lengths, shows that the SMS with Mark 5 performs similarly or better.
- Since Mark 5 fulfils the ISO-5167 requirements and gives good Cd performance at 15D, this FC can be applied in Short Metering Systems.

ACKNOWLEDGEMENTS

The authors wish to acknowledge the contributions of Dr. Paul Wilcox from K-Lab who initiated the project in 1987 and Dr. Trond Weberg from IFE who was the main architect behind the theoretical design model.

REFERENCES

- /1/ - Kreith, F. and Sonju O.K.
- The decay of turbulent swirl in a pipe.
- J. Fluid Mech. 25 (1965) 257.
- /2/ - Hannisdal, N.E.
- Metering study to reduce topsides weight
- North Sea Flow Measurement Workshop, 1992.
- /3/ - Gallagher J.E. and Beaty R.E.
- Orifice metering research - a user's perspective
- North Sea Flow Measurement Workshop, 1992.
- /4/ - Wilcox P., Weberg T. and Erdal A.
- Short gas metering systems using K-Lab flow conditioner.
- 2nd International Symposium on Fluid Flow Measurement in Calgary, June 6-8, 1990.
- /5/ - Wilcox P. and Erdal A.
- Seminar on installation effects on flow metering.
- NEL, October 22, 1990.
- /6/ - Thomassen D. and Prein B.
- Examination of the performance of three cylinder pitot probes in swirling flow.
- Report no.: IFE/KR/F-87/171
- /7/ - Bates I.P.
- Field use of K-Lab flow conditioner
- North Sea Flow Measurement Workshop 1991.
- /8/ - Laws E., Onazzane A.K., Erdal A.
- Shortening Installation lengths using a low loss flow conditioner.
- North Sea Flow Measurement Workshop 1994.

DESIGN OF A TUBE BUNDLE CONDITIONER FROM AERODYNAMIC CONCEPTS

P. GAJAN^{*}, A STRZELECKI^{*}, M BOSCH^{**}, D. DONAT^{***}

^{*}ONERA/CERT/DERMES, 2 avenue Edouard Belin, 31055 Toulouse cedex, France

^{**}Gaz du Sud Ouest, 49 avenue Dufau, B.P 522 64010 PAU cedex, France

^{***}Centre d'essai de Gaz de France, 3 chemin de villeneuve, 94140 Alforville, France

Summary

This paper presents an investigation on the behaviour of a tube bundle flow conditioner from experimental and flow modelling analyses. For a given geometry, the method of calculation gives the velocity profiles and the flow development downstream of the conditioner. From these results, two devices were designed and tested both in laboratory and industrial environment. For a fully developed upstream flow or for a swirling flow obtained downstream of two bends in different planes, the comparison between the prediction and the experiments is satisfactory. When the upstream flow is non symmetric like downstream of a U bend, the results show that the flow conditioner does not cancel entirely the flow asymmetry.

Introduction

Since twenty years, many studies have investigated the influence of the flow characteristics on the behaviour of different flowmeters. They have shown the necessity to place important lengths of straight pipe upstream of the metering device in order to ensure accurate flow counting. Nevertheless these lengths, which may reach 100 pipe diameters, can not always be achieved and the use of special devices called flow straightener or flow conditioner seems to be necessary.

As indicate in [1], while a number of such conditioner are included in international Standards ISO 5167 and ASME/ANSI 2530, there are considerable differences between installation lengths recommended in these two Standards. Furthermore, HUMPHREY[2] and SMITH[3] have shown that in many cases, the distance indicated in Standards are not sufficient to ensure the flow metering accuracy expected. Nevertheless, as pointed out by LAWS[1], in most studies, the performance of the flow conditioner was judged, not by the quality of the flow produced, but by the effect on the flow metering.

In order to improve the behaviour of such a device in many industrial configurations, recent works were undertaken to analyse the flow up and downstream of different flow straighteners and classify their performance[1,4,5,6]. In these studies new types of devices are proposed. Nevertheless, despite of the great number of results presented, no information is provided to answer the following questions: How these straighteners are designed? What are the useful geometrical parameters which influence the flow mixing and the flow development? In particular, even if in a recent paper LAWS[1] pointed out the role of the turbulence profile on the flow development, no result provides information about the « best » turbulence profile to be achieved close downstream of the conditioner.

Although, following the conclusion of recent work[1,5,7], it seems that the perforate plate flow conditioner are more efficient in terms of flow quality and pressure loss than tube bundle devices, we present in this paper a study performed between 1984 and 1988 with the financial support of Gaz de France and Gaz du Sud Ouest on the design of a tube bundle flow conditioner/orifice plate package. The tube bundle system is of the same type than SENS and TEULE [8] and HEBRARD and BOSCH[9] conditioners. This means that, contrary to the tube bundle systems proposed in Standards, the length of the different tubes depends on their radial positions. So, the outlet of the different tubes are not in the same plane. The aim of this work is to understand how such a system works? and what are the optimal geometrical parameter (tube length distribution, tube diameter) which ensure a « good flow » with the lower pressure loss?. From this study, two systems were designed and tested in industrial environment on the Gaz de France facilities

1. Experimental analysis of the flow conditioner behaviour.

1.1 Description of the flow conditioner

The geometry of the flow conditioner is presented in figure 1. It is made of concentric rings of small tubes with an internal diameter d_i . The radial position of the i^{th} ring is r_i . These tubes are combined so that one face of the flow conditioner is flat.

1.2 Description of the flow through the conditioner

The flow through the conditioner is schematised in figure 2. It can be divided in four zones. In the first one, upstream of the system, the fluid accelerates due to the diminution of the section. The static pressure decreases to a minimum value corresponding to the contraction of the flow at the inlet of the small tubes. In the second zone, in each individual tubes, the flow characteristics move from the inlet conditions (velocity, pressure) to fully developed ones. From the experimental results of DIESSLER[10], it is possible to calculate for each tube the static pressure variation between the inlet and the outlet [11]. In the third zone, the mixing of the

small jets issued from each tube occurs. The static pressure increases due to the flow expansion. This flow region is essential in the behaviour of the flow conditioner and was studied in details. In the fourth zone, downstream of the jet mixing zone, the flow develops to the steady conditions. This flow development is mainly influenced by the flow conditions occurring at the end of the mixing jet region and in particular by the velocity gradients.

1.3 Experimental study of the mixing zone

The aim of this study is to understand the role of the decay of the outlet of the small individual tubes on the mixing of the small jets and so on the flow conditions obtained at the end of this region. For this, a simplified flow conditioner was built with only a central tube and two rings (six tubes on the first and twelve on the second). These tubes have the same length and the same diameter d_t . At the inlet of each individual tube, a same small perforated plate is placed in order to ensure a same flowrate in each of them. The internal diameter d_i of the tubes is 11 mm and their length is 300 mm. The set-up used permits to place the outlet of each individual tubes at a given longitudinal position and so to impose a given decay between two rings. This device is placed in a 100 mm pipe. The velocity and turbulence profiles are measured with a constant temperature anemometer (CTA).

Detailed results may be found in [11]. Nevertheless the main conclusions of this work are:

- The shape of the velocity profile obtained at the end of the mixing zone is greatly dependant on the decay between the outlet of the small tubes. In particular, the maximum in the velocity profiles is achieved at the radial location corresponding to the most shifted tubes(figure 3).
- The pipe wall influences the mixing process.
- In a given pipe section, the static pressure is approximately constant
- The static pressure can be described by an analytical expression given by TYLER and WILLIAMSON[12].
- The length of this zone depends on the tube diameter and on the radial distance between two rings.

1.4 Experimental study of the flow development downstream of the mixing zone

The length of this zone i.e. the distance between the end of the mixing zone and the section where the flow is fully developed mostly depends on the flow characteristics obtained at the end of the mixing zone¹. In order to analyse the influence of these flow characteristics on the flow development, many tests were performed with different flow conditions (velocity profile, turbulence profile). In figures 4 to 7, the flow development obtained for different initial conditions are plotted. These results show that the rate of development of the flow towards steady conditions depends on the intensity and the location of the velocity gradients. The existence of steep velocity gradients induces an important production of energy of turbulence and therefore an increase in the turbulence levels. Furthermore, the existence of high levels of turbulence produces a radial diffusion of momentum. Consequently, it seems preferable to obtain at the end of the mixing zone, not a smooth velocity profile but flow conditions with steep radial gradients which ensure a rapid development of the flow.

2 Optimisation of the flow conditioner

In the study presented in the previous paragraph, the different parameters which may modify the performance of the flow conditioner were pointed out. Nevertheless, in order to perform a quite exhaustive analysis of these parameters, it is necessary to develop numerical methods.

The method used is divided in two parts. In the first part, the velocity profile obtained at the end of the mixing zone is calculated from an integral method. The choice of the first method was done in consideration of the complex 3D phenomena occurring in the jet mixing zone. In this method an balance equation for momentum is solved for each ring. The interaction of two different jets is modelled from the experimental results. In the second part, the flow development further downstream is predicted with a classic k - ϵ method in axisymmetric form. The correlation between the inlet U -profile and the inlet conditions for turbulent quantities (energy k and rate of dissipation ϵ) has been fixed from experimental results.

Details about these methods of flow modelling may be obtained in [11, 13].

¹ The development is also influenced by the pipe roughness but this factor has not be taken into account in this study

These different tools were then used in the following steps. At first, the $k-\epsilon$ method was applied to define the optimal U-profile needed at the end of the mixing region. Then the integral method was used to fix the geometry of the conditioner (shape, tube diameter). This choice imposes the pressure loss induced by the flow conditioner. Two straighteners were defined with two tube diameters (CERT 1: $d_t = 5$ mm and CERT 2: $d_t = 10$ mm respectively). The internal pipe diameter D is equal to 100 mm.(figure 8). In both cases, the length of the smaller tubes was fixed to 40 mm. These two flow straighteners were tested in laboratory environment with different upstream flow conditions (fully developed profile, uniform profile, swirling flows, non-symmetric profile). Figure 9 shows a comparison between the flow development obtained experimentally downstream of the first flow conditioner ($d_t = 5$ mm) with an upstream uniform profile, and the prediction given by our numerical method. At 6.5 pipe diameter D , the flow characteristics have been judged to be sufficiently closed to the fully developed conditions to ensure good accuracy with an orifice plate flow conditioner². For this reason the overall length of the package has been fixed to 6.5 pipe diameters. The pressure loss coefficient $K (= \Delta P / (1/2\rho U_0^2))$ for the first device varies from 3.9 to 3.7 for Reynolds numbers between 30,000 and 80,000.

3 Tests of the CERT flow conditioners

These two flow conditioners were tested both in laboratory and industrial environment for different upstream flow conditions. These tests included velocity and turbulence measurements and metering error with an orifice plate placed 6.5 pipe diameter downstream of the flow conditioner. The upstream flow perturbations were created either by flow generators (swirling flows, non symmetric flows) or by bend arrangement (two bends in different planes or a U bend). In this last case the flow conditioner is placed just at the outlet of the second bend.

3.1 Flow measurements

In figure 10, the U-profile obtained in gas downstream of the first flow conditioner with an upstream flow condition fully developed is plotted. It is compared with the flow measured downstream of 300 D of straight pipes. It can be noted that the CERT flow conditioner do not modify the fully developed conditions near the wall. On the centreline, a slight deficit can be noticed.

²These reasonable flow conditions were obtained from an analysis of different works on orifice plate measurements [11, 14]. This analysis try to link metering errors obtained downstream of various devices with flow conditions measured at different locations downstream of this devices.

In figure 14, the turbulence levels u/U_0 are presented. They are compared with the results of LAWS [1] (50% porosity Laws plate preceded by vanes positioned 0.5 D upstream) It can be seen that the first CERT conditioner gives better results than the second. When compared to LAUFER's results ($Re = 50,000$), the LAWS conditioner seems to be more efficient than the two CERT devices.

The flow conditions obtained when the conditioner is placed downstream of two bends in different planes are plotted in figure 12. It can be seen that, as for in fully developed flows, the velocity near the wall is well described. Nevertheless, in the centre of the pipe the velocity is too weak. In this case, the LAWS conditioner gives better results.

The behaviour of the flow conditioners with an upstream non symmetric flow is investigated in figure 13. The characteristics of the flow at the outlet of the U bend are not available. If the CERT conditioner attenuate the upstream flow perturbation, it is evident that they does not remove it entirely. Nevertheless the comparison between the profiles obtained for different conditions shows that the «signature» of the flow conditioner is always noticeable (figure 14). Although the results obtained by LAWS show that the asymmetry, still appears 5.5 D downstream its plate, its device is obviously more efficient.

3.2 Metering error

These tests were performed with an orifice plate flowmeter placed 6.5 diameters from the downstream face of the conditioner. For non symmetric flows, the β ratio is fixed to 0.57. For swirling flows, a 0.4 β ratio is considered. These results are plotted in figure 15. It can be seen that for a non symmetric flow, the metering error is about 1% for the two flow conditioner. This results confirmed the poor efficiency of these devices concerning such flows. For swirling flows, the errors obtained is near 0.5 %. This is due to the shape of the velocity profile and in particular the low velocities near the pipe axis. This is confirmed by a recent study on orifice plate flow meters in which the metering error has been linked to the velocity deficit on the pipe axis[15]. In this work the C_D deviation is compared to the variation of the dynamic pressure ($1/2 \rho U^2$) on the pipe axis due to the flow acceleration. between an section located upstream of the orifice plate and the vena contracta. When the upstream flow is flatter than a fully developed flow, this variation rises. This increase of the dynamic pressure variation corresponds to an increase of the pressure difference measured between the two faces of the plate and so, a decrease of the discharge coefficient. In this study, a good correlation is obtained between the discharge coefficient variation measured from ΔP measurements and the discharge coefficient variation computed from the flow acceleration on the pipe axis. For an orifice plate of β ratio equal to 0.4 the discharge coefficient variation obtained for a flat profile is about 0.5%. These recent studies permit to quantify the influence of an upstream velocity profile

distortion on the flow counting by an orifice plate. Such information were not available in 1988. This may explain the poor efficiency of this package.

Conclusions

This paper presents an attempt to design a flow conditioner from aerodynamic concepts. It shows how, from a detailed analysis of the flow through the straightener, it is possible to determine the shape which corresponds to the best compromise between its efficiency, its pressure loss and its cost. This definition needs flow modelling methods to analyse the influence of all the geometric parameters. The results show a good correlation between the flow condition predicted and the experiments. For symmetric flows, the tests in industrial conditions have confirmed these conclusions. Nevertheless it seems that these devices do not permit to eliminate the non symmetric flow perturbation. The use of three dimensional flow computation may be consider in order to improve the efficiency of the flow conditioner.

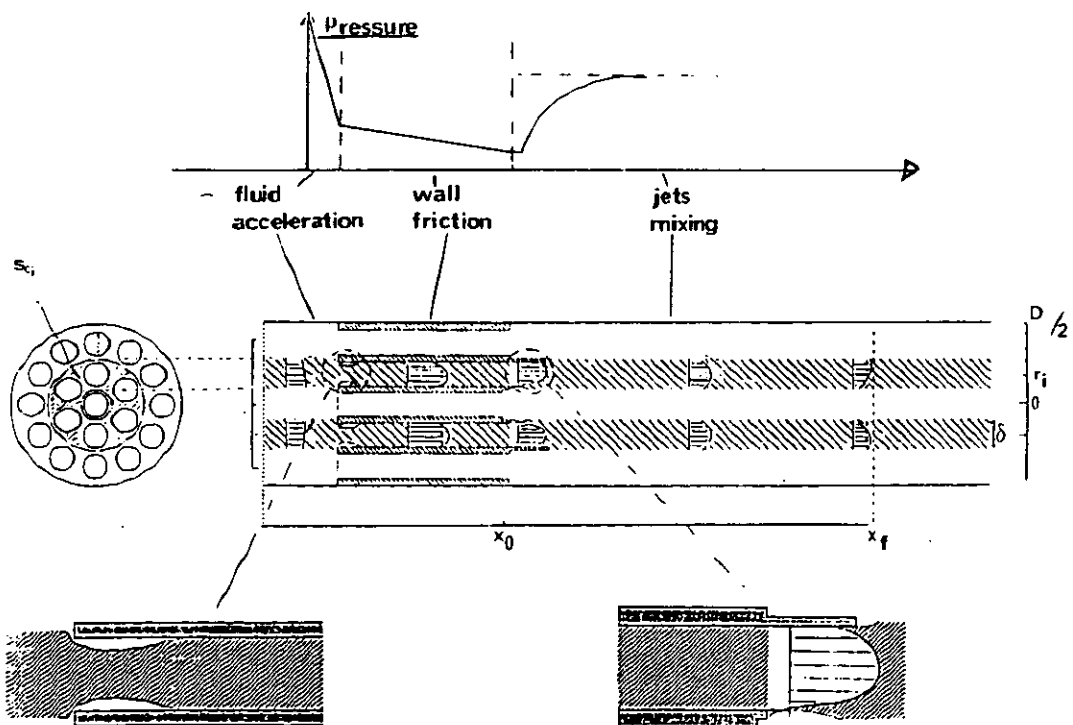
In the present work, the « good » flow condition to be produce by the flow conditioner has been defined from an bibliographical analysis of the different studies on flow metering and fluid mechanics available at this time. This extrapolation done from the different results taken into account was not sufficiently accurate to ensure a precise flow counting with an orifice plate flow meter. Nowadays, more recent works on orifice plate can be used to precise the actual flow condition needed downstream of a flow conditioner.

References

- [1] LAWS E.M., OUAZZANE A.K.: *Compact installations for differential flowmeters*, Flow Meas. Instrum., Vol 5, N 2, 1994
- [2] HUMPHREY J.S., HOBBS J.: *An investigation of the effectiveness of flow conditioners*, Int. Symp. on Fluid Flow Meas., AGA, Washington, 1986.
- [3] SMITH D.J.M.: *The effect of flow straighteners on orifice plates in good flow conditions*, Int. Symp. on Fluid Flow Meas.in the Mid 80's., vol 1, Glasgow, 1986
- [4] LAWS E.M., OUAZZANE A.K: *Effect of plate depth on the performance of a Zanker flow straightener*, Flow Meas. Instrum., Vol 3, N 4, 1992
- [5] SPEARMAN EP., SATTARY J.A., READER-HARRIS M.J.: *Comparison of velocity profiles downstream of perforated plate flow conditioners*, Flomeko'94., 1994
- [6] STUART J.W.: *Experimental results of an improved tube bundle flow conditioner for orifice metering*, Flomeko'94., 1994

- [7] LAWS E.M.: *The effect of length on the performance of Tube bundle flow conditioners*, FLOMIC report., August 1990
- [8] SENS M., TEULE C.: *Theoretical and experimental study of a new flow straightener*, ATG Conference, Paper 7.1, FRANCE, 1975
- [9] BOSCH M., HEBRARD P.: *Experimental and theoretical study of a new flow conditioner*, Proc. Int. Conf. Metering of Natural Gas and Liquefied Hydrocarbon Gases, February 1984
- [10] DIESSLER R.G.: *Analysis of the turbulent heat transfer and flow in the entrance regions of smooth passages*, NACA TN 3016, 1953
- [11] GAJAN P : *Amélioration du comptage d'un fluide par diaphragme : Approches aérodynamiques expérimentales et théoriques*, Thèse d'état N° 1383, Université Paul Sabatier, TOULOUSE, FRANCE, 1988
- [12] TYLER R.A., WILLIAMSON R.G. : *Confined mixing of coaxial flows*, Aeronautical Report LR - 602 NCR N°18831, 1980
- [13] GAJAN P , HEBRARD P.: *Experimental and theoretical study of a new flow conditioner*, Flucom'88, Sheffield, Pp 347-351, September 1988
- [14] GAJAN P , HEBRARD P., PLATET B.: *Orifice measurement in pertubated conditions: Sources of error and possible corrections*, Flucom'88, Sheffield, Pp 347-351, September 1988
- [15] GAJAN P , HEBRARD P., MILLAN P., GIOVANNINI A., AL ISBER A., STRZELECKI A., TRICHET P.: *Basic study on flow metering in pipe containing an orifice plate*, Final report GRI-90/0073, 1991

Figure 1: Sketch of the flow conditioner



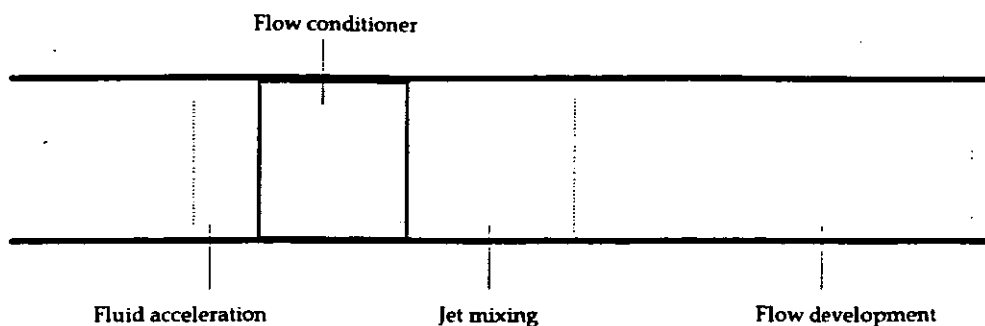


Figure 2: Sketch of the flow patterns through the flow conditioner

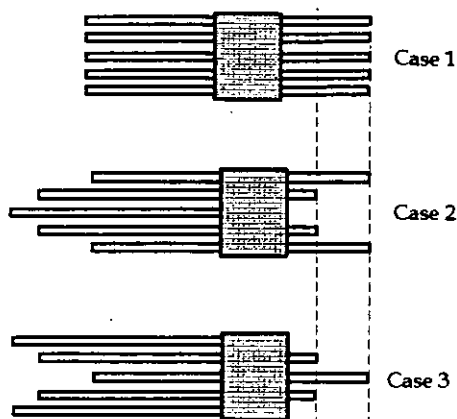


Figure 3: Study of the jets mixing
U profile at the end of the mixing region ($x/d_j = 18.5$)

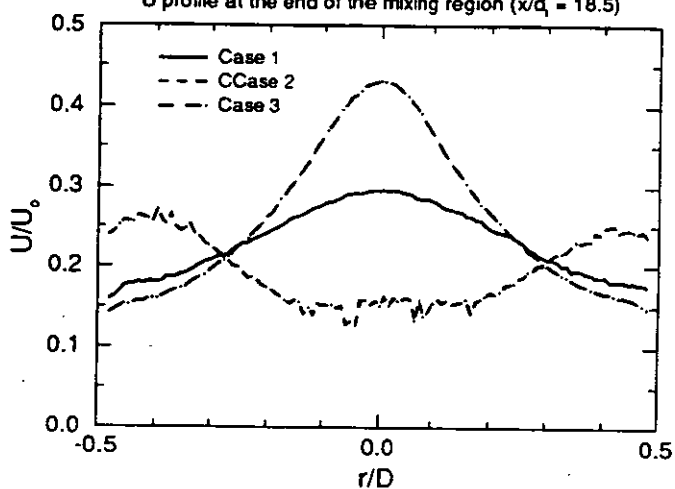


Figure 4: Flow development downstream of the mixing zone

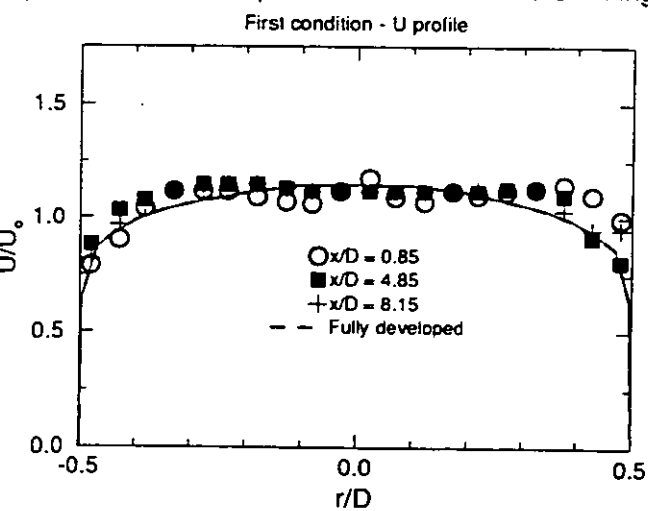


Figure 5: Flow development downstream of the mixing zone

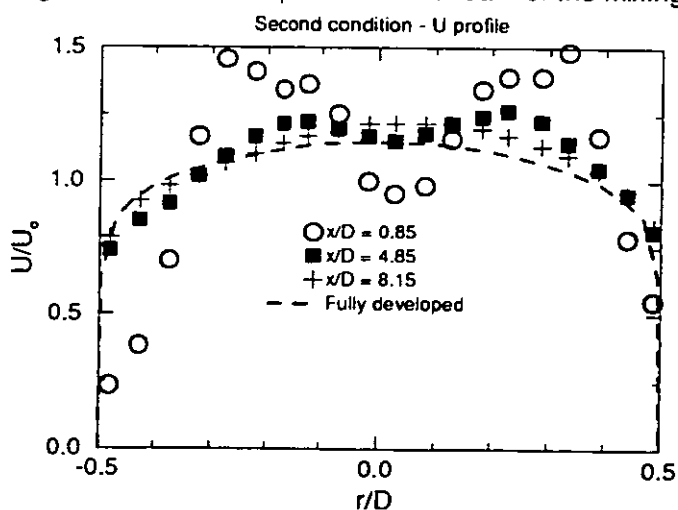


Figure 6: Flow development downstream of the mixing zone

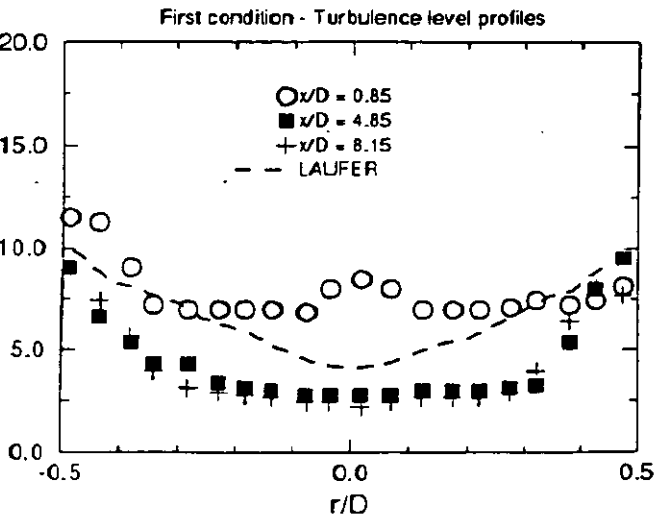


Figure 7: Flow development downstream of the mixing zone

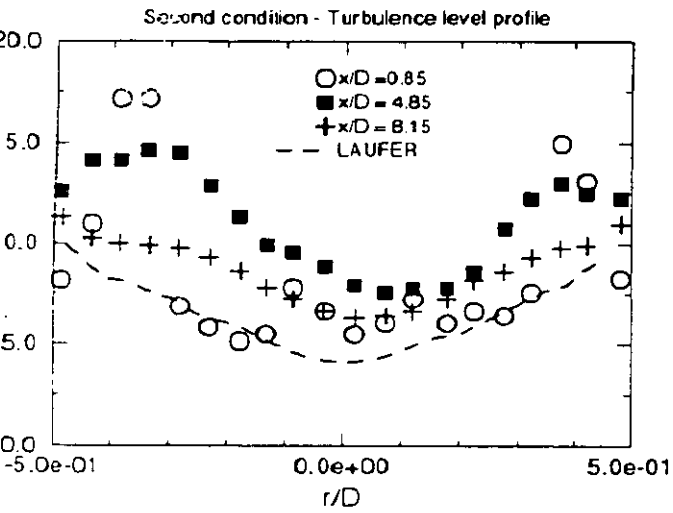


Figure 8: First CERT flow conditioner

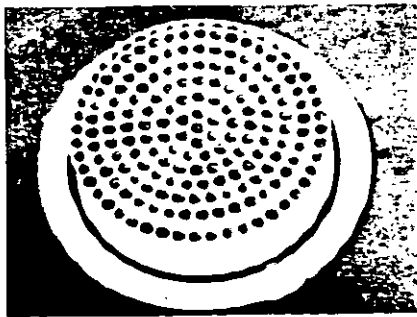


Figure 9: First CERT flow conditioner
Comparison between predictions and experiments

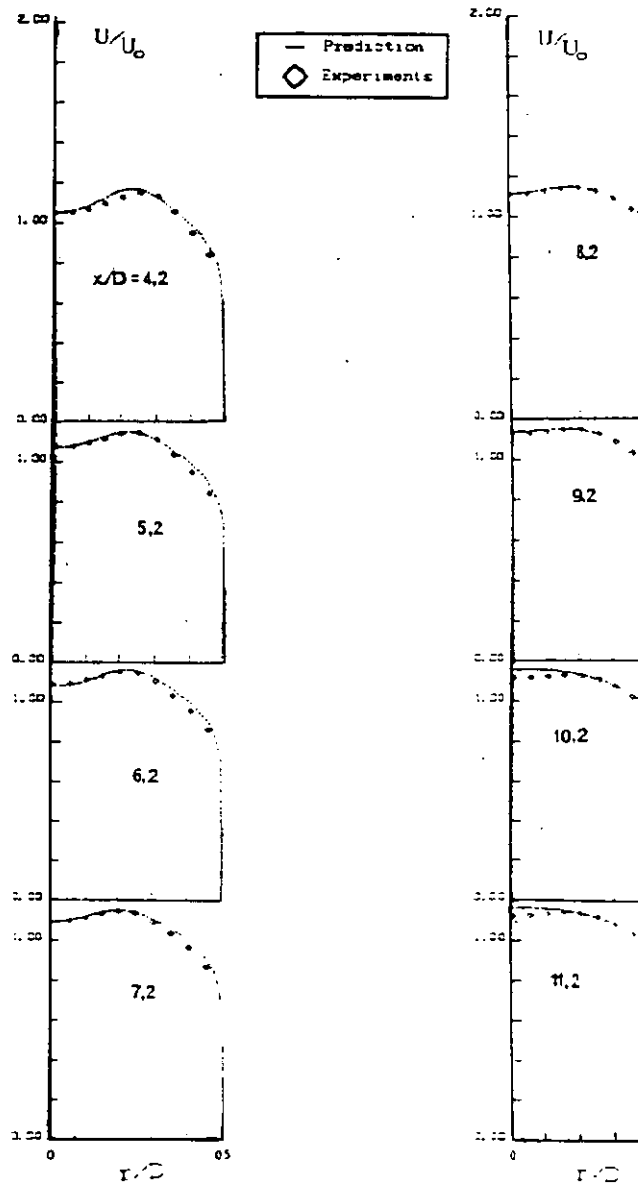


Figure 10: CERT 1 flow conditioner

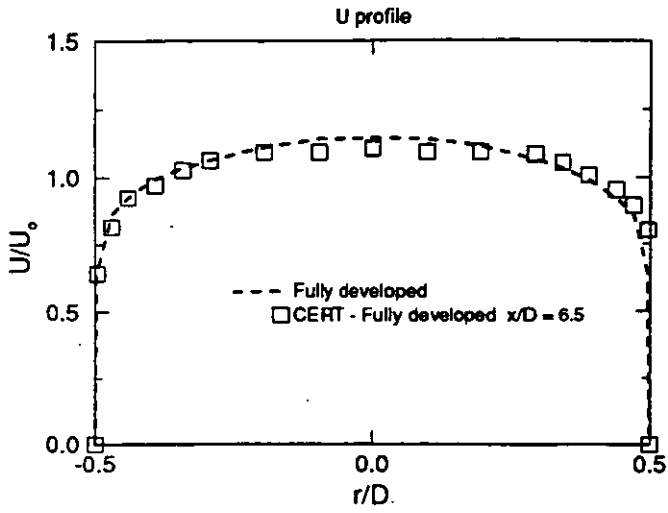


Figure 11: Turbulence quantities

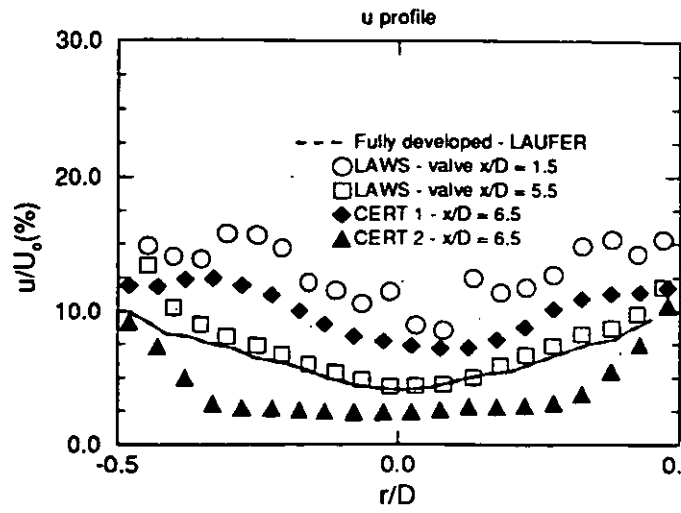


Figure 12 : Swirling flows : Two bends

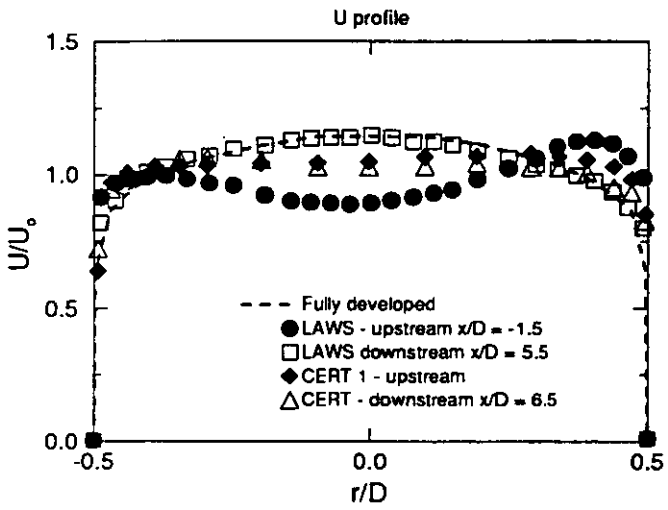


Figure 13: Non symmetric flows

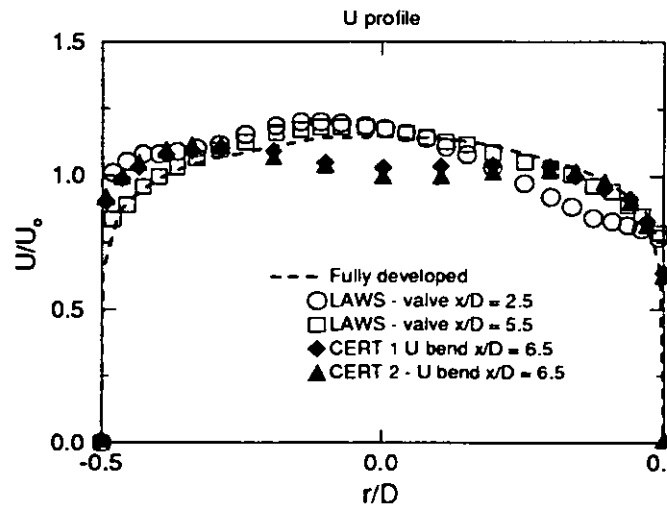


Figure 14: Influence of upstream conditions

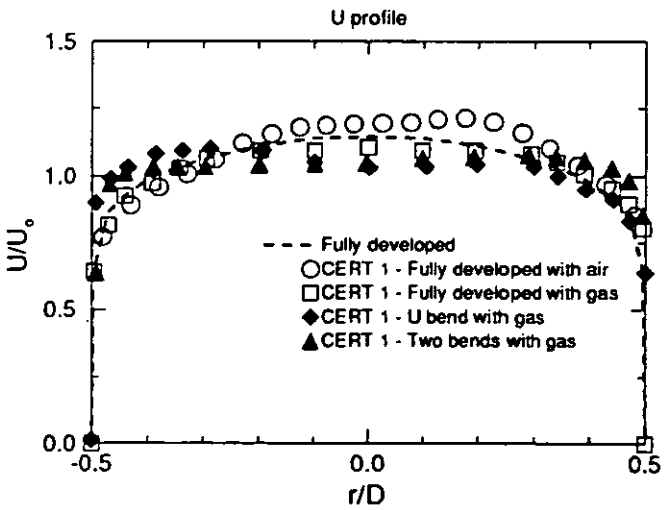
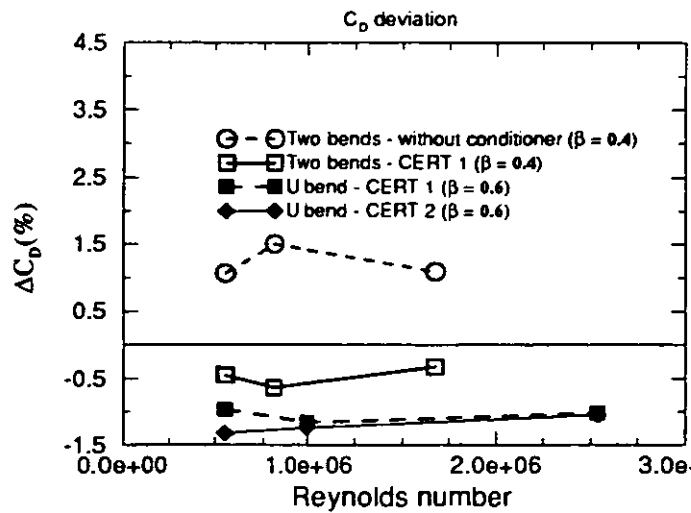


Figure 15: Orifice plate flow meter



THE GALLAGHER FLOW CONDITIONER

James E. Gallagher, P.E. - Shell USA
Paul J. LaNasa - CPL & Associates
Ronald E. Beaty, P.E. - Amoco Production

SUMMARY

This paper describes the design theory, third party research results and pending evaluations for the Gallagher Flow Conditioner (GFC).

Experimental results for the GFC indicate a maximum metering uncertainty of approximately plus or minus one-tenth of one percent (+/- 0.10%) due to upstream flow disturbances on orifice meters. The GFC has exhibited this performance irrespective of the upstream disturbance or sensing tap location.

Based on independently conducted research results, it is the authors' opinions that the GFC is a true "isolating" flow conditioner.

1. INTRODUCTION

The North American natural gas industry produces, transports, and distributes approximately 700 billion cubic meters of gas each year (25 trillion standard cubic feet). The Western European market transports and distributes 250 billion cubic meters of gas each year (9 trillion standard cubic feet). Because of the importance of gas measurement for industry operations and fiscal accountability, it is essential that metering be accurate, reliable, and cost efficient over a range of conditions.

For over sixty years, the concentric orifice meter has remained the predominant meter of choice for natural gas production, large volume gas flow and chemical metering applications. In fact, it is estimated that over 600,000 orifice meters are being used for fiscal measurement applications associated with the petroleum, chemical and gas industries in North America.

2. INSTALLATION EFFECTS

All flowmeters are subject to the effects of velocity profile, swirl and turbulence structure. The meter calibration factors or empirical discharge coefficients are valid only if geometric and dynamic similarity exists between the metering and calibration conditions or between the metering and empirical data base conditions (i.e., fully developed flow conditions). In fluid mechanics, this is commonly referred to as the Law of Similarity.

In the industrial environment, multiple piping configurations are assembled in series generating complex problems for standard writing organizations and flow metering engineers. The challenge is to minimize the difference between the actual or "real" flow conditions and the "fully developed" flow conditions in a pipe to maintain a minimum error associated with the selected metering device's performance. One of the standard error minimization methods is to install a flow conditioner in combination with straight lengths of pipe to "isolate" the meter from upstream piping disturbances.

Research programs in both Western Europe and North America have confirmed that many piping configurations and fittings generate disturbances with unknown characteristics. Even a single elbow can generate very different flow conditions from "ideal" or "fully developed" flow depending on its radius of curvature (mitred or swept). In addition, the disturbance generated by piping configurations is influenced by the conditions prior to these disturbances.

The research programs by the respective measurement communities do not fully

compliment each other in their direction due to design differences between measurement standards. However, they have clearly indicated that the requirements specified in both standards are erroneous as stated by Sattary ⁽¹⁾ -

"The work reported here indicates that the minimum straight length specifications in the Standards are in urgent need of revision."

As a result, the current focus of today's measurement community is to lower uncertainty levels associated with "non-ideal" flow conditions. A special emphasis has been placed on retrofitting existing installations.

3. MEASUREMENT STANDARDS

Present domestic and international measurement standards provide installation specifications for pipe length requirements and flow conditioners upstream of orifice meters (American National Standards Institute's 2530⁽²⁾ and International Standard Organization's 5167⁽³⁾). Unfortunately, considerable disagreement over straight length requirements exist between these highly respected documents.

With respect to installation effects and the near term flow field, the correlating parameters which impact similarity vary with flowmeter type and design. However, it is generally accepted that the concentric, square-edged, flange-tapped orifice meter exhibits a high sensitivity to time average velocity profile, turbulence structure, bulk swirl and tap location.

In North America, current design practices utilize short upstream piping lengths with a specific flow conditioner, A.G.A. tube bundles, to provide "pseudo-fully developed" flow in accordance with the applicable measurement standard (ANSI 2530/A.G.A. 3/API MPMS 14.3). Most North American installations consist of ninety degree elbows or complex header configurations upstream of the orifice meter. Tube bundles in combination with piping lengths of seventeen pipe diameters (17D) have been installed to eliminate swirl and distorted velocity profiles. Ten diameters (10D) of straight pipe is required between the upstream piping fitting and the exit of the tube bundle, and seven diameters (7D) of straight pipe is required between the exit of the tube bundle and the orifice meter (Figure 1).

In Western Europe, two design practices are currently employed to provide "pseudo-fully developed" flow in accordance with the applicable measurement standard (ISO 5167) - long upstream piping lengths with or without flow conditioners. Most Western European installations consist of complex header configurations upstream of the orifice meter. Piping lengths of one hundred pipe diameters (100D) without flow conditioners or piping lengths of forty-two pipe diameters (42D) in combination with flow conditioners have been installed to eliminate swirl and distorted velocity profiles. Three types of flow conditioners have been utilized - tube bundles, Zanker and Sprengle designs. Twenty diameters (20D) of straight pipe is required between the upstream piping fitting and the flow conditioner, and twenty-two diameters (22D) of straight pipe is required between the flow conditioner and the orifice meter (Figure 2).

ISO 5167 allows other configurations provided that the flow quality at the primary device is within +/- 5% of u/u_{max} of fully developed flow and the swirl angle is less than two degrees. Here the notation u is used for the local velocity and u_{max} for the maximum velocity at the centerline. However, recent research by Morrow⁽⁴⁾, Karnik⁽⁵⁾ and Morrison⁽⁶⁾ have indicated that the flow conditioning error is a function of time averaged velocity profile, swirl angle, tap sensing location and turbulence structure. As a result of these new findings, a significant improvement into flow conditioner performance has been achieved over other devices which were designed on velocity and swirl alone.

4. PSEUDO-FULLY DEVELOPED FLOW

The classical definition for fully developed turbulent flow is stated by Hinze⁽⁷⁾ as follows -

"For fully developed turbulent flow in pipe the mean-flow conditions are independent of the axial coordinate, x and axisymmetric, assuming a uniform wall condition."

From a practical standpoint, we generally refer to fully developed flow in terms of swirl-free, axisymmetric time average velocity profile in accordance with the Power Law or Law of the Wall prediction. However, one must not forget that fully developed turbulent flow requires equilibrium of the forces to maintain the random "cyclic" motions of turbulent flow.

Unfortunately, fully developed pipe flow is only achievable after considerable effort in a research laboratory. To bridge the gap between research and industrial applications, we will refer to the term pseudo-fully developed flow defined as -

"a swirl-free, axisymmetric flow with time average velocity profile and turbulence structure whose values approximate those found in fully developed flow and are shown to be independent of the axial coordinate."

Stated another way, **pseudo-fully developed flow** exists when -

"the slope of the orifice meter's discharge coefficient deviation or meter factor deviation asymptotically approaches zero ($\pm 0.10\%$) as the axial distance from the flowmeter to the upstream flow conditioner increases"

This pragmatic definition infers that the random cyclic forces generated by the conditioner produce a self-maintenance mechanism for the time average velocity profile and turbulence structure (Figure 3).

5. OPTIMAL FLOW CONDITIONER

To truly "isolate" flowmeters, the optimal flow conditioner should achieve the following design objectives:

- (1) low permanent pressure loss (low head ratio)
- (2) low fouling rate
- (3) rigorous mechanical design
- (4) moderate cost of construction
- (5) elimination of swirl
- (6) independent of tap sensing location
- (7) pseudo-fully developed flow for both short and long straight lengths of pipe

When the swirl angle is less than or equal to two (2) degrees as conventionally measured using pitot tube devices, swirl is regarded as substantially eliminated.

When the empirical discharge coefficient or meter calibration deviation for both short and long piping lengths is approximately plus or minus one tenth of one percent ($\pm 0.10\%$) and shown to be independent of axial position and orifice sensing tap location, it is assumed to be at a "minimum" and pseudo-fully developed.

6. FLOW CONDITIONERS

In order to provide background information so that the present device may be completely understood and appreciated in its proper context, reference may be made to a number of flow conditioner publications over the past sixty years.

As shown in the following tabular summary, the field is crowded with attempts to "isolate" flowmeters from piping induced disturbances. Despite these efforts, the current flow conditioners are not optimal and have exhibited unsatisfactory attenuation of flow disturbances.

6.1 Classification of Flow Conditioners

All flow conditioners may be grouped into three general classes based on their mechanical design - tube bundles, vanes/screens and perforated plates.

| | <u>Head Ratio</u> |
|------------------------|-------------------|
| I. Tube Bundles | |
| A.G.A. | 1 |
| ISO | 2 |
| Sens & Teule | 10 |
| Bosch & Hebrard | 10 |
| PG&E | 1 |
| II. Vanes/Screens | |
| Etoile | 1 |
| AMCA | 8 |
| Screens | - |
| III. Perforated Plates | |
| Sprenkle | 15 |
| Bellinga | 20 |
| Zanker | 5 |
| Akashi et al. | 2 |
| Kinghorn | - |
| K-Lab's Mark | 2 |
| Laws | 2 |
| Spearman | 3 |
| Gallagher (GFC) | 2 |

Note:

Head ratio is the dimensionless permanent pressure loss associated with the flow conditioner.

6.1.1 Tube Bundles

A.G.A. & ISO^(2,3)

The ISO and A.G.A. designs, shown in Figure 4 respectively, are intended to eliminate swirl. Both designs consist of a bundle of tubes having the same length and diameter.

For the A.G.A. design, the length of the bundle must be at least ten times the tube diameter. For 75 mm (3 inches) meter runs and larger, the bundle consists of nineteen (19) tubes arranged in a circular pattern with a bundle length of two to approximately three pipe diameters (2D to 2.7D). For smaller meter runs, the bundle consists of seven (7) tubes arranged in a circular pattern with a bundle length of three (3D) pipe diameters.

For both the ISO and A.G.A. designs, the permanent pressure loss is low, the mechanical design is rigorous, the cost of construction is low, the fouling rate is low, and swirl is eliminated.

Sens & Teule, Bosch & Hebrard^(8,9)

The Sens & Teule and the Bosch & Hebrard tube bundles were designed to "isolate" piping disturbances from flow meters. Both designs consist of a bundle of tubes of different lengths and diameters arranged in a circular array. The designs are not currently used in the global measurement community (industry, fiscal, research).

For both designs the permanent pressure loss is high, the cost of construction was very high and the prototype designs were rigorous and complex. While swirl is eliminated, the fouling rate is unknown for these designs. Geometric scaling is a problem when considering a range of pipe sizes.

Pacific Gas & Electric⁽¹⁰⁾ (PG&E)

The PG&E tube bundle was designed to "isolate" piping disturbances from flow meters. The prototype is similar to the Sens/Bosch approach --- a bundle of tubes of different diameters but with a constant length arranged in a circular array.

The fouling rate is unknown for these designs. Geometric scaling is a problem when considering a range of pipe sizes as well as undefined specifications for the tubes --- twist, roughness, diameter, blockage, etc.

6.1.2 Vanes/Screens

Etoile⁽³⁾

The Etoile is primarily designed to eliminate swirl in pipe. Three flat plates of equal length and width are assembled in a star-shaped pattern by means of a central hub. The length of the flat plates should be at least one pipe diameter (1D) for optimum elimination of bulk swirl. Some industrial applications currently use this design in Western Europe.

The permanent pressure loss is low, the mechanical design rigorous and the cost of construction is low. The fouling rate is low, and swirl is eliminated.

6.1.3 Perforated Plates

Sprenkle⁽¹¹⁾

The Sprenkle was intended to "isolate" piping disturbances from flow meters for steam flow. Some fiscal applications currently use this design in Western Europe.

The Sprenkle consists of three perforated plates spaced one diameter (1D) apart and connected by rods. Each plate has a porosity of fifty percent (50%) with regularly distributed perforations in a specified hexagonal pattern. The perforations consist of holes whose diameter is five percent of the pipe diameter (0.05D).

The permanent pressure loss is very high, the mechanical design rigorous and complex and it has a high cost of construction. The fouling rate is moderate, and swirl is eliminated for all piping configurations.

Bellinga⁽¹²⁾

The Bellinga is a modified Sprenkle design. This invention was intended to "isolate" piping disturbances for natural gas turbine meter applications. Some fiscal turbine meter applications currently use this design in Western Europe.

The permanent pressure loss is very high, the mechanical design rigorous and complex. The cost of construction is high. The fouling rate is moderate and swirl is eliminated for all piping configurations.

Zanker⁽¹³⁾

The Zanker was designed to "isolate" piping disturbances for pump efficiency testing. Some fiscal applications currently use this design in Western Europe.

The Zanker consists of a perforated plate connected to a downstream grid

or crate.

The perforated plate is comprised of thirty-two (32) holes with five (5) different diameters. A specified location for each hole is called for by the design.

A complex crate, similar to the AMCA design, approximately one pipe diameter (1D) in length is attached to the downstream side of the perforated plate. The crate is assembled from flat plate in a manner that does not overlap the numerous holes in the perforated plate.

The permanent pressure loss is high, the mechanical design rigorous and complex and it has a high cost of construction. The fouling rate is low, and swirl is eliminated for all piping configurations.

Akashi⁽¹⁴⁾

The Akashi, as shown in Figure 4, was designed to "isolate" piping induced disturbances for flow meters. The Akashi is sometimes referred to as the Mitsubishi. No known fiscal applications currently use this design.

The Akashi consists of a single perforated plate with thirty-five (35) holes. The hole size is thirteen percent of the pipe diameter (0.13D). The perforated plate thickness is equal to the hole diameter (0.13D). The plate has a porosity of approximately fifty-nine percent (59%). The hole distribution is dense in the middle (center of pipe) and sparse around the periphery (pipe wall). The upstream inlets of the holes are beveled.

The permanent pressure loss is low, the mechanical design rigorous and simple and it has a moderate cost of construction. The fouling rate is low to moderate, and swirl is eliminated for all piping configurations.

Kinghorn⁽¹⁵⁾

The Kinghorn flat plate was designed to "isolate" piping disturbances on flow nozzles for compressor efficiency testing. No known fiscal applications currently use this design.

The Kinghorn consists of a single perforated plate or two perforated plates in series. The hole size is four percent of the pipe diameter (0.04D). The perforated plate thickness is equal to the hole diameter. The plate has a porosity of approximately forty percent (40%). The hole distribution is dense in the middle (center of pipe) and sparse around the periphery (pipe wall). The upstream inlets of the holes are square and sharp.

The permanent pressure loss is unknown, the mechanical design rigorous and simple and it is estimated to have a moderate cost of construction. The fouling rate is moderate to high, and swirl is eliminated for all piping configurations.

K-Lab's Mark V⁽¹⁶⁾

The Mark V, a further development of the Wilcox patent, was designed to "isolate" piping induced disturbances for flow meters. No known fiscal applications currently use this design.

The Wilcox patent calls for a flow conditioner comprised of tubular passages with the area between specific tubes blocked referred to as the Mark I. Further development of the Wilcox concept has resulted in the evolution of additional models. The latest development, the Mark V, is at present considered a trade secret and, therefore, the design is unknown.

The permanent pressure loss is low, the mechanical design is rigorous

and simple, the cost of construction is moderate to high and swirl is eliminated for most piping configurations.

Laws⁽¹⁷⁾

The Laws, as shown in Figure 4, was designed to "isolate" piping induced disturbances for flow meters. Some fiscal applications currently use this design in Western Europe.

The Laws design consists of a single perforated plate several holes. The perforated plate thickness is approximately twelve percent of the pipe diameter (0.12D). The plate has a porosity of approximately fifty percent (50%). The plate is perforated with a variety of holes arranged in two radially spaced circular arrays around a central hole. The upstream inlets of the holes may be beveled. Further evolution of the design has resulted in anti-swirl vanes attached to the faces of the perforated plate.

The permanent pressure loss is low, the mechanical design rigorous and simple and it has a moderate cost of construction. The fouling rate is considered to be low, and swirl is eliminated.

7. GFC DESIGN

In attempting to achieve the optimal flow conditioner objectives, the Gallagher Flow Conditioner (GFC) maintains pseudo-fully developed flow with respect to the axial position. The reason is fundamental - **the random cyclic forces generated by the conditioner produce a self-maintenance mechanism for the velocity profile and turbulence structure within a short axial distance.**

The Gallagher Flow Conditioner, as shown in Figure 5, was designed to "isolate" piping induced disturbances. The GFC consists of an anti-swirl device, settling chamber and profile device mounted sequentially in the pipe. The anti-swirl device and the flow profile device are considered to be separate devices. This approach maximizes the efficiency of both swirl elimination and profile generation.

The anti-swirl device provides an assurance of swirl elimination. A tube bundle anti-swirl device is preferred, thus eliminating geometric similarity concerns and providing for low manufacturing costs. The design generates reproducible turbulence intensities and turbulence shear stresses, regardless of the upstream piping disturbance. For some installations, the anti-swirl device may be omitted without any loss in performance.

Downstream of the settling chamber is the profile device, which generates a pseudo-fully developed flow - time average velocity profile and turbulence structure. A flat plate is preferred when considering manufacturing costs. The interaction of porosity, hole location and hole diameter are critical success factors. As a result, the profile device is based on a series of combined theoretical/empirical interactive equations.

Downstream of the profile device is the flowmeter. The dimensionless distance, X/D , between the profile device and the flowmeter is critical. The GFC provides for X as low as three nominal pipe diameters (3D) or seven nominal pipe diameters (7D) depending on the flowmeter design. This short distance is important, especially in retrofitting short meter tubes or in fitting new meter tubes in an area where space is limited.

The flow conditioner may be preassembled into a unit or module that is then installed into a pipeline at a predetermined distance upstream of the flowmeter and beyond a predetermined distance downstream of the nearest source of flow disturbance (valve, elbow, tee, complex pipe configuration, etc.) upstream of the flowmeter. This preassembly concept is highly desirable when considering retrofitting of existing fiscal metering facilities.

The flow conditioner exhibits a low permanent pressure loss and has a rigorous, simple mechanical design. Fouling rate is anticipated to be low and swirl is eliminated. Manufacturing cost is expected to be low to moderate.

8. EXPERIMENTAL RESULTS

Research results from unbiased, highly reputable sources will be referenced for empirical performance data for several commercially available flow conditioners.

Several flow conditioners have been evaluated by the Gas Research Institute for comparison purposes⁽¹⁸⁾ as part of their Installation Effects Research Program. For these tests, the same test loop or apparatus was utilized to provide consistency between experiments.

For the test loop, gas enters a stagnation bottle and flows to a straight section of pipe (Figures 6a and 6b). The gas then enters a ninety-degree elbow or tee followed by a meter tube and flowmeter. The flow conditioners tested were positioned at various upstream distances, X, from the orifice plate. To obtain dimensionless terms, the distance X was divided by the meter tube nominal pipe diameter, D.

For the experiments, the selected flowmeter was a concentric, flange tapped square-edged orifice meter with Betas of 0.67 and 0.75. The internal diameter of the meter tube, IDp, was 102.29 mm (4.027 inches) and the length of the meter tube, L1, was seventeen nominal pipe diameters (17D). For certain A.G.A. tube bundle measurements, the length of the meter tube, L1, was increased to 45D and 100D lengths. The flow disturbance was created by either a ninety degree elbow or a tee installed at the inlet to the meter tube.

By way of explanation, the designation Cd deviation (%) refers to the percent deviation of the empirical coefficient of discharge or meter calibration factor from fully developed flow to the disturbed test conditions. Desirably, this deviation should be as near to zero as possible. As explained above, a "minimal deviation" is regarded as plus or minus one-tenth of one percent (+/- 0.10%).

8.1 Analysis of Results

The results obtained for the A.G.A. design, using meter tube lengths of 17D, 45D and 100D, (Figure 7) indicate a "minimal deviation" when:

$$\begin{aligned} L1 &= 17D; \text{ and } X/D = 12 - 15 \\ L1 &= 45D; \text{ and } X/D = 8 - 9 \\ L1 &= 100D; \text{ and } X/D = 8 - 9 \text{ or } > 45 \end{aligned}$$

Tests on four flow conditioners in a 17D long test pipe with a tee were funded by GRI. The Beta for the orifice meter was 0.67 and the Reynolds number was approximately 900,000.

The A.G.A. design does not produce pseudo-fully developed flow conditions for short piping configurations. This was evidenced by the instability of the coefficient performance (Figure 8). Similar results for the ISO tube bundle design are anticipated based on our current understanding of the physics.

These results are not surprising in light of our current understanding of pipe flows. The tube bundle does an excellent job in eliminating swirl. However, the fixed diameter tubes generate an unstable turbulence structure which begins to redevelop rapidly. Also, the constant and high radial porosity does not offer a method to redistribute any asymmetric flow patterns.

The Mark V conditioner does not produce pseudo-fully developed flow conditions for short piping configurations (Figure 9). This was evidenced by the

instability of the coefficient performance.

The Laws conditioner is useful at distances of X/D greater than about 12 (Figure 10). The Laws performance for minimal deviation from the empirical discharge coefficient for short piping lengths is unacceptable, but completely acceptable for long piping lengths.

With respect to the Laws conditioner, it is important to note that the 100mm design tested by GRI is not similar to the 250mm design tested by NEL and funded by Amoco in 1992.

In analyzing the Laws and Mark V results, it would appear that these highly respectable devices were designed to attain the ISO 5167 time average velocity profile and swirl criteria. Unfortunately, when the criteria was adopted into ISO 5167, it was based on an understanding rather than hard experimental evidence. Research subsequent to the development of the Laws and Mark V flow conditioners have conclusively linked two additional influence quantities --- turbulence structure and sensing tap location.

The GFC produces pseudo-fully developed flow conditions for both short and long piping configurations. This is evidenced by the slope of the orifice meter's discharge coefficient deviation or meter factor deviation asymptotically approaching zero as the axial distance from the flowmeter to the upstream flow conditioner increases (Figure 11). The GFC has also demonstrated an insensitivity to tap sensing location confirming the presence of pseudo-fully developed flow.

The GFC has the benefit of being the most recent evolution in the design of flow conditioners. As such, one would expect to have significant performance improvements over existing flow conditioners (Figure 12). The design should and does exhibit this improved performance as a result of a considerable parametric study for sensitivity (profile device design, settling chamber length, etc.), as well as the added insights attained over the last four years.

9. OTHER EVALUATIONS

Several commercial and research evaluations have been completed or are currently underway to further assess the performance of the GFC on both gas and liquid fiscal metering applications.

9.1 Completed Evaluations

The first evaluation called for testing in both a 75 mm (3 inch) and 100 mm (4 inch) orifice meter runs with complex out of plane headers at variable oblique angles. The tests, funded by Amoco Production Company, were conducted at the Colorado Engineering Experiment Station Incorporated (CEESI) facility in Nunn, Colorado in the summer of 1994. The test results⁽¹⁹⁾ showed the GFC eliminated piping induced disturbances and produced a maximum uncertainty due to installation effects of +/- 0.075% for a Beta of 0.67. These results are similar to the previous GRI research.

A second series of experiments called for testing the GFC in combination with a 250 mm (10 inch) helical turbine meter and straight bladed turbine meter run in series. The program, funded by Shell, was conducted at Capline's St. James, Louisiana facility. Capline is the largest imported crude oil pipeline in North America. They currently handle approximately 100 crude types with a daily throughput of 1,200,000 barrels. The GFC⁽²⁰⁾ has been successfully utilized to "isolate" any disturbances associated with the upstream piping and turbine meter, thereby eliminating a variable in the fractional factorial experimental pattern.

9.2 Planned Evaluations

An evaluation currently underway calls for the GFC to be tested as part of the GRI Orifice Meter Installation Effects Program. Current tests will assess a double elbow out of plane header configuration in conjunction with velocity profile and turbulence measurements. The experiments are limited to a 100 mm (4 inch) orifice meter run. Preliminary results⁽²⁾ indicate that the GFC has exhibited a maximum error of +/- 0.10% due to installation effects for a single elbow, a single tee and double elbows out of plane.

A second evaluation underway calls for the GFC to be tested as part of the NEL Header Consortium Project. The GFC will be installed in a 250 mm (10 inch) orifice meter run in order to produce pseudo-fully developed flow regardless of the upstream piping disturbance. Separate asymmetric and bulk swirl experiments are planned for three Beta ratios. The pipe Reynolds number will be approximately 900,000 with Beta ratios of 0.40, 0.60, and 0.75.

The third evaluation currently funded calls for testing a 250 mm (10 inch) multipath ultrasonic meter (USM) in series with "best" turbine meter out of the research project stated above. The GFC will be utilized to "isolate" any disturbances associated with the upstream piping and to provide a pseudo-fully developed flow. It is believed that the GFC will improve the USM performance or ensure the manufacturer's stated performance without relying heavily on Lagrangian-Gaussian integration techniques.

A fourth evaluation calls for the GFC to be tested in a 450 mm (18 inch) straight bladed liquid turbine meter run. The research, funded by Capline, is being conducted at their Salem, Illinois facility. Problems of asymmetry associated with prover return lines located immediately upstream of the A.G.A. tube bundle indicate a possible bias.

A fifth evaluation currently funded calls for the GFC to be tested in both 250 mm (10 inch) and 150 mm (6 inch) straight bladed turbine meter runs. The project is funded by LOOP Inc. and will be conducted at their Clovelly, Louisiana facility. Asymmetry associated with prover return lines located immediately upstream of the A.G.A. tube bundle has shown to produce a bias.

10. CONCLUSION

The GFC has exhibited an ability to "isolate" flowmeters from piping-induced disturbances, thereby allowing more accurate metering of fluids flowing in pipelines. The device achieves the optimal flow conditioner objectives previously stated and maintains pseudo-fully developed flow in a pipeline with respect to the axial position.

Based on the independently conducted research results, it is the authors' opinions that the GFC is a true "isolating" flow conditioner.

REFERENCES

1. Sattary, J.A., "Progress Report No. 10 on The Effect of Installations and Straighteners on the Discharge Coefficient of Orifice Plate Flowmeters", Department of Trade and Industry, National Engineering Laboratory, East Kilbride, Scotland, March, 1991.
2. API MPMS Chapter 14 Section 3 Parts 1 - 4 (ANSI 2530, A.G.A. Report No. 3), "Concentric, Square-Edged Orifice Meters", American Petroleum Institute, Washington, D.C., USA, 1990.
3. International Standard ISO 5167-1, "Measurement of Fluid Flow by Means of Orifice Plates, Nozzles and Venturi Tubes Inserted in Circular

Cross-Section Conduits Running Full", International Standards Organization, Geneva, Switzerland, 1992.

4. Morrow, T.B., Park, J.T., McKee, R.J., "Determination of Installation Effects for a 100 mm Orifice Meter Using a Sliding Vane Technique", Flow Measurement and Instrumentation, Volume 2, Number 1, January, 1991.

5. Karnik, U., Jungowski, W.M., Botros, K.K., "Effects of Flow Characteristics Downstream of Elbow/Flow Conditioner on Orifice Meter", 9th North Sea Flow Measurement Workshop, Department of Trade and Industry, National Engineering Laboratory, East Kilbride, Scotland, 1991.

6. Morrison, G.L., DeOtte, R.E., "3-D Laser Anemometer Study of Compressible Flow Through Orifice Plates", GRI Report 91/0177, Gas Research Institute, Chicago, IL, December, 1991.

7. Hinze, J.O., "Turbulence", second edition, McGraw-Hill, New York, NY, 1975.

8. Sens, M., Teule, C., "Theoretical and Experimental Study of a New Flow Straightener", Association Technique de L'Industrie du Gaz en France, 1975.

9. Bosch, M., Hebrard, P., "Experimental and Theoretical Study of a New Flow Conditioner", Proceedings of the International Conference on the Metering of Natural Gas and Liquified Hydrocarbon Gases, February, 1984.

10. Stuart, J., "Improvements in Flow Conditioner Design for Orifice Metering", A.G.A. Operations Conference, 1993.

11. Sprenkle, R.E., Courtright, N.S., "Straightening Vanes for Flow Measurement", Mechanical Engineering, NY, NY, 1958.

12. Bellinga, H., Stronk, H.B., "The Practical Application of Flow Straighteners with Turbine Flowmeters for Gas", Paper BFL242, Presented at the IMEKO VII Congress, London, UK, May 10-14, 1976.

13. Zanker, K.J., "The Development of a Flow Straightener for Use with Orifice Flowmeters in Disturbed Flow", Paper D-2, Symposium on Flow Measurement, Scotland, 1969.

14. Akashi, K., Watanabe, H., Koga, K., "Flow Rate Measurement in Pipe Line with Many Bends", IMEKO Symposium, Flow Measurement and Control in Industry, Tokyo, Japan, 1979.

15. Kinghorn, F.C., Blake, K.A., "The Design of Flow Straightener - Nozzle Packages for Discharge Side Testing of Compressors", NEL Report, 1978.

16. Wilcox, P. L., Weberg, T., Erdal, A., "Short Gas Metering Systems Using K-Lab Flow Conditioners", 8th North Sea Flow Measurement Workshop, Department of Trade and Industry, National Engineering Laboratory, East Kilbride, Scotland, 1990.

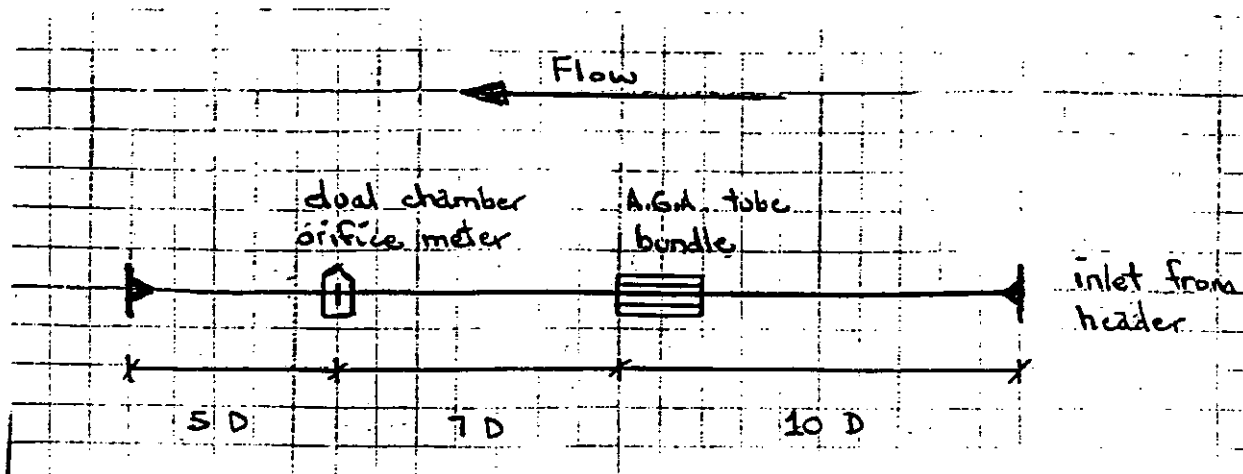
17. Laws, E.M., "Flow Conditioning - A New Development", Flow Measurement and Instrumentation, Volume 1, April, 1990.

18. GRI's Technical Advisory Committee, Summer 1994 Meeting, Southwest Research Institute, San Antonio, Texas, USA.

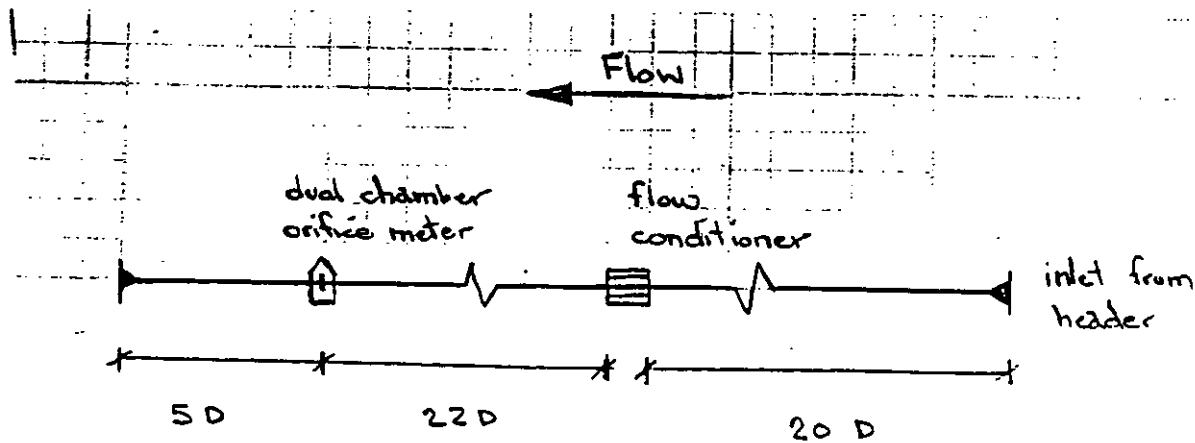
19. Private Communication with Amoco's Mr. David Simpson, July, 1994.

20. Internal Shell Research Report, September, 1994.

21. Private Communication with GRI's Mr. John Gregor, September, 1994.



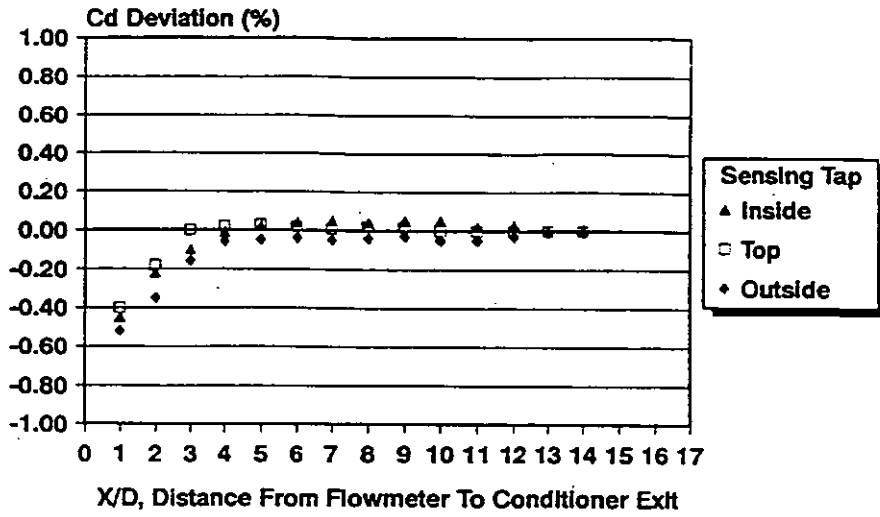
North American Practice
Figure 1



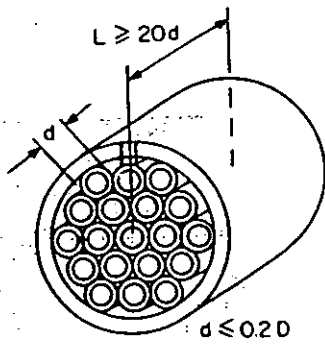
ISO 5167 Requirement
Figure 2

Pseudo-Fully Developed Flow

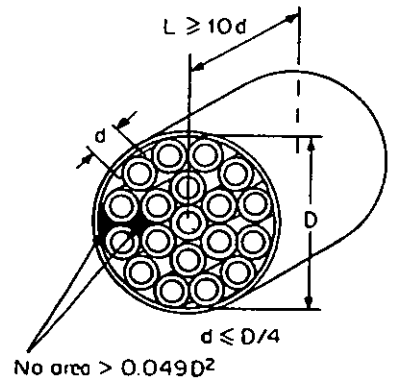
17 D Long Meter Tube



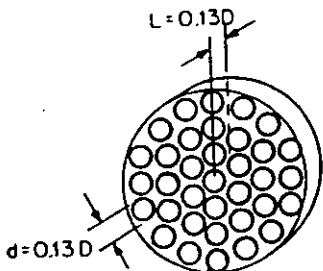
Pseudo-fully Developed Flow
Figure 3



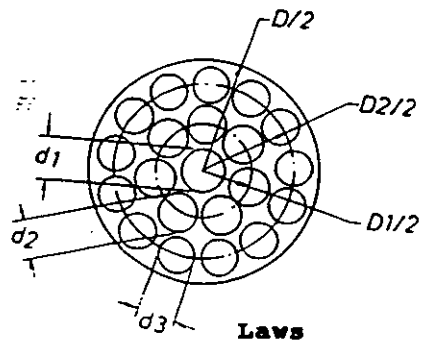
ISO



A.G.A.



Akashi

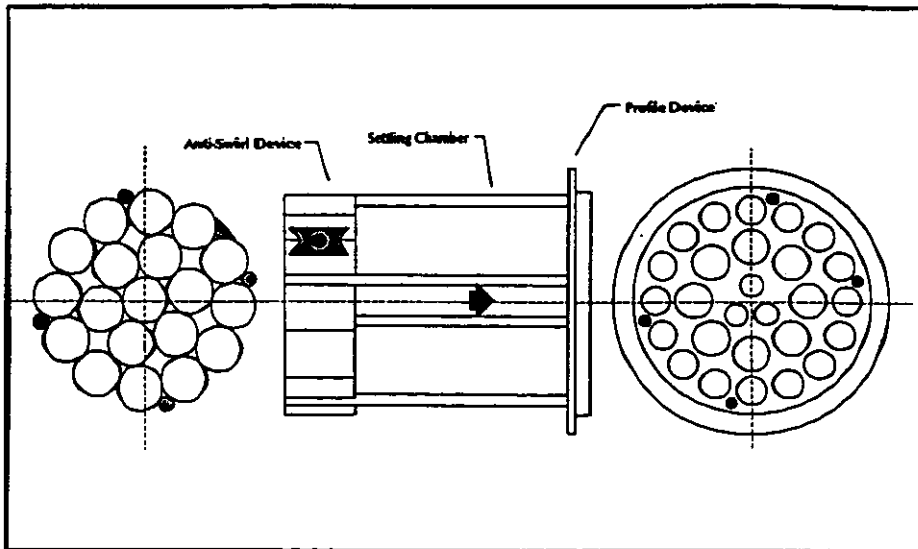
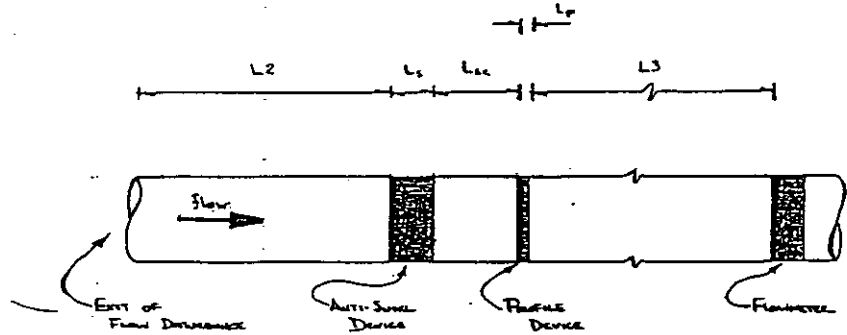


Laws

Flow Conditioners
Figure 4

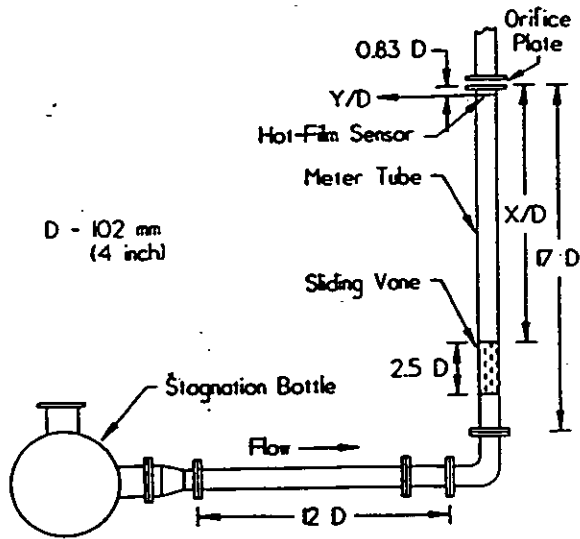
[L2] + [Anti-Swirl Device] + [Lsc] + [Profile Device] + [L3]

- * L2 - Settling chamber, or distance from piping disturbance to inlet of "anti-swirl device".
- * Anti-Swirl Device
A device designed to eliminate swirl. The most efficient designs are vanes, tubes, honeycombs or crates.
- * Lsc - Settling chamber, or distance from the "anti-swirl device" to the "profile device".
- * Profile Device
A device designed to generate an axisymmetrical, "pseudo-fully developed" flow profile (in particular velocity profile and turbulence).
- * L3 - Settling chamber, or distance from the "profile device" to the flowmeter.



Gallagher Flow Conditioner
Figure 5

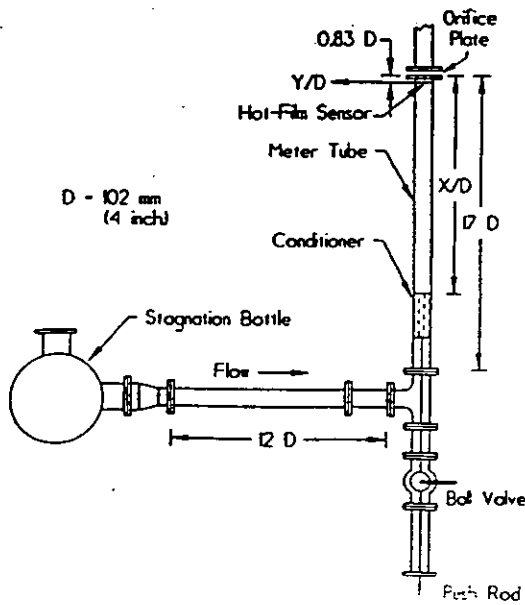
MRF UPSTREAM EFFECTS RESEARCH



MRF Orifice Meter Installation for Tube Bundle Flow Conditioner Location Tests Downstream of a 90-Degree Elbow.

Figure 6a

MRF UPSTREAM EFFECTS RESEARCH



MRF Orifice Meter Installation for New Flow Conditioner Location Tests Downstream of a Tee.

Figure 6b

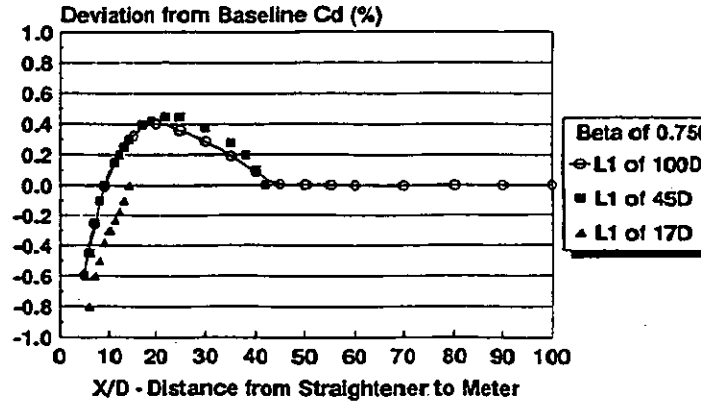
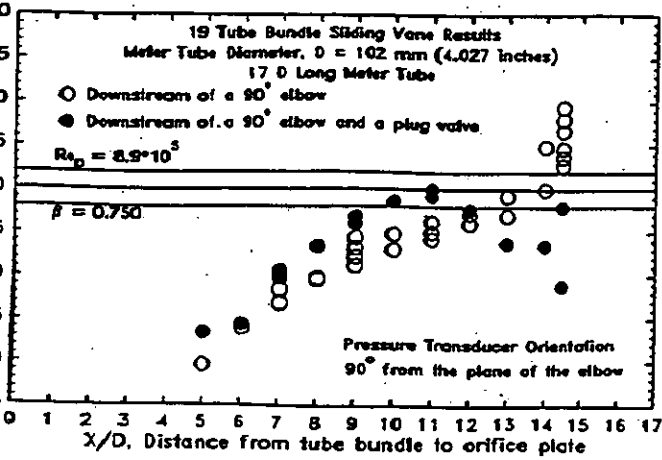


Figure 7

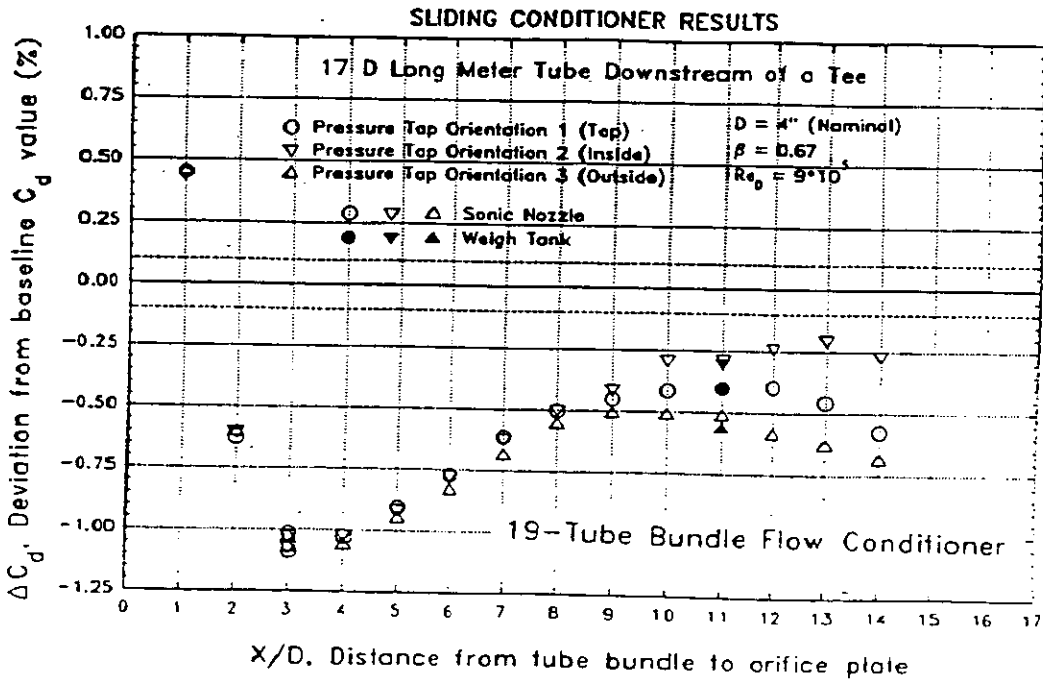


Figure 8

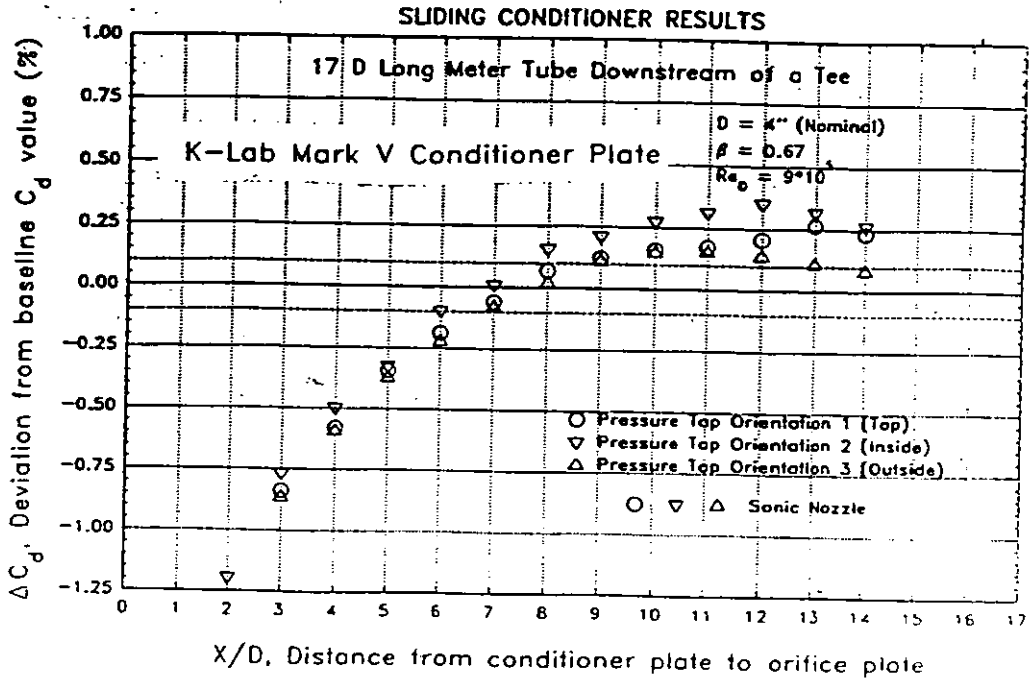


Figure 9

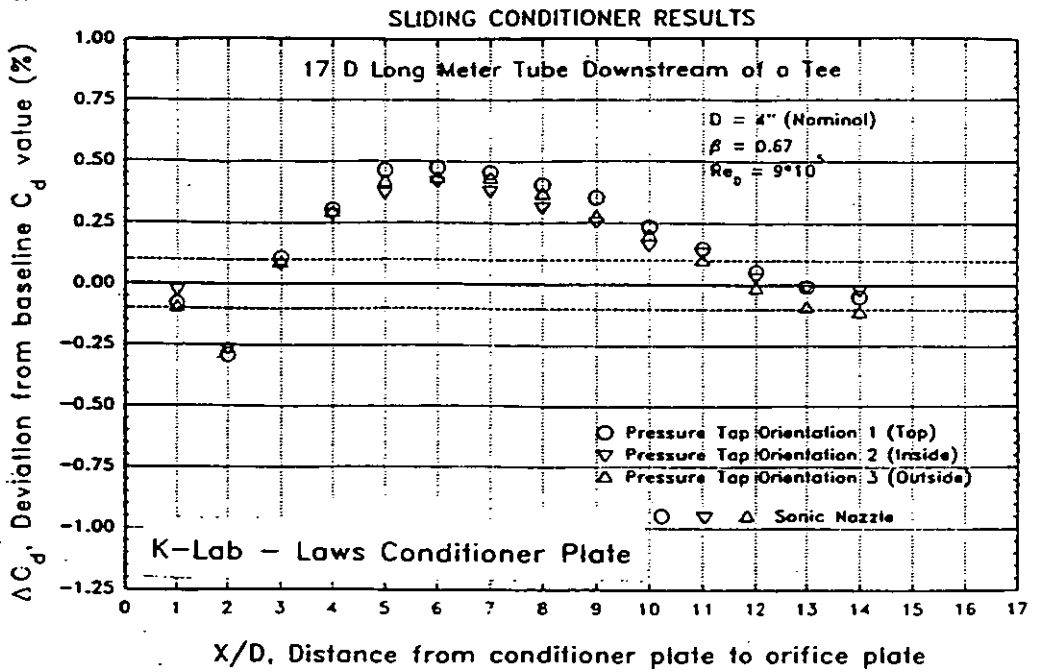


Figure 10

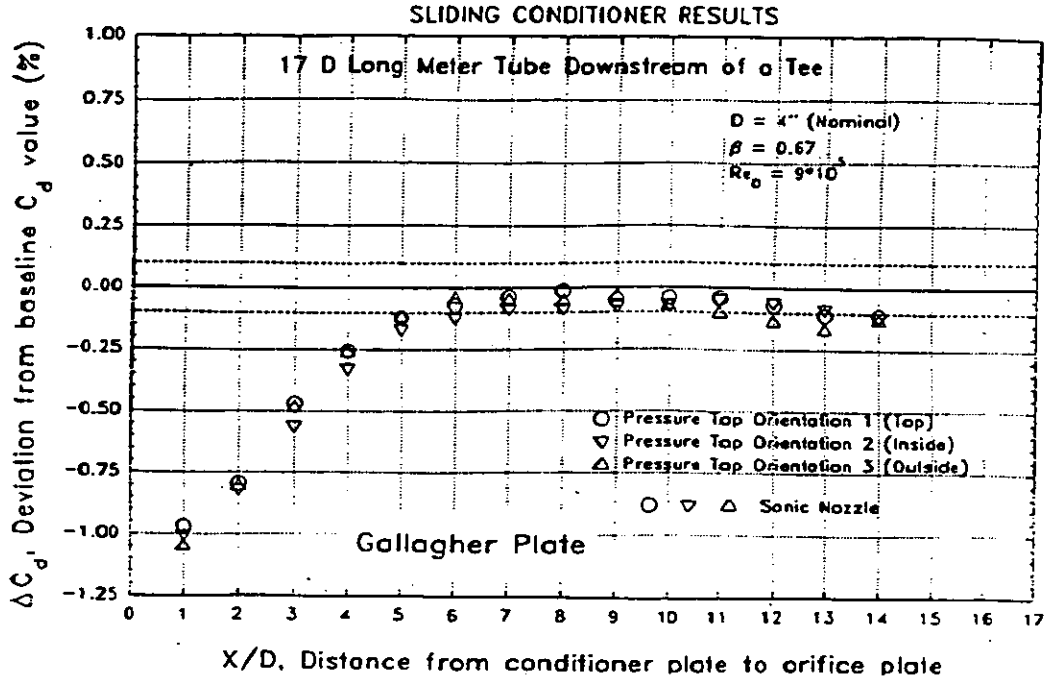


Figure 11

Flow Conditioner Comparison

17 D Long Meter Tube w/ Tee

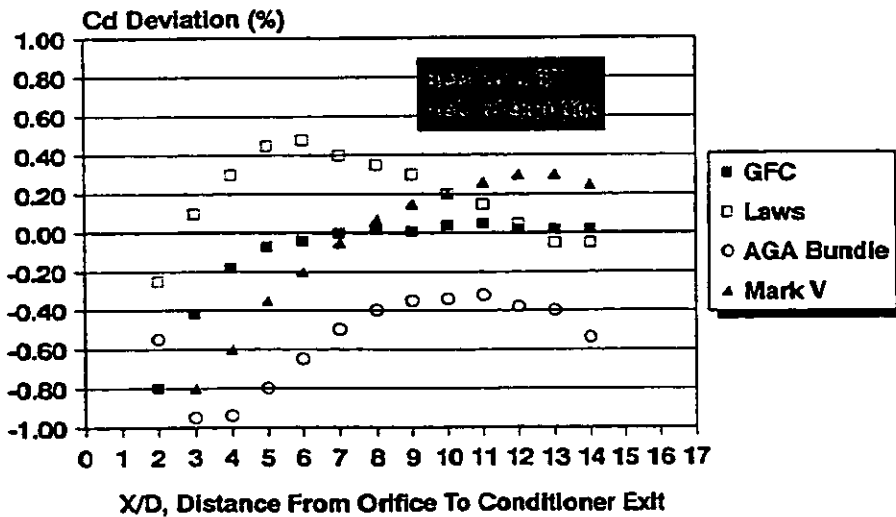


Figure 12

SESSION 3

MULTIPHASE TECHNOLOGY

Chairman - R Paton, NEL

NORTH SEA FIELD TEST OF A MULTIPHASE FLOWMETER

Andreas Hatlo, Flow Technology, Kongsberg Offshore a.s. (KOS)
Sven Sørensen, Production Programming, Mærsk Oilie & Gas a.s. (MOG)

1. SUMMARY

The KOS MCF 350 Multiphase Flow meter has been tested in the Danish part of the North Sea at the Dan F platform in co-operation with Mærsk Oil & Gas. Test results are showing some promising results for further use of the KOS MCF 350 Multiphase meter for offshore application. However, some performance limitations with regards to flow regimes and watercuts were seen as expected.

A prediction of the actual multiphase flow regimes on the test site is important to avoid installation of the multiphase meter in applications outside the operational range of the meter. In addition, identification of the flow regime for the well stream on test is of major importance. Both requirements was met for the KOS MCF 350 meter for the Dan F test.

The test separator used for reference measurement was equipped with conventional metering equipment. The accuracy of the reference measurement was not verified, but the expected accuracy is given. The influence of the reference measurement accuracy on the deviation between the KOS MCF 350 measurement and the test separator is discussed.

2. INTRODUCTION

Development of the MCF Multiphase Flow meter

Kongsberg Offshore a.s (KOS) has in co-operation with Shell Research (KSEPL) and A/S Norske Shell developed the KOS MCF 350 Multiphase Flow meter. The development of the MCF Multiphase Flow meter technology started in 1991 and the first commercial KOS MCF 350 meter was available in 1993 after extensive laboratory and field testing.

Further development of the MCF technology is ongoing (October 1994), and a new version of the MCF Multiphase Flow meter, the KOS MCF 351, will be commercially available early 1995.

The aim for the development of the MCF technology is to establish a MCF meter in the market which will meet the requirements from the users regarding range of flow rates, flow regimes and different watercuts. (For more detailed information see ref. /1/).

The field test at Dan F was initiated by MOG and KOS in co-operation to verify the performance of the KOS MCF 350 Multiphase Flow meter in an offshore environment. The aim of the test was for MOG to evaluate the operability of the MCF 350 Multiphase Flow meter and to evaluate the possibilities of using this type of meter for testing of wells on satellite platforms. Hence the operational range of the meter is limited to the slug flow regime some effort was put into determining the flow regime for each single well prior to the test.

The test was initially planned for a period of three months. During this period more wells producing within the operational range of the MCF 350 meter were identified. It was therefore decided to extend the test period for another three months. Detailed investigations regarding the use of MCF 350 on another satellite platform is ongoing.

Previous onshore field tests

| Test site | Country | Company | Test period |
|-----------------------|---------|-------------|------------------------|
| Marmul | Oman | PDO | Sept. - Oct. 1992 |
| Marmule / Ramlat Rawl | Oman | PDO | Feb. - Mar. 1993 |
| Rabi | Gabon | Shell Gabon | Mar. - April 1993 |
| Ramlat Rawl | Oman | PDO | March 1993 - (ongoing) |
| Lekhwair | Oman | PDO | Dec. 1993 - (ongoing) |

Table 1 Overview of previous onshore field tests, KOS MCF 350 Multiphase Flow meter.

For further details see ref. /2/ which describes test results and findings for tests performed in Gabon and Oman.

The meter has been tested in well flows with high wax content and sand production and for a wide range of well flow behaviour, fluid properties and environmental conditions. These different process conditions, within the operational range of the KOS MCF 350 meter, has not been a limitation for the performance of the MCF meter or the quality of the measurements. For extreme wax production KOS can recommend steam cleaning of pipe unit, injection of wax inhibitor or pre-heating of the multiphase flow to avoid wax deposition. The MCF has consequently proven to be a reliable equipment for onshore field conditions performing within the specification for the meter.

3. PREDICTION AND IDENTIFICATION OF FLOW REGIMES

The need of flow regime prediction and identification.

The actual flow regimes of the well stream routed through the multiphase meter must be predicted prior to the installation of the meter. This must be done to avoid installations of multiphase meters for production rates outside the operational range of the meter. The time used at the actual field application can then be more effectively used testing wells within the operational range of the meter.

The operational range of the KOS MCF 350 Multiphase Flow meter is limited to slugging flow. The prediction of the flow regime prior to the installation is therefore important. In addition the identification of the flow regime of the actual well just before test start was essential for the field test at Dan F. Through this routine wells which had changed production out of the operational range of the meter was identified and excluded from the MCF 350 test programme.

General description of multiphase flow regimes

Multiphase flow is divided into different flow regimes dependant on its physical and visual characteristics. Both for vertical and horizontal two and three phase flow the different flow regimes are defined based on the combination of liquid and gas flow rates, often given as superficial velocity. Fluid properties, such as gas and liquid viscosity, gas and liquid densities, effects from pressure gradients, pipe inclination and pipe diameters will also have influence on the boundaries between the different regimes.

General flow regime maps for horizontal and vertical flow, Figure 1 and Figure 2, indicate the differences between the flow patterns for the two different situations.

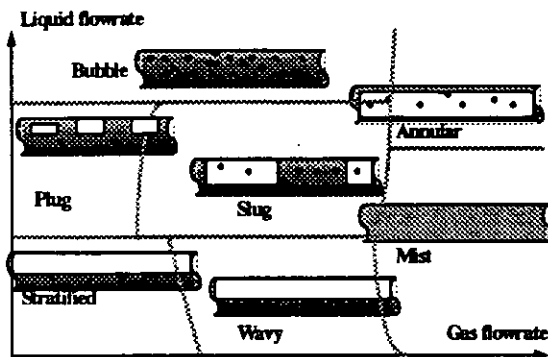


Figure 1 Flow regime map horizontal flow.

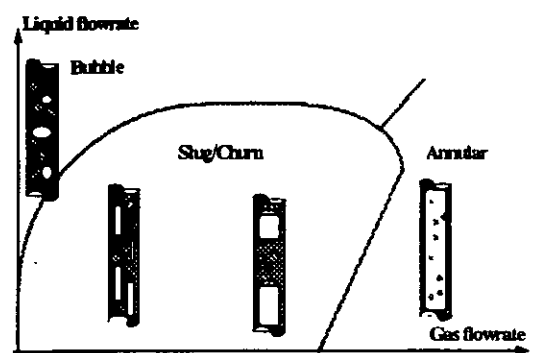


Figure 2 Flow regime map vertical flow.

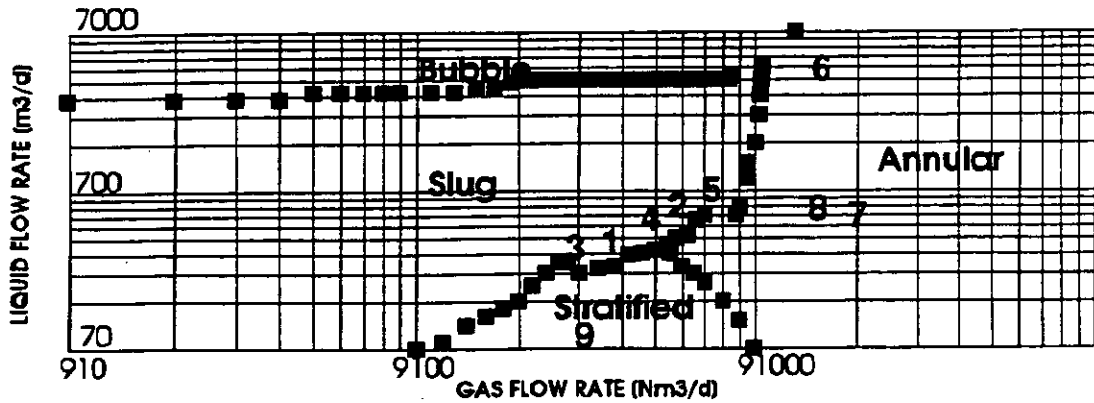
The measuring principle of the MCF 350 Multiphase Flow meter requires a slugging flow and the meter must be installed in a horizontal section. The MCF 350 meter is only depended on slug flow as such, and does not set any requirements to the slugs through the meter. This paper will therefore discuss only the horizontal flow regimes with special attention on the horizontal slug flow regime.

Regime prediction and identification at Dan F

Prior to the installation of the MCF 350 Multiphase flow meter at Dan F a detailed investigation of the actual volume flow was done based on the well test data available. Through this exercise a number of wells were found to be within the operational range of the MCF 350 meter. Some wells, with either high gas production or low oil production or a combination of both, were predicted to produce outside the operational range of the MCF 350 meter.

To perform an evaluation of the flow regime for the different well production effects from fluid properties, pipe inclination and pipe diameter must be taken into account. For this purpose a software based flow regime prediction tool was used. This is a useful tool in order to successfully modelling of the changed regime borders caused by the actual fluid properties, flow conditions, etc.

The predicted flow regime map with the different well production rates based on available welltest information from Dan F is shown in Figure 3.



| Identification of well predictions | | | |
|------------------------------------|--------|--------------------|--------|
| Slug flow regime | | Other flow regimes | |
| 1 | Well 1 | 6 | Well 6 |
| 2 | Well 2 | 7 | Well 7 |
| 3 | Well 3 | 8 | Well 8 |
| 4 | Well 4 | 9 | Well 9 |
| 5 | Well 5 | | |

Figure 3. Flow regime map for Dan F wells

Through the ongoing development project of the MCF multiphase metering technology with Norske Shell and Shell Research (KSEPL) the flow regime prediction was performed by Shell Research on their Shell developed Regime Prediction Tool.

Similar flow regime prediction was done on a software tool being developed at Kongsberg Offshore a.s. The KOS Flow Regime Prediction Tool is based on correlation and theoretical models from open literature. The two prediction tools gave matching results.

4. PROCESS CONDITIONS AT Dan F

Due to a number of reasons the wells on Dan F are tested on different choke settings.

Consequently the production rates from the wells also changed.

Initial predictions of flow regimes indicated for some wells production in the boarder area of the operational range of the MCF. These wells were therefore closely monitored and the flow regime was identified to be either within or outside the operational range.

The fluid characteristics for the Dan field:

- Density of the oil: 850 to 885 kg/m³ at 15degC
- Density of the gas: (natural gas)
- Viscosity of the oil: 8 cP at 30°C (down to 2 cP can occur)
- Viscosity of the gas: (natural gas)
- Density of production water: 1020 - 1030 m³/kg at about 30°C
- Salinity: from 2% to 3%
- Pressure: about 13 bar (test separator pressure)
- Temperature: 15 to 60 degC

Surging well.

For the Dan F wells with heavy surging the production rates varied from production within the operational range to production outside the operational range of the MCF. This effected the total accuracy of the specific well measurement as further discussed in chapter 6.

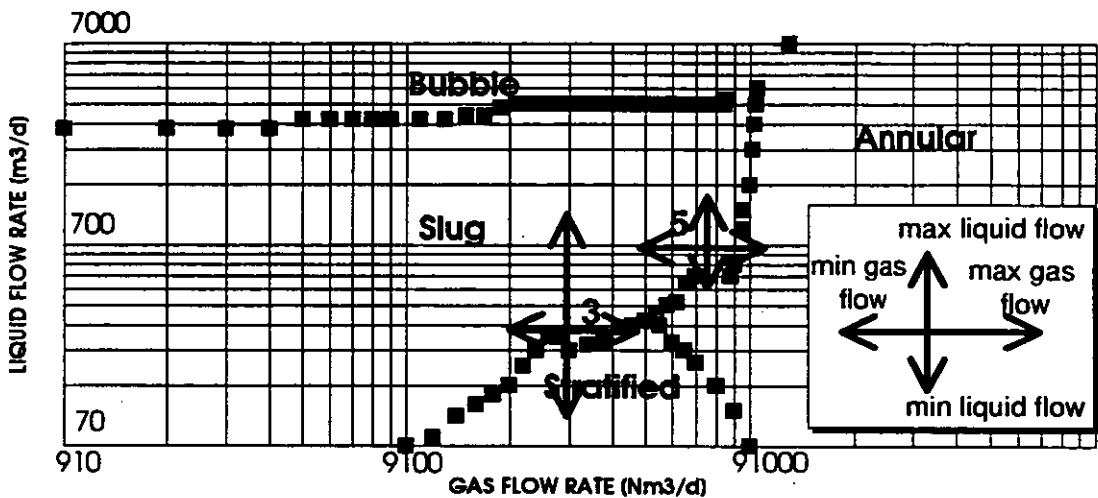


Figure 4 Example of flow variation in surging well production.

Sand production.

All wells at Dan F produced larger or smaller amounts of sand. The sand production gave erosion on the intrusive sensor plates of the KOS MCF 350 meter. During the six month period a wear of 0.5 to 1.0 millimetres was found on the upstream edge of the on the PCB sensor plate. Such erosion does not effect the quality of the measurements as the sensor is designed with upstream edges to withstand moderate sand production for upto three years.

Due to a production failure in the moulding process of the sensor used at the Dan F field the core of the sensor elements was directly exposed to process flow. The smaller sand erosion of the upstream edge led to an opening between the outer and inner PCB layers on the sensor element. This unexpected malfunction was indicated by a shift in the measurements and the sensor was replaced immediately.

A development programme for alternative sensor materials is now being finalised at Kongsberg Offshore a.s. The new sensor is designed to withstand sand erosion as well as high pressure and temperature.

Wax deposition.

Some of the wells gave wax deposition due to low temperature at the MCF 350 installation point upstream the test separator (for mechanical installation see chapter 5, Figure 5). The sensor elements were therefore manually cleaned regularly. An increasing wax layer on the sensor plate gave a shift in the calibration value. However, such wax deposition is easily detected by inspection of capacitance signal from the sensor, and did therefore not influence the quality of the well tests performed.

As an alternative to the manual cleaning procedure of the sensor plates used for the DanF test capacitance signals for a gas filled pipe can be inspected through the MCF 350 system. Any consistent shift in the measured values compared to corresponding gas calibration values will indicate a wax deposition on the sensor plates.

(More detailed description of different methods to avoid wax deposition or remove such wax layer on the sensor plates are shown in ref. /2/).

5. Dan F TEST INSTALLATION

The MCF was installed at the test separator deck on the Dan F platform. An overview of the test installation is shown in Figure 5.

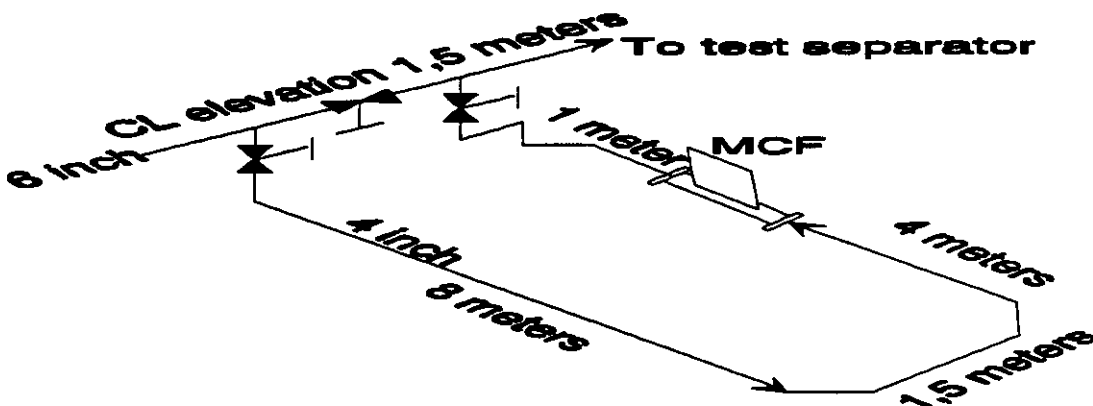


Figure 5. Mechanical layout of test installation.

The MCF system tested at Dan F consisted of:

- KOS MCF 350 Field Unit, 4 inch
- KOS MCF 350 Signal Conditioning Unit
- KOS MCF 350 Control System

The KOS MCF 350 Field Unit was installed upstream of the test separator in a purpose made bypass loop. The well flow from the test header was then either routed through the KOS MCF 350 meter and to the test separator or directly into the test separator.

The KOS MCF 350 Field Unit was connected to the KOS MCF 350 Signal Conditioning Unit in the Central Control Room through a purpose made cable. The cable length from Signal Conditioning Unit to Field Unit was 100 meters.

Test separator instrumentation.

The test separator instrumentation was as listed below.

- The oil metering system for the test separator consisted of:
 - 1 off 1 inch turbine meter, Hydril.
 - 1 off 2 inch turbine meter, Hydril.
 - 1 off 3 inch turbine meter, Hydril.

- The gas metering system for the test separator consisted of:
 - Standard Daniel Junior Orifice fitting with manual replacement of orifice plate.

- The water metering system for the test separator consisted of:
 - 1 off 1 inch Electromagnetic flow meter, Krone.
 - 1 off 3 inch Electromagnetic flow meter, Krone.

The size of the used reference meters on the gas, oil and water leg was chosen and optimised dependent on the actual flow. Only one meter was used for oil and one for water at the time.

All instrumentation on the test separator has for this test period (December 1993 to May 1994) been subject to ordinary maintenance such as re-calibration of pressure transmitters and replacing of turbine meters. Action was taken to increase level stability of the test separator. The level indicators were opened to drain to give a very low circulation of crude to prevent wax, sand and others to block the level transmitters.

Repeatability tests on the reference measurements using wells with stable production was performed. From these tests it was concluded that the repeatability of the reference measurement was varying through the whole test period.

Accuracy figures for the reference measurements could not be directly derived from these tests. However, results from these tests and judgement done by metering specialists in Mærsk Oil & Gas the accuracy of the reference measurement was expected to be:

- ± 5 - 7 % for oil volume flow rate
- ± 10 - 15 % for gas volume flow rate
- ± 8 - 10 % absolute for Watercut

6. TEST RESULTS

Test results for well production within the operational range of the meter are shown in Figure 6 a) and 6 b) with the corresponding reference measurements at the test separator.

A number of measurements from 5 different wells are presented from test period, November 1993 to May 1994.

There were 38 wells available at Dan F for this test period. An overview of the number of wells tested and welltests performed is given in table 2.

| | Test separator | KOS MCF 350 |
|---------------------------------|----------------|-------------|
| no. of wells tested | 30 | 5 |
| tot. no. of welltests performed | 124 | 22 |

Table 2 Overview of Dan F wells tested and welltests performed from Nov. '93 to May. '94.

This discussion will highlight the performance of the KOS MCF 350 Multiphase Flow meter based on wells tested in the test period.

The accuracy specification for the **KOS MCF 350** :

± 10 % for liquid volume flow rate

± 10 % for gas volume flow rate

± 3 % absolute for Watercut

To evaluate the quality of the MCF readings its important to take in to consideration the expected accuracy of the reference measurements as given in chapter 5 above.

In Figure 6 a) and 6 b) the readings for the five different wells are shown as the test separator measurement on the abscissa axe and the corresponding MCF measurement on the ordinate axe.

The specified accuracy of the MCF 350 multiphase flow meter of ± 10 % of the flowrate for liquid (oil and water) and gas is shown graphically. In addition the different wells with surging production are marked. The behaviour of these wells are described further in chapter 4.

A full verification of the specified accuracy of the KOS MCF 350 meter was not possible. Such verification can only be done based on special designed reference measurement system with the required stability and repeatability.

The acceptance of the actual deviations between the MCF 350 measurement and the test separator must therefore be based on the specified accuracy of the MCF 350 combined with the expected accuracy of the test separator as independent measurements.

Deviation larger than the specified ± 10 % on the liquid and gas flow has therefore been closely examined and accepted.

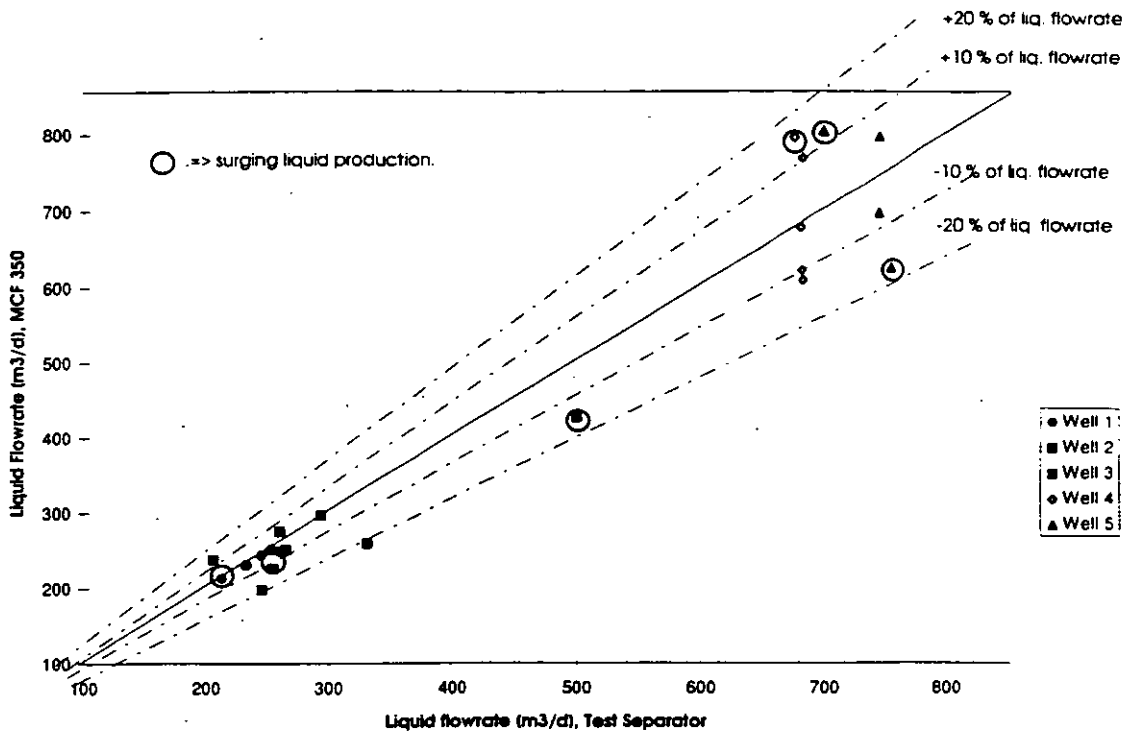


Figure 6 a) Test results for liquid flowrate.

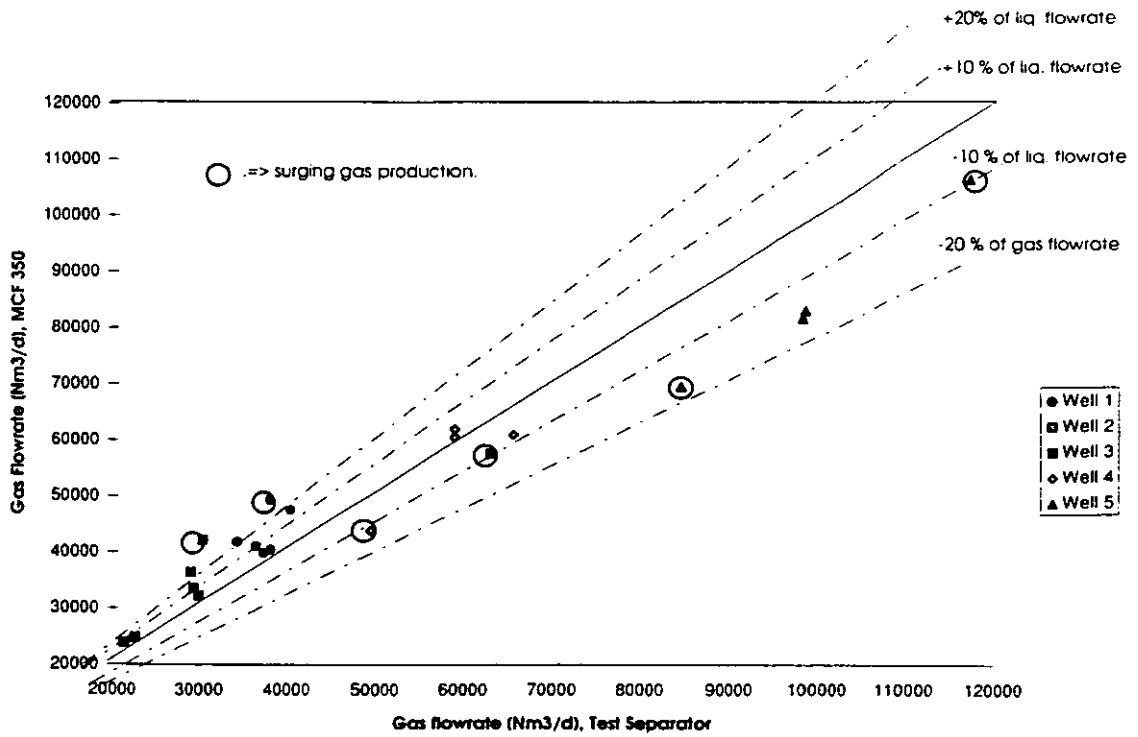


Figure 6 b) Test results for gas flowrate

The larger deviations shown in Figure 6 a) and 6 b) are mainly caused by surging well behaviour. Surging well production gave larger deviations as the well partly produced in flow regimes outside the operational range specified for the MCF.

The other test results are acceptable based on combination of the specified accuracy of the MCF 350 and the expected accuracy of the reference measurements.

As shown, repeated measurements on identical production has for the majority of the wells was not possible due to a number of reasons.

The Dan F wells tested produced from 10 % to 40 % water in the total liquid. The MCF 350 meter measured in average a lower watercut with a 10% absolute deviation relative to the test separator. The systematic underreading was small for the lowest watercuts and increasing with increasing water content in the produced total liquid (watercut).

The recorded systematic underreading is thought to be an effect of both overreading on water flows at the separator and a systematic underreading by the MCF 350. The underreading by the MCF 350 has been examined closely and found to be minor and caused by high gas volume fraction. This is a subject for optimisation for later tests in similar flow conditions with high gas volume fraction (GVF). A possible solution for this phenomena has been found.

Generally a stable deviation was found for the MCF and the test separator for the different wells at a stable production level. Changed production rates gave a shift in the deviation reflecting the accuracy for the different flow rates both for the MCF and the reference measurements.

7. Acknowledgement

This paper has only been possible to realise through a close and open co-operation between the Production Programming group in Mærsk Oil and Gas and Kongsberg Offshore a.s. Further we will like to acknowledge the staff at the Dan F installation for all practical help and for the flexibility shown during the active test periods at their installation.

We would also like to acknowledge the assistance and advises given by David Brown at Shell Research KSEPL prior to the performance of the tests.

8. References:

- / 1/ D. Brown, J.J.den Boer and G. Washington: "A multi-capacitor multiphase flow meter for slugging flow",
The North Sea Flow Measurement Workshop, October 1992.
- /2/ D. Brown: "Field experience with the multi-capacitor multiphase flow meter",
The North Sea Flow Measurement Workshop, October 1993
- /3/ C.J.M. Wolff: " The required operating envelope of multiphase flowmeters for oil production measurement",
The North Sea Flow Measurement Workshop, October 1993.

USING THE MFI MULTIPHASE METER FOR WELL TESTING AT GULLFAKS B

Ole Økland, Statoil Research Centre, Trondheim, Norway
Hans Berentsen, Statoil technology division, Stavanger, Norway

SUMMARY

Results from offshore testing of a multiphase meter is reported. The objective of the test was to investigate the multiphase meter's ability to perform well testing in a more time efficient manner than with a test separator. The results show that it is possible to test all the wells at Gullfaks B within 2 hours with very satisfactory results.

The paper presents a sequence where five wells are tested within 20 minutes. Testing the same wells using the conventional procedure for well testing takes some 20 hours. By optimizing the multiphase meter against the test separator it is possible to obtain an accuracy on the oil rate within 5 % compared to the reference oil rate. This accuracy is based on a 3 minutes logging interval for the multiphase meter compared with a four hour conventional welltest. For most of the wells the accuracy is within 4 % for all three phases.

1 INTRODUCTION

1.1 Background

Some years ago the main discussion in multiphase metering focused on the possibility to succeed in developing a reliable and accurate multiphase meter. Today there exist several commercially available first generation meters. In the last two years many oil companies have gained experience with different meters from field applications and tests. The main issue now is to investigate the performance of the various meters in terms of accuracy and reliability, and finding "the application envelope" with respect to flowrates, composition and flowregimes. The oil industry is about to enter the application phase of multiphase meters using them both topside on existing platforms and subsea on satellite fields on a permanent basis.

If we consider various multiphase meter applications we can divide these into two groups:

- * **WELL TESTING** - By this we mean testing of a well's performance over a period of time. The information is used for reservoir management and well operation purposes.
- * **ALLOCATION** - This refers to "fiscal" metering where the multiphase meter measurement is used to calculate taxation or to apportion production between partners in a field, multiphase pipeline network or for satellite tie-ins to a process platform.

The experience gained from working with different multiphase meters at Gullfaks B (GFB), has taught us that these meters are very efficient for well testing. The time necessary to perform one well test is reduced to the well change-over interval and a short test time.

1.2 Previous work

The first tests with multiphase meters on GFB, the Fluenta MPFM 1900 and the Multi-Fluid International (MFI) LP-Meter, took place in December 1992 and in March 1993, respectively.

The results from these tests have been published earlier [1,2,3].

To summarize the experience with these two electromagnetic meters, they both measure the composition of the oil-continuous wells at GFB with a satisfactory accuracy. The LP-meter can also be used to measure flow rates. From a user's viewpoint these tests indicate that the time is approaching when qualified multiphase meters can be implemented.

In July 1993 new tests on the same two meters took place and showed the same conclusions on overall accuracy and performance. The results presented in this paper showing the MFI LP-meter's ability to perform time-efficient well tests and are from these second experiments.

2 THE GULLFAKS B MULTIPHASE METER TEST RIG

Presently about 20 wells on GFB are producing a total of 30.000 Sm³/d of oil through two identical first stage separators and the test separator. The test separator is normally used for several purposes. Its main activity is the well test programme. But, it is also used in well maintenance programs and for drilling purposes. Upstream of the inlet to the test separator a 4" bypass loop has been connected to the test line. The test section in the bypass loop is shaped like a vertical "U". The multiphase instruments can be placed in both vertical legs and in the horizontal leg.

Figure 1 shows a picture of the MFI LP meter in the test rig. In the background it is possible to observe the test separator and the 8" testline. For information on the test rig, details can be found in [3].

3 TEST PROCEDURES FOR WELL TESTING

Each well on GFB is tested sequentially in a test programme. The X-mas trees at GFB are situated on the platform deck, and there is a very short distance between the manifolds and the separators. The different wells are routed into the test separator or into two identical first stage production separators via a manifold system controlled from the central control room. This means that the time required to change a well from the production separator to the test separator is short.

The stability time for a well is solely dependent on the separator. It normally takes half an hour after change-over before a log can be started. During this time the test separator control system will stabilize the single phase flows rates for the new well. The control room operator is responsible for running well tests and for changing between wells by remotely operating the manifold valves on each well. An official well test has a duration of four hours. To ensure correct gas measurement, orifice plates of four different borings are used. The test separator readings are totalized at 30 minutes intervals to give volume production rates for oil, water and gas.

Analysis of several well tests show that it is possible to reduce the test duration. Including preparation and stability time, each well test using the test separator could be reduced to approximately 3 hours.

Figure 2 is showing a sequence where well B21 has been tested and the operator wants to test next well, B10.

4 THE MFI LP- MULTIPHASE METER

The MFI LP meter is a compact, full-bore meter for direct measurement of wellstream from live oil and gas wells. The meter is only applicable to oil-continuous flow. Multiphase flow rates are calculated by measuring

the composition of the flow mixture (oil, water and gas volume or mass fractions) and the velocity at which the multi-phase mixture is flowing through the meter. These readings are processed to provide flow rates of oil, water and gas at actual conditions.

The composition meter consists of a microwave sensor element for measuring mixture dielectric properties and a gamma densitometer for measuring mixture density. The dielectric properties of the multiphase flow are most sensitive to water and the density reading is sensitive to the gas-liquid ratio. These complementary properties are measured very accurately by the MFI LP Meter to give precise information about the composition of multiphase flows. In the meter, the dielectric measurements, adjusted according to the temperature and pressure conditions, are combined with the density measurements to yield the instantaneous ratios of oil, water and gas.

MFI's way of measuring velocity is based on dielectric measurements from two cross-sections that are analysed with cross-correlation routines to determine the average time it takes the oil, water and gas mixture to flow from the first to the second section. The distance between the two measurement sections is known, and the production rates of the components can be found.

Physically, the MFI meter consists of a short spool-piece with microwave, density, temperature and pressure sensors, and a box housing the electronics system. The electronics comprises a system generating and processing microwave signals and a computer that does the data processing. The meter calculates flowrates, compositions every second. To reduce the amount of data the programme average 10 samples such that data recording is taken every tenth second.

Later this autumn, MFI and Statoil, are planning a test at Gullfaks B on a new MFI Full-Range meter, which can also be used in water-continuous flow. This development has been sponsored by the oil-companies BP, Elf, Philips, Saga, Total and Statoil.

5 CALIBRATION OF THE MULTIPHASE METER

After the installation of the MFI LP meter a calibration is required. This was performed in December 1992 on the gamma densitometer in air at atmosphere condition, and the whole procedure was finished after about 10 minutes. There has been no further calibration of the meter since this first calibration.

It is also necessary to enter available data about the process fluids into the flowcomputer. The necessary data consists of densities at process conditions and water conductivity. No attempts have been made to discriminate between the oil, water and gas in the different wells tested.

Based on results from earlier tests of the meter [1, 2] some efforts were made to improve the accuracy. The results from the composition metering were very satisfactory showing accuracies within +/- 2 % absolute deviation on all three phases. For most tests the velocity readings were systematically high by 8 - 12 %. It was therefore decided to introduce a velocity calibration factor. In this way the meter could be tuned to Gullfaks B conditions aiming for an overall accuracy within 5%.

6 RESULTS USING THE MULTIPHASE METER FOR WELL TESTING

6.1 Objectives

The main objective of the test was to show that by introducing a multiphase meter after the test manifold, it is possible to perform testing of all the wells at GFB in 2 hours.

A second objective was to show that it is possible to tune a multiphase meter to give an accuracy in well testing better than $\pm 5\%$ of actual rates for all three phases. If this accuracy can be achieved it can open up for using multiphase meters for "allocation" purposes.

6.2 The test sequence

The test programme consists of several test series where two different wells are tested sequentially. The period of change-over are logged on data files. A full well test on the test separator is run for each well to obtain accurate reference production data for comparison.

In this presentation the data from three test series are used to illustrate the performance of the meter:

- * Well test: B21 - B10
- * Well test: B9 - B25
- * Well test: B25 - B9

To show the overall accuracy of the meter and the possibilities a reliable multiphase meter offers, emphasis has been given to the flowdata from the MFI LP-meter taken from the change-over period between the testing of two wells.

In this test set-up the results from the multiphase meter are based on only a few minutes test interval with stable flow. The reference measurements are official well tests over a four hour period.

6.3 Change-over from well B21 to B10

The figures 3a,b,c give detailed information from the tests on well B21 and well B10 in three different ways.

Figure 3a shows the production rates using a 10 second sampling interval. Looking into the details it can be observed that there is natural variations in the production rates. The flow variations seem to follow a cyclic behaviour. If the flow data from the multiphase meter is studied, it can be observed that the phase fractions are stable over one cycle period. The flow velocity on the other hand is following a cyclic pattern and therefore will create the same pattern for the flowrates.

In figure 3b a sliding window of 100 seconds has been used. Comparing the two figures it can be seen that the latter gives the necessary flowrate information without disturbances from the smaller fluctuations in the velocity. By increasing the average sampling time local periodical flow variations can be dampened.

In figure 3c the results are averaged from the beginning of the test. In this figure it can be observed that B10 is stable four minutes after start of the change-over. The change-over period can be separated into two parts which not easily can be discriminated. The first part contains the time it takes the operator to operate the 4 valves to route a new well from the production separator into the test separator and vice versa. The second period is the time needed to stabilize the flow from the new well after the valve operations are finished. In the B21-B10 change-over it can be observed that the time needed is 4.5 minutes. In this situation the operator used quite a long time in the operation of the valves compared with later similar operations. Other similar change-overs indicate that this operation can be reduced to approximately two minutes.

Fig 3d shows the time needed to perform similar well tests with the test separator. The total operation lasted 9 hours. It is possible to reduce this time to a total duration of 3 - 4 hours for two wells. Included is the time for manual work like changing orifice plates, taking samples etc.

A question of major importance when new equipment is introduced concerns performance, i.e. accuracy and reliability. In figure 3c the test separator readings are superimposed and the reference flowrates shown in frames. Table 1 (B21, B10) shows the accuracy using the two different methods.

It is not straight forward to evaluate the performance of multiphase meters. If one of the phases contributes only a few percent of the total flow it is not very meaningful to refer the accuracy for that phase to the reference measurement of the single phase. The accuracy data are therefore presented in two different ways. The first method compares each individual phase with the reference phase, while the second method compares the phase readings with the total flow. The results from the two wells are measured very satisfactory within $\pm 1.5\%$ compared with total flow and within 3% for the oil and gas rates compared with reference single phase flowrates.

Well no. B21 has a very low watercut and can be used as a good example that clearly illustrates the problem in defining accuracy figures for multiphase meters.

The deviation on water is quite large (40%) using the single phase flowrates as a reference and nearly negligible when referred to total flow (0.6%). This is because the water content in the well is only 1.5% (volumetric). From fiscal metering it is well-known that the a 4" reference turbine meter is not very accurate for such low water flowrates.

6.4 Testing five wells in 20 minutes

Since the instrument is excellent for trending of a well performance, the special sequence, "Testing five wells in 20 minutes", was set up to show that the LP-meter has ability to test many different wells in a short period of time. Figure 4a shows a 20 minutes test sequence with 5 different wells. Superimposed in the figure are readings from the test separator for each well.

In figure 4b the same test using the test separator is shown. Using this method 20 hours of testing was needed to complete the programme. The test programme was started when B21 was tested. After a 4-hour test was finished, next well B10 was routed into the test separator for a complete test. The first test of B9 was abruptly when the multiphase meter gave no readings, indicating water continuous flow and the official well test was abruptly. B25 was the next well for test, followed by a new test of B9.

B9 was tested twice in this sequence to illustrate an important limitation Statoil has experienced using electromagnetic multiphase meters in oilwells having a watercut between $30 - 50\%$ and injection of production chemicals.

B9 has a watercut around 30% . When 10 PPM of a corrosion inhibitor was injected the multiphase meter stopped to function indicating water continuous flow. Stopping the injection pump caused the well immediately to become oil-continuously, and the meter started to measure the flowrates again. Investigations later has shown that this chemical has an unwanted effect on the surface active properties of the emulsion.

In our case we have concluded that the transition point between oil-continuous emulsion and water-continuous emulsion has been moved down on the watercut scale.

Table 1 shows the accuracy for each well. The overall accuracy are essentially within $\pm 5\%$ using each phase as a reference and within $\pm 4\%$ using total flow as a reference. B25 has been divided into two parts. The results shown in table B25a is referring to the output from the multiphase meter during the beginning of the test, while table B25b is referring to the last minutes of the test before a new well was replacing B25. The gas fraction at actual condition referring to the test section for the various wells at GFB, varies from $30 - 50$ volumetric percent. The flow regime is most likely bubble-flow in the testsection. The difference in the flowrates seen by the multiphase meter for B25 might be caused by slip flow. B25 is produced from a different reservoir and has a higher gas-content than the other wells. Comparing test results also show that the results for this well is worse than the results from the others. For the other wells the accuracy are far better than the requirement on $\pm 5\%$.

This experiment shows that during 20 minutes five well tests of different wells can be performed. That gives an average of about four minutes for each well. Comparing the two different methods for well testing we can conclude that significant improvements can be obtained by starting to use multiphase meters.

7 CONCLUSION

Statoil has gained experience in multiphase meters using the MFI LP meter on Gullfaks B from December 1992 to March 1994. For Gullfaks B flow condition, the meter is qualified for use in well testing. Compared to the conventional method using the flow readings from the test separator it is possible to optimize the time needed for well testing and thereby releasing the test separator for other purposes. The change-over period needed before steady production rates for a new well is achieved is less than 4 minutes for the majority of the wells. After the valve operation period is finished it takes 1 - 2 minutes before the meter has obtained stable production rate readings for the new well routed into the test line. The stability time needed between two well tests is dominated by the time needed for the valve operation. This will be very different on a satellite field having a dedicated test line from the subsea template. Here the stability time will be dominated by the multiphase flow transport phenomena. Of course this could be eliminated if the multiphase meters were installed subsea.

Five wells are tested within 20 minutes with the meter compared with 20 hours needed using the test separator. This indicates the possibility of testing all the wells on Gullfaks B within 2 hours. Adequate data from prior testing has been used to formulate a correction factor which gives results with an acceptable accuracy. In this way the performance of the multiphase meter has been optimized to give 5 % maximum deviation on flowrates used on Gullfaks B.

Using electromagnetic multiphase flowmeters, that only function in oil continuous conditions, it is important to know that corrosion inhibitors or other chemicals may have an unwanted effect on the multiphase flow. By injecting small quantities of some chemicals in wells having a watercut around 30 - 40 %, the flow can become water-continuous causing the meter to malfunction.

The results of this test demonstrate the usefulness of multiphase meters in one application, using multiphase meters in line with test separators or replacing test separators for well testing. This makes it possible to use existing test separators as production separators of hydrocarbons.

REFERENCES

1. Økland, O. and Berentsen, H. Experience from water-in-oil monitors and multiphase meters, Automation Conferance (NIF-IFEA), Sandefjord 9 - 10. September 1993
2. Gaisford, S., Berentsen, H. and Amdal J. Offshore multiphase meters nears acceptable accuracy level, Oil & Gas Journal, 17 May 1993
3. Økland, O. Gullfaks B - Field test facility for multiphase meters, Multiphase meters and their subsea applications, London 14. April 1993.

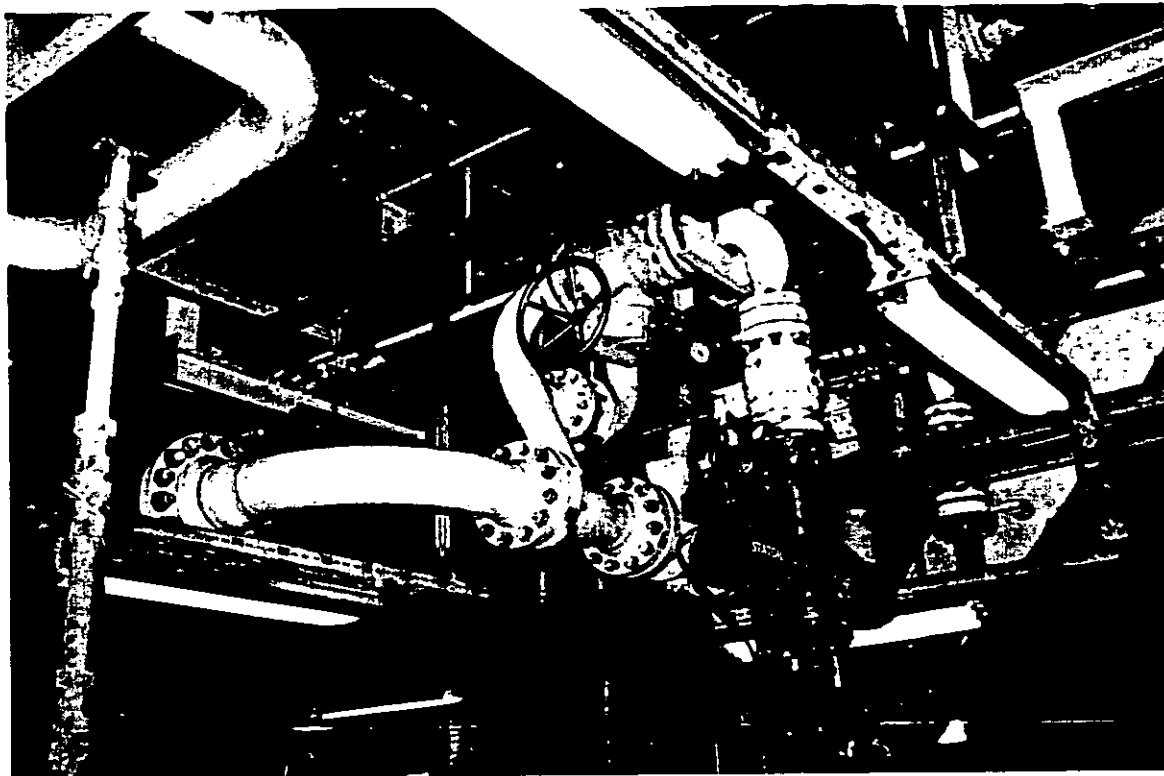


Fig. 1 MFI LP-meter at Gullfaks B

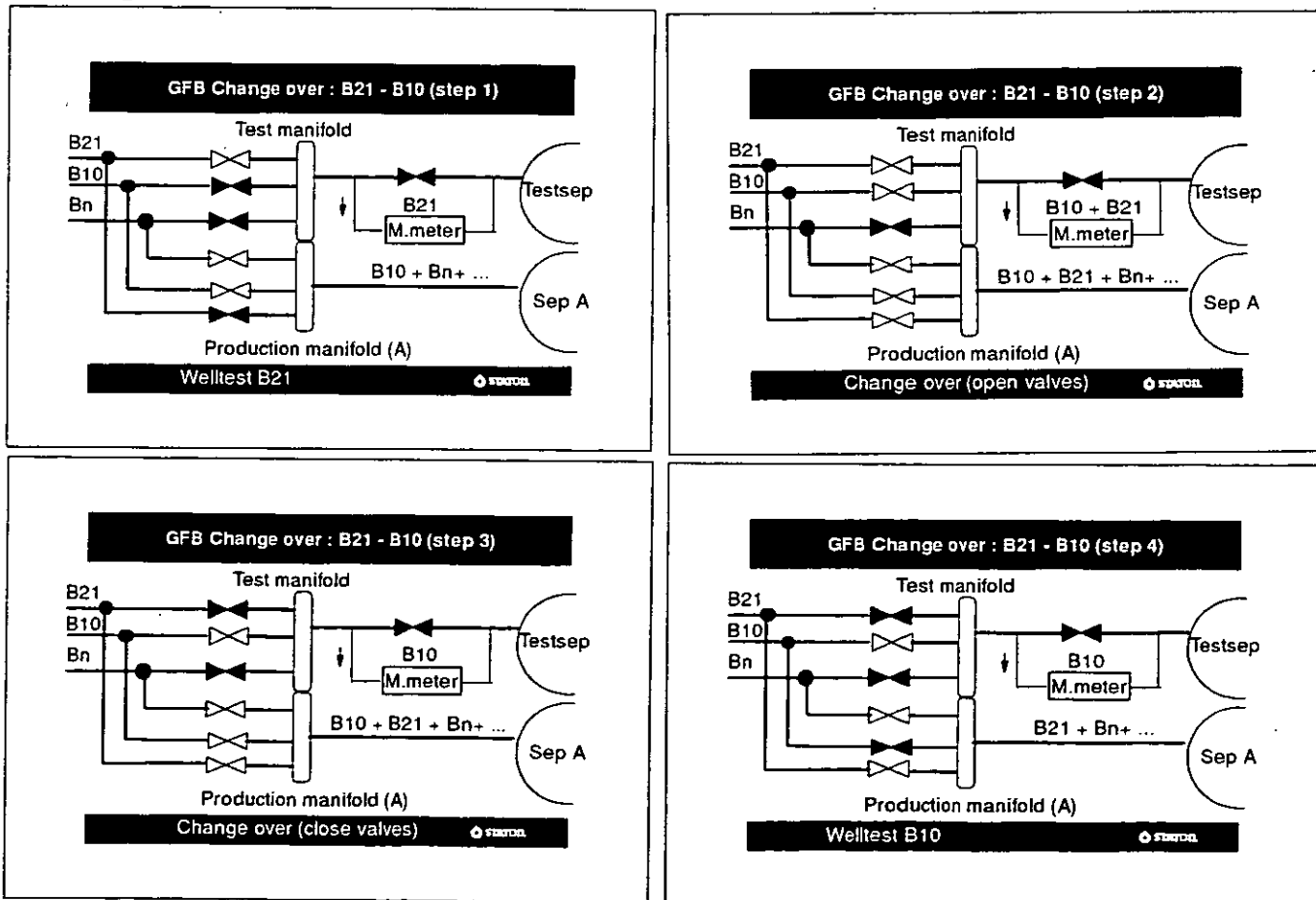


Figure 2. Change sequence B21 - B10

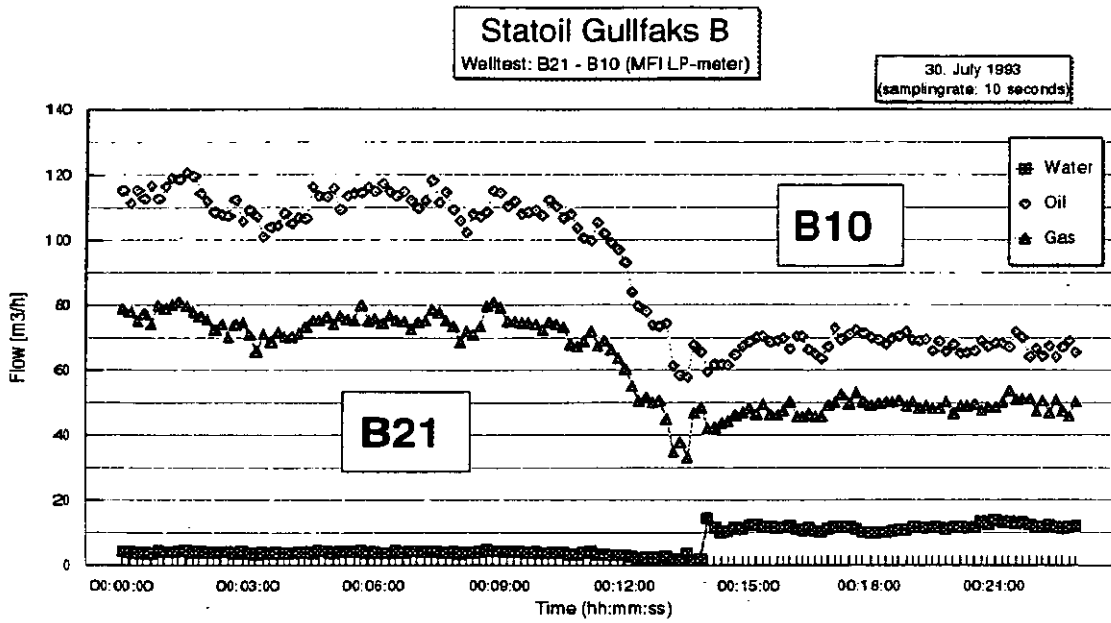


Fig. 3a Inst.flowrates (10 seconds sampling interval)

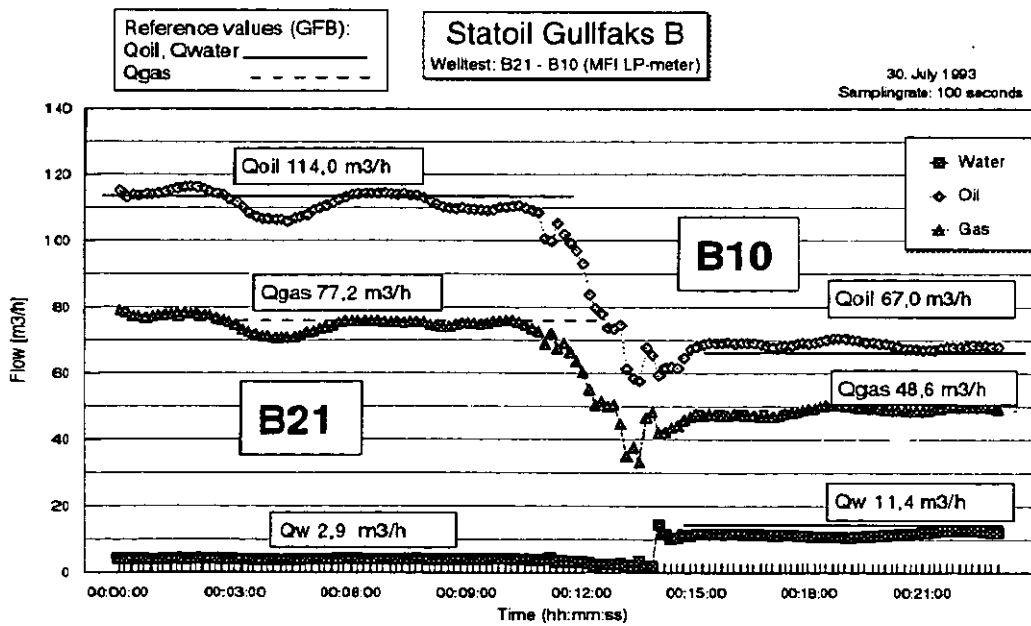


Fig. 3b Inst.flowrates (100 seconds sampling interval)

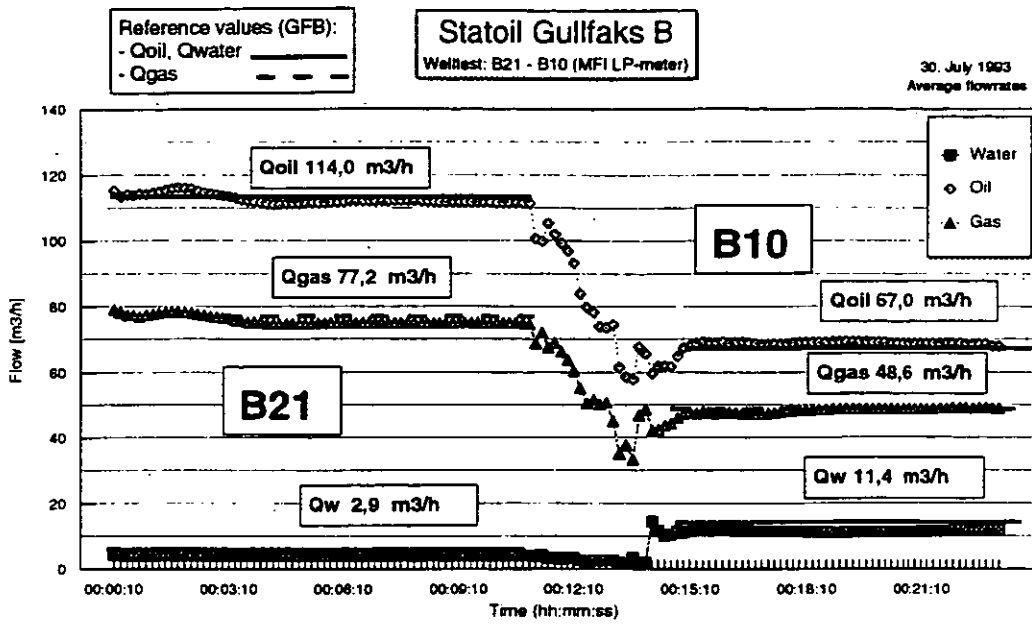


Fig. 3C Average values B21-B10

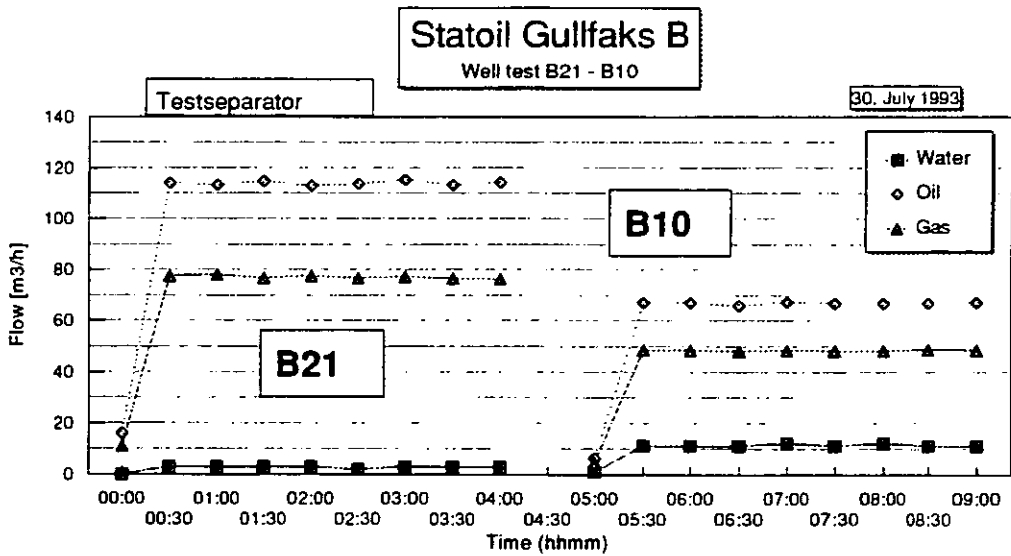


Fig. 3d Well: B21 - B10 Testseparator

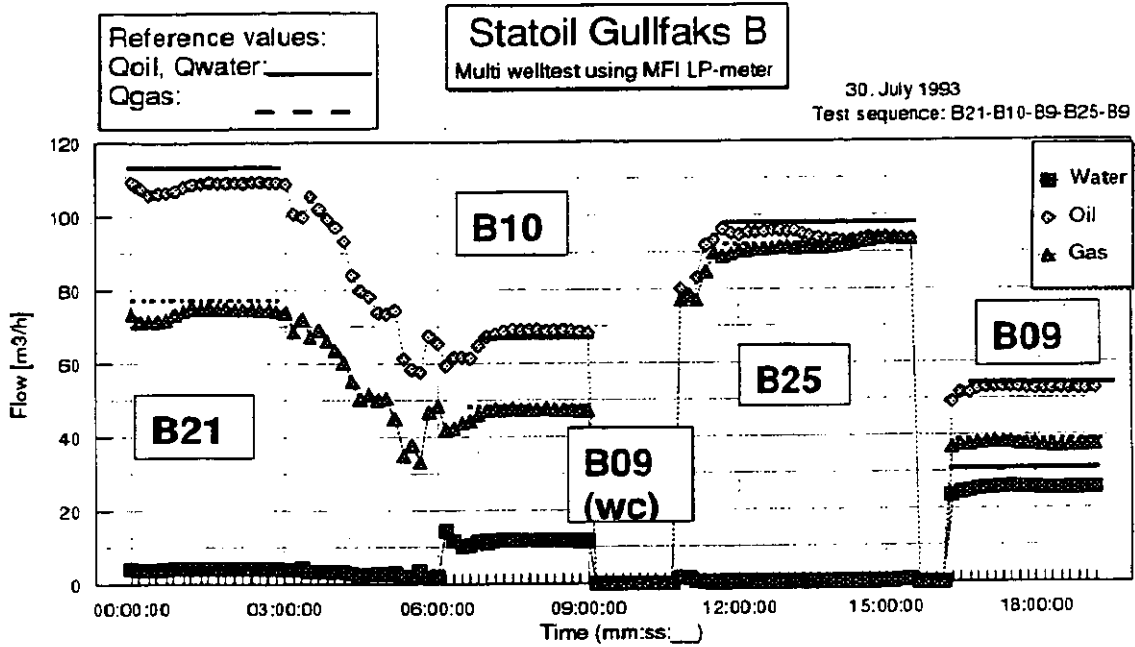


Fig. 4A Testsequence 5 wells

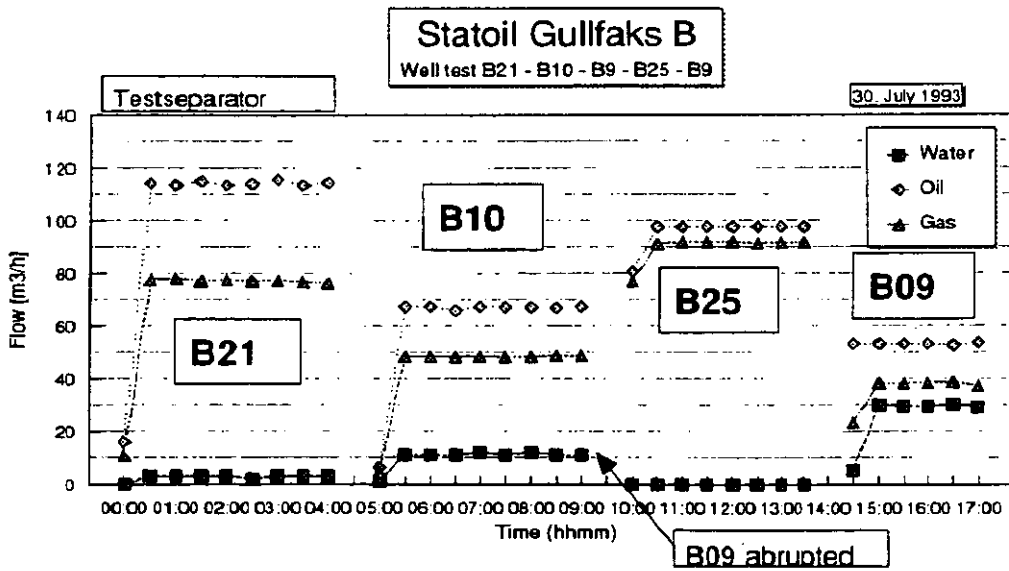


Fig. 4B welltesting using testseparator

Using the MFI LP meter for well testing

Test 30, July 1993

Accuracy MFI LPmeter - GFB reference

Well B21 - B10 - B25 - B09

B21

MFI B21
GFB B21
Accuracy (Ref Qtot)
Accuracy (Ref Qphase)

| Qoil | Qgas | Qwater |
|--------|--------|--------|
| [m3/h] | [m3/h] | [m3/h] |
| 111,54 | 75,06 | 4,10 |
| 114,05 | 77,20 | 2,92 |
| -1,29 | -1,10 | 0,61 |
| -2,20 | -2,77 | 40,41 |

| Fractions (absolute) | | |
|----------------------|-------|---------|
| % Oil | % Gas | % Water |
| 58,49 | 39,36 | 2,15 |
| 58,74 | 39,76 | 1,50 |
| -0,25 | -0,40 | 0,65 |

B10

MFI B10
GFB B10
Accuracy (Ref Qtot)
Accuracy (Ref Qphase)

| Qoil | Qgas | Qwater |
|--------|--------|--------|
| [m3/h] | [m3/h] | [m3/h] |
| 67,70 | 48,57 | 11,53 |
| 66,95 | 48,52 | 11,36 |
| 0,59 | 0,04 | 0,13 |
| 1,12 | 0,10 | 1,50 |

| Fractions (absolute) | | |
|----------------------|-------|---------|
| % Oil | % Gas | % Water |
| 52,97 | 38,00 | 9,02 |
| 52,79 | 38,26 | 8,96 |
| 0,19 | -0,25 | 0,07 |

B09 (WC)

Corrosion inhibitor -> Well B09 water cont.

B25-a

MFI B25
GFB B25
Accuracy (Ref Qtot)
Accuracy (Ref Qphase)

| Qoil | Qgas | Qwater |
|--------|--------|--------|
| [m3/h] | [m3/h] | [m3/h] |
| 93,46 | 92,11 | 0,00 |
| 97,49 | 91,59 | 0,00 |
| -2,13 | 0,28 | 0,00 |
| -4,13 | 0,57 | 0,00 |

| Fractions (absolute) | | |
|----------------------|-------|---------|
| % Oil | % Gas | % Water |
| 50,36 | 49,64 | 0,00 |
| 51,56 | 48,44 | 0,00 |
| -1,20 | 1,20 | 0,00 |

B25-b

MFI B25
GFB B25
Accuracy (Ref Qtot)
Accuracy (Ref Qphase)

| Qoil | Qgas | Qwater |
|--------|--------|--------|
| [m3/h] | [m3/h] | [m3/h] |
| 90,33 | 94,59 | 0,00 |
| 97,49 | 91,59 | 0,00 |
| -3,79 | 1,59 | 0,00 |
| -7,34 | 3,28 | 0,00 |

| Fractions (absolute) | | |
|----------------------|-------|---------|
| % Oil | % Gas | % Water |
| 48,85 | 51,15 | 0,00 |
| 51,56 | 48,44 | 0,00 |
| -2,71 | 2,71 | 0,00 |

B09

MFI B09
GFB B09
Accuracy (Ref Qtot)
Accuracy (Ref Qphase)

| Qoil | Qgas | Qwater |
|--------|--------|--------|
| [m3/h] | [m3/h] | [m3/h] |
| 53,52 | 37,31 | 25,84 |
| 53,24 | 38,30 | 29,84 |
| 0,23 | -0,82 | -3,30 |
| 0,53 | -2,58 | -13,40 |

| Fractions (absolute) | | |
|----------------------|-------|---------|
| % Oil | % Gas | % Water |
| 45,87 | 31,98 | 22,15 |
| 43,86 | 31,55 | 24,58 |
| 2,01 | 0,43 | -2,44 |

Table 1 - Accuracy MFI LP meter versus test separator Gullfaks B

BP MULTIPHASE METER TEST EXPERIENCE

Dr W J Priddy
BP Exploration Operating Company Ltd

SUMMARY

The paper summarises test data obtained for the BP-developed multiphase metering system. The eight-year test programme included a rigorous and comprehensive flow loop investigation using an independent multiphase flow meter test facility and field tests at Wytch Farm, England and Prudhoe Bay, Alaska.

The paper highlights key findings along the development path which have enabled the system to evolve. Latest field test data from Prudhoe Bay demonstrate a measurement capability of comparable accuracy to a reliable test separator reference. Calibration for this was on a simple basis using water as the flowing medium.

The Alaskan data cover the most difficult of multiphase flow conditions, involving gassy flows exhibiting violent slugging and annular regimes. Gas volume fraction ranged from 62% to 95% and fluid pressure varied from 200 psig to 2300 psig. In combination with the previous testing, the trial gave confidence in reliability and demonstrated resilience of the calibration.

NOTATION

| | |
|--------------|--------------------------------------|
| GOR | Gas/oil ratio |
| GVF | Gas volume fraction (%) |
| ρ_g | Gas phase density |
| ρ_{mix} | Total stream mixture density |
| ρ_o | Oil phase density |
| ρ_w | Water phase density |
| V | Instantaneous total volume flow rate |
| V_g | Instantaneous gas volume flow rate |
| V_o | Instantaneous oil volume flow rate |
| V_w | Instantaneous water volume flow rate |
| WC | Water cut (fraction) |

1 INTRODUCTION

Multiphase flow metering offers the potential for significant savings in capital expenditure in the development of oil fields. Several multiphase metering techniques are under development with the principal aim of replacing the conventional test separator and its associated piping and systems for reservoir management and well allocation flow measurements. A successful multiphase meter is expected to give significant improvements in operational efficiency and reduction in maintenance burden compared to conventional separation systems, with further savings in costs and a potential enhancement of production revenues.

The development of metering hardware beyond the basic phase separation and measurement approach is hampered by the complex nature of multiphase flows. The tendency of the phases to segregate results in generally non-reproducible, unsteady spatial distributions of the phases, which flow at different bulk velocities from each other and exhibit highly unsteady non-uniform velocity profiles. This complex behaviour is often over-simplistically described as the term "slip".

The BP-developed multiphase metering system is based on fundamental principles which overcome these inherent difficulties in measuring unprocessed multiphase streams. The philosophy of this measurement technique is to produce repeatable measurement response to oil, water and gas flow rates such that calibration is possible and is, indeed, meaningful in that it applies universally to subsequent applications in the field.

At the heart of the technique is a positive displacement meter. The development of this meter and, in particular, the principle of the flow constraining influence of its mechanical elements, was described in (1). It is combined with a gamma densitometer which measures mixture density and, as such, can measure the total stream mass flow rate. However, its intended use, as a system, is to measure the flow rates of oil, water and gas. For this purpose, it uses an additional measurement of water cut.

An account of the field testing at Wytch Farm and some of the laboratory flow loop results was reported earlier (1,2). This work facilitated the development of field prototypes of the positive displacement meter and a separate phase fraction measurement cell from which the water cut could be derived. The work exposed deficiencies in the system, particularly with regard to a characteristic but test-site dependent bias error, but also demonstrated a high degree of confidence in mechanical reliability. It showed that measurement accuracy suitable for well testing could be achieved and improvements to effect this were identified.

Following the Wytch Farm trial, the bias measurement error was investigated at BP Research. Subsequently, the opportunity arose to test the system at the Prudhoe Bay oil field which offered a significant extension in the range of flow conditions compared to the previous test facilities in Europe. This trial allowed further investigations of the shortcomings already identified and the chance to test design modifications to address these.

This paper presents significant findings from the overall test programme on the prototype multiphase meter system and the latest results from the testing at Prudhoe Bay. The data show that the principles of the metering technique work in practice.

2 MULTIPHASE METER SYSTEM

The positive displacement meter is shown installed at the Prudhoe Bay test site in Figure 1, with a phase fraction cell situated downstream in the background. Both devices have been described in the previous references (1,2). These prototypes were 4" designs, suitable for ANSI C1 1500 service as at the Prudhoe Bay test location.

The system uses a novel combination of a fast response (0.1 secs) gamma densitometer with the positive displacement meter. The gamma beam senses across maximum cross-sectional coverage of the multiphase mixture within a specially shaped chamber which is located integrally within the swept volume elements. This ensures that mixture density and total stream volume flow rate are measured simultaneously at a point where the phases are constrained to move at a single velocity. The fast response of the densitometer was selected on the basis of BP experience of tracking multiphase flows using nucleonic gauges.

The instantaneous oil, water and gas volume flow rates at meter pressure and temperature are derived from the following three equations. These can be deduced from simple summations relating total mass and volumetric flow rates to the phase flow rates and densities and from the equation defining the water cut. The relationships rely on the assumption of zero phase slip at the measurement point, as ensured by the integrated positive displacement - gamma densitometer system:

$$V_o = \frac{V \cdot (\rho_{mix} - \rho_g) \cdot (1 - WC)}{WC \cdot (\rho_w - \rho_o) + (\rho_o - \rho_g)} \dots\dots\dots(1)$$

$$V_w = \frac{V \cdot (\rho_{mix} - \rho_g) \cdot WC}{WC \cdot (\rho_w - \rho_o) + (\rho_o - \rho_g)} \dots\dots\dots(2)$$

$$V_g = V - \frac{V \cdot (\rho_{mix} - \rho_g)}{WC \cdot (\rho_w - \rho_o) + (\rho_o - \rho_g)} \dots\dots\dots(3)$$

The water cut is derived by a second sensing means, such as a phase fraction measurement device, as in the example of Figure 1.

A pressure transmitter mounted at a side tapping into the central densitometer chamber of the positive displacement meter gives the pressure at the multiphase flow measurement point. The

line temperature may be measured by a transmitter located in piping close to the multiphase meter. These readings are used to derive the single phase fluid densities which appear in the above equations.

Volume formation factors for the oil, water and gas and solution GOR may also be computed from the measured pressure and temperature at the multiphase meter to convert the line phase flow rates to stock tank quantities. The instantaneous phase flow rates are typically sampled at 0.1 second interval and integrated over the well testing period (which can be for many hours) to derive average flow rates.

3 TEST EXPERIENCE

The following account presents measurement data taken during the course of the entire test programme to establish the principles of the multiphase metering system and validate the associated calibration methods.

The analysis of measurement errors is used to assess the performance of the separate components as well as the phase flow rate measurement accuracy of the combined multiphase meter system.

Specifically, the positive displacement meter is evaluated in terms of relative error in total volume flow rate measurement.

The mixture densitometer reading and, in particular, adherence to the no-slip principle are assessed by the relative error in total mass flow rate measurement. This must account for any total volumetric error characteristic of the positive displacement element which contributes within the product of density x volume.

The means of measuring the water cut required by the system has also been evaluated.

Finally, relative errors in individual phase flow rate measurements are presented to analyse the accuracy of the multiphase meter system as a whole.

3.1 Error Definition

Here, the test data are plotted as measurement errors as determined by the difference between multiphase meter reading and reference reading of average flow rate. These errors are defined in "relative" terms; that is, they are expressed as a percentage of actual reading or flow rate (not as a percentage of full scale reading). (Note that, in the analysis of errors in individual phase flow rate measurement that follows, the term relative means percentage of actual phase flow rate and **not** of actual total stream flow rate).

3.2 Volumetric Evaluation

The purpose of this part of the analysis is to assess the accuracy and repeatability of the positive displacement element of the multiphase measurement system.

The average total (oil + water + gas) swept volume measurement through the positive displacement meter is compared with the sum of the oil, water and gas single phase measurements by the reference metering system.

The results from the Prudhoe Bay tests are shown in Figure 2, together with those taken from earlier controlled flow loop tests conducted using the independent multiphase meter test facility. There, the single phase reference metering was calibrated to accurate traceable national standards.

The volumetric "K-Factor" curve of the multiphase meter used in this graph was established from the single phase water testing in the independent flow loop facility. The capability of the positive displacement meter, calibrated in this simple way, to repeat multiphase total swept volume measurements to within $\pm 5\%$ relative is clearly demonstrated over a turn-down of 7:1.

Note that the flow loop tests covered pressures ranging 15 to 90 psig and involved the full range (0% to 100%) of gas volume fractions (GVFs) and flow regimes. The Prudhoe Bay data include

points for pressure ranging from 200 psig to 2300 psig and were entirely in the most difficult high void fraction range of multiphase flows.

The repeatability of the data in Figure 2 between test sites and periods is especially noteworthy. It confirms insensitivity to multiphase flow pattern and conditions and how the positive displacement design is accurate for extremes of unsteadiness and low pressure gas (where fluid leakage past clearances is expected to be at its worst).

Further, through the test programme in Europe and Alaska, 12,000 run hours have accumulated using the prototype meter. Although the original internal bearing system has been modified at various stages to improve performance (resulting in a proven design run for 2000 hours at Prudhoe Bay in 1993) all other components were not changed. Thus, the data demonstrate the ruggedness and reliability of the meter and the resilience of its calibration curve.

Details of the Prudhoe Bay field trial given in (3) describe the reference metering system and procedures used to ensure good quality measurement data. Accurate and reliable reference metering was not available for the gas phase during the earlier trial at Wytch Farm to enable total volumetric accuracy assessments. This trial was primarily used during the development stages to evolve a rugged and reliable mechanical design.

During the Alaska trial in July 1993, for one particular well - H21, the meter exhibited apparently high readings of total throughput. These tests were repeated in October 1993 with the same choke settings but the error data fell in with all the other points and the discrepancy was not repeated. The reason for the erroneous points is unknown but one possible cause can be identified.

A clear possibility is that the gas reference (a turbine meter with no direct means of calibration checking) was in some way affected for this particular well (e.g. liquid carry-over at the separator gas outlet). The same tests do not exhibit corresponding errors in total mass measurement (see next section). The mass comparison is primarily influenced by the liquid reference metering whereas the total volume analysis is particularly sensitive to the gas reference owing to the high gas volume fraction of the well streams at Prudhoe Bay. Any error effect attributable to the multiphase meter could be expected to manifest itself in both the total volumetric and mass analyses.

Immediate repeat measurements of wells tested confirmed the errant data for H21 in July 1993. By October that year, the water cut of this well had risen from 65% in July to 77%, possibly further away from inversion-point emulsion viscosity effects which could have existed in July and affected separator performance.

The overall good and repeatable agreement between the multiphase meter measurements of total volume flow rate and the reference derived values throughout the tests confirms a high degree of confidence, not only in the multiphase positive displacement meter, but also in the reference metering systems. This confidence extends to the fluid property equations used to compensate for differences in pressure and temperature between test section and reference.

3.3 Total Mass Evaluation

All the test data, excluding Alaskan tests conducted in 1993, are plotted in Figure 3. The characteristic 'U' shaped bias error as a function of void fraction has been reported previously (1). The bias appears to be test site specific, the data otherwise exhibiting repeatability to within $\pm 5\%$ about the offset over most of the GVF range. Although plotted against GVF, they represent a number of different wells, flow rates, wide ranging pressures and water cuts and the full range of multiphase flow regimes.

Between the testing at the independent facility in 1990 and the two-year programme at Prudhoe Bay commencing in 1992, the mass bias characteristic was investigated during two-phase (air-water) flow loop tests at BP Research in 1991. Specifically, the geometry of the central section of the positive displacement meter was temporarily modified to investigate variations in the flow path through the gamma beam of the density gauge. From the analysis of the positive displacement meter total volume flow rate results, it was clear that the mass biasing error was primarily associated with the mixture density measurement.

Subsequently, in 1992, other work published in the literature (4) and an analysis by the supplier of the nucleonic densitometer highlighted a theoretical source of error exhibiting a 'U' shaped bias characteristic when plotted against GVF similar to the observed test results.

This evidence and observations arising from the air-water experiments identified a potential significant source of biasing of the mixture density measurement associated with the packaging and swirling actions of the positive displacement meter. Although constraining the level of phase slip, it is believed that the rotor action segregates the gas and liquid phases within the positive displacement chambers to produce perturbations in multiphase composition at the gamma beam. The frequency of these is related to rotor speed and is significantly higher than the response capability of the current detector technology. Coupled with the logarithmic characteristic of the density gauge, the averaging of photon counts can introduce a bias.

The theoretical work used modelling of compositional fluctuation amplitude to study this biasing effect. In practice, the amplitude of compositional fluctuations within the positive displacement meter, unlike the "packaging" frequency, is unknown. It depends on several variables of the flow stream, such as flow regime, composition and phase distribution pattern (and fluctuation of these) at entry to the meter and fluid properties such as gas density and liquid viscosity. All these factors vary between installations, which is one explanation for the site-specific nature of the biasing seen in Figure 3.

On the basis of the experiments conducted at BP Research, the path length of the gamma beam within the flow stream was reduced. This was intended to produce a more linear response characteristic of the densitometer in order to minimise the biasing effect. The modification of the flow cross-section was also intended to address a suspicion of localised phase segregation and slippage effects at the gamma beam. These aspects are described in more detail in (3).

Following the 1992 tests at Prudhoe Bay, the meter was returned to the UK in order to implement the design change. A number of well tests were then conducted at Prudhoe Bay following re-commissioning of the modified meter in 1993. The resulting total mass flow measurement error data are plotted in Figure 4 for comparison with the 1992 results.

As these data show, significant improvement in the performance of the multiphase meter resulted from the alterations to the gamma beam chamber. The data indicate that the characteristic bias error of the gamma densitometer system has apparently been fully eliminated.

(Note: ten percent of the bulk 15% negative error observed in Figure 3 for the Alaskan data is attributed to the gamma densitometer measurement. The remaining -5% is attributable to the use of a constant volumetric K-factor deduced from an original positive displacement meter calibration using a refined oil. For the Prudhoe Bay flows, this gives a 5% under-read on average compared to the calibration curve for tap water. This was not corrected in Figure 3 so as to give a consistent comparison with the earlier data from the field trials at Wytch Farm and air-water laboratory tests. These used the oil calibration factor and are subject to varying volumetric deviation from the water based calibration. The applicability of the water K-factor curve was demonstrated in the previous section and has been used in plotting Figure 4. Calibration philosophy is discussed in more detail in (5)).

The multiphase metering system is scheduled for testing as part of the UK National Engineering Laboratory "Multiflow" joint industry programme to independently evaluate multiphase meters. These tests will enable a check for elimination of the 'U' bias characteristic over the full range of gas void fraction.

3.4 Water Cut Measurement

The water cut measurement required within the BP multiphase metering system can be provided from a choice of measurement means. These range from full-bore phase fraction cells (BP has been involved in the development of alternative devices as part of its overall multiphase meter technology programme (2, 6)) to sampling methods.

For accurate results using any of these methods, the oil and water phases should ideally be well mixed together in the flow stream. This ensures representivity for sensors using only a sample or close adherence to mixture field models where, for example, full-bore dielectric techniques are used. Equally important, it ensures the absence of slip between the oil and water phases so that their quantity ratio is represented by the water cut deduced, even if the gas phase slips relative to the liquid phases within the sensing zone. For certain multiphase flow regimes, the shearing

actions between the gas and liquid phases can ensure that this is the case. Fluid sample data obtained during the independent flow loop testing of the BP multiphase meter on oil, water and gas show how the internals of the positive displacement meter ensure thorough mixing of the oil and water across the full range of flow regimes.

During these flow loop tests, manual fluid samples were drawn from a side-tapping located on the multiphase meter body at the gamma beam section. This was achieved by means of a simple ball valve arrangement from which fluid could be momentarily drained during the course of testing. Table 1 compares water cuts derived from 250 ml graduated jars, once the sample liquids had stratified, with reference values determined from the accurately measured single phase flow rates at entry to the flow loop.

The agreement between the sample and reference water cuts is good. The observed deviations would be acceptable for practical oil field well test use. The tests shown cover a wide range of gas void fractions, regimes and flow rates and oil-continuous and water-continuous emulsions. Such agreement could only be achieved with thorough mixing of the oil and water phases, especially given the unsophisticated nature of the manual sample measurements.

On the basis of this evidence, it is concluded that the various water cut measurement techniques can be used provided the fluids are sensed or sampled in close proximity downstream of the multiphase meter.

This aspect of the system was investigated further at Prudhoe Bay using the phase fraction cell shown in Figure 1. Specifically, a method of dynamically tracking the water cut in the high GVF streams was tested. Limited data were obtained (before a fault occurred with the fraction cell) which show that water cut can be measured accurately downstream of the positive displacement meter in high gas content multiphase streams. The tracking technique and the results are described in (3).

At this stage, practical sensor techniques giving accurate water cut measurement for oilfield multiphase streams have not been fully established, especially for high water cuts (near oil-water inversion point and water-continuous conditions). BP is still involved in joint-industry programmes to evaluate emerging technology.

3.5 Multiphase Measurement Evaluation

The results presented in the preceding sections have allowed the evolution of an understanding of the behaviour of multiphase flow through the multiphase metering system and its influence on sensor measurements. By analysing the measurement components separately, error sources have been isolated and practical calibration methods have been established. Latest understanding culminated in a final design of meter tested at Prudhoe Bay in 1993.

For the purpose of assessing the central multiphase flow measurement system in terms of its accuracy in measuring the phase flow rates, the latest Prudhoe Bay test data have been analysed using the water cut reading deduced from the test separator reference system. This allows an examination of the accuracy of oil, water and gas flow rates derived from the total volume and mixture density readings of the multiphase meter, given an accurate reading of water cut.

The 1993 test results have been analysed following the successful elimination of the bias error previously associated with the gamma densitometer as described in the section on total mass analysis.

The relative error data for oil, water and gas flow rates are plotted against reference total volume flow rate in Figures 5a, 5b and 5c respectively.

In Figure 5a, the relative errors show a scatter band achieving the $\pm 5\%$ level. This is a range quoted for multiphase meters intended to replace the test separator as a means of well testing and allocation measurement. In fact, the errors seen in Figure 5a are within the uncertainty levels associated with the reference metering system, which thus limits the capability to judge the multiphase meter beyond the scatter band observed.

Similarly, the error data for the water flow rate measurement, Figure 5b, on the whole exhibit a $\pm 5\%$ scatter, although a few points deviate significantly from this level. These outlying points represent low water cut wells (1% and less). They arise since the water flow rate is a small quantity in the total multiphase stream and its measurement is prone to magnification of error

sources. This can occur even though the reference water cut has been used in the breakdown of the phase flow rates because of small errors in the other sensor readings on which the water flow rate depends. Also, the conversion of the reference water cut at test separator pressure and temperature to an in-situ value at multiphase meter conditions is susceptible to errors in oil and water formation volume factor calculations.

The gas phase flow rate error data plotted in Figure 5c largely comply with the $\pm 5\%$ band, within the uncertainties of the reference system. The outlying high readings all reflect the apparently high total volumetric readings observed in July 1993 when testing well H21. With the high gas volume fraction of the Prudhoe Bay well streams (62% to 95%) the error behaviour in gas phase flow rate measurement is mainly dependent on the accuracy of the total volumetric reading. (The liquid error data in multiphase flow measurement in general more closely mimic the corresponding total mass data). The high volumetric readings for H21 in July 1993 have already been discussed.

In all three graphs, the repeatability of the tests between July and October 1993 should be noted. Any remaining bias levels and uncertainty levels are within the uncertainties of the reference measurement system and a deeper investigation of error patterns is considered to be not worthwhile.

These data confirm that, given an accurate measurement of water cut, the positive displacement multiphase flow meter system can measure the flow rates of oil, water and gas to an accuracy comparable to a test separator system. At Prudhoe Bay, this has been achieved under the most arduous multiphase flow conditions, particularly in terms of gas voidage. The high volumetric gas contents make the measurement of the liquid phases particularly susceptible to error.

3.6 Calibration and Use in Practice

In order to obtain the above results, the gamma densitometer (a standard Cs-137 system) was laboratory calibrated by filling the meter with mains water and recording the detector reading and then repeating this measurement with the meter drained (giving a density reference from air at atmospheric pressure). Thus, including the water based calibration for the positive displacement meter K-Factor (section 3.2), the basic multiphase meter can be calibrated on a simple and practical basis.

Prior to safe-out procedures and pressurisation of the meter at the start of the field trials, it was a simple matter to check the "empty" air densitometry reading in-situ. The basic calibration of the densitometer unit mounted on the prototype meter for field and independent loop testing was first established in March 1990 (using air and tap water). The detector calibration count readings have been repeatable to within $\pm 0.5\%$ up to and including the last checks at Prudhoe Bay on all occasions. These have included mounting and disassembly at the Wytch Farm oil field and the independent test loop site. No faults have arisen with the densitometer equipment throughout the trials programme.

During the test work, simple procedures were established which could form the basis of in-service calibration checking. These can be applied to the mixture property sensing devices such as the densitometer and water cut sensors, where these are mounted vertically and can be isolated in a by-pass piping arrangement. (The thrust bearing design of the BP multiphase meter positive displacement mechanism is such that it must be mounted for vertical down-flow).

The method basically consists of a series of repeat valve operations where, in by-pass mode, the sensor spool is filled with single phase fluid at line pressure and temperature. For example, in downflow, with the upstream isolation valve shut and the downstream valve open, the sensor fills with vapour phase. Conversely, it fills with liquid with the reverse valve configuration. A combination of repeat valve operations and settling periods ensures stratification with the phase interface levels clear of the sensing region. The presence of a single phase fluid is confirmed when repeatable readings are observed each time the measurement section is exposed to production at one end and then isolated.

This was initially attempted at Wytch Farm and then on several wells at Prudhoe Bay giving a range of fluid pressures and temperatures. Line density measurements for the oil and gas phases obtained from the densitometer of the BP multiphase meter are plotted in Figure 6 against reference values derived from site sample and PVT data. The agreement, generally within $\pm 6\%$ relative, is within uncertainty figures quoted with the reference data.

At both sites, the procedure only required one or two iterations with the valving and took about half an hour. It was possible to isolate the oil, water and gas phases in turn to measure the density of each. In practice, the method could form an additional part of well testing procedure whereby sensor calibration could be checked when required.

Furthermore, the method provides a means of checking or directly measuring the phase densities used in equations (1) to (3) to derive the phase flow rates. These otherwise rely on equation-of-state calculations and sample data. It can be used in installations where the pipe section can be isolated and purged with service fluids to provide a more reliable reference fluid calibration if the properties of the injectant are accurately known.

(It should be noted that the exponent of the gamma beam decay law of the densitometer is a product comprising density (the measurand), path length and mass absorption coefficient. This coefficient depends, to a limited extent, on the atomic make-up of the attenuating medium, although it is particularly influenced by the presence of hydrogen. Using an average mixture or bulk value for the coefficient (as determined by calibration on air and water) can lead to $\pm 2\%$ error in density when reading at the extremes of 100% oil or 100% water. The effect can be corrected by an iterative procedure when the three phase flow rates (and hence their ratios) have been measured by the multiphase measurement system. This refinement was not made for the BP test programme but its inclusion in later versions of the system could improve even further on the flow rate error levels observed).

3.7 Pressure Drop

Through the course of the BP test programme, confidence has been established in the performance of the multiphase meter for an envelope of gas-liquid flow rates, see Figure 7. This envelope covers the full spectrum of flow regimes, from all liquid to annular flows. The pressure drop across the meter depends on where in this envelope it is operating and can fluctuate in intermittent flow regimes. Pressure loss also depends on fluid properties and the nature of the variation in its level during intermittent flows can depend on the behaviour of a particular well and the topography and components of the entire flowline. Maximum continuous and peak pressure differentials of 35 psi have been observed across, and tolerated by, the meter during extended periods of well testing. The meter has been subjected to violent surges continuously for several days during some well tests at Prudhoe Bay (cycling over seconds in some cases and tens of minutes in others).

4 CONCLUSIONS

The principles of the multiphase flow meter system developed by BP were adopted in order to overcome the complex and generally non-reproducible nature of multiphase flow streams. Key observations, arising out of an eight year test programme, have enabled these principles to be realised in practice. The test data, presented in this paper, show that flow rate measurements within $\pm 5\%$ relative error can be obtained on the basis of simple and practical calibration procedures. This level of scatter is within the uncertainties of the separate phase reference metering and meets the target level specified for well test and allocation purposes in order to replace the conventional test separator system. At the Prudhoe Bay oil field, this has been achieved under the most difficult multiphase flow conditions in terms of reliability and accuracy.

BP Exploration is now targeting specific application opportunities where multiphase metering will add value. In common with several other multiphase meter systems developed, the prototype BP system is a 3" to 4" nominal design and further experience will be required in order to confirm its capability for larger line sizes. Flow rate operating envelopes requiring larger designs have been identified in some applications. These cases include examples of total field production measurement for allocation. Furthermore, acceptable accuracy of water cut measurement has only been demonstrated for oil-continuous liquid conditions. The development of techniques for full-range (0-100%) water cut measurement continues.

REFERENCES

1. GOLD, R.C., MILLER, J.S.S. and PRIDY, W.J. Measurement of multiphase well fluids by positive displacement meter. Paper SPE 23065 presented at "Offshore Europe" conference, Aberdeen, September 1991.

2. DYKESTEEN, E. and FRANTZEN, K.H. Multiphase fraction meter developed and field-tested. Oil & Gas JI, February 1991.
3. PRIDDY, W.J. Field trials of multiphase metering systems at Prudhoe Bay, Alaska. Paper SPE 28514, 69th SPE Annual Technical Conference, New Orleans, Louisiana, 25-28 September 1994.
4. TAYLOR, D.J.N. and FLITTON, V. Bias removal in two phase flow density measurements by signal deconvolution. ISA paper 92-0181, 38th Instrum. Soc. Amer. Int. Instrum. Symp. Proc., p.395, 1992.
5. PRIDDY, W.J. Multiphase flow metering and calibration philosophy. Measurement + Control, 26(10), p.293, December/January 1993/94.
6. GAISFORD, S. Multiphase fraction metering solved? A report of the latest results achieved with a new technology. North Sea Flow Measurement Workshop, National Engineering Laboratory, East Kilbride, Scotland, 23-25 October 1990.

ACKNOWLEDGEMENTS

This paper is presented on behalf of the teams responsible for the work, including current and former personnel of BP Exploration, ARCO Alaska Inc., and BP Group Research and Engineering, with special acknowledgement of the contribution of prototype designer and manufacturer Mr Robert Maurer. Contributions from Christian Michelsen Research and Shell Research during the test programme are also acknowledged.

COPYRIGHT

Parts of this paper are reproduced from reference (3) presented at the 69th SPE Annual Technical Conference in September 1994. Copyright of that material reproduced is held by the SPE. The author acknowledges the permission granted by the SPE to reproduce material from reference (3).

DISCLAIMER

The techniques and/or conclusions are those of the authors and may or may not be shared by the Prudhoe Bay Unit Working Interest Owners.

TABLE 1

| TEST | TOTAL FLOW | GVF | REFERENCE | SAMPLE WATER | DEVIATION |
|------------------------------|------------|------|-----------|--------------|-----------|
| | | | WATER CUT | CUT | WATER CUT |
| | m3/h | % | % | % | % |
| < 45% WATER CUT (OIL CONT.) | | | | | |
| 202 | 77.1 | 22.4 | 18.1 | 19.3 | 1.2 |
| 213 | 182.2 | 91.0 | 28.4 | 29.9 | 1.5 |
| 219 | 153.3 | 98.2 | 29.8 | 30.3 | 0.5 |
| 223 | 61.0 | 42.5 | 29.4 | 28.3 | -1.1 |
| 224 | 122.9 | 52.4 | 29.4 | 29.5 | 0.1 |
| 225 | 58.9 | 61.3 | 29.0 | 28.8 | -0.2 |
| 230 | 63.8 | 53.2 | 38.4 | 38.6 | 0.2 |
| 242 | 169.4 | 62.3 | 28.8 | 30.2 | 1.4 |
| >45% WATER CUT (WATER CONT.) | | | | | |
| 210 | 173.4 | 58.8 | 65.6 | 65.5 | -0.1 |
| 217 | 194.4 | 95.1 | 55.4 | 55.4 | 0.0 |
| 232 | 122.6 | 43.8 | 59.5 | 60.2 | 0.7 |
| 233 | 128.6 | 45.8 | 57.1 | 57.1 | 0.0 |
| 243 | 168.4 | 62.6 | 61.5 | 59.2 | -2.3 |

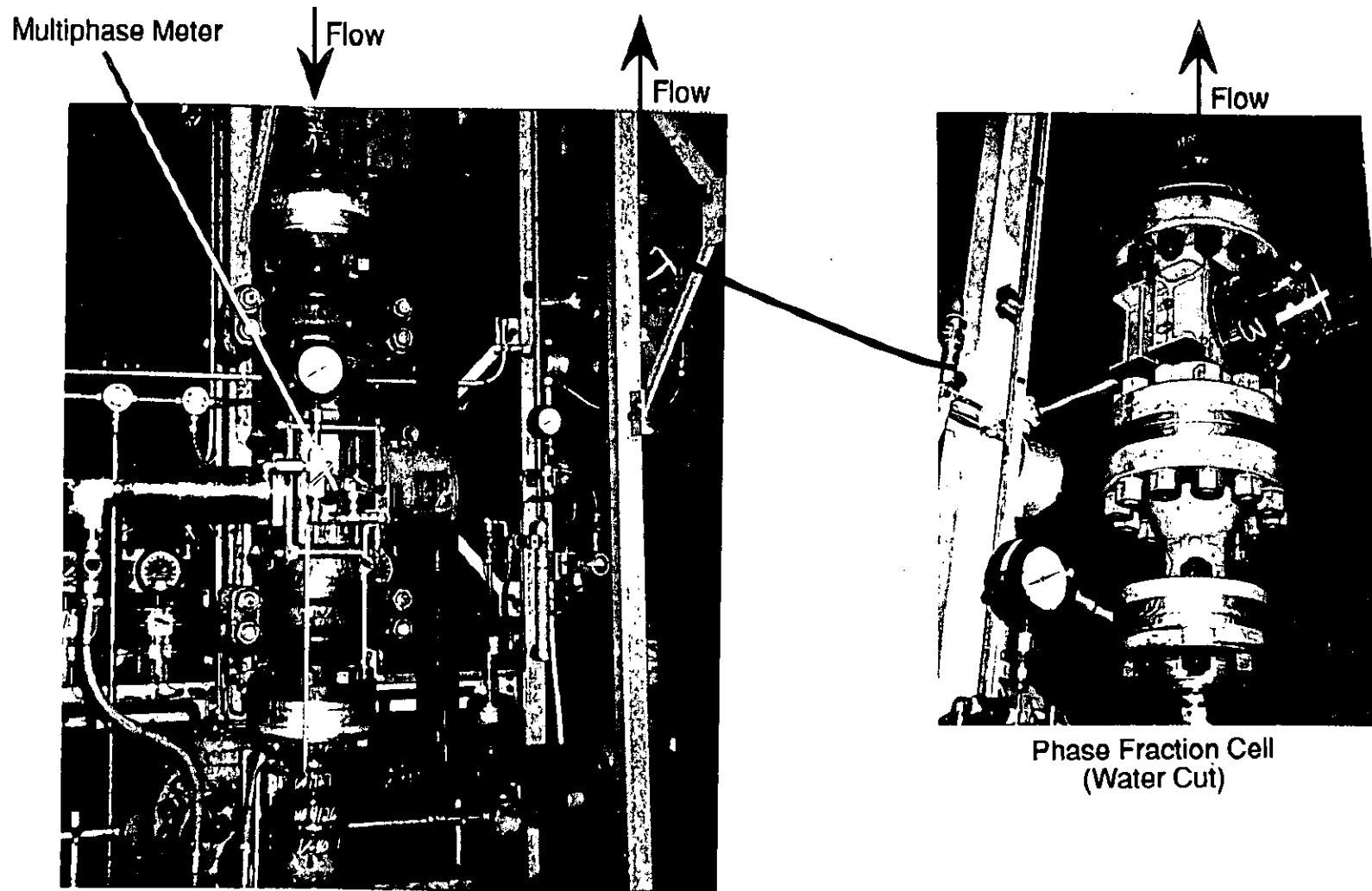


Figure 1. Test Multiphase Meter System

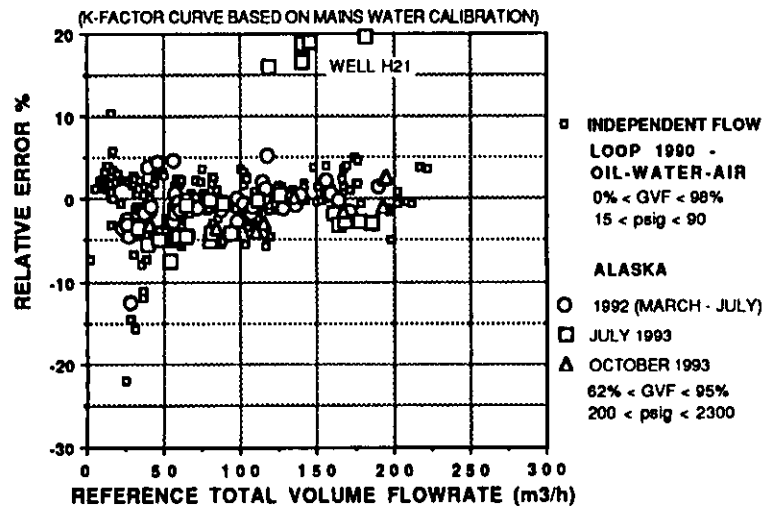


Figure 2. Volumetric Performance of Multiphase Flow Meter

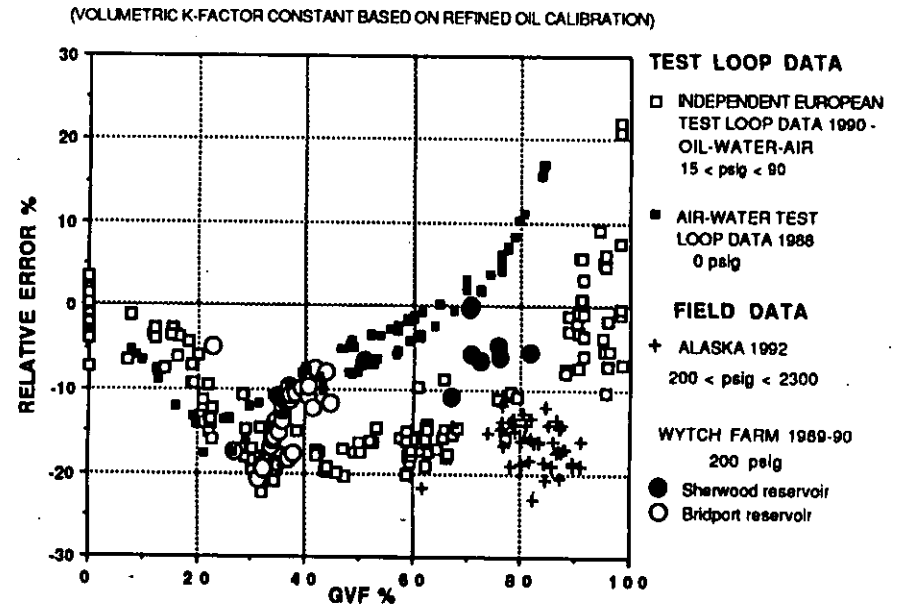


Figure 3. Total Mass Measurement Performance of Multiphase Meter

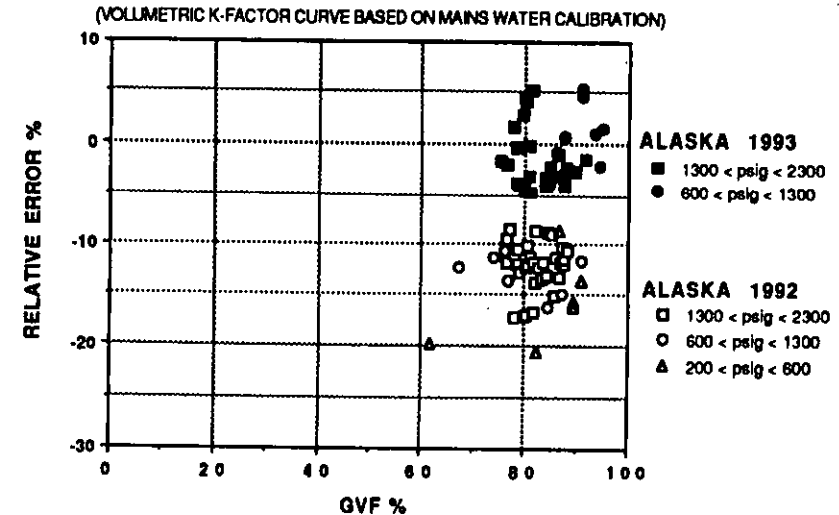


Figure 4. Total Mass Measurement Performance - Alaska

COPYRIGHT 1994 SPE
 Figures 2, 3 and 4 taken from Reference 3.

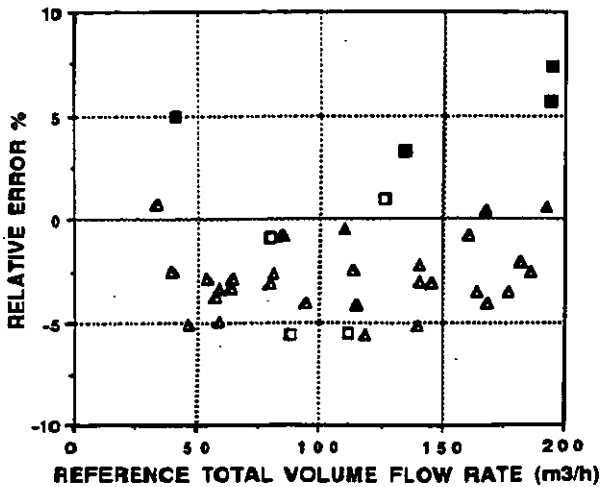


Figure 5a. Oil

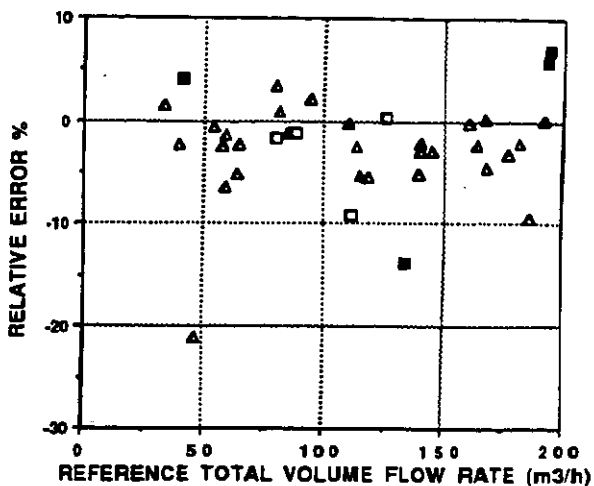


Figure 5b. Water

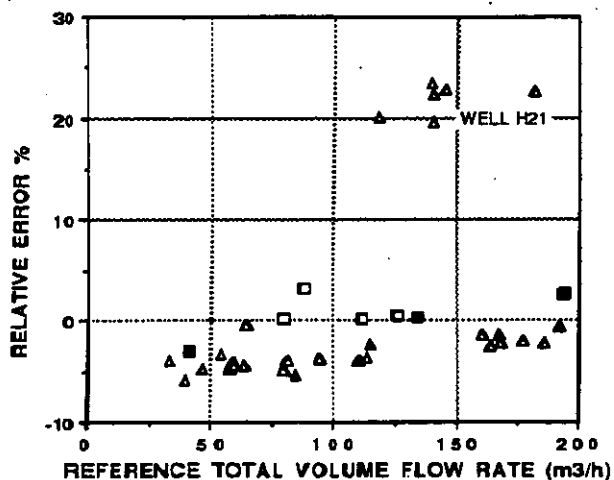


Figure 5c. Gas

JULY 1993

□ 600 < psig < 1300
 ▲ 1300 < psig < 2300

OCTOBER 1993

■ 600 < psig < 1300
 ▲ 1300 < psig < 2300

(75% < GVF < 95%)

(VOLUMETRIC K-FACTOR CURVE BASED ON MAINS WATER CALIBRATION)

Figure 5. Relative Error in Phase Flow Rate - Alaska

COPYRIGHT 1994 SPE
 Figure 5 is taken from Reference 3.

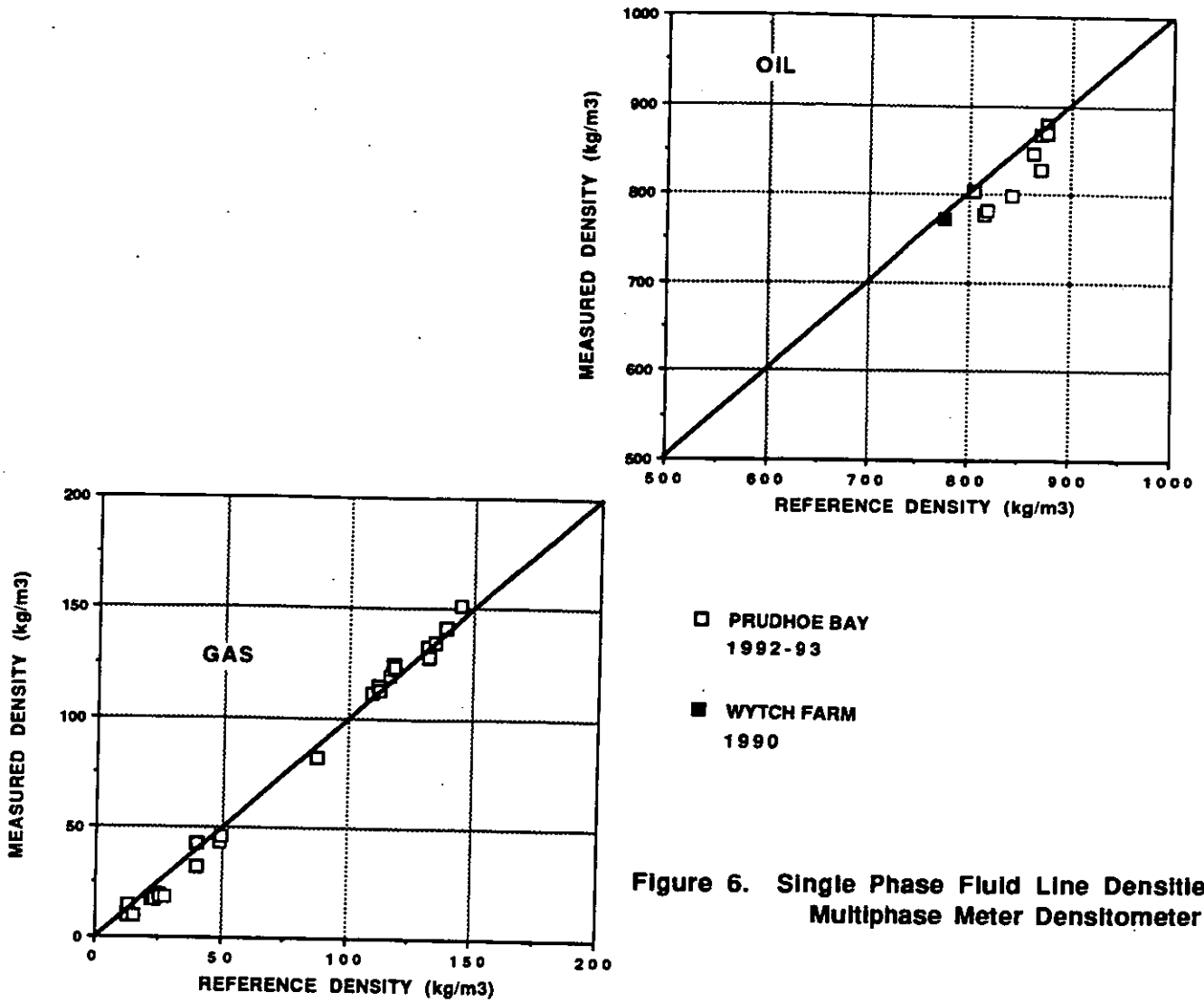


Figure 6. Single Phase Fluid Line Densities
Multiphase Meter Densitometer

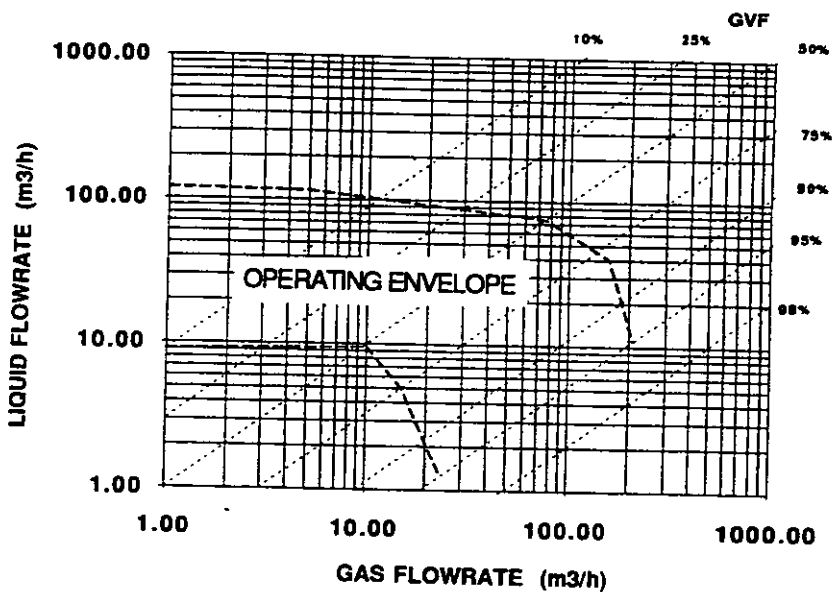


Figure 7. Operating Envelope of the BP Multiphase Meter

PAPER FROM CHRISTIAN MICHELSEN RESEARCH AS

Presented at North Sea Flow Measurement Workshop in Scotland October 1994.

3.4

An evaluation of some static mixers in multiphase flow.

Tested using on-line evaluation equipment

Authors:

Sigmund Hjermann, Christian Michelsen Research
Eivind Dykesteen, Christian Michelsen Research

Bergen, 26. September 1994
Ref.nr.: CMR-94-A10017

ABSTRACT: In multiphase flow measurement there may be a need to homogenise the mixture of the three phases upstream of the measurement point. This is attempted in many applications by installing a static mixer upstream of the measuring instrument. Most of the commercially available static mixers are designed for liquid-liquid mixing, and their performance in multiphase flow is not well documented. On this background Statoil, Agip and Elf initiated a research project at CMR to evaluate the performance of a range of available mixers. The mixing efficiency of the different mixers with respect to pressure drop, homogeneity, interphasial slip etc. is tested over a wide range of flowrates and compositions. Reference instrumentation includes high speed video, isokinetic sampling, gamma density measurement and capacitance cross-correlation velocity measurements. In addition, chemometric analysis has been implemented for on-line determination of how the quality of the flow develops downstream of the mixer. The mixing capability of both a V-cone meter and a classical venturi were evaluated. The presentation will give the background and criteria for the work. The reference measurement system and the test facility will be described. The development of the evaluation method and the evaluation test will be described. High speed video of multiphase flow in the test section will be presented.

1. Evaluation of static mixers for preconditioning of multiphase flow

This paper is a result of a research project completed at Christian Michelsen Research on the behalf of our clients Statoil, Elf Aquitaine, and AGIP. The background for the project is the need for development and qualification of new technology for multiphase transport of oil, water and gas in connection with the potential use of new development concepts for marginal oil and gas reservoirs in the North Sea. One such new technology is the measurement of multiphase volume flow. Several multiphase meters currently under development will require an upstream mixer, or at least give improved performance when installed downstream of a mixer. It is however not evident that commercially available mixers are suitable for this application.

Our clients engaged CMR to evaluate the performance of available multiphase mixers through an extensive test program, and found the multiphase flow facility at Christian Michelsen Research suitable for the objective of such a test programme. The project was completed in winter 1994.

There are several classes of commercially available mixers. A very rough grouping is to classify them as either

- static mixers, which requires no energy input, and with no moving parts, or
- dynamic mixers, which require energy input, and which generally have moving parts.

A further grouping is as mixers with

- radial mixing effect, that is that they create a homogeneous phase and velocity distributions over the pipe cross-section downstream of the mixer, or
- with axial mixing effect, that is that they act as a "filter" for phase distributions along the pipe, thereby smoothing e. g. slug flow.

The performance of a particular mixer can be dependent on both the installation and the application. Typically, the performance of a mixer can be dependent on if the application

- is in vertical upwards flow
- is in vertical downwards flow
- is in horizontal flow
- has fully developed flow at mixer inlet

and on the pipe configuration upstream of the mixer inlet. In addition, the performance of a mixer can be dependent on the application flowrates and phase composition.

To evaluate all types of mixers for a large number of applications would be a very challenging task, as well as quite time consuming and costly. In the evaluation project described in this paper, the objective therefore was to concentrate the effort to a limited number of mixing devices for the specific application of installation in vertical upwards flow.

The objective of the project was

to test and evaluate static mixers for installation in vertical upwards multiphase flow over a wide range of flowrates and compositions, and for varying inlet flow conditions.

For this purpose there were identified and developed a set of measurement methods suitable for characterisation of important characteristics of a multiphase flow, for example

- bubble size distribution
- velocity profile
- interphasial slip
- axial and radial phase distribution

These different flow characteristics were integrated into a reference measurement test section for characterisation of the multiphase flow immediately upstream and downstream of the mixer. Considering these measurements, the aim was to evaluate the different mixers in terms of homogeneity downstream of mixer, and overall mixer efficiency. These objective measurement methods were also supported by subjective "measurements" by installing perspex sections and using high speed video techniques.

In addition to the actual testing of the different static mixers under various conditions as described above, we also aimed to give a technical description of each mixer and its operating principle. In the final evaluation, also operating parameters like pressure drop and operational limits for flowrates and/or compositions were evaluated.

2. Test set-up

A customised test section was developed and a data acquisition system was developed on an IBM PC compatible computer. The test section was integrated in the existing multiphase flow rig at Christian Michelsen Research. To implement the on-line evaluation tool, a setup for measuring different calibration quantities off-line has been developed.

This chapter contains a brief description of the tested mixers and a description of the technical implementation of the different data acquisition systems and how they work together.

2.1. Reference system and model calibration

The on-line evaluation tool was established by relating off-line reference measurements and evaluation methods to the on-line signals from the capacitance detector pairs. The test section developed for this purpose is shown in Figure 2.1.

This test section is placed directly at the outlet of the mixer and the capacitance detector pair arrangement is aimed at observing how the flow develops in vertical upwards flow at the outlet of the mixer. For reference, another capacitance detector pair is placed at the inlet of the mixer.

To relate the on-line capacitance detector pair signals to how well the flow is mixed, several parameters are used. From the on-line capacitance detector pair signals, two very important parameters can be extracted directly. These are

- Cross-correlation velocity, V_x
- Local gas fraction, α

These two parameters are directly linked to the behaviour of the flow. Several other parameters can also be extracted from the capacitance detector pair signals, like

- Permittivity average value, e_{mean}
- Permittivity standard deviation, $estd$
- Permittivity maximum, e_{max}
- Permittivity minimum, e_{min}
- Permittivity span, $e_{max} - e_{min}$
- Permittivity signal center frequency, f_c
- Permittivity signal whiteness, $f_w (f_{max} - f_{min})$
- Power spectrum symmetry, $f_{w-s} ((f_{max} - f_c) / (f_{max} - f_{min}))$

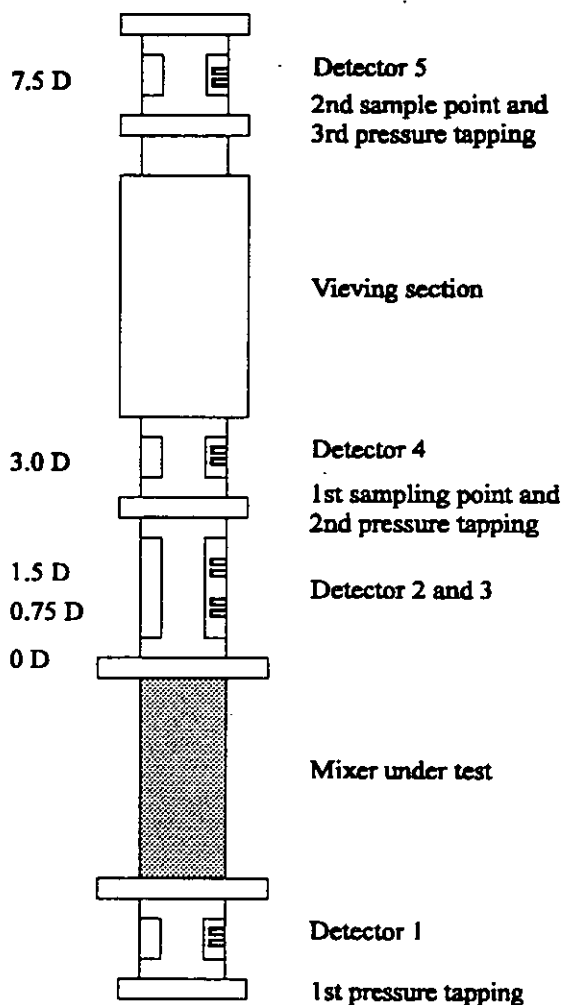


Figure 2.1 The mixer test section.

The definitions of the variables extracted from the time domain are given in Figure 2.2.

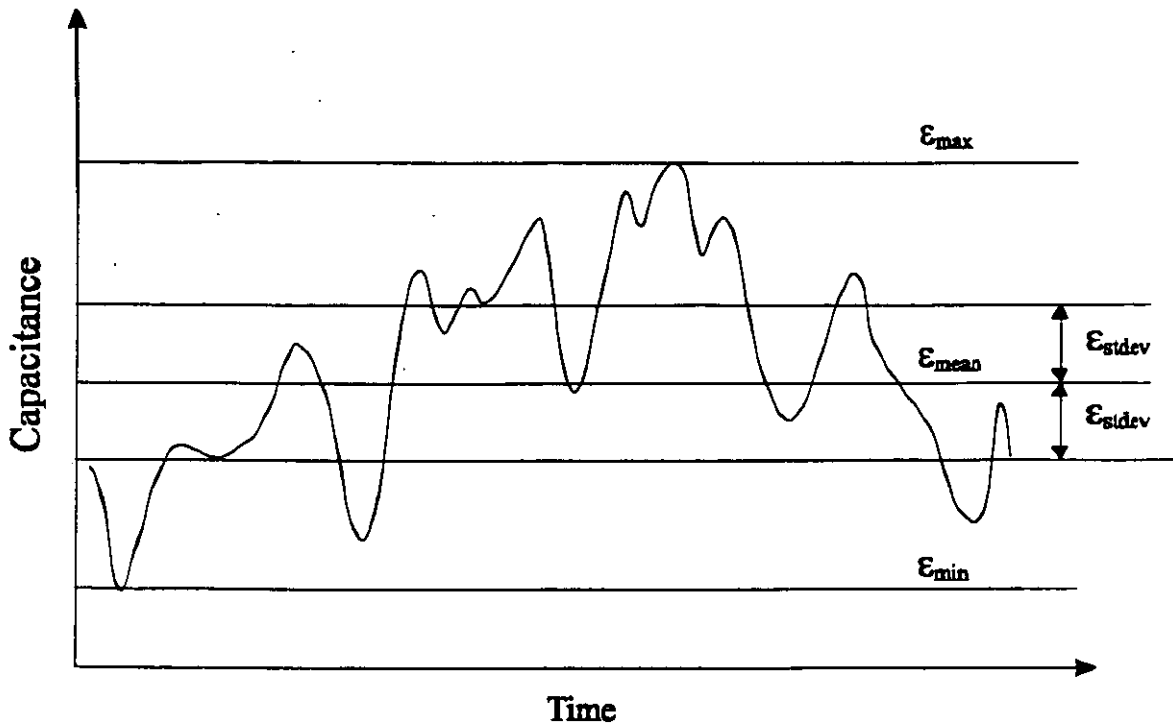


Figure 2.2 A capacitance time domain signal and the variables extracted from this signal.

The definitions of the variables extracted from the frequency domain are given in Figure 2.3.

These signals are indirectly linked to the phenomena that is studied in this project. The average value, standard deviation, maximum, and minimum of the permittivity are derived from the permittivity time domain signal. The center frequency, bandwidth, and cut off frequency is derived from the power spectrum of the permittivity time domain signal.

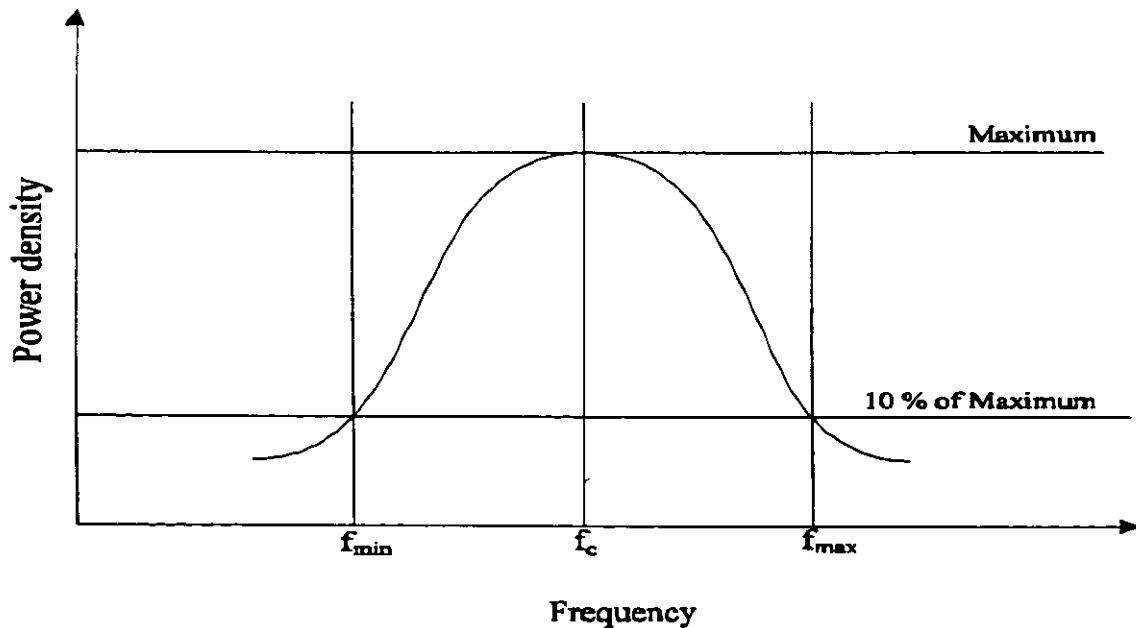


Figure 2.3: A capacitance signal power spectrum and the variables extracted from this signal.

If a mixer creates a well-mixed flow at the mixer outlet, the flow will start to develop towards a bubbly or churning flow shortly after the mixer outlet in a vertical upwards flow. One of the important differences to look for from mixer to mixer is the time (or distance) it takes before this development becomes significant. The mixer evaluation test section is designed to monitor these local variations.

The task of linking variations in all the seven indirect variables to the flow conditions at all test points in the mixer test section and for all flow rates and flow conditions is time consuming and requires a complex set of laboratory routines. In addition, the evaluation will be subjective and can thereby be influenced by the operator.

To avoid this, a statistical model relating these indirect variables and a term called radial gas distribution (RGD) was developed. When developing this model, all the information available from the reference system was used to relate the on-line signals from the capacitance detector pairs to the RGD. The actual model was established by the UNSCRAMBLER statistical modelling software package from CAMO of Trondheim in Norway.

In this way, the evaluation of the indirect variables is performed by a computer, and the possible subjectivity included in the statistical model will be imposed equally on all the mixers.

When using this statistical model, the RGD can be divided in five main categories. These categories are defined in Table 2.1.

To make this software generate the statistical model, a set of input signals (derived from the permittivity signal) and the output signal (RGD) must be available. The input signals can be recorded in the laboratory. The RGD is not a physical variable and can not be measured directly, hence it must be generated through the modelling process.

Table 2.1: RGD categories.

| | |
|---------------|----------|
| No mix | 0 - 20 |
| Bad mix | 21 - 40 |
| Fair mix | 41 - 60 |
| Good mix | 61 - 80 |
| Excellent mix | 81 - 100 |

To be able to quantify the RGD, the on-line input signals are logged for a wide range of flow rates and conditions that cover the conditions that are to be applied in the mixer test. At every single point, a set of off-line reference data is recorded. All this information is then presented to a panel of experienced scientists, and this panel determines the RGD for each test point, see also section 2.3 below. This process is repeated in two different and independent panels and the results are combined. This set of RGD values is then used in the statistical modelling to generate the model coefficients.

2.2. Evaluation parameters

Each capacitance detector contains a pair of detectors, and the signals from both detectors in these pairs are cross correlated. The velocity read from this cross-correlation is an indication of the velocity of the large bubbles in the flow. In a well-mixed flow, the bubble size should not vary significantly and there should be a neglectable slip between these bubbles and the liquid. Hence, the velocity detected from cross-correlation will be close to the reference multiphase flow velocity. In a badly mixed flow, the bubble size varies a lot, and there will be a slip in order of magnitude meters pr. second between the large bubbles and the liquid. Then the cross-correlation velocity will be larger than the reference multiphase flow velocity.

The two capacitance detectors in a detector pair are combined to generate a better sensitivity in the detector when the permittivity is measured. The permittivity measurement is used to measure the local gas fraction. In a well-mixed flow the local gas fraction will be the same as the gas fraction calculated from the single phase reference meters. If there is a slip, a part of the gas will travel at a higher velocity, hence it will stay a shorter time in the capacitive detector and the local gas fraction will decrease. From this difference in gas fraction the slip can be calculated.

For the same nominal gas fraction, the measured average permittivity will vary due to the homogeneity of the flow. If a small change in the permittivity is due to a change in the nominal gas fraction, this may incorrectly be interpreted as a change in homogeneity.

To avoid this effect, all permittivity variables were normalised versus the permittivity average prior to predicting the homogeneity using the statistical model. The variables extracted from the permittivity time domain signal to be used as inputs to the statistical model are then:

- $\epsilon'_{std} = \epsilon_{std} / \epsilon_{mean}$
- $\epsilon'_{max} = \epsilon_{max} / \epsilon_{mean}$

- $\epsilon'_{\min} = \epsilon_{\min} / \epsilon_{\text{mean}}$
- $\epsilon'_{\text{span}} = (\epsilon_{\max} - \epsilon_{\min}) / \epsilon_{\text{mean}}$

The average value of the permittivity is directly linked to the gas fraction, hence it can be analysed by itself. These normalised values are then relative to the actual gas fraction.

For the variables extracted from the power spectrum, the same rationale is valid concerning the conflict between the local variations and the nominal set-point for the gas fraction. In this case, the variables are normalised versus the center frequency. The variables extracted from the power spectrum and used as input to the statistical model are then:

- Permittivity signal whiteness, $f_w ((f_{\max} - f_{\min}) / f_c)$
- Power spectrum symmetry, $f_{w-s} ((f_{\max} - f_c) / (f_{\max} - f_{\min}))$

2.3. Test set-up and equipment

The test rig used is shown in Figure 2.4. The path through pump 2 and the mixer test section is used in this project. The tests were performed in oil continuo's diesel oil. The valves at the water and oil outlet were continuously controlled to provide a constant water cut of 5% in the diesel oil measured by the WIOM (Fluenta Water In Oil Monitor). The 5% water cut was added to enhance the resolution in the capacitance measurements by increasing the difference in permittivity from the liquid phase to the gas phase. The distribution of the water in the liquid phase is *not* an issue in this study. The gas used was air from the on site compressor.

To generate two different inlet conditions, two gas injection points have been established. Gas injection point no. 1 is used to generate slug flow at the mixer inlet when the flow is *not* diverted through the vertical loop. Gas injection point no. 2 is *not* used in this project. Gas injection point no. 3 is used to generate flow without slugs at the mixer inlet when the flow is diverted through the vertical loop. When gas injection point 3 is used, the flow into the mixer has a uniform axial gas distribution, and when gas injection point 1 is used, the flow into the mixer has a *nonuniform* axial gas distribution.

All the tests were performed at atmospheric pressure and room temperature.

The instrumentation on the rig is used as reference measurements in this project. The instruments used are:

- The Fluenta WIOM (Water In Oil Monitor) is used as a reference measurement for the water cut (water fraction in liquid phase).
- The liquid turbine meter gives the liquid flow rate in m^3/h .
- The gas turbine meter gives the gas flow rate in m^3/h .

The mixer test section is shown in Figure 2.1. The electrodes in the five pairs of capacitance detectors have an internal distance between 32 and 34 millimetres. The sampling probe and the high speed video were used when gathering information for use when calibrating the statistical model.

A fifth pair of capacitance detector electrodes was placed directly upstream of the mixer. The purpose of this detector pair is to provide a 'reference measurement' for the flow condition at the inlet of the mixer. By comparing the signals from the four detector pairs downstream of the mixer with the signals from the detector pair upstream of the mixer, the development of the flow parameters when the flow passes through the mixer under test can be investigated.

All test points in the calibration test matrix were recorded by high speed video. This camera records 200 frames pr. second, eight times as many as conventional video. By replaying these recordings at regular speed, the panel of scientists could view the details of flow and observe the degree of homogeneity in the flow.

The isokinetic sampling probe was used to extract samples of the flow at two radial points and at two axial positions in the mixer test section during the calibration test. Four samples were taken from the flow at each flow condition during the calibration test. These samples were extracted

- 1 cm from the wall at 1st sampling point
- In the tube center at 1st sampling point
- 1 cm from the wall at 2nd sampling point
- In the tube center at 2nd sampling point

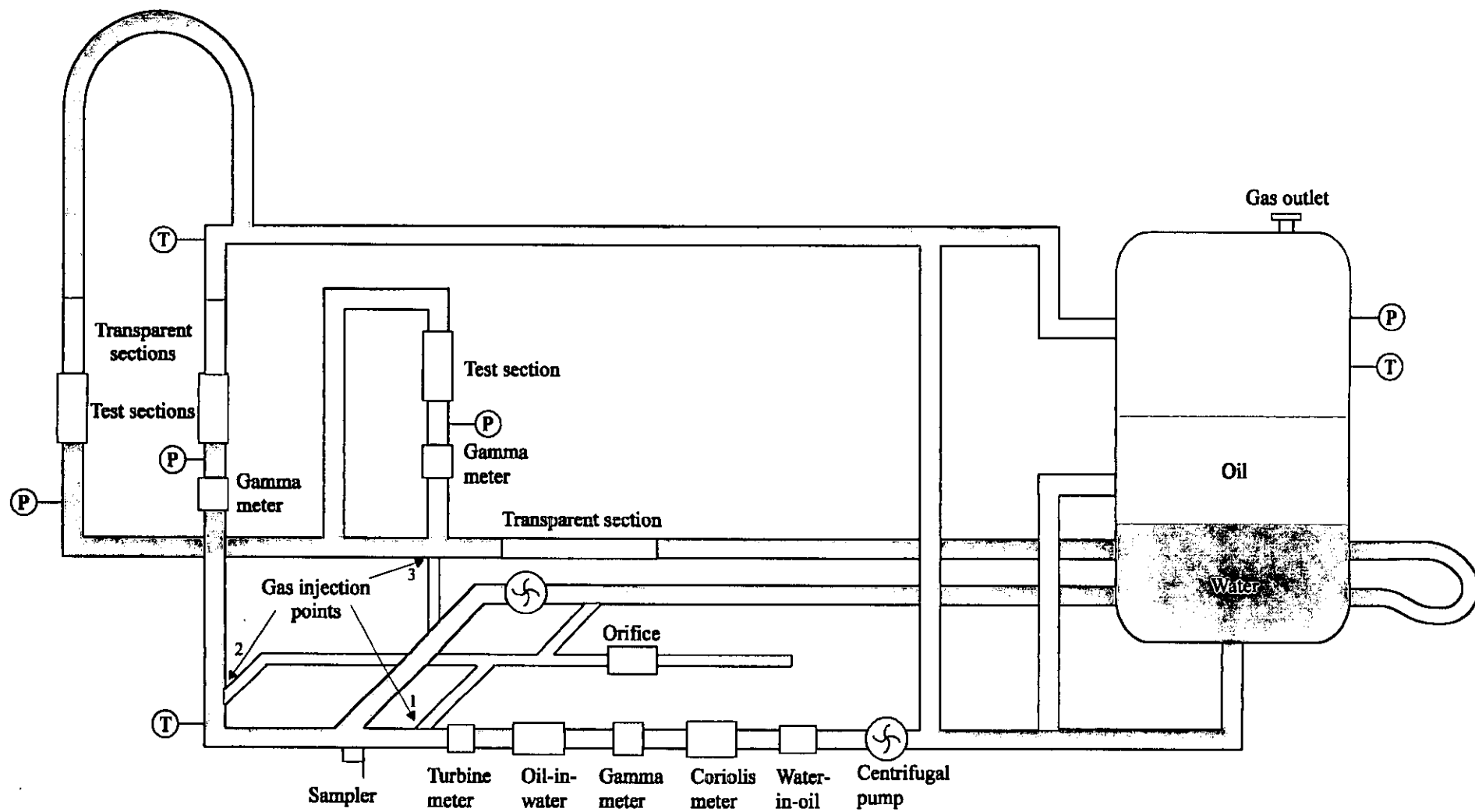


Figure 2.4: The multiphase test-rig used.

To achieve isokinetic conditions at the probe point, a suction pump was used to 'pull' the sample from the flow. Obvious outliers collected using this method were discarded.

The details from the video, the sampling results, and all the recorded values from the capacitance detectors were used as the information basis for determining the RGD during the calibration test.

3. Model verification

To be practically applicable the generated model needs to be properly validated. The validation gives a measure of how good the model is, and how accurate predictions can be made from the model. To verify that the model was properly calibrated, a verification test was performed.

Verification of the statistical model was done by running 12 tests covering the valid model range. Since a reference for the RGD needs to be known, the predicted objects were selected as repeated test points from the calibration tests. The results are shown in Figure 3.1.

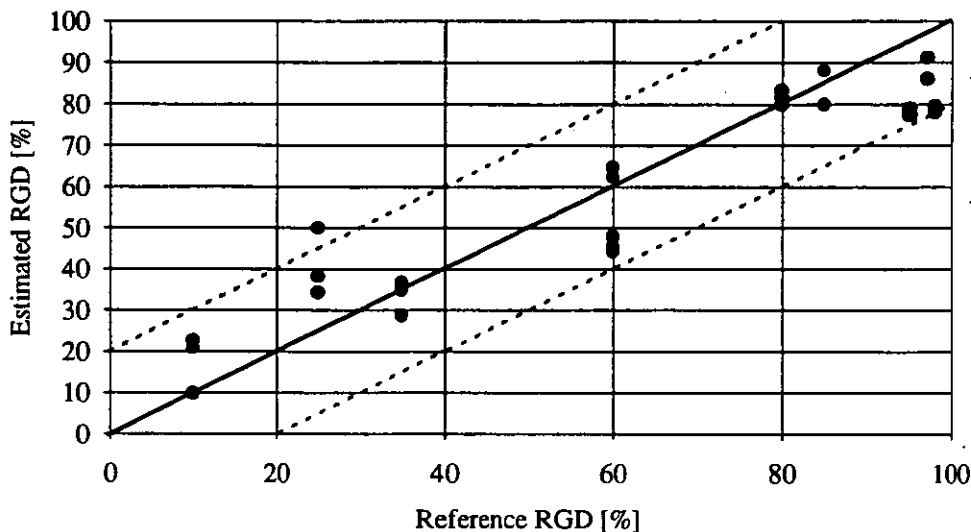


Figure 3.1: Validation test at the multiphase loop of the multivariate model. Test results of estimated radial gas distribution (RGD) compared to off-line determined references are shown.

It is observed that the uncertainty of the model is $\pm 20\%$ in absolute percentage terms. The radial gas distribution is a fuzzy quantity whose exact value is very difficult to determine. Therefore, the relatively large uncertainty of the estimation most likely comes from the off-line subjective evaluations of the radial gas distribution during the calibration test. However, the repeatability of the estimations has been found to be good.

4. Static mixer tests

The evaluation of the test results is based on the

- Gas fraction considerations
- Slip considerations (related to cross-correlation velocity)
- Differential pressure
- Radial gas distribution based on the statistical model.

Table 4.1 Mixer test matrix.

| Liquid flow | Gas flow | Nominal gas fraction |
|-------------|----------|----------------------|
| 10 | 1.1 | 10 |
| 10 | 3.3 | 25 |
| 10 | 10 | 50 |
| 10 | 30 | 75 |
| 10 | 90 | 90 |
| 25 | 2.8 | 10 |
| 25 | 8.3 | 25 |
| 25 | 25 | 50 |
| 25 | 100 | 80 |
| 50 | 5.6 | 10 |
| 50 | 17 | 25 |
| 50 | 50 | 50 |
| 50 | 93 | 65 |
| 75 | 8.3 | 10 |
| 75 | 25 | 25 |
| 75 | 75 | 50 |

For each test point, the software wrote five measurements to file at a 30 seconds' interval. All measurements written to file are an average over these 30 seconds. If all these five measurements are approximately the same, the conditions are said to be stable. If they have unrealistic values, or are clearly unstable, all five measurements are discarded.

The test matrix used is shown in Table 4.1.

4.1. Interpreting the data plots

The amount of data to be analysed in this analysis is extensive. The data have been compressed into a set of three-dimensional plots. The cross-correlation velocity, the gas fraction and the RGD have been plotted for each of the five capacitance detectors.

Two kinds of plots are used to describe the mixers:

- Surface plot. One plot for each capacitance detector pair, with an X-Y plane covering the tested range of flow rates and compositions. Examples of these plots are found section 4.3.
- Mean and standard deviation. A plot showing the development in the different analysis parameters relative to the input condition along the pipe downstream of the mixer. An example of these plots section 4.3.

4.1.1. Interpreting surface plots

If absolute values are used in this kind of surface plot, the plot does not give a good indication of how the different parameters develop downstream of the mixer. To improve this, only the plot of the parameter at the mixer inlet contains absolute values. The rest of the plots are made relative to this value at the input of the mixer.

For the ideal mixer, the development should be:

- An increase in gas fraction
- A decrease in cross-correlation velocity
- An increase in RGD

In addition to this, the information about the pressure loss is plotted in a separate plot. All these plots are generated for both well mixed and slugging flow at the mixer inlet.

The plots are placed in a vertical series on the page to illustrate the vertical upwards flow. The relative plots of gas fraction for the detectors downstream of the mixer have been compensated for the pressure loss across the mixer. By doing so, a gas fraction increase due to this pressure loss does not favour the mixers with a high pressure loss.

4.1.2. Interpreting the mean and standard deviation plots

This two dimensional plot shows the development of the parameter relative to the inlet condition along the pipe downstream of the mixer. The values plotted are the average values, and the error bars are the standard deviation.

This plot then contains the information about the mixer at all flow rates and compositions. If a mixer influences a parameter differently from flow condition to flow condition, the standard deviation will increase.

4.2. Test data pressure compensations

All the tested mixers generate pressure drop, although this varies a lot from mixer to mixer. This pressure drop also causes the gas to expand, and this expansion turns out to generate some effects that have to be eliminated.

If the slip is reduced by a mixer, the gas fraction will increase and the cross-correlation velocity will decrease, and vice versa. The pressure drop over the mixer will also cause the gas volume to increase, and this increase is ideally proportional to the pressure drop, if the liquid phase is not saturated with gas. Hence, a mixer that generates large pressure drop may appear to reduce the slip, and may get a better evaluation than it deserves. This effect was removed by transforming the gas fraction measured at detector 2 in Figure 2.1 with respect to pressure to the condition at detector 1, and then make the measured gas fraction relative to the gas fraction measured at detector 1.

The influence on the cross-correlation velocity due to the pressure loss is more complex. As the gas fraction increased due to the pressure drop, the total multiphase volume flow rate increased. In this study, the changes in the flow characteristics were studied, and a change in flow velocity is interpreted as a change in flow characteristics. Hence, the change in flow velocity due to gas expansion had to be eliminated from the velocity measurements to avoid misinterpretation of the gas expansion effect. By transforming the flow condition at the output of the mixer to the flow conditions at the input of the mixer, and then performing the comparison of the flow characteristics at that flow condition, this was achieved. It was shown that the change in velocity due to gas expansion can be eliminated by the equation 4.1.

$$v_1^* = v_1 \cdot \frac{(1 - \alpha_1)}{1 - \left(\alpha_1 \cdot \frac{P_1}{P_2} \right)} \quad (4.1)$$

where

- v_1^* = velocity transformed from mixer outlet to mixer inlet
- v_1 = velocity at mixer inlet
- α_1 = gas fraction measured at the mixer inlet
- P_1 = pressure at the mixer inlet
- P_2 = pressure at the mixer outlet

In the plots described in section 4.1.1 and 4.1.2, these transformed values of gas fraction and cross-correlation velocity were used.

4.3. Test data example

Figure 4.1 shows an example of the data overview plots from an example mixer. As described in section 4.1, the plotted data in the four top rows are columnwise relative to the absolute data shown in the bottom row. Hence, in any column, the brown, green, yellow, and blue plot are all relative to the red plot. The gas fraction and cross-correlation velocity data are compensated both for the static head and for gas expansion effects as described in section 4.2.

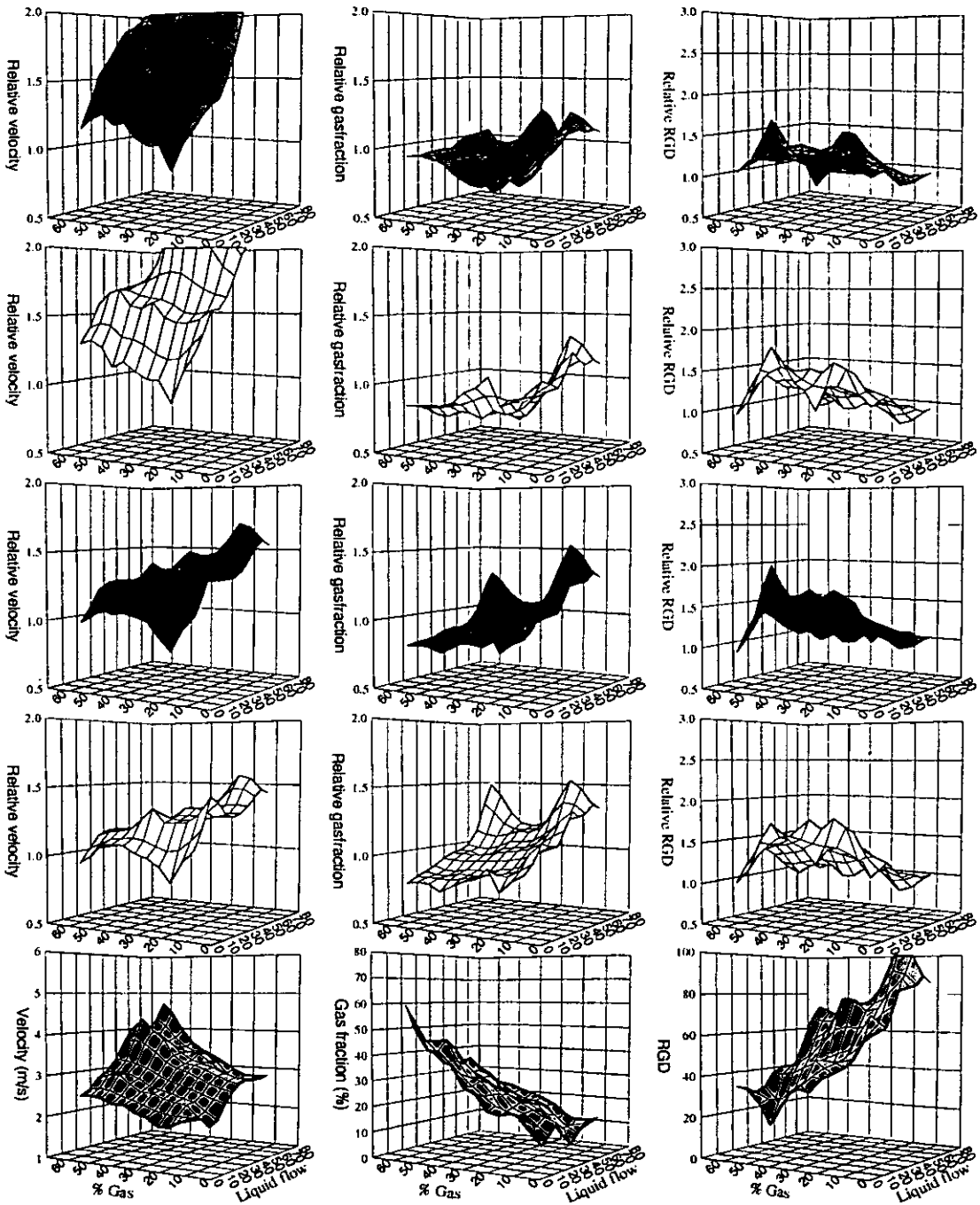


Figure 4.1: The example mixer performance, with gas injection point 3.

4.3.1. Relative gas fraction, velocity, and RGD development

In Figure 4.2 shows the mean and standard deviation of the relative gas fraction development across the example mixer. The standard deviation shown is a measure for the influence this mixer has on the gas fraction over the different flow conditions tested. If the standard deviation is large, the mixer creates a change in gas fraction

that is dependent on the flow rate and composition, hence the gas fraction measured is dependent on the mixer itself. This effect is denoted as uniform or non-uniform mixer performance over the tested flow range.

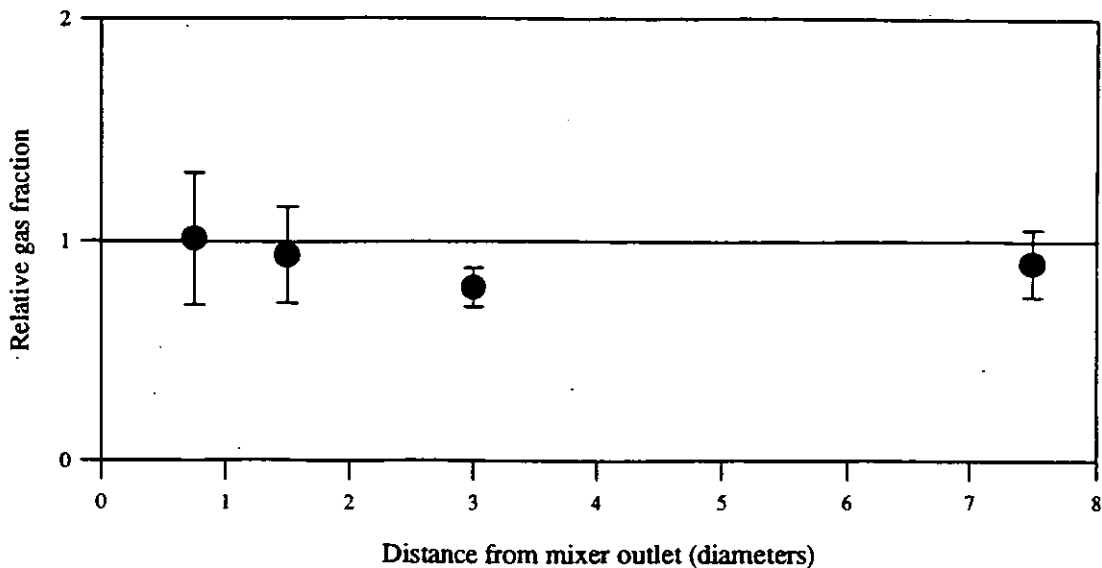


Figure 4.2: Relative gas fraction development downstream of the example mixer with gas injection at point 3.

Figure 4.2 shows a decrease in gas fraction as the distance from the mixer outlet increases, which indicates slip. Also, the standard deviation is higher close to the mixer, which indicates non uniform performance at this position over the flow range tested.

In Figure 4.3 the mean and standard deviation of the relative cross-correlation velocity development across the example mixer are shown. If the standard deviation is large, the mixer creates a change in cross-correlation velocity that is dependent on the flow rate and composition, hence the velocity at the measuring point is dependent on the mixer itself.

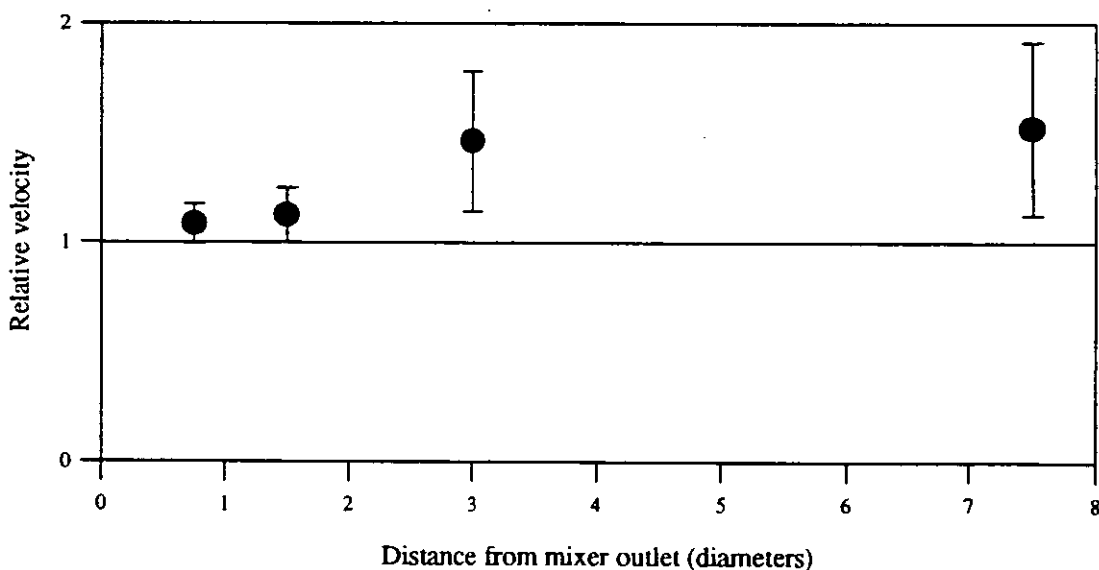


Figure 4.3: Relative velocity development downstream of the example mixer with gas injection at point 3.

Figure 4.3 show an increase in cross-correlation velocity as the distance from the mixer outlet increases, which indicates slip. Also, the standard deviation is higher far from the mixer, which indicates non uniform performance at this position over the flow range tested.

In Figure 4.4 the mean and standard deviation of the RGD across the example mixer is shown. If the standard deviation is large, the mixer creates a change in RGD that is dependent on the flow rate and composition, hence the RGD at the measuring point is dependent on the mixer itself.

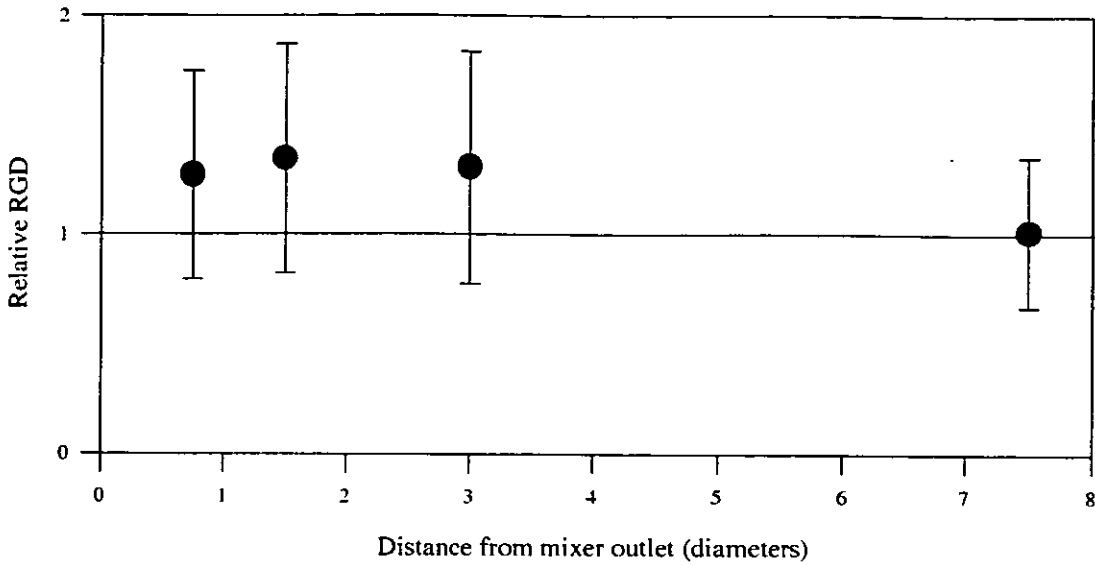


Figure 4.4: Relative RGD development downstream of the example mixer with gas injection at point 3.

Figure 4.4 shows a decrease in RGD as the distance from the mixer outlet increases. The statistical model is not calibrated to interpret swirl, so the results from the model may be misleading.

4.3.2. Pressure drop across mixer.

The development of the pressure drop with the example mixer over flow range tested is shown in Figure 4.5. This figure shows a remarkably low pressure drop over the mixer, although this mixer is one of the devices with the largest pressure drop among the tested mixers.

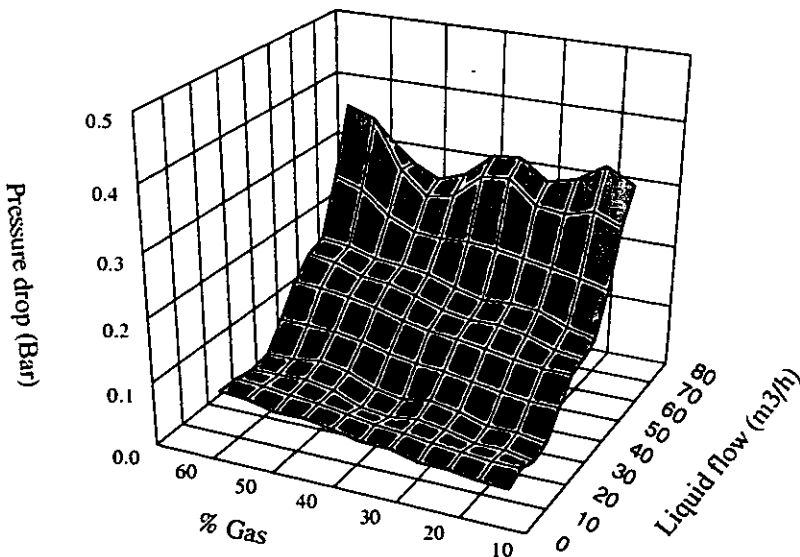


Figure 4.5: Pressure drop across example mixer.

4.3.3. Example mixer conclusions

Highlights:

- Velocity increase along pipe downstream of mixer
- Gas fraction reduction along pipe downstream of mixer
- RGD best close to mixer outlet
- Heavy swirl at mixer output excludes the mixer from multiphase applications

From the high speed video it can be seen that the example mixer generates heavy swirl. This together with that the gas fraction decreases and the cross-correlation velocity increases as the downstream distance to the mixer outlet increases, leads to the conclusion that the example mixer concentrates the gas in the pipe center.

This is the same effect as is utilised for separation in a hydrocyclone. The centrifugal force throws the liquid towards the pipe wall, and the gas is concentrated in the pipe center. As the gas is concentrated in the center of the pipe, the buoyancy effect becomes more dominant, which generates an increase in cross-correlation velocity and a decrease in gas fraction.

The example mixer has the best performance at high gas fractions within 2 diameters downstream of the mixer outlet. The pressure drop is relatively high with an average of more than 120 millibar and a maximum of 450 millibar.

5. General conclusions

The mixers included in this evaluation have been developed for different applications. The efficiency of static mixers as a preconditioner in multiphase flow is heavily influenced by the design criteria given in the intended application. This work does not contain any conclusions regarding the efficiency of the static mixers when used in the application they are specifically designed for.

In the following, our general experiences with the static mixers we tested are discussed.

5.1. Radial mixing

Using a single static mixer, reasonably good radial gas distribution can be achieved over a limited flow composition range. Our experience is that the influence of most mixers on the slip and the local gas fraction will change if the flow rate and composition are altered. Hence, if a mixer is used as a preconditioner for a multiphase flow meter, it may be necessary to calibrate the flow meter for the varying performance of the mixer.

5.2. Axial phase distribution

The static mixers have marginal effect on the axial distribution of the phases. A large body of gas or liquid, 10D or more with only one phase occupying almost the entire cross section, will pass through such a mixer with the internal mix in the body being modified, but without any interchange of mass with the preceding or succeeding bodies of flow.

A liquid and/or gas hold-up volume must be introduced in the flow line to improve the axial gas distribution. This can be done by using a device as developed by FRAMO Engineering or by careful design of the upstream piping.

5.3. Pressure drop

The tested devices generated less pressure drop than expected. The pressure drop tapping downstream of the mixer was placed at a distance $2.5D$ from the mixer outlet, at which pressure recovery should be completed. In crude oil environments, the instant pressure drop at the outlet of the mixer could cause boiling, but that effect has not been studied in this project.

The highest pressure drop recorded during these tests was 496 millibar. The mixer with the lowest pressure drop had a maximal pressure drop of 44 millibar. We found no correlation between the pressure loss and the efficiency of the mixer.

5.4. Secondary flow effects

Static mixers generating heavy swirl is practically useless in vertical upwards multiphase flow, due to the fact that heavy swirl in effect is a hydrocyclone separator. The liquid will be thrown towards the pipe wall and, due to the large difference in density, the gas will be forced towards the center of the pipe. This gas will then coalesce and form larger bubbles, which will accelerate relative to the liquid and create a large interphasial slip.

Static mixers generating turbulence appears to have a positive effect on the conditions for measuring multiphase flow. The plausible cause of this is that turbulence will both split larger bubbles in the flow and reduce small bubble coalescence, hence preventing large interphasial slip.

We have not studied the performance of these devices in any other configuration than vertical upwards multiphase flow, hence our experiences may not be relevant in other flow configurations.

6. Acknowledgements

The authors would like to acknowledge the contributions from this projects clients, and their representatives in the project steering committee. The steering committee representatives were:

| | |
|-----------------------|-----------------------|
| Ole Økland (chairman) | Statoil, Norway |
| Agostino Mazzoni | AGIP, Italy |
| Bernhard LeMoullec | Elf Aquitaine, Norway |
| Philippe Jouve | Elf Aquitaine, France |

The authors also acknowledge the assistance and inspiration of our colleagues at CMR, and particularly naming Mr. Øyvind Midtveit, Ms. Jannicke Hilland, and Mr. Martin Halvorsen for their contributions to the project.

7. References

- [1] Hjermann S., Hilland J., Halvorsen M., Midtveit Ø. (1994): *Evaluation of Static Mixers as Preconditioners in Multiphase Flow*, CMR Ref. No. CMR-93-F15015.
- [2] Hjermann S., Midtveit Ø. (1993): *Evaluation of Static Mixers as Preconditioners in Multiphase Flow*, Executive Summary, CMR Ref. No. CMR-93-F15023.
- [3] Berntsen H. (1989): *Multivariate calibration as an identification method and its relationship to the extended Kalmanfilter*. Proceedings of the 28th Conference on Decision and Control, Tampa, Florida. Vol. 1 (IEEE, New York), pp. 640-645.

- [4] Martens H., Næs T. (1989): *Multivariate calibration* (Wiley).
- [5] CAMO (Computer Aided Modelling) AS (1993), *UNSCRAMBLER User's guide*, Trondheim, Norway.
- [6] Hammer E. A., Hjertaker B. T., and Ahadzi G. (1992); *Volume Flow Measurement in Three Phase Flow*, International Conference on Electronic Measurement & Instruments, Tianjin University, China.

DEVELOPMENT AND TRIAL OF MULTIPHASE FLOW METERS FOR OIL, WATER AND GAS IN PIPELINES

S.L. Ashton, N.G. Cutmore, G.J. Roach, J.S. Watt and H.W. Zastawny

CSIRO Division of Mineral and Process Engineering
PMB 5, Menai, NSW, 2234, AUSTRALIA

ABSTRACT

The CSIRO has developed two meters for the measurement of the flow of multiphase fluids in oil well pipelines. The gamma-ray multiphase flow meter (MFM) is based on single and dual energy gamma-ray transmission, and the microwave/gamma-ray MFM is based on microwave and gamma-ray transmission. Both have been trialed at the oil field facilities on Thevenard Island where they were installed on an 140 mm bore pipeline carrying the full flow from each of seven wells and approximately eleven commingled well streams. Measurements were made over a wide range of water cuts (25-96 %) and flow rates of liquids (6600-33000 BPD).

For the gamma-ray MFM mounted on the vertical upflow (downflow) pipeline, the flow rates were determined to 4.0 (3.3) % relative for liquids, 7.5 (6.1) % for oil, 4.5 (4.5) % for water and 7.9 (7.7) % for gas. Water cut was determined to 3.6 (3.7) % relative. For the microwave/gamma-ray MFM mounted on the vertical upflow (downflow) pipeline, water cut was determined to 3.3 (5.4)% and oil and water flow rates to 5.5 (6.6) % and 5.9 (5.6) %.

1. INTRODUCTION

The CSIRO Division of Mineral and Process Engineering is involved in the development, trials and commercialisation of gamma-ray and microwave techniques for the measurement of the flow of multiphase fluids in oil well pipelines. The main criteria for these developments has been that the multiphase meter be compact and mounted directly on the production pipeline; the meter be non-intrusive and hence not obstructing flow; the measurement not require an homogenised flow; the technique be applicable to the majority of flow regimes; and the meter determines the flow rate of each component to within 5-10% relative.

Use of such a meter should lead to

- a) the replacement of the need for test separators, initially in non-critical applications and later, after the MFM technology has been proved to be dependable, on most new offshore platforms,
- b) the reduction in the cost of subsea piping because the outputs of two or more wells can be commingled and flow through a single flowline from satellite platform to central facility,
- c) the reduction in capital costs of new platforms because the heavy and bulky test separator can be replaced by the light and compact MFM,
- d) better reservoir management, production allocation, and optimisation of total oil production over the field lifetime.

Various organisations are developing multiphase flow meters for oil, water and gas in pipelines [1-8]. Most of these techniques have been tested on laboratory loops; some have had limited testing on production pipelines, none covering all the flow conditions occurring in pipelines from oil wells.

This paper describes results of trials of two multiphase flow meters, one based on gamma-ray transmission, and the other on microwave and gamma-ray transmission. The trials were undertaken from September to December 1993 at WAPET's oil production facilities on Thevenard Island. The current status of development of the MFMs is discussed.

2. GAMMA-RAY AND MICROWAVE/GAMMA-RAY MFMs

There are two main components in the determination of the flow rates of oil, water and gas [4,5]: determination of water cut (WC) and determination of flow rates of liquids and gas. In the gamma-ray MFM, water cut is determined by dual energy gamma-ray transmission (DUET). In the microwave/gamma-ray MFM, water cut is determined either by microwave phase shift and gamma-ray transmission or by microwave phase shift and attenuation. The flow rates of liquids and gas are determined from measurements of mass per unit area of liquids across a diameter of the pipeline by single energy gamma-ray transmission, cross-correlation of the outputs of two gamma-ray transmission gauges to determine flow velocity, and measurements of the operating pressure and temperature in the pipeline. These measurements are combined with models of flow regime to determine liquids and gas flow, and oil and water flow are respectively determined by multiplying liquids flow by (1-WC) and by WC.

The gamma-ray multiphase flow meter consists of two non-intrusive gamma-ray transmission gauges mounted about a pipeline (Figure 1). One of these gauges depends on measurement of the transmitted intensity of 662 keV gamma-rays (^{137}Cs) through the pipeline. The other depends on measurement of the transmitted intensities of 59.5 and 662 keV gamma-rays respectively from ^{241}Am and ^{137}Cs . The scintillation detectors are housed in flameproof enclosures, and electrical pulses from the detectors were routed via armoured cable to processing electronics and computer located in the plant room. The transmitted intensities of gamma-rays were determined every five milliseconds. This data was then grouped into approximately 17 second blocks for processing. The flows of liquids, gas, oil and water, and the water cut, were continuously displayed graphically on the MFM computer.

The microwave and gamma-ray technique has been described previously [8]. A schematic of the prototype microwave/gamma-ray MFM used in the Thevenard Island trial is shown in Figure 2. The MFM comprised the two gamma-ray transmission gauges with a single microwave transmission gauge mounted between them.

The microwave transmitter and receiver sensors of the microwave gauge were mounted in a pipeline crosspiece so that they were diametrically opposite and flush with the internal bore of the pipeline. These non-intrusive sensors were designed to comply with oil industry standards for integrity and safe operation. All the microwave circuitry associated with the MFM was housed in a flameproof enclosure mounted on the pipeline adjacent to the microwave gauge. The transmission of microwave signals between the sensors and this enclosure was via microwave cable enclosed in flameproof conduit. In routine operation, the phase shift and attenuation of an

~2.3 GHz microwave signal, transmitted across the diameter of the pipeline, was determined at approximately 30 ms intervals. This data was then grouped into ~14 s blocks for processing. The gauge electronics was housed in a flameproof enclosure located adjacent to the pipeline. The operation of both microwave gauge, and all data logging, was controlled by a plant room computer that was linked to the field enclosures via a armoured communications cable.

3. THEVENARD ISLAND TRIAL

West Australian Petroleum Pty. Ltd. (WAPET) produces oil from the Saladin, Yammaderry and Cowle oil fields near Thevenard Island, North West Shelf, Western Australia (Figure 3). At the time of the trial, eight oil wells were in operation, three on the Island and five offshore. The offshore wells produce from small platforms, and single or commingled flows are carried via pipelines on the sea bed to Thevenard Island. The processing facilities for all wells are on the Island.

3.1 MFMs and test pipeline

Two gamma-ray MFMs were used in each of the three phases of the trial. These were mounted on a 'test pipeline' joining the test manifold to the test separator (Figure 4), the density gauges being on steel spool pieces and the DUET gauges on glass reinforced epoxy (GRE) spool pieces. Individual streams from each well, and commingled streams from two or three wells, were routed through the test pipeline.

One of the gamma-ray MFMs was installed on the vertical (upflow) pipeline for the whole trial (position C, Figure 4). The other was moved to a different position on the test pipeline after completion of each phase of the trial. In Phase 1, the second gamma-ray MFM was mounted on the horizontal pipeline with a long straight length of pipe (12.4 metres) upstream of it (position B). In Phase 2, it was mounted on the vertical downflow pipeline (position D). In Phase 3, it was mounted on the horizontal pipeline about 1.4 metres downstream of a 90° bend (position A). The two gauges were spaced about 1100 mm apart on spool pieces of 139.8 mm bore.

The microwave gauge was installed in a cross piece of the spool piece on which the gamma-ray density gauge was mounted, between the two gamma-ray gauges of one of the gamma-ray MFMs. It was mounted on the horizontal (Position B) pipeline for Phase 1 of the trial, on the vertical downflow pipeline for Phase 2, and on the vertical upflow pipeline for Phase 3.

3.2 Test conditions during trial

The test separator on Thevenard Island is a horizontal type with an internal diameter of 2.7 metres and length 9.5 metres, and operates at a pressure of about 10 atmospheres. The single phase outputs from the separator are monitored by conventional turbine meters for oil and water, and orifice plates for gas.

The range and mean of test conditions during the periods in which the MFM measurements were made during Phase 2 of the trial are detailed in Table 1. These are typical of the whole trial. The ranges of flow rates for liquids, oil, water and gas were large.

During the trial, WAPET became aware that the test separator was overestimating the flow rates of oil. The separator was opened up late in December 1993, and holes found in its oil bucket from failure of repair work done in June 1993. Water was leaking through these holes into the oil bucket. Production accounting routines indicate that the leak rate increased with time. Using an 'oil decline' method, WAPET estimated the leakage rates during the trial based on production data obtained prior to June 1993 and after fixing the separator in 1994. CSIRO used in its calculations a simplification of this method, assuming that, over the short period of each Phase of the trial, the leak rate was constant and equal to the mean of the WAPET oil decline predictions for the various wells. The average corrections corresponding to the times of Phases 1, 2 and 3 of the trial were to subtract respectively 543, 1036 and 1128 BPD from the oil flow rates measured by the separator, and to add the same BPD to the water flow rates.

In each of the three phases of the trial, measurements with the gamma-ray and microwave/gamma-ray MFMs were made on all single well flows except for Saladin 7 during Phase 3. Some pairs of wells chosen for commingling were different between each phase depending on availability at the time of measurement. Measurements on Saladin 2 well flow during Phases 1 and 2 were discarded since during this period the water flow of this well was far too low to be measured accurately by the separator water meter. During Phase 1 of the trial, measurements were made on each single well stream at normal operating pressure in the pipeline, and at one or two higher pressures. The aim was to cover a greater range of operating conditions. In practice, the maximum change in flow rate achieved was relatively small. For Phases 2 and 3 of the trial, Saladin wells 4, 5 and 6 were each measured at two pressures, whilst the other single wells were measured only at the normal operating pressure.

The microwave/gamma-ray MFM data for Saladin 4 and Saladin 7 wells during Phase 1, and Saladin 2 well during Phase 3 were discarded due to insufficient data being available as a result of gauge malfunction during data logging. Data from one commingled stream (Cowie 2/Saladin 6) was also excluded from the Phase 3 data as inadequate mixing of the component wells resulted in unacceptable errors for the microwave/gamma-ray MFM.

3.3 Setting up the gamma-ray MFM

The procedures for off-line calibration of the gamma-ray MFM were refined between the first and second phases of the trial. This change would be expected to lead to more accurate results for determination of flows and water cut during Phases 2 and 3 compared with Phase 1. In particular, the determinations based on off-line calibration of the MFM would be very considerably improved and, to a lesser extent, determinations based on the on-line calibration.

Some of the count rates measured with the DUET gauges during Phase 1 of the trial were considerably higher than desirable for accurate measurement. This did not effect the liquids or gas flow measurements much, but directly affected the water cut determination and, via this, determinations of the oil and water flow rates. For Phases 2 and 3, the count rates were reduced by use of a smaller diameter collimator than that used in Phase 1.

4. PROCESSING OF RESULTS

The outputs of the MFM and separator output meters were processed by comparing the mean readings of each averaged over a period of 60 minutes. The determinations of liquids and gas

flow rates for both gamma-ray and microwave/gamma-ray MFMs were based on the gamma-ray transmission measurements.

4.1 Gamma-ray MFM

There are four ways in which the results of the gamma-ray MFM were compared with those of the separator output meters:

- a) The MFM was calibrated off-line based on measurements on static samples of oil, well water and gas, and models of the flow in the pipeline. The standard deviation between the flow rates predicted by the MFM and by the separator output meter was calculated.
- b) Least squares regression was used to obtain the best fits, separately for water cut and for liquids flow rate, comparing the MFM predictions in a) above with the corresponding separator output meter results. The r.m.s. differences so determined by this 'one variable fitting' do not include linear offsets in calibration caused by either or both the MFM and the separator.
- c) Water cut was determined as in b) above (i.e., one variable fitting), but liquids flow rate was determined by least squares regression using the predicted MFM flow and the additional (linear) parameter of pressure. This is called 1-2 variable fitting.
- d) Both water cut and liquids flow rate were determined by least squares regression, each with two parameters, one being the MFM result from a). This is called 2-2 variable fitting.

When a second variable measured by the MFM is included (c and d above) in the least squares regression, not only is compensation made for linear offsets as in b) but also for any linear error in the MFM or separator which depends on the second variable. In general, the larger the number of MFM measured variables incorporated into the least squares regression, the more the chance that there will be a better correction for separator errors and hence a lower r.m.s. difference between the results of the MFM and the separator. However, this does not make the calibration of the MFM more accurate; in practice it incorporates into the MFM calibration the errors of the separator.

The results given in Sections 5-7 are expressed as the ratio of r.m.s. difference to the mean of the flow rates or of the water cuts of all multiphase mixtures measured. For simplicity, this ratio in the rest of this paper is called the relative error, even though the ratio includes not only errors of the MFM but also those of the separator and separator output meters. For the determinations of oil and water flow rates, the MFM flow rates were the product of the MFM determinations of liquids flow rate and the oil or water cut.

4.2 Microwave/gamma-ray MFM

The error in the microwave/gamma-ray MFM predicted water cut was determined by direct correlation of the MFM data with the separator data. Consequently, the r.m.s. errors determined include the errors of the separator output meters, however, they do not include offsets in the estimation of the water cut due to either or both the MFM and the separator.

The r.m.s. errors were calculated using conventional linear least squares fitting and using non-linear fitting based on optimisation of the correlation using neural net fitting techniques.

5. LIQUIDS AND GAS FLOW RATES

5.1 Mass per unit area and velocity

Figure 5 shows the results of the determinations of mass per unit area (g cm^{-2}) of fluids in the gamma-ray beam versus time, for three different flows. The higher mass per unit area regions are slugs which are interspersed with lower mass per unit area regions of film. The top two plots of mass per unit area versus time for the onshore wells are very different to the bottom two plots which show two 17 second records of the commingled flow from two offshore wells. The former have approximately regular slugging with several slugs in the 17 second periods; the latter shows part of a very long slug (second from bottom) and part of a very long film (bottom). The latter flow was piped for more than a kilometre along the sea bed prior to surfacing at Thevenard Island. Long slugs build up in the seabed pipeline, and these are interspersed by long periods of film. The pattern of slug and film, seen on plots over much longer periods than 17 seconds, is very irregular.

Velocity is determined by cross-correlation of the two gauge outputs of transmitted intensities of ^{137}Cs gamma-rays which gives the time displacement, and the distance between the two gauges on the pipeline. Velocities are determined each 17 seconds. The range of velocities for flows from different individual and commingled wells was 4.4 to 23 metres per second.

5.2 Liquids and gas flow rates

The flow rate of liquids versus time for three streams are shown in Figure 6. The upper plot is for a well on Thevenard Island; the middle plot for commingled flows of two wells also on Thevenard Island; and the bottom plot for the commingled flows of two wells from an offshore platform. The upper and middle plots show reasonably constant flow over a 60 minute period, each point corresponding to one 17 seconds interval. The bottom plot shows the very large changes in flow rates which are more typical of the flow from offshore wells, due to the terrain slugging in the long pipeline along the sea bed.

The plots of the one-two variable fitting results of liquids and gas flow rates in the vertical upflow pipeline for the Phase 2 trial are shown in Figure 7. The plot for the liquids shows a very good correlation, with a relative error of 3.7%. The plot for gas flow has fewer data points because of lack of suitable orifice plates for the higher flows of gas. The relative error is 7.1%. These relative errors include errors both MFM and separator errors.

The relative errors for all MFM measurements of liquids and gas flows, based 2 variable fitting, are detailed in Table 2. The results of liquids flow in the vertical upflow pipeline average 4.0% over the three Phases of the trial. The results for the vertical downflow pipe is 3.3% (Phase 2), and for the two positions on the horizontal pipe worse at 5.3 and 6.2%. The one variable fitted results (not shown) for the vertical upflow pipeline are only slightly worse than those for the 2 variable fitting. The off-line calibration (not shown) is significantly worse, due to a linear offset in either or both the separator and the MFM. The results for one variable fitting in the vertical downflow pipeline are somewhat worse than for the two variable fitting, but the off-line

calibration is considerably worse. The one variable fitting results for the horizontal pipeline are much worse than for the two variable fitting, probably because of the lack of a good flow model for flows in the horizontal pipe.

The relative errors for the gas flows are given in Table 2. The ratios average 7.4%. There are relatively few experimental points, due to lack of suitable orifice plates to measure the higher gas flows from commingled streams.

6. WATER CUT

6.1 DUET gauge

Figure 8 shows a plot of water cut, determined in the vertical upflow pipeline by the gamma-ray MFM, and water cut determined by the separator (Phase 2). The relative error is 3.7% for the very wide range of water cuts of 25-96%.

The relative error for all MFM measurements of water cut, averaged over a period of one hour per measurement, are detailed in Table 2. For the vertical upflow stream, one variable fitting is used; for the horizontal and vertical down flow streams, two variable fitting. The results of water cut in the vertical upflow pipeline average 3.6% over the three Phases of the trial, with the relative error increasing with time probably due to the increase with time of the leak rate of water to the oil bucket in the separator. The relative error for the vertical downflow pipe is 3.7% (Phase 2), and for the two positions on the horizontal pipe at 6.6 and 2.7%. The high value of 6.6% is due to the very high count rates in the DUET gauge in Phase 1 of the trial. The count rates were reduced before the start of Phase 2 of the trial.

6.2 Microwave/gamma-ray gauges

An example of the trial data for a 14 s logging period on a commingled well flow (Saladin 6 + Saladin 7 + Yammaderry 2) is shown in Figure 9. The phase shift and attenuation data was determined by the microwave gauge and the liquids thickness was determined by the gamma-ray gauge (Figure 2). Due to the physical separation of the microwave and gamma-ray gauges on the pipeline there is a time lag of approximately 50-250 ms (depending on the flow velocity) between the data from these gauges. However, this delay is too small to be obvious in Figure 9. The data in Figure 9 indicates that there is a correlation between the phase shift, attenuation and gamma-ray data, with a very similar response to the thickness variation of the fluid flow due to the passage of slugs. This result also indicates that, as expected, there is little variation in the water cut over the 14 s period shown.

The data from the ~14 s blocks of data was averaged over the total logging period (~1 hour) for each well (or well mixture) to enable a comparison to be made with the separator data for the corresponding period.

The % relative errors (ratio of the r.m.s. difference to the mean) in the determination of the water cut by the microwave/gamma-ray MFM are shown in Table 3. In Table 3, separate errors are given for calculation of the water cut based on either linear or non-linear fitting of the microwave data. The non-linear fit, based on optimisation of the correlation using artificial neural net fitting techniques, is the more accurate, with errors typically less than half those

obtained using a linear fit. The best results for the determination of the water cut were obtained when the MFM was installed on the vertical upflow position. A plot of the microwave and gamma-ray predicted water cut for Phase 3 (vertical upflow), using the non-linear fit in Table 3, is shown in Figure 10.

7. OIL AND WATER FLOW RATES

7.1 Gamma-ray MFM

The oil and water flow rates determined, in the vertical upflow pipeline, in Phase 2 of the trial, are shown in Figure 11 (1-2 variables fitting). The flow rates determined by the MFM closely correlate with those of the separator. The flow rates for oil are determined to about 7.3% (Table 2), and water to about 4.7%. These averages exclude the results for the horizontal pipeline in Phase 1, which were the worst affected by the too high count rates (Section 3.3). For the vertical upflow pipeline, the results (not shown) of the one parameter fits for oil and for water are slightly worse than for the 1-2 parameter fits, while the results for the off-line calibration are significantly worse because of a linear offset error due to the MFM or separator, or both.

7.2 Microwave/gamma-ray MFM

The calculation of liquids flow rate, from liquids thickness and flow velocity, was performed by the same method as used in the gamma-ray MFM. The calculated flow rates for oil, water and gas during Phases 1, 2 and 3 of the Thevenard Island trial are given in Tables 4-6. The liquids flow rate has been calculated from the liquids mass per unit area, determined by gamma-ray transmission, and the flow velocity determined by cross-correlation of the outputs of the two gamma-ray transmission gauges. The oil and water flow rates have been determined from the product of the liquids flow rate and the respective oil and water cuts (using the non-linear fitting results in Table 3).

The results in Tables 4-6 indicate that over all three phases of the trial the microwave/gamma-ray MFM determined the oil and water flow rates, of the Thevenard Island wells and well mixtures, with errors of 6.8 % and 6.8 % relative respectively. The best results were obtained when the MFM was installed on either the vertical upflow or downflow positions. However, acceptable measurement accuracy was obtained for horizontal, vertical upflow and vertical downflow installations.

8. SUMMARY AND COMMENTS: GAMMA-RAY MFM

8.1 Accuracy

The gamma-ray MFM has now been proved in two trials on oil production pipelines: on the Vicksburg offshore oil platform [4-6] and on Thevenard Island. The flow rates of liquids for the two trials were very different; and the total range over which the MFM has now been proved is 1,400 to 33,400 BPD. Water cuts have ranged in the two trials from 17 to 96%. For the Thevenard Island trial, the flow rates were determined in the vertical upflow (downflow) pipeline to 4.0 (3.3) % relative for liquids, 7.5 (6.1) % for oil, 4.5 (4.5) % for water and 7.9 (7.7) % for

gas. Water cut was determined to 3.6 (3.7) % relative. These relative errors include errors not only due to the MFM but also due to the separator and its output meters.

The results for the vertical downflow, and horizontal flows, are roughly the same as for the vertical upflows, but depended on the use of 2-2 variable fitting.

8.2 Calibration

The mounting of the MFM on a vertical pipeline is preferred because the models for describing the flow regime in vertical pipelines are much simpler and better understood than those for horizontal pipes. The results of the present trial show that a simple one parameter calibration determines flow rates with sufficient accuracy for many practical applications. This is possible because the basic principles, including the mathematical equations, of gamma-ray transmission in liquids and gases are very well understood. There is a reasonable possibility that off-line calibration on static samples of oil, well water and gas will give sufficient accuracy. This has not been definitely established mainly because of the uncertainty of the absolute accuracy of the test separator.

8.3 Operating envelope

The operating envelope of a multiphase flow meter is the region in which the MFM determines the flow rates and water cut with acceptable accuracy for the application. Wolff [9] has defined one important parameter of the operating envelope of the MFM as the area on the two phase map of gas and liquid flow rates where the MFM measures flow rates with sufficient accuracy; the gas flow rate in this case is the gas volume flow rate at the pipeline operating pressure. The complete operating envelope of the gamma-ray MFM on this two phase map has not yet been established due to lack of sufficiently different flow conditions in the Vicksburg platform and Thevenard Island trials. However, the results of the trials on the Vicksburg platform (74 mm bore pipe) and on Thevenard Island (140 mm bore pipe) can be used to show at least some of the operating envelope covered by it (Figure 12).

Based on current experience with the gamma-ray MFM, gas volume fractions (GVFs) up to 0.9 should not limit the accuracy of the MFM determinations. We do not have any experience with GVFs above 0.9 and hence cannot make any predictions other than that there is a better chance of accurate measurement if the flow regime is not a misty annular flow. The limitation at very high GVFs is inaccuracies in determination of water cut by the DUET gauge; there is insufficient mass per unit area (g cm^{-2}) liquids in the gamma-ray beam. [The microwave/gamma-ray gauge can determine water cuts at much lower mass per unit areas of liquids; its main limitation being at high water mass per unit areas where the high absorption of microwaves prevents accurate measurement of transmitted microwave intensity.] The determination of liquids and gas flow rates is not a problem because the single energy gamma-ray transmission measures mass per unit area very sensitively; and since the determination of velocity by cross-correlation is also based on two single energy gamma-ray transmission measurements.

8.4 Pipe bores

The gamma-ray MFM can operate over a wide range of pipe bores, with limitation at small and very large pipe bores. With small pipe bores, less than approximately 75 mm but depending on

the GVF, there is insufficient mass per unit area of liquids in the gamma-ray beam for the accurate determination of water cut. At very large pipe bores, larger than about 300 mm, insufficient ^{241}Am gamma-rays will penetrate the very large mass per unit areas of liquids in the pipe (assuming the pipe is full of liquids with no gas) and hence the intensity of gamma-rays cannot be accurately measured. The liquids and gas flow rates can be determined accurately over a much wider range of pipe bores than possible for water cut.

9. SUMMARY AND COMMENTS: MICROWAVE/GAMMA-RAY MFM

A prototype microwave/gamma-ray MFM has been developed and successfully trialed at the Thevenard Island oil production facility for in-pipe measurement of oil, water and gas flow rates on production pipelines. The microwave/gamma-ray MFM determined the oil and water flow rates with errors of 6.8 and 6.8 % relative respectively for the wide range of wells and flow conditions during the trial period. The technique has been demonstrated to have acceptable accuracy for reservoir management purposes and the gauge design has been proven to be reliable in an industrial environment.

The water (or oil) cut and liquids thickness can be directly determined from a measurement of both microwave phase shift and attenuation [8]. However, compared to the microwave/gamma-ray transmission technique this approach was previously limited by the accuracy of the microwave attenuation measurement. As a result of developments during the Thevenard Island trial of the microwave/gamma-ray MFM, significant advances were made in the accuracy of the on-line determination of both microwave phase shift and attenuation. These developments led to a reassessment of a microwave MFM based on a simultaneous measurement of microwave attenuation and phase shift. In this technique, a transmission measurement of microwave attenuation and phase shift by a single microwave sensor is sufficient to determine water (or oil) cut and liquids thickness, and the cross-correlation of the output of two such sensors is used to determine flow velocity. The oil, water and gas flow rates are then determined from combining liquids thickness, water cut, pressure and temperature data in an appropriate flow model.

A preliminary assessment of the viability of the technique was based on a calculation of the water cut for the Thevenard Island Phase 3 data from microwave attenuation and phase shift measurements alone. A non-linear correlation of the measured attenuation and phase shift data with the separator water cut, using an artificial neural net fitting technique, gave a 3.2 % relative error in the predicted water cut for the Thevenard Island data. This error was comparable to that obtained by the microwave/gamma-ray MFM (Table 3). This result confirmed the viability of the technique for determination of water cut. However, a trial of a prototype microwave MFM is required to establish the accuracy of this technique for the direct determination of the flow rate of oil, water and gas in production pipelines.

A schematic of the prototype microwave MFM spool piece that is presently under development is shown in Figure 13. The microwave MFM is comprised of two independently operated microwave sensors mounted in pipeline crosspieces. The two microwave sensors are aligned so that they measure over the same transmission path and are flush with the internal bore of the pipeline. The attenuation and phase shift of a microwave signal transmitted across the diameter of the pipe at each sensor is used to determine the liquids thickness and the volume fractions of oil, water and gas in the measurement path. The fluids flow velocity is determined from the cross correlation of the outputs from each microwave sensor. Measurements of oil, water and gas

volume fractions and the flow velocity are then combined using an appropriate flow model to determine the flow rate of each component.

10. 1994 TRIAL

Trials of both the gamma-ray and microwave MFMs will be undertaken on the West Kingfish platform in the Bass Strait operated by ESSO Australia. There are 24 oil wells flowing to this platform with a wide range of flow conditions and water cuts. The facility to increase gas lift and thereby gas volume fractions will allow further definition of the operating envelope of the MFM. The 1994 trial is scheduled to commence late in September, and last for about four months.

The gamma-ray MFM to be trialed is an advanced prototype, equivalent to a commercial prototype. The aim of the trial is to demonstrate the accuracy of the gamma-ray MFM equipment in long-term operation, and to assess further the calibration techniques based on off-line measurements on static samples. The gamma-ray MFM outputs of flow rates of liquids, oil, water and gas, and water cut, will be routed to the ESSO computer in the platform control room.

The aim of the trial of the microwave MFM is to assess the accuracy of on-line determination of oil, water and gas flow rates over a range of wells and flow conditions.

11. CONCLUSION

The gamma-ray MFM has now been demonstrated in trials on the Vicksburg offshore oil platform and at the oil production facilities on Thevenard Island. Flow rates and water cut are determined to an accuracy sufficient to meet the oil industry's requirements for optimisation of oil production over the whole field life. The hardware and software of the MFM have been demonstrated to be reliable under field conditions, giving continuous and instantaneous display of water cut and flow rates. An advanced prototype, equivalent to the commercial prototype, of the gamma-ray MFM will be trialed at the West Kingfish offshore oil platform late in 1994.

A prototype microwave and gamma-ray MFM has been developed and successfully trialed at the Thevenard Island oil production facility for in-pipe measurement of oil, water and gas flow rates on production pipelines. The microwave and gamma-ray MFM determined the oil and water flow rates with errors of 6.8 and 6.8% relative respectively for the wide range of wells and flow conditions during the trial period. The technique has been demonstrated to have acceptable accuracy for reservoir management purposes and the gauge design has been proven to be reliable in an industrial environment. A microwave only MFM is presently being developed and an industrial prototype gauge will undergo a platform trial in late 1994.

ACKNOWLEDGMENTS

The authors wish to thank Mr. D. Stribley, the Australian Mineral Industries Research Association Ltd., for coordination of the Project. Project Sponsors are the Energy Research and Development Corporation of the Australian Government, ESSO Australia Ltd., The Shell Company of Australia Ltd., West Australian Petroleum Pty. Ltd. and Western Mining Corporation. These Sponsors have contributed greatly by sound advice and (in part) financial support. The authors wish to thank WAPET staff at Perth and Thevenard Island for their

enthusiastic support, help and encouragement which made possible the success of the trial; and CSIRO electronics staff Al McEwan and Vic Sharp.

REFERENCES

1. Brown, D. - The multi-component multiphase flow meter. The North Sea Flow Measurement Workshop, Peebles, Scotland, October, 1992.
2. Dykesteen, E. and Midttveit, O. - A flow regime independent multiphase flowrate meter. The North Sea Flow Measurement Workshop, Peebles, October, 1992.
3. Gaisford, S., Amdal, J. and Berentsen, H. - Offshore multiphase meter nears acceptable accuracy level. *Oil & Gas Journal* 91 (20): pp. 54-58, 1991.
4. Roach, G.J., Watt, J.S., Zastawny, H.W., Hartley, P.E., Ellis, W.K., McEwan, A., and Sharp, V. - Platform trial of a multiphase flow meter. The North Sea Flow Metering Workshop, Bergen, October, 1993.
5. Roach, G.J., Watt, J.S., Zastawny, H.W., Hartley, P.E. and Ellis, W.K. - Multiphase flowmeter for oil, water and gas in pipelines based on gamma-ray transmission techniques. *Nuclear Geophysics* 8 (3) pp. 225-242, 1994.
6. Roach, G.J., Watt, J.S. Zastawny, H.W., Hartley, P.E. and Ellis, W.K. - Trials of a gamma-ray multiphase flow meter on Thevenard Island. SPE 1994 Asia Pacific Oil and Gas Conference, Melbourne, 7-10 November, 1994.
7. Torkildsen, B.H. and Olsen, A.B. - Framo multi-phase flow meter. The North Sea Flow Measurement Workshop, Peebles, October, 1992.
8. Ashton, S.L., Cutmore, N.G., Roach, G.J., Watt, J.S. and Zastawny, H.W. - Development and trial of microwave techniques for measurement of multiphase flow of oil, water and gas. SPE 1994 Asea Pacific Oil and Gas Conference, Melbourne, 7-10 November, 1994.
9. Wolff C.J.M. - Required operating envelope of multiphase flow meters for oil well production measurement. The North Sea Flow Metering Workshop, Bergen, Norway, October 26-28, 1993.

Table 1. Range and mean of flow parameters at times corresponding to MFM measurements.

| PARAMETER | RANGE | MEAN | UNITS |
|------------------|------------|--------|-------------------|
| Liquids | 7233-32346 | 18,278 | BPD |
| Oil | 445-16020 | 8,095 | BPD |
| Water | 3715-20630 | 10,184 | BPD |
| Gas | 1423-4494 | 3,074 | MSCF/D* |
| Water cut | 25.4-95.6 | 58.2 | % |
| Gas to oil ratio | 379-2960 | 749 | SCF/Barrel |
| Pressure | 1123-1595 | 1,219 | kPa |
| Temperature | 24-78 | 60 | °C |
| Velocity | 4.4-19 | 11.3 | m s ⁻¹ |

*thousand standard cubic feet per day

Table 2. Relative errors (r.m.s. difference σ/mean) for flow rates and water cuts determined by the gamma-ray MFM. The r.m.s. difference is the combined errors of the MFM and the separator.

| Phase | MFM | σ/mean (%) | | | | |
|-------|------------|--------------------------|-----------|-------|-------|-----|
| | | Liquids | Water cut | Oil | Water | Gas |
| 1 | Vertical ↑ | 4.0 | 3.1 | 6.9 | 5.2 | 8.0 |
| | Horiz.(B) | 5.3* | 6.6* | 10.4* | 9.2* | 7.5 |
| 2 | Vertical ↑ | 3.7 | 3.7 | 7.1 | 3.7 | 7.1 |
| | Vertical ↓ | 3.3 | 3.7 | 6.1 | 4.5 | 7.7 |
| 3 | Vertical ↑ | 4.4 | 4.1 | 8.4 | 4.5 | 8.6 |
| | Horiz.(A) | 6.2 | 2.7 | 8.1 | 5.6 | 5.7 |

* too high count rates

Table 3. Results of the water cut determined by the microwave/gamma-ray MFM for Phases 1, 2, and 3 of the Thevenard Island trial.

| TRIAL | % RELATIVE ERROR IN WATER CUT* | |
|-----------------------------|--------------------------------|----------------|
| | Non-linear fitting | Linear fitting |
| Phase 1 (horizontal B) | 5.2 | 10.5 |
| Phase 2 (vertical downflow) | 5.4 | 12.2 |
| Phase 3 (vertical upflow) | 3.3 | 9.2 |

*ratio of the r.m.s. difference to the mean (%)

Table 4. Phase 1: % relative error for microwave/gamma-ray MFM mounted in the horizontal position.

| PARAMETER | HORIZONTAL (Position B) | |
|--------------|-------------------------|-------------------------|
| | % Relative Error | Correlation Coefficient |
| Liquids Flow | 3.2 | 0.993 |
| Oil Flow | 8.4 | 0.994 |
| Water Flow | 9.0 | 0.973 |

Table 5. Phase 2: % relative error for microwave/gamma-ray MFM mounted in the vertical downflow position.

| PARAMETER | VERTICAL DOWNFLOW (Position D) | |
|--------------|--------------------------------|-------------------------|
| | % Relative Error | Correlation Coefficient |
| Liquids Flow | 3.2 | 0.997 |
| Oil Flow | 6.6 | 0.994 |
| Water Flow | 5.6 | 0.992 |

Table 6. Phase 3: % relative error for microwave/gamma-ray MFM mounted in the vertical upflow position.

| PARAMETER | VERTICAL UPFLOW (Position C) | |
|--------------|------------------------------|-------------------------|
| | % Relative Error | Correlation Coefficient |
| Liquids Flow | 4.1 | 0.991 |
| Oil Flow | 5.5 | 0.993 |
| Water flow | 5.9 | 0.982 |

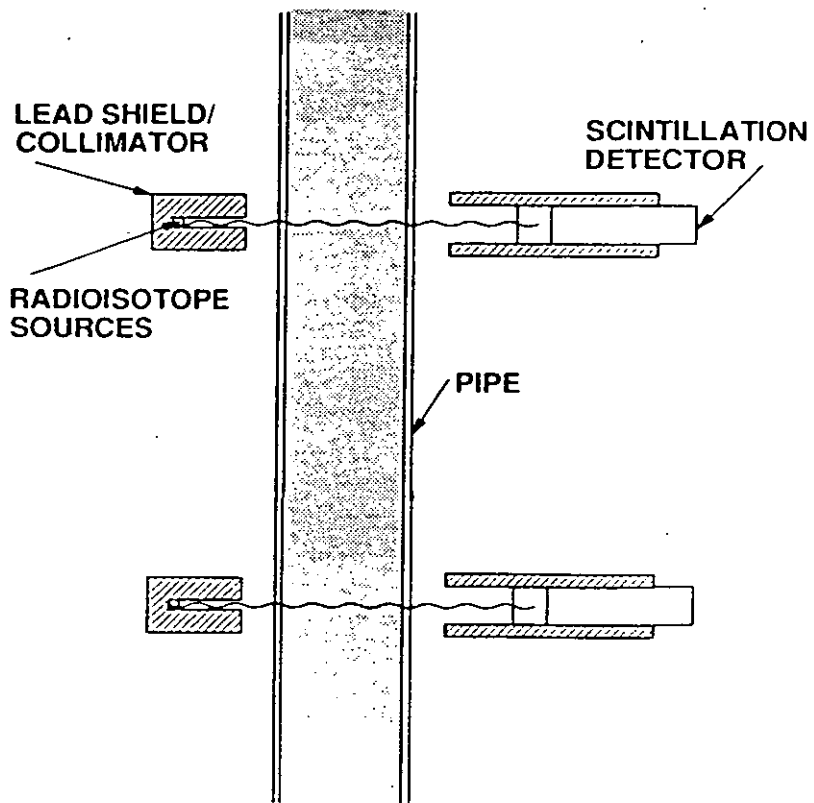


Fig. 1. Schematic of the gamma-ray MFM.

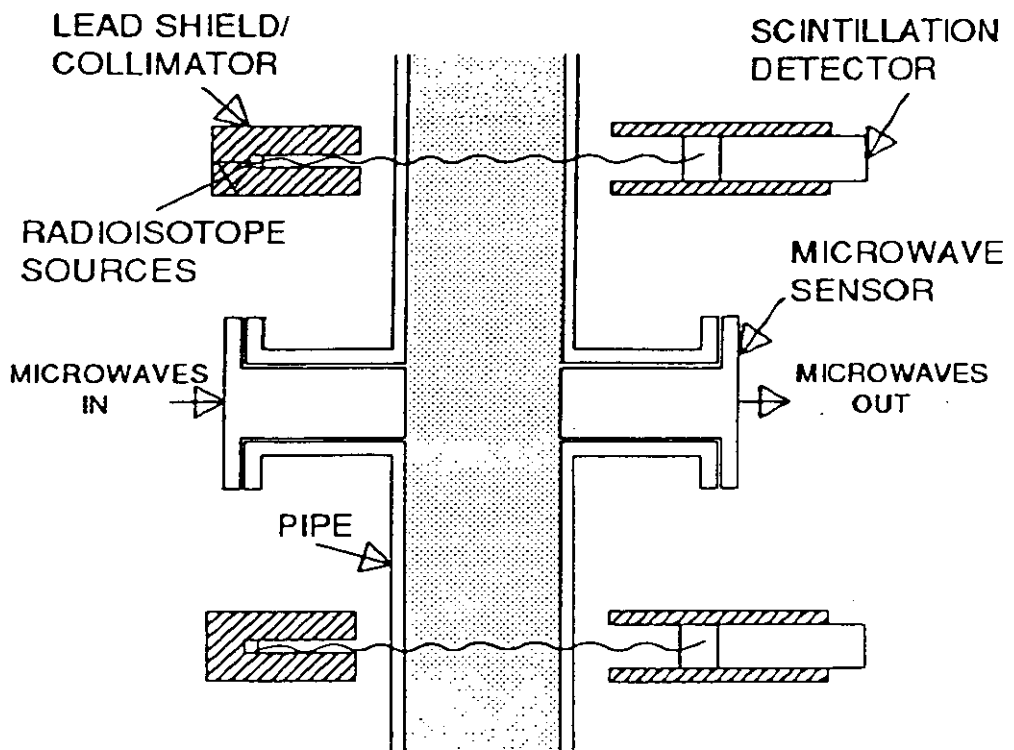


Fig. 2. Schematic of the prototype microwave/gamma-ray MFM used in the trial on Thevenard Island.

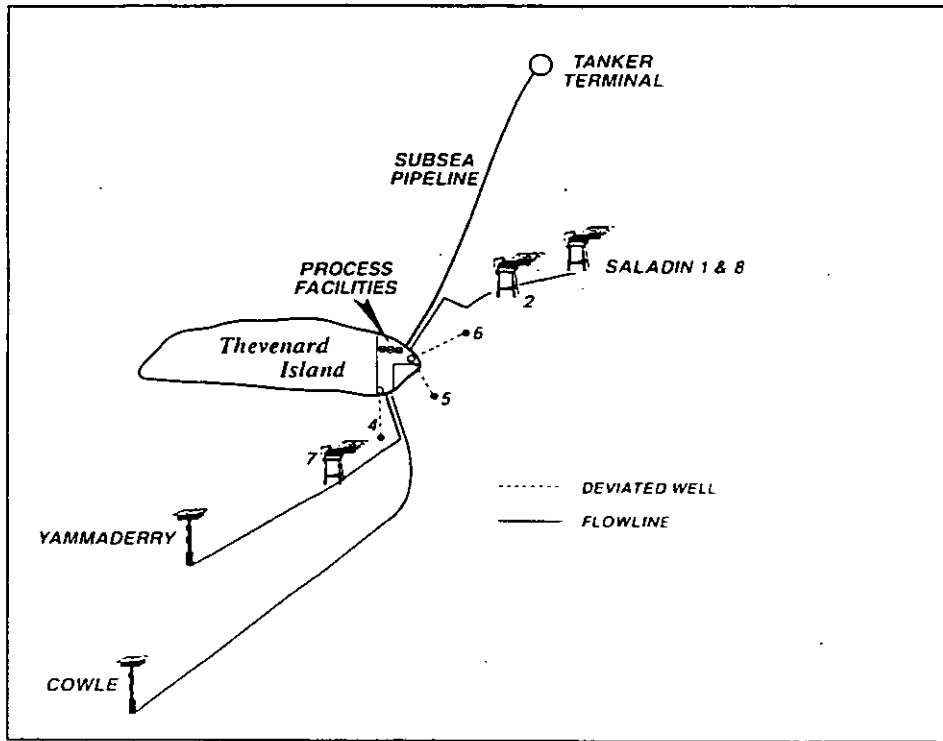


Fig 3. Schematic showing the Saladin, Yammaderry and Cowle facilities near Thevenard Island.

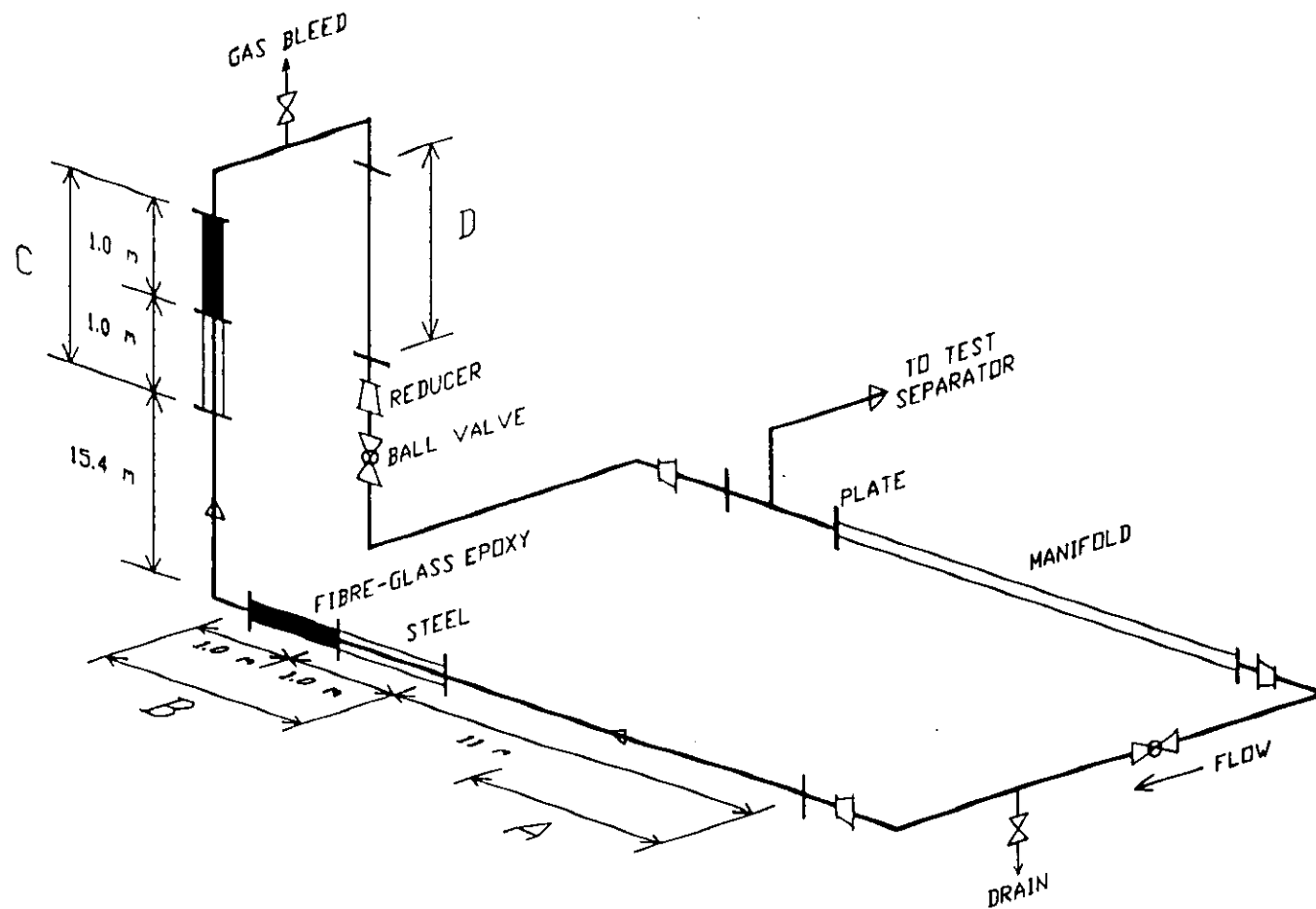


Fig. 4. Schematic of the test pipeline at Thevenard Island. A, B, C, and D are the positions at which the two-gamma-ray multiphase flow meters were mounted during the trial, with one MFM always in position C.

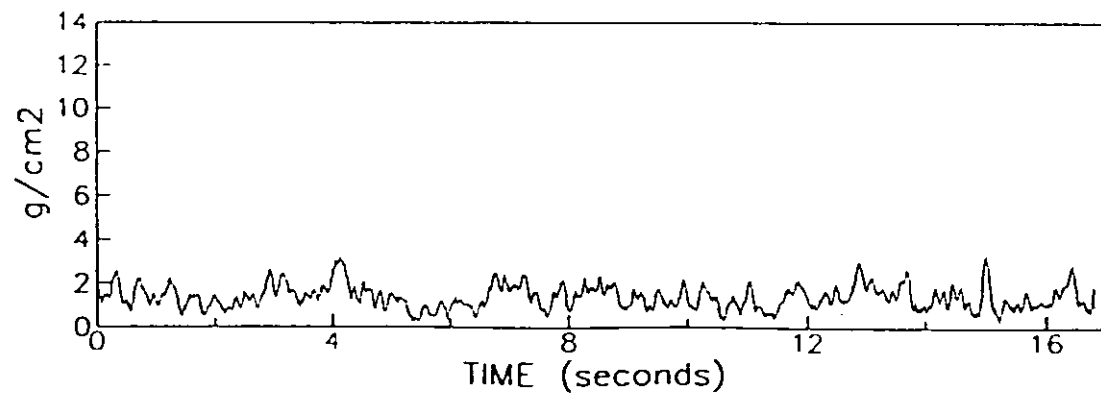
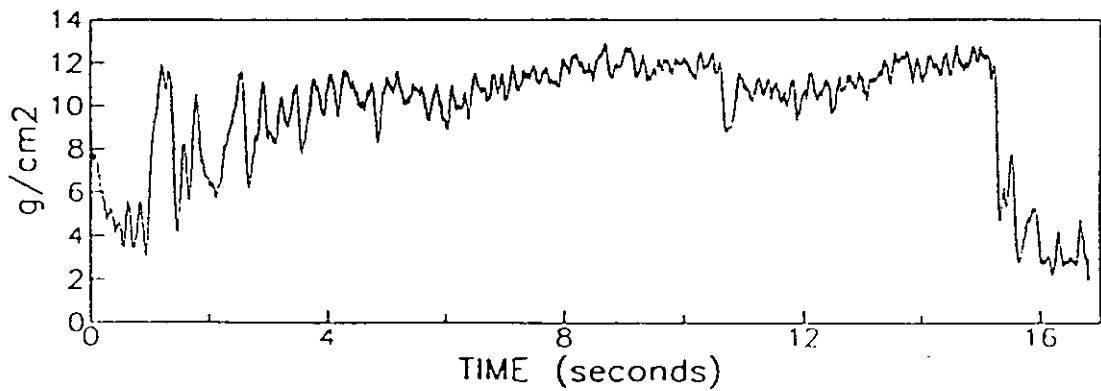
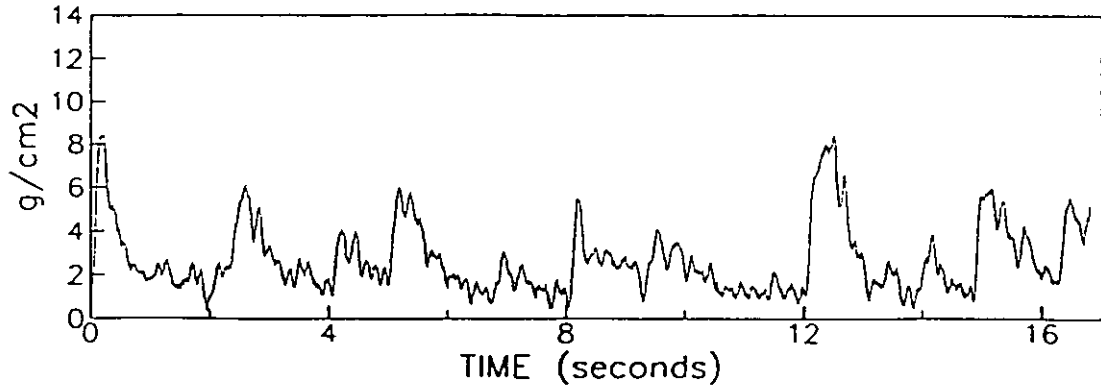
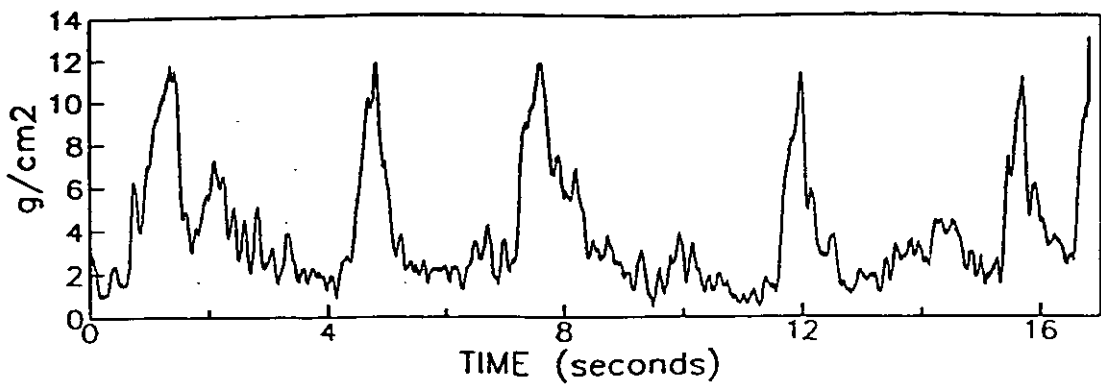


Fig. 5. Mass per unit area (g cm^{-2}) of fluids versus time for the flow of the Saladin 4 well (top), for the commingled flow of the Saladin 4 and 5 wells (second from top), and for the commingled flow of the Saladin 7 and Yammaderry 2 wells (bottom two).

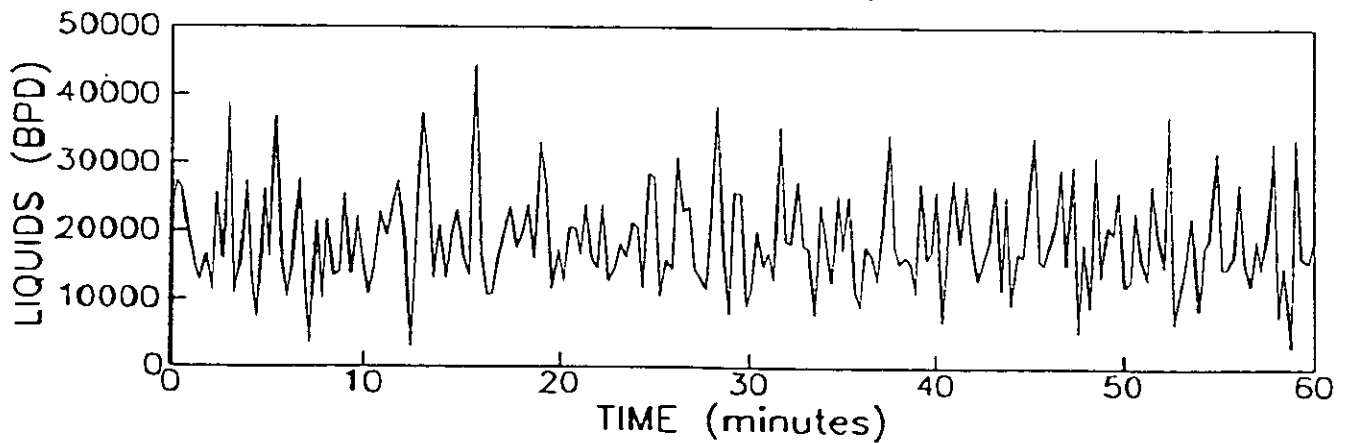
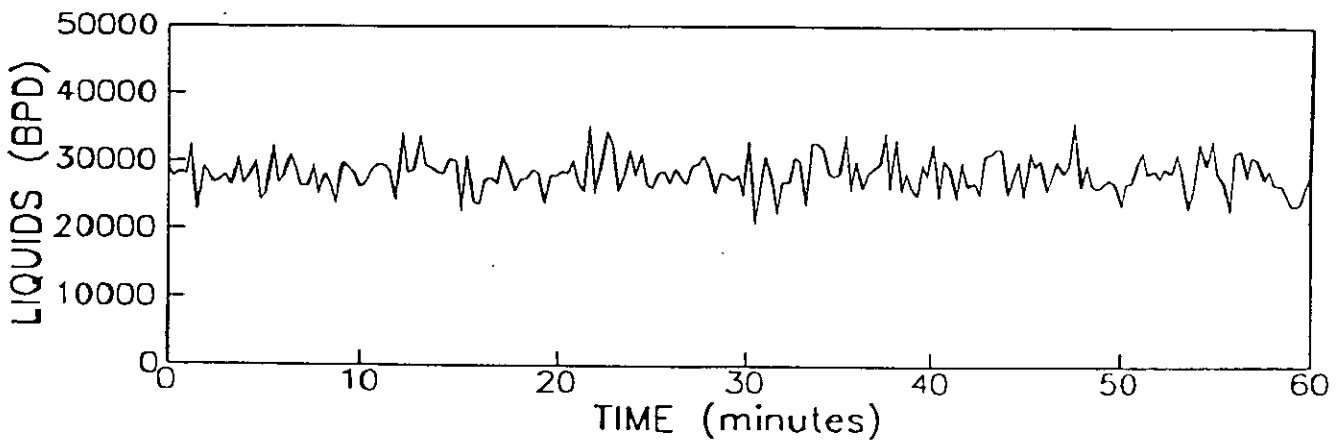
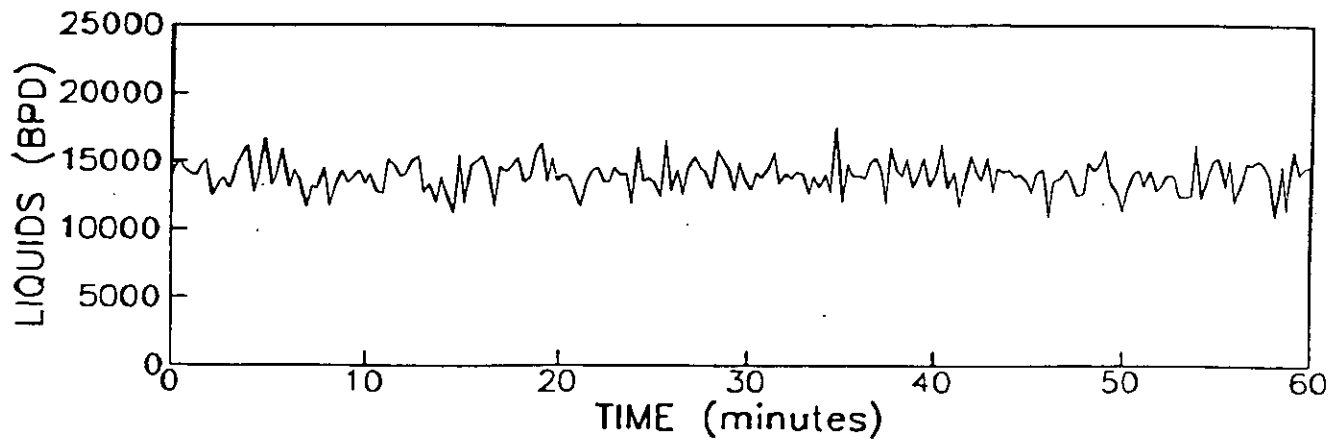


Fig. 6. The flow rate of liquids versus time for the flow from the Saladin 4 well (top), for the commingled flows of the Saladin 4 and 6 wells, and for the commingled flows of the Saladin 7 and Yammaderry 2 wells.

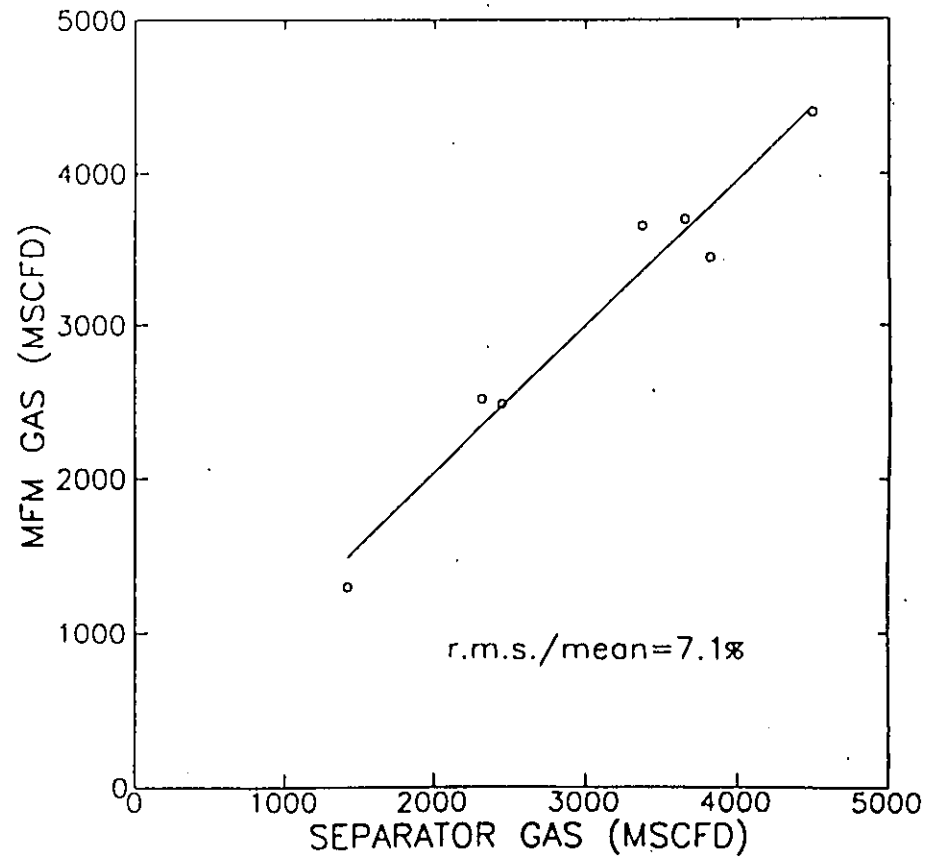
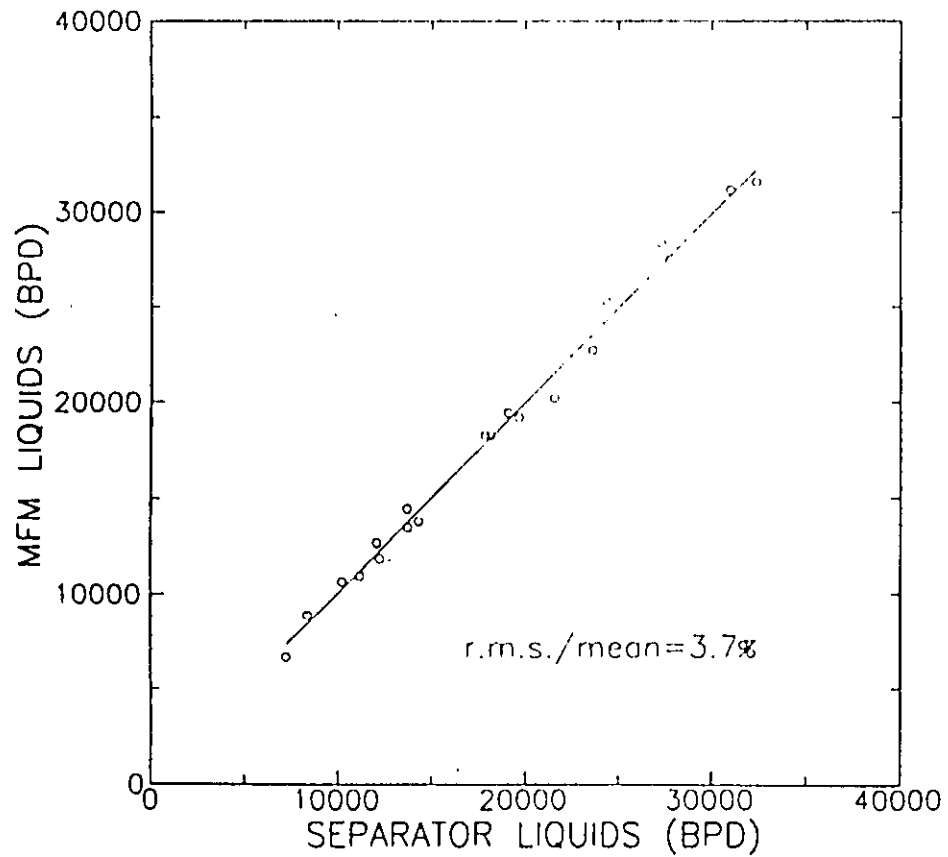


Fig. 7. Liquids and gas flows for the gamma-ray MFM mounted about the vertical upflow pipeline: Phase 2 of the trial.

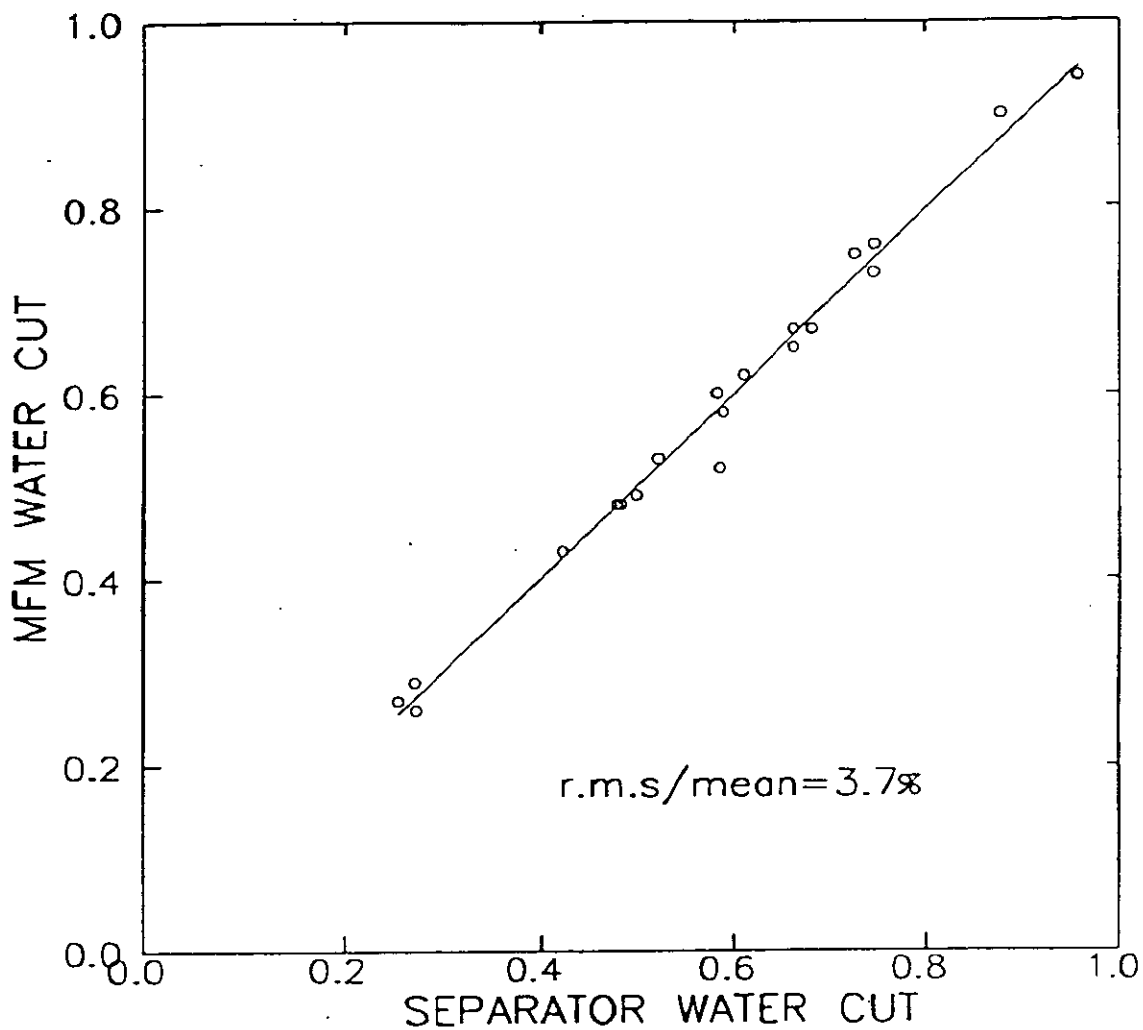


Fig. 8. Water cut for the gamma-ray MFM mounted about the vertical upflow pipeline: Phase 2 of the trial.

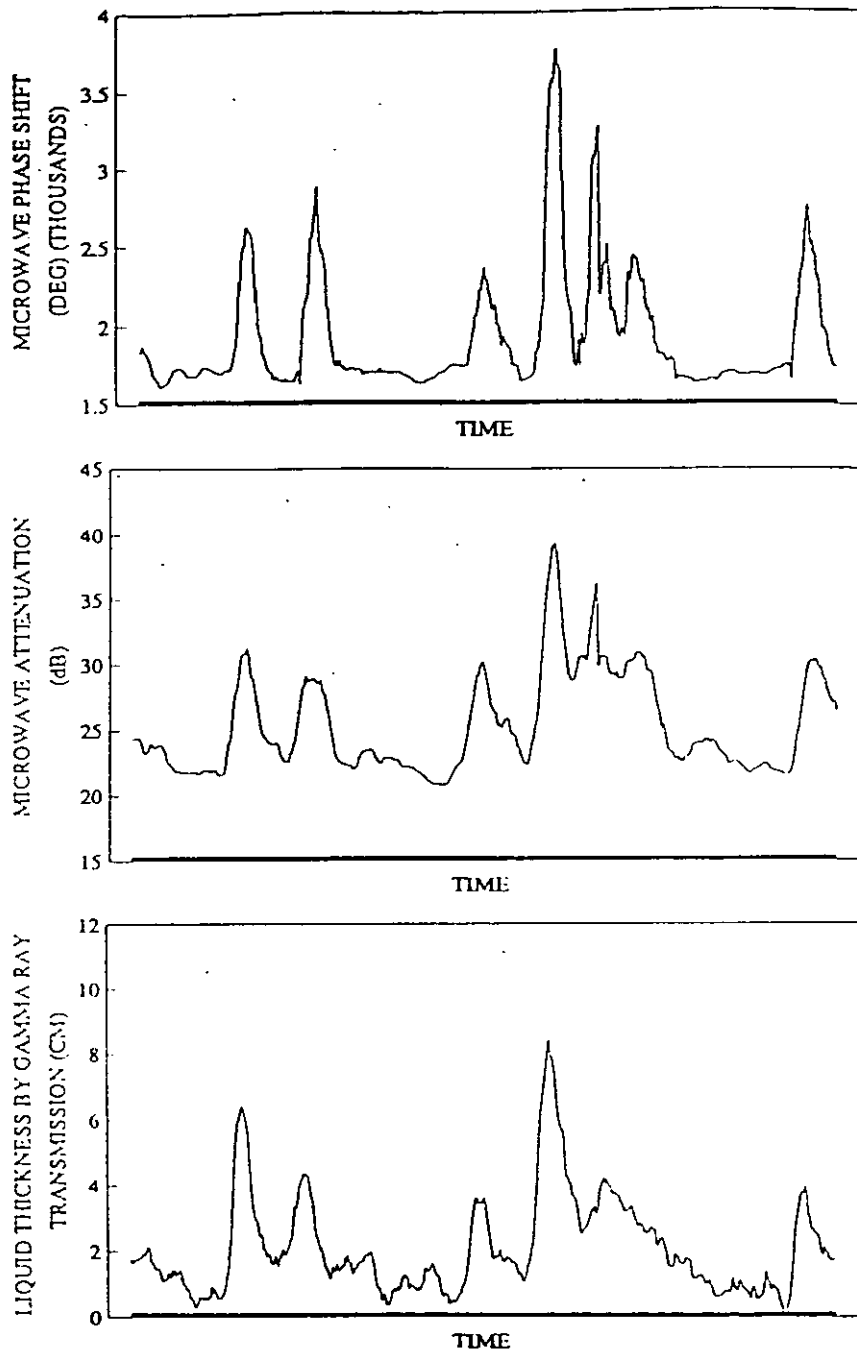


Fig. 9. Plot of microwave/gamma-ray MFM data for an ~14 s logging period of a commingled (Saladin 6+Saladin 7+Yammaderry 2) well flow during the Thevenard Island trial. The phase shift and attenuation gamma data were measured by the microwave gauge of the MFM and liquids thickness by the gamma-ray gauge of the MFM.

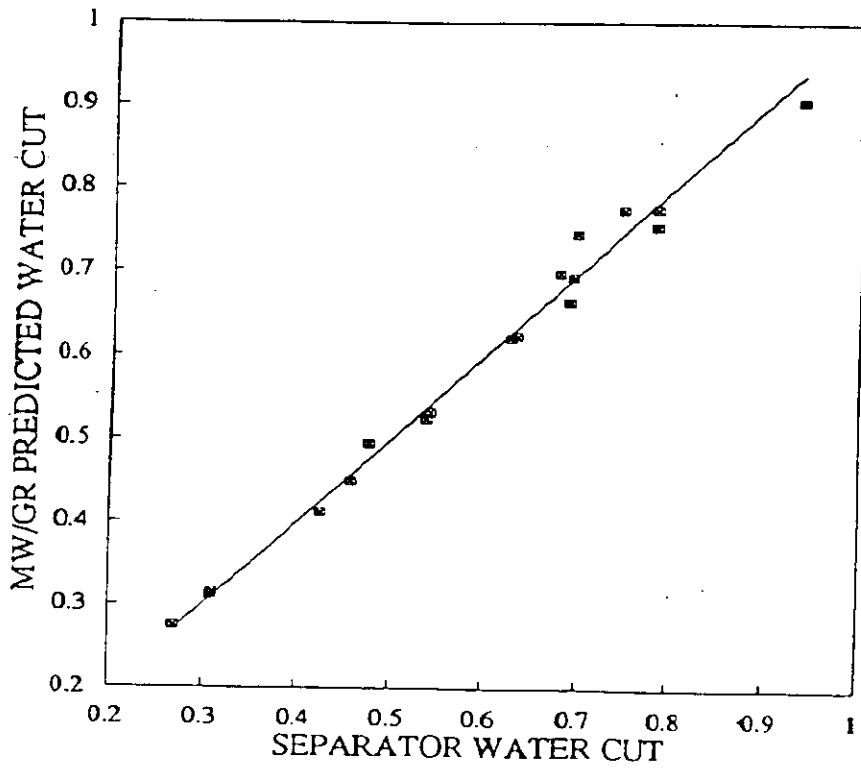


Fig. 10. Plot of the microwave/gamma-ray MFM predicted water cut versus the separator water cut during Phase 3 of the Thevenard Island trial.

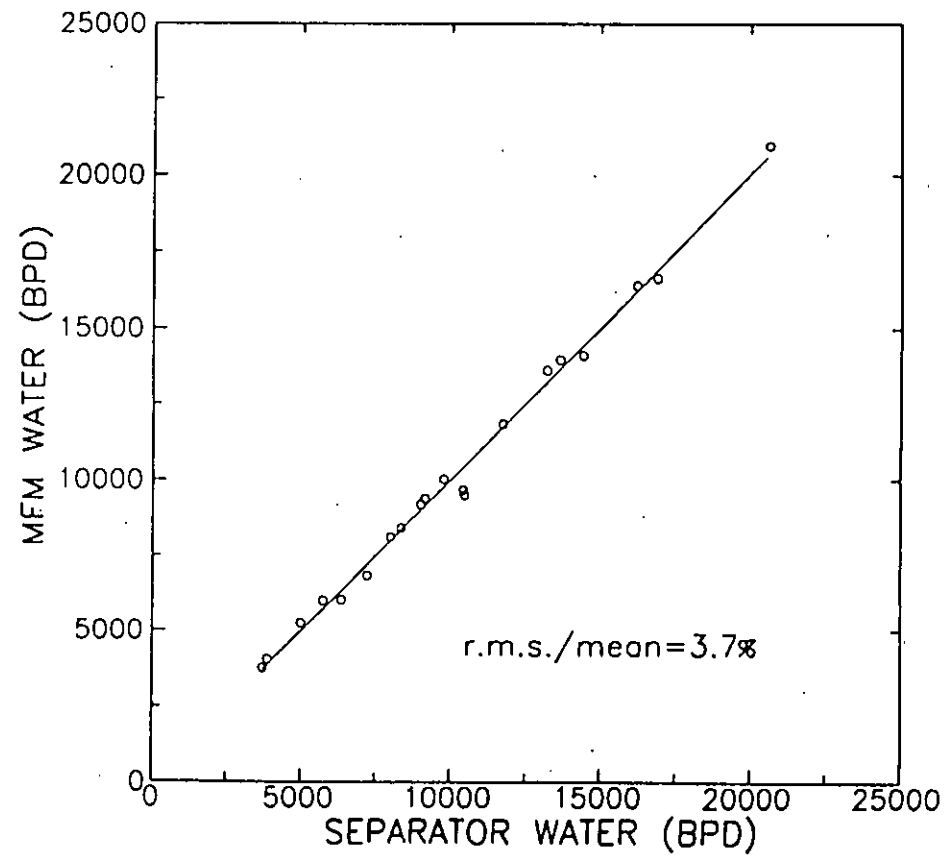
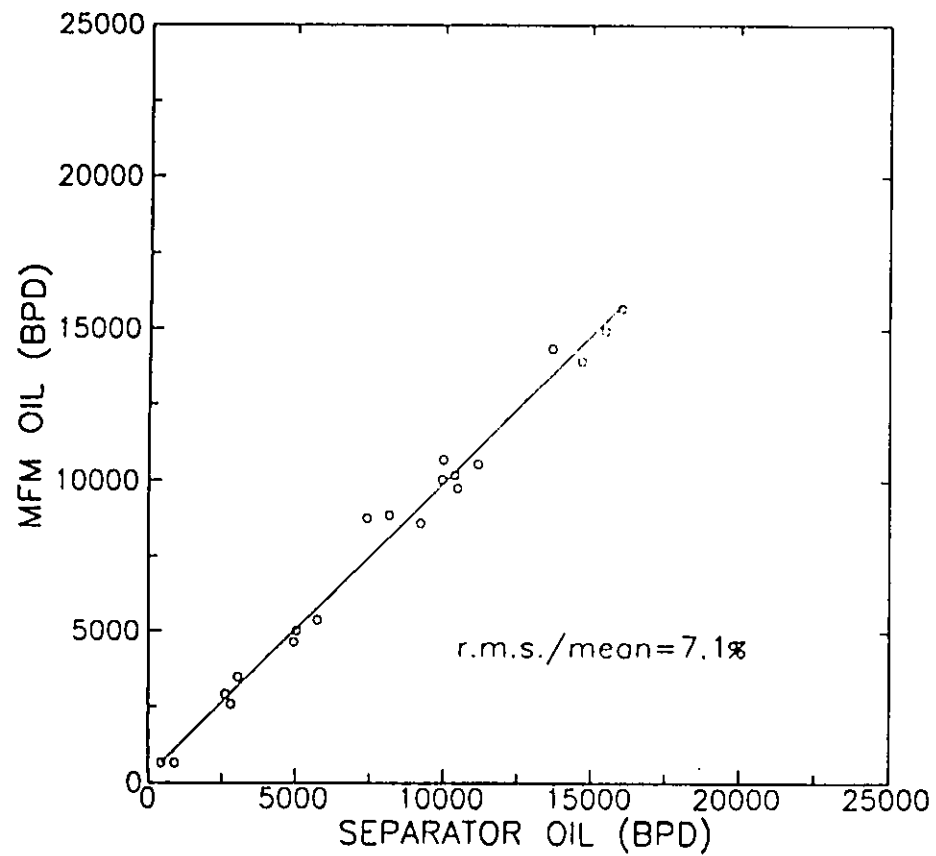


Fig. 11. Oil and water flows for the gamma-ray MFM mounted about the vertical upflow pipeline: Phase 2 of the trial.

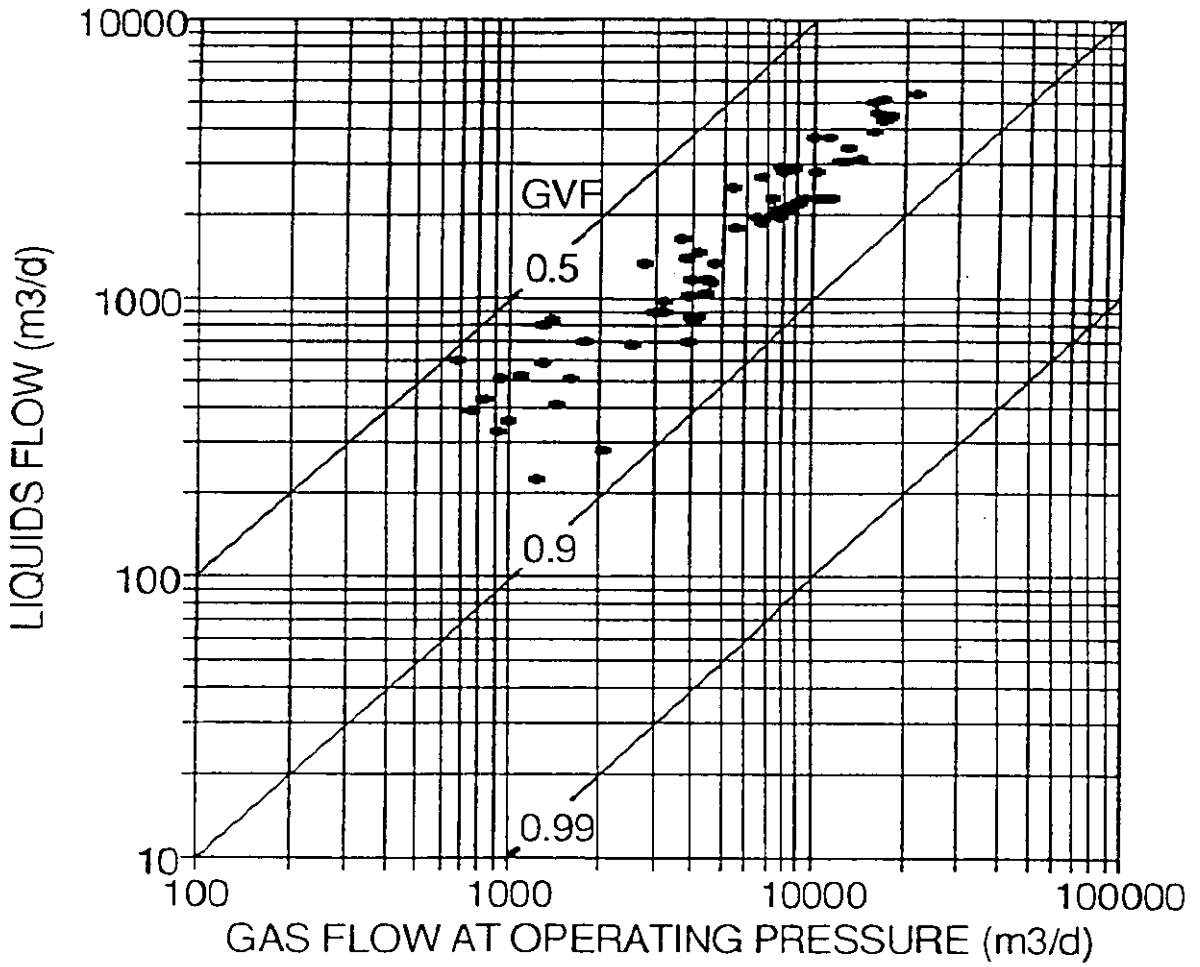


Fig. 12. Flow rates of liquids and gas (at operating pressure in pipeline) during the Vicksburg platform and Thevenard Island trials.

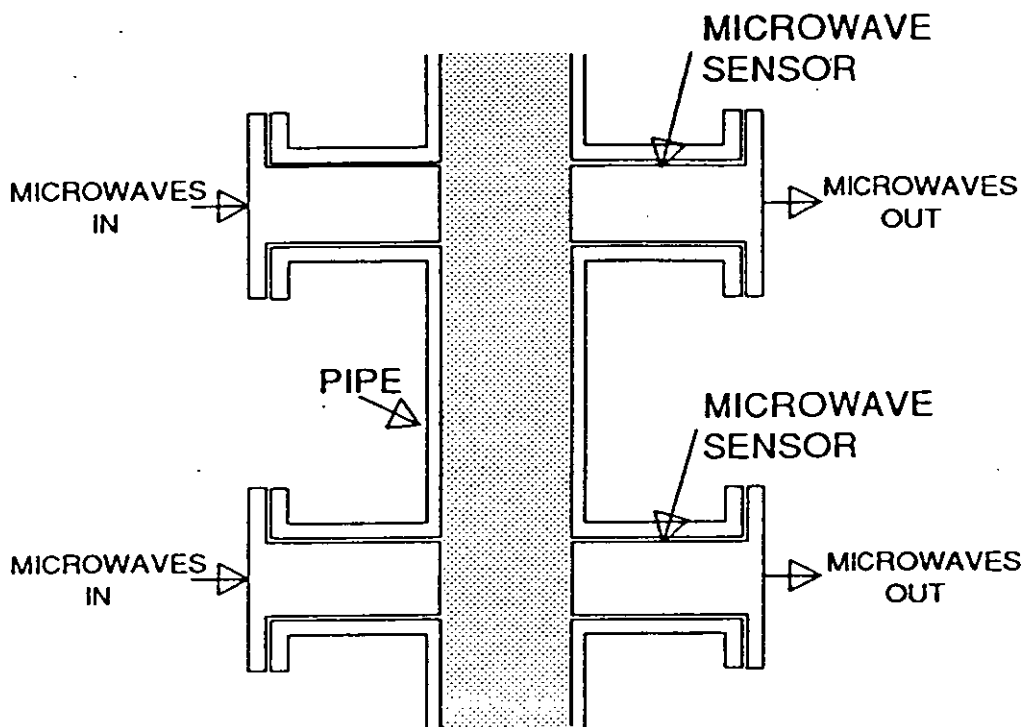


Fig. 13. Schematic of the prototype microwave MFM to be used in the West Kingfish platform trial.

SESSION 4

FLOWMETERS

Chairman - L N Philp, Dept of Trade and Industry

V-Cone meter : Gas measurement for the real world

Maron J. Dahlstrøm

Phillips Petroleum Company Norway

Summary

This paper describes the performance of the V-Cone meters used for Embla test separator gas measurement, starting May 1993. The advantages and disadvantages for use of this technology on the partially processed gas at an offshore platform is discussed.

It has been shown in tests that the V-Cone meter functions well with wet gas conditions. The long term repeatability of the meter is documented. Also the low influence from upstream disturbance is confirmed. It is shown that calibration curve fit to ISO5167-1 based equations, can give dry gas accuracy inside the fiscal requirements for gas at Reynoldsnumber above 1 million. The experience from Embla shows that the V-Cone meter tolerates rough operation : The V-Cone meter dimensions certified at six month intervals identifies no changes to the meter. Also the flow calibrations carried out at the same time intervals presents no significant changes ; the results match close to the accuracy of the equipment used in the flow calibrations.

1 Introduction

The remote operation of the Embla platform was a challenge in selection of reliable equipment with low maintenance requirements for the test separator measurement used in fiscal allocations. The gas measurement criterias ; no moving parts and high tolerance to particles and condensate, is not complied with by any of the well proven measurement equipment.

Our thorough evaluation of the V-Cone meter design for this application showed no apparent weakness, apart from possible vortex noise introduced by the V-Cone holder. The design with the central cone allows for the liquid to continue along the wall, and liquid buildup can therefore be avoided. The thin film of condensates at the wall will not introduce upsets to the flow pattern. Also the contineously increasing velocity up to the minimum area by the edge of the V-Cone, produces a uniform flow profile at higher flow-rates; thus the requirement for upstream straight lenghts is reduced or eliminated. In a gas experiment by McCrometer, it is documented on video that the profile is smoothend out before the edge of the V-Cone, and that the swirl appears to be removed . In any case, the vortex noise would be seen as stochastic and eliminated thru square rooth averaging of the differential pressure.

Previous tests by Phillips Petroleum in New Mexico over months of operation showed repeatable long term results. We were therefore satisfied that the V-Cone meter would fulfill the requirements on Embla. On this background, it was decided to qualify the V-Cone meter for the Embla gas measurement.

The V-Cone meter functional performance was verified at the Rogaland Research wet gas test loop facilities , where both installation tolerance and tolerance to liquid in the gas were tested in the spring of 1992.

Calibration of the V-Cone meters before offshore installation at Embla and every six months for the first year, was agreed with the NPD. Initial testing with high differential pressures were carried out at K-Lab in the first part of 1993. Certification of the coefficient of discharge was carried out at NMI, Bergum before startup of Embla in the summer of 1993, and recertification was carried out by NMI in the end of 1993 and again in the summer of 1994. Dimensional certification procedure was developed by Con-Tech and the V-Cone meter certification was performed each time before the flow calibration certification of the coefficient of discharge.

2 *Phillips Petroleum New Mexico comparison with orifice*

Early gas measurement comparison tests where the V-Cone meter was put in series with an Orifice meter, was carried out in 1991 by Phillips Petroleum New Mexico. The monthly mass comparison from May to July repeated within $\pm 0.01\%$ and the daily comparison was mainly within $\pm 0.1\%$. However, a consistent bias of approximate $+0.75\%$, made it clear that traceable calibration close to operating conditions would be required for accurate measurement.

BIAS

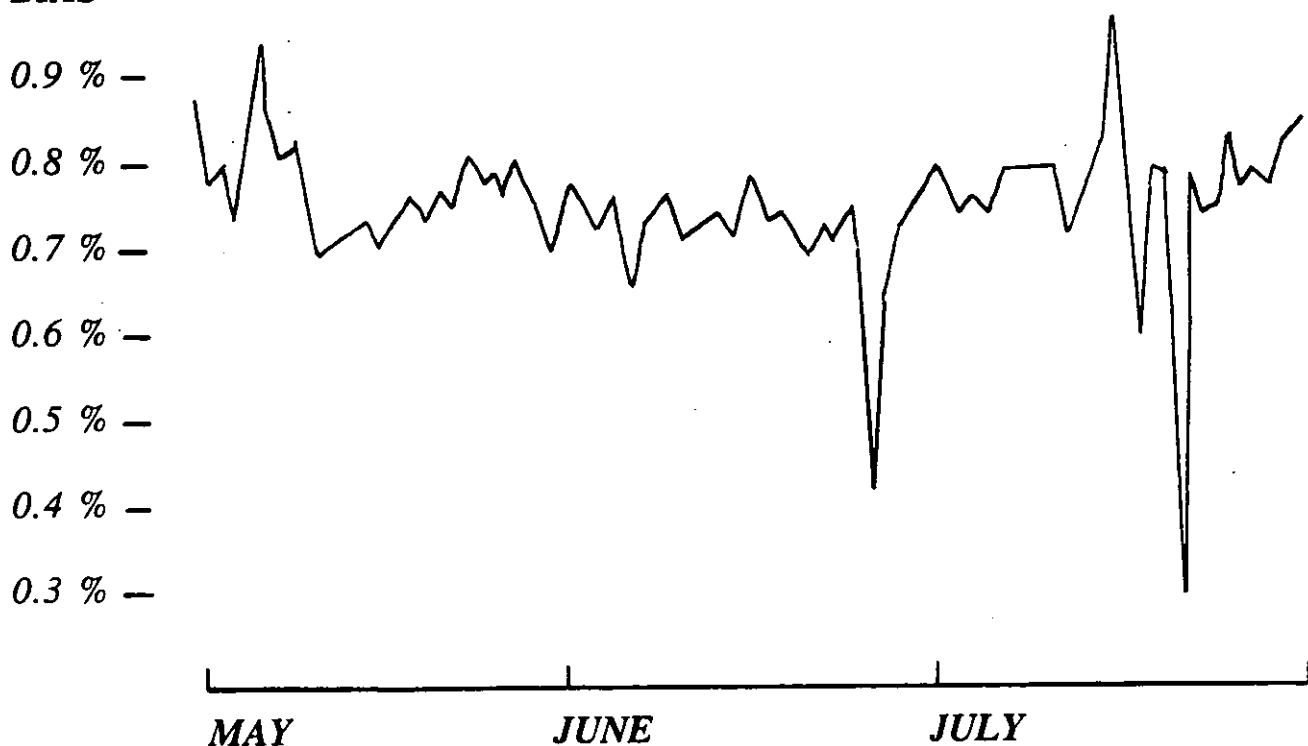


FIGURE 1 *COMPARISON OF V-CONE WITH ORIFICE 1991*

3 *V-Cone meter functional performance verification at RF*

The functional performance test at Rogaland Research was carried out to quantify the V-Cone meter tolerance to free liquid in gas, and also to check the tolerance to upstream disturbance and eccentric profile. In the closed loop wet gas testing facilities, a V-Cone meter was tested in series with an Orifice meter. It should also be noted that the vortex noise imposed on the

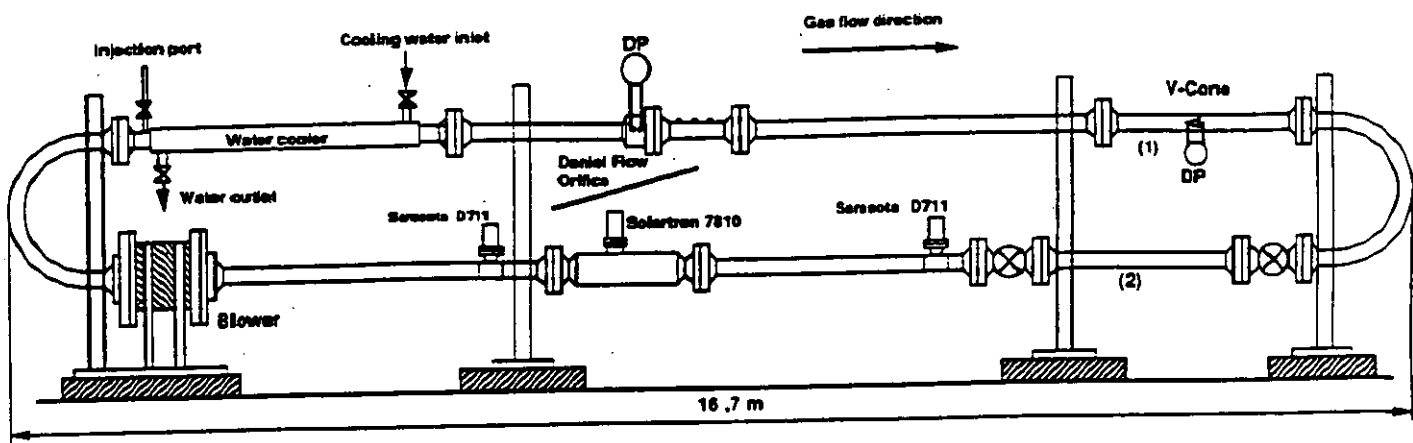


FIGURE 2 THE WET GAS TEST LOOP WITH V-CONE

differential pressure can be removed. This was confirmed by the consistency wherever averaging over more than 30 readings was performed . Possible vortex effect can therefore be removed over short time.

Before the first functional performance test , a dry nitrogen reference ratio between the V-Cone meter and the Orifice meter differential pressure at three flowrates was established at Rogaland Research ; using long straight upstream lengths upstream of the V-Cone meter (Position 1).

With the V-Cone meter remaining in the same position, high amounts of water was injected, only to show that the smoother flow profile effect that liquid causes on the Orifice meter , is not similarly imposed on the V-Cone meter. The relative reduction in differential pressure for the Orifice meter was 3.5 % at the end of the water injection.

The second functional performance test at Rogaland Research checked for the uneven profile and swirl effects , with the V-Cone meter installed immediately downstream of a U-bend (Position 2). The block valve between the U-bend and the V-Cone meter was used for further flow disturbance . With full open valve, the average offset from the ratio at highest flowrate in dry gas, was below 0.2 % for all three flowrates. No significant effect was registered up to 25 degrees valve choking. Approximate 1 % effect was seen at 30 degrees choked block valve. With the block valve close to the V-Cone meter, the pressure drop across the block valve is regaining when the gas reached the V-Cone edge. Significant pressure loss must be avoided 10 diameters upstream of the V-Cone meter. Uneven profile and swirl effect was not detected, in line with the findings presented by Ketema at the 1992 NSF MW .

The functional performance test data from Rogalands Research, supported by the long term comparison data from Phillips Petroleum New Mexico, strongly indicate that the V-Cone meter can be better than Orifice meter, providing that the flow coefficient is determined thru third party calibration with pure gas. In particular the V-Cone meter will be superior in wet gas service.

4 Dimensional certification procedure developed by Con-Tech

Installed inside the meter, the practical limitation for the determination of the V-Cone diameter at the outer edge was found to be +/- 0.04 mm, which is negligible for larger meters. For the 3 inch meter this amounts to +/- 0.2 % of the minimum flowing area. However, using the certified dimensions in the calibration for determination of the discharge coefficient, any error in the dimensional certification is almost eliminated. The dimensional certification is therefore intended mainly for identification of mechanical changes. A typical certificate is shown in Attachment A.

5 Initial testing with high differential pressure at K-Lab and certification of the coefficient of discharge by NMI

The initial testing at 20 BarG of the two V-Cone meters for Embla, carried out at K-Lab, showed some very surprising results. With a modified ISO 5167-1 based equation, using the Venturi meter expansibility factor, as advised by the manufacturer McCrometer, the discharge coefficient found at 20 BarG pressure showed a continual rising value as a function of Reynolds-number. From 1 to 6 million Reynoldsnumber, the coefficient of discharge increased by more than 5 %. It should be noted that the differential pressure at 6 million Reynoldsnumber was approximate 3 bar.

Since this discharge coefficient characteristic seen, was not in line with the earlier findings for a V-Cone meter tested at 55 BarG pressure; the V-Cone meters for Embla were reverified at 85 BarG pressure. Now the continuous rising discharge coefficient with rising Reynolds number at the 20 BarG tests was proven to be wrong. In the 85 BarG tests where similar Reynolds numbers were achieved with much lower differential pressure ratio, the discharge coefficient characteristic was almost flat. As the coefficient of discharge for one particular meter is mainly a function of Reynolds number, it was decided to run new independent tests at NMI in Bergum for the two V-Cone meters for Embla. Calibration at 50 BarG confirmed the almost flat

discharge coefficient characteristic. At the 20 BarG reverification, the high differential pressure ratio was not allowed. However, in the range tested, the 20 BarG results from NMI matched the 50 BarG flat characteristic as well as the K-Lab results at 20 BarG. At the lower differential pressures the NMI results showed high coefficient of discharge, indicating offsets in the differential pressure reading.

When information was received from McCrometer that the phenomenon with different findings for the coefficient of discharge characteristic, at different pressures, had been observed in a number of earlier cases, it was evident to us that the Venturi equation used for expansibility is not valid for V-Cone meters.

To determine a more correct expansibility factor, the correct coefficient of discharge must be found as a function of Reynolds numbers. For the two V-Cone meters for Embla, data points were selected from 20 BarG data at NMI and K-Lab, 50 BarG data from NMI, and 85 BarG data from K-Lab, where the expansibility factor was still close to 1 and also where differential pressure offset errors would not add significant additional uncertainty.

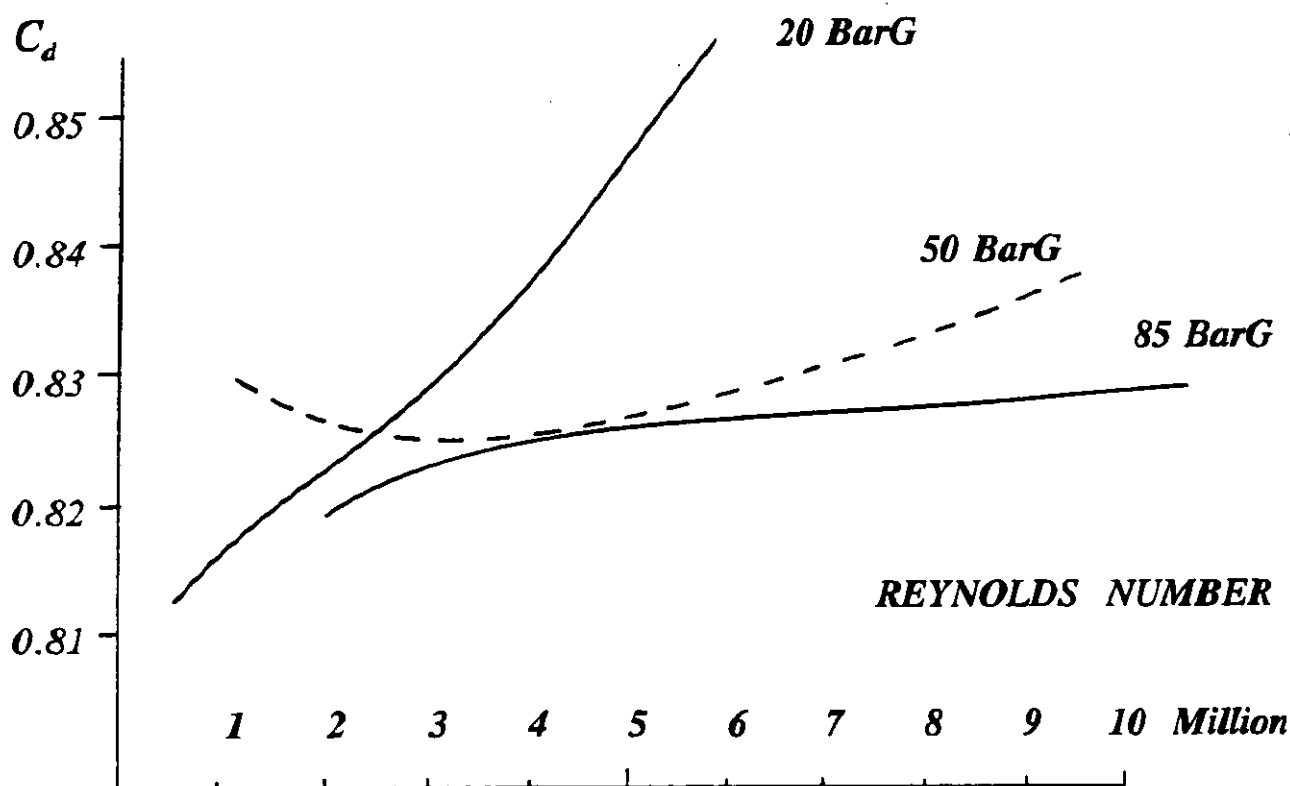


FIGURE 3 TYPICAL FINDINGS FOR DISCHARGE COEFFICIENT , USING VENTURI METER EXPANSIBILITY FACTOR

Using the function found for the coefficient of discharge based on the selected data, the expansibility factor required to give correct flowrate was plotted for the remaining points with high differential pressure to pressure ratio. The resulting expansibility factor characteristic found, was crystal clear: The expansibility factor for the V-Cone meters was linear with differential pressure to pressure ratio divided by heat ratio. Furthermore the expansibility for the V-Cone meter was found to be almost mid between that for the Venturi meter and the Orifice meter per ISO 5167-1.

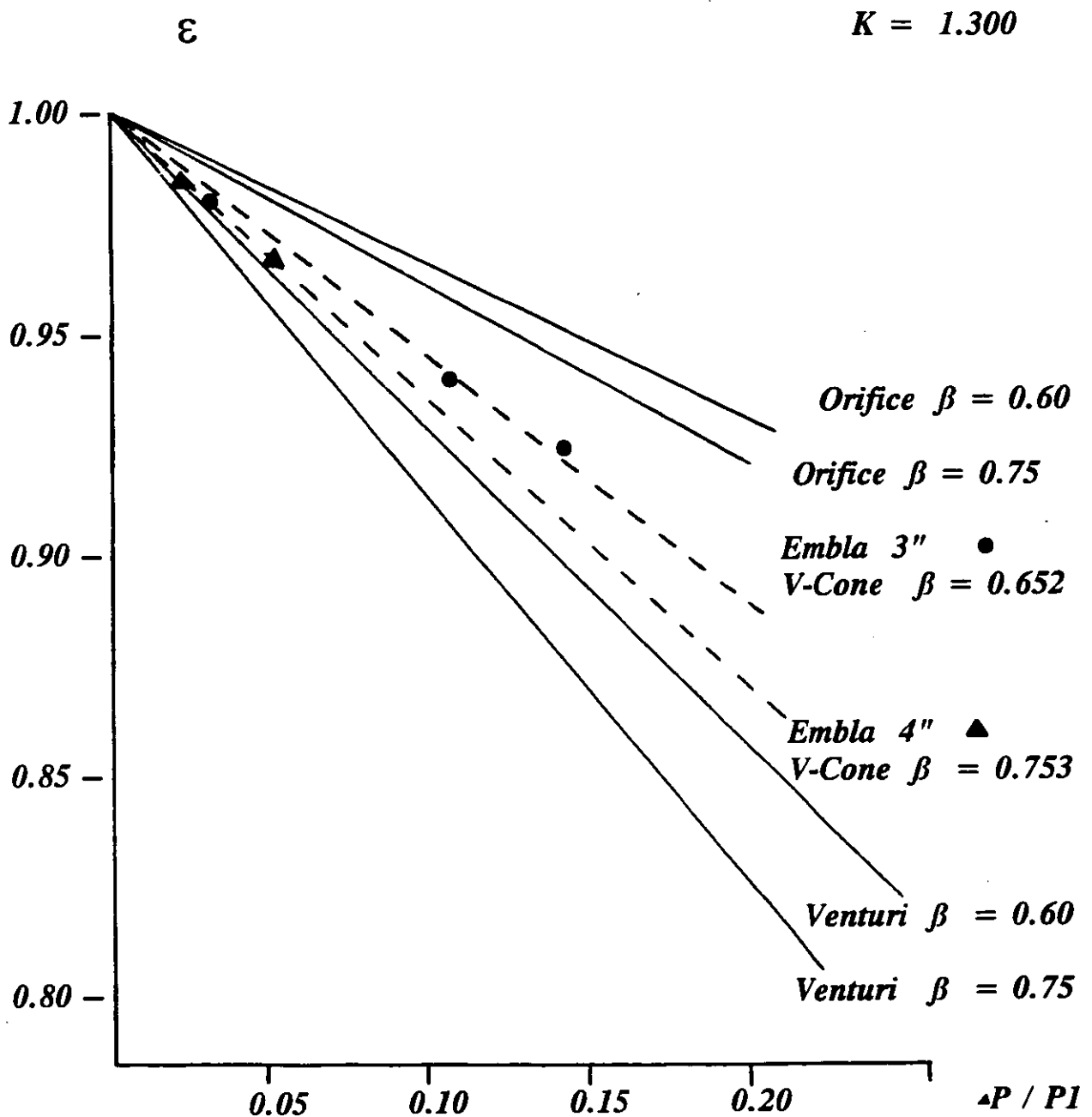


FIGURE 4 EXPANSIBILITY FACTOR PLOT FOR THE V-CONE

Based on the expansibility factor plot for the two V-Cone meters for Embla an equation for the expansibility factor was developed:

$$\epsilon = 1 - (C_{\epsilon 1} + C_{\epsilon 2} * \beta^4) * X / 1300$$

$$X = (1.3 * \Delta P) / (K * P1)$$

This equation has a similar form to the expansibility factor used for the Orifice meter. However, X is made as an universal variable which will make it easier to compare data from different test facilities. The best fit for $C_{\epsilon 1}$ and $C_{\epsilon 2}$ is ; $C_{\epsilon 1}$ equals 0.60 and $C_{\epsilon 2}$ equals 0.75 . This is also confirmed with two different V-Cone meters. However, these other V-Cone meters did not have quite as high differential pressure to pressure ratio.

The V-Cone flow calculations, based on ISO 5167-1, and the V-Cone meter expansibility factor equation developed, as shown in Attachment B, has been used for all further determination of the coefficient of discharge. The plot of the coefficient of discharge determined from K-Lab and NMI data for the two V-Cone meters for Embla now showed more consistent results.

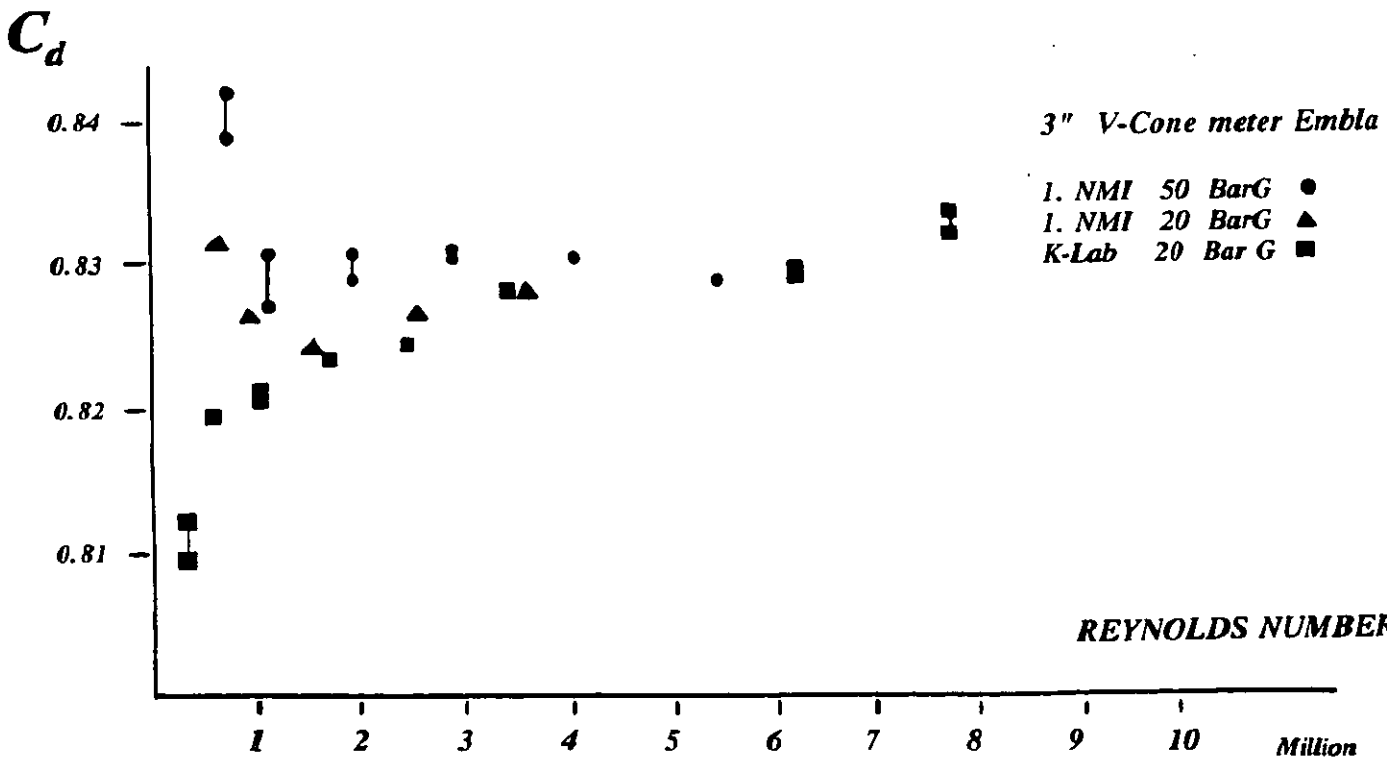


FIGURE 5 DISCHARGE COEFFICIENT FOR 3 " V-CONE METER

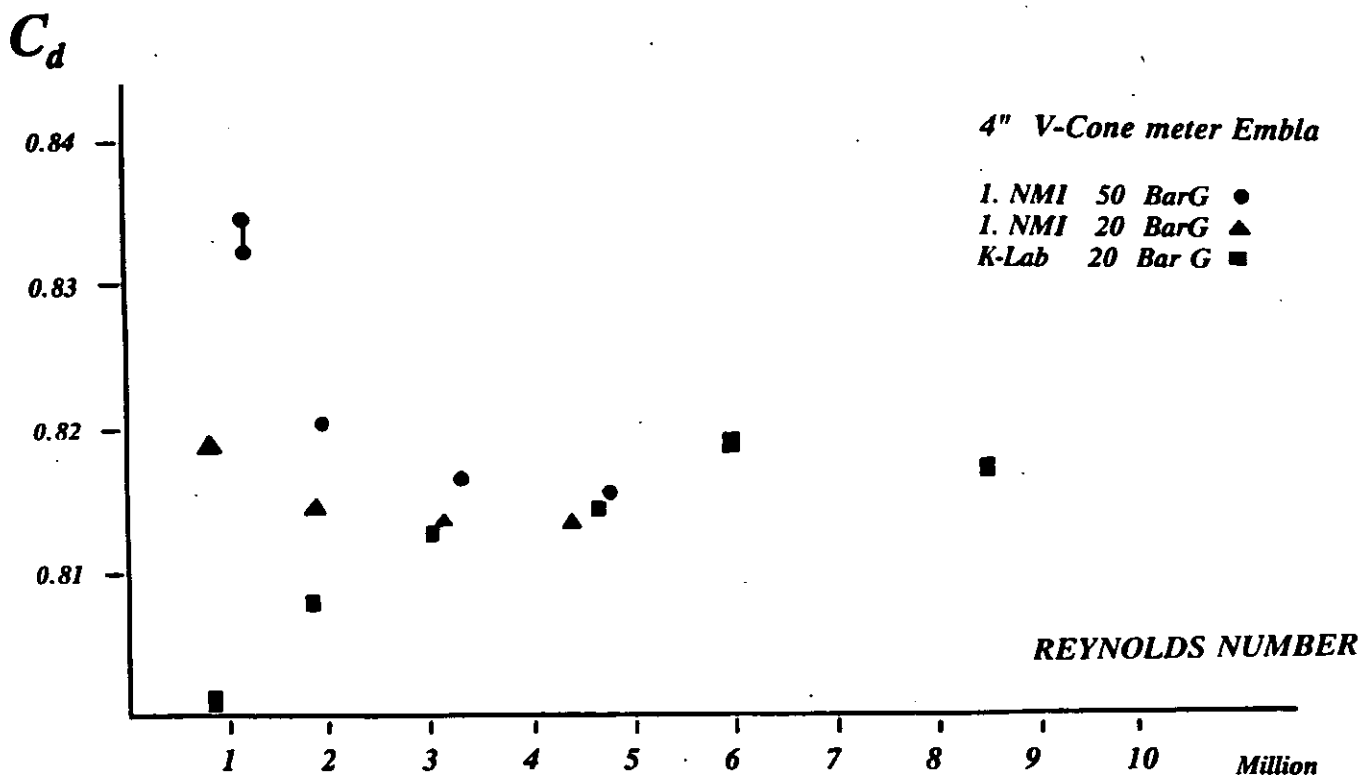


FIGURE 6 DISCHARGE COEFFICIENT FOR 4" V-CONE METER

6 Experience from Embla operation

The 3 inch and 4 inch V-Cone meters were designed to cover approximate 30 % and 70 % respectively, installed in parallel. This increase in rangeability that this gave, helped to cover the different well flowrates, thus avoiding changeout of V-Cone meter to match. Smart transmitters were used with direct digital communication for optimum rangeability accuracy.

Turning on new wells for testing at Embla crashed the turbine meters in the first phase, before strict procedure for pressure equalisation between the test separator and the export line was established. The V-Cone meters stood thru this period without any damages. Our earlier experience is that in these situations, the Orifice plates would be buckled and relocated to some downstream restricting passage position.

No damages; wear, burrs or scratches have been found in the visual inspections carried out for either of the two meters during the almost eighteen months of operation.

7 Recertification after each six months of operation

The dimensional recertification after six and twelve months of operation showed identical results to the original certification, within the dimensional determination tolerance. There was no clear trend indicating increasing or decreasing dimensions.

The recertification of the discharge coefficient was carried out by NMI immediately after the six and twelve months dimensional recertification. The coefficient of discharge curvefit with Reynoldsnumber are within a band of +/- 0.5 % for all calibrations and tests at different pressures for each V-Cone meter, with the exception of where differential pressure uncertainty contribution take the data points outside this band for lower differential pressures. It became apparent that data points below 20 milliBar reading require a very strict procedure to be of any value in the calibration for the coefficient at discharge. In the recertification after twelve months, NMI adjusted their procedure ; at each flowrate datapoint the differential pressure static pressure zero offset was recorded and corrected for. Phillips brought in a special calibrated smart transmitter with digital readout, and confirmed the official corrected differential pressure used by NMI. The low differential pressure data points were , almost without exception , inside the +/- 0.5 % band for the discharge coefficient. The comparison between all tests and calibration points for the 3" and 4" V-Cone meters at Embla is shown in Attachment C and Attachment D respectively.

8 Recommendation for further work to standardize V-Cone meter

Presently the equation for expansibility is based on data from a limited number of V-Cone meters. Before using the equation developed for traceable calibration , it must be confirmed for each individual V-Cone meter: Verify that the discharge coefficient determined at low static pressure and high differential pressure to pressure ratio, is within tolerance from the discharge coefficient determined at the same Reynoldsnumber with high static pressure and low differential pressure to pressure ratio. An international data bank with this type of data is required to give the best fit C_{e1} and C_{e2} factors in the expansibility equation.

No direct comparison of different pipewall roughness effect is performed. Further work is needed in this area. Untill this is done, the pipe wall should be smooth in the minimum flowing area passage by the V-Cone outer edge.

High accuracy calibration and research data is only available in a limited β -ratio range from 0.65 to 0.75 , and in a limited size range. For β -ratio required outside this range, the V-Cone meter performance should be reaffirmed. Obviously, with millimeter distance between V-Cone and pipe-wall, the V-Cone meter tolerance to wet gas effects will be low.

9 Conclusions

V-Cone meters selected with proper distance between V-Cone and pipewall and with V-Cone large enough to suppress the bluff body effects from the V-Cone holder, for a verified Reynoldsnumber range, and inside a verified β -ratio range, the V-Cone meter can be better than Orifice meter for gas service, providing that the flow coefficient is determined thru third party calibration with gas. In particular the V-Cone meter will be superior in wet gas service and in service with high kickoff flowrates.

10 References

- * Pipe elbow effects on the V-Cone flowmeter
North Sea Flow Measurement Workshop , Peebles 1992
S A Ifft and E D Mikkelsen , Ketema Inc*
- * V-Cone video
McCrometer*
- * Erfaringer med V-Cone måler
Akkreditering, Flerfasemåling og Forenklet måling i Olje og Gass-
industrien , Stavanger 1994
M J Dahlstrøm , Phillips Petroleum*

Acknowledgement

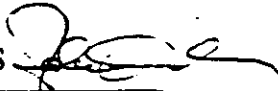
K-Lab; their stamina in verification of the V-Cone meter characteristics made it possible to develop methods for accurate calibration of the V-Cone meter without recreating the identical operating conditions.

MEASUREMENT OF "V-CONE"

METER MODEL : "V-CONE", Size 3"

METER SERIAL NO : 92012003

CLIENT : Phillips Petroleum Co.N.

MEASURED BY : John Eide, Con-Tech a/s 

MEASURED DATE : June 15, 1994.

- A and B = Diameter at weld
- C = Diameter upstream of cone
- D = Diameter downstream of cone
- E = Diameter of cone

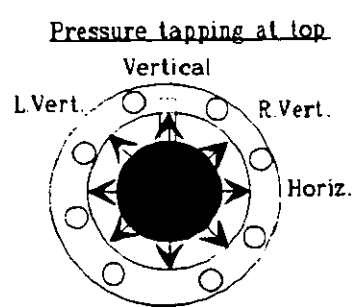
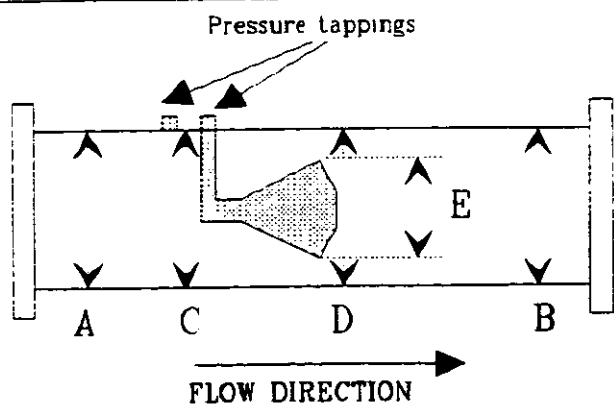
Measurements done at 20,0 deg.C

Radius cone edge = 0,200 mm

| Readings | Pos A | Pos B | Pos C | Pos D | Pos E |
|-----------|----------|----------|----------|----------|---------|
| Vertical | 77,320 | 77,300 | 78,136 | 78,635 | 59,55 |
| L.Vert. | 77,180 | 77,400 | 78,433 | 78,566 | 59,49 |
| R.Vert. | 77,400 | 77,590 | 78,471 | 78,510 | 59,60 |
| Horiz. | 77,200 | 77,290 | 78,705 | 78,423 | 59,53 |
| Avg.diam. | 77,275mm | 77,395mm | 78,436mm | 78,534mm | 59,54mm |

Measurement uncertainty: Position A - D = +/- 0,002 mm & Position E = +/- 0,04 mm

Measurements refers to gauge blocks traceable to national standards



V-Cone Flow Calculations, Based On ISO 5167-1

$$D_R = D_{R,CAL} (1 + E_{xR} (T_L - 20))$$

$$d_C = d_{C,CAL} (1 + E_{xC} (T_L - 20))$$

$D_{R,CAL}$ Calibrated pipe internal diameter at downstream cone tap; mm 20°C

$d_{C,CAL}$ Calibrated cone diameter at the downstream bevel start; mm , 20°C

E_{xR} Metal width dimensional expansion factor for the pipe; per °C .

E_{xC} Metal width dimensional expansion factor for the cone; per °C .

T_L Measured line temperature , °C

The discharge coefficient C_d , to be determined from calibration and curvefit for C_1 and C_2 :

$$C_d = C_1 - C_2 * (10^6 / Re)^{0.75}$$

Note that the exponent is presently fixed to 0.75 from experience in the Reynoldsnumber range 1,000,000 to 10,000,000 .

$$\beta = (D_R^2 - d_C^2)^{0.5} / D_R$$

Expansion factor:

$$\varepsilon = 1 - (C_{\varepsilon 1} + C_{\varepsilon 2} * \beta^4) * X / 1300$$

$$X = (1.3 * \Delta P) / (K * P1)$$

$$\text{Present : } C_{\varepsilon 1} = 0.60 , C_{\varepsilon 2} = 0.75$$

ΔP Differential pressure in mBar

$P1$ Upstream pressure in BarA

K Isentropic exponent

Reynolds number:

$$Re = \frac{4 * 10^6}{\pi} \frac{qm}{D_R * \mu}$$

qm Massflow in Kg/sec

μ Dynamic viscosity in CentiPoise

Massflow in Kg/sec :

$$qm = C_{ONST} * C_d * (1 - \beta^4)^{0.5} * \epsilon * (D_R^2 - d_c^2) * (\Delta P * \rho)^{0.5}$$

$$C_{ONST} = 10^{-5} * (\pi/4) * \sqrt{2} = 1.110720734 * 10^{-5}$$

ρ Density in Kg/m³.

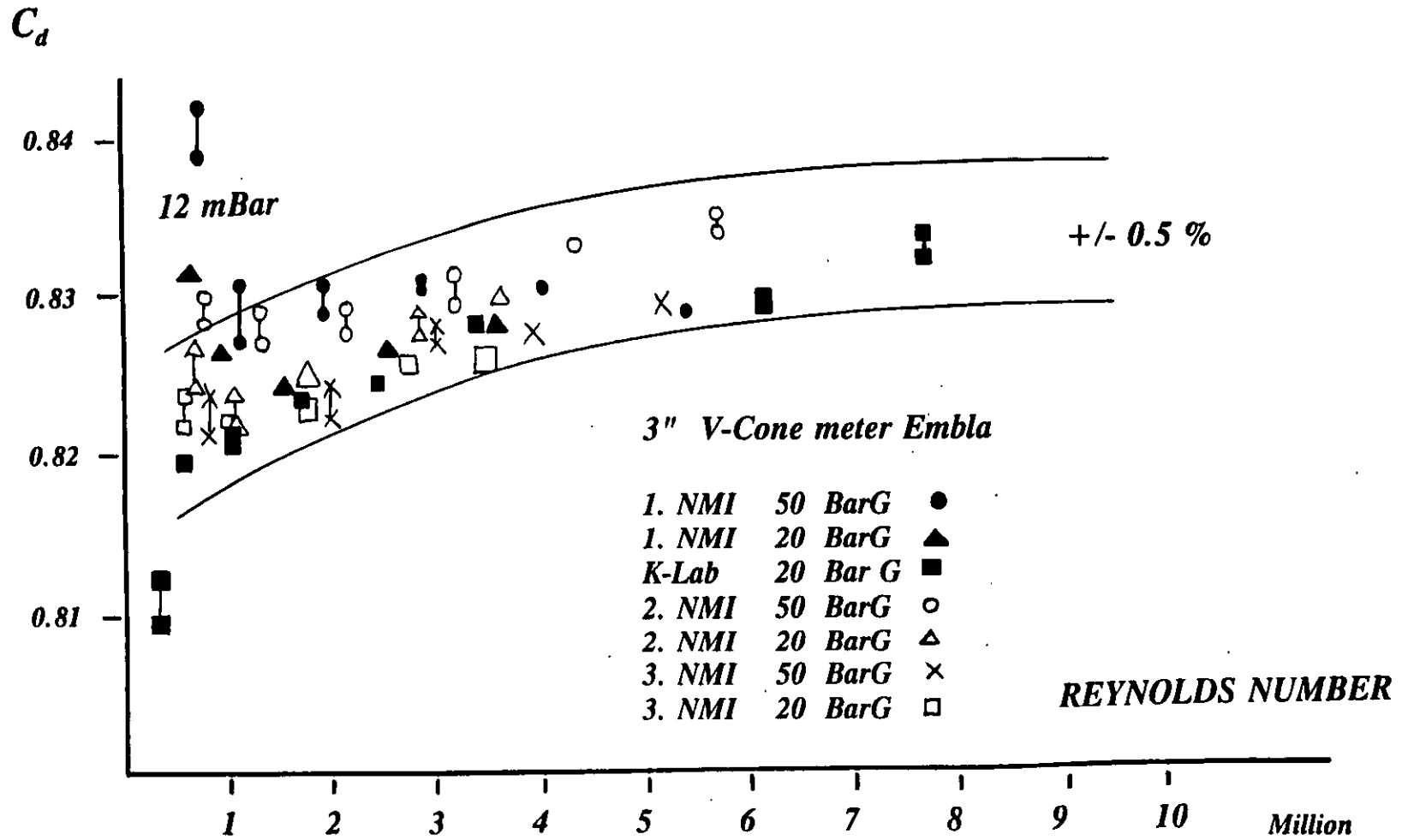
LEAST SQUARE CURVEFIT FOR C_d CONSTANTS C_1 & C_2

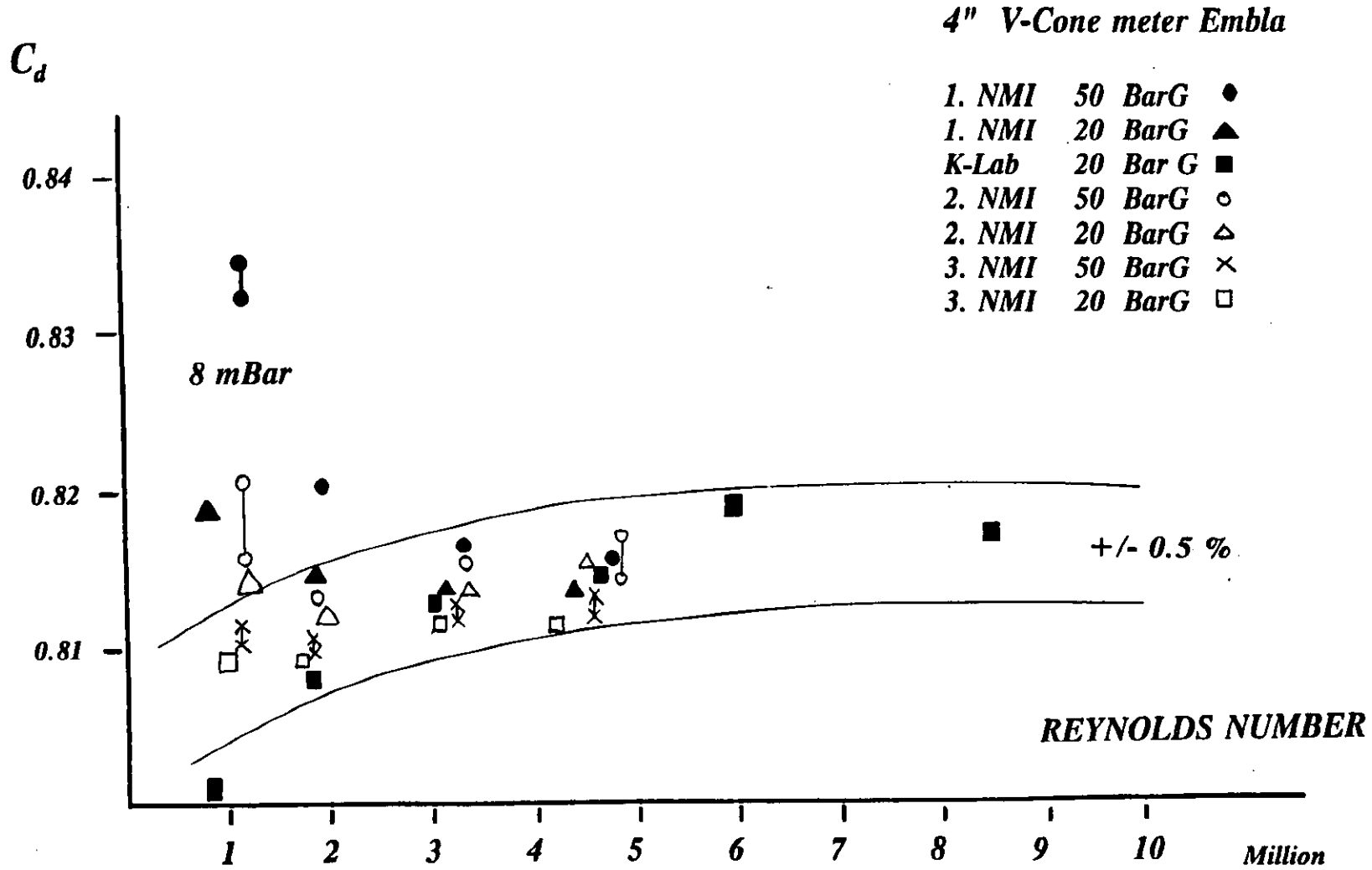
For points where ΔP accuracy is better than 0.3 % (Recommended above 20 mBar , except where sufficient accuracy can be verified; as for Smart Transmitters with direct digital reading where 10 mBar is realistic).

$$C_1 \sum (1) - C_2 \sum \frac{10^6}{Re}^{0.75} = \sum (C_d)$$

$$C_1 \sum \frac{10^6}{Re}^{0.75} - C_2 \sum \frac{10^6}{Re}^{1.5} = \sum (C_d * \frac{10^6}{Re}^{0.75})$$

*However if C_2 is found to be < 0 ; then $C_2 = 0$, and $C_1 = 1/n \sum (C_d)$
 C_d is the average C_d in one Reynoldsnumber calibration point.*





INSTALLATION EFFECTS ON MULTI-PATH ULTRASONIC FLOW METERS: THE 'ULTRAFLOW' PROJECT

K. van Bloemendaal and P.M.A. van der Kam

N.V. Nederlandse Gasunie, Groningen, the Netherlands.

SUMMARY

'ULTRAFLOW' was a Joint Industry Project aimed at establishing the effect of installation conditions on multi-path ultrasonic flow meters. An extensive test series was performed at 5 test facilities on 6" and 12" meters operating on natural gas at pressures from 10 to 60 bar. All test facilities and procedures are reviewed by an independent international Quality Assessment Team, comprising experts from legal metrological authorities, to ensure that the work was appropriate to support International Standards activity.

This paper is a condensed version of the projects final report describing the project and test results. The tests in ideal flow conditions pay attention to meter stability and effects of signal averaging and pressure. From the error shifts in the tests with upstream disturbances (1 or 2 bends, step changes in pipe diameter and pressure reduction) values for uncertainties due to the presence of these disturbances are proposed.

NOTATION

| | | |
|------------------|---|--------|
| A, B | After, Before disturbance tests | |
| AV, NA | With, Without signal averaging applied | |
| CW, ACW | Clockwise, Anti-clockwise swirl | |
| CH, CV | Chords Horizontal, Chords Vertical | |
| D | Pipe diameter | [inch] |
| Di.Err.% | Shift in meter error due to a specific installation effect | [%] |
| Dm.Err.% | Deviation of an individual calibration from mean of all calibrations | [%] |
| Err.% | Meter error | [%] |
| r | Repeat test | |
| Δp | Differential Pressure | [mbar] |
| $xD(p)$ (graphs) | x represents the distance between the disturbance and meter inlet and p represents the test pressure | |
| [a] (graphs) | indicates that tests at, or beyond that flow rate were limited by meter operation. | |
| [b] (graphs) | indicates that tests were limited by the test facility capacity. | |

1 INTRODUCTION

Only recently, multi-path ultrasonic gas flow meters have been developed to a point where they may be considered to be a realistic alternative to orifice plate or turbine meters for high accuracy large volume gas flow measurement. In principle, upstream disturbances should have little effect upon a multi-path ultrasonic meter but there is little evidence available to quantify this. Such evidence is an important pre-requisite to the development of the installation standards.

The project 'ULTRAFLOW' was undertaken in order to address this problem and provide data on the effect of disturbances as upstream bends, swirl, step changes in pipe diameter and pressure reduction on a multi-path ultrasonic meter. The Joint Industry Project, involved 6 user companies (British Gas (BG), Gaz de France (GF), Ruhrgas (RG), Nederlandse Gasunie (GU), BP, NAM)

and a meter manufacturer. The project was managed by BP and received financial support from the EC.

The objective of the project was to perform a series of tests to demonstrate the effect upon the meter of upstream disturbances like asymmetries, caused by 90° and 180° bends, swirl caused by double bends out of plane, small pipe diameter step changes and upstream pressure reduction. To be able to determine these effects, calibrations in ideal flow conditions at the appropriate pressures are performed to serve as a reference. These calibrations also serve for determination of calibration stability and pressure dependency. The overall aim of the project was to identify whether the uncertainty of the multi-path ultrasonic meter reading does not exceed 1% under defined installation conditions.

The tests were carried out on meters of nominal size 6" and 12" selected as representing a range likely to be employed in practice, and also suitable for the available test facilities. Testing was performed over a range of pressures from 10 to 60 bar. The work was carried out on 5 high pressure flow testing facilities of 4 of the participants over the period March 1993 to March 1994. Table 1 shows the agreed division of work.

TABLE 1 - DIVISION OF WORK BETWEEN LABORATORIES

| | | | 20 bar | 40 bar | 60 bar | 10 bar | 35 bar | 50 bar | 60 bar |
|---|--------------------|-----|----------------|----------|----------|----------------|--------|--------|--------|
| TEST | | | 12" METER | | | 6" METER | | | |
| 1. "Ideal" calibration at start and end of measurement series | | | BG RG GF | RG GF | BG GU | GU RG GF | GU | RG | GU |
| 2. 90° bend Asymmetry | CH, CV | 5D | BG | | BG | RG | | RG | |
| 90° bend Asymmetry | CH, CV | 10D | BG | | BG | RG | | RG | |
| 180° bend Asymmetry | CH, CV | 5D | BG | | BG | RG | | RG | |
| 180° bend Asymmetry | CH, CV | 10D | BG | | BG | RG | | RG | |
| 3. Low Level Swirl | CH, CV | 5D | | | GU | GU | GU | | GU |
| Low Level Swirl | CH, CV | 10D | | | GU | GU | GU | | GU |
| High Level Swirl | CH, CV | 5D | | | GU | GU | GU | | GU |
| High Level Swirl | CH, CV | 10D | | | GU | GU | GU | | GU |
| 4. Diameter Step | increase, decrease | 0D | GF | GF | | GU | GU | | |
| Diameter Step | increase, decrease | 5D | GF | GF | | GU | GU | | |
| 5. Pressure Reduction | 3 Δp's | 5D | GF | | | GF | | | |
| Pressure Reduction | 3 Δp's | 10D | GF | | | GF | | | |

A Quality Assessment Team (QAT) was set up independently of the participants in the project. The team comprised experts from PTB (Germany), NMi (the Netherlands), Ministère de l'Industrie (France) and DTI (UK) together with a representative of the ULTRAFLOW-participants. This group critically examined the installation, traceability, instrumentation, data acquisition and data acceptance criteria of each test facility, to ensure the quality of the work. The QAT reviewed each of the test facilities involved and came to the conclusion that data derived from the testing are of adequate quality for reference data to support meter standards work.

2 DESCRIPTION OF THE METERS TESTED

The meters tested were of 6" and 12" nominal size. Maximum flow capacity was 1400 [m³/h] for the 6" meter and 5500 [m³/h] for the 12" meter (maximum mean gas velocity of 21 [m/s]). The meters comprise a spool piece housing the ultrasonic transducers which measure the gas velocity across four paths or chords arranged crosswise. Each chord has two transducers which serve alternately as transmitter and receiver to measure the transit time with and against the direction of gas flow. This permits determination of the mean gas velocity across the chord. For determination of the flow rate, the Westinghouse integration method is used.

3 PIPEWORK CONFIGURATIONS FOR TESTS

Each facility undertook tests on the meters operating in "ideal" conditions with a substantial length of straight pipework upstream and at varying pressures where appropriate. These tests were performed prior to the disturbance tests, and in most cases repeated at the conclusion of the series of disturbance tests. The following sections describe the configurations for the disturbance tests. Normally the parallel planes through the chords are oriented horizontally. In some tests, the chords have been oriented both horizontally (CH) and vertically (CV). To achieve uniform definitions, the definitions of CH and CV in this paper are related to the direction of the final bend before the meter. Note that in the case of the swirl testing the final bend was vertical, so that CH means that the chords are actually vertical, related to the earth.

3.1 Disturbances due to 90° and 180° Bends (Asymmetry)

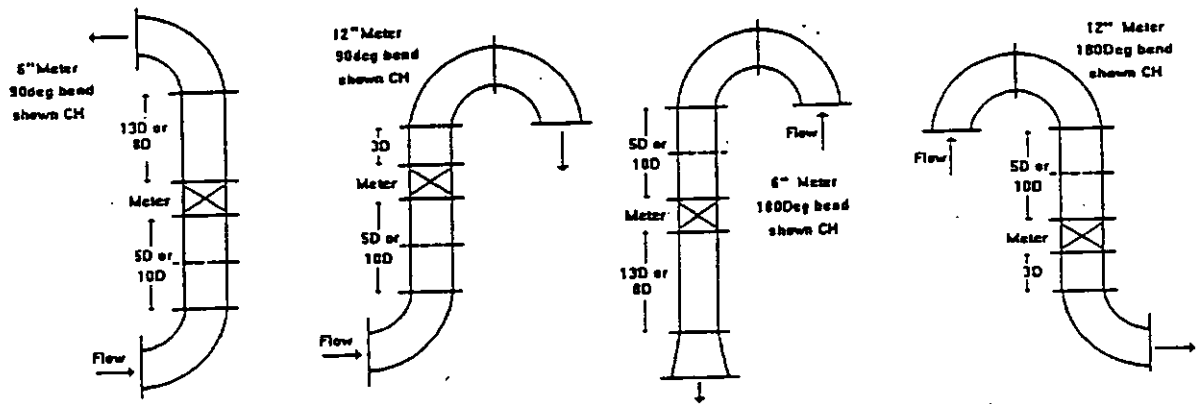


Figure 1 - 90° and 180° Bend Test Configurations

Both CH and CV tests were carried out with the meter situated 5D and 10D downstream of 90° and 180° bends. Figure 1 shows plan views of the meter installations used.

3.2 Disturbances due to Bends in Two Planes (Swirl)

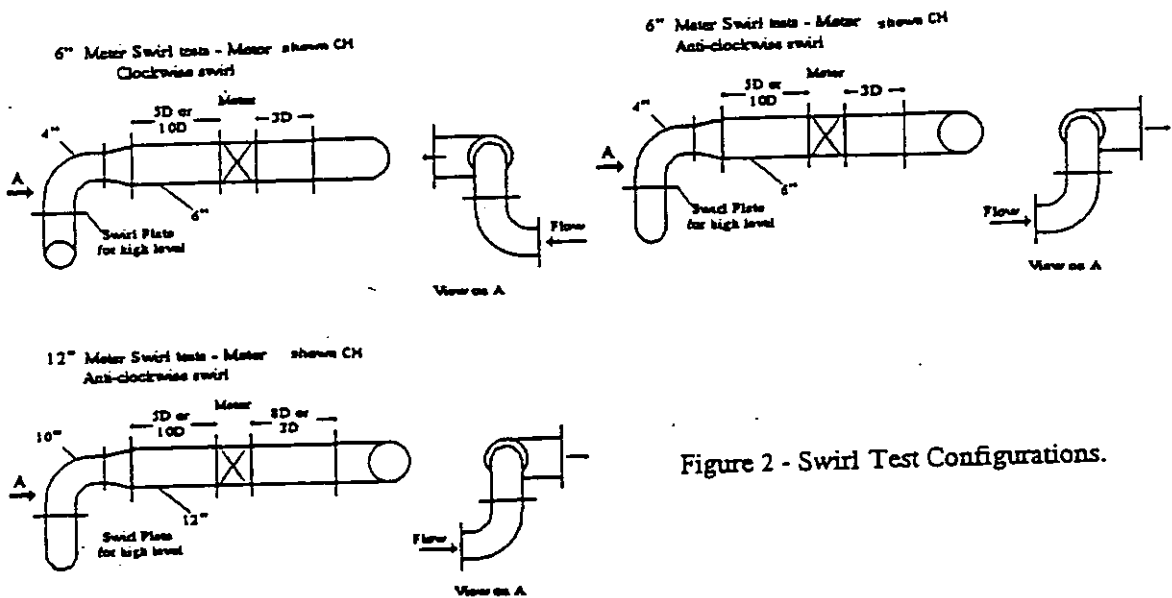


Figure 2 - Swirl Test Configurations.

Figure 2 shows side- and end-elevation views of the meter installations used for swirl tests, based on ISO 9951. Both CH and CV tests were carried out with the meter situated 5D and 10D downstream of pipework configured to induce swirl either CW or ACW (clockwise or anti-clockwise). Two levels of swirl were generated. "Low level swirl" was produced by two 90° bends mounted

with their planes perpendicular to each other. From earlier work with this configuration, swirl angles may be estimated to be about 20. "High level swirl" was produced by addition of a half area plate between the bends causing estimated swirl angles of about 30°-40°.

3.3 Disturbances due to Steps in Pipe Diameter

5 mm Diameter step changes are assumed to be typical for tolerances in pipe wall thickness and the tests were conducted with the steps at 0D and 5D from the meter (see figure 3).

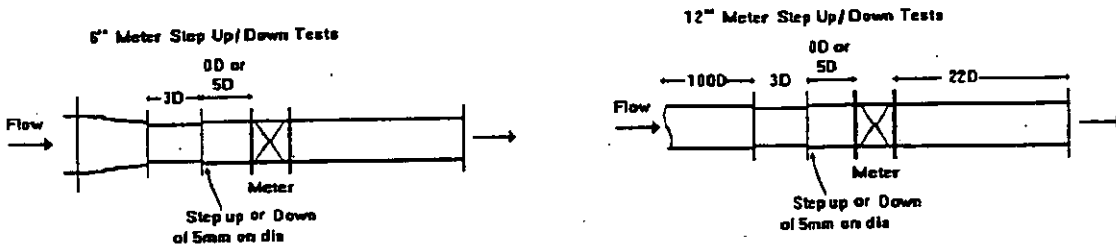


Figure 3 - Step Up and Step Down Test Configurations

3.4 Disturbances due to Pressure Reduction Valves

The pressure reducing valve used was of a type known from previous experience to generate a combination of high level acoustic noise, profile asymmetry and swirl. The valve was placed 5D and 10D upstream of the meter. The same 4" pressure reducing valve was used with both 6" and 12" meters. Figure 4 shows a plan view of the meter installation used.

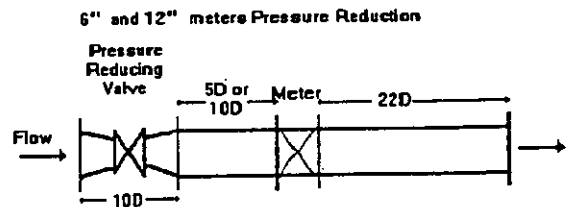


Figure 4 - Pressure Reduction Test Configuration

4 TEST RESULTS - METER OPERATING IN IDEAL FLOW CONDITIONS

Each laboratory conducted at least one but usually two ideal calibrations at each pressure to serve as a baseline for the disturbance tests. This way, a large number of ideal calibrations was obtained during a period of 12 months. It was not the aim of this project to look critically at the shape of the calibration curve associated with the particular meter under test. Therefore, in figure 5, the results are shown in terms of deviations from the mean of all ideal calibration curves (Dm.Err.%) against flow rate, expressed as percentage of maximum. The value of Dm.Err.% was determined at each flow rate from $Dm.Err.\% = Err.\% - Ref.Err.\%$, where Err.% is the mean of data points of an individual calibration and Ref.Err.% is the mean of data points of all calibrations.

The overall spread of results between sites is within about $\pm 0.5\%$ over a 5:1 turndown ratio and 0.6% over a 10:1 turndown ratio. This spread includes effects of pressure (10 to 60 bar), transport between sites, meter transducer removals for inspections and transport, location of temperature thermowells at 1.5D downstream of the meter, pressure tapings at the meter body or within 3D of the meter and small differences in ideal calibration installation pipework configurations. Analysis of the data showed that tests, on the same facility and at the same pressure, before and after the disturbance tests indicated no significant calibration drift. The meters were tested over a period of 12 months without any noticeable long term deterioration in calibration or performance. No pressure dependency can be concluded from the data. From this, it is concluded that if the meter is installed in well developed flow conditions free of swirl that a meter uncertainty at the 95% confidence interval of 0.6% over a 10:1 turndown independent of pressure can be given.

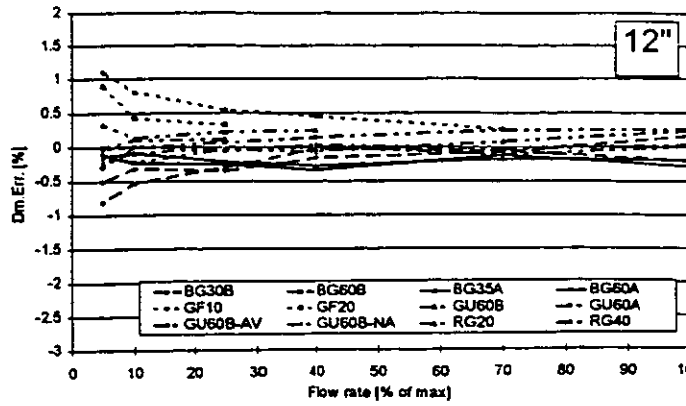
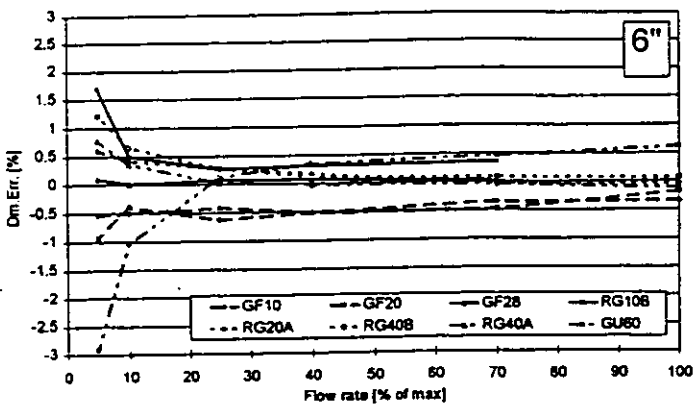


Figure 5 - Deviation of Each Individual Calibration from the Mean of Ideal Calibrations.

5 TEST RESULTS - DISTURBANCE TESTS

In this section, all results are shown in terms of error shifts (Di.Err.%) due to the disturbance. The value of Di.Err.% was determined at each flow rate from $Di.Err.\% = Err.\% - Ref.Err.\%$, where Err.% is the mean of data points of specific test and Ref.Err.% is the mean of data points of the ideal calibration at the same pressure at the same laboratory.

The ideal calibrations were performed mainly to serve as base line for disturbance tests. From an analysis of the results of these calibrations follows that any "disturbance error" Di.Err.% in excess of $\pm 0.2\%$ may be regarded as a significant effect of the disturbance. At low flows (below 10% of maximum) a Di.Err.% in excess of about 0.5% is needed before it can be attributed to the disturbance. These figures are estimates based on spread in ideal calibration curves, the known repeatability of each of the test facilities' and the repeatability specification of the meters.

It can be noted that for a particular installation producing asymmetric flow profiles the errors are repeatable and can be considered as systematic therefore if calibrations were performed they could be calibrated out. However for the purposes of this work the errors will be viewed as an additional uncertainty which can be added to the base uncertainty observed in the ideal flow situation.

5.1 Asymmetry: 90° Bend

The results of the asymmetry tests with 90° bends are shown in figure 6.

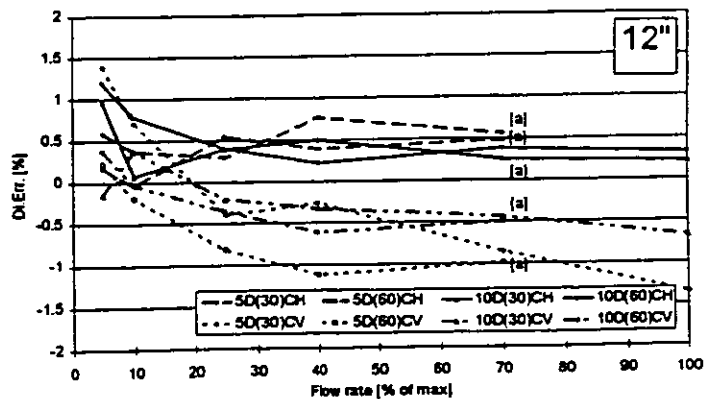
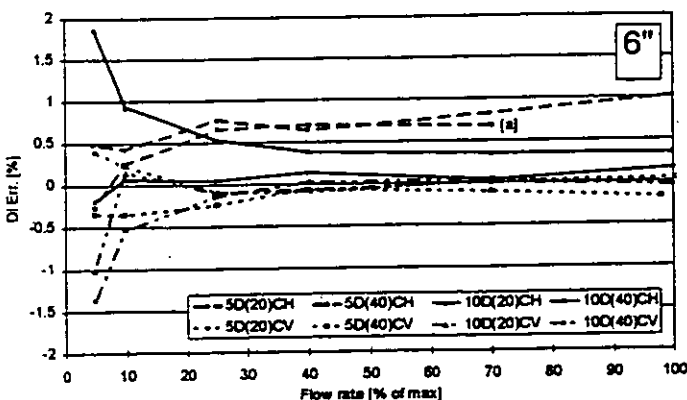


Figure 6 - Meter Downstream of a 90° Bend.

The tests show generally consistent results. There is a general reduction in error shift as the meter is moved further away from the disturbance which is indicative of the flow profile re-establishing itself. The orientation of the meter chords with respect to the plane of the bends appears to have some effect. This effect can be explained by the meter geometry employed. The plane of symme-

try of the disturbance with respect to the meter chord directions will result in different measured average linear velocities for each chord which will produce differences in the way the chord arrangement cancels over- and undermeasurement of the profile due to the disturbance.

There also appears to be some differences in magnitude of the errors associated with the meter size. In general, the 6" meter displays less sensitivity to asymmetry than the 12" does. This may be due to the relative sizes of the ultrasound beams to the meter cross sections i.e. the smaller the meter the more the chord linear average velocity represents the cross sectional area it is associated with in the flow integration process.

5.2 Asymmetry: 180° Bend

The results of the asymmetry tests with a 180° bend are shown in figure 7. The results differed substantially for the 6" and 12" meters.

In this configuration there is a general reduction in error shift as the meter is moved further away from the disturbance, which is consistent with results in the 90° bend. The orientation of the meter chords with respect to the plane of the bends appears to have some effect. For the 180° bend the 6" meter tests had the final bend in the same orientation as the 90° tests and similar results are evident. However, the 12" meter 180° bend test was in the opposite direction with the result of a tendency for the error shifts to be in the opposite direction when shifting from CH to CV. This phenomena can also be explained by the meter geometry.

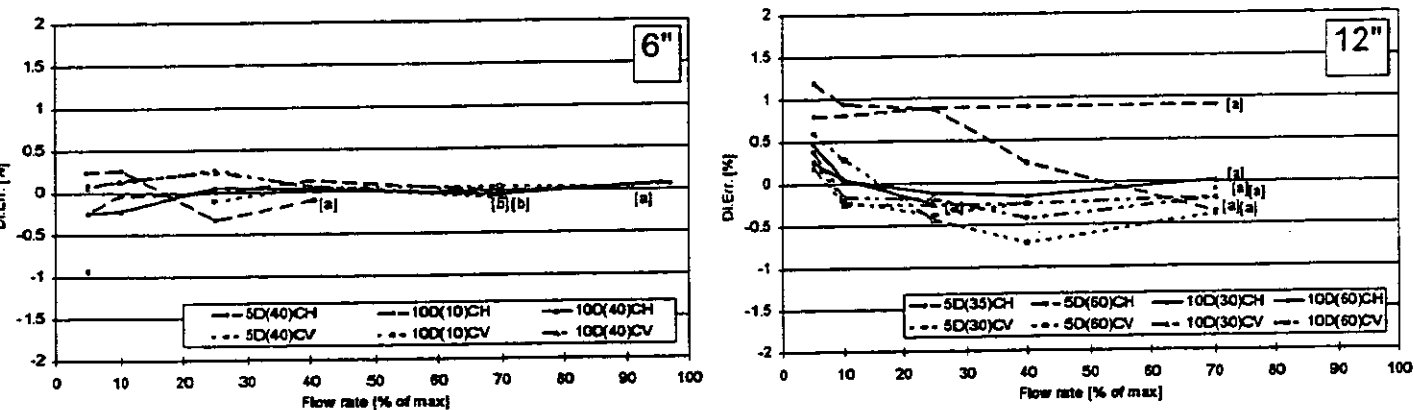


Figure 7 - Meter Downstream of a 180° Bend.

The overall error shifts due to asymmetric flow profiles are generally small regardless of meter size and orientation and with due allowance for medium term reproducibilities and day to day test site uncertainties associated with repeatabilities error shifts are generally within 1.0 % at 5D and 0.5% at 10D over a 5:1 turndown with the meter operating correctly.

5.3 Low Level Swirl Tests

The results of the meters in low level swirl are given in figures 8 (6" meter) and 9 (12" meter). The swirl appears to be rather severe. In the ISO 9951 document this low level test was intended to represent the most severe case to occur in normal pipework configurations. However, it seems it is not a realistic representation of field installation conditions.

The meter errors, especially at 5D, will be a combination of effects which confuses the issue. The flow is not only swirling, but has also asymmetry in the profile. The swirl generator is known to produce instabilities in the flow with severe turbulence, affecting the meter in both chord failures and increased fluctuations in the meter output (which necessitated repeat tests with changes made to the signal handling statistical checking). Anti-clockwise swirl results in larger error shifts than

clockwise swirl. The changes in errors between anti-clockwise and clockwise can be attributed on the meter geometry as mentioned with the asymmetry tests. The error shift generally tended to fall somewhat between the 5D and 10D tests but this was not always the case.

It is difficult to draw definite conclusions from these variable results. It is suggested that the most severe swirl from normal pipework installations may increase the uncertainty by 2.5%. No recommendations for upstream pipe lengths can reasonably be given.

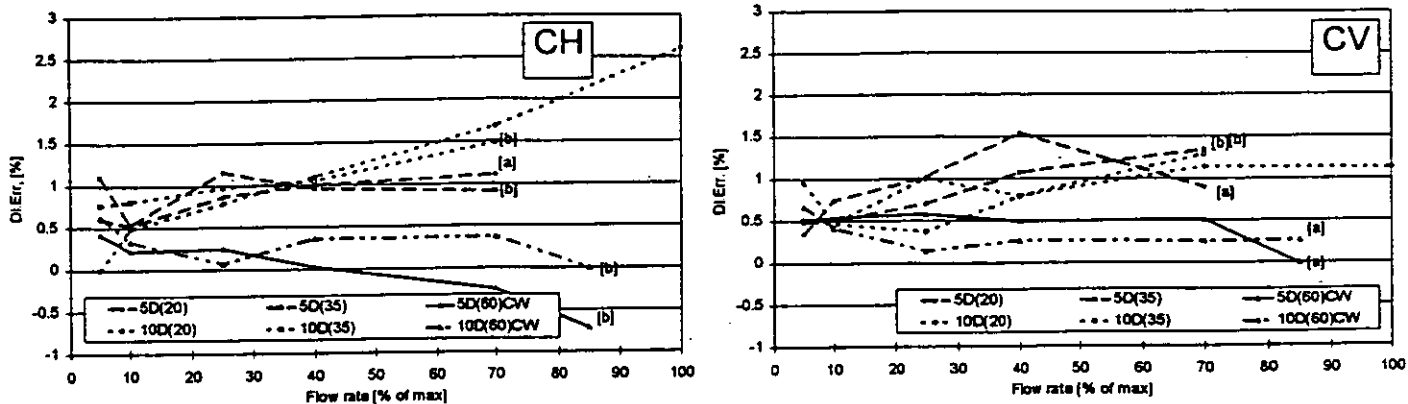


Figure 8 - 6" Meter in Low Level Swirl.

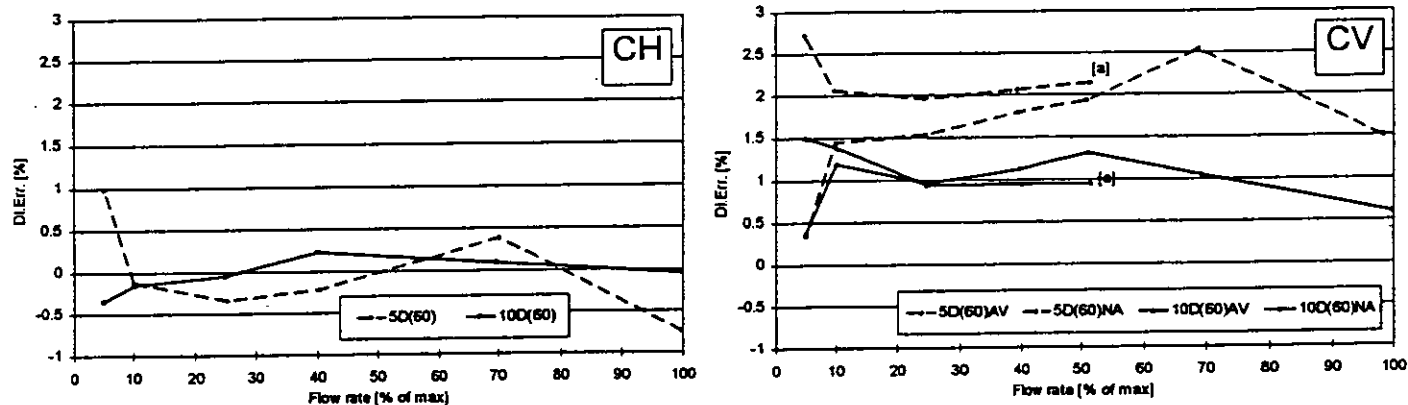


Figure 9 - 12" Meter in Low Level Swirl.

5.4 High Level Swirl Tests

The results of the tests in high level swirl are given in figures 10 (6" meter) and 11 (12" meter).

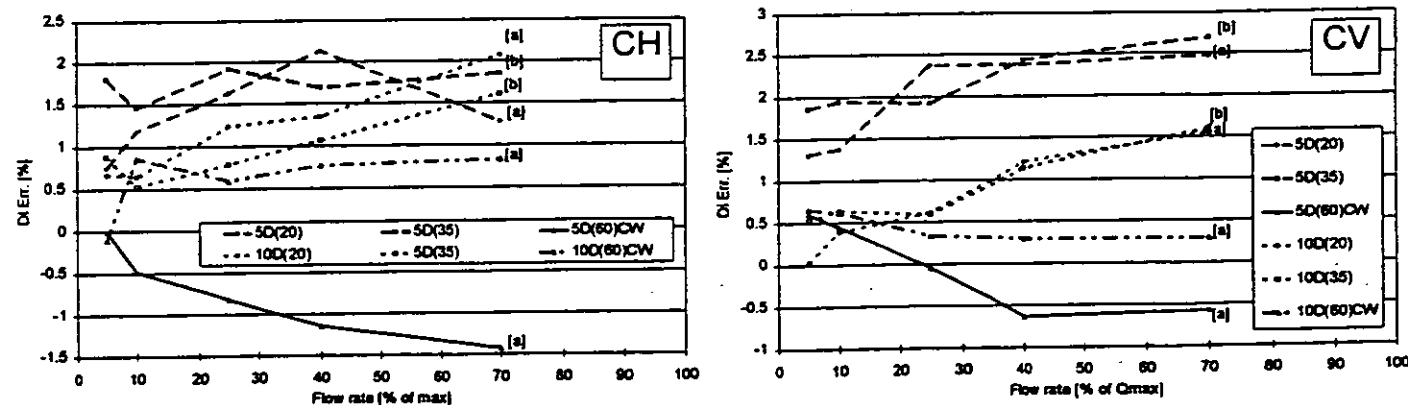


Figure 10 - 6" Meter in High Level Swirl.

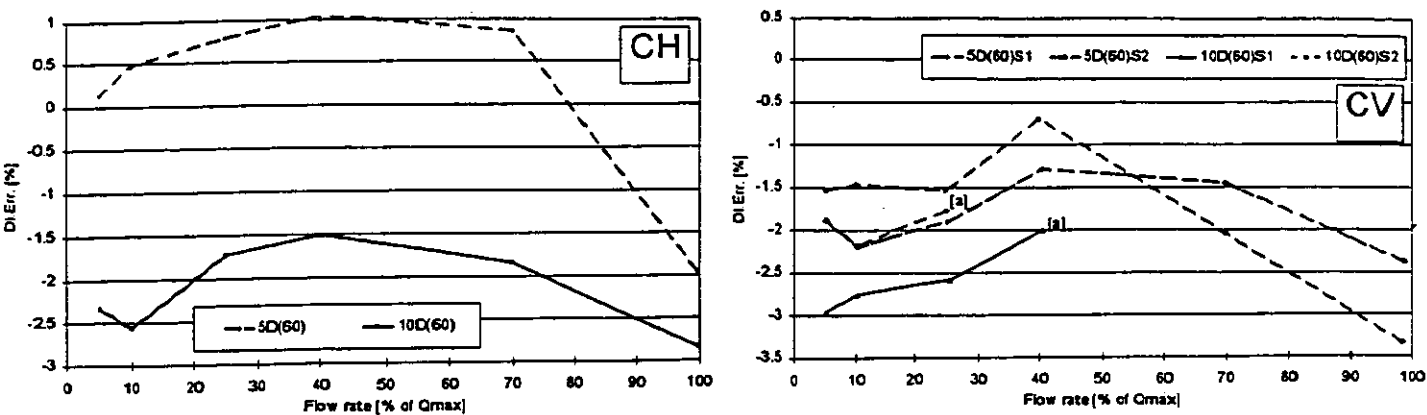


Figure 11 - 12" Meter in High Level Swirl.

For high level swirl it is even more difficult to propose an additional uncertainty than it was for low level. The half area plate not only enhances the swirl, but also very strongly the asymmetries, instabilities and turbulence. The instabilities caused severe signal handling problems. The high level swirl test results differed considerably between the 6" and 12" meters. The error shifts were both positive and negative and in the range $\pm 3\%$. The error shift tended to fall between the 5D and 10D tests but this was not always the case, and there is a definite switch between CV and CH error directions. Since intention of the ISO test for high level swirl was to represent a pressure regulator these results should be compared with those for the pressure reducer. If this is done it is seen that in general terms the results are similar.

5.5 Diameter Step Up and Down

The results of these tests are given in figure 12 for both the 6" and 12" meters. For a step up or step down of 5mm in pipe diameter at the meter inlet, or at 5D upstream no additional uncertainty is added. Over 10:1 turndown all test results were within the area of medium term reproducibility and no significant error shifts could be measured.

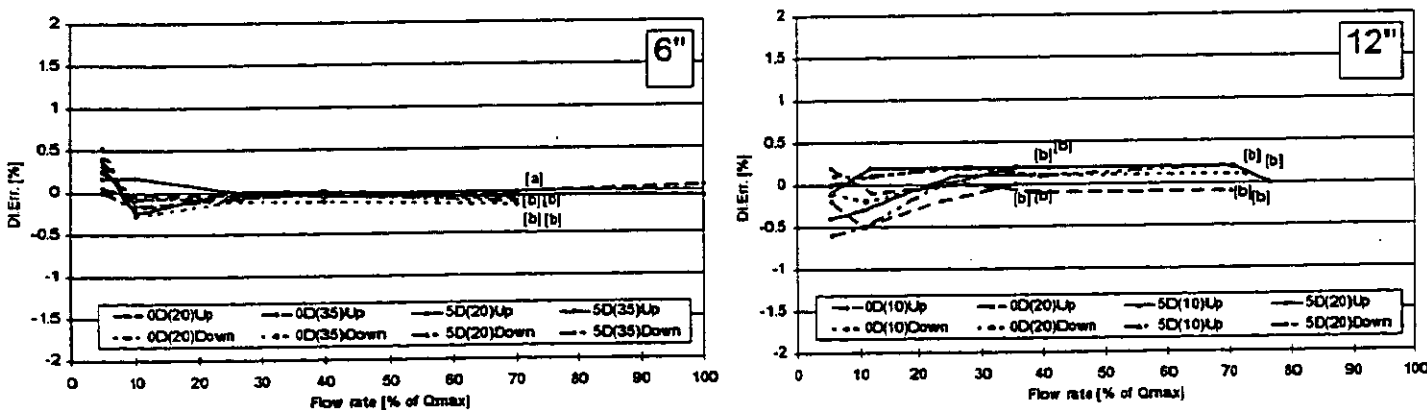


Figure 12 - Meter with Step Up or Down.

5.6 Pressure Reduction Tests

The results of the meters placed downstream of a 4" pressure reducer are given in figure 13. The pressure reducer subjects the meter to swirl, asymmetry and ultrasonic noise. The pressure reducer tests were curtailed because the meters would not operate correctly with a pressure reduction in excess of 2 bar. Only low level pressure reduction tests at 900 mbar could be completed and even then special filtering techniques were needed for the meter to handle the signal.

The 6" meter was much more seriously effected than the 12" meter, which may well have been due to the fact that the same size pressure reducing valve was used. At present it must be suggested that the meters should not be installed in close proximity to any substantial pressure reduction. If this is essential then for a limited pressure reduction an additional uncertainty of perhaps 2% is introduced.

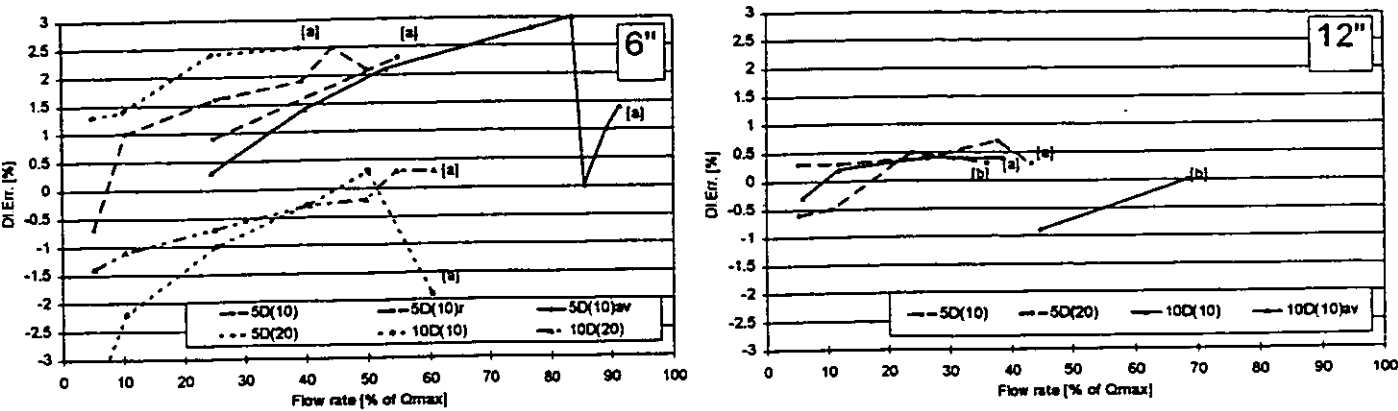


Figure 13 - Meter with 900 mbar Pressure Reduction.

5.7 Meter Signal Handling Techniques

In many of the disturbance tests results could not be obtained at high flow due to excessive chord fails on the meters. These can be alleviated, however, by appropriate setting of the meter averaging or statistical acceptance limits, at the expense of longer up-date times or larger variations in output. The results indicate that these do not influence the "ideal" calibration of the meter, although perhaps this does need to be more convincingly demonstrated in the highly disturbed flows, such as swirl or pressure reduction.

6 PROPOSAL OF ADDITIONAL UNCERTAINTIES DUE TO DISTURBANCES

The additional uncertainties proposed in the previous chapter are summarized in table 2. All figures are given in percentages. Overall figures represent uncertainties required if meter orientation is not defined as part of the installation requirement.

TABLE 2 -
SUMMARY OF PROPOSED ADDITIONAL UNCERTAINTIES DUE TO DISTURBANCES

| | 90° Bend | | 180° Bend | | LL Swirl | | HL Swirl | | Diam. Step | | Press.Red. | |
|---------|----------|-----|-----------|-----|----------|-----|----------|-----|------------|-----|------------|-----|
| | 5D | 10D | 5D | 10D | 5D | 10D | 5D | 10D | 0D | 5D | 5D | 10D |
| 6" CH | 1.0 | 0.5 | 1.0 | 0.5 | 1.0 | 2.5 | 2.0 | 2.0 | 0.0 | 0.0 | 3.0 | 2.0 |
| 6" CV | 0.5 | 0.5 | 0.5 | 0.5 | 1.5 | 1.5 | 2.5 | 1.5 | NT | NT | NT | NT |
| 12" CH | 1.0 | 0.5 | 1.0 | 0.5 | 1.0 | 0.5 | 2.0 | 2.5 | 0.0 | 0.0 | 0.5 | 1.0 |
| 12" CV | 1.5 | 0.5 | 1.0 | 0.5 | 2.5 | 1.5 | 3.5 | 3.0 | NT | NT | NT | NT |
| Overall | 1.5 | 0.5 | 1.0 | 0.5 | 2.5 | 2.5 | 3.5 | 3.0 | 0.0 | 0.0 | 3.0 | 2.0 |

7 CONCLUSIONS

Ultrasonic meters can be installed in well developed flow conditions in the absence of swirl and provide meter uncertainties of 0.6% without recourse to reference calibration methods. All that is required is accurate determination of meter dimensions and setting of meter zero under no flow conditions. From the results, additional uncertainties are proposed to be used for standardization work in case the meter is to be installed in non-ideal conditions. There may be advantages gained in defining meter orientation but this cannot be certain.

- The diameter step tests have shown that ultrasonic meters are insensitive to small changes in upstream pipe diameters such as that which would be experienced from use of standard scheduled pipe and installation of full bore ball or plug valves immediately adjacent to the meter.
- For the disturbance tests of asymmetry, swirl and pressure reduction the results at 5D all are at or exceed 1% additional uncertainty. It is not recommended that ultrasonic meters are installed with only 5D of straight pipe from the disturbing pipe configurations.
- If ultrasonic meters are placed with 10D of straight pipe after a bend in a single plane (90° or 180°) an additional uncertainty of 0.5% must be added to the base calibration uncertainty.
- From present results conclusions on swirl cannot be clearly drawn. If the meters are installed 10D from the disturbance an additional uncertainty of 2.5% is proposed which places the meter outside the usual custody transfer accuracy requirements.
- Installing ultrasonic meters downstream of pressure reduction stations is not recommended without provisions to eliminate noise and other disturbances. Where valves are producing low pressure reduction (< 1 bar) the meters can operate but with no additional flow conditioning an additional uncertainty of 2% is indicated with the disturbance 10D from the meter.

The test programme has demonstrated that the meter geometry and integration techniques also play an important role in the meter response to particular disturbances. The above conclusions may therefore not be fully representative for other meter types. Any conclusions apply specifically to 4 path meters, with criss-cross chord arrangements using the Westinghouse integration method.

8 FUTURE WORK

- The swirl tests seem to be more severe than that found in actual practice. Testing of more realistic swirl conditions like headers and extension of the upstream pipe straight lengths is recommended because the results indicate that these might result in the required uncertainty being maintained below the 1% limit. Also the benefits of flow straighteners should be investigated. Suggested spacings are 0D, 5D and 10D.
- The pressure reduction tests highlighted the problem of ultrasonic noise and demonstrated a need to address methods of reducing this if ultrasonic meters are to operate successfully downstream of pressure reducing valves. Like swirl the pressure reduction tests need also to establish acceptable upstream lengths to maintain uncertainty within the 1% limit.
- The programme was limited to a single meter type and it is apparent from the results that meter geometry and integration technique plays a role in response to disturbances. It is important that future programmes look at different meter types. These should be backed up by theoretical and practical work on profile effects to help predict meter performance and understand the results.
- There does appear to be a need for work on optimisation of the meter signal processing for different disturbed conditions. There may be a need to indicate a possible down-rating of the meter capacity in disturbed conditions.

ACKNOWLEDGEMENTS

The authors wish to thank all who contributed to the success of this project either by discussion, by carrying out work, or by financial support.

REFERENCES

- 1 Project Ultraflow, Installation Effects on Multi-Path Ultrasonic Flow Meters - Synthesis Report EC Contract no. 3443/1/0/193/91/8-BCR-UK(30). M.B. Wilson, BP International Ltd, Research and Engineering Centre, Sunbury, UK. To be published end 1994.
- 2 ISO 9951 - Measurement of Gas Flow in Closed Conduits - Turbine Meters. 1993.
- 3 GERG - Intercomparison Exercise of High Pressure Test Facilities within GERG, GERG TM6 1993.

DEVELOPMENTS OF MULTIPATH TRANSIT TIME ULTRASONIC GAS FLOW METERS

K. J. Zanker, Daniel Industries UK
W. R. Freund Jr. Daniel Electronics USA

SUMMARY

Ultrasonic meters that do not need flow calibration are being developed for fiscal gas measurement. As with any other new technology the lack of recognised standards is hampering this effort. Evidence is presented to advance the use of uncalibrated meters and performance validation. The meter was originally designed for distribution, i.e. clean dry sales gas at 60 Bar and ambient temperature. It is being extended into gas production where moisture can cause practical problems. Some ongoing research on the measurement of wet gas is presented.

NOTATION

| | |
|-------|--|
| c | Velocity of sound in the gas (VOS) |
| D | Pipe internal diameter |
| L | Ultrasonic path length between transducers |
| q | Actual volumetric flow rate |
| R | Pipe internal radius (D/2) |
| t_1 | Transit time against flow component |
| t_2 | Transit time with flow component |
| V | Chord velocity |
| V_m | Average velocity |
| W | Weighting factor, for integration |
| x | Axial component of ultrasonic path in the flow |

1. INTRODUCTION

The multipath meter was developed by British Gas in the early 1980's (Ref 1 to 5) and licensed to Daniel Industries in 1986 (Ref 6 to 9). The first commercial production meters were sold in 1989. These meters had analog electronics and used a simple threshold to detect the ultrasonic signals. In 1993 Daniel introduced digital electronics with automatic gain control (AGC) and digital signal processing (DSP) to reduce electrical noise, greatly improve the signal detection and hence increase the timing accuracy. The advantage of AGC was to eliminate pressure sensitivity.

This year Daniel have released a MkII design where the drive unit electronics are installed in a Flameproof Enclosure that is directly mounted onto the meter body, instead of into a 19" rack located in the safe area. This eliminates an expensive 8-core cable, improves immunity to electrical noise and produces a smart flow transmitter.

Three developments are considered:

- Ultrasonics is a relatively new method of gas flow measurement and although capable of meeting fiscal requirements, no accepted standards exist and hence they must be developed.
- Another great attraction of ultrasonic meters is the potential for not needing a flow calibration, but this remains to be demonstrated.
- The British Gas meter was originally designed to measure clean dry gas and has been found susceptible to moisture, development is under way to extend the operation to include wet gas.

2. STANDARDISATION

The paper on the Ultraflow project by Bloemendaal & Kam, in this workshop, tackles the development of an installation standard.

The following is intended to help produce a standard for uncalibrated ultrasonic flow meters.

3. "DRY" CALIBRATION

It is not necessary to calibrate the meter with a gas flow and reference standard, basic measurements of geometry and time should suffice.

Theory of a transit time ultrasonic meter predicts (Refs 1 & 6)

For each chord the velocity $V = L^2/2x (t_1-t_2)/t_1t_2$ - (eq 1)

and the velocity of sound $c = L/2 (t_1+t_2)/t_1t_2$ - (eq 2)

A multi path meter gives several chord velocities which are then integrated to give the Average velocity $V_m = \Sigma W_i V_i$ - (eq 3)

The individual chord velocities give an idea of the velocity profile and if not very distorted, the integration technique gives an accurate average.

The actual volume flow $q = V_m * Area = V_m \pi D^2 / 4$ - (eq 4)

The accuracy depends on area from diameter (D) and velocity, which in turn is derived from distance (L, x) and time (t₁, t₂).

The meter geometry (L, x, D) can be determined with sufficient accuracy (by a coordinate measuring machine), but the transit time is not quite so straight forward.

The absolute transit time can not be measured directly because the required time is that through the gas alone, whereas the measured time includes delays due to cables, electronics, transducers and the time into the received waveform where the DSP chooses to detect the signal arrival.

The average delay time (AvgDly) for a pair of transducers is measured in a test cell or the meter body using nitrogen, where the velocity of sound is known from IUPAC tables to 0.1%.

Some orders of magnitude will help examine timing accuracy:

- With an ultrasonic frequency of 100 KHz the period $T = 10 \mu s$
- For $L = 0.4$ m and $c = 400$ m/s $t = 1000 \mu s$ (12" meter)
- In a test cell ($L = 0.2$ m) $t = 500 \mu s$ and is known to $0.5 \mu s$ (0.1%)
- A typical AvgDly = $25 \mu s$ and is also known to $0.5 \mu s$

Using these values gives:

- The delay time is a 2.5% (25/1000) correction to the transit time, and hence a 5% correction to the flow (span adjustment).
- An accuracy of $0.5 \mu s$ in delay time corresponds to 0.1% in flow.
- A skip of one period T in signal detection on both t₁ & t₂ (no effect on t₁- t₂) is a 1% (10/1000) error in the transit time, and hence a 2% error in flow.

To go further we need to consider flow e.g.

- For $L = 0.4$ m, $c = 400$ m/s and $V = 8$ m/s then $t_1 - t_2 = 20 \mu s$

Using these values gives:

- A skip of one period T in signal detection on one transit time can give 50 - 100% error ($t_1 - t_2 = 10 - 30 \mu s$).
- A typical accuracy on time measurement is 20 ns giving 0.1% accuracy in flow (at 8 m/s), which increases to 1% at 0.8 m/s.
- Note, these magnitudes depend on the meter size and gas velocity as shown by Eqs 1 & 2.

The major potential source of error is peak switching and much effort is made to avoid this in the DSP quality checks. In fact the 80 - 120 KHz frequency range was chosen to make peak switching (of $10 \mu s$) obvious when it occurs.

3.1. First step of dry calibration

- Determine AvgDly for all four chords, using the actual drive unit electronics. Enter these delay times into the flow computer and check VOS same on each chord and equal N_2 value to 0.1%.
- 0.1% on VOS gives 0.2% on flow in the meter body, if a smaller test cell is used this can be improved.
- The four VOS values are a powerful self check, especially with smaller meters.

The AvgDly for a transducer pair is not the whole story. At zero flow $t_1 - t_2$ is not exactly zero because of differences in electronics and transducers as transmitters and receivers, this lack of reciprocity giving typically a DltDly $< 0.1 \mu s$. At 8 m/s in the above example this would give 0.5% error (0.1/20), which would increase to 5% at 0.8 m/s

3.2. Second step of dry calibration (zero adjustment)

Determine the DltDly on each chord at zero flow, using the actual drive unit electronics, to at least $0.02 \mu s$. It is not easy to achieve zero flow in the field, because shut off valves are not normally close to the meter and convection currents occur due to temperature differences. Insulation will help, but zero flow is easier attained in a temperature controlled lab with blind flanges on the meter, or better still in a test cell. It may be necessary to run the zero test over varying temperatures, to estimate the range and mid value of DltDly (typically $\pm 10 ns$). A good zero should give $V_m < 0.005 m/s$, dependent on meter size.

3.3. Field check - validation

The dry calibration done in the factory should ensure that the meter works in the field. In addition field checks are possible:

- VOS should be same on all four chords.
- VOS should agree with calculations from gas composition, pressure and temperature.
- The velocity profile given by the four chords should indicate any installation problems and zero problems at low velocities.
- The standard deviation of transit time measurements is normally $< 1 \mu s$, larger values indicate disturbed flow (dependent on D).
- It is also possible to observe the received ultrasonic signal on an oscilloscope and check for amplitude, noise and distortion.

3.4. Verification by Flow Calibration

We have recently had the opportunity to flow calibrate several meters for our clients (Norsk Hydro, Statoil) that were first dry calibrated in our works:

A 6" meter at 37.5 Bar and 38.3 °C, see Fig 1 and a 12" meter at 140 Bar and 55 °C, see Fig 2, both at K-Lab.

Several 20" meters at K-Lab and British Gas Bishop Auckland.

K-Lab tested the effect of changing the pressure from 60 to 132 Bar on two meters and British Gas Bishop Auckland then calibrated them all at 60 Bar, see Fig 3.

The results showed that:

- Most meters attain 1% accuracy over 1 - 21 m/s velocity range with the factory dry calibration.
- Some problems with poor zero setting in the field especially with large meters. Fig. 3 shows that two out of five meters could have a better zero. It may not be good to zero in the field, as the effect of gas composition, pressure and temperature are not as great as thermal convection (non-zero flow) problems.
- One meter (filled square) was outside 1%, due to known problems with thermal equilibrium during dry calibration in the 20" body, it is probably better to use a smaller test cell.
- Negligible pressure effect between 60 - 130 Bar or temperature effect from 10 - 55 °C on flow calibration.

3.5 Conclusions

If the geometry is measured accurately, the timing set to give the correct VOS in nitrogen and the zero flow adjustment performed (with real zero flow), the dry calibration meets the +/- 1% accuracy spec over the 1 - 21 m/s velocity range.

4. WET GAS MEASUREMENT

The objective is to measure the gas flow, preferably unaffected by any liquid present, no attempt is made here to measure the two phase flow.

The original British Gas meter was designed for dry clean gas, with transducers recessed in ports, and further recessed by the use of transducer isolating valves (to facilitate transducer exchange). Moisture can cause several problems:

Moisture collects in the transducer ports, short circuits the acoustic isolation between transducer and body, bridges the small clearance between port and transducer, and contaminates the transducer front face.

The wet gas design aims to overcome these problems by:

- Using self draining ports, back into the body.
- Increasing the clearance between transducer and port.
- Placing the transducer face at the bore/port intersection, to both get a cleaning action from the flow and not be recessed.
- Better acoustic isolation and damping of the transducer.
- Reducing side emission from the transducer.

4.1. Testing

Two 6" meters were built for testing, with electroless nickel plating (ENP) to improve the corrosion resistance in wet gas, particularly for the air/water.

- Both were installed in horizontal lines with the chords in an horizontal plane.
- One at NEL on air and water in laboratory simulated conditions, that could be closely controlled.
- The other at Shell Bacton on natural gas with condensate, under real two phase flow conditions, dependent on production and the process plant requirements.

4.2. Test Results

- NEL injected mist, via a multitude of nozzles that atomized the water, in accurately controlled and stable conditions. Fig 4 shows a typical result (note the logarithmic scale).
- Bacton was originally conceived as a 6 month survival trial in a line attached to a gas treatment plant, see Fig 5.
- The success of the Bacton survival prompted some additional condensate injection tests, summarised in Fig 6 and shown in more detail in Fig 7.

4.3. Discussion

The Bacton trial lasted 9 months with at least 6 months of flow, which included 4 liquid slugs and complete flooding of the meter. The original concern was survival, not accuracy. When the meter showed potential for +/- 1% accuracy with wet gas, Bacton offered to do some controlled liquid injection tests. The main advantage at Shell Bacton was that known equilibrium two phase flow regimes could be established, based on previous work by KSLA.

The 2% shift in meter error after a liquid slug in Dec (Fig 5) is difficult to explain. The meter was not set up very well for the survival tests, it was reset for the liquid injection tests, showing some errors in the original set up which might have affected performance. The transducers were removed

after this slug, but inspection showed no problems with liquid retention.

Fig 6 shows that with mist flow, especially at high gas velocity, 3% liquid by volume makes the ultrasonic meter read about 3% high. The gas and condensate appear to be travelling at the same velocity and the meter reads the total volume flow.

At the lowest velocity (5 m/s) the two phase flow is stratified (i.e. a river running in the bottom of the pipe). Under these conditions 1% liquid by volume makes the ultrasonic meter read about 4-5% high, indicating that the river flows much slower than the gas and hence occupies a larger volume (hold up).

Fig. 7 shows more detail of the Bacton injection tests:

With stratified flow (5 m/s) the D-chord fails at 1.3% liquid injection. The D-chord is at the bottom of the pipe at 0.809R and the area occupied by the segment is 4.8% of the circle. The failure is due to the river flooding the transducers on the D-chord and the error (4-5%) corresponds exactly to the area occupied by the river, confirming the stratified flow.

With mist flow the D-chord and eventually the C-chord fail at higher liquid injection. The failure is due to the mist attenuating the ultrasound transmission (scattering) and not flooding of the transducers. This is further confirmed by measuring the amplitude of the received signal, the speed of sound and the standard deviation of the transit time.

The NEL tests show that the flow is stratified, despite atomizing the water, it seems to settle onto the bottom of the pipe. The errors with air/water seem to be greater than with gas/condensate, this is probably due to water having higher density, higher viscosity and higher surface tension than condensate, all increasing the hold up. Air/water is a two-component flow rather than a two-phase flow.

4.4. Further work

The wet gas development is ongoing and requires extension to:

- Commercially produce wet/sour gas transducers (so far only prototypes have been made for a 6" meter) and investigate the manufacture of other meter sizes.
- Consider vertical installation, as vertical two phase flow might eliminate stratification, giving a more homogeneous flow and the ability to measure higher liquid volume fractions.
- Examine the possibility of two phase flow measurement.

4.5. Conclusions

- Wet gas ultrasonic meter design works.
- Meter survived 9 months operation with plant upsets.
- Meter recovers from complete flooding .
- Less than 1% condensate has a small effect, typically + 1% for mist flow and the meter seems to measure the total (gas + liquid) flow.
- Different behaviour in stratified flow, larger errors (~ 5 times) than mist flow due to liquid hold up.
- Above 1% liquid D-chord (on bottom) fails giving larger errors.
- The results are understandable in terms of liquid effects on the ultrasonic signals.
- The main objective of measuring the gas flow was achieved.
- Air/water is not a good model for gas/condensate flow.
- Information probably exists in the ultrasonic meter signals to recognise two phase flow.

REFERENCES

1. NOLAN M. E. AND O'HAIR J. G. - An ultrasonic flowmeter for the accurate measurement of high pressure gas
Norflow 83. IMC Aberdeen, May 1983

2. NOLAN M. E. AND O'HAIR J. G. - The development of a multipath ultrasonic flowmeter for the measurement of high pressure gas flows.
Int Gas Research Conf. IGU London, June 1983
3. NOLAN M. E. AND O'HAIR J. G. - An ultrasonic flowmeter for the accurate measurement of high pressure gas
Flomeko 83. IMEKO Budapest. Sep 1983
4. NOLAN M.E., O'HAIR J.G., GASKELL M.C., CHEUNG W.S.& FELLOWES B. - Developments in the ultrasonic flowmeter in British Gas
The metering of natural gas and liquified hydrocarbon gases.
Oyez Sci & Tech, London, Feb 1984
5. NOLAN M.E., GASKELL M.C. AND CHEUNG W.S. - Further developments of the British Gas ultrasonic flowmeter
Int Conf on flow measurement in the mid 80's
NEL, East Kilbride, June 1986
6. NOLAN M. E., O'HAIR J. G. AND TEYSSANDIER R. - The measurement of high pressure natural gas flows using the four path ultrasonic flowmeter developed by British Gas
Int Symp on fluid flow measurement
Washington, Nov 1986
7. NOLAN M. E., O'HAIR J. G. AND PETERS R.J.W. - Ultrasonic flowmeters for the gas industry
North sea flow metering workshop 88
NEL, East Kilbride, Oct 1988
8. HOLDEN J.L. AND PETERS R.J.W. - Practical experiences using ultrasonic flowmeters on high pressure gas
Flow Meas. Instrum. Vol 2 Jan 1991
9. SAKARIASSEN R. - Practical experiences with multipath ultrasonic gas flowmeters
North sea flow metering workshop 93
NFOGM, Norway, Oct 1993

ACKNOWLEDGEMENTS

Statoil, Norsk Hydro, Aker, K-Lab, British Gas, are the end users, engineering company and test facilities involved in the calibration of the ultrasonic meters. Their contribution is gratefully acknowledged.

The Wet Gas JIP (which consists of BP International, British Gas, Shell Expro, NAM, Phillips Petroleum, Amoco Europe, & Daniel Industries) and DTI sponsored the work on wet gas, and have generously allowed this publication.

Ron Meerhoff of KSLA made a most valuable contribution to the Bacton site testing.

FIG 1. Calibration of 6" meter

Natural gas 37.5 Bar, 38.3 Deg C

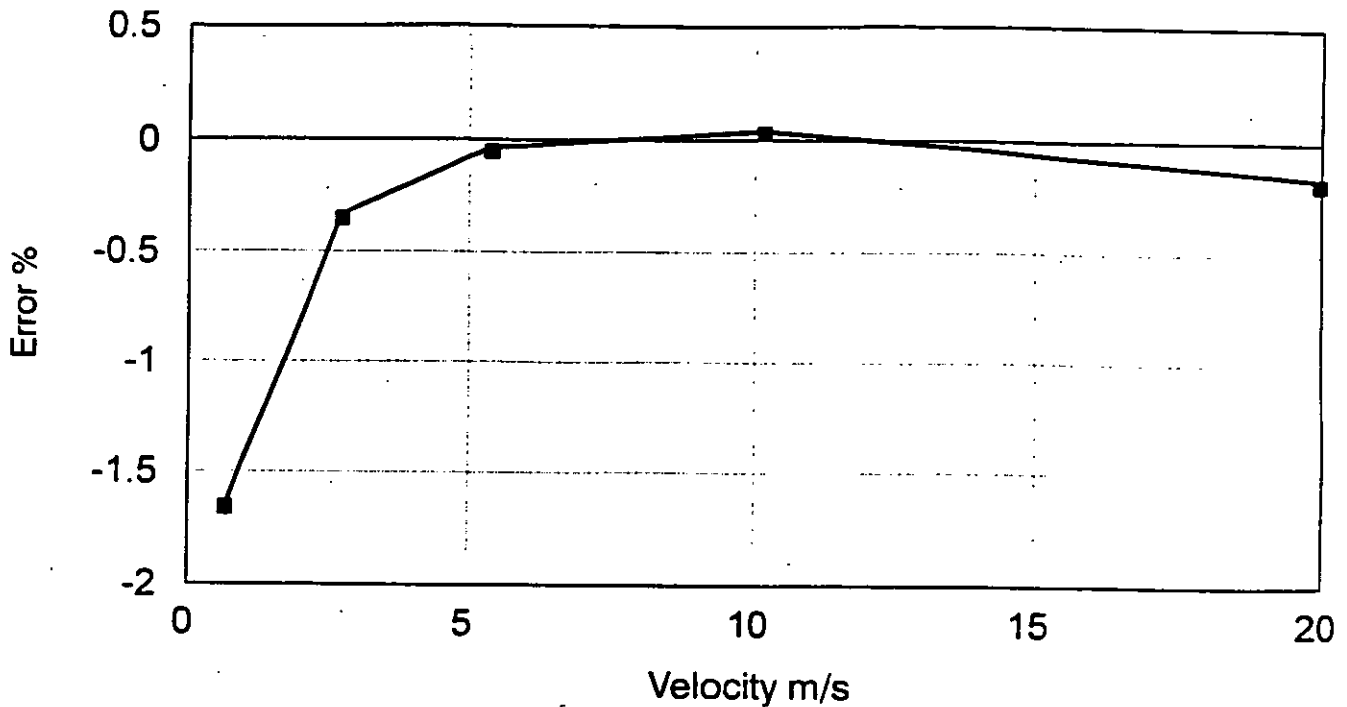


FIG 2. Calibration of 12" meter

Natural gas 140 Bar, 55 Deg C

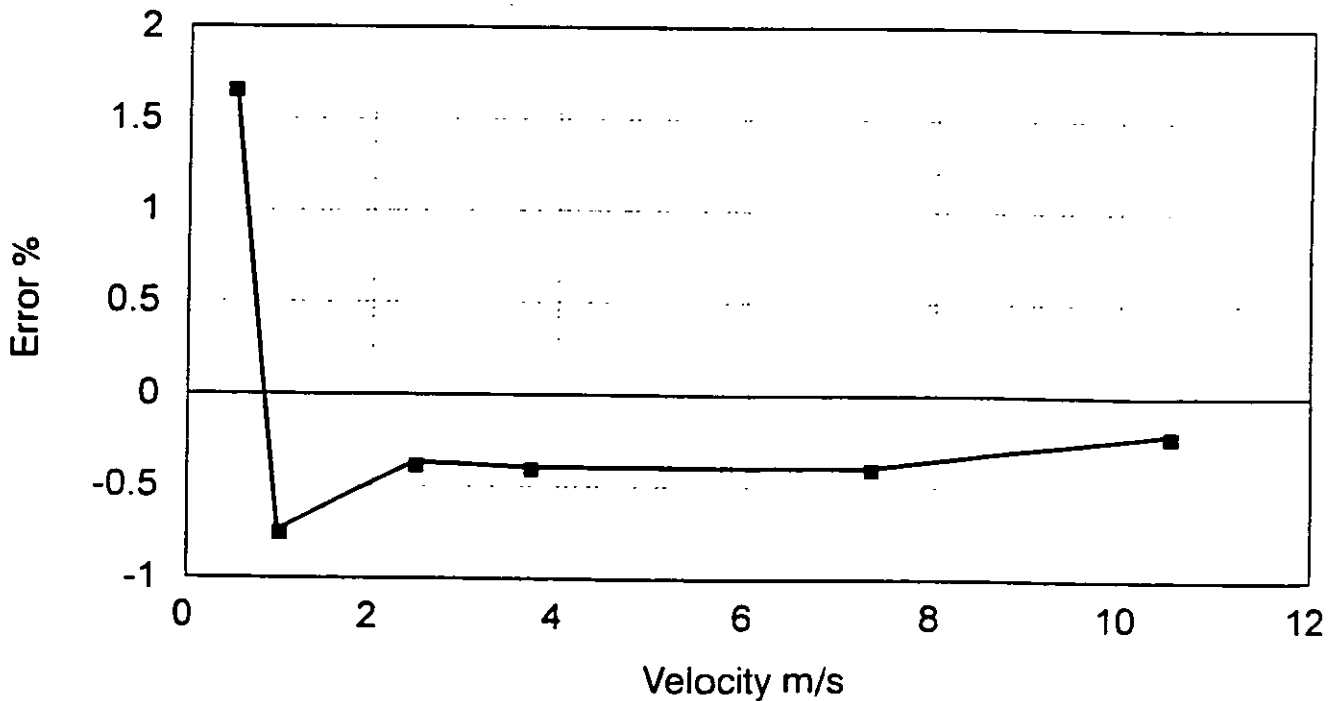


FIG 3. Calibration of five 20" meters

Natural gas 60 Bar, 10 Deg C

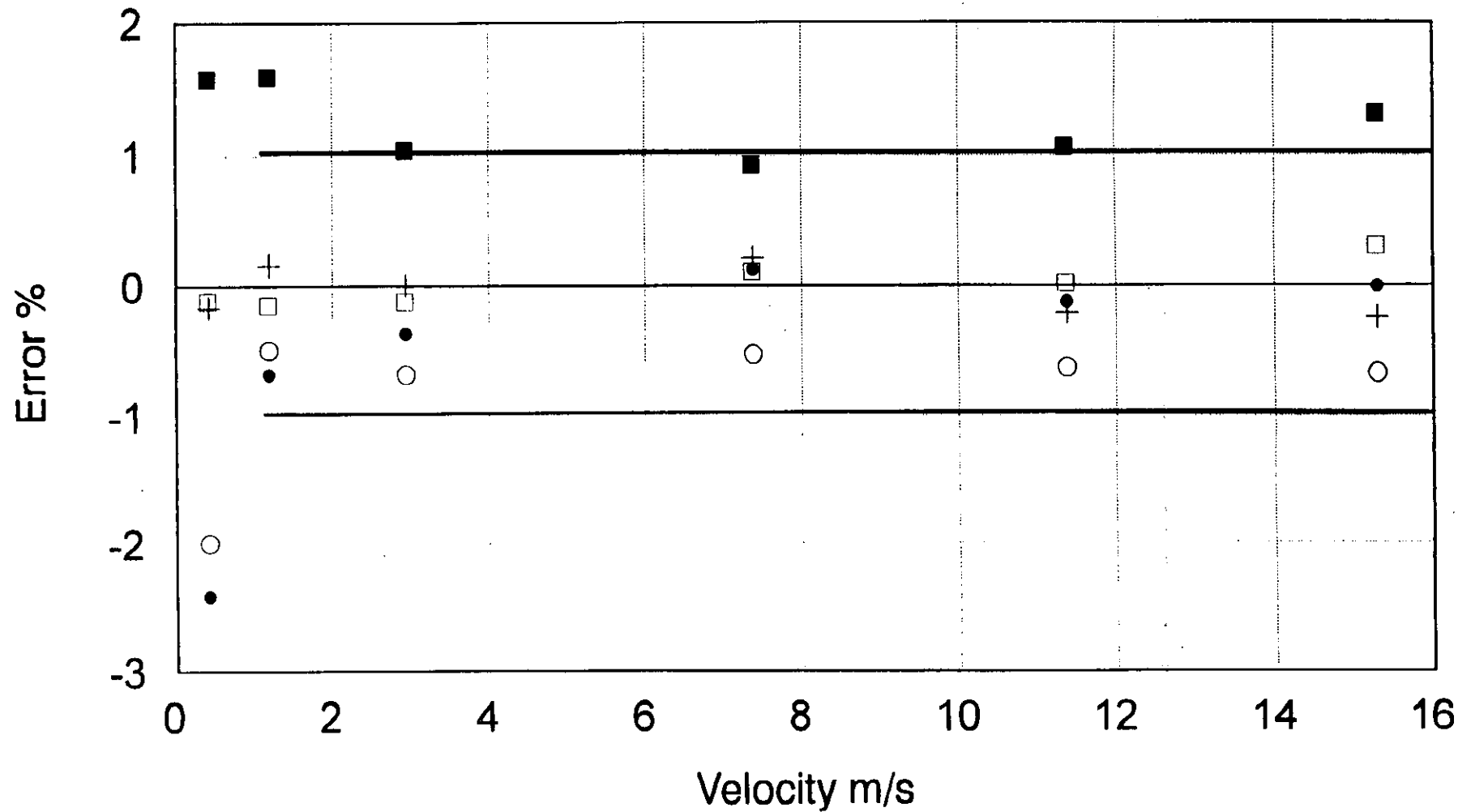
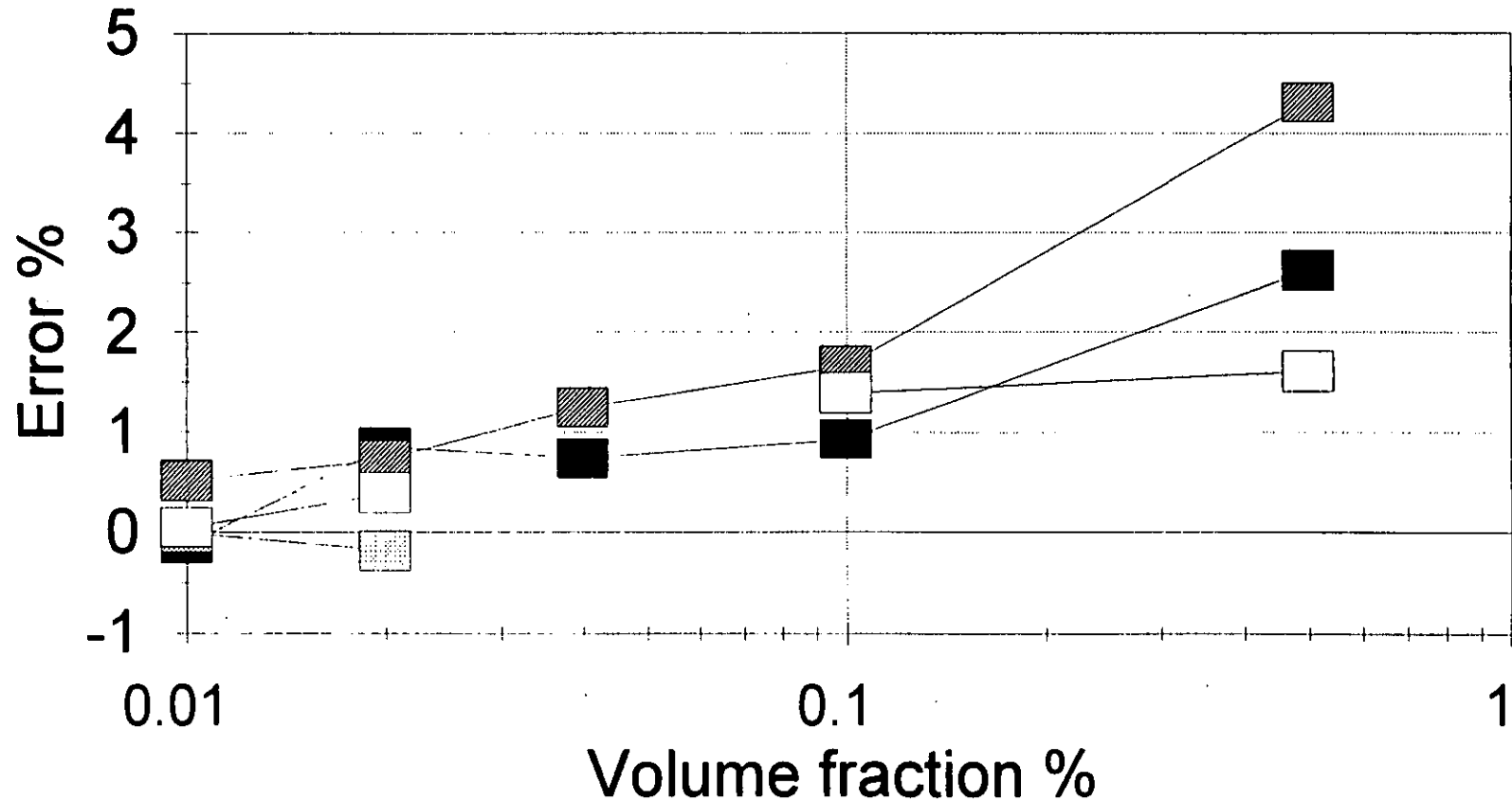


FIG 4. Wet gas tests at NEL

70 Bar air, atomized water at 50D



b

■ 1 m/s ▨ 2 m/s ▩ 5 m/s □ 10 m/s

FIG 5. Bacton Trials Overall Summary
%Error and Reference Flow Rate for Complete Test Period

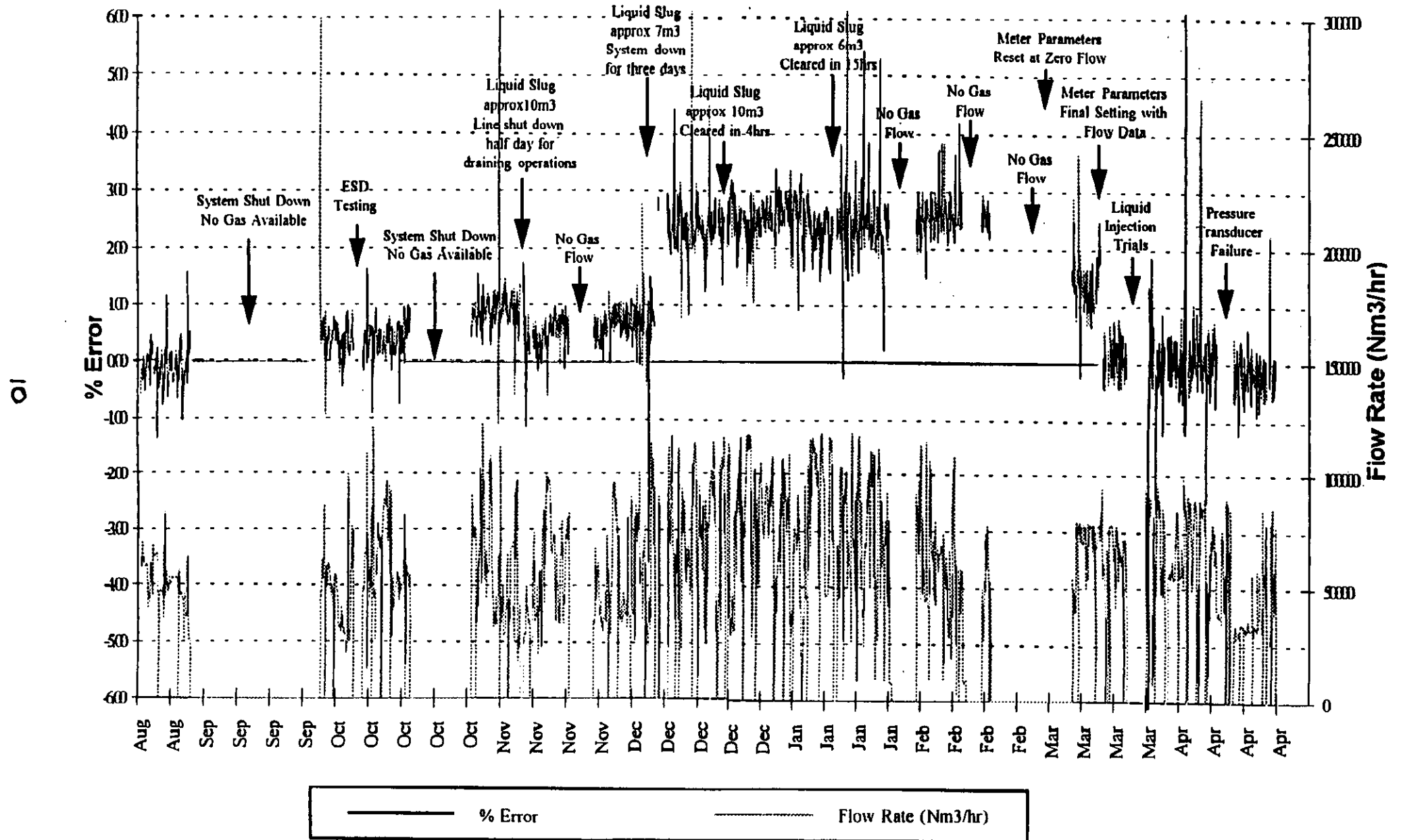
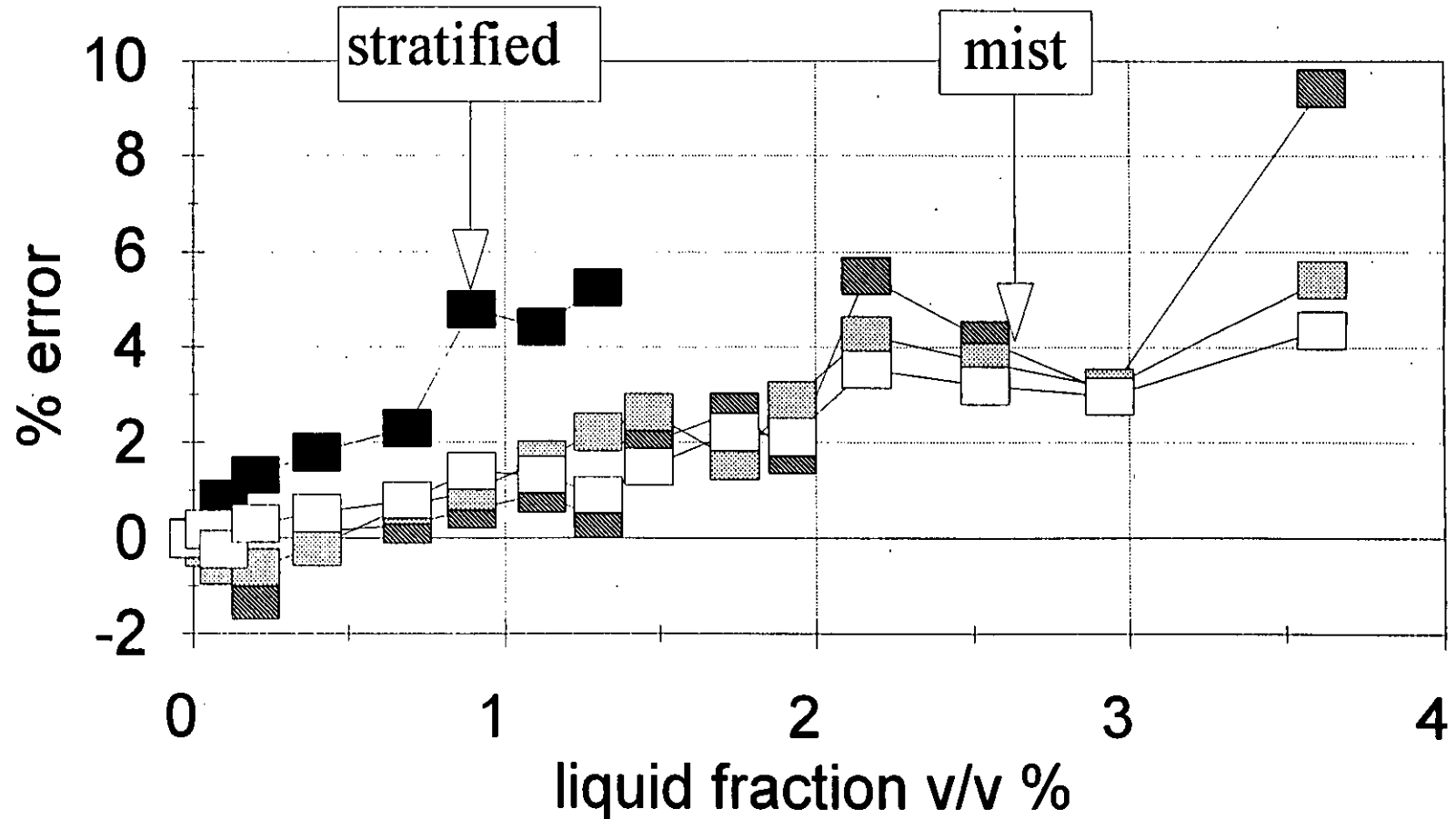
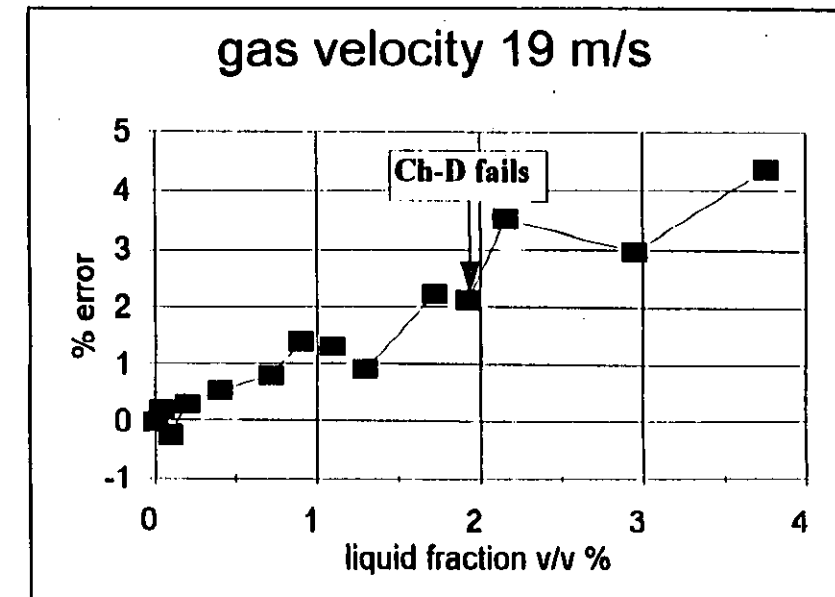
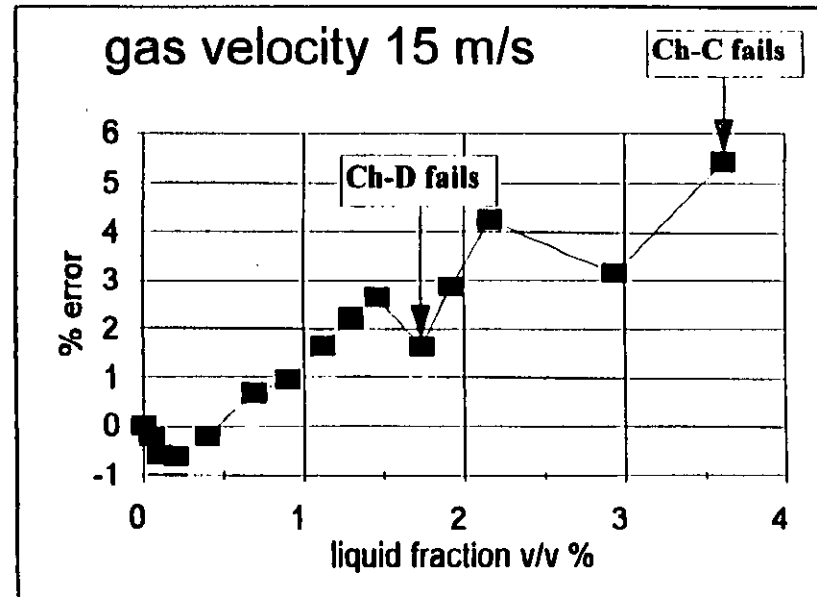
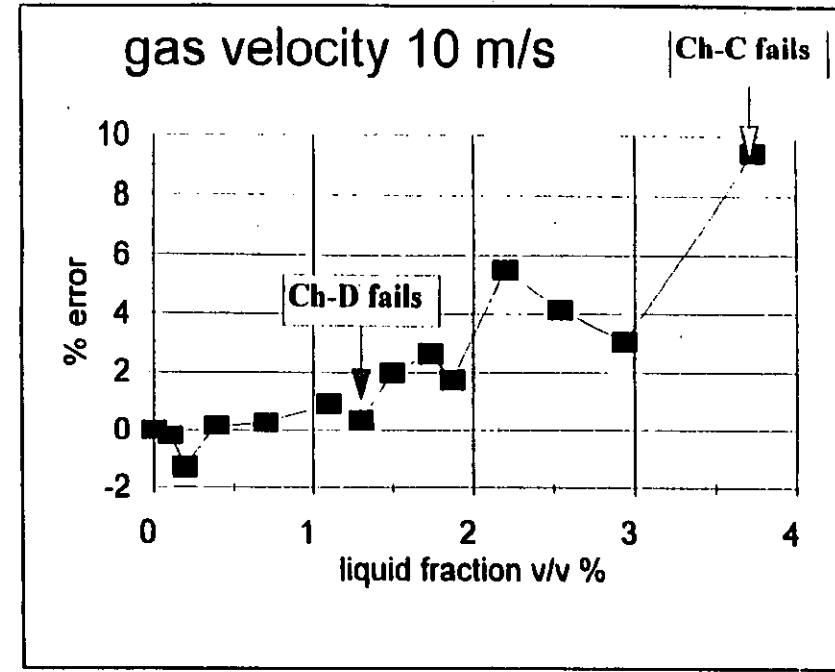
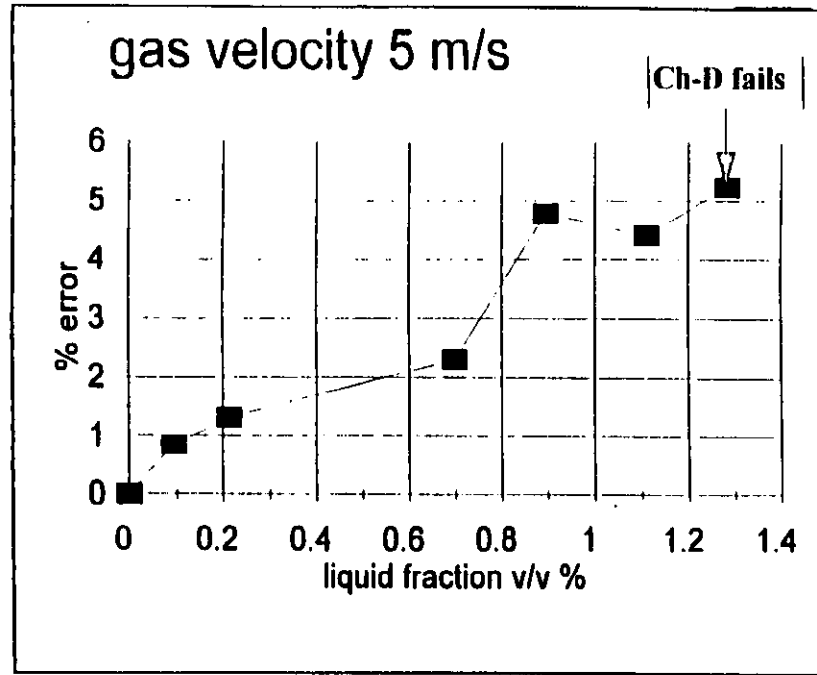


FIG 6. Bacton condensate injection



■ 5 m/s ▨ 10 m/s ▩ 15 m/s □ 19 m/s

FIG 7. Bacton condensate injection tests



THE EFFECT OF DIFFERENT PATH CONFIGURATIONS ON ULTRASONIC FLOW MEASUREMENT

by

T. COUSINS STORK FLOW MEASUREMENT Ltd. & F.J.J. HUISMANS STORK SERVEX B.V.

INTRODUCTION

For many years now liquid flow measurement using the Time of Flight of ultrasound has been accepted as an equal partner alongside other flow metering techniques. The advantages of negligible intrusion into the pipe, giving no extra pressure drop and a low chance of transducer fouling and damage, good levels of precision, repeatability, resolution and range make it an attractive method. Further, the direct link of the performance and cost reduction with improvements in electronic technology makes the possibilities for the future performance even more exciting.

Development until recently has been largely on liquid meters, due mainly to the problems of successfully transmitting ultrasound into gases, and detecting the signal. This is particularly acute for low pressure applications. The first successful application for the gas ultrasonic flow meter was the measurement of Flare gas. An application where the good range, ease of installation and low pressure drop is a major requirement. These meters are generally single path, with a modest level of uncertainty, due mainly to the lack of ability to determine the exact pipe size. Meters were then developed for such applications as gas blending, compressor measurement etc., all however being generally single path meters with an uncertainty in the region of 1-2%.

The advantages of multi-path ultrasonic meters have been clear from very early in their development. In 1971, a five-path meter was described by Westinghouse ¹ for fiscal measurement of liquids. Further developments showed that a high level of precision could be obtained, even under adverse installation conditions, if several paths were chosen across the pipe, forming chords, and an appropriate algorithm obtained. It has only, in the last five years, been possible to successfully design a multi-path meter for gas measurement. The resultant meter produces results of a "fiscal" standard, for custody transfer.

The paper describes the design of Stork Servex ultrasonic flow meters, which are both novel and advanced in their approach to the problems of both single and multi-path methods of metering using ultrasonic time of flight.

MEASURING METHOD

The meter works on the Time of Flight principle, an absolute digital travel time method. The basic system is shown in Fig.1. Transducers are placed on opposite sides of the pipe, such that the piezo-crystal faces are opposite each other. Pulses of ultrasound are generated simultaneously by both transducers.

At zero flow the time taken for the sound to travel from A to B (t_{AB}) is the same as for B to A (t_{BA}), thus:-

$$t_{AB} = t_{BA} = \frac{L}{C} \text{ ----- (1)}$$

If there is a flow as shown in Fig1, the travel time from A to B (t_{AB}) will decrease and B to A (t_{BA}) will increase as below :-

$$t_{AB} = \frac{L}{C + V_a \cos \theta} \text{ ----- (2)}$$

$$t_{BA} = \frac{L}{C - V_a \cos \theta} \text{ ----- (3)}$$

The simultaneous transmission of the pulses is essential, as small changes in velocity of sound, due for example to changes in gas content, temperature or pressure, will cause errors in the calculation of the fluid velocity. The velocity of sound is thus eliminated by combining equations 2 and 3 in the following way :-

$$V_a = \frac{L}{2 \cos \theta} \left(\frac{1}{t_{AB}} - \frac{1}{t_{BA}} \right) \text{ ----- (4)}$$

This method is essentially therefore based on the primary measurements of distance and time. The ultrasonic pulses can be considered as a gating mechanism for timing of the measurement of time of flight. Due to the digitalisation of the received signal this method is able to check the quality of the transmission of every single pulse individually against built pre-set standards. Thus each set of measurements can be assessed and either accepted or rejected, the record being a good indicator of the meters overall performance.

GAS MEASUREMENT

Signal Detection

The measurement of gas flow using ultrasonics presents some particular problems. There is a large mismatch in acoustic impedance between gas and the transducer resulting in very low levels of signal transmission. This problem increases as the gas pressure reduces. The result is, that the received signal is very low, particularly compared to ultrasound transmitted through other paths, such as the pipe walls. It is conventional wisdom to increase the signal transmission and transducer sensitivity by using high "Q" resonant transducers. Unfortunately, the performance of such transducers is very dependent on the surrounding fluid, and the received signal can become distorted, with excessive ring times. The solution is to use wide band transducers. While such transducers require more power to drive them they retain a very well defined signal with a wide variety of surrounding fluid. At manufacture the signal they produce is checked against a digital signal signature (or footprint). If they are within defined parameters they are acceptable. As the signal shape remains constant it can be

compared in the meter processing electronics with the standard digital footprint signal. This enables the detection of very low level signals in high noise conditions. The signals received from sources other than directly through the fluid can be removed by using a time window to catch the actual signal. As the "ringing" of the signals is short this does not extend into the time window to add noise to the received signal.

Solid and Liquid Particles

Under working conditions gas generally contains quantities of solids and liquids when being transported. Offshore gas, in particular, contains large quantities of liquid, and as those who deal with orifice plates will testify, onshore gas contains quantities of solids that erode orifice plate edges. By using digital pulse recognition techniques, the ultrasonic meter can be made relatively immune to solid and liquid deposits. While ultimately too much solid and liquid content will attenuate the signal beyond the point of measurement, until the point of lack of signal the digital processing system ensures the continued accuracy of the meter.

Acoustic Interference

As with all types of gas ultrasonic meters, this system is not immune to the effect of "low noise" valves. Such valves achieve this performance by pushing the audible noise up into the ultrasonic region particularly when they are nearly closed. The use of digital signal processing techniques helps to alleviate this problem although it is still advisable to place the meter as far a way as possible and preferably upstream of the meter.

Mass Flow Measurement

From the proceeding equations it is quite clear that the meter measures **actual velocity** and thus in the majority of gas applications needs to be corrected, obviously for area, but also for density changes due to gas content, pressure and temperature. There are a number of ways in which this can be done.

Velocity of Sound

The simplest method is to use the knowledge of the velocity of sound obtained from the meter to determine the density. This is done at the same instant as the flow velocity is measured, and in the same plane as the metering. Also, with this technique, the molar mass can also be calculated. The speed of sound is related to the fluid density with the following equations :-

$$\rho = \frac{k.P}{C^2} \text{----- (5)}$$

and

$$M = \frac{k.z.R.T}{C^2} \text{----- (6)}$$

ρ = Density, M = Molar Mass, T = Temperature, P = Pressure,

R = Universal Gas constant, k = Poissons ratio,

C = Sound Speed, z = Compressibility

The overall uncertainty of mass flow measurement thus depends on the uncertainty of the volume flow measurement, pressure measurement and Poisson ratio. The uncertainty of measuring Poisson ratio is dependent on the gas composition. With Flare gas, for example if a mean range of C_1 to C_8 is taken then a maximum error of approximately 4% could be expected.

Mass Flow Computation

A more precise method for correcting the output is to use pressure and temperature inputs and flow computation to produce a compensated or mass flow output. The meter can thus be treated in the same way as a standard orifice plate or turbine meter within the measuring system. Higher precision compressibility can be taken into account using one of the many "standard" methods such as NX-19, AGAB etc. It is usual to use this method for Custody Transfer Applications.

Density Meter

Again for more precise compensation, the meter can be used in conjunction with a density meter, feeding into a flow computer. The combination of the actual volume flow and the density output will give either a mass or compensated flow output.

SINGLE PATH METERS

At present, the most common configuration for the transducers is single path, cutting a chord across the pipe cross-section, usually across the centre, Fig.2. The path cuts across the velocity gradient of the pipe with each component of velocity modifying the flight time. The result is a line integral of velocity across the line of transmission. As can be seen however the flow through a pipe with a fully a developed flow profile is axi-symmetric about the centre line, and a line integral does not give full weighting to the velocities towards the outside of the pipe. Thus, the velocity output is always high

relative to the mean. At high Reynolds numbers the ratio of recorded velocity to mean velocity remains relatively constant as the changes in profile are small. At lower Reynolds numbers the curve begins to increase as the profile becomes more "peaky". Under conditions of fully developed symmetrical profiles therefore the curve is determined largely by the pipe Reynolds number. The curve obtained is shown in Fig.3. To linearise the curve the velocity obtained has to be modified by a calculated K-factor such that mean velocity $V_m = V_a/K$.

The value of K is a function of chordal position and duct velocity profile. As can be seen in Fig.3, a large number of meter factors were tried to obtain the best fit for the experimental results. The curves K1 to K3 were obtained using theoretical Prandtl type velocity profiles. These curves converge well at high Reynolds numbers but as the number reduces show increasing deviations from the experimental results. The K4 curve developed by Rothfus and Monrad⁴ incorporates the influence of the laminar sub-layer, unlike the previous three. The result is a close fit over the Reynolds number range tested.

Acoustic Path Configurations

The configuration of the acoustic path is essential to the effect of installation on the measurement of an ultrasonic meter. The conventional path configuration is shown in Fig.4a. The sound is fired directly at the receiver across the pipe, either at the centreline or along a predetermined chord. Such a configuration is subject to error due to both velocity profile and swirl. A variation is to reflect the signal from the opposite wall, Fig. 4b. This configuration is still sensitive to profile variations but effectively cancels out the rotational velocity induced by swirl. The introduction of swirl adds a component along the flight path, either speeding up or retarding the sound speed dependent on the direction of swirl. Providing that the reflected path is in a plane parallel to the direction of the pipe axis and the other path, the effect on each path will be equal and opposite. Thus, cancelling out the swirl component. The same effect can be achieved with two sets of transducers, but the **same rules with regard to the plane of flight apply**. This rule is particularly applicable in the case where swirl breaks into two contra-rotating cores Fig.5. There are further configurations applicable, Fig. 4c and 4d. These involve multiple reflections, 4c has two and 4d has four. The benefit of these configurations are a better averaging of distorted flow but are subject to a swirl component error. Configuration 4d is also very impractical as an installation, however 4c is acceptable within the concept of a "spoolpiece" meter, but is not practical for "insertion" type installation. With the use of contra-rotating double reflection paths it is possible to determine the swirl component itself, as will be described in the multi-path Q.sonic meter.

Practical Design

The practical design is a function of both pressure and pipe size. Where possible, hot tap single path Stork installations use the single reflection method. This has the following advantages:-

- This configuration alleviates the effect of the swirl component of velocity.
- The transducers are installed from one side, making the installation easier particularly for buried pipes.
- A longer path length. giving greater timing resolution.

Such a configuration is possible for most pipe sizes at high pressures, but for low pressure applications such as Flare metering the maximum pipe size for such a configuration is 15", above which the configuration should revert to the conventional direct transmission.

The meters, the Gassonic 400 and the Flaresonic, are installed into the existing line using either a high or low pressure insertion mechanism, Fig. 6, usually by hot tapping the meter offtakes. A spoolpiece single path meter, the P.Sonic is also available.

Performance

A large number of tests have been carried out at the high pressure test facility of the Dutch Gasunie at Westerbork and Groningen and by Oval Engineering Inc. in Yokohama. These tests are detailed in reference 2.

The performance of a single path meter with a variety of straight pipe (SP) configurations and flow straightener (FS) positions is shown in Fig. 7. Over most of the range the linearity is within 1%. There are small shifts with installation of a flow straightener, but all data is contained within a 1% band.

A summary of the effect of bends in different planes is shown. Fig. 8 shows a schematic of the variations of installation tested and Fig. 9, the results achieved. The results are plotted as the difference between the achieved results and a preferred installation.

Effect of Different Bend Configurations at 20 Pipe Diameters

The effect of different bend configurations, 20 pipe diameters upstream of the meter, are shown in Fig.9a. It should be noted that the effect is to generally retain the Reynolds number curve, that is the linearity, but to push the calibration negative. The data for the cross plane configuration with a single bend does show an increase in linearity at the lower flows. The general shift in calibration at higher Reynolds numbers is between is approximately 2% .

Effect of Change in Upstream Pipe Length.

As shown in Fig 9b, the effect of moving the bend to within 10 diameters of the meter is to depress the calibration further, but still retain the calibration shape. The curve is still retained within 3% at higher Reynolds numbers.

Pulsating Flow

Due to the linear nature of the principle, the absence of moving parts and high repetition, rate the ultrasonic time of flight meter is ideally suited to measure pulsating flows. Aliasing effects, between the pulsating frequency and the sampling rate, can be eliminated by using an asynchronous sampling technique. An example of the measurement of pulsating flow is shown in Fig.10. The results are from two single path Gassonic 400 meters installed in the inlet and outlet ducts of a compressor, about 3 metres from the compressor itself. The inlet flow is relatively stable, while the outlet shows the oscillations of the flow produced by the compressor.

MULTI-PATH METERS

As can be seen the performance of the single path meter is subject to profile variations due both to Reynolds number and installation. While the repeatability, range and the resolution are better than most meters, the overall measurement uncertainty is not within the limits required for Fiscal (Custody Transfer) applications. The solution is readily evident, the use of more than one path across the fluid will improve the data available about the flow profile.

Conventional Multi-Path Configuration

In general, conventional meters use between four and five paths, forming chords across the pipe cross-section, Fig.11. In some cases the transducers fire as X-paths but only to save room on transducer installation. As they are not in the same plane they cannot be used to give detail of the swirl in the pipe. The positioning of the pipe and the weightings of the various paths is done by a numerical Gaussian quadrature method. The advantages of this method are :-

- No additional information about flow profile is required.
- The weighting factors are fixed, relieving the processor of a large volume of computational work.

The drawbacks are :-

- The flow velocity is assumed to be axially symmetrical.
- The additional information with respect to Reynolds Number is lost.
- As the weightings are optimised for a symmetrical profile errors occur when the profile deviates from this optimum.

Because of these drawbacks Stork Servex B.V. have developed a novel design based on a matrix of reflected paths.

Double Reflection Configuration

As discussed previously, a double reflection gives benefits in regard to variation of the performance with velocity profile. It is not, however, a feasible installation for a low cost single path "insertion" meter. For a fiscal meter in which the transducers can be installed permanently into a Spoolpiece it gives valuable extra data. In particular the double reflection meter produces an output that gives data on the degree of swirl being produced in a pipe line. Fig. 12 shows variation in output with angle of flow of swirl flow disturber. Over much of the range the relationship is almost linear. The experiment was set up with two pairs of transducers, transmitting in clockwise and anti-clockwise directions. The reaction to the swirl is opposite and symmetrical. This is clearly shown in Fig.13, comparing the velocity output from the two, changing the swirl from a clockwise angle of 5° to an anticlockwise swirl of 10° . The intermediate region results from the two step procedure of adjusting the flow disturber. The swirl strength and direction can be obtained from the difference between the two paths.

The Five Path Matrics Method

As stated the flow path is likely to compose a number of distortions, asymmetry, swirl and pulsations. The five path matrics meter three single reflection paths and two double reflection paths. From these it is possible to detect the type of velocity profile and measure the strength of any distortions. As can be seen, the double reflection paths give detail of the swirl strength, independent of the profile. The use of three single reflection paths placed symmetrically around the pipe circumference shows detail of the profile, Fig.14, independent of any swirl. The deviations from both path types are taken into account in the computation of bulk mean flow.

The calculation matrix has been developed to use information from:-

- The flow Reynolds Number.
- The individual velocities along different paths.
- The measured swirl strength.
- Pulsation strength along certain paths.
- The flow asymmetry.

The development of the matrix method is based on experimental measurements and a number of sets of data that classify the different flow profiles encountered in actual installations.

The setup of the five paths are shown in Fig. 15. The advantages of this method are :-

- The close spacing of the acoustic path network, giving a high coverage of the cross-section.
- The measurement is insensitive to the orientation of the meter with respect to the piping.
- The path lengths are much longer, resulting in a more accurate measurement of flow velocity.

Implementation

The meter developed by Stork Servex BV is the Q.sonic. It consists of a spoolpiece with the three single reflection paths at 120° intervals around the tube and two double reflection paths. The Q.sonic is placed in the hazardous area with the basic data processing electronics. The meter can then either talk to a remote unit in the safe area which provides the power supply to the meter and additional computation, or the meter can be supplied separately with a power supply, +/- 15V, 12Vdc or 24Vdc, and the data taken to a flow or control computer. In both cases data can be transferred using a serial RS485 link, up to 700m or an optical fibre, 3Km.

From the Remote unit the data available is via a 4-20mA output, a 0-10Khz frequency, both of which are freely configurable, an RS232 output with all necessary information, flow direction, relay output, and data validity, relay output. Pressure and Temperature can be connected to the remote unit, galvanically separated, or to the local unit, not galvanically separated.

The same outputs are available direct from the meter, except that the flow direction and validity outputs are opto-isolated open collector outputs. In this form the meter is configured and serviced via the RS485 connections. A P.C. is used to configure the meter. As with the remote unit the P&T corrections can be made locally or into the electronics in the safe area, such as a flow computer.

Performance

Some of the results using the, preliminary theoretical computations, of the calibration of a 20" five path Q.sonic meter, tested at the Bernoulli station of Gasunie with different pipe configurations, are shown in Fig. 16. For a straight pipe, Fig.16a, the accuracy of the meter was found to be within 0.3% for most of the range. Each of the points shown is composed of three independent measurements, too close to show as separate values on the scale chosen. The effect of a single and double bend 5.5 pipe diameters upstream are shown in Figs 16b and 16c. The maximum deviation over most of the range is less than 0.3%. As a result of this data improved computations have been developed that significantly improve on these results. An orifice plate to retain the discharge coefficient within the specified uncertainty would require between 15 and 30 diameters of straight pipe after such disturbances, dependant on the area ratio. Data indicates an error of as much as 1% if placed as close as 5 pipe diameters downstream of a single bend, again dependent on the area ratio.

ACCURACY

From equation 4, it can be seen that the errors in flow measurement are due to the uncertainty of the measuring path length, the timing and the angle of transmission. In converting the acoustic velocity into a volumetric flow the "K" factor is required and the area of the pipe both of which carry uncertainties. The errors can be divided into two parts:-

- Transit time measurement errors.
- Errors due to installation parameters.

Transit Time Measurement

Any timing error in the instrument will cause an error in the velocity measurement. This results from two sources, the timing resolution and the precision with which the signal can gate the timer. With the use of wide band piezo-ceramics and high speed digital processing a timing error of less than 10ns can be achieved. The relation between the timing error and the velocity error is linear. Assuming the velocity of sound and transmission angle remain constant the error as a function of pipe diameter due to the timing is :-

As can be expected, the error decreases as the pipe size increases.

Installation Parameters

The installation errors are largely independent, and so the total error will be the RMS. of the individual errors. The total volumetric error E_Q is given by:-

$$E_Q = \sqrt{E_{V_m}^2 + E_A^2 + E_K^2}$$

where E_A is error in measurement of area, E_K is K factor error and

$$E_{V_m} = \sqrt{E_D^2 + E_\theta^2}$$

E_D is the diameter error and E_θ is the error in measuring the transmission angle.

The magnitude of these errors is quite clearly a function of the meter type. A "hot-tap" insertion meter will obviously carry larger errors than a spoolpiece where the dimensions are under the control of the meter manufacturer.

Practical values for these errors for insertion type meters are:-

$$E_A < 0.5\%$$

$$E_D < 0.5\%$$

$$E_\theta < 0.2\%$$

$$E_K < 2.0\%$$

This gives a worst case error of Volumetric flow measurement of 2.1%.

Generally it has been found that the results are better than this. As good as 1% with a flowstraightener and 10 pipe diameters upstream and 5 downstream. Without a straightener these pipe lengths must be doubled.

With a carefully manufactured spoolpiece these are reduced significantly to less than 0.5% as shown with Q.sonic.

APPLICATIONS

With the wide range of variations available from the basic concept from low cost, low pressure insertion type meters to sophisticated multi-path meters the range of applications is extensive. These include for the single path meters Flare and Flue gas monitoring, underground natural gas storage, vapour return metering, leakage detection, compressor efficiency, custody transfer checkmetering and general process control. The multi-path meters are obviously aimed at providing a Fiscal standard of metering for Custody transfer both onshore and offshore, consumption metering for gas fired power stations, bulk gas supply to heavy industrial users etc. It is worth considering a few of these applications in detail.

Flare Gas Metering

Flare metering is an application strewn with failed techniques. This is partly due to the lack of desire to carry out such measurements and the consequent use of the cheapest possible instruments. However, it is clear now that there are tangible benefits to measuring flare gas, not only due to environmental concerns but as a process control mechanism and an indicator of plant efficiency. With the reducing cost of ultrasonic meters and ease of installation it is becoming very viable not only to place them in the main Flare line but also the feeders from the various processes, giving a much clearer idea of where the flare gas is being generated. The good performance at medium and low velocities makes the meter very attractive for flare metering. Also, as was shown in equation 5, the density can be obtained from the velocity of sound, pressure and the Poissons ratio. Further, knowing the temperature it is possible to measure the Molar mass, and indication of the gas quality. Poissons ratio varies with gas content but by taking a mean default mixture it is possible for most applications to obtain an answer within 5%.

Compressor Stations

Because of the ability of the ultrasonic meter to measure unsteady flows, it is ideal for metering flow from compressors. As the pipework is usually very tight the fact that the meter can be installed by "hot tapping" and can be close to the compressor and still give good answers make it ideal. The results shown in Fig. 10 are from a Tenneco station in Texas.

Gas Mixing

In many countries a variety of gas qualities are used to make up the final mix. Often the pipe line is underground. The ability to insert both transducers from the same side combined with installation under pressure and a good level of precision, make the meter very suitable for these applications.

Level Detection

Again the "hot-tapping" installation combined with the lack of added pressure drop make this type of meter useful for leak detection on gas transport systems. When installed large distances apart, 50km, a long term comparison of the results gives a good indication of the presence of small leaks.

CONCLUSIONS

New flow meter concepts, such as ultrasonic time of flight meters, have had their problems in the early days of development and application. However, technology has caught up with these problems very quickly and solved the majority of them. The result is a meter that is becoming well proven as a technology, particularly in the medium precision range of metering. Custody transfer metering is now also becoming feasible with the development of multi-path methods to enhance the accuracy. The major advantages of the technique are the wide dynamic range, negligible pressure drop, lack of sensitivity to liquid droplets and solid particles in the flow, high repeatability, good precision and a variation in design to suit different applications. A major feature for the future is the strong relationship between the meter performance and advances in electronic and computer technology. This ensures that the meters will continue to improve their performance and economic viability.

REFERENCES

- 1.0 Malone J.T. ,1971 US Patent 3,564,912
- 2.0 Drenthen J.G, Huijsmans F.J.J., Gassonic-400 Single Path Ultrasonic Flow meter, Stork Servex B.V.
- 3.0 Drenthen J.G, Huijsmans F.J.J , Gassonic-400 & P.sonic & Q.sonic Ultrasonic Gas Flow Meters, Stork Servex BV.
- 4.0 Rothfus R.R, Monrand C.C, Correlation of Turbulent Velocities for Tubes and Parallel Plates, Indust. and Engng. Chem. 47 1955 1144

ACKNOWLEDGEMENTS

The authors wish to thank Stork Servex BV for permission to publish this paper

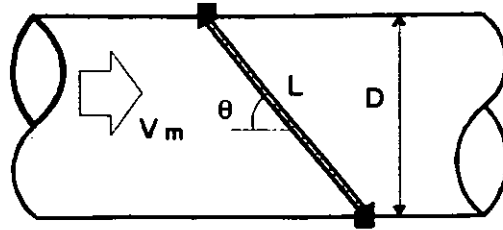


Fig. 1 BASIC SYSTEM

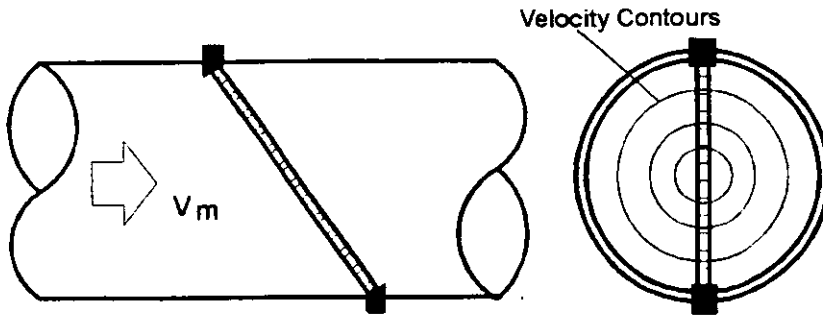


Fig. 2 SINGLE PATH TRANSMISSION

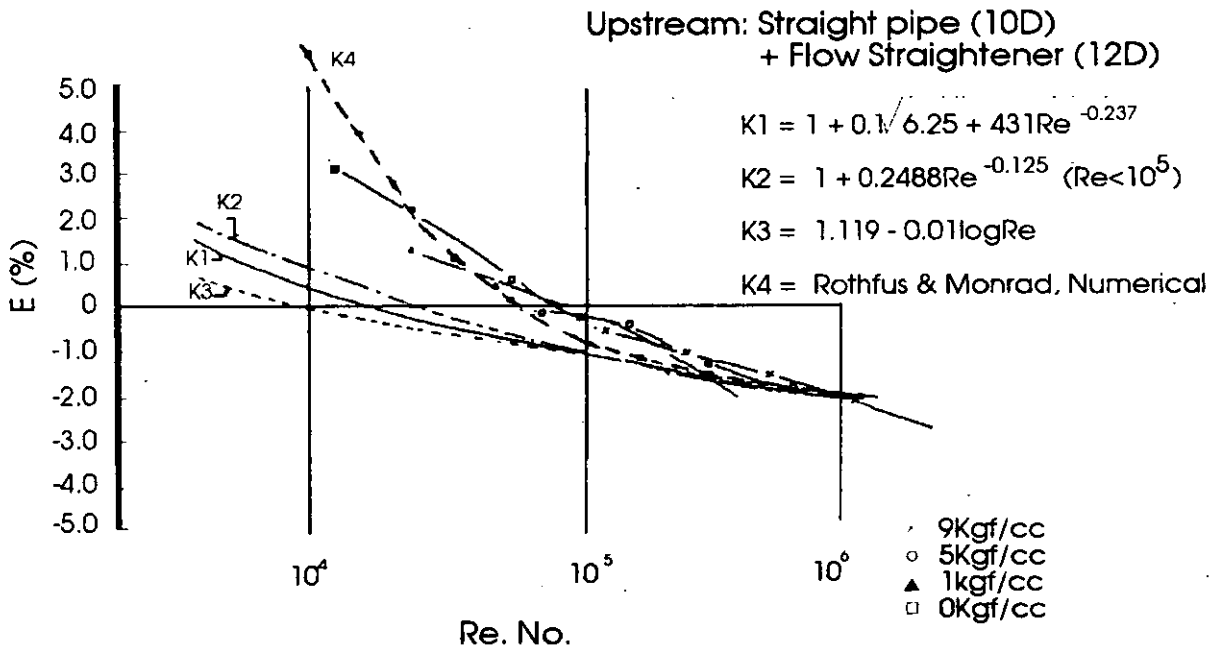


Fig. 3 CHARACTERISIC OF REYNOLDS NUMBER

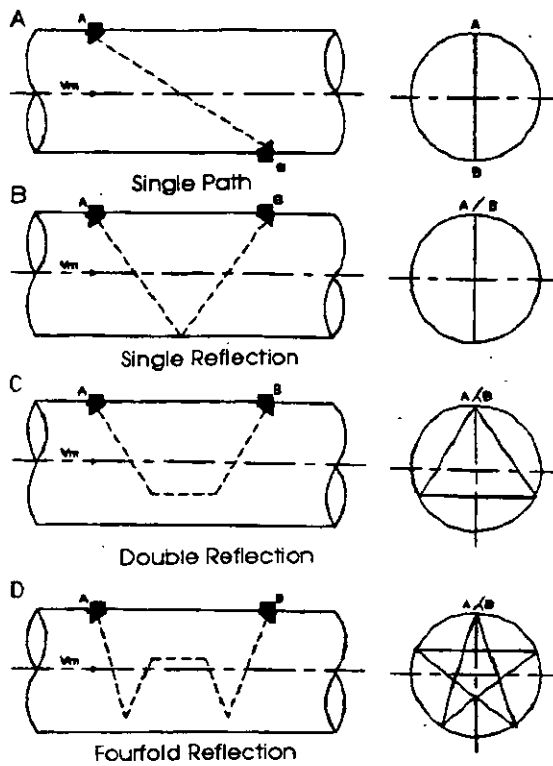


Fig. 4 PATH VARIATIONS

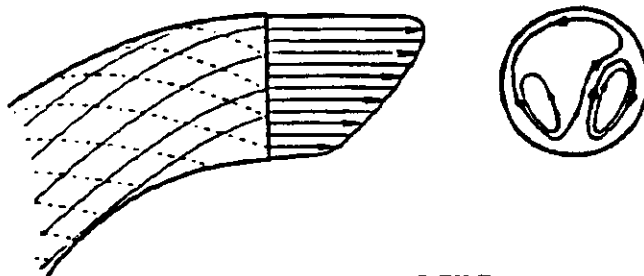


Fig. 5 SWIRL PROFILE

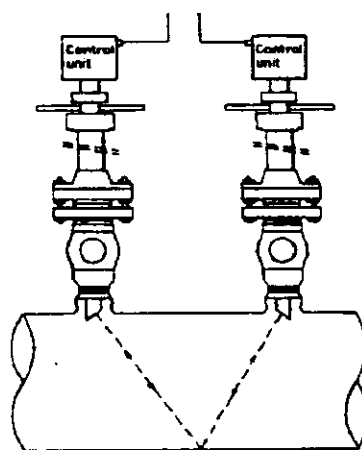


Fig. 6 GASSONIC 400 INSTALLATION

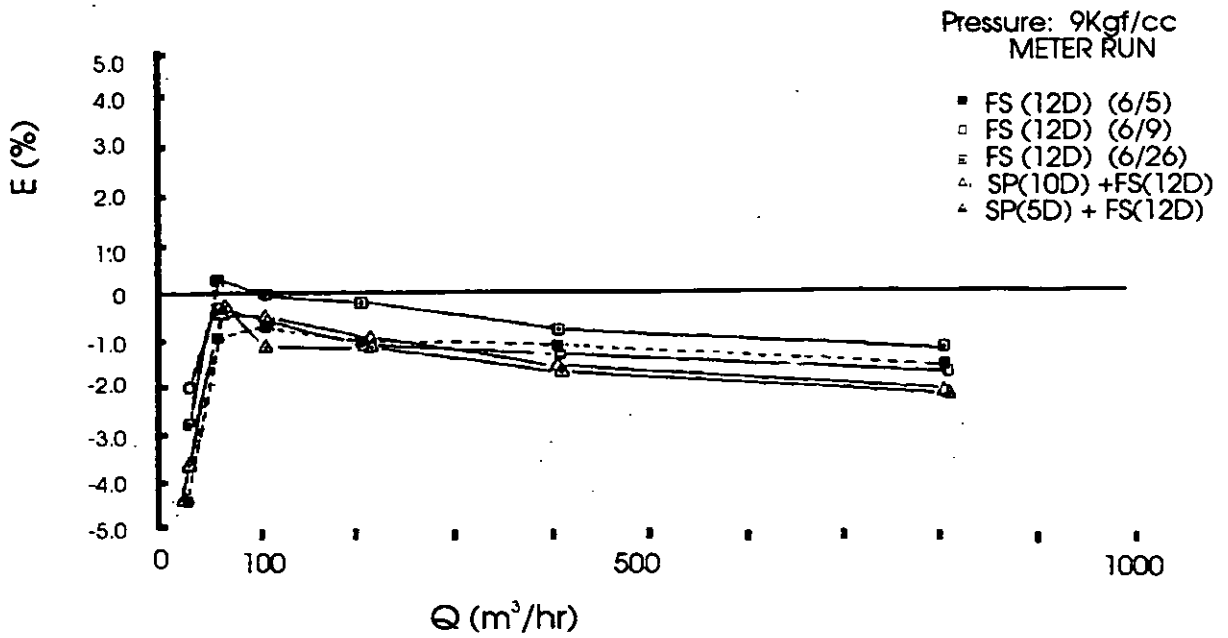
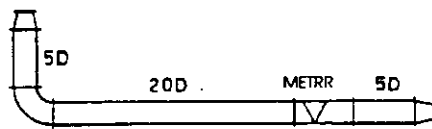
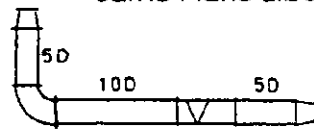


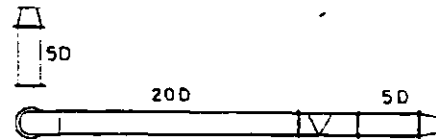
Fig. 7 CALIBRATION WITH VARIOUS PIPE ARRANGEMENTS



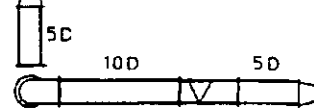
Same Plane Elbow SP20D



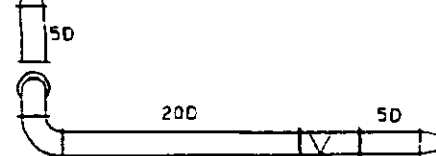
Same Plane Elbow SP10D



Cross Plane Elbow SP20D



Cross Plane Elbow SP10D



Complex Planes Elbow 20D

Flow Direction →

Fig. 8 PIPE ARRANGEMENTS

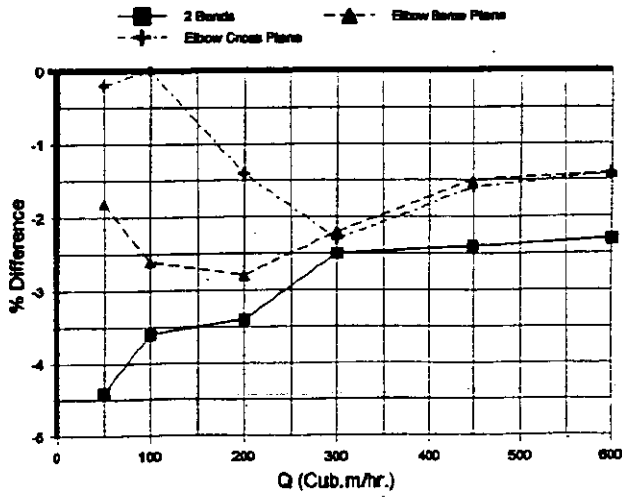


Fig.9a CHANGE IN CALIBRATION WITH VARIOUS BEND CONFIGURATIONS AT 20D

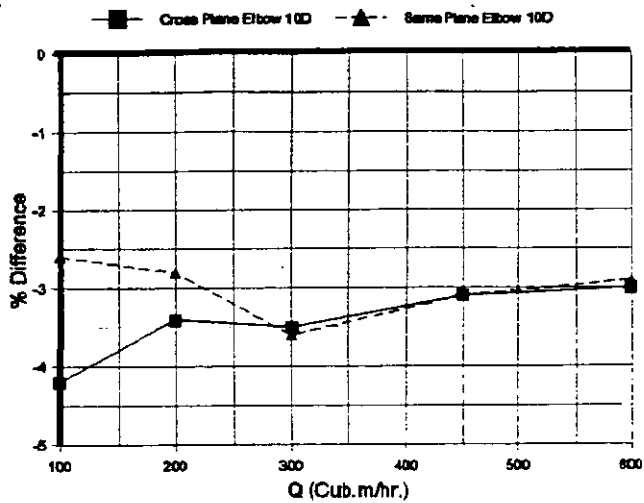


Fig. 9b CALIBRATION CHANGE WITH ELBOWS AT 10D

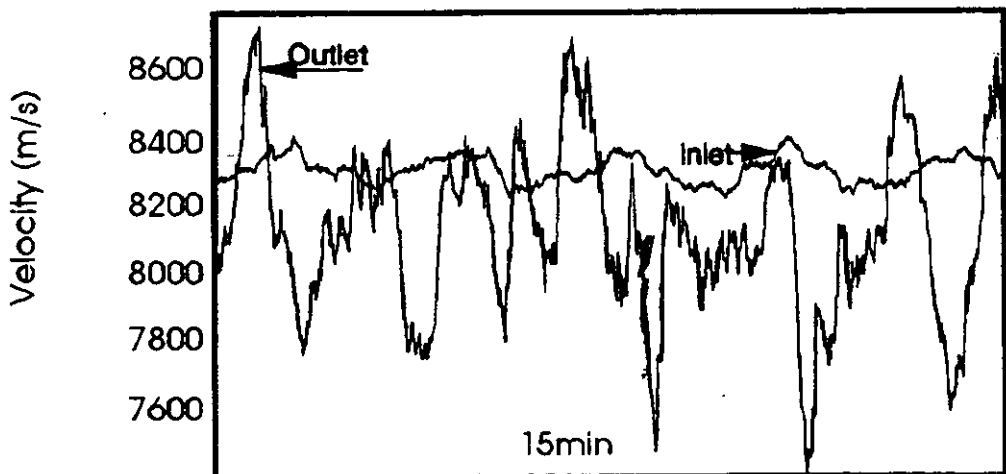


Fig. 10 PULSATING FLOW

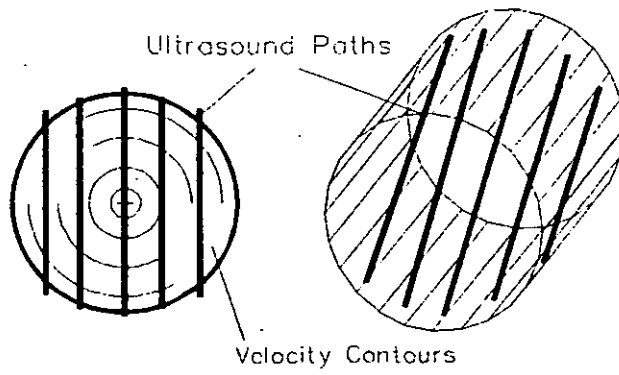


Fig. 11 CONVENTIONAL MULTI-PATH CONFIGURATION

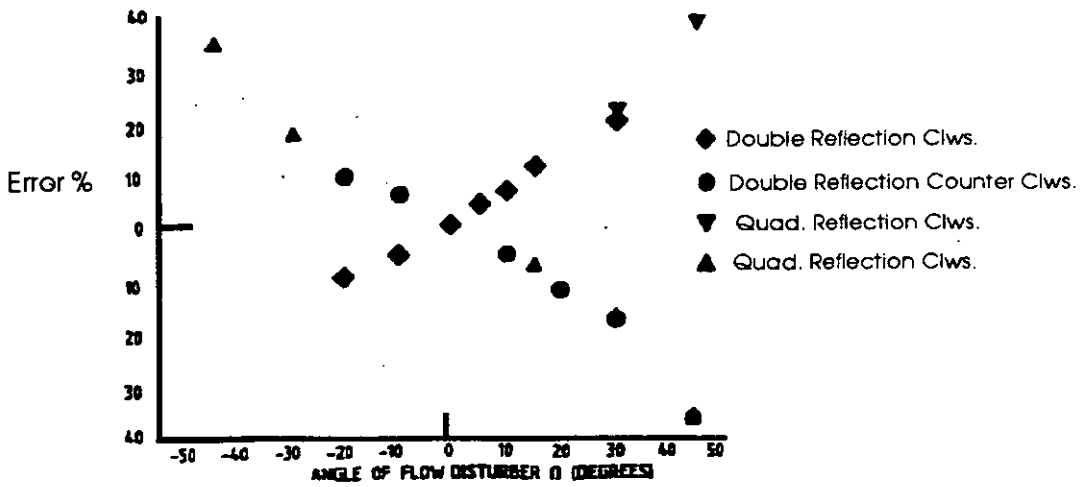


Fig. 12 OUTPUT ERROR WITH SWIRL ANGLE MULTI-REFLECTORS

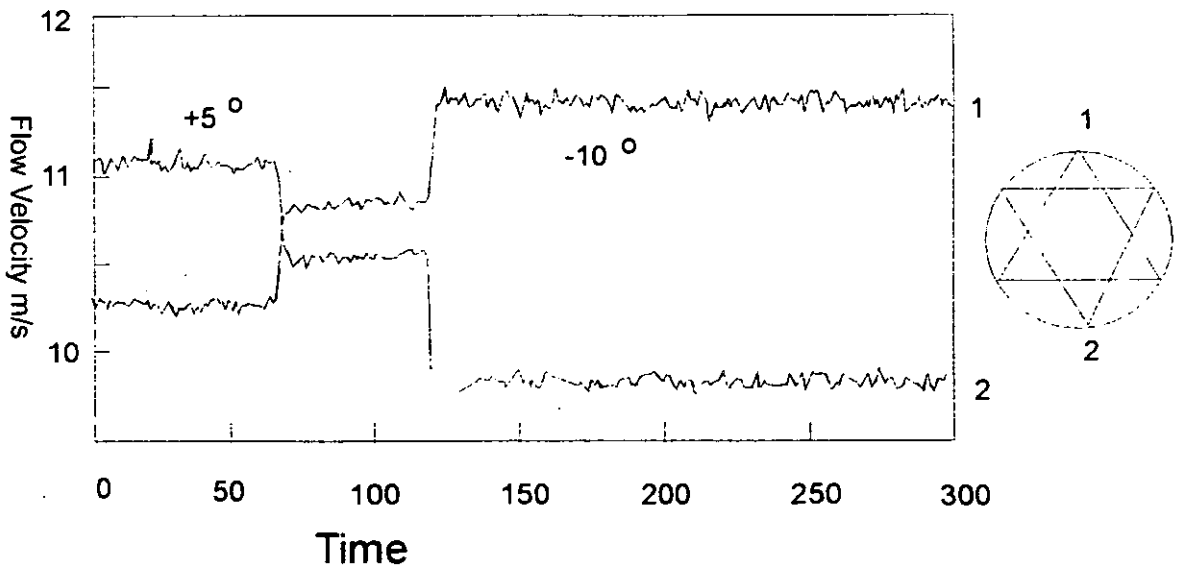


Fig. 13 SWIRL EFFECT ON DOUBLE REFLECTION PATHS

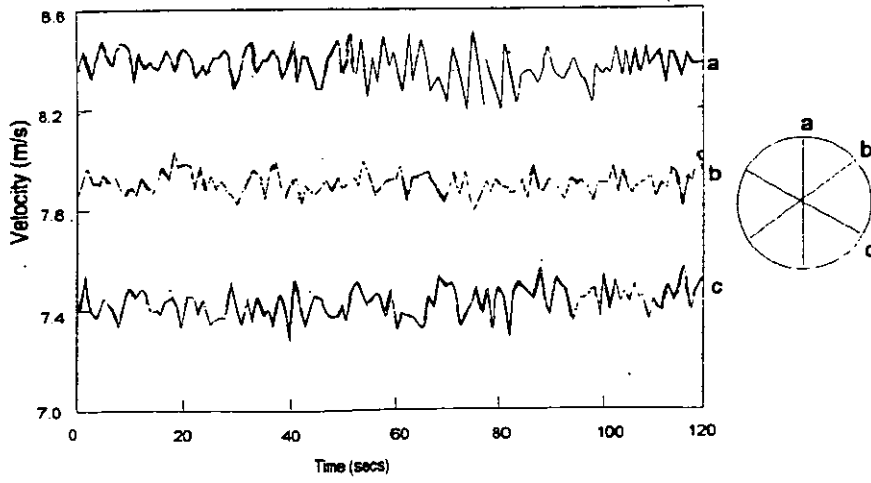


Fig. 14 PROFILE EFFECT ON SINGLE REFLECTIONS

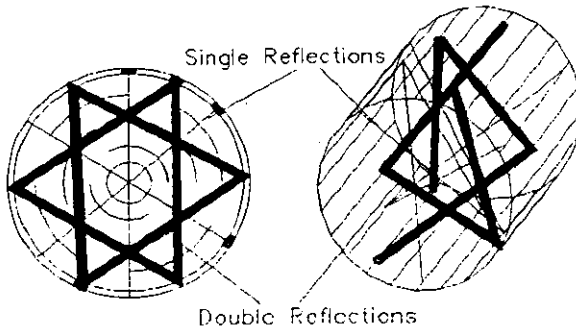


Fig. 15 Q.SONIC PATH CONFIGURATION

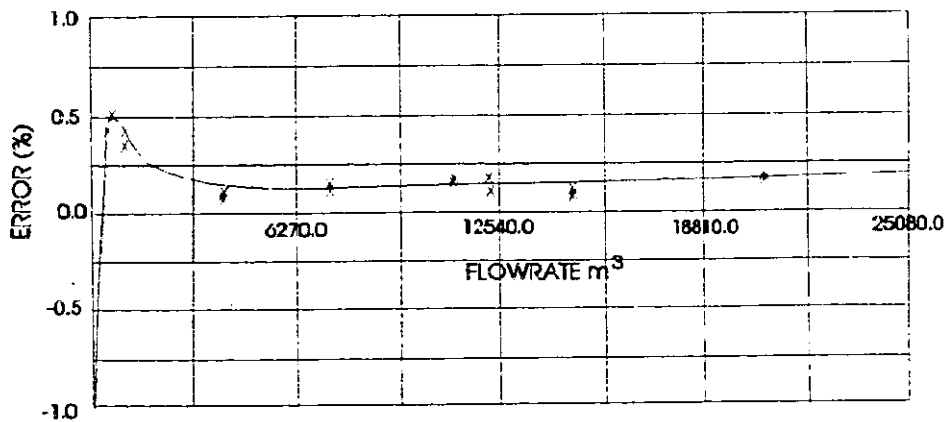


Fig. 16a CALIBRATION OF Q.SONIC METER

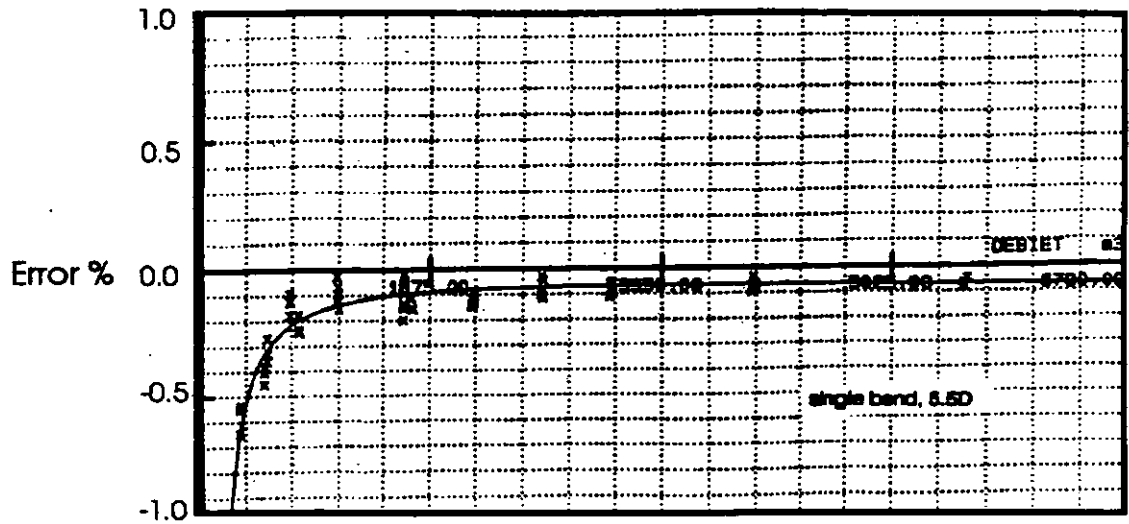


Fig 16b SINGLE BEND (PRELIMINARY RESULTS)

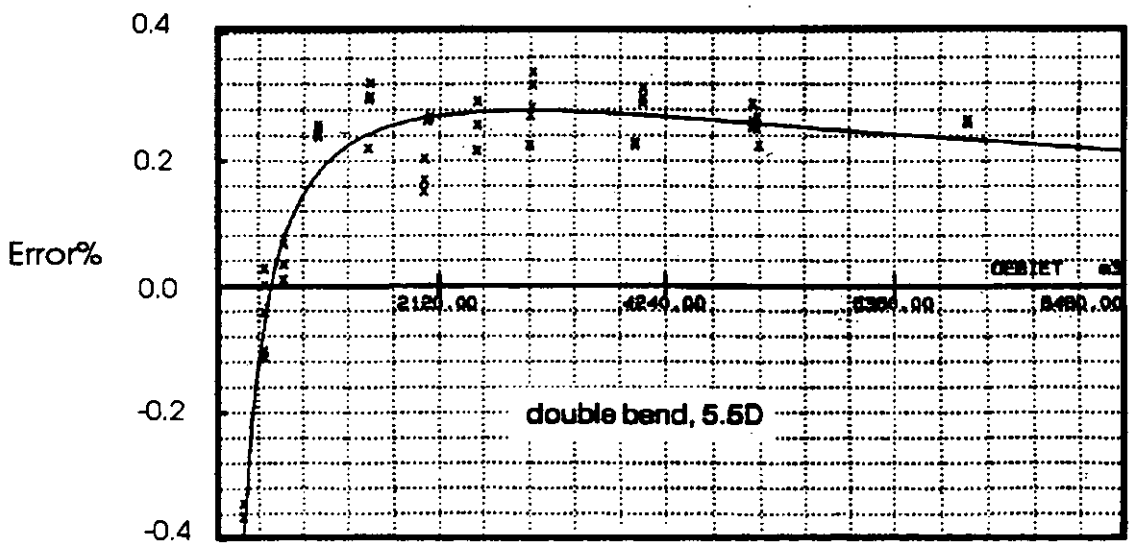


Fig. 16c DOUBLE BEND (PRELIMINARY RESULTS)

SESSION 5

SAMPLING

Chairman - A W Jamieson, Shell UK

WATER IN OIL: ON-LINE MEASUREMENT. THE MFI WATER CUT METER IN OFFSHORE APPLICATION.

R Purvey

British Petroleum Research, Sunbury-on-Thames, Middlesex.

1. SUMMARY

BP is currently investigating the performance of the MFI water cut meter for fiscal water content measurement of pressurised crude oil. A series of tests have been carried out to determine meter performance with reference to the ISO3171 (1) fiscal accuracy criteria. Manual sampling techniques have been developed in order to validate meter accuracy in measurement of instantaneous produced water content. Simultaneous flow rate, temperature, pressure, density and water content data were logged and flow weighted water content values calculated on a daily basis. The MFI daily average water cut was then compared with results obtained using the fiscal automatic sampling system. This paper presents the results and findings of a series of tests carried out on a 2 inch MFI water cut meter, installed in the fiscal sampling flow loop on the BP Forties Charlie platform. Data relate to the periods October 1993 and May to July 1994.

2. INTRODUCTION

2.1 Background

BP and Multi-Fluid International (MFI) have been in co-operation throughout the period of development of the on-line water cut meter. Early work on validating instrument accuracy was encouraging and BP Research, Sunbury, became involved with meter testing under actual service conditions. Following successful tests in measuring the produced water content of a variety of stabilised crude oils at Grangemouth and Rotterdam Refinery, together with results obtained by Statoil at Mongstad (2), BP Forties agreed on a long term trial to assess the meter's performance in an offshore environment.

A 2 inch MFI water cut meter was first installed in the fiscal sampling flow loop on the BP Forties Charlie platform in October 1993. After fiscal metering, Forties Blend crude oil is exported from Forties Charlie to Kinneil, Grangemouth. Typical, flow-loop oil temperature and pressure conditions are 35°C and 100 barg respectively. The original, prototype, meter was upgraded to allow compensation for changes in line pressure and oil density, and was installed in May 1994. The upgraded device incorporated an auto-zero function which enabled the instrument to calculate the flowing oil dry oil dielectric constant (ϵ) with reference to the measured density and simultaneous water content. Thus, the instrument zero is automatically 'calibrated' and updated according to changes in the flowing oil composition (dry oil density).

2.2 MFI Water Cut Meter: Operating Principle

Full details of the MFI water cut meter operating principle are given in the Manufacturer's Literature (3). Briefly, the meter uses a cavity resonator for measuring dielectric constant (ϵ). The meter utilises the large difference in the values of ϵ , for oil and water, to determine water content. The value of ϵ for dry oil sets the instrument zero, and the value of ϵ for the produced water sets the instrument span.

2.2 Compatibility of Data

Pressurised oil manual sampling techniques were developed to facilitate representative 'spot' sampling for accurate measurement of the instantaneous water content of the flowing oil.

The MFI water cut meter measures the saline water content of the flowing oil. The accuracy of the MFI meter was investigated by comparison with Karl Fischer coulometric titration (KF) which determines pure water content. Sample handling methodology was carried out in accordance with Forties Field Analysis (FFA) procedures. The actual KF analysis followed the procedures of IP386 (4) and therefore provided a traceable standard. Direct comparison of the KF, FFA, pure water content, %weight (%w/w), was made after conversion of the KF value to the equivalent saline produced water content, %volume (%v/v), see Appendix 1. The meter was deemed to indicate the 'correct' water content if the agreement between the KF and the MFI was within the ISO3171 fiscal acceptance criteria as follows:-

- produced water content 0 - 1 %v/v : ± 0.05 %v/v absolute.
- produced water content > 1 %v/v : ± 5 % relative.

Since comparisons of data are between results obtained from two separate sampling/measurement systems, each required to operate within an accuracy specification of $\pm 5\%$, a more appropriate relative acceptance limit of $\pm 7\%$ (ie. $\sqrt{2} \times \pm 5\%$) could be applied.

3. MFI WATER CUT METER

3.1 Instrument Calibration

The main set-up calibration was carried out by input of the dry oil density (for instrument calculation of the corresponding dielectric constant, ϵ) and the produced water conductivity. These data set the instrument zero and span respectively. The meter measures water content in the range 0-20 %vol.

3.1.1 4-20mA Signals

Prior to datalogging, all the 4-20mA signals were calibrated. In order to maximise accuracy of each measurement, each signal span was set to the minimum acceptable range. Flow rate, density and line pressure signals were taken from the local control room computer. Temperature and water content signals were measured directly from the MFI unit. Particular attention was paid to the calibration of the 4-20mA output for the water cut signal. An accurate current loop meter was used for the calibration, which was carried out in accordance with the manufacturer's published procedures (3). The MFI water content 4-20mA output signal calibration was re-checked at the end of the trial period and no change was detected in the signal accuracy.

3.1.2 On-Line Water Content Calibration

The parameters required for on-line calibration were the flowing oil density and temperature, and the corresponding pipeline pure water content. Oil density and temperature data were obtained from the in-line fiscal densitometers and the MFI calibrated thermal sensor respectively. Comparative, instantaneous, oil water content determination was carried out by KF analysis of a pressurised oil manual 'spot' sample. On completion of input of the calibration data the MFI meter calculated a 'new' value for ϵ , and the corresponding water content correction to be applied to the 'old' measurements. The instrument then displayed an option to save the 'new' value for ϵ . When saved, all subsequent measurements were carried out using the updated calibration data.

3.2 Auto-Zero Function

The MFI meter utilises a relationship between dry oil dielectric constant (ϵ) and density. The instrument manufacturer has developed an automatic calibration method where the instrument is linked to the output of an in-line fiscal standard densitometer and compensates for changes in ϵ by relating to measured changes in the dry oil density of the flowing fluid. The dry oil density is itself calculated within the meter's software and is related to the metered water cut. The instrument automatically re-zeros according to changes in the composition of the flowing oil stream. Thus, the MFI water cut signal should be maintained at optimum accuracy.

4: DATA ACQUISITION AND SAMPLING METHODOLOGY

4.1 MFI / Datalogging

A Magus 2000 datalogger was used to log daily data (18:00-18:00) commensurate with the automatic sampler 'daily' sample accumulation period. Flow rate, pressure, oil density, temperature and MFI water content data were logged at 5 second intervals. A real time display graph was used to monitor the data collection and observe production and water content stability. Data were recorded on a daily basis and calculations of the flow weighted average MFI water content were carried out.

4.2 Manual 'Spot' Sampling

In order to acquire independent data on the instantaneous water content of the flowing oil, pressurised manual 'spot' samples were taken for KF analysis. Figure 1 shows the MFI water cut meter installation in the fast-loop pipework. The fiscal densitometers and the MFI installation are shown in Figure 1A. Figure 1B shows a close-up of the MFI meter and a 50 ml Piston Internal Mixing Receiver (PIMR) installed for manual sampling for calibration or instantaneous water content comparison purposes. Figure 2 shows the MFI electronics enclosure and the location of the two automatic samplers.

A 50ml PIMR was connected to the pressurised oil manual sampling point, adjacent to the MFI meter, using a 30cm length of 1/4" OD flexible pressure hose. Oil was allowed to flow straight through the PIMR, via the internal mixing baffle plate, such that the sample chamber was not filled. When the instantaneous water content was observed to be constant (within about 0.05-.10 %v/v) the PIMR outlet valve was closed and pressurised oil was collected in the sample chamber. The PIMR sample was then allowed to cool and water content analysis was carried out in accordance with the FFA methodology.

On-line calibration and investigation of MFI water content data accuracy was carried out by comparison of instantaneous water content measurements. Manual 'spot' samples were obtained and corresponding MFI data recorded during the sampling period (5 - 10 seconds). Prior to sampling, the MFI water content reading was monitored via a portable computer terminal. The stability of the flowing oil water content was determined by observation and a 'spot' sample was taken at an appropriate time. Immediately the 'spot' sample was obtained, the actual time (synchronised with the datalogger clock) was recorded. The concurrent MFI water content measurement, together with the related line conditions (ie. pressure, temperature and density) were obtained from the datalogger by averaging the results over the sampling period. Water content stability was confirmed by observation of the datalogger results around the sampling time. If acceptable stability was not achieved, then a replacement manual sample was taken.

4.3 Automatic Sampling

The fiscal automatic sampling system on Forties Charlie comprises two flow proportional cell samplers installed in the sampling fast-loop, and spaced about 30 cm apart. Under normal operating conditions, 1 litre 'daily' and 3 litre 'weekly' samples are obtained. The samples are of pressurised oil and are collected in PIMRs. For the duration of the trials, arrangements were made to operate both automatic samplers at the same 'daily' sampling rate.

MFI flow weighted 'daily' water content results, calculated from the logged data, were compared with corresponding fiscal measurements obtained from the automatic sampling system. Test comparisons were made using the two concurrent 'daily' 1 litre PIMR samples to 'confirm' daily automatic sample representativity, thus providing 'valid' results.

MFI/Automatic sampler 'daily' water content data comparisons were deemed valid if none of the following faults were identified with either the sampling, measuring or datalogging equipment:

- | | |
|---------------------------------------|---|
| (i) Sampler operation suspect: | Monitored by grab size and visual inspection. |
| (ii) Sample representativity suspect: | Deemed representative if both samples agreed within $\pm 5\%$ relative. |
| (iii) MFI over-ranged: | Produced water content $> 20\%v/v$. |
| (iv) MFI down-time: | Data off line. |
| (v) Datalogger fault: | Data loss due to logger down time (eg. power loss). |

5. RESULTS

5.1 MFI / Manual 'Spot' Samples

5.1.1 Auto-Zero Off / Not Installed

A summary of the comparative data, obtained prior to fitting and enabling the MFI auto-zero function, is presented in Table 1. Figure 3 shows the absolute difference between the MFI water content values and the comparable reference 'spot' samples. These data are presented with reference to the ISO3171 limits of $\pm 5\%$. Calibration data are identified separately, as indicated in Figure 3.

Overall the data indicate very good agreement with the reference manual 'spot' sampling results and are within the $\pm 5\%$ acceptance criteria, for produced water contents in the range 0-10.6 $\%v/v$. The data reflect the findings of previous BP trials and the Statoil tests (2), carried out on stabilised crude oils.

5.1.2 Auto-Zero On

Comparative data, obtained after initialising the auto-zero function, are presented in Table 2 and shown in Figure 4.

It is observed that these data show a obvious improvement on the results obtained without the benefit of the auto-zero option. The average absolute difference between the MFI and reference water content was just 0.005 $\%v/v$ for the 14 data points. The results covered the range 0-7 $\%v/v$ produced water content, and indicate remarkable agreement between the MFI and reference manual 'spot' sample results. The data clearly demonstrate that the MFI water cut meter (auto-zero function enabled) provides instantaneous water content measurement well within the fiscal acceptance limits of ISO3171.

5.2 MFI / Automatic 'Daily' Samples

Data obtained from the comparison of MFI and automatic sampler 'daily' water content determinations are presented in Table 3.

Figure 5 shows the absolute differences between the MFI and the comparable autosampler average 'daily' samples. With the auto-zero on, 4 of the 19 data points are outside the acceptance criteria of $\pm 5\%$. Since comparisons of data are between results obtained from two separate sampling/measurement systems, each required to operate within an accuracy specification of $\pm 5\%$, a more appropriate relative acceptance limit of $\pm 7\%$ (ie. $\sqrt{2} \times \pm 5\%$) could be applied. Referring to the less stringent accuracy limits, just 1 of the 19 data points lies outside the acceptance band. These results are most encouraging, and consideration of the observed accuracy in the measurement of instantaneous water content reinforce the view that the MFI meter provides an accurate measure of the flowing oil produced water content.

5.3 'Daily' Logged Data

The datalogger was programed to log 'daily' data files of flow rate, pressure, oil density, temperature and MFI water content. All data channels were logged at 5 second intervals. 'Daily' data files comprised a log of 1 minute average values from the logged data channels. The 'daily' data files were imported into spreadsheet format and plots of 'instantaneous' pipeline water content and oil density made. A change in flowing oil density will occur as a result of a change in the produced water content. Thus water content and oil density should show the same instantaneous trend. The equivalent oil dry oil density at 0 barg and 15°C was also computed. Major change in dry oil composition should only occur as a result of a major alteration in production. Thus the dry oil density (at standard conditions) should remain essentially constant. A demonstration plot is shown in Figure 6. MFI water content and oil density data are plotted against time for the 24 hour period of automatic sampling for Test A8. The water content and density data have been scaled to show peaks of comparable amplitude. Clearly the MFI water content and fiscal densitometer plots show almost identical trends. Furthermore the computed dry oil data show an essentially constant value despite observed differences in pipeline oil density of up to 0.015 kg/l.

Although the data do not prove instrument accuracy, the graphs presented in Figure 6 demonstrate consistency of MFI data. Combined with the accuracy in measurement of instantaneous water content, verified from the results of the comparisons with the reference manual 'spot' samples, it appears that the MFI meter should readily satisfy fiscal accuracy requirements for determination of daily average water content.

5.4 Operational Considerations

During the BP trials, there were several instances of instrument down-time as a result of software limitations. These problems are currently being addressed by the manufacturer and should be overcome in due course. Continuous trouble free service, with the minimum of maintenance, is as important as accuracy of determination in an on-line monitoring/measurement system. Long term trials are needed to prove instrument acceptability for both accuracy and operational requirements.

6. CONCLUSIONS

The results of the BP Forties offshore application trials have demonstrated that the MFI water cut meter is capable of accurate water content measurement of a pressurised oil stream. The test instrument had a range of operation from 0-20 %vol and worked well, within the operational range. Unstable water content is common on Forties Charlie and water contents above 20 % are not unusual. In order to provide a fair test of the MFI meter, stability of production was required providing continuous water content below the maximum 20 % throughout daily sample accumulation periods.

Problems associated with instrument down-time have been attributed to limitations in software and corrective action is currently being taken by the manufacturer. Long term stability and trouble free operation are important factors for on-line measurement systems. Ongoing trials should provide the data needed to confirm acceptance for fiscal measurement within the oil industry.

7. REFERENCES

1. **INTERNATIONAL STANDARD ISO 3171: 1988(E)**
Petroleum Liquids - Automatic Pipeline Sampling.
2. **OKLAND, O. BERENTSEN, H. and OLSEN, O. - Testing Water in Oil Monitors at the Mongstad Terminal.**
North Sea Flow Measurement Workshop 1993, 26-28 October, Bergen.
3. **MFI WATER CUT METER. INSTALLATION AND USER'S MANUAL**
Multi-Fluid International AS, PO Box 112, N-4033 Forus, Norway.
4. **STANDARD METHODS FOR ANALYSIS AND TESTING OF PETROLEUM AND RELATED PRODUCTS**
Designation IP386/90 (ASTM D4928-89)
Determination of Water Content of Crude Oil-Coulometric Karl Fischer Method.

APPENDIX I

CONVERSION OF WATER CONTENT:

(%WEIGHT PURE WATER TO % VOLUME SALINE WATER)

$$(i) \quad \%v/v^* = (\%w/w^*/Db_{(T,P)}) / ((\%w/w^*/Db_{(T,P)}) + ((100 - \%w/w^*)/Dd_{(T,P)}))$$

$$ie. \quad \%v/v^*_{(T,P)} = \frac{\text{Volume Produced Water}_{(T,P)}}{\text{Volume Produced Water}_{(T,P)} + \text{Volume Dry Oil}_{(T,P)}}$$

$$(ii) \quad \%v/v^* = \%w/w \times SCF \times Dl_{(T,P)} / Db_{(T,P)}$$

$$ie. \quad \%v/v^*_{(T,P)} = \% \text{Weight Pure Water} \times \text{Salt Correction Factor} \times \frac{\text{Line Density}_{(T,P)}}{\text{Brine Density}_{(T,P)}}$$

Where: $\%v/v^*$ is the %volume of produced/saline water at line conditions.
 $\%w/w^*$ is the %weight of produced/saline water at line conditions.
 $Db_{(T,P)}$ is the produced/saline water density at line conditions.
 $Dd_{(T,P)}$ is the dry oil density at line conditions.

Equations (i) and (ii) are equivalent, and represent the calculations used by MFI and the Forties System Allocation Schedule of Analysis (FSASA) respectively.

(Auto-Zero Off / Not Installed)

| Test Ref No | Sample Water Content | | MFI Reading (%v/v) | MFI Water Content (%v/v) | Diff (MFI-Sample) (%v/v) | Relative Diff (%) |
|-------------|----------------------|----------------------|-----------------------|-----------------------------|--------------------------------|----------------------|
| | (pure) (%w/w) | (produced) (%v/v) | | | | |
| M1 | 4.70 | 4.04 | 5.62 | 4.10 | 0.06 | 1.4 |
| M2 | 3.58 | 3.07 | 4.59 | 3.07 | 0.00 | 0.0 |
| M3 | 4.59 | 3.94 | 4.12 | 4.12 | 0.18 | 4.6 |
| M4 | 0.90 | 0.77 | 0.64 | 0.76 | -0.01 | -0.7 |
| M5 | 9.29 | 8.05 | 8.38 | 8.38 | 0.33 | 4.1 |
| M6 | 10.67 | 9.28 | 9.40 | 9.40 | 0.12 | 1.3 |
| M7 | 4.86 | 4.15 | 4.26 | 4.26 | 0.11 | 2.7 |
| M8 | 4.79 | 4.08 | 4.23 | 4.23 | 0.15 | 3.6 |
| M9 | 5.69 | 4.88 | 5.07 | 4.90 | 0.02 | 0.5 |
| M10 | 5.52 | 4.72 | 5.03 | 4.86 | 0.14 | 2.9 |
| M11 | 10.61 | 9.19 | 9.32 | 9.32 | 0.13 | 1.5 |
| M12 | 8.67 | 7.48 | 8.05 | 8.05 | 0.57 | 7.7 |
| M13 | 3.55 | 3.02 | 3.01 | 3.01 | -0.01 | -0.5 |
| M14 | 11.72 | 10.18 | 10.50 | 10.50 | 0.32 | 3.2 |
| M15 | 8.95 | 7.70 | 8.06 | 8.06 | 0.36 | 4.7 |
| M16 | 11.67 | 10.16 | 10.56 | 10.56 | 0.40 | 4.0 |
| M17 | 10.34 | 8.93 | 9.30 | 9.30 | 0.37 | 4.1 |
| M18 | 9.40 | 8.11 | 8.22 | 8.22 | 0.11 | 1.3 |
| M19 | 12.21 | 10.61 | 10.64 | 10.64 | 0.03 | 0.3 |
| M20 | 9.33 | 8.05 | 8.17 | 8.17 | 0.12 | 1.5 |
| M21 | 6.78 | 5.81 | 5.88 | 5.88 | 0.07 | 1.2 |
| M22 | 5.30 | 4.54 | 4.78 | 4.57 | 0.03 | 0.6 |
| M23 | 4.31 | 3.68 | 3.62 | 3.62 | -0.06 | -1.6 |
| M24 | 3.14 | 2.67 | 2.60 | 2.60 | -0.07 | -2.7 |
| M25 | 2.85 | 2.43 | 2.47 | 2.47 | 0.04 | 1.8 |
| M26 | 3.10 | 2.64 | 2.59 | 2.59 | -0.05 | -2.0 |
| M27 | 3.20 | 2.73 | 2.63 | 2.63 | -0.10 | -3.6 |
| M28 | 2.92 | 2.49 | 2.51 | 2.51 | 0.02 | 0.9 |
| M29 | 0.60 | 0.51 | 0.31 | 0.51 | 0.01 | 1.2 |
| M30 | 11.45 | 10.00 | 10.31 | 10.31 | 0.31 | 3.1 |
| M31 | 7.36 | 6.35 | 6.65 | 6.65 | 0.30 | 4.8 |
| M32 | 7.86 | 6.77 | 6.62 | 6.62 | -0.15 | -2.3 |
| M33 | 3.17 | 2.71 | 2.80 | 2.80 | 0.09 | 3.2 |
| M34 | 4.36 | 3.74 | 4.00 | 4.00 | 0.26 | 6.9 |
| M35 | 3.17 | 2.71 | 2.82 | 2.71 | 0.00 | 0.1 |

(Auto-Zero On)

| Test Ref No | Sample Water Content | | MFI Reading (%v/v) | MFI Water Content (%v/v) | Diff (MFI-Sample) (%v/v) | Relative Diff (%) |
|-------------|----------------------|----------------------|-----------------------|-----------------------------|--------------------------------|----------------------|
| | (pure) (%w/w) | (produced) (%v/v) | | | | |
| M36 | 1.83 | 1.56 | 1.83 | 1.57 | 0.01 | 0.5 |
| M37 | 2.15 | 1.83 | 2.10 | 1.84 | 0.01 | 0.5 |
| M38 | 4.17 | 3.57 | 3.87 | 3.61 | 0.04 | 1.1 |
| M39 | 6.60 | 5.69 | 5.95 | 5.69 | 0.00 | 0.0 |
| M40 | 5.66 | 4.86 | 4.95 | 4.93 | 0.07 | 1.4 |
| M41 | 5.05 | 4.34 | 4.29 | 4.29 | -0.05 | -1.2 |
| M42 | 6.16 | 5.31 | 5.30 | 5.30 | -0.01 | -0.1 |
| M43 | 6.65 | 5.71 | 5.55 | 5.55 | -0.16 | -2.8 |
| M44 | 6.42 | 5.48 | 5.61 | 5.61 | 0.13 | 2.4 |
| M45 | 8.12 | 6.97 | 6.97 | 6.97 | 0.00 | 0.0 |
| M46 | 1.40 | 1.19 | 1.24 | 1.24 | 0.05 | 4.0 |
| M47 | 3.54 | 3.03 | 2.97 | 2.97 | -0.06 | -2.1 |
| M48 | 2.71 | 2.31 | 2.35 | 2.35 | 0.04 | 1.6 |
| M49 | 1.77 | 1.51 | 1.52 | 1.52 | 0.01 | 0.7 |

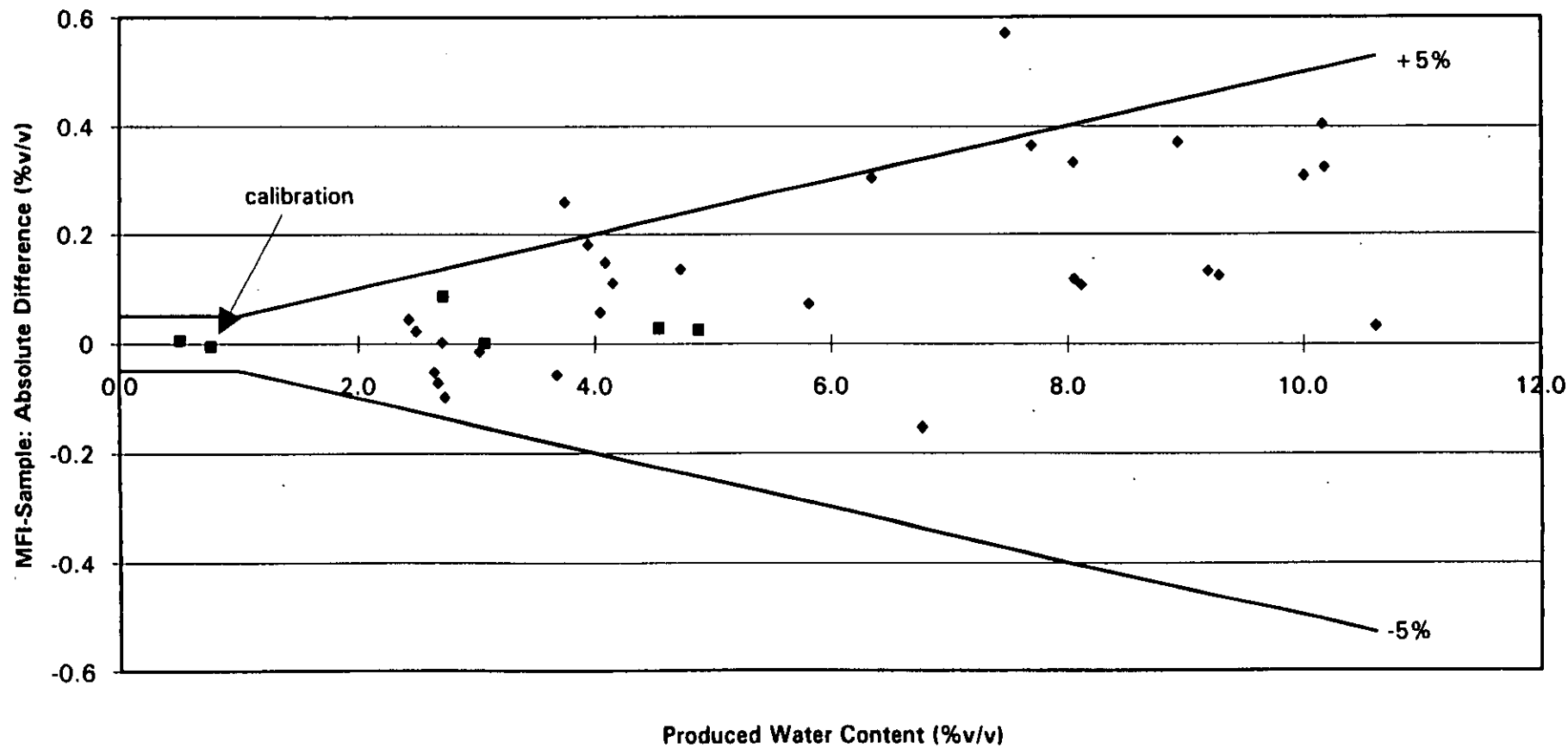
MFI / AUTO SAMPLER 'DAILY' WATER CONTENT COMPARISON

TABLE 3

| Test Ref No | Auto Sample Water Content | | | | | MFI Water Cut (2) (%v/v) | Absolute Difference (2)-(1) (%v/v) | Relative Difference (2)-(1) (%) |
|-------------|---------------------------|--------------|---------------------|------------------|-----------------------------|-----------------------------|---------------------------------------|------------------------------------|
| | Sampler No 1 | Sampler No 2 | Relative Difference | Average | Average | | | |
| | (%w/w) | (%w/w) | (%) | (pure) (%w/w) | (1) (produced) (%v/v) | | | |
| A1 | 11.140 | 11.652 | -4.6 | 11.396 | 9.970 | 10.500 | 0.530 | 5.3 |
| A2 | 7.604 | 7.585 | 0.2 | 7.595 | 6.652 | 6.980 | 0.328 | 4.9 |
| A3 | 6.751 | 6.937 | -2.8 | 6.844 | 5.900 | 6.290 | 0.390 | 6.6 |
| A4 | 5.655 | 5.748 | -1.6 | 5.702 | 4.899 | 5.170 | 0.271 | 5.5 |
| A5 | 5.183 | 5.287 | -2.0 | 5.235 | 4.492 | 4.719 | 0.227 | 5.1 |
| A6* | 4.938 | 4.908 | 0.6 | 4.923 | 4.224 | 4.227 | 0.003 | 0.1 |
| A7 | 3.267 | 3.232 | 1.1 | 3.250 | 2.783 | 2.789 | 0.006 | 0.2 |
| A8 | 3.565 | 3.638 | -2.0 | 3.602 | 3.085 | 3.217 | 0.132 | 4.3 |
| A9 | 5.899 | 6.096 | -3.3 | 5.998 | 5.166 | 5.317 | 0.151 | 2.9 |
| A10 | 6.087 | 6.347 | -4.3 | 6.217 | 5.337 | 5.255 | -0.082 | -1.5 |
| A11 | 3.603 | 3.607 | -0.1 | 3.605 | 3.081 | 2.956 | -0.125 | -4.1 |
| A12 | 7.137 | 7.204 | -0.9 | 7.171 | 6.200 | 6.322 | 0.122 | 2.0 |
| A13 | 5.407 | 5.158 | 4.6 | 5.283 | 4.527 | 4.420 | -0.107 | -2.4 |
| A14 | 6.352 | 6.392 | -0.6 | 6.372 | 5.485 | 5.507 | 0.022 | 0.4 |
| A15 | 5.293 | 5.301 | -0.2 | 5.297 | 4.509 | 4.271 | -0.238 | -5.3 |
| A16 | 3.214 | 3.250 | -1.1 | 3.232 | 2.762 | 2.503 | -0.259 | -9.4 |
| A17 | 3.476 | 3.514 | -1.1 | 3.495 | 2.982 | 3.038 | 0.056 | 1.9 |
| A18 | 6.405 | 6.528 | -1.9 | 6.467 | 5.549 | 5.869 | 0.320 | 5.8 |
| A19 | 5.101 | 5.109 | -0.2 | 5.105 | 4.379 | 4.431 | 0.052 | 1.2 |
| A20 | 5.530 | 5.345 | 3.3 | 5.438 | 4.676 | 4.840 | 0.164 | 3.5 |
| A21 | 6.077 | 5.986 | 1.5 | 6.032 | 5.182 | 5.140 | -0.042 | -0.8 |
| A22 | 5.558 | 5.650 | -1.7 | 5.604 | 4.819 | 4.755 | -0.064 | -1.3 |
| A23 | 4.779 | 4.655 | 2.6 | 4.717 | 4.042 | 3.970 | -0.072 | -1.8 |
| A24 | 2.832 | 2.854 | -0.8 | 2.843 | 2.423 | 2.262 | -0.161 | -6.6 |

* MFI Auto-Zero Function Enabled

MFI / MANUAL 'SPOT' SAMPLE (Auto-Zero Off/Not Installed)



[FIGURE 3]

MFI / MANUAL 'SPOT' SAMPLE (Auto-Zero On)

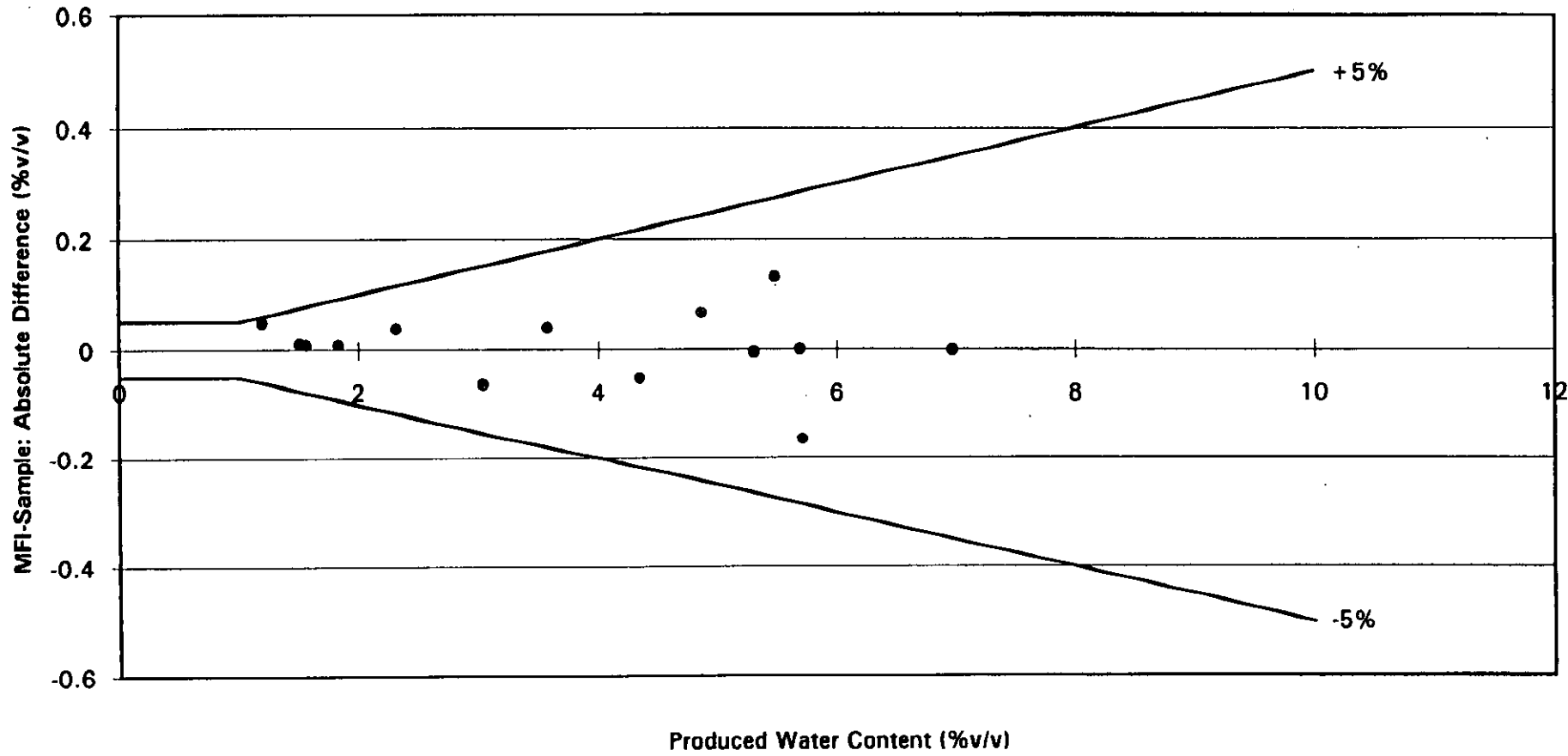


[FIGURE 4]

MFI / AUTO 'DAILY' SAMPLE

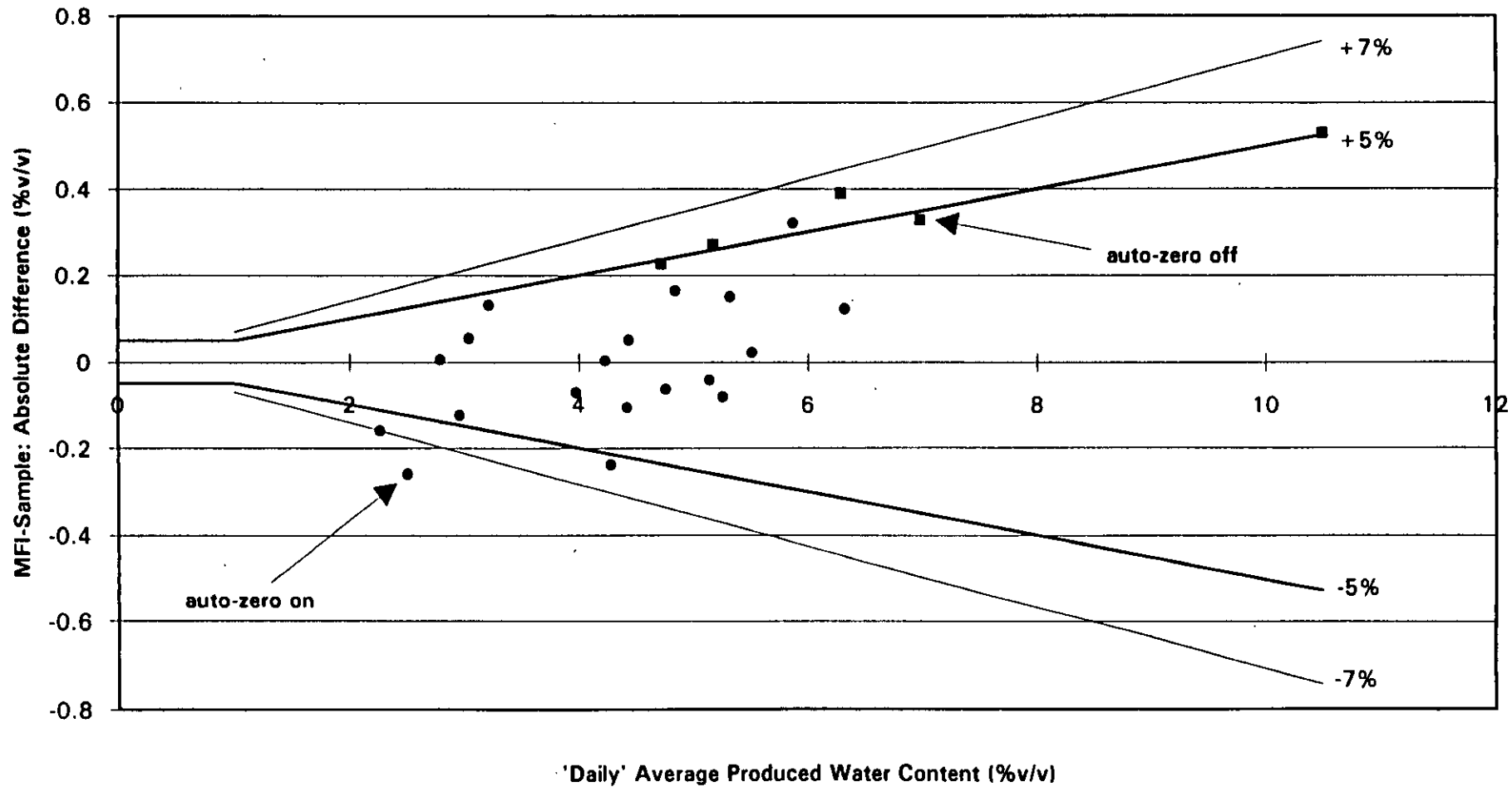


[FIGURE 5]

MFI TEST A8: WATER CONTENT AND OIL DENSITY DATA

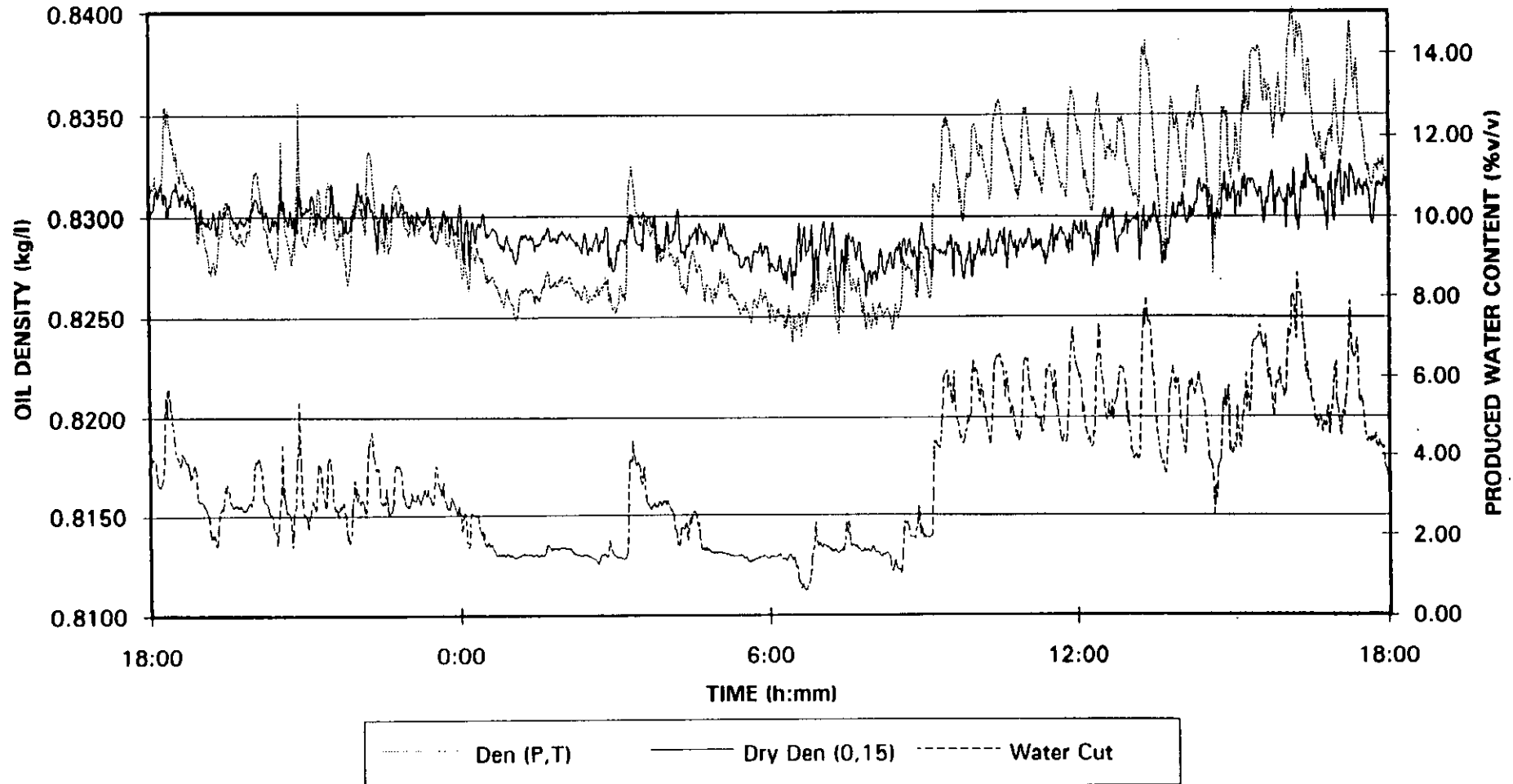


[FIGURE 6]

11.

MFI WATER CUT METER INSTALLATION

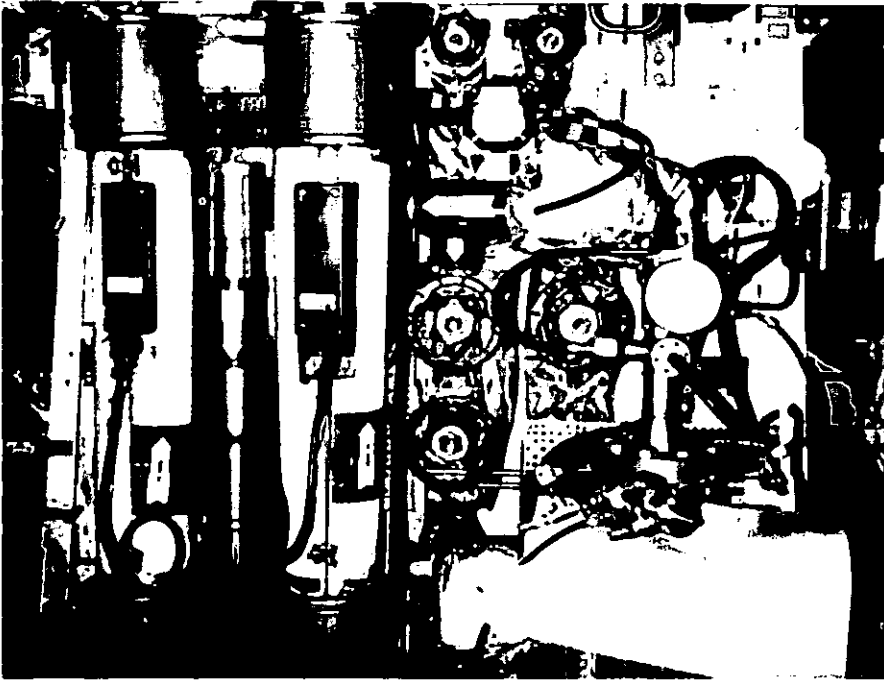


FIGURE 1A: FISCAL DENSITOMETERS AND MFI METER INSTALLATION

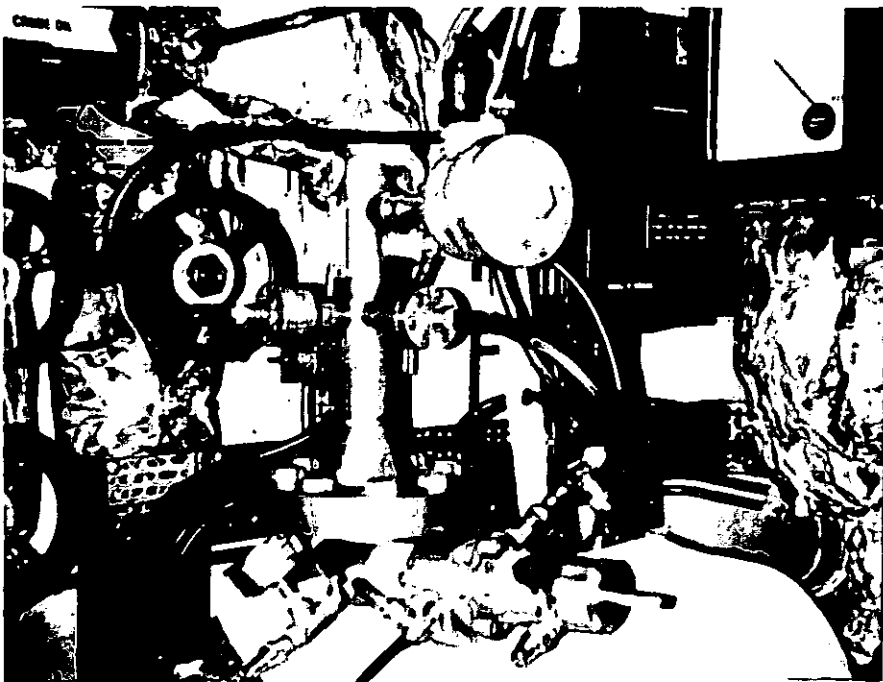
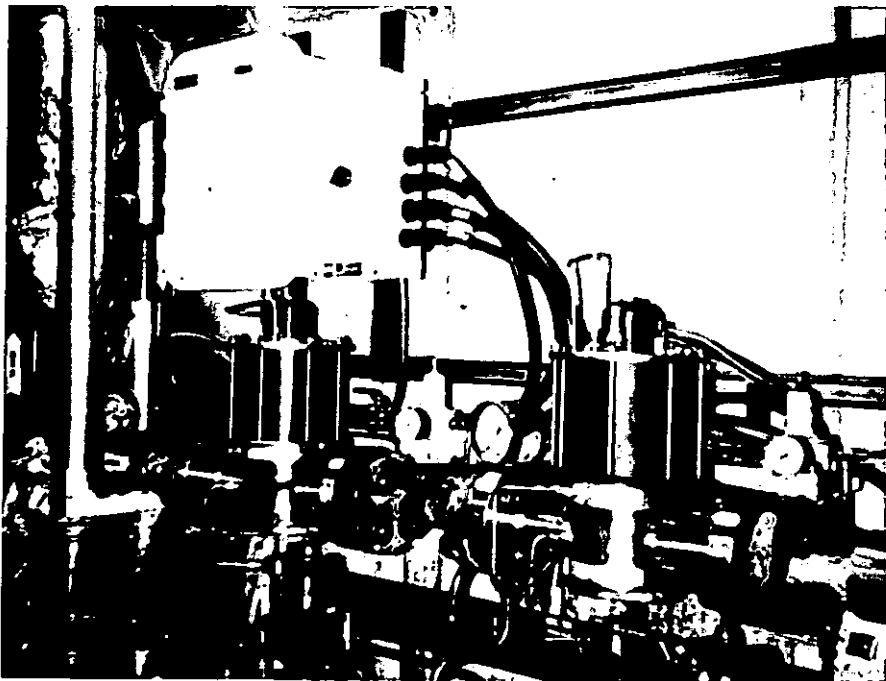
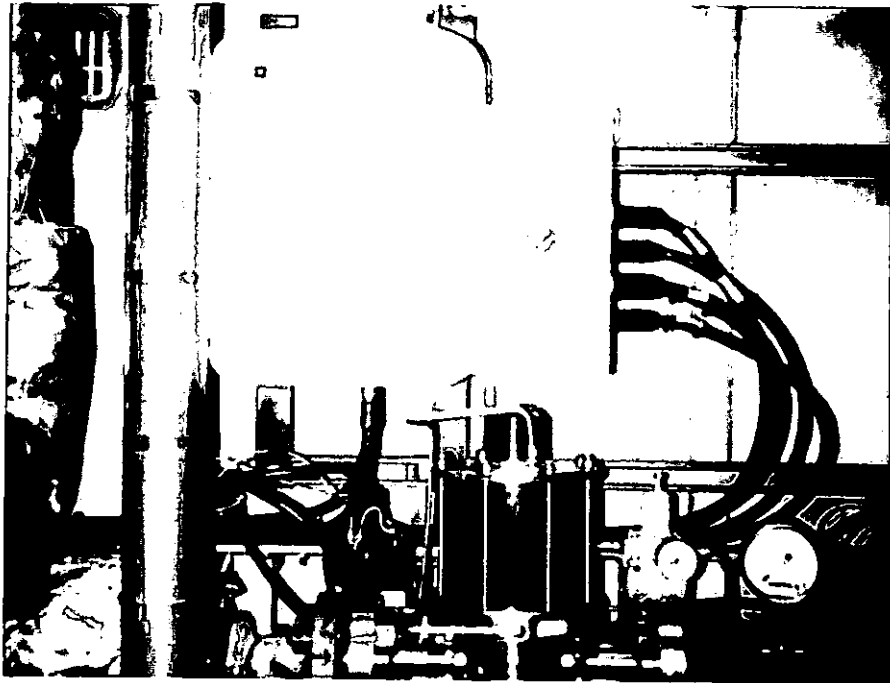


FIGURE 1B: MFI METER AND 50ml PIMR (FOR 'SPOT' SAMPLING)

[FIGURE 1]

AUTOMATIC SAMPLERS AND MFI ELECTRONICS ENCLOSURE



[FIGURE 2]

L Farestvedt: Field testing of the Fluenta WIOM 300 - Water-In-Oil Monitor
The North Sea Flow Measurement Workshop, October 1994

SUMMARY

The Fluenta WIOM 300, High Precision Water-In-Oil Monitor, is a full-bore, in-line, real-time and non-intrusive watercut (BS&W) monitor that meets the requirements of fiscal and custody transfer metering of oil. The monitor is delivered in two versions; one covering 0 to approximately 70% watercut, the other covering the full 0-100% watercut range.

The paper includes a brief technical introduction to the WIOM 300, after which typical results from four of the more recent installations are presented.

These are: Statoil - Gullfaks A, where it was tested for long term stability
 Statoil - Mongstad, where it was tested for high accuracy applications
 Mærsk - Gorm E, where it was tested with unpredictable mixtures of crude oils
 Schlumberger - France, where it was tested with high watercuts and free gas

The conclusion of these and other tests is that the Fluenta WIOM 300 is a reliable and field proven instrument for essentially any watercut measurement application.

CONTENTS

- 1 INTRODUCTION
 - 1.1 Principle of operation
 - 1.2 Applications
 - 1.3 Recent improvements

- 2 FIELD TESTING OF THE FLUENTA WIOM 300
 - 2.1 Statoil - Gullfaks A; long term stability
 - 2.2 Statoil - Mongstad; high accuracy applications
 - 2.3 Mærsk - Gorm E; unpredictable mixtures of crude oils
 - 2.4 Schlumberger - France; high watercuts and free gas

- 3 CONCLUSIONS

**L Faresvedt: Field testing of the Fluenta WIOM 300 - Water-In-Oil Monitor
The North Sea Flow Measurement Workshop, October 1994**

1 INTRODUCTION

The Fluenta Water-In-Oil Monitors are non-intrusive and full-bore watercut meters (BS&W) that continuously measures the water content of water/oil mixtures. They have no objects intruding into the flow, and no by-pass lines are required.

Two versions are available; the **High Precision Water-In-Oil Monitor, WIOM 300**, and recently also the **Full Range Water-In-Oil Monitor, WIOM 300F**. As the names imply, the WIOM 300 is optimized for the lower watercut range (where it meets the requirements of fiscal and custody transfer metering of oil), while the WIOM 300F covers the full 0-100% watercut range. Both versions have wide temperature and pressure ranges, and are reliable instruments with essentially no maintenance requirements.

1.1 Principle of operation

The WIOM 300 consists of a capacitance sensor, sensor electronics, cables, safety barriers, and a system computer. The arrangement, and the location of the different components, are shown in figure 1.

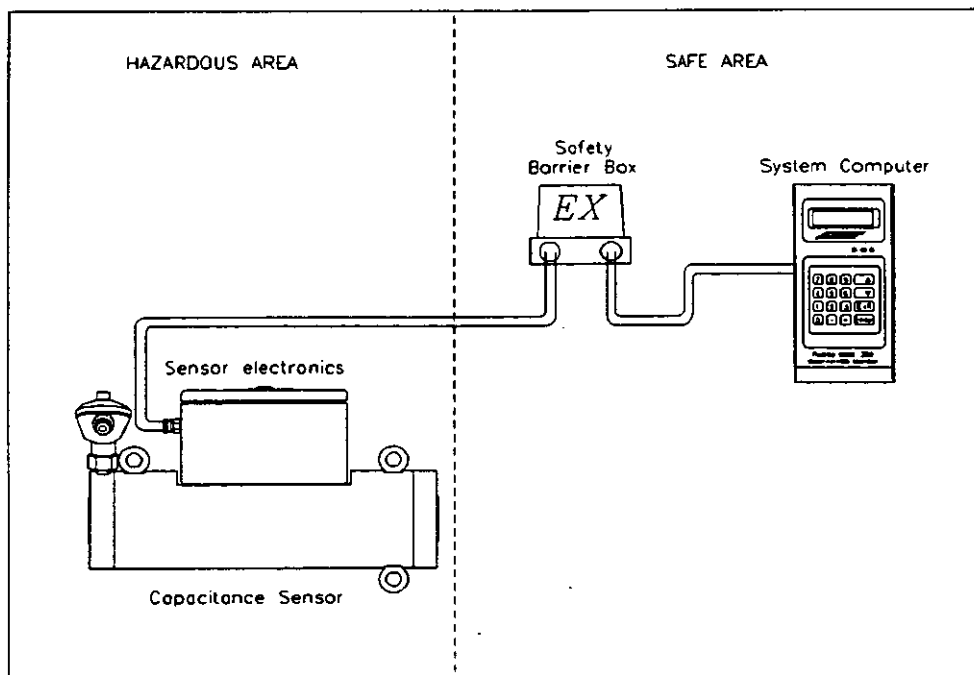


Figure 1: Arrangement of the WIOM 300.

The purpose of the capacitance sensor is to position the oil/water mixture as the dielectric in a capacitor, in such a way that as much as possible of the electrical field induced by the sensor passes through the mixture. The permittivity (dielectric constant) of the mixture can then be determined.

**L Farestvedt: Field testing of the Fluenta WIOM 300 - Water-In-Oil Monitor
The North Sea Flow Measurement Workshop, October 1994**

By placing an electrode on each side of the pipe, and allowing the mixture to flow through the pipe, the electrical field between the electrodes will be affected by the permittivity of the water/oil mixture, and the capacitance measured between the electrodes will vary according to the amount of water in the mixture.

The electrical field is not affected by the velocity of the mixture, and experiments at Christian Michelsen Research (CMR) have shown that the sensor concludes with the same water fraction at a velocity of 3 m/sec as at 0 m/sec. After a period with no flow, however, the readout will change as a result of the water separating from the mixture. Furthermore, a capacitance sensor, such as the WIOM 300, will not be affected by the salinity of the water. This corresponds with the theory, and has also been verified by tests.

The WIOM 300F utilize the same capacitance sensor as the WIOM 300, but in addition also makes use of an inductance sensor. By placing two toroids on the outside of a non-conductive liner, a constant current is induced through the oil/water mixture. Two potential electrodes (placed between the two toroids) detect the voltage drop, which is dependent of the conductivity of the oil/water mixture. Since the conductivity is very different from water to oil, the differential voltage measured will vary according to the amount of water in the mixture. These readings are not affected by the velocity nor the pressure of the mixture. Each of the two spool pieces of the WIOM 300F have separate sensor electronics, cables and safety barriers, while they are both run by the same system computer.

The relation between watercut and permittivity/conductivity is shown in figure 2.

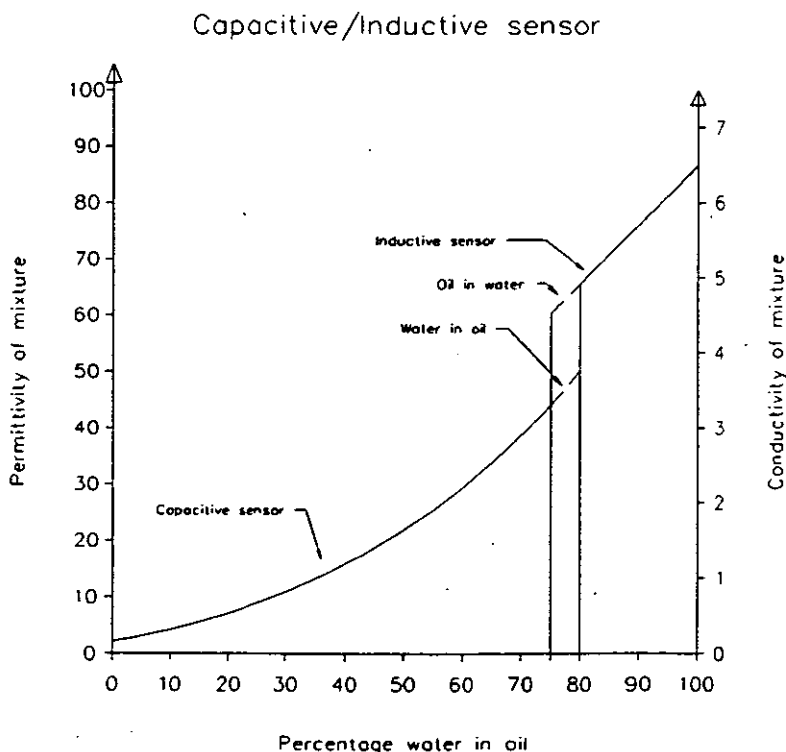


Figure 2: Measurement range for capacitance and inductance sensors.

**L Faresvedt: Field testing of the Fluenta WIOM 300 - Water-In-Oil Monitor
The North Sea Flow Measurement Workshop, October 1994**

1.2 Applications

The WIOM 300 and WIOM 300F, with their high accuracy and wide measurement range, are suitable for a number of applications. Figure 3 and 4 presents the uncertainty for the 0-10 and 0-100% watercut range.

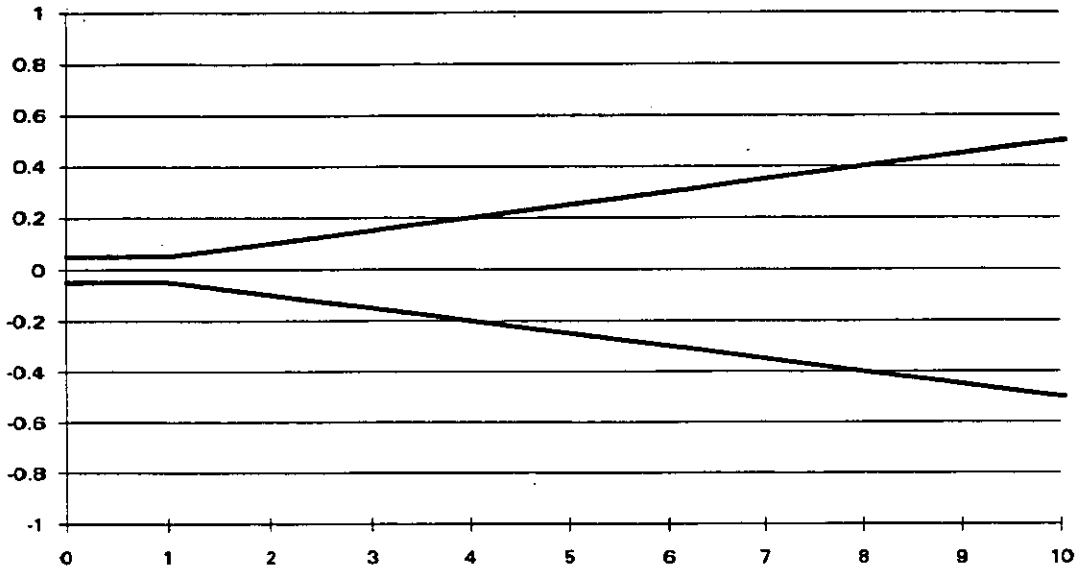


Figure 3: Absolute uncertainty for 0-10% watercut.

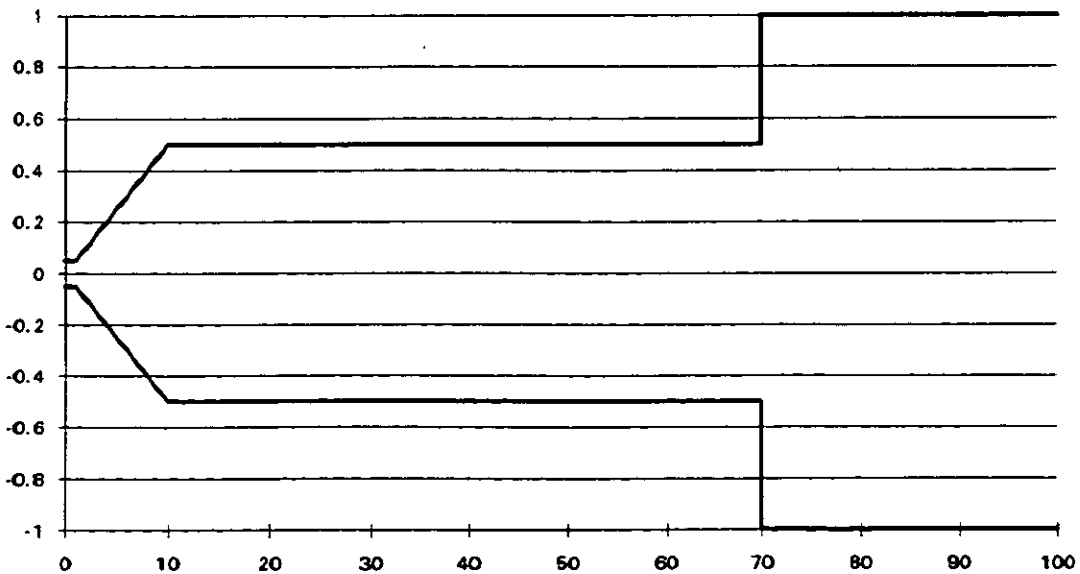


Figure 4: Absolute uncertainty for 0-100% watercut.

L. Farestvedt: Field testing of the Fluenta WIOM 300 - Water-In-Oil Monitor
The North Sea Flow Measurement Workshop, October 1994

The following are some of the applications for the WIOM 300 and WIOM 300F:

- * The extremely low uncertainty makes the WIOM 300 a reliable instrument for fiscal and custody-transfer metering of oil.
- * The full-profile, non-intrusive and very accurate sensor makes the WIOM 300F well suited for continuous and accurate monitoring of the liquid legs of a separator. The WIOM 300F consists of two spool-pieces, one capable of measuring the water content of the oil leg, and one capable of measuring the oil content of the water leg. A single flow computer performs the algorithms from both sensor units.
- * The high measurement range and the full-profile, non-intrusive design guarantees the user a correct and optimized production metering for allocation, and will also ensure an optimized water-flood production.
- * The full-profile design enables installation in pipelines of 1" to 16" inner diameter without having to build a by-pass loop. The high temperatures and pressures that sometimes are present in these pipelines, are also handled with the high temperature and high pressure versions.

For these and many other applications, the Fluenta Water-In-Oil Monitors will increase the efficiency substantially, and result in significant cost-reductions and profit gains. The WIOM 300 and WIOM 300F are certified by BASEEFA according to European Standards, suitable for zone 0 area (corresponding to Division 1 in North America), for temperature class T4 (EEx ia T4).

1.3 Recent improvements

Since the market introduction in 1989, the WIOM 300 series has been through a number of design improvements. The latest of these is in regards to the non-conductive liner, which enables us to use the capacitance technology to detect the watercut, and at the same time also have a completely non-intrusive design.

The first version of the WIOM 300 made use of a ceramic liner. However, for some applications we experienced a surface film developing on the inside of the liner. This resulted in an increased capacitance, and over-estimation of watercut. The ceramic liner has thus been changed to a TK2 coated Boro Cilicate liner, with which the surface film does not occur.

L Farestvedt: Field testing of the Fluenta WIOM 300 - Water-In-Oil Monitor
 The North Sea Flow Measurement Workshop, October 1994

2 FIELD TESTING OF THE FLUENTA WIOM 300

The WIOM 300 has been on the market since 1989, and has since been installed and tested at a number of installations. Some of these are discussed on the following pages.

2.1 Statoil - Gullfaks A; long term stability

Statoil purchased a WIOM 300, which was installed on the Gullfaks A platform in the North Sea during the beginning of August 1992. The WIOM 300 continuously monitors the water content of the exported oil, and the operators are very satisfied with the Fluenta instrument. Some of the initial results are shown in figure 5.

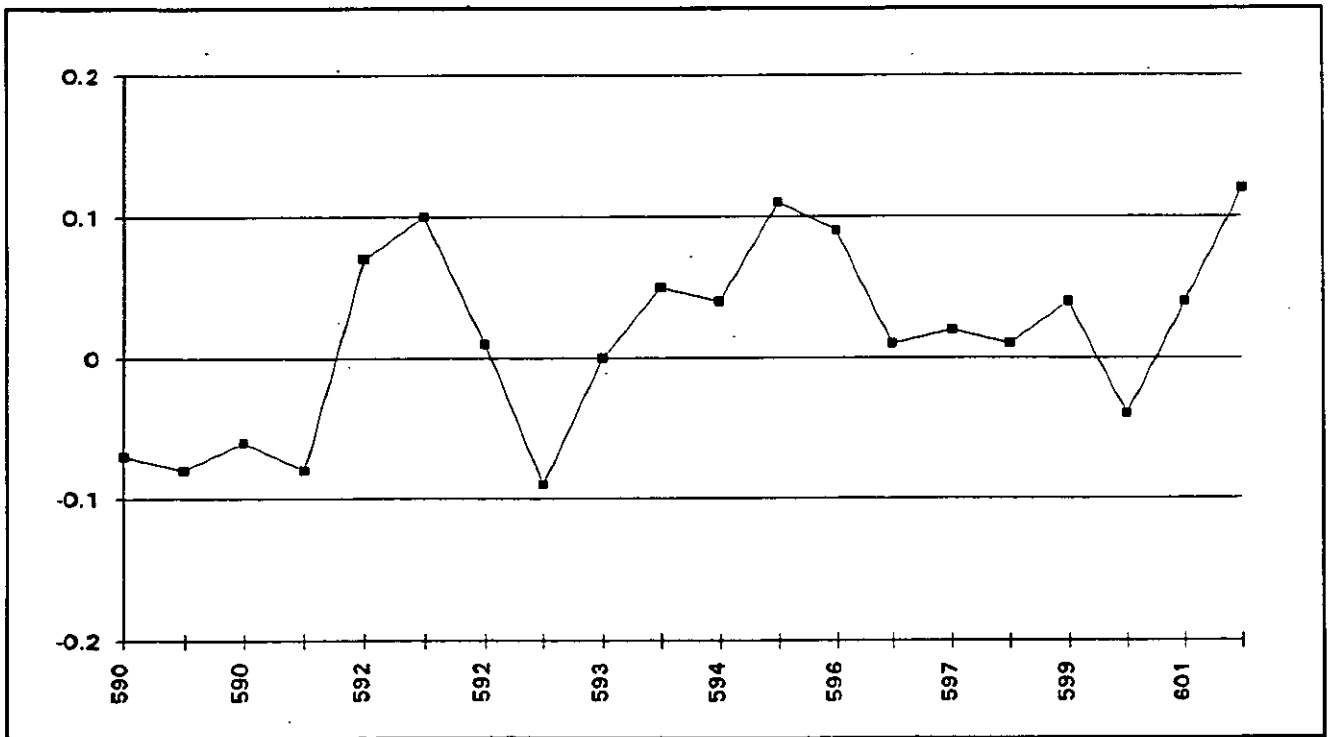


Figure 5: Deviation for different Cargo's during August / September 1992.

The monitor has also since performed to the operators satisfaction. It has shown a slight dependency on temperature variations, and the operators have to adjust for this during loading of the oil tankers. The offset is in the order 0.2%, and is constant throughout the tanker loading.

Since the installation at Gullfaks A, Fluenta has improved the temperature calibration routines, and the dependency to temperature variations is now essentially eliminated (ref. Statoil - Mongstad test described in part 2.2 of this paper).

As the monitor has performed without any problems for over two years, it has proven the stability of the essentially "maintenance free" WIOM 300.

L Faresvedt: Field testing of the Fluenta WIOM 300 - Water-In-Oil Monitor
 The North Sea Flow Measurement Workshop, October 1994

2.2 Statoil - Mongstad; high accuracy applications

The Fluenta High Precision Water-In-Oil Monitor, WIOM 300, was during the time period September -92 to February -93 thoroughly tested through a field test performed by Statoil at the Mongstad refinery outside Bergen. The tests included testing of three different crude oils, with watercut varying from 0 to 10%. The different crudes (Gulfaks A/B, Gulfaks C and Statfjord crude), have quite different electrical and physical properties. The test has thus enabled us to check the instrument's performance for a variety of different crude oils. Results from testing Gulfaks C crude are shown in figure 6.

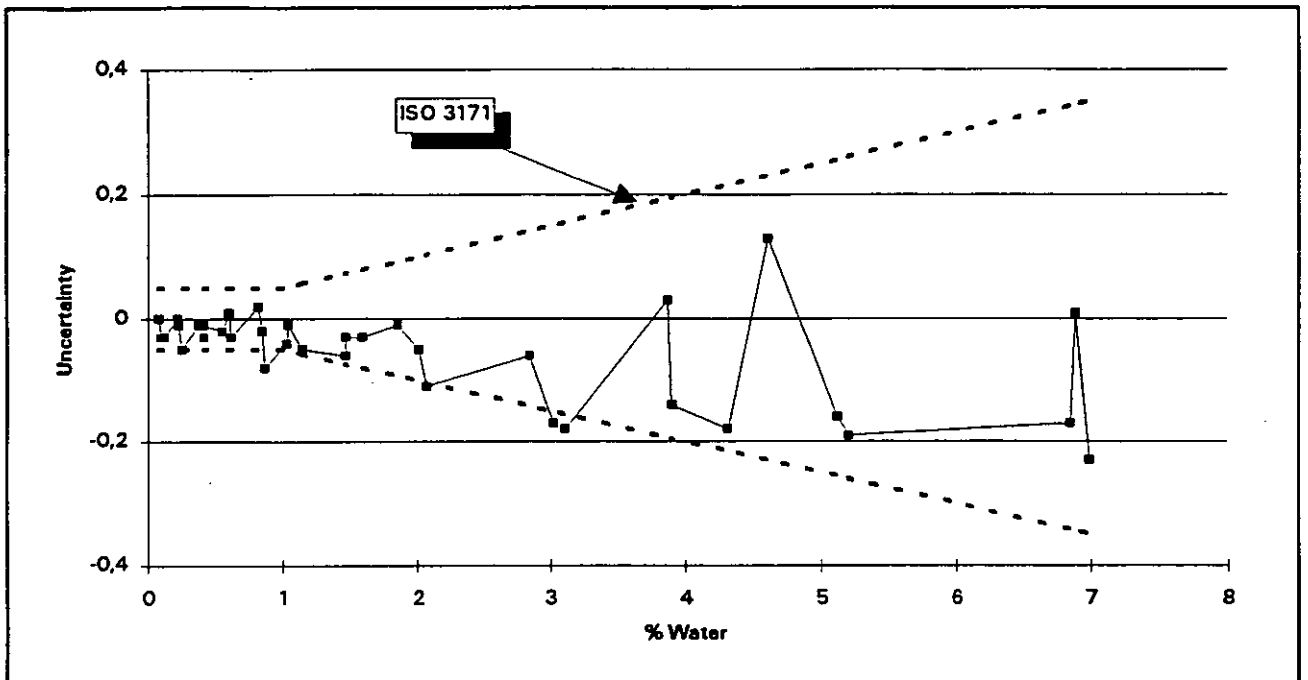


Figure 6: Deviation from Karl Fisher titration for 0-7% watercut.

In addition to the above mentioned tests, the WIOM 300 was tested in regards to temperature variation of the flow and the electronics, and to variation of pressure and flowrate. The monitor proved to be independent of pressure, flowrate and flow temperature. Furthermore, the monitor had only a minor dependency to the electronics temperature, where a variation of 20°C resulted in an error of 0.06% water.

L Farestvedt: Field testing of the Fluenta WIOM 300 - Water-In-Oil Monitor
 The North Sea Flow Measurement Workshop, October 1994

2.3 Mærsk - Gorm E; unpredictable mixtures of crude oils

A WIOM 300 was installed at the offshore Gorm E platform in the middle of January 1993, and was tested for approximately one year. The WIOM 300 monitors the watercut of the export line transporting crude from the different oil producing fields in the Danish sector of the North Sea to shore. The crudes have very different electrical properties, which makes this installation complex and difficult for an in-line and continuous watercut monitoring. The rapid changes in oil type and watercut also makes it difficult to test the monitor, as the sampled oil/water mixture often is not representative to the mixture in the monitor.

The readings from the WIOM 300 has been checked every 4 hours against the water content of samples, determined by the centrifuge method. Due to the variations in crude composition, and with basis in the samples taken, the monitor has been re-calibrated once every two weeks to obtain a best possible coherence with the samples.

Typical results from the installation period are shown in figure 7, where the specified absolute uncertainty also is plotted.

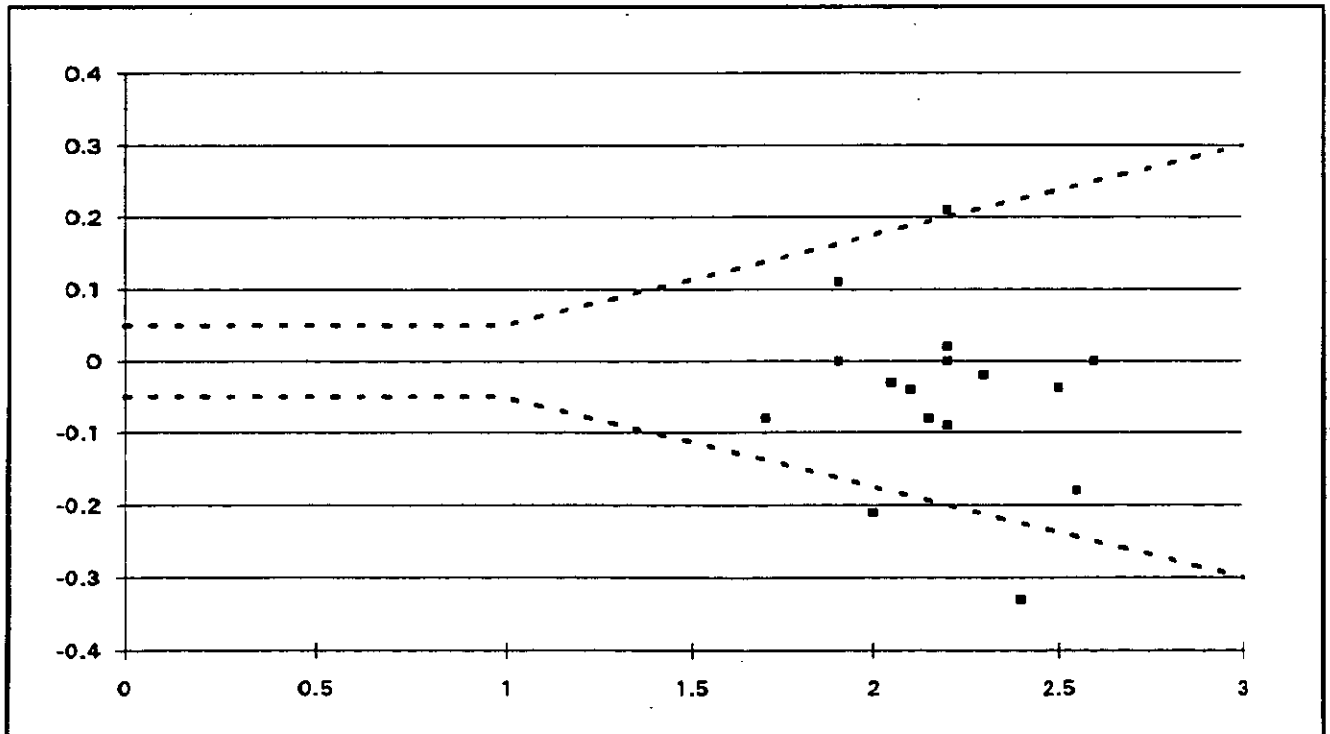


Figure 7: Deviation from centrifuge.

The conclusion of the test is that the application is extremely difficult due to the great variation of oil type, and to the rapid variation of watercut. The major problem is, however, not the monitor's ability to determine the watercut of the mixture, but to verify that the measured value is correct. As the conditions change constantly, it is virtually impossible to get a representative sample.

L Farestvedt: Field testing of the Fluenta WIOM 300 - Water-In-Oil Monitor
 The North Sea Flow Measurement Workshop, October 1994

2.4 Schlumberger - France; high watercuts and free gas

Schlumberger tested a WIOM 300 in the time period March to July 1993. The program included testing for watercuts of 5-30% and void fractions of 0-40%. The test showed that the WIOM 300 performed within its specified uncertainties for the entire watercut range.

Figure 8 presents the results for 3 to 25% watercut.

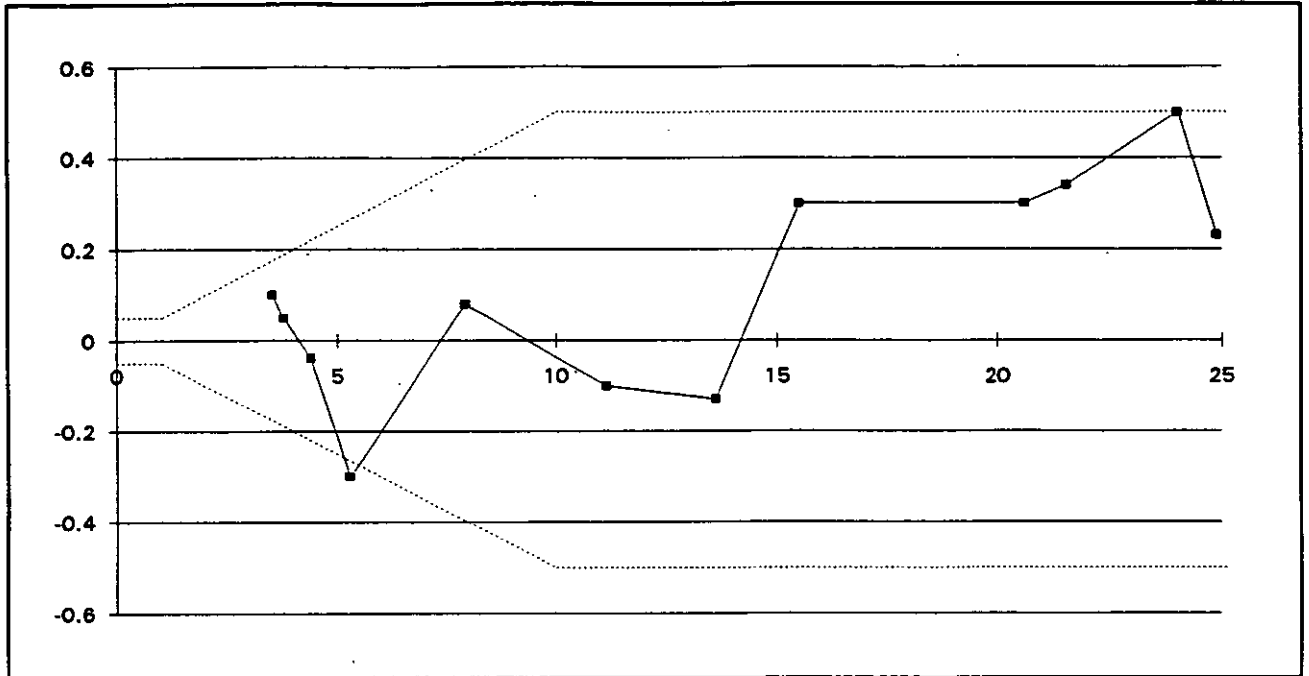


Figure 8: Deviation for watercuts of up to 25%.

The WIOM 300 was also tested for void fractions of up to 40%. It proved to be a linear dependency to the volume of free gas up to approximately 15% gas fraction. Above that level, the monitor had substantially higher uncertainties. As figure 9 shows, the WIOM 300 has a dependency of free gas in the water/oil mixture where 1% gas results in a negative error of approximately 0.1% watercut.

L Farestvedt: Field testing of the Fluenta WIOM 300 - Water-In-Oil Monitor
 The North Sea Flow Measurement Workshop, October 1994

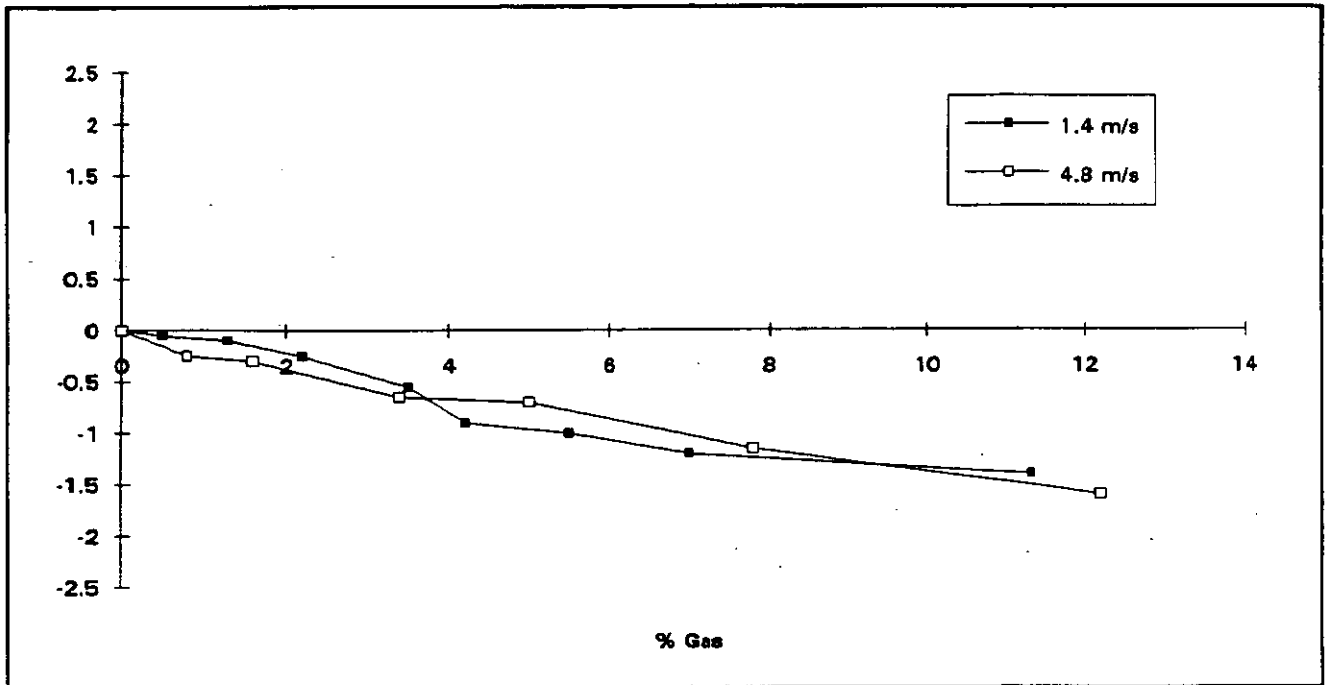


Figure 9: Deviation for 10% watercut.

3 CONCLUSIONS

As the tests described in part 2 of the paper show, the Fluenta WIOM 300 is a fully field proven instrument that can be used for a number of different applications.

The monitor is extremely reliable and essentially maintenance free. It can be used for applications where fiscal accuracy is required, and also for applications where water content is expected to vary over the full 0-100% watercut range.

FRAMO MULTIPHASE FLOW METER - FIELD TESTING EXPERIENCE FROM STATOIL GULLFAKS A AND B PLATFORMS AND TEXACO HUMBLE TEST FACILITIES

Main Index

Arne B. Olsen and Birger V. Hanssen
Framo Engineering AS, Bergen, Norway

SUMMARY AND CONCLUSIONS

The tests performed at the Gullfaks A and B platform and Texaco's test facilities at Humble have given important experience with the FRAMO Multiphase Flow Meter system at field conditions.

At the Gullfaks B platform, the meter was installed in series with a test separator system. Phase flow rates from wells were measured with the multiphase flow meter with the test separator as reference.

The scope of work for the test at Gullfaks A is to verify the operational stability of the meter over at least a 6 months period at an offshore installation.

In the tests at Texaco's Humble test site, a test matrix was followed and the objective was to investigate the meter behaviour at varying gas fractions, water cuts, flow rates and flow conditions.

The tests has shown that we are able to reproduce the good accuracy and repeatability obtained with the FRAMO multiphase flow meter in previous multiphase flow loop tests.

The tests performed at the Gullfaks A and B platform and Texaco's test facilities at Humble have given important experience with the FRAMO Multiphase Flow Meter system at field conditions.

1.0 ABBREVIATIONS

| | | | |
|--------------------|---|-----------------------|-------------------|
| GVF | = | Gas Volume Fraction | % |
| OVF | = | Oil Volume Fraction | % |
| WVF | = | Water Volume Fraction | % |
| Q _{tot} | = | Total flow rate | m ³ /h |
| Q _{oil} | = | Oil flow rate | m ³ /h |
| Q _{gas} | = | Gas flow rate | m ³ /h |
| Q _{water} | = | Water flow rate | m ³ /h |
| MPFM | = | Multiphase Flow Meter | |

2.0 INTRODUCTION

This document includes a summary of the test experience gained from three extensive field test programmes using the Framo Multiphase Flow Meter.

The main objectives of the field testing were as follows:

- To operate the flow meter in actual well environments.
- Investigate meter performance in dynamic operating conditions and under various upstream flow regimes.
- Investigate the influence of various fluid compositions.
- Verify the test results gained from in-house testing.
- Establish meter turn-down capabilities.
- Establish the repeatability and stability performance.

The following test sites were used:

| Site | Customer | Period |
|------------------------|----------|--------------------|
| Gullfaks B | Statoil | March - April 1994 |
| Humble test facilities | Texaco | March - May 1994 |
| Gullfaks A | Statoil | May 1994 - |

For reference purposes a full technical description of the Framo flow meter concept as well as test results from the in-house testing have been included in Appendix.

3.0 STATOIL GULLFAKS B TEST

3.1 Test conditions and programme

The flow meter was tested on well fluids from six different wells on Gullfaks B. All wells produce by the use of water injection. One of the wells produces with zero water cut while the rest have water break through and, hence, produce at different water cuts.

The flow meter was installed downstream a test manifold in a by-pass loop located upstream the test separator as shown in Figure 9. The test separator was equipped with dedicated instrumentation for the measurements of the individual flow rates of oil, water and gas.

The test was sponsored by Statoil, Shell, Conoco, BP, Elf and Norsk Hydro.

The following basic design conditions apply for the test meter used at Gullfaks B:

| Parameter | Unit | Design | Range |
|----------------------|---------------------|--------|--------|
| Pressure | (bar) | 300 | 5-300 |
| Temperature | (°C) | 90 | 15-90 |
| Gas Volume Fraction | (%) | 20-60 | 0-100 |
| Water Cut | (%) | 5-90 | 0-100 |
| Total vol. flow rate | (m ³ /h) | 200 | 20-300 |

Table 1: Design parameters for the MPFM used in the Gullfaks B test

Selected wells were routed through the meter into the test separator with flow conditions as given in the table below:

| Well ID | Q _{tot} (m ³ /h) | GVF (%) | OVF (%) | WVF (%) | WC (%) |
|---------|---|------------|------------|------------|-----------|
| Well 1 | 200 | 43 | 57 | 0 | 0 |
| Well 2 | 95 | 20 | 17 | 63 | 79 |
| Well 3 | 100 | 25 | 30 | 45 | 60 |
| Well 4 | 100-140 | 26-30 | 40-43 | 23-25 | 41 |
| Well 5 | 140 | 34 | 56 | 10 | 15 |
| Well 6 | 55-60 | 28 | 44 | 28 | 39 |

Table 2: Test matrix at Gullfaks B

Average flow measurements from the test separator were carried out in intervals of approximately ten minutes and, hence, the same intervals apply for flow meter measurements.

3.2 Test results

A comparison of flow rate measurements taken from the Framo meter and the test separator are shown in the figures 1 through 6. Figures 1 through 3 show individual component volumetric flow rate compared to test separator while figures 4 through 6 show the same test points, but now presented together with the test separator measurements for the individual wells, all as function of time.

The straight line represents the test separator measurements. This has been done for presentation purposes even though it would have been more correct to use a band to visualise the inaccuracy in the test separator system.

Looking at the individual wells, the scatter around the mean value is small, thus the repeatability is good. Assuming the reference data are correct, some deviation in the average error can be anticipated due to using the same set of calibration values for all wells.

A variation in water salinity from well to well was discovered during the tests. Although salt content will affect the attenuation coefficient for water, these variations were not adjusted for during the test. The same set of calibration constants were used for all wells. The sensitivity to water salinity appeared less than expected.

3.3 Discussion of results.

The Gullfaks B field test has shown that the Framo multiphase flow meter operates satisfactory at field production conditions and the meter performance, as established in previous flow loop tests, has been re-produced.

The test has also verified that the mass attenuation coefficient for oil seems to be independent of actual oil (crude, dead crude, diesel, Exsol D80) and furthermore, the mass attenuation coefficient for natural gas is equal to that of oil. Another interesting finding is that the Barium spectre contains information which can be utilised for determining the salinity of water. These findings will contribute to simplify the calibration requirements of the meter in the future.

No sensitivity to flow regimes, sand, chemicals have been observed during the test.

The deviation around the mean value for single wells indicates excellent repeatability.

4.0 TEXACO HUMBLE TEST

4.1 Test conditions and programme

The Framo Multiphase flow meter was tested by Texaco at the Humble test facility in Texas, USA in April and May 1994 as part of a project sponsored by Statoil, Svenska Petroleum, and the Norwegian KAPOF programme.

The Humble test facility allows multiphase testing with live fluids - natural gas/oil/water and the ability to measure field typical flow regimes. The test rig flow schematic is shown in figure 10.

Flow loop specifications:

| | |
|--|---|
| Oil/crude flow rate: | 0-20.000 bbl/d (0-133 Sm ³ /h) |
| Water flow rate: | 0-20.000 bbl/d (0-133 Sm ³ /h) |
| Gas flow rate: (nitrogen/natural gas) | 0-13 nmscf/d (0-15340 Sm ³ /h) |
| System pressure: | 50-1500 psi (3,4 - 103,4 bar) |
| Slug length: | Field typical |

The objective with the test was to investigate the meter performance at the following conditions:

- Variable water cut
- Variable gas volume fractions
- Variable flow rates (flow turn-down test)
- Field typical flow regimes

The test matrix was as follows:

| | |
|-----------------------------|---|
| Water cut: | 50%, 60%, 70%, 80%, 90% |
| Gas volume fractions (GVF): | 60%, 80%, 90%, 96% |
| Flow rates: | 4 from low to high limit of meter (50 to 300 m ³ /h) |

The multiphase flow meter used in the test is a topside version of the Framo meter with a 2" venturi section.

The following design conditions apply for the meter used at Humble:

| | Unit | Design | Range |
|--|----------------------|---------|-----------|
| Flow line pressure, P | bar | 10,3 | 3,4 - 250 |
| Production temperature T | °C | 25 | 15 - 70 |
| Gas Volume Fraction (GVF) | - | 60 - 96 | 0 - 100 |
| Water Cut | % | 5 - 90 | 0 - 100 |
| Total flowrate (all phases) Q _{tot} | m ³ /hour | 150 | 50 - 400 |

4.2 Test results

The main difference between the GULLFAKS B test and the test at Humble was the flow regimes and the Gas Volume Fraction (GVF). At Gullfaks B the GVF was below 50% while at Humble they concentrated on 50% and higher with severe slugging included as part of the test.

The meters capability to measure water cut was tested by varying the GVF from 50% to 90% and at each step, vary the water cut from 5% to 90%. The total volumetric flow rate was kept constant during this test. The results are shown in figure 7 (measured water cut vs. reference water cut).

In the tests at Humble, three different configurations were used to prepare the inlet flow conditions for the multiphase flow meter. Homogeneous flow was created by mixing the three components just upstream the meter. Short slugs were generated by mixing in a 100 meter riser, and long slugs by mixing in a 100 meter riser followed by a 600 meter terrain pipeline upstream the meter. Although the meter interfaces to a 4" pipeline, the dominating pipe diameter in the loop is 6".

The data presented in figure 8 represent the results from tests on different GVFs comparing reference oil flow rate to metered oil flow rate under homogeneous and slugging conditions.

4.3 Discussion of results

Results from the three-phase oil, water and gas tests at Humble show that phase flow rates are predicted with good accuracy over the whole range tested. The error in oil and water flow rates relative to the actual total flow rate are within +/- 5% which are comparable to the GULLFAKS B results. This is also true for the gas flow rates less than about 70%.

As in the GULLFAKS B test and in inhouse testing the meter has a tendency to measure lower gas flow rates than the reference system at high gas volume fractions (70 to 100% gas). This trend was foreseen and is systematic.

Due to the built-in flow mixer which always provides homogenous flow to the measuring section, the meter seems to measure with good repeatability over the whole test range, even at extreme slugging conditions.

5.0 GULLFAKS A TEST

5.1 Test Conditions and Programme

The Framo Multiphase Flow Meter was installed on Gullfaks A as part of the Poseidon multiphase pump skid in May 1994. As for the test at Humble, this test was sponsored by Statoil, Svenska Petroleum, and KAPOF.

The objective of this test was to get long term experience with the meter under real offshore conditions and to enable online monitoring of the pump performance.

The meter was hence located downstream the pump where the conditions are as follows:

| | | |
|-------------|---|------------------------------|
| Total flow | : | 120 - 140 m ³ /hr |
| GVF | : | 30 - 35% |
| WC | : | 50% |
| Pressure | : | 70 bar |
| Temperature | : | 70 - 80_C |

Only one well is being boosted by the multiphase pump.

5.2 Test Results

So far we have received a limited number of test points which has been compared to the test separator.

The results we have got are, however, within the specified accuracy of the meter which is $\pm 5\%$ of actual total flow.

The meter has been in operation for about 1200 hours so far. Further testing will continue throughout the rest of 1994 and possibly into 1995.

Appendix 1 - Framo multiphase flow meter description and test results

FRAMO Multiphase Flow Meter

A considerable amount of research effort lies behind the development of reliable, flexible and accurate multiphase flow meters. This is now available from Framo Engineering AS for both topside and subsea applications.

The multiphase flow meters offer the following advantages compared to conventional methods of well testing:

- On-line well monitoring
- Improved well control
- Optimized production control
- Improved allocation methods
- Reduced OPEX and CAPEX
- Reduced space and weight requirement for topside installations

The FRAMO multiphase flow meter is capable of measuring all combinations of oil, water and gas in a well stream.

The system consists of a multi-energy level gamma fraction meter and a venturi momentum meter in combination with an in-line static mixing unit.

Flow mixer

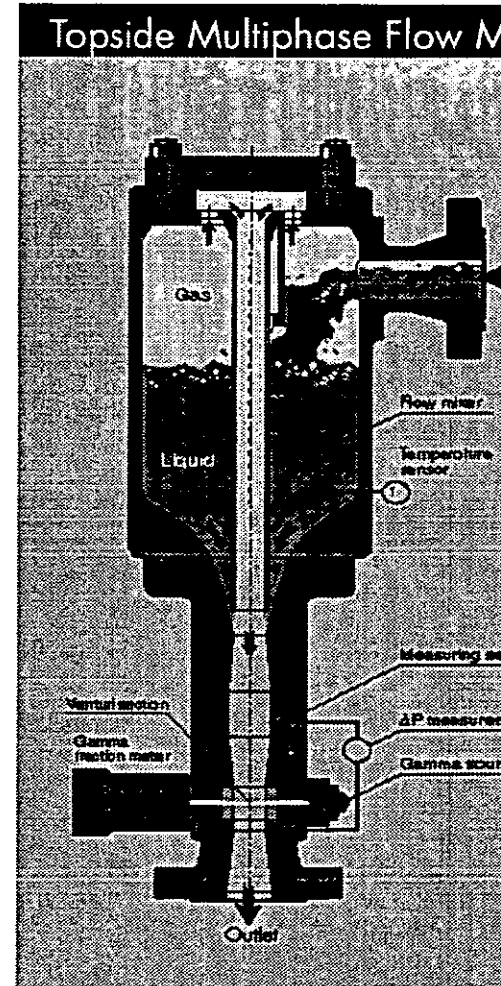
The mixing unit makes the metering system completely independent of upstream flow regimes and provides a homogeneous flow to the metering section.

The flow mixer is a purely static device. The most dense part of the fluid is drained from the bottom of the mixer via an ejector, while the lightest fraction is drained from the top and directed via a pipe back to the ejector, where it is mixed with the dense fluid, according to the ejector ratio.

Multi-energy gamma meter

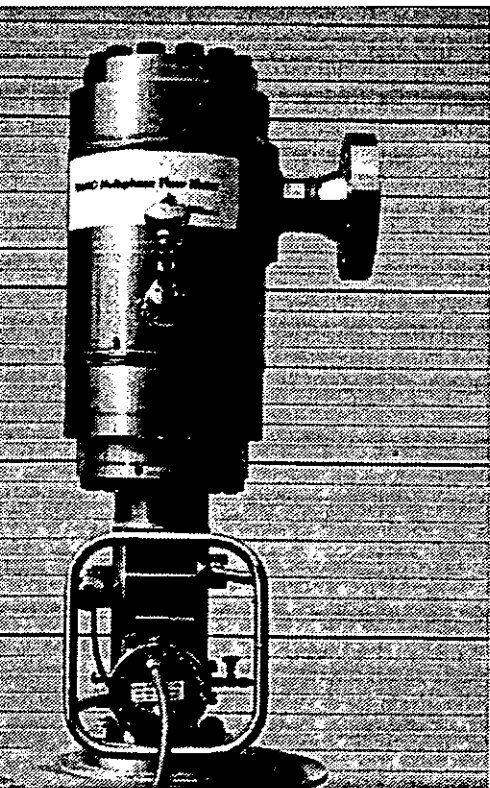
The multi-energy gamma meter determines the fractions of oil, water and gas in the well stream. The gamma meter is located immediately downstream the flow mixer, and these fractions can be treated as volume fractions.

Calculation of the oil, water and gas fractions is based on the relative attenuation of different



gamma energy levels. The gamma meter consists of a gamma isotope and a ruggedized detector.

The combination of two different energy levels is sufficient to determine three fractions, since the third fraction can be deducted by subtracting the first two from 100%.



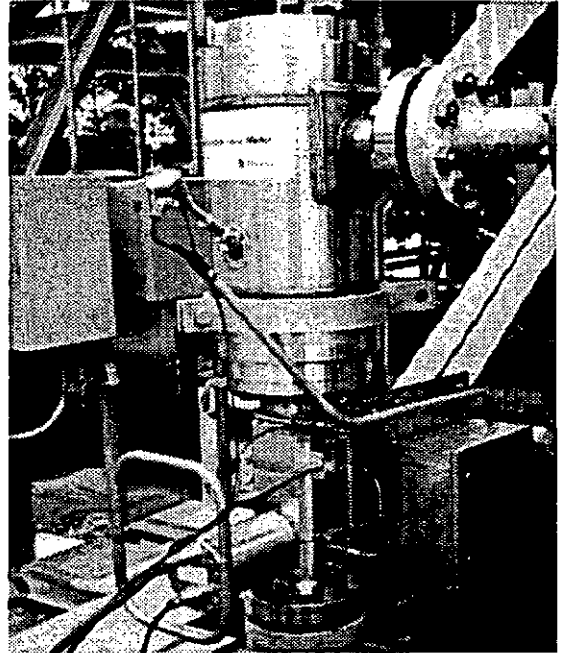
Venturi meter

A venturi meter is used in combination with the gamma fraction meter to obtain the flow rates of oil, water and gas. This can be done since the venturi meter is located immediately downstream the flow mixer. Multiphase mixtures have the same properties as single phase mixtures of similar density, and the single-phase venturi relation can therefore be utilized.

The basic venturi meter configuration is equipped with high-precision pressure sensors for both venturi differential pressure and absolute pressure.

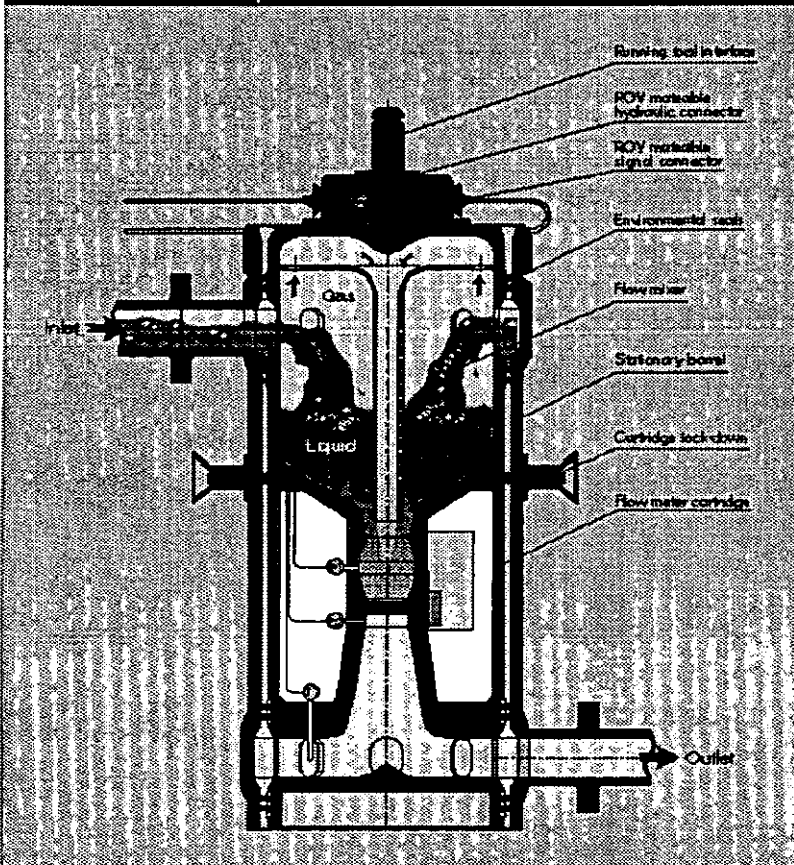
Design parameters:

- Accommodates any flow regime
- 0 - 100% Water Cut
- 0 - 100% GVF
- Subsea and topside designs available

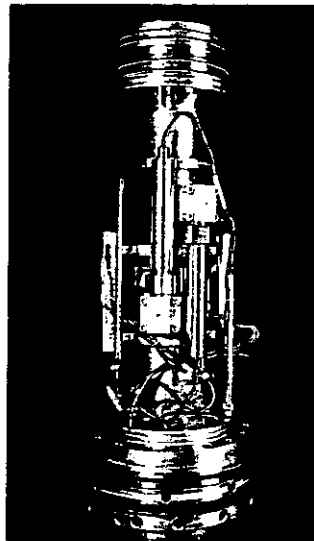


FRAMO topside multiphase flow meter successfully tested at Humble field in Texas

Subsea Multiphase Flow Meter



Measuring section of the subsea meter



For further information, please contact: Framo Engineering AS P.O. Box, N-5051 Nesttun, Norway
Phone: +47 55 99 98 00 • Telefax: +47 55 99 99 10 • Telex: 42 078 framon

FRAMO Multiphase Flow Meter
Test at Gullfaks B - April-May 94

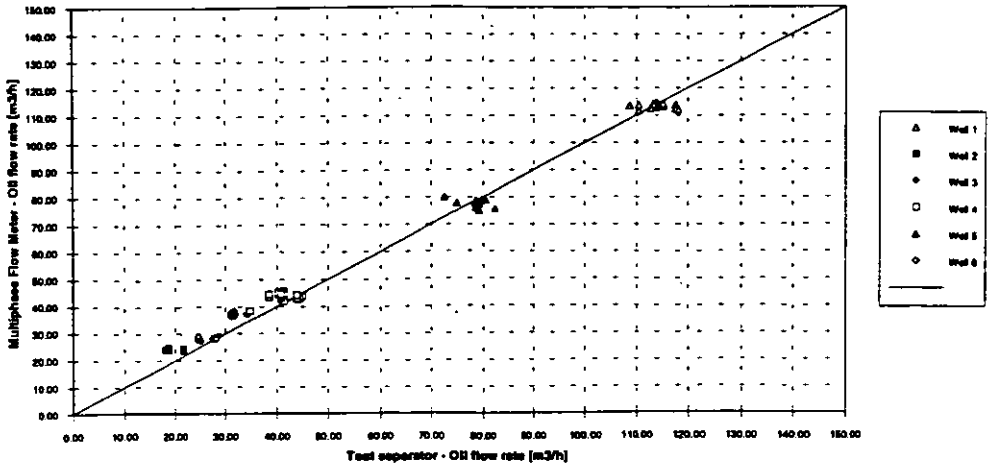


Figure 1 Measured oil flow rate vs. test separator oil flow rate, Gullfaks B

FRAMO Multiphase Flow Meter
Test at Gullfaks B - April-May 94

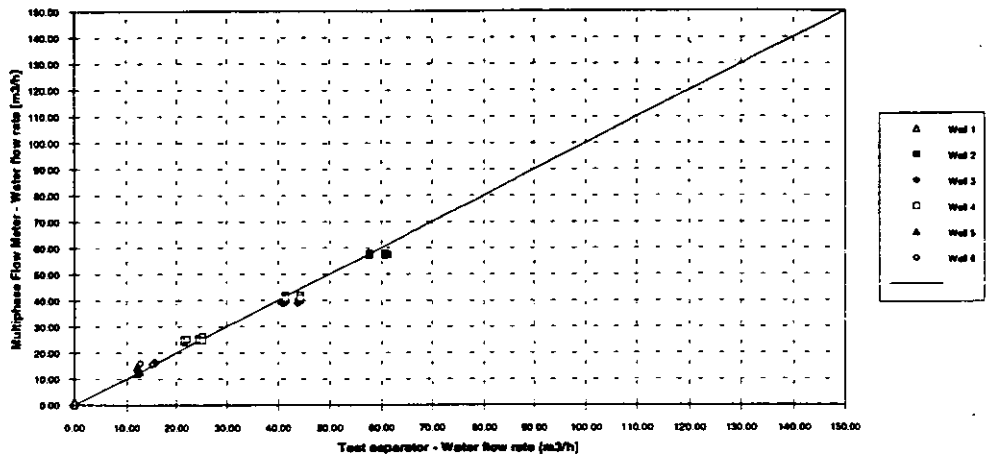


Figure 2 Measured water flow rate vs. test separator water flow rate, Gullfaks B

FRAMO Multiphase Flow Meter
Test at Gullfaks B - April-May 94

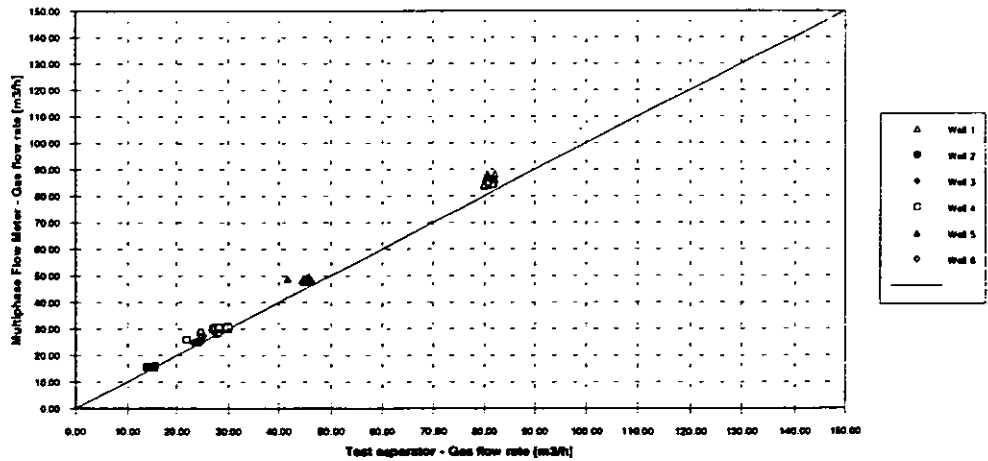


Figure 3 Measured gas flow rate vs. test separator gas flow rate, Gullfaks B

FRAMO Multiphase Flow Meter
Test at Gullfaks B - April-May 94

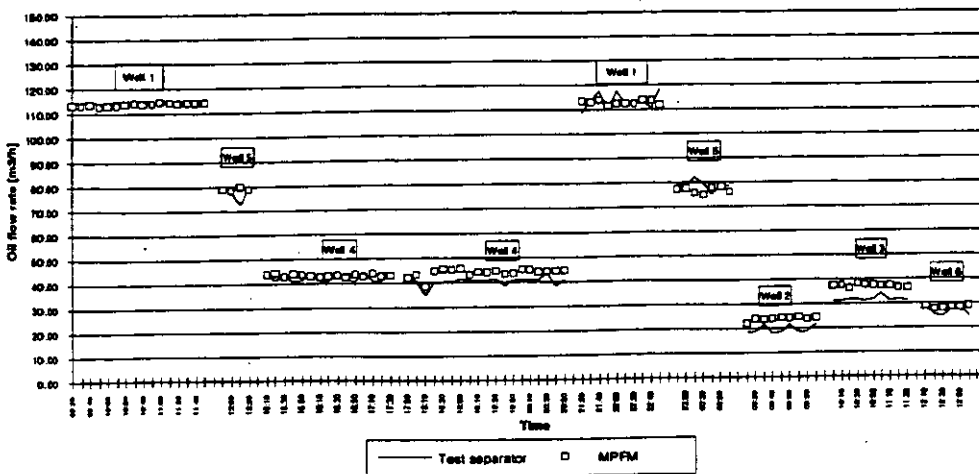


Figure 4 Multiphase flow meter and test separator oil flow rate vs. time, Gullfaks B.

FRAMO Multiphase Flow Meter
Test at Gullfaks B - April-May 94

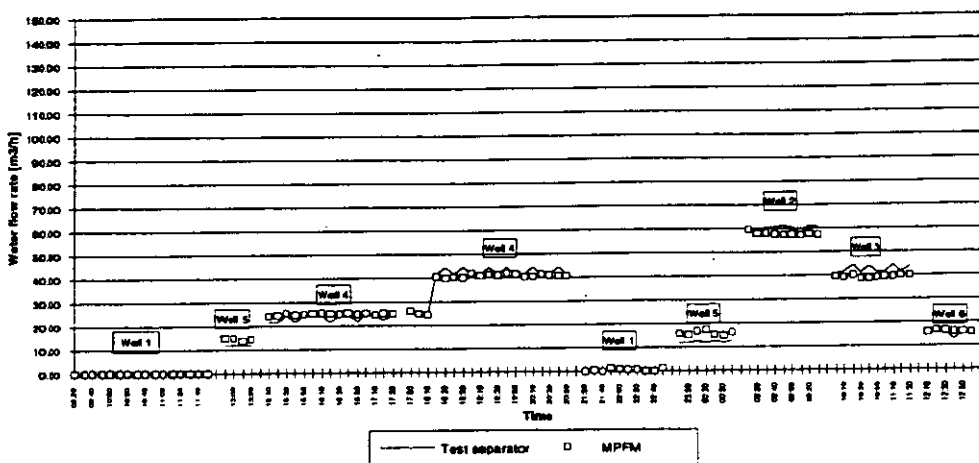


Figure 5 Multiphase flow meter and test separator water flow rate vs. time, Gullfaks B.

FRAMO Multiphase Flow Meter
Test at Gullfaks B - April-May 94

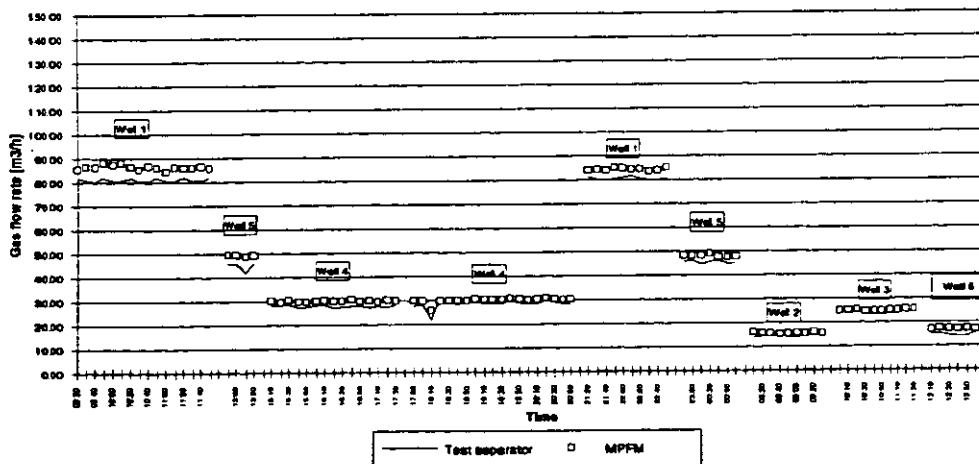


Figure 7 Multiphase flow meter and test separator gas flow rate vs. time, Gullfaks B.

Measured water cut vs. reference water cut
(Total flow rate = 270 m³/h, variable GVF)

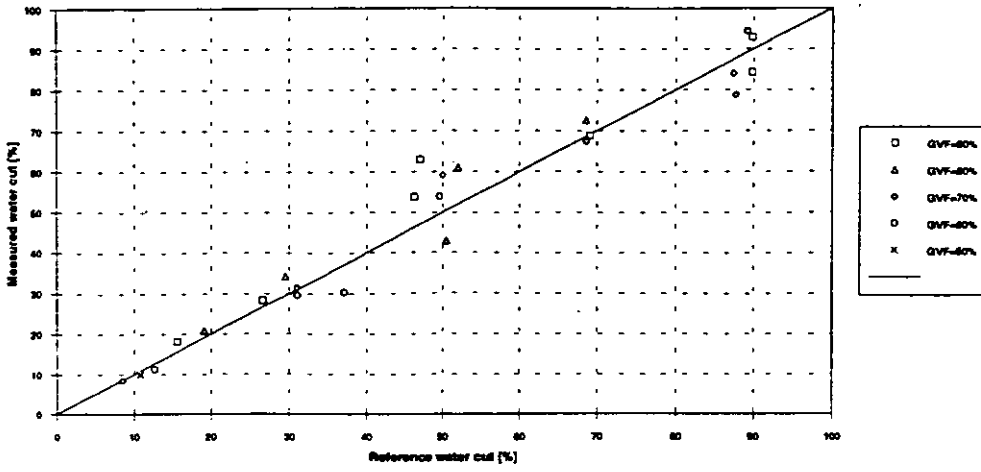


Figure 7 Measured water cut vs. reference water cut, Humble.

Turndown oil rate, variable flow regime

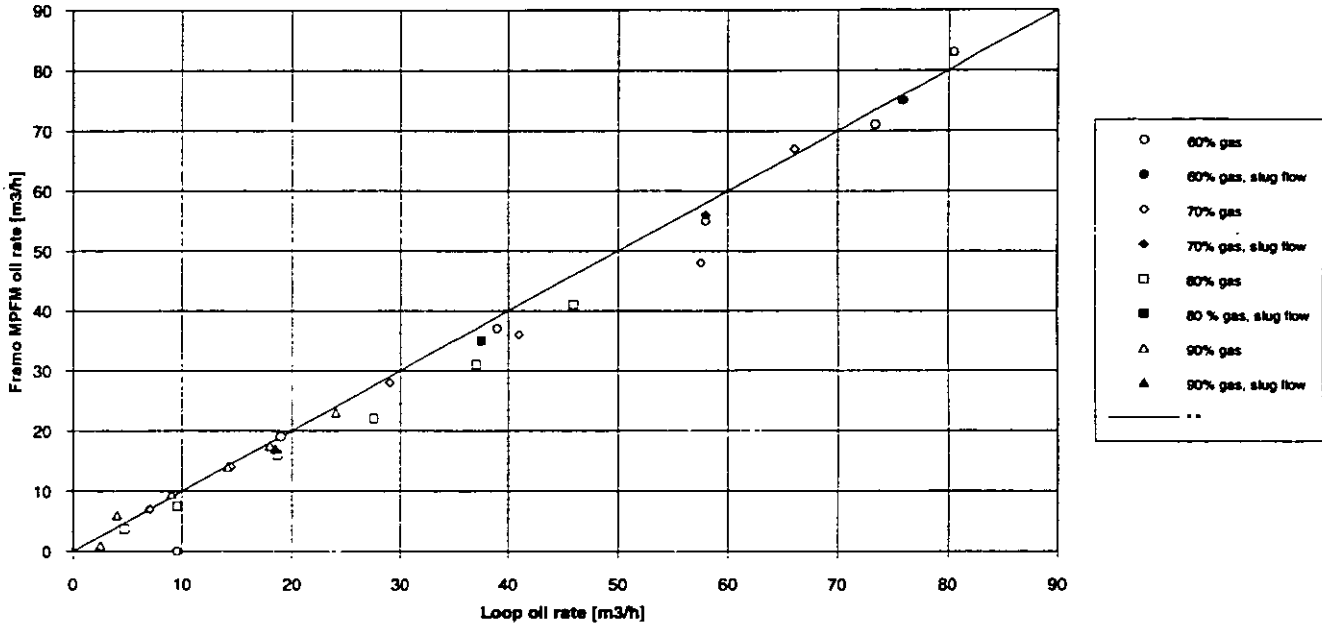
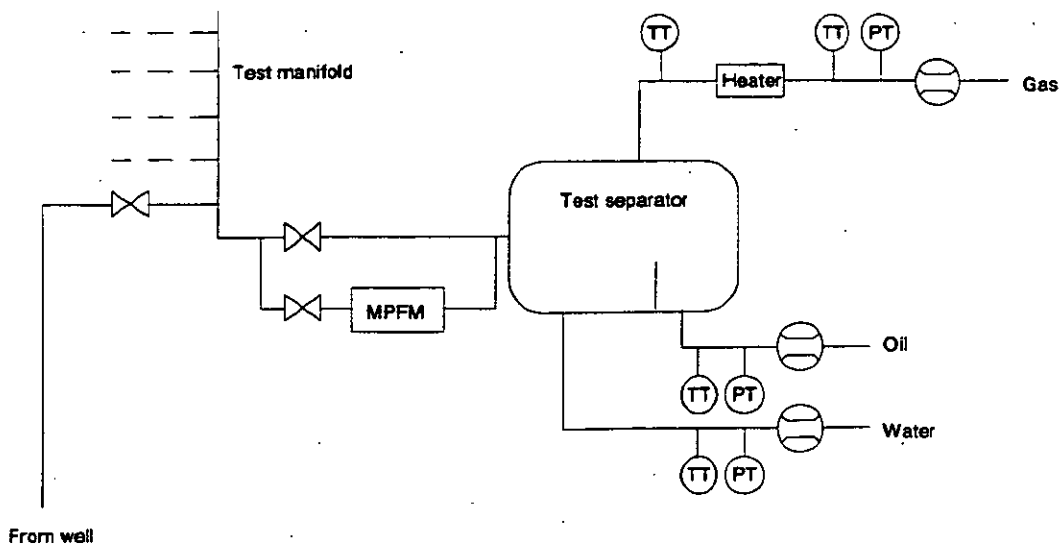


Figure 8 Measured oil rate vs. reference oil rate at variable flow regimes, Humble.



From well

MPFM = Multiphase Flow Meter

TT = Temperature Transmitter

PT = Pressure Transmitter

Single Phase Flow Meter

Figure 9. Test set-up at Gullfaks B.

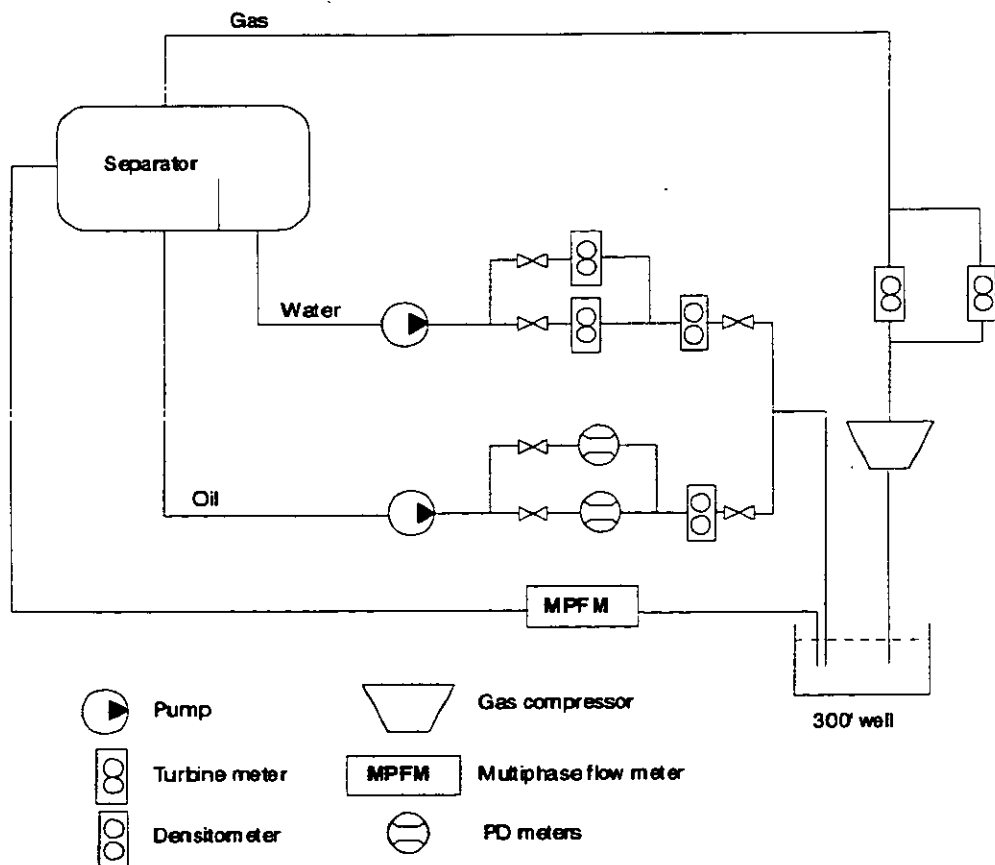


Figure 10 Multiphase test loop at Humble test site.

A Cooperative Approach To New Product Development

W. Letton
Daniel Industries
Houston, Texas
USA

S u m m a r y

In times past, development of new products for our and other industries could be described as **serial and compartmental**. It was serial in the sense that all major developmental activities - design, laboratory testing, field testing, regulatory approvals - were conducted sequentially, one following the other. It was compartmental in the sense that the parties involved - suppliers, users, governmental authorities, independent test laboratories - had access to and communicated only a portion of the total body of knowledge of the new product. The net result has often been that the new product was stillborn, or introduced years after it might otherwise have been.

The intent of this paper is to propose a better methodology to develop new products than this serial-compartmental model. What is suggested is a cooperative model, where the key participants come together early in the development program, discuss the issues involved, and formulate an introduction plan which satisfies the requirements of users, suppliers, and regulators in order to commercialize the new product in as expeditious a fashion as possible.

1 Introduction

The intent of this paper is to propose a better way of new product development for our industry than that we have traditionally used in the past. Here we suggest that a partnership between the three primary participants - suppliers, users, and regulatory authorities - can be the optimal means of commercializing innovative new technology in a manner which satisfies the needs of all three.

In what follows we first consider the primary needs of suppliers, users, and authorities, where they are in harmony and where they are not. Next we discuss a model for new product development used in former times (perhaps still in use today in some places?), and give examples of where and how it failed. We then consider a better methodology for developing new products which can overcome the deficiencies of its predecessor. The two halves of Project Ultraflow are used to illustrate the process.

2 Basic Needs of Suppliers, Users, and Regulatory Authorities

It should be apparent that users, suppliers, and authorities each have a set of needs which they

attempt to satisfy. In some cases these needs are identical for each participant - the need for product safety, for example - while in other cases they may be quite different. Table I is a partial list of needs for suppliers, users, and authorities. As noted above, there are certain needs which exist on more than one list, sometimes on all three. We do not suggest that each list is complete or absolute in any sense; one could argue for a different set.

There are several points we try to make here. The first is that supplier, user, and authority have needs which, though sometimes similar, often diverge. The second is that each is a necessary player in bringing the new technology to market; without the affirmation and participation of each, the common goal of commercialization can't be achieved. A third point follows from the first two: some form of accommodation among the participants must take place to bring the product to a commercial state.

In what follows, we describe two models of new product development. In both cases all three participants play a role, each striving to achieve the maximum on their needs list. The difference between the two is that, in the second model, the participants recognize the need for cooperation. In so doing, they come together early to develop a plan for bringing the new product to a state whereby it can be sold commercially and used for its intended purpose. In this way, they create a "Win-Win-Win" situation.

3 The Old Model of New Product Development

By the expression "Old Model" we simply mean the way new products were often developed in the 1970's and 1980's. There is no intended suggestion that all new products were developed this way, but our personal experience was that a significant number experienced some of the characteristics described below.

In both models, the source of the major innovation can be either supplier or user. Although we often think of the supplier as the innovator, in some high-technology areas it has been estimated that as many as 80% of the innovations came from users [1]. Indeed, among the products we have heard described here, the Daniel Multipath Ultrasonic Meter and the Kongsberg Multicomponent Flowmeter (MCF) are good examples of such.

In the Old Model, the three main participants typically did their work in series. First, the supplier did the bulk of his development work, taking the product far along before turning it over to the user for evaluation. Once the user was satisfied, the authorities whose approval was needed became involved. Lack of early extensive interaction among the three often proved costly in both time and money.

In the Old Model, the notion of secrecy was paramount. Intellectual property rights were precious, and neither user nor supplier was willing to divulge much, lest it give away the technology advantage. Users were reluctant to sign non-disclosure agreements, and suppliers declared that anything communicated to a customer was "as good as in the hands of our competitor." Often user and supplier companies were represented by personnel from their

respective research laboratories, hence the real users were not dealing with the real suppliers. If the innovation was from the supplier, often it was the result of a technology push rather than a market pull. Instead of looking for technology which might satisfy a perceived need in the user domain, an enthusiastic researcher at the supplier company would take some new technological starburst (fiber optics? micromachined silicon? neural networks?) in search of a problem he might solve. Such an approach is often unsuccessful; the dead product files of many a high-technology company are littered with such corpses. If the supplier was fortunate, he exposed the "hot new product" to user scrutiny at an early stage, at which time its deficiencies were highlighted. At times, however, the technology push within the supplier company is so great that the development can't or won't be stopped. This can be due to any of several reasons.

Poor feedback during prototype testing. If the supplier doesn't avail himself of the user community when he finally has something to test, he may proceed blithely on toward production, assuming all is well, when in reality the product should have been killed or substantially modified. This can result from very little or no user testing - perhaps a manifestation of the paranoia over secrecy - or can be due to testing with the wrong users. More about user selection will be said later.

Wrong-headed technical management. Sometimes the urge to push the technology into a commercial form is overpowering. Those in powerful positions who believe in the technology may convince themselves and others that the market will develop around the product once it has been introduced. While this is sometimes true, it is a dangerous strategy. If the product is really good, the user community should be able to affirm this.

Wrong-headed general management. After investing much time and money on prior development, general management may not be receptive to suggestions of major changes in the program. Considerable pressure may be brought to bear to complete the product development process, reduce engineering expenses, start production, and begin to recoup some of the cost of development.

Whatever the cause, any new product development which is a technology push is a potential drain on the supplier's resources. In the worst of cases, large sums may be spent in development, then spent again in re-work. Two good examples of this phenomenon are found in wireline well logging.

(1) **LINAC.** In the first case, a downhole linear accelerator was developed ostensibly to replace an existing nuclear radiation instrument [2]. Called the LINAC, it accelerated electrons into a special target to generate bursts of gamma rays 100 times more intense than those from the existing tool, the Lithology-Density Tool (LDT). This meant that it could eliminate many of the statistical variations typically seen by nuclear instruments, move through the borehole much faster than the LDT, and turn its gamma radiation off when not in use (the Cesium source in the LDT radiated continuously and could be quite dangerous). However the LINAC was three times as expensive as the LDT and twice as large; an extra operator would have been required simply to maneuver the tool, had it proceeded to commerciality. The

program was killed after building two prototypes and performing limited testing. Very little was learned from prototype testing which wasn't predicted; the same decision could have been made before any money was spent.

(2) **SDT.** A second, more expensive example of a technology push gone awry was the development of a Digital Sonic Tool (SDT) in the early 1980's [3]. Here, as with the LINAC, the drive to introduce new technology overwhelmed the forces of reason, which asked only, "What will it do for the user?" It was well known that by observing how sound propagates in and around a borehole, one could conceptually learn much about mechanical properties, such as shear and compressive strengths of the rocks, cement bond quality behind casing, and so on. The technology to digitally capture acoustic waveforms downhole had been developed, so that all the power of digital signal processing could be applied to extract the relevant information. Prototypes were built, huge amounts of data were acquired and processed, and the SDT went straight into production. Unfortunately, the technology to acquire raw data was far ahead of the ability to process it. A more serious problem, however, was the lack of "answer products" from the SDT. The customer had no interest in acoustic waveforms, and only a little interest in the basic mechanical properties of the rock; what he wanted was someone to tell him when his production zone might collapse in a heap of sand, and when it would not. Unfortunately, years passed before these kinds of answers were available. In the meantime, the SDT struggled to do the job of its simpler predecessor, at twice the cost. In the end, it was actually the next generation acoustic waveform tool which was successful in achieving the goals set out originally for the SDT.

The two cases described above illustrate the point that pushing technology can be an extremely expensive exercise.

Neither of these examples required involvement of the authorities as part of the development process. Under the Old Model, however, taking such a new product to the authorities would probably have taken place after some amount of re-work had satisfied the user's needs. It is not inconceivable that the authorities might also require changes, in which case another round of re-work would be necessary.

4 A Better Model

As mentioned earlier, the source of innovation for the new product can be either supplier or user. Whichever the case, we shall assume the supplier is convinced that this technology has strong commercial prospects. What should he do next?

If we can assume that the supplier's technical and general management are enlightened rather than wrong-headed, the place he is most likely to falter is in testing the new product, and in gaining good feedback from both users and authorities on the test results. In general, suppliers can do only limited testing on their own; they need facilities and, more importantly, experience in similar product use that only the user community has.

In the new way of doing things, then, the essence of our problem is establishing a close working relationship early on between supplier, user, and the appropriate authorities. In the abstract it all sounds rather straightforward, however there is still one thing that can ruin the process: poor user selection.

To understand the importance of connecting the supplier of the new product with the proper users for testing, it is useful to consider Eric von Hippel's concept of lead users [4]. He defines lead users of a novel product, process, or service as those who display both of the following traits with respect to it:

- (1) They face needs that will be general in the marketplace, but months or years before the bulk of that marketplace faces them.
- (2) They expect to benefit significantly by obtaining a solution to those needs.

Lead users will not only follow the test program of the product with a keen awareness, they will be a constant source of new ideas about which features are missing from the product and must be added. They are also a thoughtful sounding board for new ideas from the supplier. Primarily, they will be involved.

Finding a group of such users to test the new product and provide feedback sounds like normal, common-sense advice. Why would a supplier not look to those users who satisfy these criteria?

The answer is simply that it is often a good deal more work to line up a group of lead users than to assemble a user test group with no such selection criteria. To determine who those lead users are for a specific product - and they obviously will vary from product to product - the supplier will need to perform an analysis of the market. If, as is often the case, the Sales Department is responsible for finding test opportunities for the new product, one can almost guarantee the test group will consist of three types of users: (1) the supplier's largest clients, (2) clients with whom most recent sales contact has been made, and (3) clients to be seen in the near future. None of these users inherently has a need for the new product, hence getting the strong user interaction required may be difficult for the supplier. These non-lead users may agree to test the new product, perhaps as a favor, however their lack of need for the product will do nothing but impede real progress, as the testing will likely yield very little. If no true lead users are engaged in the test program, an important step in the development cycle will have been skipped. At a later point in time this omission may result in a re-design of the product to correct faults which should have been uncovered during the development program.

Also important in getting the hot new technology into a form that it can be used commercially is identifying the appropriate authorities who will need to be persuaded, and including them during the period of testing the product. If a strong core group of lead users has been identified, they probably have very clear ideas about where it will be of use to them, and hence which authorities will need to approve it. These people should be included from the very beginning in whatever test programs are arranged between suppliers and users, and can thereby have a

major positive impact on the development program.

V Project Ultraflow

The Project Ultraflow has been a good example of many of the ideas proposed here. Begun in 1989, this Joint Industry Project had the goal of bringing high-accuracy multipath ultrasonic flowmeters to a point of acceptance as a viable means of fiscal metering of natural gas. Early in the program it was recognized that there were really two distinct sets of objectives among the interested users, hence two separate JIPs were formed inside Project Ultraflow, the so-called Wet and Dry Gas Projects you have already heard described here.

In each of the Ultraflow projects, the members were lead users almost by definition. Each member paid a substantial sum simply to participate and to have access to the results. Had these users not recognized the benefits to be derived from this new form of gas flow measurement and believed they would benefit significantly from its introduction, it seems doubtful they would have spent such a considerable sum. In each of the Ultraflow groups, it was the users who defined the environment in which the meter was required to perform and specified how it was to be tested, whether in third-party test laboratories, their own laboratories/test facilities, or through actual field installations. Decisions on how to proceed at key points during the development were made by supplier and users together, in consultation with third-party lab personnel as required. Early in each project it was decided that certain improvements to the meter would be permitted, but only if it could be shown that these did not invalidate earlier results. This was a crucial and correct decision; when a product is sailing through uncharted waters, it is essential that alterations be permitted to take advantage of what is learned during testing. Both groups met often during the course of development. Wet Gas met ten times in 33 months, Dry Gas eight times in 23 months.

The role of the authorities in both Wet and Dry Gas groups has been fundamental from their beginnings. The DTI was involved from the very start of the Wet Gas activities, and has kept a close watch on results obtained both at NEL and at the Bacton field test site throughout the development. On the Dry Gas side, the following statement was highlighted in the group's first separate meeting on 1 March 1990:

"The objective of the work programme to be proposed is for ultrasonic meters to be approved, by the appropriate European authorities, for fiscal metering applications."

To achieve this goal, representatives from DTI, PTB, NMI, and the French Ministry of Industry were direct participants in the project as members of the Quality Assessment Team required by the EEC.

As soon as the Dry Gas effort began, the group informed the convenor of the ISO TC30/WG20 of the work planned and of its relevance as the basis for a draft standard. In fact, the Synthesis Report of results has recently been provided ISO for just that purpose.

A brief word needs to be said about secrecy. If the liaison between supplier and user(s) is for the purpose of further developing the technology, accommodation must be made for protecting information which is revealed during that development. Without this, the supplier will be reluctant to enter into the kinds of discussions necessary to move the technology forward.

VI Conclusion

So in the end we conclude that we all have more to gain by working together to develop new high-technology products. On the surface, this certainly doesn't sound controversial or revolutionary. After all, aren't we encouraged from the time we are small children to cooperate with one another, that more can be accomplished working together than individually?

The simple fact is, however, that what is suggested here is contrary to certain aspects of human behavior. If we work in a cooperative way with those outside our own company, we will likely be required to share some our secrets with them, albeit within the protection of a confidentiality agreement. Furthermore, if we work side by side in the development as proposed, there may be times when our partner sees our "dirty laundry." And since the individual partners have differing goals for the development, there will be times when they must compromise on the execution of the development activity. For all these reasons and more, companies may find it difficult to participate in a cooperative development program, even though the concept sounds simple.

Finally each company must decide if this cooperative development model is workable. The cost to be paid is the sacrifice of a certain amount of one's autonomy in new product development. However, sooner or later the market may make one wish the sacrifice had been made.

REFERENCES

- 1 VON HIPPEL, E. *The Sources of Innovation*. Oxford University Press, New York, 1988.
- 2 KING, G., BECKER, A., CORRIS, G., BOYCE, J., and BRAMBLETT, R. Density Logging Using an Electron Linear Accelerator as the X-Ray Source. *Nuclear Instruments and Methods*, B4-25, pp. 990-994, 1987.
- 3 MORRIS, C. F., LITTLE, T. M., and LETTON, W. A New Sonic Array Tool for Full Waveform Logging. *Oilfield Review*, 33(1), pp. 19-25, 1985.
- 4 VON HIPPEL, E. New Product Ideas from "Lead Users." *Research-Technology Management*, 32 (3), pp.24-27, May-June 1989.